1999

Quality of gas metal arc welds for rapid prototyping and wear replacement

Suprana Frank Jacono

University of Wollongong

Quality of Gas Metal Arc Welds for Rapid Prototyping and Wear Replacement

A thesis submitted in fulfilment of the requirements for the award of the degree

Honours Masters of Engineering

from

UNIVERSITY OF WOLLONGONG

by

Suprana Frank Jacono, B.E. (Hons)

Department of Mechanical Engineering

1999

Some people spend their money freely and still grow richer. Others are cautious, and yet grow poorer.

Be generous, and you will be prosperous. Help others, and you will be helped.

Proverb 11:24-25

This thesis is dedicated in memory of Caroline; Someone to whom I gave all my love to...but...time will tell...the truth shall reveal...

Abstract

Rapid prototyping by Gas Metal Arc Welding is a method of making a prototype by creating layers of welds to form a desired shape. The work in this thesis investigates the feasibility of a robotic Gas Metal Arc Welding cell for rapid prototyping and wear replacement applications.

The experiments were divided into two categories, ie. thin walled objects and solid objects. The optimal range of welding parameters for the two types of objects were investigated extensively for their suitability for rapid prototyping and wear replacement applications. The experiments include investigations of the mechanical property, surface temperature and surface regularity of the welded steel created by rapid prototyping and wear replacement techniques. The importance and the significance of selecting the correct welding parameters for rapid prototyping and wear replacement applications are demonstrated in this thesis.

In the experiments, it was found that the welding parameters lie within a narrow range. It was also determined that the suitable settings are in the short-circuit transfer mode. However, in the case of the solid objects it was determined that spray transfer is a suitable transfer mode for the fill.

Acknowledgments

First of all I would like to express many thanks to my supervisors, Dr. Friso De Boer and Professor John Norrish, for their support, professionalism, attention and comment which helped me to write this thesis. Their comments and suggestions helped to improve this thesis significantly.

Many thanks to Joe Abbott for his excellent technical support, professionalism and assistance in the Manufacturing Research Laboratory throughout the experiments and also my colleague Michael Siminski for his excellent collaboration and help in programming the ABB robot. I would also like to thank Mirjam Jonkman, Ian Kirby, Tony Kent, Keith Maywald, Roma Hamlet, Jenny Robertson, Nadine Jurd, Edward Biyik, Graeme Dash, and Ron Young for their help and generosity.

Many thanks also to Greg Tillman of the Materials Engineering Department for his help with the preparation of specimens, macro etching and taking photographs. Thanks also to Max Conyngham of Materials Engineering Department for his advice in metallurgy and macro etching. I would also like to thank Ron Kinell of the Materials Engineering Workshop for his assistance of making and testing tensile and Charpy specimens.

Finally, I would also like to say many thanks to my wife Caroline for her faith, sacrifice, support and my family for their courage and faith in me all of these years.

<u>HOWEVER,</u>

On 18 March 2000, something happened, Caroline decided to leave and went on her own separate way. On that day she said something which I could never forget till the day I blow my last breath. She said, "Frank I regret to marry you, I don't feel anything for you anymore, I don't care about you anymore and I don't love you anymore". My heart was broken when I heard those words from someone whom I love with all my heart and my life. I have been searching for the answer why, but I never found it. Perhaps God does not want me to know the real reason behind it as it would probably hurt my heart even more. I guess life is a constant change and people change their heart. Like people say, some things are meant to be and some things are not meant to be; why? You just can't find the reason why and you just have to let nature takes its course. So long Caroline...May God bless you.

I wish to acknowledge the University of Wollongong for providing the necessary facilities and friendly atmosphere during many years of my study. I would like to express many thanks to Cooperative Research Center for Material Welding and Joining for sponsoring and financing the research and the Mechanical Engineering workshop for providing support and technical assistance.

Contents

List of Tables

List of Formulas

List of Figures

List of Symbols

Symbol	Description	Unit
θ	Angle of the first order of polynomial fit	Degrees
μm	Distance	μm
°	Angle	Degree
C	Temperature	Celsius
l	Capacity	Litres
m	Distance	metre
min	Time	minute
mm	Distance	millimetre
sec	Time	second
Std.Dev	Standard deviation	
t	Time	second
x	x-axis coordinate of the profile projector	μm
X	x-axis coordinate after angle compensation	μm
y	y-axis coordinate of the profile projector	μm
Y	y-axis coordinate after angle compensation	μm

Chapter 1

Introduction

1.1 An Overview of Welding Processes

The work in this thesis will demonstrate the capability of a robotic welding cell using Gas Metal Arc Welding for rapid prototyping and wear replacement applications. Two types of objects were investigated to determine the weld quality using rapid prototyping techniques. These are a thin walled sample and a solid sample. The thin walled sample represents the suitability to create hollow objects and the solid sample represents the suitability to create solid objects using rapid prototyping technique. The experiment was carried out by using various welding parameters to determine the range of the optimal settings for rapid prototyping and wear replacement applications. This includes choosing the suitable transfer mode, finding the optimal region for the application, investigating the mechanical property of the weld specimen and determining the method of defining weld quality.

Over the last century, there has been rapid development in joining technology. A number of new joining techniques have been developed and what was once known as a 'black art' has now become a sophisticated manufacturing technology.

Welding is an efficient way to join metals and it is widely used in industry. Welding can also be used in repairing or rejoining products made of metals. Welding and joining are essential in many industries to manufacture various components. Typically, the joining process may be divided into the following categories: mechanical joining, adhesive bonding, brazing, soldering and welding.

Definitions of a weld vary from book to book. For example, a weld may be defined as a *union between two pieces of metal rendered plastic or liquid by heat or pressure or both. A filler metal with melting temperature of the same order of that of the parent metal may or may not be used [11]* or, alternatively, *a weld can be defined as a localised coalescence of metal or non-metals produced either by heating the material to the welding temperature, with or without the application of pressure, or by the application of pressure alone, with or without the use of a filler metal [32].*

Utilising the two definitions above, welding processes may be classified into those that rely on the use of pressure and those that use elevated temperatures only to achieve the bond. The most important welding processes are shown in figure 1.1.

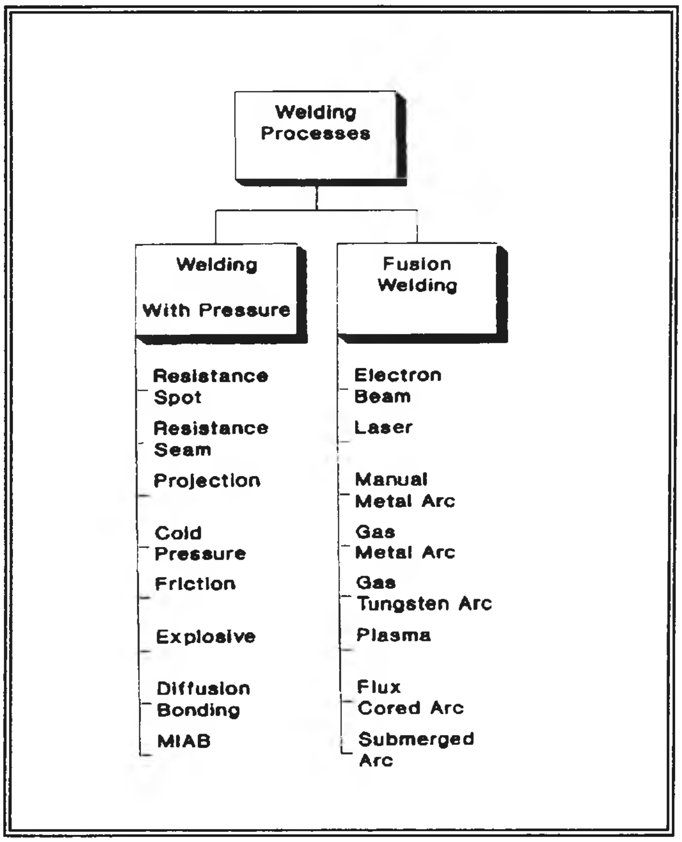

Figure 1.1

Important welding processes [1]

1.1.1 Welding with Pressure

For this type of welding, though the process is undertaken at an elevated temperature, little or no melting takes place in the joint region of the components. Examples are Resistance Welding, Cold Pressure Welding, Friction Welding, Explosive Welding, Diffusion Bonding and Magnetically Impelled Arc Butt Welding (MIAB).

1.1.2 Fusion Welding

Fusion welding processes require high temperatures to locally melt the components which are to be joined. A filler metal may be used in fusion welding, depending on the geometry of the two mating surfaces. Some of important factors that need to be considered are the thickness of the material and the gap between the mating surfaces. Examples of fusion welding processes are Gas Metal Arc Welding (GMAW), Oxy Acetylene (OA), Thermit Welding, Electroslag Welding, Gas Tungsten Arc Welding (GTAW), Shielded Metal Arc Welding (SMAW), Plasma Welding, Submerged Arc Welding (SAW) and Electron Beam Welding (Power Beam). A more detailed description of the welding process used in this thesis, Gas Metal Arc Welding will be given in the following section.

1.2 Gas Metal Arc Welding Process and Characteristic

'Gas metal arc welding uses the heat by an electric arc to fuse the join area. The arc is formed between the tip of a consumable, continuously fed filler wire and the workpiece and the entire area is shielded by an inert gas' [1]. GMAW may be used to join carbon steel sheet, ranging from 0.5 mm to 20 mm in thickness. This welding process has a number of advantageous features such as it only requires a low heat input compared with Shielded Metal Arc Welding (SMAW) and Submerged Arc Welding (SAW). The process can perform a continuous operation, has a high deposition rate, does not build heavy slag which greatly reduces post-weld cleaning and is a low hydrogen process which reduces the risk of cold cracking.

'Gas metal arc welding (GMAW) is an electric arc welding process which produces coalescence of metals by heating them with an arc established between a continuous filler metal (consumable) electrode and the work' [6]. It is also mentioned in the welding handbook edited by Kearns [6] that Shielding of the arc and molten weld pool is obtained entirely from an externally supplied gas or gas mixture. An external gas or gas mixture is supplied to provide shielding to the process, surrounding the arc to protect it from contamination from the atmosphere. The GMAW welding process is shown in figure 1.2.

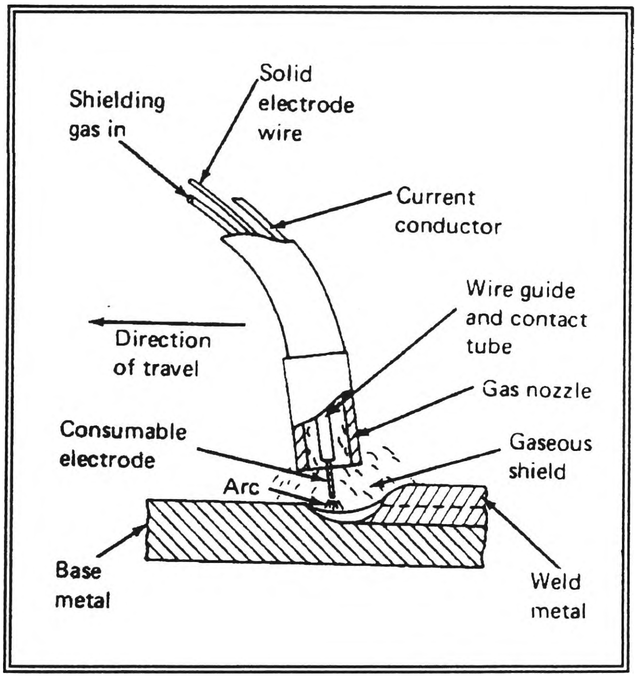

Figure 1.2

GMAW process [6]

The GMAW process was first introduced in the 1940s and has become one of the most popular arc welding processes in industry. GMAW is quite a flexible welding process. It can be used in semiautomatic and automatic mode. This type of welding process is suitable for high production welding operations and capable of welding most commercial available metals such as carbon steel, stainless steel, aluminium and copper.

It is mentioned by Norrish [1] that GMAW has the following important features:

- low heat input (compared with SMAW and SAW)
- continuous operation
- high deposition rate
- no heavy slag → reduced post-weld cleaning
- low hydrogen → reduces risk of cold cracking

One limitation of gas metal arc welding is that lack of fusion occurs more easily compared with other welding processes due to the lower heat input. It is mentioned in Cary [3] that GMAW can be used to weld most metals ranging from 0.13 mm upward. The short circuit and the pulsed arc variation are used for welding thin materials.

There are several types of metal transfer in the GMAW process. These are:

- Spray metal transfer
- Globular metal transfer
- Short-circuit metal transfer
- Pulsed-spray metal transfer

The type of metal transfer depends on the welding current density, which relates to the electrode wire size and the welding current. Each of these different metal transfer mode has its own set of welding parameters, such as travel speed, wire feed rate, voltage and applicable welding positions. The mechanism of transferring liquid metal across the arc gap is controlled by surface tension, the plasma jet, gravity and electromagnetic force, which provides the pinch effect [3]. The combinations of the forces mentioned above that act on the molten droplet determine the transfer mode.

1.2.1 Spray Metal Transfer

'Spray transfer, sometimes called axial spray, is a very smooth mode of transfer of molten metal droplets from the end of the electrode to the molten weld pool' [3]. This type of transfer occurs when very fine droplets of electrode metal are transferred rapidly through the welding arc from the electrode to the puddle. It requires argon and small amounts of oxygen gas mixtures; higher current density is also required for this type of transfer. 'The spray transfer occurs because the argon shielding gas exhibits a pinch effect on the molten tip of the electrode wire' [3]. The pinch effect limits the size of the molten ball that will form at the end of the electrode wire, see figure 1.3. It is also mentioned in Kearns [6] that the droplet diameter is equal to or less than the electrode diameter. The reduction in droplet size increases the rate of droplet detachment.

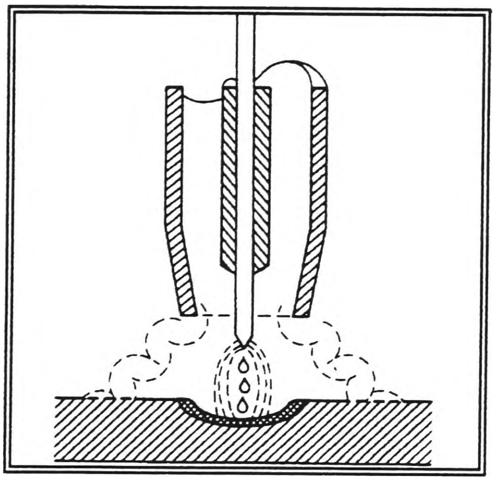

Figure 1.3

Spray metal transfer [3]

1.2.2 Globular Metal Transfer

'With positive electrode, globular transfer takes place when the current density is relatively low, regardless of the type of shielding gas. It is also mentioned in Kearns [6] that carbon dioxide (CO_2) shielding yields this type of transfer at all usable welding currents. There are two variations of globular [3], one known as drop transfer, where gravity is the dominant force. The other is known as the repelled transfer, where the forces due to the plasma jet occur although gravity force is a factor.

This process is encountered when CO_2 is used with argon additions. The force called "cathode jet" occurs in this process because the CO_2 arc is longer. An argon atmosphere is intended to reduce the length. As the globule is transferred along the arc, it is subjected to force in the arc and takes on an irregular shape and a rotating motion, which sometimes causes the globule to reconnect with the electrode as well as the work. In this type of transfer the arc is sometimes extinguished. The drawback of the Globular transfer is that it produces spatter which comes from both the molten puddle and the transferred metal and excessive fumes, see figure 1.4. Generally, this is not a desired metal transfer mode for welding.

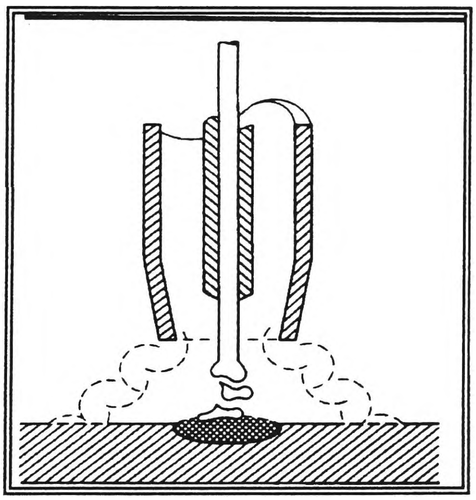

Figure 1.4

Globular metal transfer [3]

1.2.3 Short-circuit Metal Transfer

'Short circuiting arc welding uses the lowest range of welding currents and electrode diameters associated with GMAW' [6]. It is also mentioned in Kearns [6] that this transfer mode produces a small, fast freezing weld pool that is generally suited for the joining of thin sections, for filling of large root openings and for out-of-position welding.

In the short circuit metal transfer, the molten tip of the electrode wire is supported by the cathode jet mentioned previously. This type of metal transfer occurs at low values of welding current or voltage, typically less than 200 Amperes. 'Electrode wire is fed at a high rate of speed so that the molten tip of the electrode will occasionally come in contact with the puddle before the globule can separate from the electrode' [3]. Thus in short circuit mode, there is no metal transposed across the arc gap. The only time when there is a metal transfer from the electrode to the workpiece is when the electrode is in contact with the weld pool, see figure 1.5.

Short circuit transfer is very popular in GMAW because it can produce good weld quality with low heat input. However, the welding process is quite sensitive to the setting of the welding parameters.

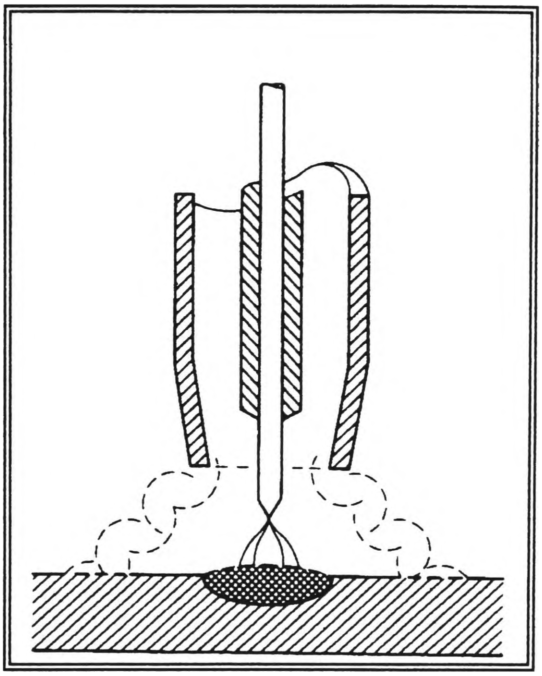

Figure 1.5

Short-circuit metal transfer [3]

1.2.4 Pulsed-spray Metal Transfer

'This transfer mode was developed in England in the late 1960s to overcome the limitations of the three types of metal transfer mentioned above' [3]. This mode gives 'spray transfer' characteristic with a low average current, permitting use on thin materials out of position [3]. This transfer mode is suitable to weld most metals.

In the pulsed-spray transfer mode, the welding current is rapidly switched from a high current to a low background current level. These currents must be adjusted for stable operation. Metal is transferred across the arc during the high current. Therefore the transfer is regulated and matches the pulsing rate which causes droplets to cross the arc, see figure 1.6. An advantage of this process is that it allows larger electrode wires with metal transfer across the arc in small particles at a regular rate. These features have advantages for aluminium welding and for welding high nickel alloy steels where argon is usually used for the shielding gas.

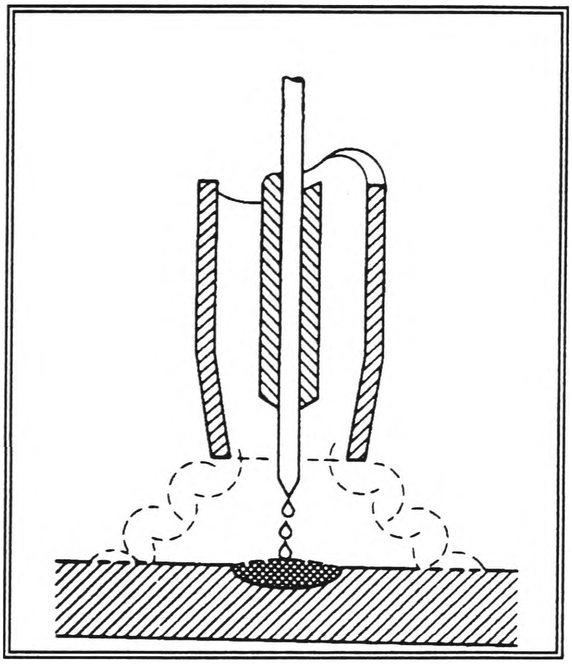

Figure 1.6

Pulsed-spray metal transfer [3]

The latest development of this transfer mode is known as synergic pulsed-spray metal transfer. The shape of the waveform of the pulse, the duration of the peak pulse and the pulse frequency are matched to the arc atmosphere and the electrode feed rate. This characteristic makes this transfer mode produce a controllable weld pool and a smooth weld with virtually no spatter.

1.3 The History of Robots

'The word robot was first used by a Czehoslovakian dramatist, Karel Capek, in his 1921 play "Rossum's Universal Robots"' [7]. Besel [9] defines a robot as a self-governing, programmable electromechanical device that offers the advantages of performing a task more *quickly, cheaply and accurately* than a human counterpart. Robots are capable of operating in locations, or under conditions, hazardous to human health, ranging from areas of the factory floor in industry to the ocean depths and outer space.

In his book, Klafter [8] mentioned that 'the robot age' began in 1954 when Devol patented the first manipulator with a playback memory. This device was capable of performing a controlled motion from one point to another. One of the first true robots was an experimental model called SHAKEY, designed by researchers at the Stanford Research Institute in 1968. It was capable of arranging blocks into stacks through the use of a television camera as a visual sensor, processing this information in a small computer. This device also had the ability to understand and react to verbal commands in English.

Nowadays robots are extensively used for automated welding. In the last few years, the use of robotic Gas Metal Arc Welding has grown significantly in industry.

1.4 An Overview of Rapid Prototyping

Nowadays it is essential to develop a product from a concept to market as quickly and inexpensively as possible. Rapid prototyping (RP) technology is one of the methods that aid this process. Wohler [10] refers to rapid prototyping as a relatively new class of technology used for building physical models and prototype parts from 3D computer aided design (CAD) data. He also mentioned that there are 481 rapid prototyping systems around the world, with at least 32 universities and corporations such as the University of Wollongong developing various forms of rapid prototyping technology.

1.5 An Overview of Rapid Prototyping by Robotic Gas Metal Arc Welding

There is practical case study of rapid prototyping using GMAW done at Cranfield University by Fernando Ribeiro and John Norrish [13], proving the viability of rapid prototyping using fusion welding. The method uses a CAD package to draw a component and then to print it in 3D using gas metal fusion arc welding robot. The robot is used to deposit successive layers of metal to form a 3D solid component as drawn in the CAD package, see figure 1.7.

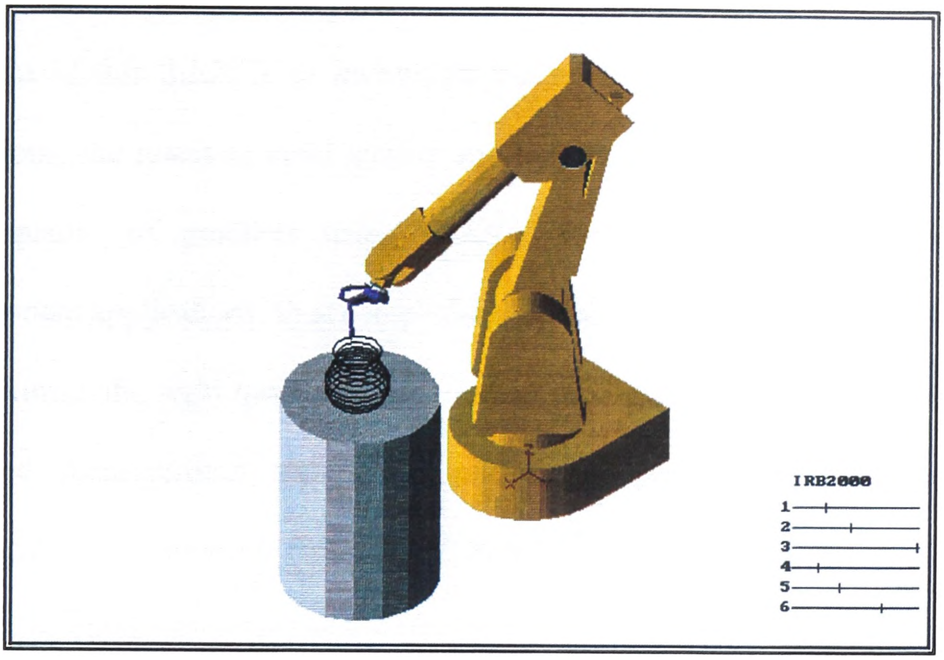

Figure 1.7

Rapid prototyping using robotic welding [14]

Although the practical case study mentioned above proved the feasibility of rapid prototyping technique, there was no method established to determine the quality of the weld parts produced, optimal operating conditions and the resulting weld quality using this method.

In this thesis, the relation between process operating conditions and the resulting weld quality of the resulting component for a rapid prototyping process using a GMAW robotic welding cell will be investigated in more detailed.

1.6 Aim

The aim of this thesis is to investigate the relation between process operating conditions, the resulting weld quality and measurement techniques to determine weld quality of products using GMAW for rapid prototyping and wear replacement applications. In accomplishing the aim, several tasks were carried out to determine the weld quality of the product produced using this method. These included measurement techniques, performing preliminary experiments to investigate the important factors that influence the weld quality, making thin walled and solid specimens, and performing mechanical destructive testing.

1.7 Outline of the Thesis

The outline of the thesis is summarised in the following points below:

- Measurement techniques to determine weld quality (Chapter 2)
- Preliminary experiments (Chapter 3)
- Description of the experimental setup (Chapter 4)
- Experiments making thin walled objects (Chapter 5)
- Experiments making solid objects (Chapter 6)
- Conclusions and further research (Chapter 7)

Chapter 2

Measurement Techniques to Determine Weld Quality

2.1 Introduction

In this chapter, several measurement techniques were established to determine weld quality. This included performing mechanical testing (Hardness, tensile and Charpy V-notch) and establishing a method of approximating surface regularity. There are two types of sample prototypes examined in the experiments. These are thin walled and solid specimens. The detailed description of the two sample prototypes will be discussed further in Chapter 5 and Chapter 6.

In order to determine weld quality, the following factors are considered:

- Physical defects: These include defects such as porosity, inclusions, excess material, spatter and lack of penetration
- Surface regularity
- Process stability
- Mechanical property: These include properties such as tensile strength, toughness and hardness

The prototypes produced using rapid prototyping technique were investigated for defects, surface regularity, process stability, porosity and mechanical properties.

Mechanical destructive tests such as tensile test, Charpy V-notch, and Vickers hardness test were used in the experiment to evaluate the quality of a weld metal built-up. A profile projector was used to give an indication of the surface regularity of the weld specimen. Visual inspections were also performed to analyse the physical defects such as porosity, spatter, inclusions, excess material and lack of penetration. The detailed description of these measurement techniques will be described further in this chapter.

2.2 An Overview of Mechanical Testing

Generally there are three purposes for making mechanical tests according to Fenner [17]. First, they are used to provide data for design that is useful for the designer to formulate a fairly precise estimate of the loads that a structure will be required to handle. Secondly, mechanical tests may be useful to provide solutions for trouble-shooting. It could become necessary to establish the cause of some service failures, to verify that the material was in fact used correctly. Thirdly, it is a tool for the metallurgist for developing new alloys, for metal-physicists researching the microscopic mechanism of fracture in materials and for engineers researching the macroscopic behaviour of materials in structures.

Mechanical destructive tests will be used in this thesis to assure the quality of the weld built-up. The tests will reveal the mechanical properties of the weld specimens such as yield strength, ductility or toughness of weld build-up.

There are a number of terms commonly used with reference to mechanical testing. These terms are summarised below.

- *Mechanical properties* of a material can be defined as the behaviour of a material under applied forces. These forces are usually expressed in terms of quantities that are functions of stress or strain or both.
- *Stress* can be defined as force per unit area over which the force is applied.

- *Strain* can be defined as the change in a dimension per unit dimension of a stressed body. This property means that strain has no units. It can be used for elastic, plastic or for the combination of the two.
- *Proportional limit* can be defined as a region where stress is proportional to strain. This can be shown at the first part of the stress-strain graph as shown in figure 2.1, where the relation between stress and strain may be approximated as a straight line. The stress at the limit of proportionality (point P) is known as the proportional limit.
- *Yield stress* is the point where the plastic deformation continues to occur at almost constant force. This point is point Y in the stress-strain diagram shown in figure 2.1.
- *Yield strength (Y)* is 'the stress at which a material exhibits a specified limiting deviation from the proportionality of stress and strain' [2]. Usually this yield strength corresponding to 0.5% of the total strain or 0.2% offset strain, see figure 2.2

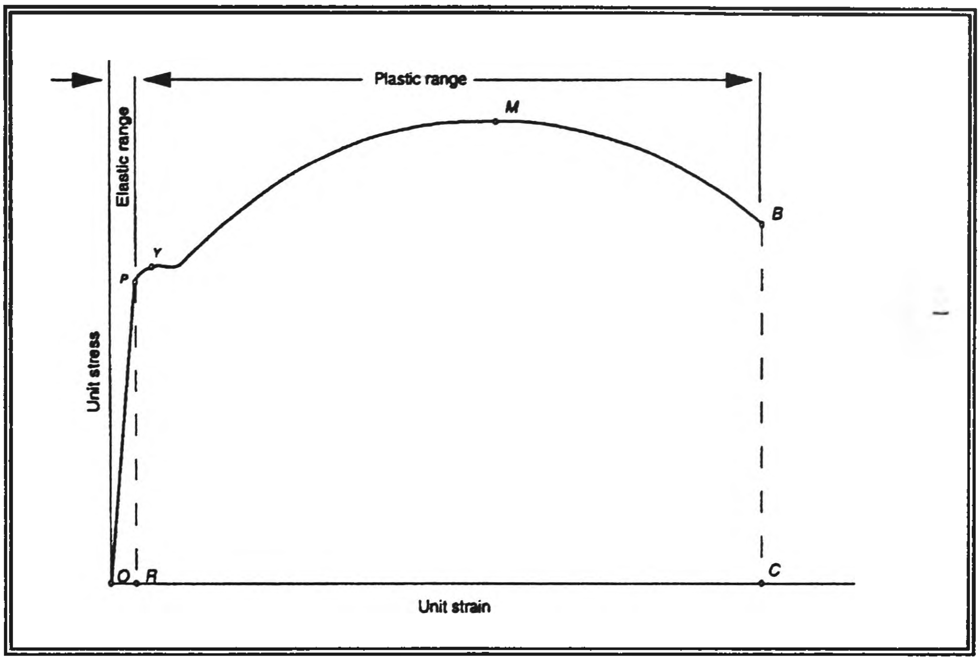

Figure 2.1

Stress-strain diagram for a ductile steel [2]

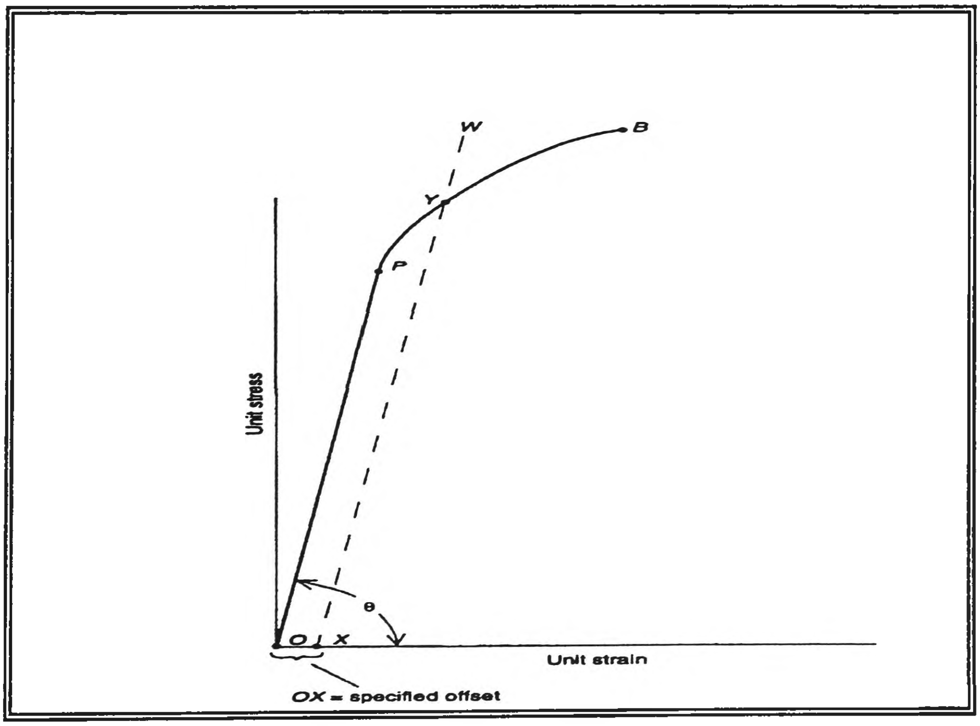

Figure 2.2

Stress-strain diagram for brittle material [2]

- *Ultimate tensile strength,* this point is shown as point M in figure 2.1. Point M is the maximum point of the graph. This is where for a ductile material necking occurs or for brittle material where fracture of the specimen occurs.
- *Breaking strength (B)* can be determined by dividing the breaking load by the original cross-section area. In the case of a ductile material the breaking strength is always less than the ultimate tensile strength and in the case of brittle material the ultimate tensile strength coincide with the breaking strength as shown in figure 2.2.
- *Ductility,* 'The ductility of a material indicated by the amount of deformation that is possible until fracture' [2]. Determination of ductility is investigated by using tension test by measuring the elongation and reduction in the cross-sectional area.
- *Modulus of elasticity or Young's Modulus* can be defined as proportionality between stress and strain below the proportional limit. This property gives an indication of the stiffness of the material. Young's modulus is given by measuring the slope of the straight line of the stress-strain curve.
- *Toughness* can be defined as 'a measure of a material's ability to resist fracture by initiation and/or propagation of a crack' [2]. Brittle material can be defined as low resistance material to fracture whereas ductile material can be define as high resistance material to fracture.
- *Hardness* can be defined as ' the resistance of metal to penetration by an indentor under load' [2].

2.3 Tensile Test

Tensile tests were performed in this thesis to determine a material's properties of the weld specimen. This test was done by straining the specimen in uni-axial tension at room temperature. The method reveals the material's modulus of elasticity, proportional limit, elastic limit, yield strength, tensile strength, elongation and reduction in cross-sectional area. 'The quantities derived from a tensile test are best considered by a reference to the deformation behaviour of a test piece when subjected to a continuously increasing tension load till it breaks' [17].

The principal tensile testing machine consists of machinery to pull a test piece coupled to a device which measures the load. The machine may be driven by hydraulics with a piston carrying one of the test piece grips, or it could also consist of a screw, driven in an axial direction by the rotation of a nut. The principle of operation of a single-lever testing machine is shown in figure 2.3.

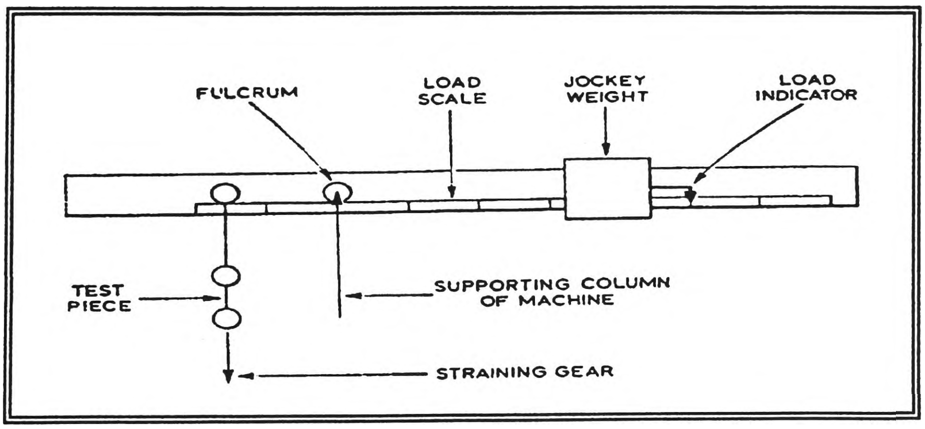

Figure 2.3

Principle operation of single-lever testing machine [17]

Tensile tests can be used for various materials and it is worth noting that low carbon annealed steels behave differently to high carbon steels after the proportional limits is reached [2]. With low carbon annealed steels the material yields discontinuously and the applied loads drops at the initiation of yielding. High carbon steels and some other steel materials and non-ferrous materials do not possess a well-defined yield point as for these materials, the maximum useful strength is the yield strength.

The tensile test used in the experiment is according to Australian Standard 2205.2.2-1997 (All-weld-metal tensile test methods for destructive testing of welds in metal). The Australian Standard 2205-1997 is also linked to the Australian Standard 1391-1991 (Method for tensile testing of metals) where dimensions, preferred shape of the standard piece and all of the procedures are explained in more detailed. The general dimensions of the circular standard piece are shown in figure 2.4.

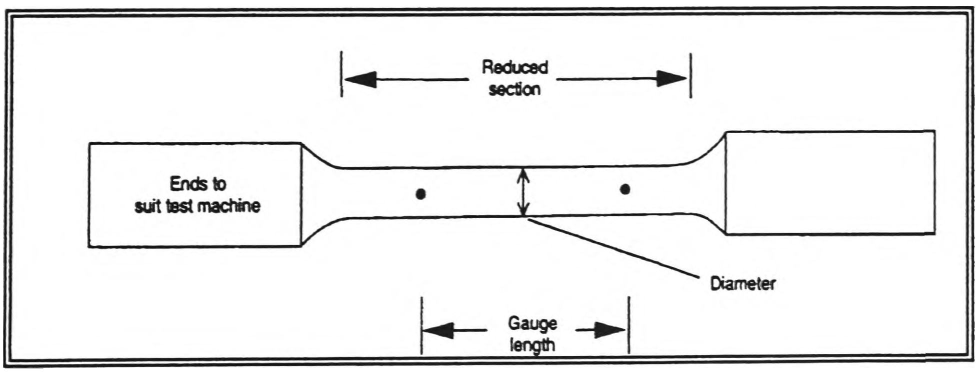

Figure 2.4

General dimensions of circular tensile test specimen [2]

The gauge length (L_o), the original cross-sectional area (S_o), diameter (d), and the minimum transition radius (r) is shown in figure 2.5. The dimensional requirements and the relationship between L_o and S_o of a circular section test piece is shown in table 2.1

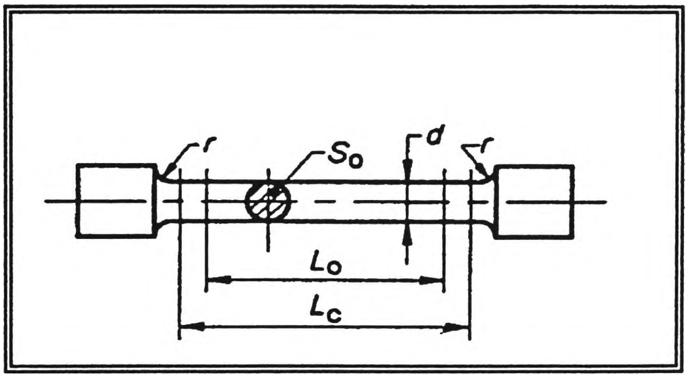

Figure 2.5

Test piece of circular cross-section [16]

Diameter d [mm]	Maximum variation of diameter of parallel length [mm]	Original gauge length $L_o = 5.65\sqrt{So}$ [mm]	Minimum parallel length $L_c = L_o + 0.5d$ [mm]	Minimum free length between grips L_o+d [mm]	Minimum transition radius r [mm]
20.0 ±0.4	0.05	100 ±2.0	110	120	20
15.0 ±0.3	0.04	75 ±1.5	83	90	15
10.0 ±0.2	0.03	50 ±1.0	55	60	10
5.0 ±0.1	0.02	25 ±0.5	28	30	5

Table 2.1

Dimensional requirements for circular section test piece [16]

2.4 Charpy V-notch Impact Test

The Charpy impact test is widely used in industry because it is relatively simple. A Charpy machine is shown in figure 2.6. In this test a stress-concentrating notch is machined into a small test piece as shown in figure 2.7. This notch is made to promote brittle failure of the specimen when subjected to a high impact force. The sample is broken in the testing machine, which has a pendulum like a hammer that swings in a vertical arc. The specimen is placed in the machine as shown in figure 2.6 such that the hammer strikes the specimen on the side opposite the notch at the bottom of the vertical arc. The enlarged picture of the notch is shown in figure 2.8. After the hammer strikes the specimen, the toughness value can be read on the dial in energy units of Joules. This dial indicates the energy used by the hammer to fracture the specimen. Note that the energy used by the hammer is about equal to the energy absorbed by the specimen. Therefore the higher the energy absorbed by the specimen means the higher the toughness of the metal.

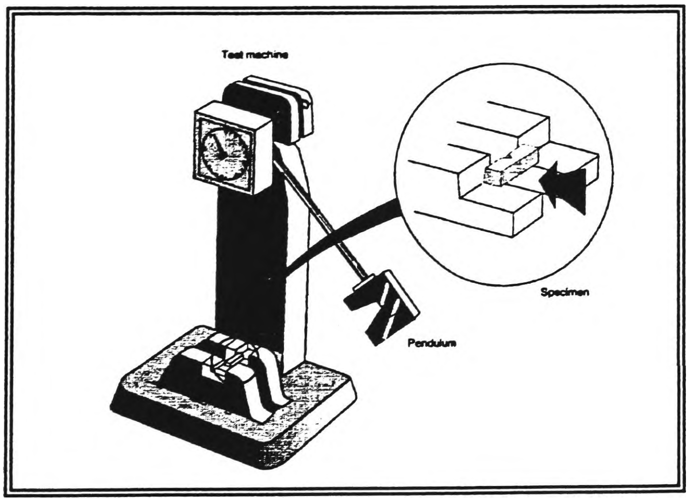

Figure 2.6

Charpy impact test machine [2]

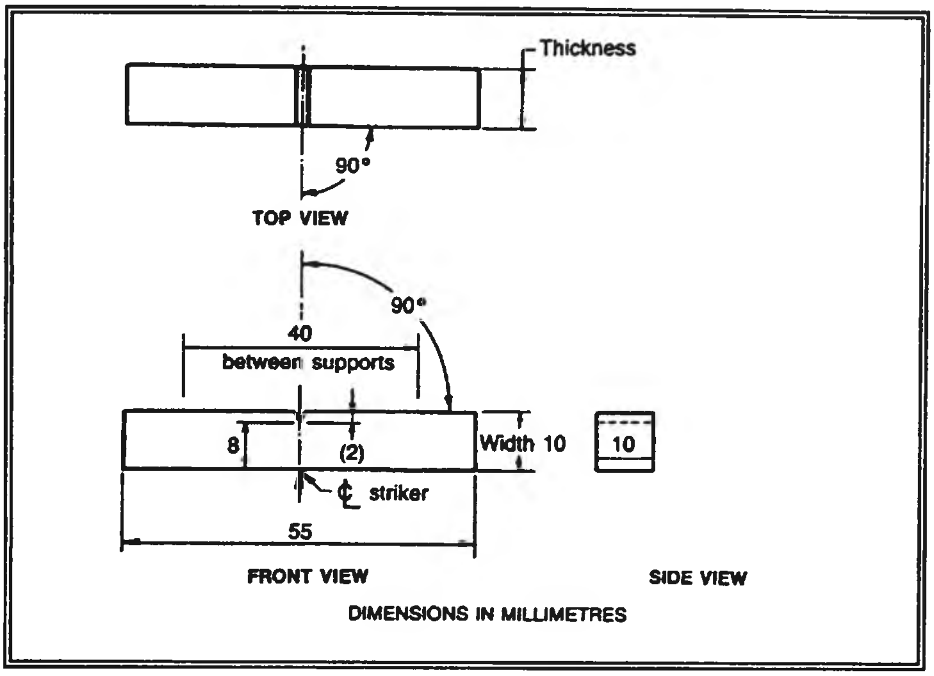

Figure 2.7

Standard Charpy test piece [15]

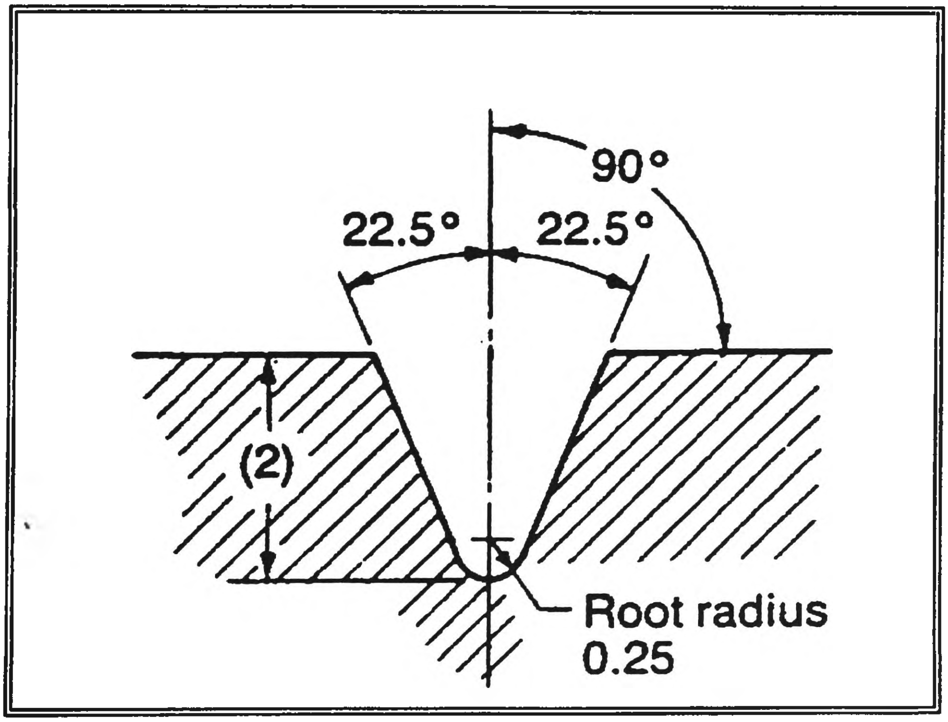

Figure 2.8

Enlarged view of notch in test piece [15]

The experiment was carried out according to Australian Standard 1544.2-1989. The dimensions and tolerances of standard test piece is shown in the table 2.2 [15]:

Characteristic	Nominal dimension	Machining tolerance
Length	55 mm	± 0.60 mm
Thickness	10 mm	± 0.11 mm
Width	10 mm	± 0.06 mm
Root radius of notch	0.25 mm	± 0.025 mm
Depth below notch	8 mm	± 0.06 mm
Distance of centre of notch from one end of test piece	27.5 mm	±0.42 mm
Angle between plane of symmetry of notch and longitudinal axis of test piece	90°	± 2°
Angle of notch	45°	± 2°
Angle between adjacent longitudinal faces of test piece	90°	± 20°

Table 2.2

The dimensions and tolerances of standard test piece [15]

The experiment was conducted at room temperature (20 ±2° C) and 'the location of the test piece lies with the notch squarely against the reaction supports so that it will be struck on the face opposite the notch' [15], see figure 2.9.

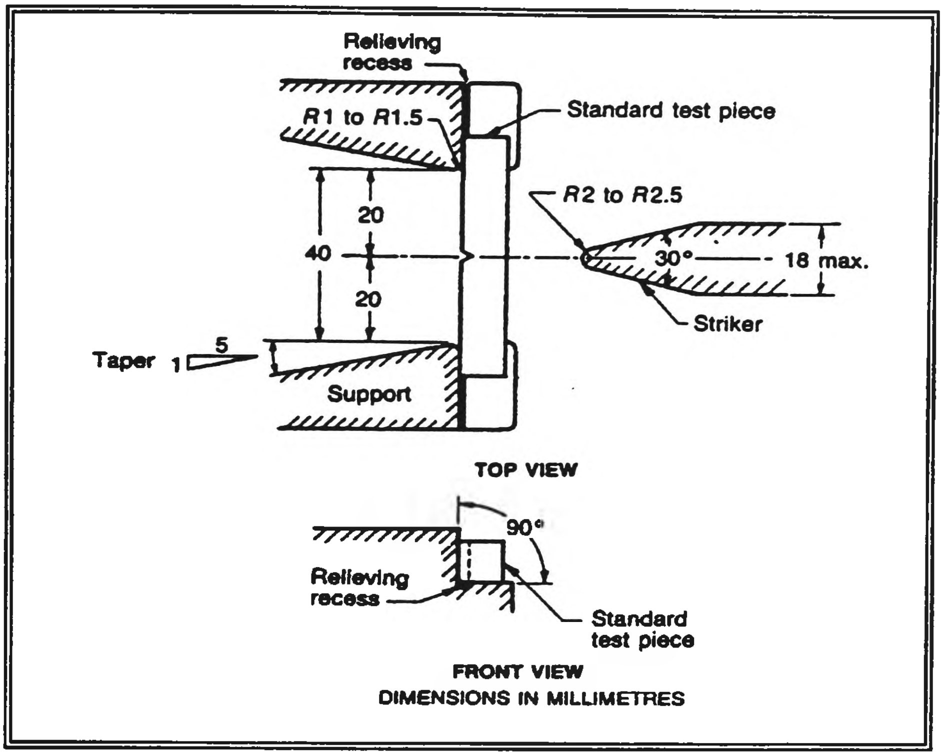

Figure 2.9

Arrangement of supports, test piece and striker [15]

2.5 Vickers Hardness Test

There are three common method of measuring hardness of materials. These testing methods are Brinnel, Rockwell and Vickers hardness tests.

In Brinell hardness test, a steel bar is used to indent the metal by using hydraulic press forces. The ball is 10 mm in diameter and it is usually made of tungsten carbide. Load of 3000 kg is applied for 10-15 seconds for ferrous metals and load of 500 kg is applied for 30 seconds for softer non-ferrous metal. The hardness value is given in terms of Brinell Hardness Number (BHN), this hardness value ranging from 50 for a soft metal to about 700 for very hard metals.

In Rockwell hardness testing the depth of indenter penetration is measured by means of a dial-gauge connected to a vertical ram which drives the indenter into the specimen. There are two types of loads used in this test, minor and major loads. At first, the specimen is placed in the testing machine and raised against the indenter until a minor load of 10 kg is reached and then a major load is applied by the ram. There are three scales used in this test, they are known as Rockwell A, Rockwell B and Rockwell C. Each one of the scales is associated with a different combination of load and indenter.

The Vickers hardness test has more load options in comparison with Brinnel and Rockwell hardness tests. It is more suitable for small specimen as the indentation can be adjusted by using a suitable load. Therefore from the advantages mentioned above, Vickers hardness test was chosen for the experiments.

Vickers hardness test is a convenient and accurate method to measure the hardness of a material. The Vickers hardness test will be used to determine the hardness of the weld built-up. The results of the test would reveal if there is a significant change in hardness of the material compared to the original hardness properties or depending on the welding parameters.

Vickers uses a square based pyramidal diamond indentor in which the angle between the opposite faces is 136°. The loads can be varied from 5 to 120 kg. This test can be used for macro or micro specimens cut from a welded section and is widely used in a laboratory. The measurement of the hardness is in terms Vickers hardness number (HV).

The basic principle of this test involves pressing a diamond indenter into the surface of a test specimen under a certain force. The force is applied for a period of 15 seconds and then removed from the surface, two diagonals, d_1 and d_2 of the indentation and the mean value d are determined, see figure 2.10. The mean length 'd' is an estimation area of indentation of the two diagonals d_1 and d_2. In the figure 2.10 it is also shown that the indenter is a right pyramid with 136° between opposite faces.

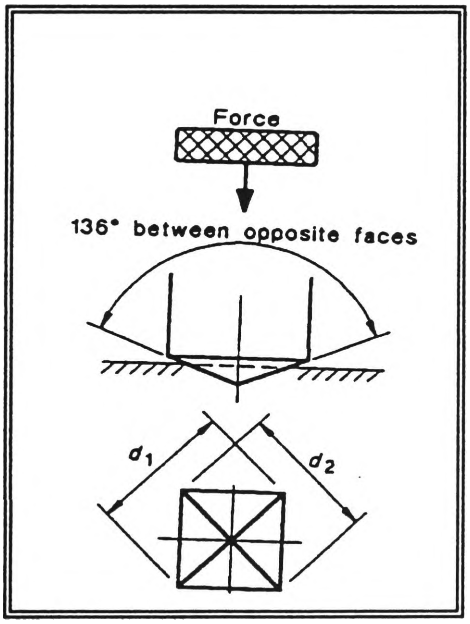

Figure 2.10

Vickers principle [18]

The hardness is computed by dividing the test force by 9.806 X 65 times the sloping area of the indentation. This may be expressed by the following equation 2.1 [18]:

$$\boxed{HV = 2F\sin\frac{136^{\circ}}{9.806\times 65\mathrm{d}^2} = 0.1891\frac{\mathrm{F}}{\mathrm{d}^2}\ \textit{approximately}} \qquad (2.1)$$

Where

HV	=	Vickers hardness
F	=	force, in Newtons
d	=	mean diagonal of indentation, in millimetres

Thus the Vickers hardness is calculated using the above formula, or by the use of tables provided. The 'Vickers hardness values are, in general, artificial quantities in that each is calculated by making the assumption that' [17]:

- The geometric shape of the intender is unaltered by the application of the test load
- No change in shape of the indentation takes place when the test load is removed

The Vickers hardness testing machine used in the experiment is a 6030LKV Vickers Hardness Testing Machine made by Indentec Hardness Testing Machine Limited. The Australian standard relating to this test is AS 1817-1991 (Metallic Materials-Vickers Hardness Test). The 6030LKV Vickers Hardness Testing Machine is depicted in figure 2.11.

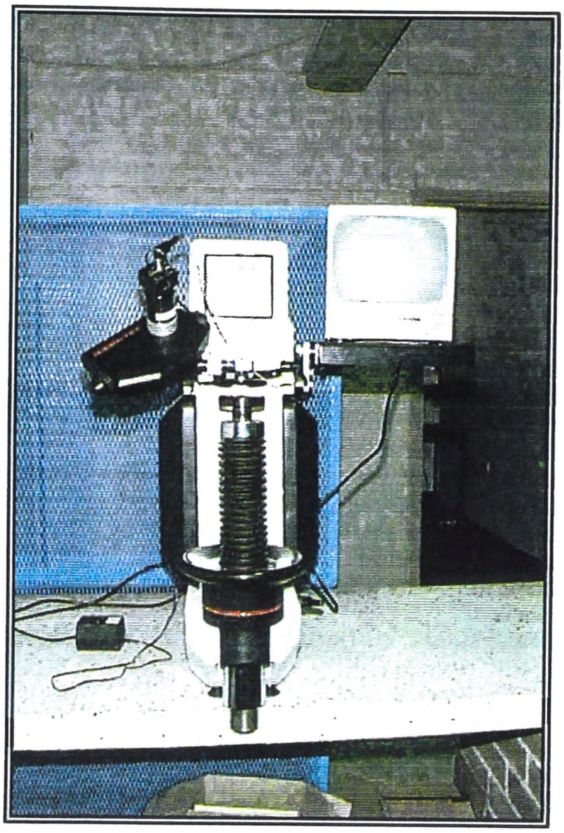

Figure 2.11

The 6030LKV Vickers hardness testing machine

The 6030LKV has six loads options available ie. 1, 2.5, 5,10,20,30 kg. The load can be determined by adjusting the lever to the appropriate position. Several trials were performed to determine the most suitable load for the specimen. It was found that the 10-kg load was the most suitable load for the specimen because it could reveal the indentation very clearly. Thus the 10-kg load was used for all of the samples. The machine calculates the hardness number automatically after both edges of the impression are measured. The size of the diamond shape impression determines the Vickers hardness number of the specimen tested.

2.6 Measurement of Surface Regularity

As mentioned previously, one of the components to determine the weld quality is a measure of surface regularity. Usually an indication of surface regularity can be obtained by using a surface texture measuring machine. The machine determines the surface profile as well as calculates a surface roughness of the sample analysed. However, in the case of the experiment it was not possible to use such a machine to analyse the samples because the surface of the weld samples were far too irregular for the machine to measure. Therefore an alternative method of measuring the surface quality was determined by using a profile projector.

The profile projector used in the experiment is a Profile Projector Model V-12 made by Nikon, see figure 2.12. The projector is equipped with two lenses of ten times and twenty times magnifications. The projector is fairly easy to use and has an accuracy of 10 micron. The specimen is placed underneath the lens as shown in figure 2.13 and the profile is measured by recording the x and y coordinates along the surface. The biggest disadvantages of using the profile projector were the limitation of the number of points the operator can measure manually and also the accuracy is only up to 10 microns. However it is sufficient to give an indication of the surface regularity for the weld samples.

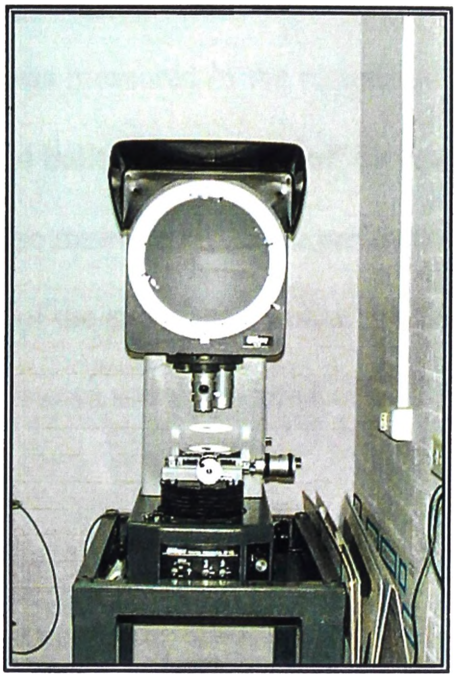

Figure 2.12

Nikon profile projector model V-12

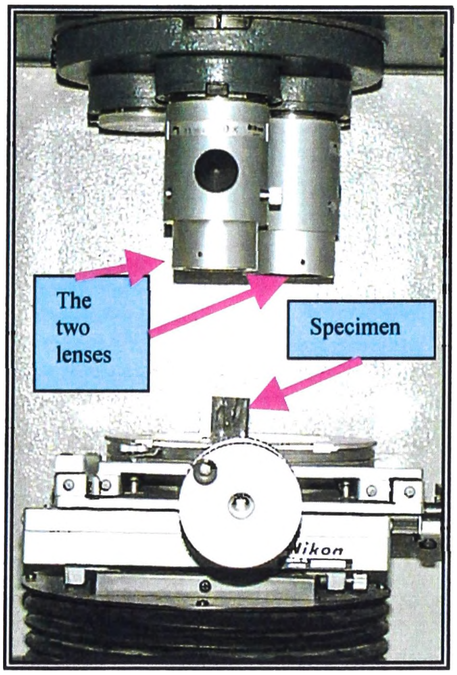

Figure 2.13

Specimen position

2.7 Surface Temperature and Standoff Measurement

The surface temperature was measured in the experiment to give an indication of the temperature of the weld built-up. The standoff distance (Distance from contact tip to the work piece) is also measured in the experiment to give an approximation of the standoff at the start of the experiment and at the last layer, so that a possible standoff variation will be known and considered.

The temperature measurement was done with a handheld digital thermometer model 305K made by Temperature Controls Pty Ltd. The thermometer has a range from -50 °C - 1300 °C. The thermometer is equipped with a thermocouple type K which is also made by Temperature Controls Pty Ltd, see figure 2.14. The surface temperature was measured by stopping the robot in middle of the last layer, see figure 2.15.

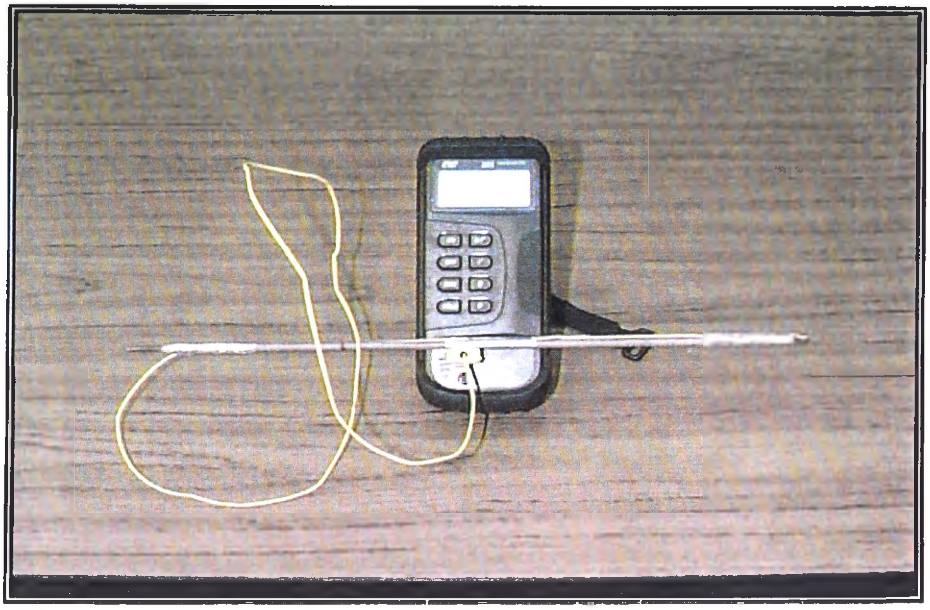

Figure 2.14

Temperature measurement probe

The standoff distance is measured at the beginning and also measured once again at the last layer to compare from the original value at the beginning, see figure 2.16 and figure 2.17 respectively.

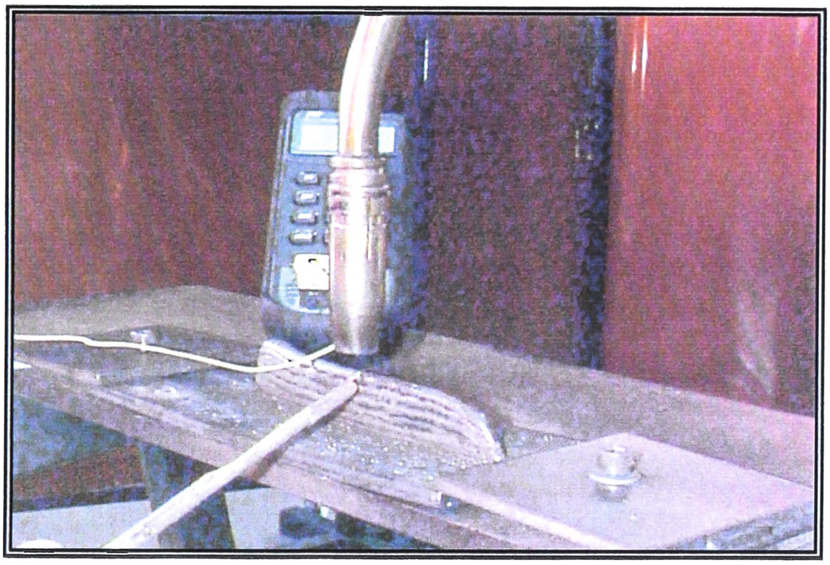

Figure 2.15

Measuring surface temperature at the last layer

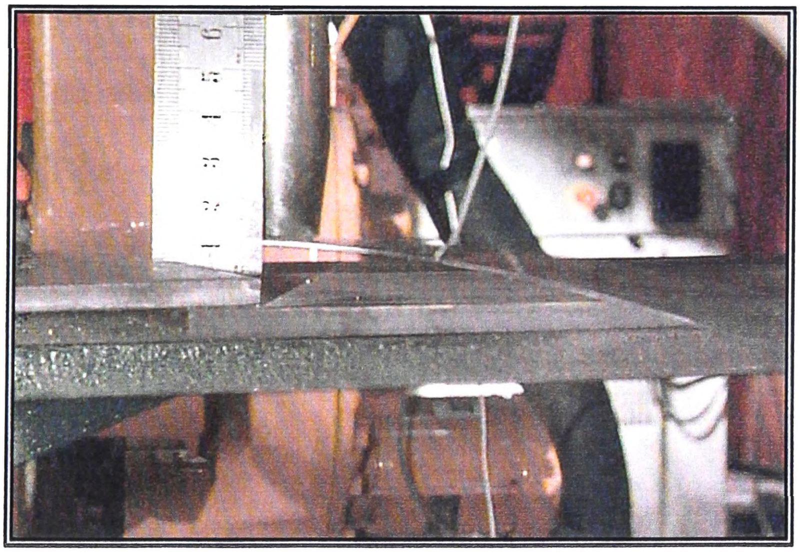

Figure 2.16

Standoff measurement at start

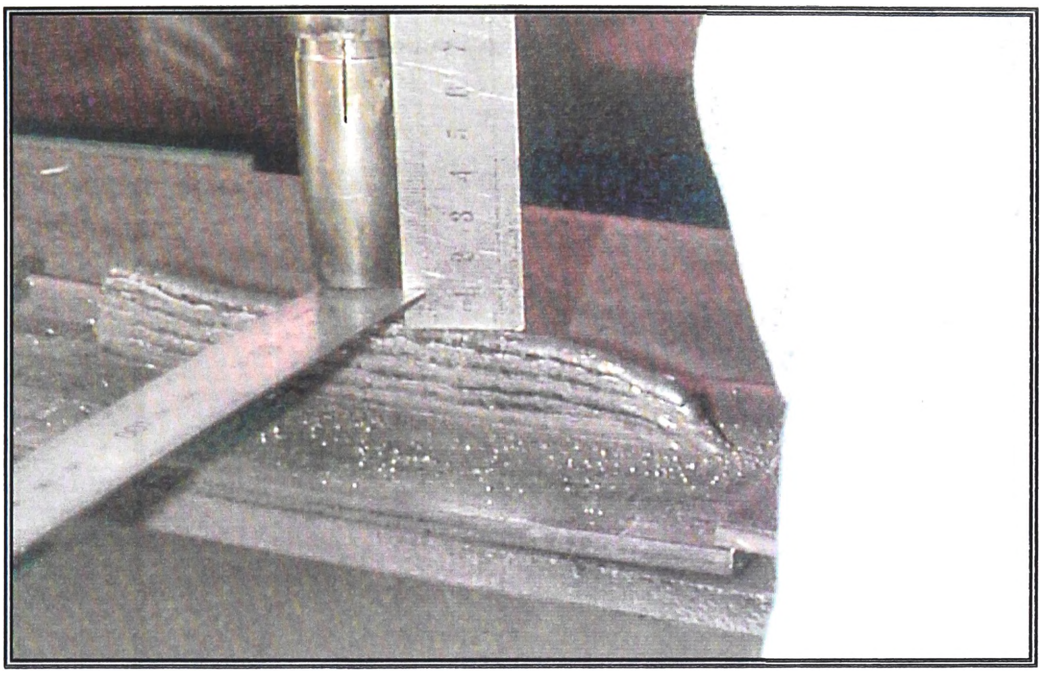

Figure 2.17

Standoff measurement at last layer

Note that the actual distance measured is the distance between the nozzle to the workpiece, however the equivalent standoff distance is known, see figure 2.18. For example in the case of the experiment, the nozzle distance of 10 mm is equal to the standoff distance of 15 mm. For the experiments throughout this thesis a suitable standoff distance for the Hitachi and IRB 1400 robots welding guns is 15 mm.

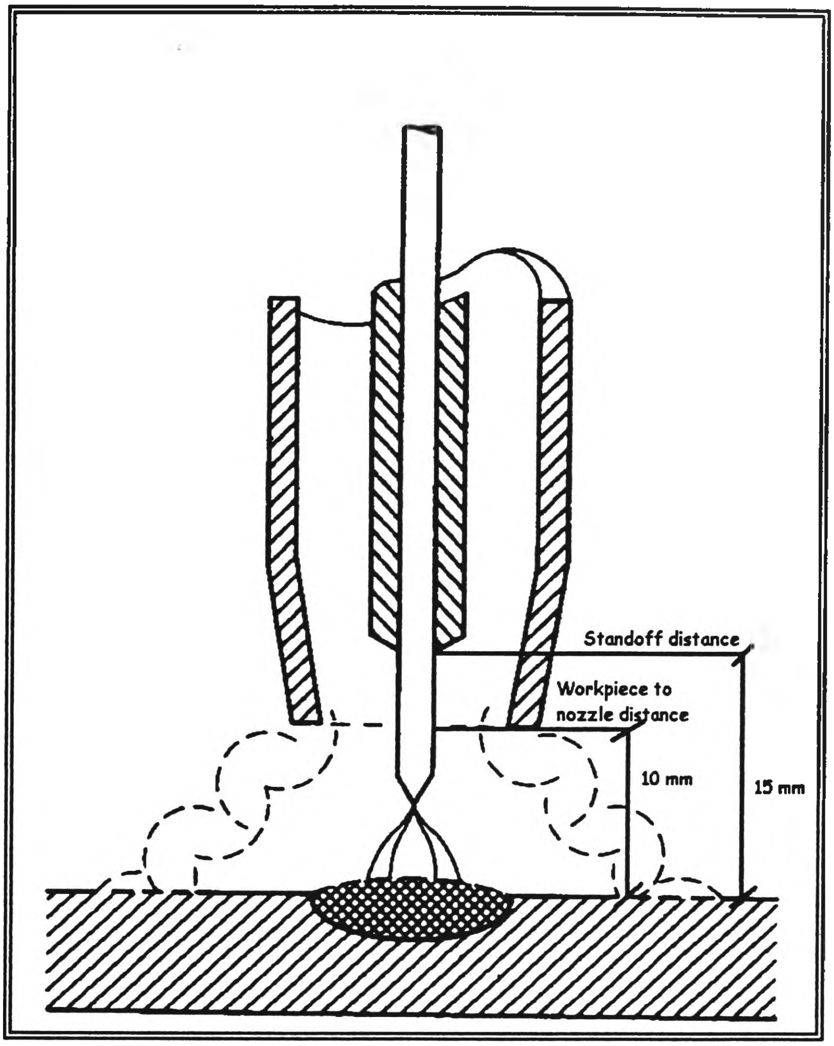

Figure 2.18

Schematic diagram of standoff and nozzle to workpiece distance

Chapter 3

Preliminary Experiments and Results

3.1 Introduction

This thesis project started in February 1997, however the propose built robotic welding cell was not available until about ten months after the project started. Therefore preliminary experiments were conducted by using the Hitachi robot. The aim of the preliminary experiment was to develop measurement techniques to determine quality of weld for rapid prototyping and wear replacement applications. The method, equipment and results obtained from the preliminary experiment will be described in more detailed in the next several sections of this chapter.

3.2 The Hitachi Robot Specifications

The Hitachi Process Robot Model M6060II is a 6-axis type robot. The features of this model are that it has a long reach and large operating space with high speed, high rigidity and high accuracy.

The robot body is capable of carrying 6 kg at 1 m/sec, its motor capacity is 1,740 Watts and it has a repeatability of ± 0.2 mm or less equipped with mechanical brakes to all axes except the twist axis. The mechanical brake can handle up to 405 kg. The dimensions of the robot body are depicted in figure 3.1.

The Hitachi robot has three coordinate systems; these are Cartesian, cylindrical and articulated and it has the ability to be programmed using linear or circular interpolation. The robot also allows gradual acceleration, deceleration and it is also equipped with a positioning function (accurate and rough positioning). The

Hitachi robot has speed ranging from 1.67 mm/sec to 167 mm/sec and it is also equipped with a timer that can be adjusted up to 99.9 second.

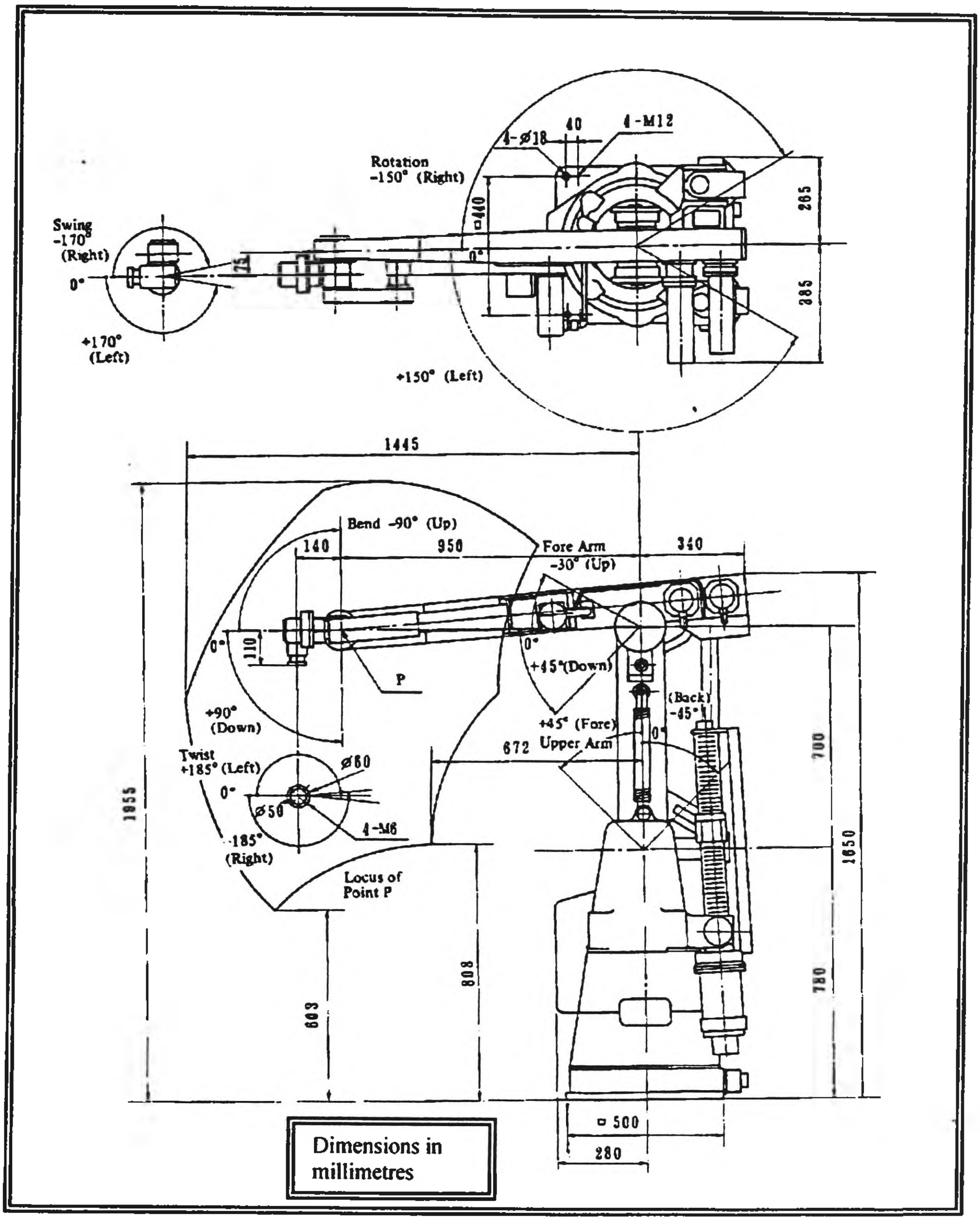

Figure 3.1

Dimensions of the robot body [24]

The robot has the ability to detect whether or not an arc has been extinguished and whether the welding torch has come in contact with the workpiece. If the robot detects any error during welding, it automatically switches itself off and tells the operator what is wrong by displaying the error on the control unit, see figure 3.2 for the Hitachi robot and figure 3.3 for a picture of Hitachi control unit. When a welding torch is attached to the end of the robot wrist, the recommended centre position of the workpiece is shown in figure 3.4.

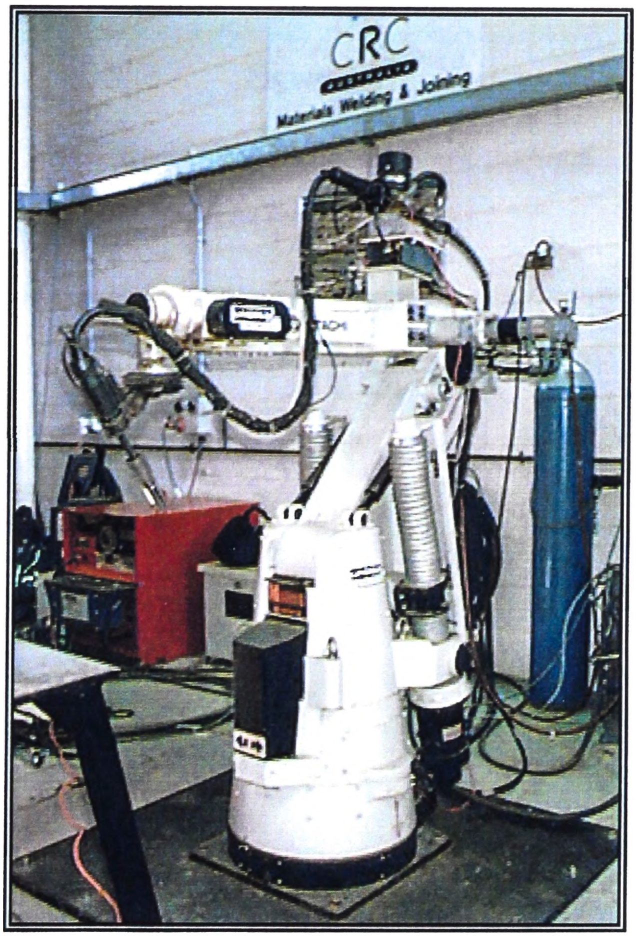

Figure 3.2

The Hitachi robot

Figure 3.3

The Hitachi controller and teach pendant

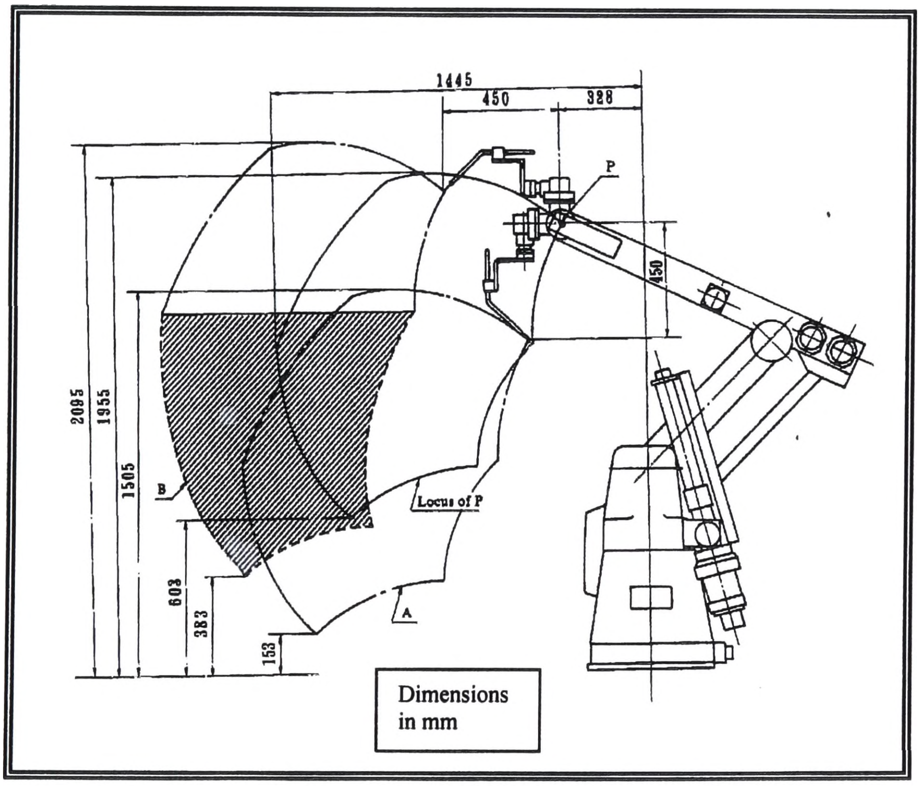

Figure 3.4

Recommended centre position of workpiece [24]

3.2 The Welding Power Supply

The welding power supply used for the preliminary experiment is the Ideal Arc® DC-400 made by Lincoln Electric. This power supply provides a pinch setting, which may be varied from a setting of 1 to 11. This pinch setting varies the internal resistance and thus can be used to change the characteristic of the power supply. The voltage and wire feed rate may be varied by the user to suit the specified welding conditions. This power supply is designed 'for all open arc processes including inner-shield, all solid wire and gas procedures and air carbon arc within the capabilities of the machine' [25]. It mentioned in the manual [25] that the power supply also has a single range potentiometer control. The power supply and its accessories are depicted in figure 3.5 and 3.6 respectively.

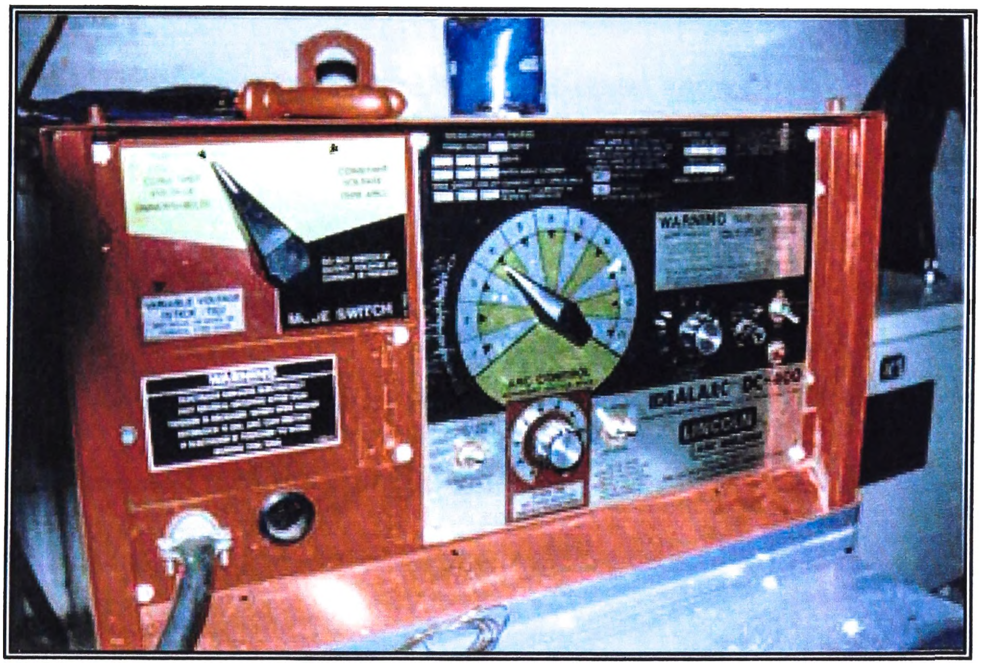

Figure 3.5

The DC-400 welding power supply

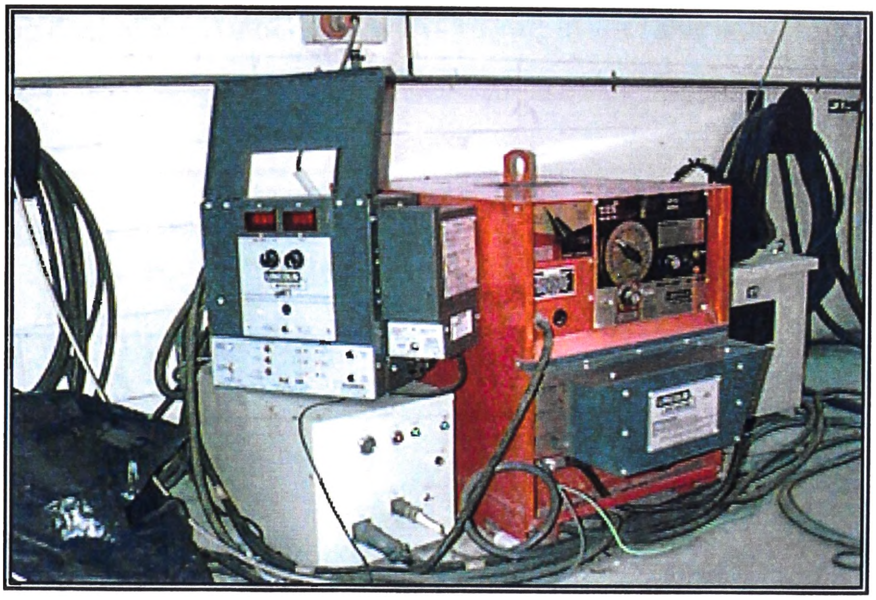

Figure 3.6

The power supply and its accessories

3.3 Filler Wire Specifications

The wire used for the preliminary experiment is Autocraft LW1 made by CIGWELD. This filler wire is suitable for gas metal arc welding of mild and low alloy steel. It is also suitable for use with short-arc, spray and pulsed-arc transfer mode.

This type of wire is suitable to be used in multi-pass Gas Metal Arc Welding of mild, low alloy and medium strength steels. Thus it can be used for building up thin wall weld specimen where multi-pass welding is involved.

The operating data of the Autocraft LW1 is shown in the table 3.1 below.

Wire Diameter [mm]	Voltage Range [Volts]	Wire Feed Speed [metres/min]	Current Range [Amps]
0.9	15-26	3.5-15	70-230

Table 3.1

Operating data of the Autocraft LW1 [22]

The Autocraft LW1 complies with Classifications *AS/NZS 2717.1: ES4-GC/M-W503AH; AWS/ASME-SFA A5.18: ER70S-4*. This type of wire has mechanical properties as shown in the table 3.2 below.

	Argoshield 51	Welding Grade CO_2
Yield Stress	420 Mpa	390 Mpa
Tensile Strength	520 Mpa	500 Mpa
Elongation	30%	31%
CVN Impact Value	110 J @ -20 °C	100 J @ -20 °C

Table 3.2

Typical weld metal mechanical properties [22]

In later stage, the mechanical properties of weld samples obtained from the experiments will be compared with the mechanical properties given in table 3.2.

Therefore change in mechanical properties can be identified and investigated further.

The Autocraft LW1 can be used with a variety of shielding gases, these are [22]:

- Argoshield 50 or Ar + 10-15% CO_2 or equivalent
- Argoshield 51 or Ar + 20-25% CO_2 or equivalent
- Welding Grade CO_2
- EN439: C1, M14, M21(1) & M24 shielding gases

3.4 Shielding Gas Specifications

The purpose of a shielding gas in the gas metal arc welding process is to shield the weld pool and molten filler wire from atmospheric Oxygen and Nitrogen. It is also functions to stabilise the arc and desired depth of penetration.

The shielding gas used for the experiments is Argoshield ™ 51, which is made by CIG. 'Argoshield ™ 51 is particularly noted for its low sensitivity to weld joint impurities and is also suitable for robotic applications' [23].

3.5 Base Plate Specifications

The base plate used in the experiment is manufactured by BHP, the product is known as BHP-300PLUS. The BHP-300PLUS grade has a minimum yield stress of 320 Mpa for plate thickness up to 11 mm, minimum tensile strength of 440 Mpa and minimum elongation of 22 %. The material contains carbon equivalent

(CE) of 0.44. The plate was cut to the length of 250 mm, width of 150 mm and a thickness of 6 mm for the experiments.

The surface of the plate was ground to ensure that it was free from contaminants, free of rust and any other substances which could affect the stability of the process and the quality of weld. The picture of the prepared base plate is shown in figure 3.7.

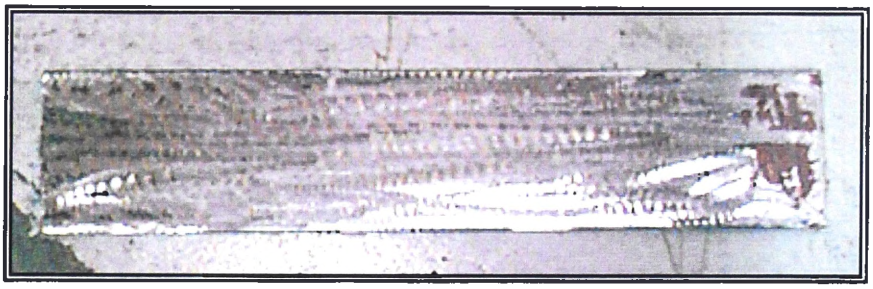

Figure 3.7

The base plate

3.6 Preliminary Experiment Procedures

The preliminary experiments were conducted using the Hitachi robot, Ideal Arc® DC-400 conventional power supply and its accessories. Several areas were looked at in the preliminary experiment. These are:

- Test object geometry selection
- Transfer mode selection
- Welding parameters selection
- Programming the Hitachi robot
- The monitoring system

- Specification and preparation of the base plate

3.6.1 Preliminary Test Object Geometry Selection

A simple test object shape was used to evaluate suitable of parameters for rapid prototyping and wear replacement applications. Several simple shapes were considered as test objects, these are square, rectangular, circular and straight-line objects.

A straight-line object was selected as the test object in the experiment because it is representative of a thin wall object and has the characteristic of a smooth shape (no curves or sharp corners). The length of the weld must also be considered. There are several factors to consider in selecting the length, such as time to cool down so that it will represent a reasonable cooling time in a real application.

After several trials were conducted, a length of 150 mm was selected for the following reasons. By using travel speed of 5 mm/sec, the welding operation will take 30 seconds per layer, then robot with will start welding on the second layer and so on up to the tenth layer is performed. By trial and error, it was found that 30 seconds is a reasonable time to allow the weld to cool down before the next layer is started. It was also determined that the temperature profile would stabilise to a certain temperature after the first two or three layers performed, see figure 3.8. It was determined from the trials that all of the temperature profiles obtained from different welding parameters have similar characteristic like the one shown in figure 3.8. Hence it can be said that ten layers were enough to represent the stable temperature.

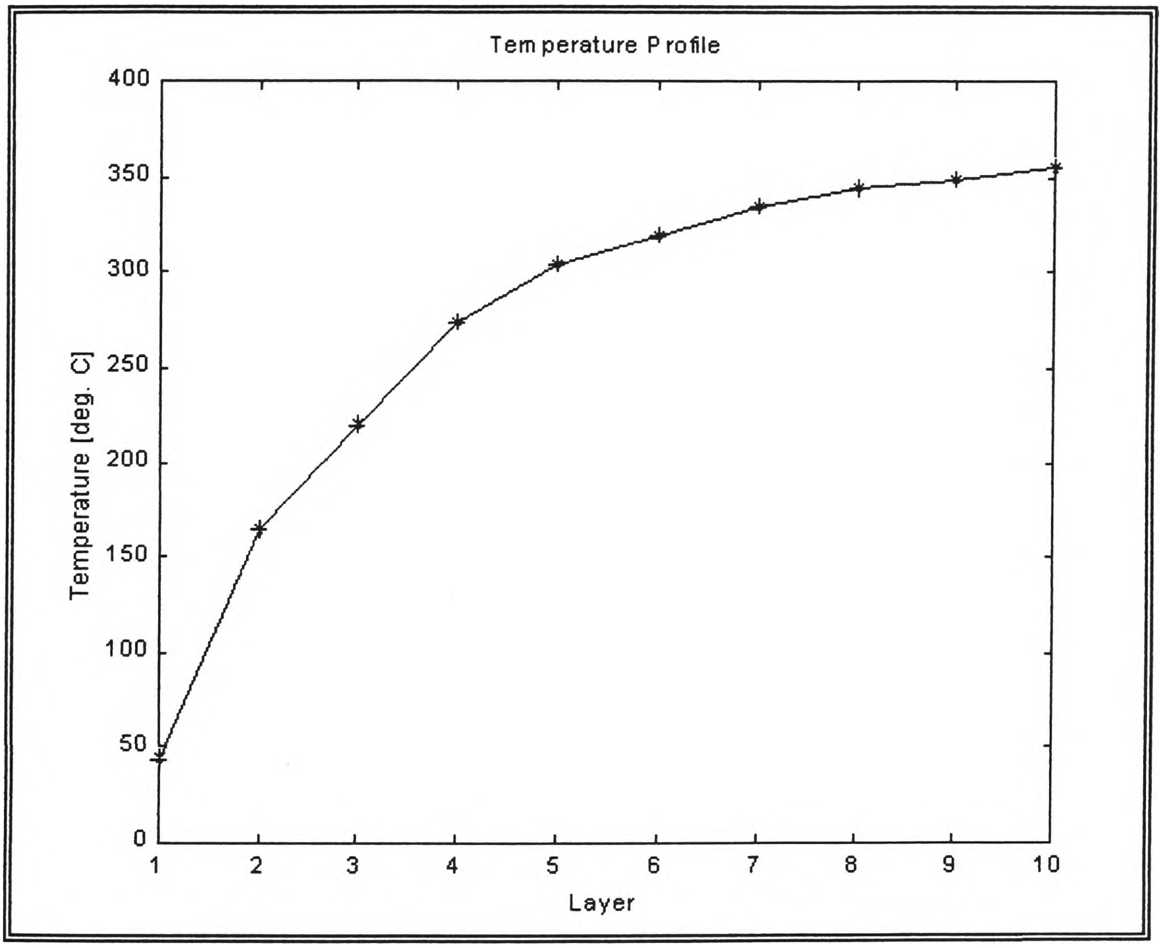

Figure 3.8

Typical temperature profile characteristic of the process

3.6.2 Preliminary Transfer Mode Selection

The transfer mode in GMAW plays an important role in controlling the heat input and droplet deposition during the process. The transfer mode also plays an important role to determine the stability of the process. For a rapid prototyping application, a low heat input, high stability, and a good control of deposition rate during the process are the critical components to achieve good quality weld.

There are several transfer modes available in Gas Metal Arc Welding, however there is only one suitable transfer mode that most suitable which fulfils the conditions mentioned above, this transfer mode is known as short-circuit transfer. In short circuit mode, the heat input is low compared to the other transfer mode such as spray transfer and globular transfer. Moreover, in globular transfer the process is relatively unstable and produces spatter, which comes from both the molten puddle and the transferred metal. Thus, it is definitely not suitable for an application that needs a good control of the transfer of metal droplets. In the case of spray transfer, though this transfer is quite stable, it produces a high heat input and deposition rate, which makes it unsuitable for building thin wall objects.

The short-circuit transfer mode was selected for the preliminary experiment because this transfer mode has characteristics which are required for rapid prototyping and wear replacement application.

3.6.3 Preliminary Welding Parameters Selection

The voltage used in the experiments range from 17 - 19 Volts. The reason is because it is a suitable voltage range used in the short circuit mode [29]. The travel speed used is 5 mm/sec because it is also a suitable travel speed used for short circuit transfer mode [29].

The wire feed rate selected in this experiment ranges from 3 to 9 m/min, the selection being based on previous experimental work by other student who used the power supply [29]. The pinch setting of four was used throughout the preliminary experiment because it was determined experimentally to be a suitable pinch setting for short-circuit transfer mode.

3.6.4 Programming the Hitachi Robot

Programming on the Hitachi Robot is done by teaching positions with the teach pendant. The program can be categorised into two major positions. These are home position and welding operation position. The different stages of the program are described in the illustration below.

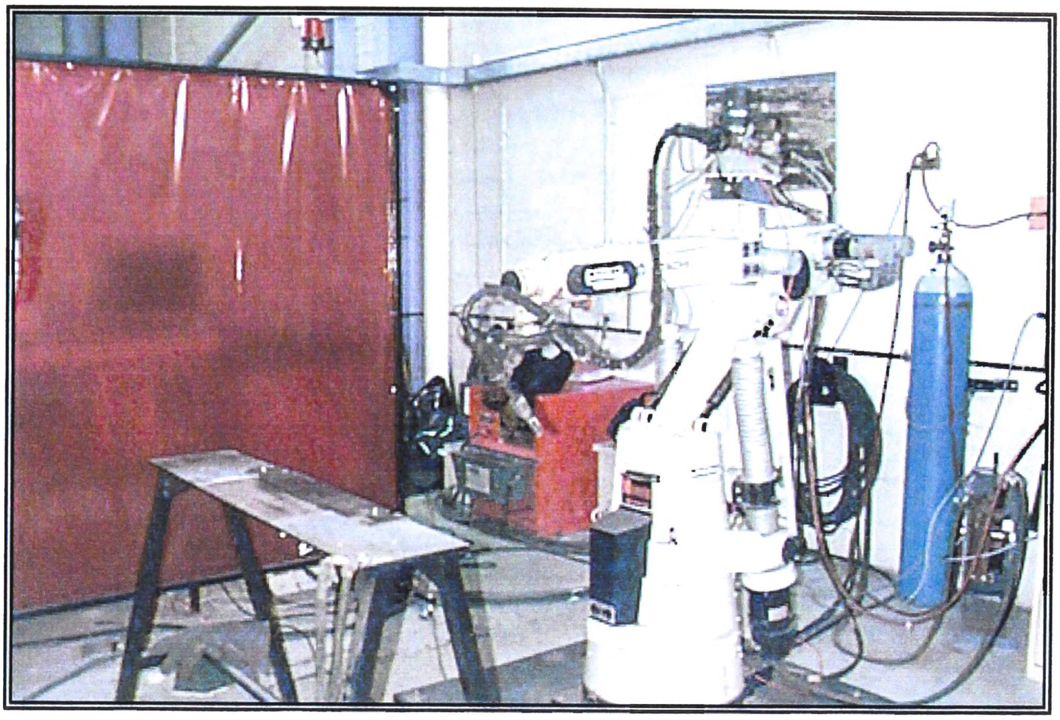

Figure 3.9

Home position of the robot

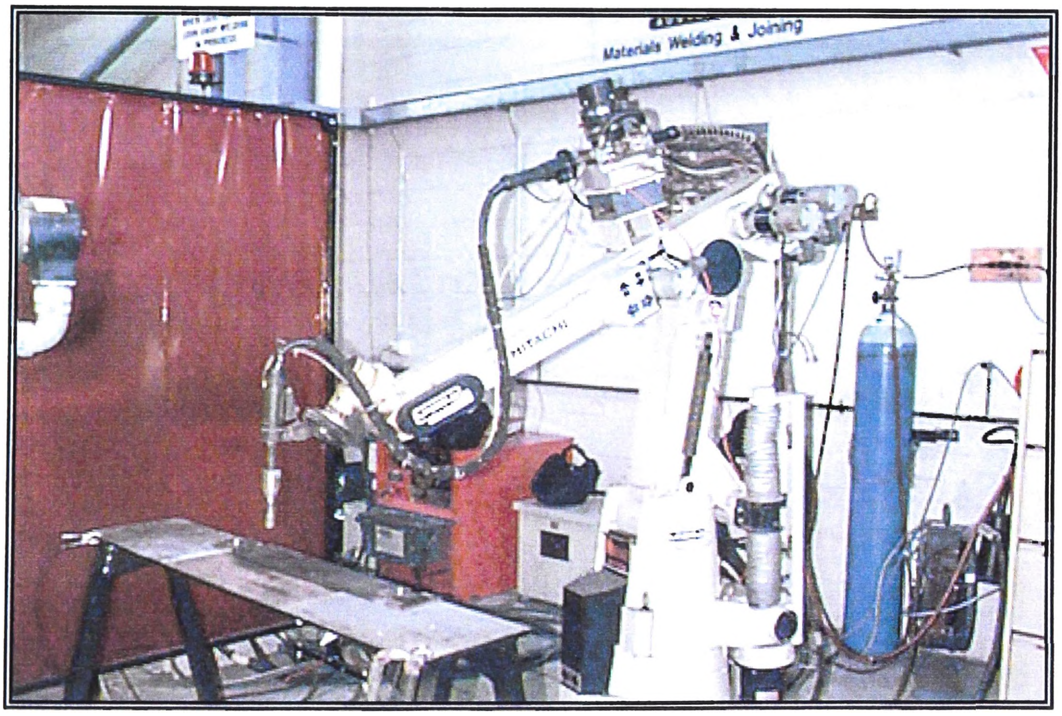

Figure 3.10

The Hitachi moves above the workpiece

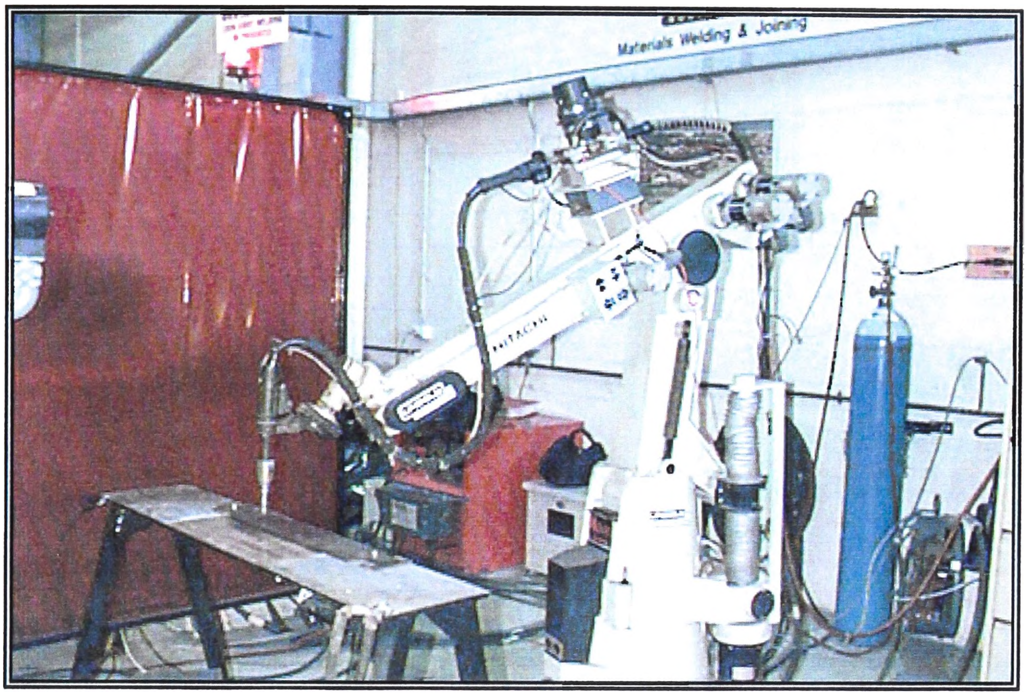

Figure 3.11

The Hitachi is at the start position before welding operation begins

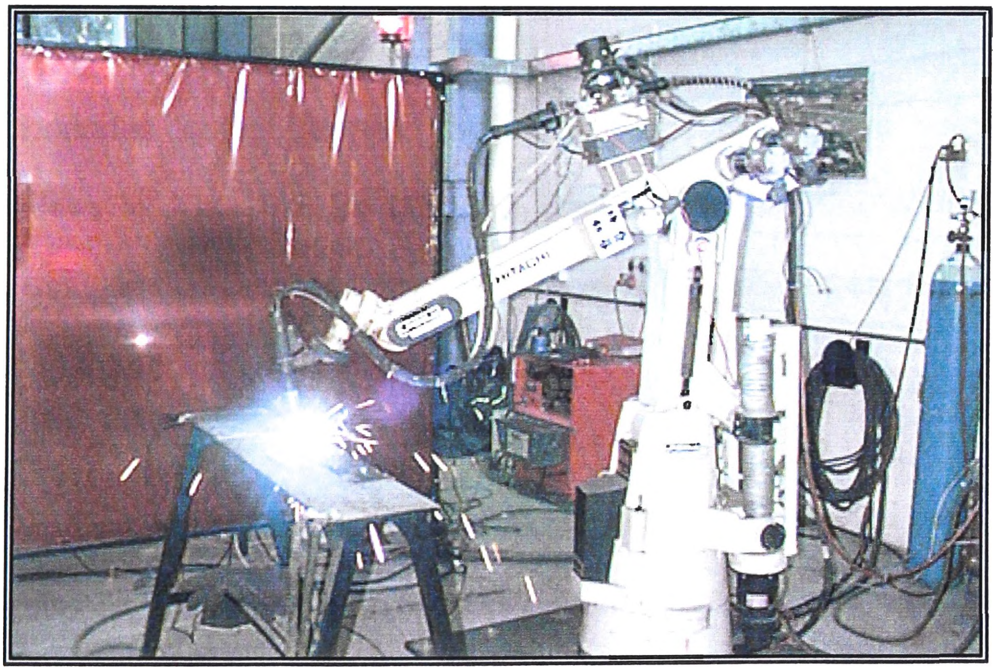

Figure 3.12

The welding operation starts

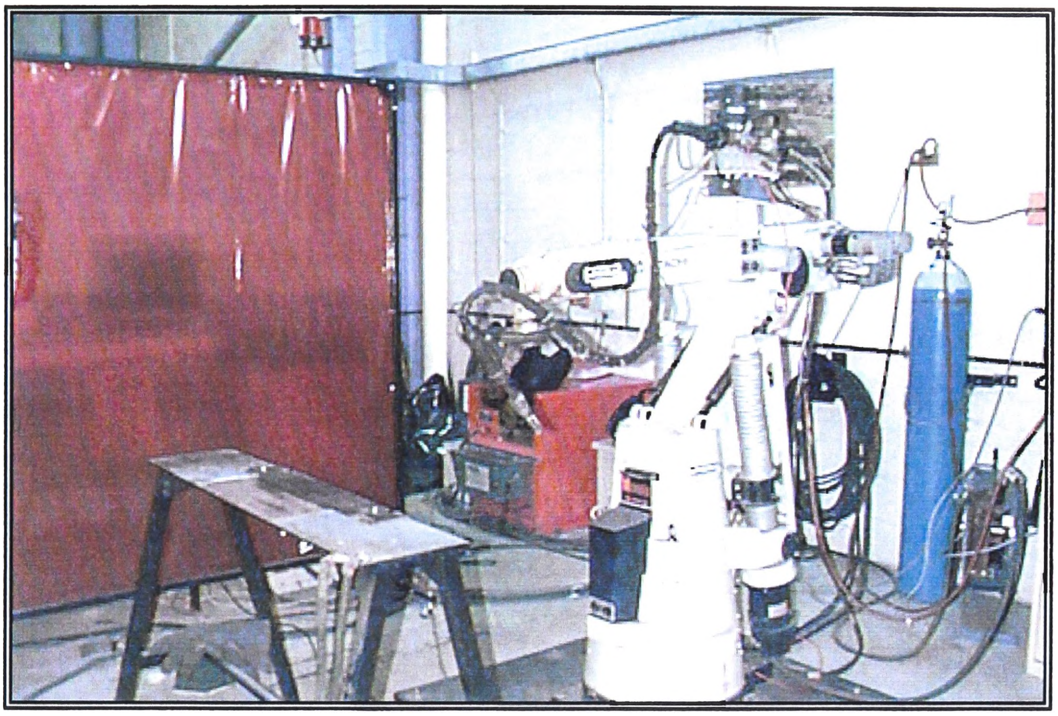

Figure 3.13

The Hitachi returns to home position after the welding operation is finished

3.6.5 The Weld Monitoring System

The monitoring system software used for the experiments was written in Labwindows by Khac Duc Do [33]. The graphical user interface of the main panel, configuration panel and monitoring panel of the program are depicted in figures 3.14, 3.15 and 3.16 respectively.

All of the functions on the graphical user interface can be reached by the mouse. By clicking the mouse on the desired location and inputting by the keyboard, the required values such as number of scans, travel speed and log time can be entered. During welding, the user can monitor on-line the actual welding parameters such as voltage, wire feed rate, travel speed, a stability histogram and heat input.

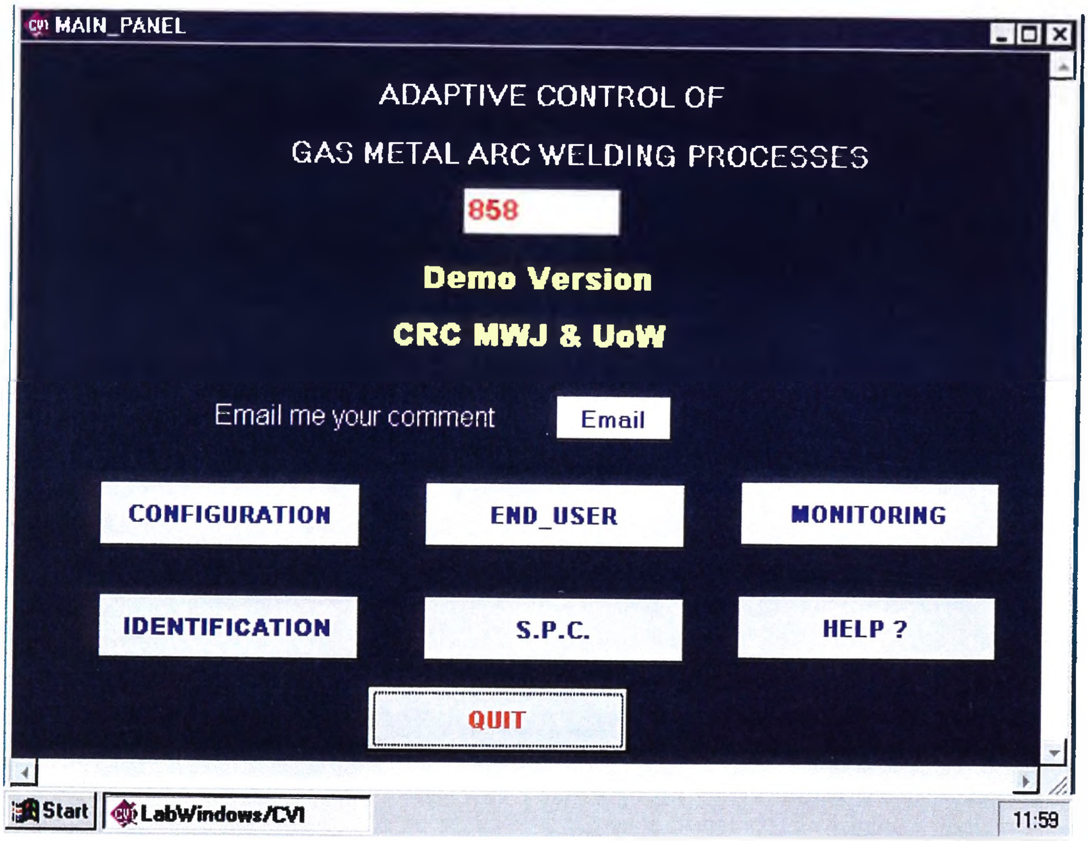

Figure 3.14

Main user interface panel

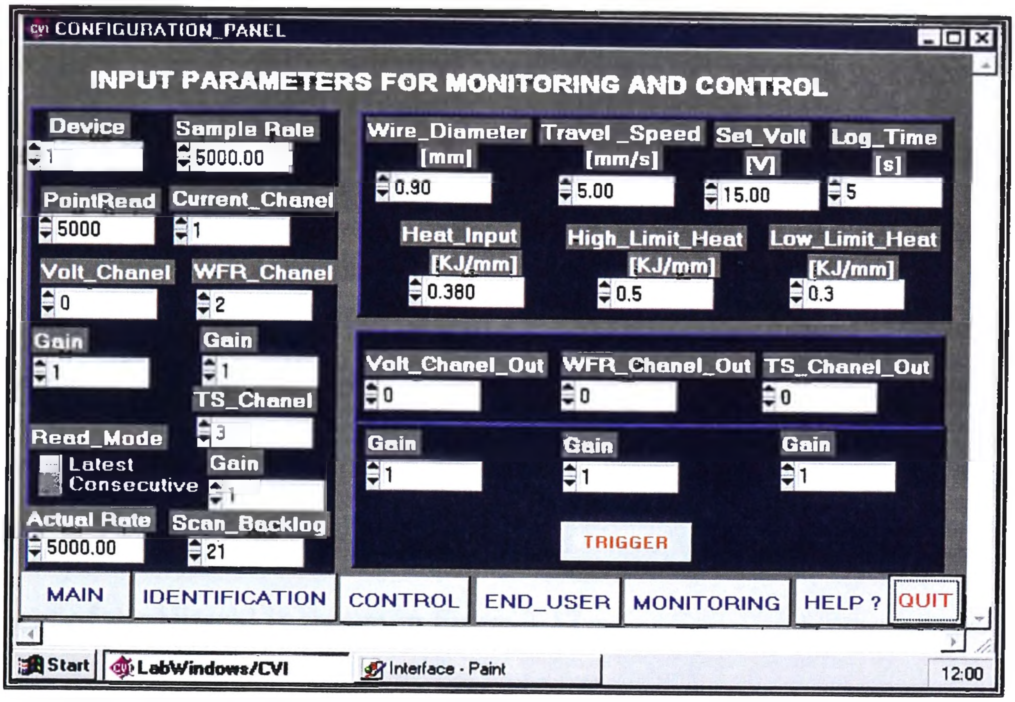

Figure 3.15

Configuration panel

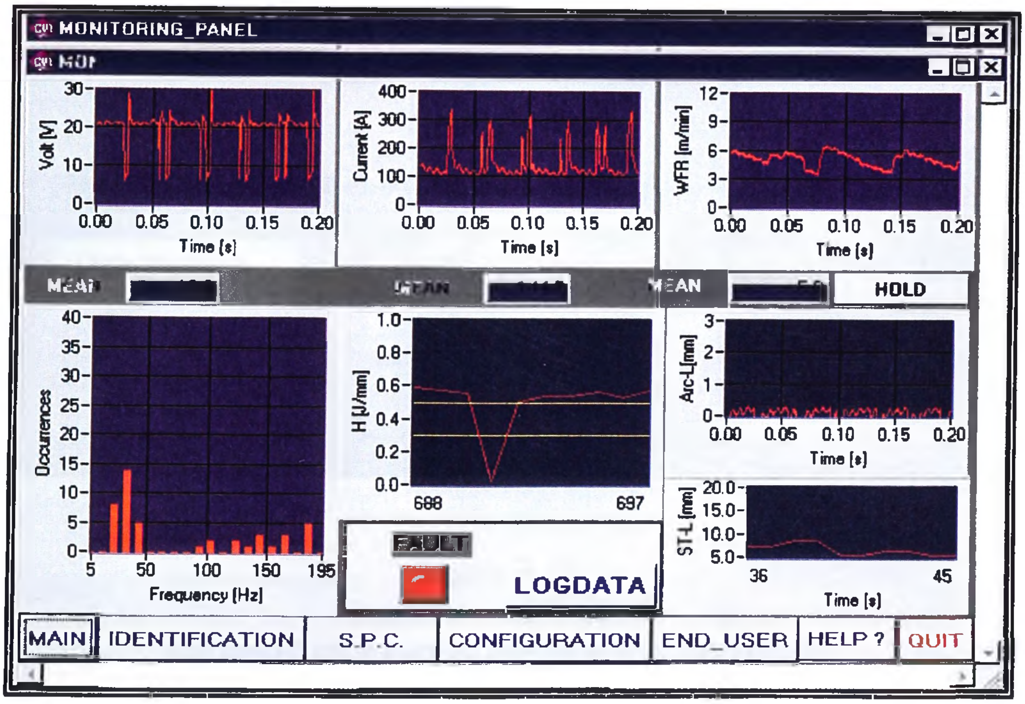

Figure 3.16

Monitoring panel

This monitoring system enables the user to record welding data (Voltage, current and wire feed rate) in the monitoring panel during the welding operation (See figure 3.16). The data is saved as a binary file. The data obtained from the experiment can then be analysed by using Matlab or other data analysis packages.

The monitoring system contains signal-conditioning box which isolates and conditions the censor signals for the analogue to digital converter. The PC is also equipped with analogue to digital converter and a monitor. The monitoring system equipment of the Hitachi is shown in figure 3.17.

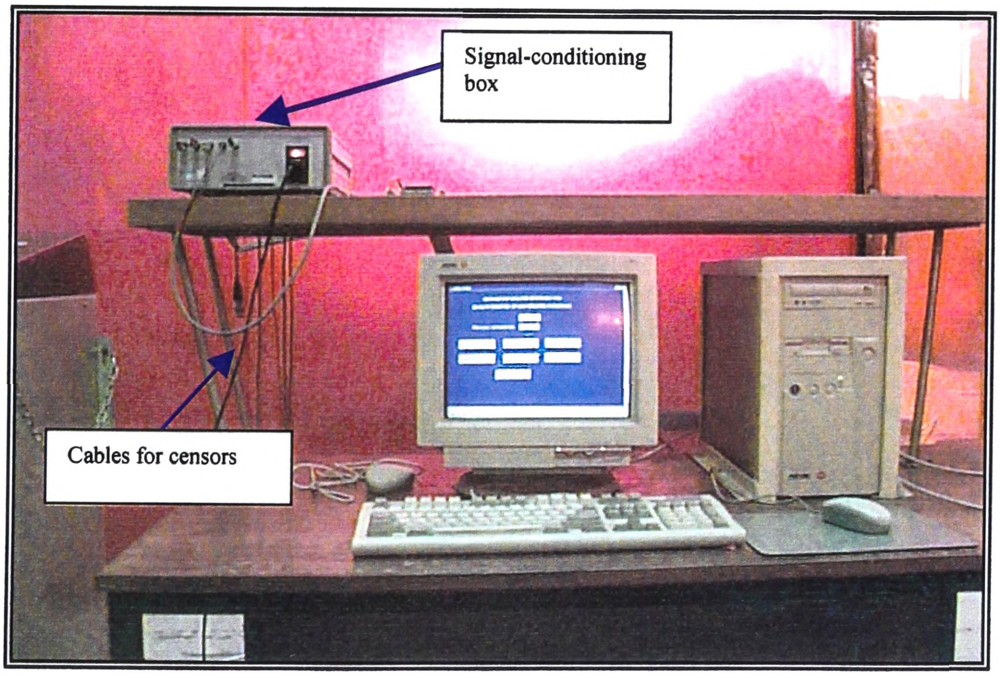

Figure 3.17

The monitoring system equipment of the Hitachi

3.6.6 Surface Temperature and Standoff Measurements

Surface temperature and standoff distance were measured during the preliminary experiments because it is expected that the surface temperature and incorrect standoff have a significant influence in determining weld quality. The method of determining these measurements had been described in detailed previously in chapter 2.

3.7 The Preliminary Experimental Results

There were twenty-seven samples made in the preliminary experiments. Therefore a coding system was established to identify the samples and data plots. The coding format chosen is described below:

p-xx-yy-zz-t, where

p	=	preliminary
xx	=	voltage setting [V]
yy	=	wire feed rate [m/min]
zz	=	travel speed [mm/sec]
t	=	pinch setting

The example of the above format is described below:

Consider the case where the coding is p-19-06-05-4. Thus, it means this is a preliminary experiment with the following parameters as described below:

- Voltage = 19 Volts
- Wire feed rate = 6 m/min
- Travel speed = 5 mm/sec

- The pinch setting = 4

An example of the layout for the particular setting above is illustrated below.

Data:			
Voltage [V]	19	Weld width [mm]	18.8
Wire feed rate [m/min]	6	Stand-off at layer 1 [mm]	15
Travel speed [mm/sec]	5	Stand-off at layer 10 [mm]	15
Number of layers	10	Temperature at layer 10 [deg.C]	473
Weld height [mm]	18	Pinch setting	4

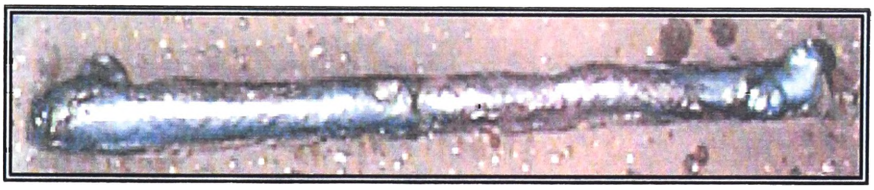

Figure 3.18

Sample p-19-06-05-4 (Top view)

Figure 3.19

Sample p-19-06-05-4 (Front view)

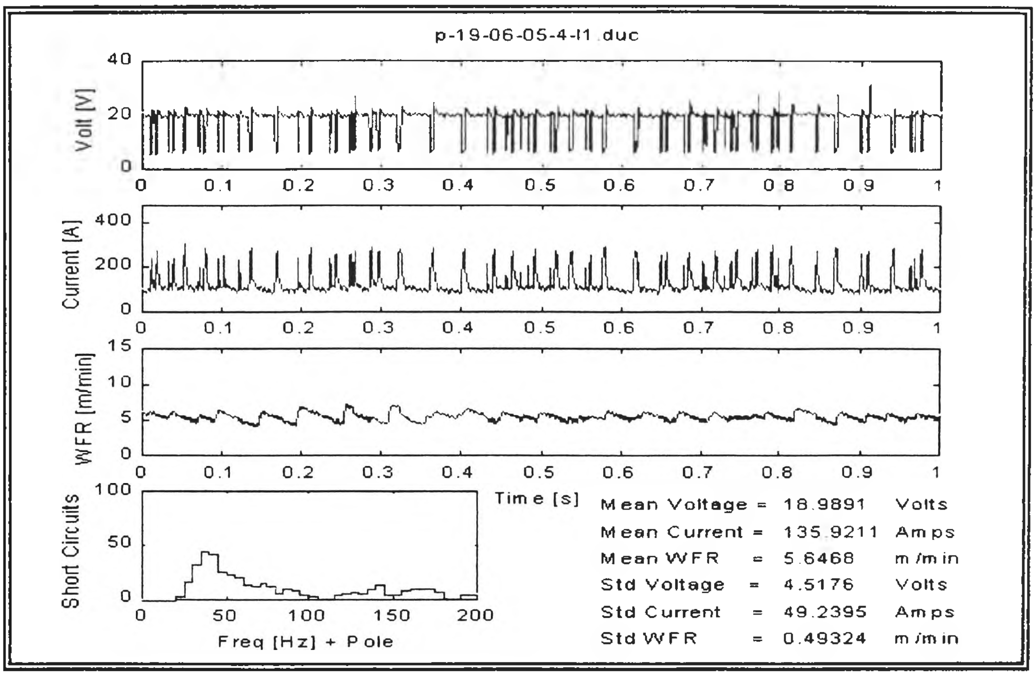

Figure 3.20

Electrical data plot of sample p-19-06-05-4 at layer 1

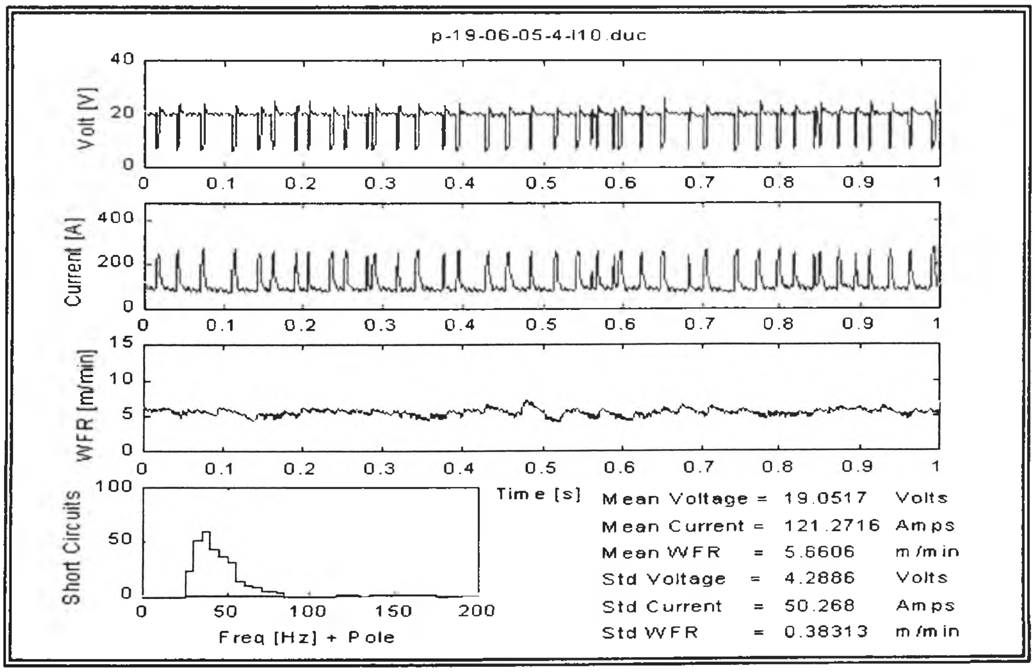

Figure 3.21

Electrical data plot of sample p-19-06-05-4 at layer 10

The pictures of all the weld samples, welding parameters and plots of the electrical data measured during the experiments are given in appendix A.

From results obtained in the preliminary experiments, several physical weld defects for building-up weld metal by robotic Gas Metal Arc Welding were identified. The defects are summarised in the paragraph below.

Spatter

Spatter was identified in many samples. This is caused by the process instability and unsuitable welding parameters for a particular sample. In addition nozzle blockage was a problem where excessive spatter was identified. This blockage will cause porosity because the blockage in the nozzle blocks the gas flow. Porosity can also be caused by an unsuitable standoff distance, if it became too large for the subsequent layers. The inappropriate standoff distance would reduce the efficiency of the shielding gas because as it makes the distance between the nozzle and the workpiece become inappropriate. An example of spatters and porosity is shown in figure 3.22 and 3.23 respectively.

Surface irregularity was also identified, this occurred particularly at the lower heat input settings. This is probably caused by the failure of power supply to maintain a stable arc during process as it is outside of its operating bandwidth. An example of surface irregularity is shown in figure 3.22.

Excess materials is a defect particular for this application. This problem particularly occurs in the high heat input settings. It is caused by the excessive heat input which made the molten weld pool to flow over the side and form excess materials along the weld metal built-up. An example of excess materials is shown in figure 3.24.

Figure 3.22

An example of spatters and surface irregularity

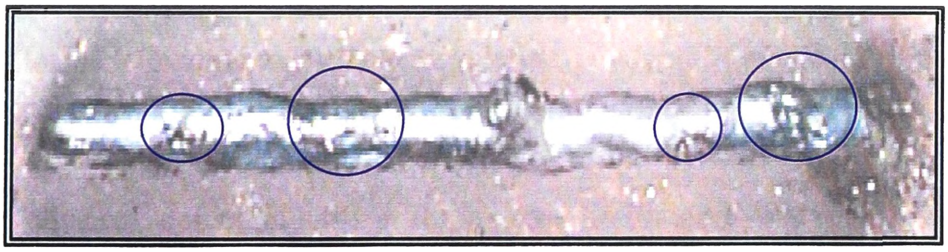

Figure 3.23

An example of porosity along the surface

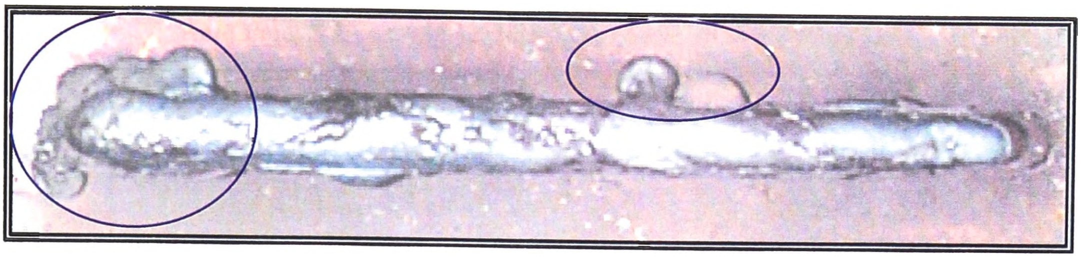

Figure 3.24

An example of excess materials

3.8 Discussion of the Preliminary Experiments

Spatters, porosity, surface irregularity, nozzle blockage and instability during the process were identified as dominant defects for this application. Nozzle blockage is a problem as it creates a build up of deposits on the tip of the nozzle. These deposits block the gas flowing through during the welding operations. This creates shielding problem, which creates porosity on the surface of the weld as is shown in some of the samples. In addition, when the nozzle is blocked, the process becomes unstable leading to surface irregularity.

Another physical defect identified during the preliminary experiments is the forming of excess materials in several samples. This defect occurred in samples with higher settings of wire feed rates and voltages. Hence, it is most probably caused by the excessive heat input which caused the molten pool to over flow as the surface temperature gets too high. The plot of heat input versus temperature for various settings is depicted in figure 3.25.

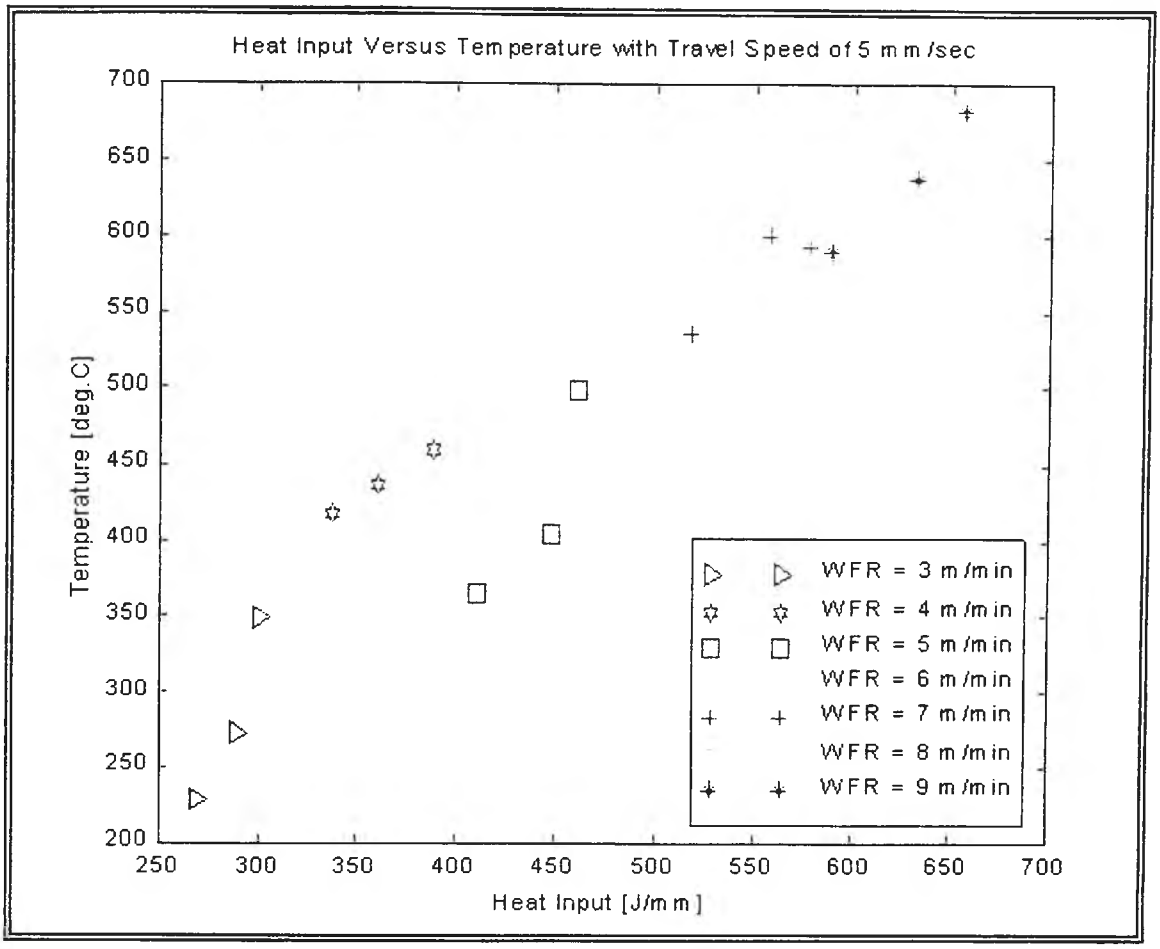

Figure 3.25

Heat input versus temperature

The Hitachi robot controller restricts the user to programming by teaching points, which makes accuracy of the increments became insufficient. Therefore it was fairly difficult to maintain a similar standoff distance on each layer because the points taught could only be determined by eye. If the standoff varies too much from the preset distance (15 mm), the standoff could become too large or too small. Then the process would result in spatter, porosity, uneven surface and instability. It was not possible to program the Hitachi robot accurately enough for the experiments to build up thin wall weld metal specimen.

A power supply which has better control over the transfer of metal droplets is required for rapid prototyping and wear replacement applications because the power supply used in the preliminary experiment failed to give satisfactory results. It is expected that building up thin walled weld metal specimen requires an appropriate amount of heat input, good stability and good control on the deposited weld metal during the process. This can be achieved by using modern inverted band power supply.

3.9 Summary

A number of problems building up thin wall weld metal objects were identified. These are porosity, spatter, surface irregularity and excess material. Nozzle blockage was also a problem, however this is mainly caused by spatter during the process and an automatic cleaning station or prevention of spatter by suitable parameter selection could overcome this.

Maintaining standoff distance was another problem identified. Standoff distance is one of the dominant factors that influence the process stability, if the standoff becomes too large or too close then the process would experience instability. Therefore, it is required to have a more accurate way to determine the standoff distance on each layer. However it was not possible to improve the standoff distance to the required accuracy because the limitation of the Hitachi robot controller which only allows the user to teach points in the program.

A better calibration of standoff, process stability and metal droplets are expected to be achieved by using the IRB 1400 robot and its synergic welding power supply which were specifically purchased for this application. A detailed description of IRB 1400 robotic welding cell will be given in the next chapter.

Chapter 4

The Experimental Setup

4.1 Description of Experimental Setup

This chapter will describe the experimental setup used for the remainder part of this thesis. The experimental work was carried out with a welding cell that had a IRB 1400 robot and accessories such as RobotWare monitoring software, a Power Wave™ 450 welding power supply made by Lincoln Electric, a Binzel welding torch, filler metal and shielding gas. A more detailed description of the equipment will be given in the following sections of this chapter.

4.2 The IRB 1400 Specifications

The IRB 1400 is a 6-axis industrial robot, the robot is made up of two main parts, these are: manipulator and controller, see figure 4.1 and figure 4.2 respectively. The IRB 1400 contains an electronics controller which controls the manipulator, external axes and peripheral equipment. The robot's manipulator and controller have a mass of 225 kg and 240 kg respectively. The controller has a volume of 950 mm X 800 mm X 540 mm, see figure 4.3.

The robot also fully complies with the health and safety standards specified in ANSI/RIA 15.06-1992. The safety system is based on a two-channel circuit which is monitored continuously. The system enables the robot to stop immediately by shutting off the electrical power and engages the brakes if there is any failure in any of the components.

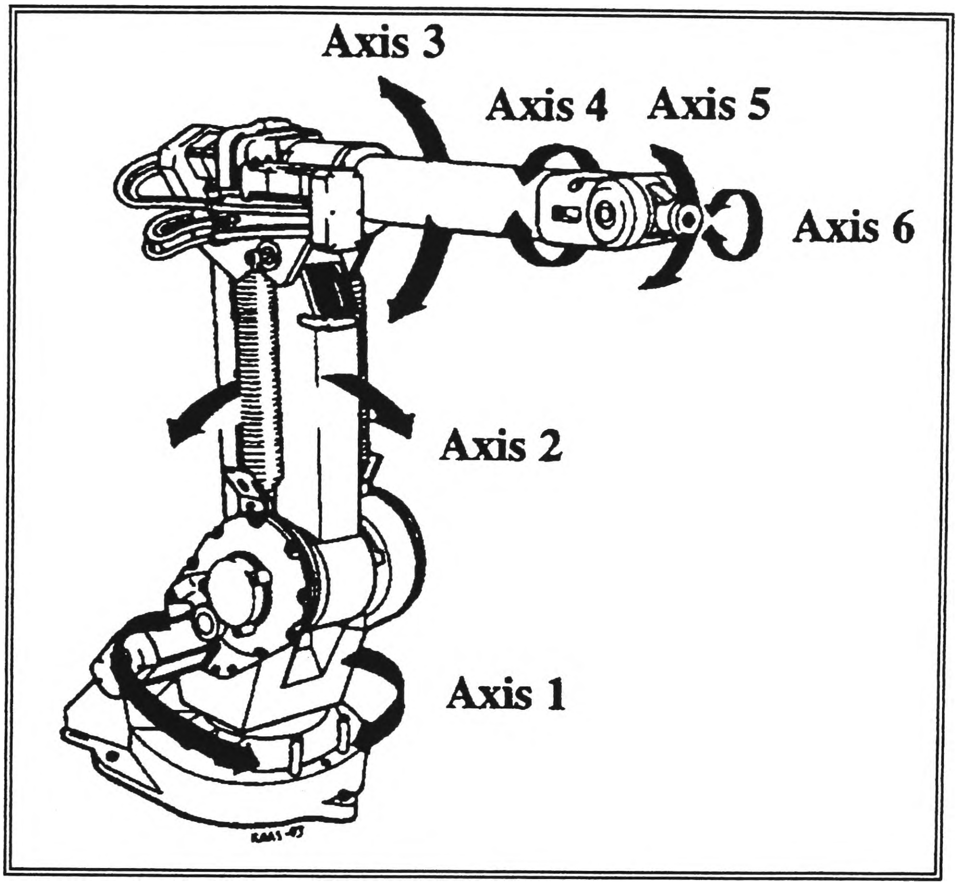

Figure 4.1

The IRB 1400 manipulator [19]

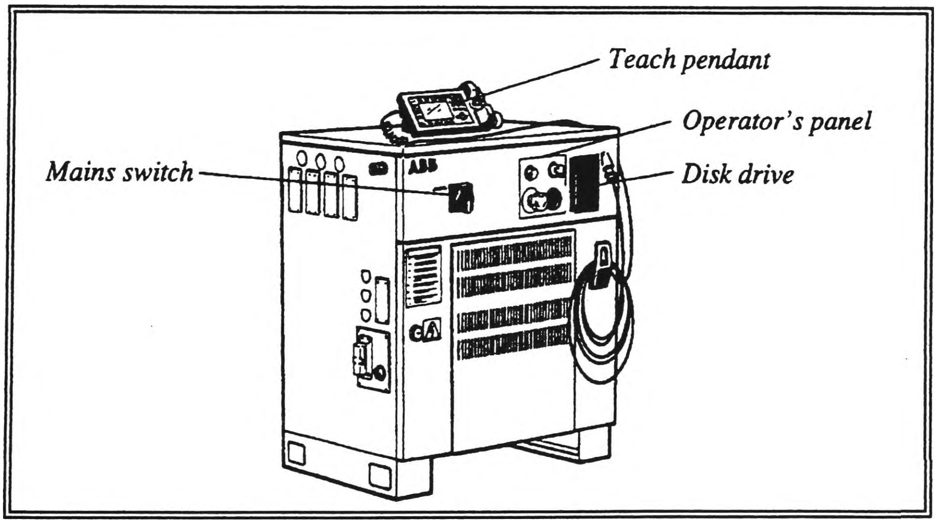

Figure 4.2

The IRB 1400 controller [19]

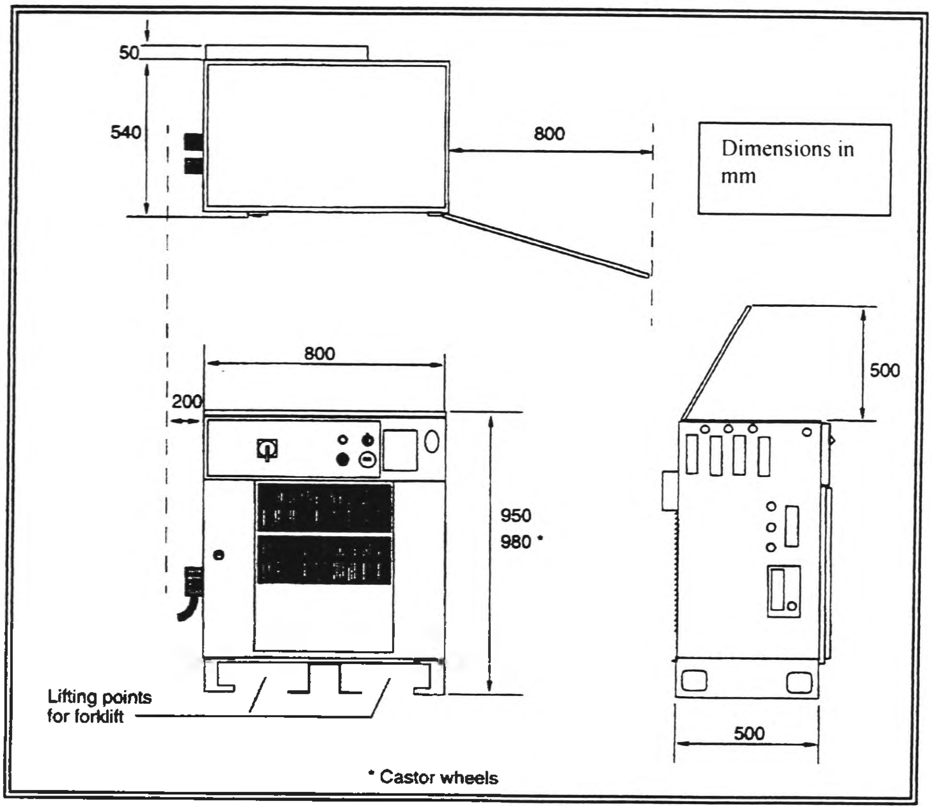

Figure 4.3

The IRB 1400 controller dimensions [19]

Each of these six axes performs different motions. The motions and the range of movements of the robot's axes are described in the table 4.1. The picture of the IRB 1400 robot and its controller are shown in figure 4.4 and 4.5 respectively.

Type of Motion	Range of Movement
Axis 1 Rotation motion	+170° - -170°
Axis 2 Arm motion	+70° - -70°
Axis 3 Arm motion	+70° - -65°

Axis 4 Wrist motion	+150° - -150°
Axis 5 Bend motion	+115° - -115°
Axis 6 Turn motion	+300 - -300°

Table 4.1

Robot motions and range of movements

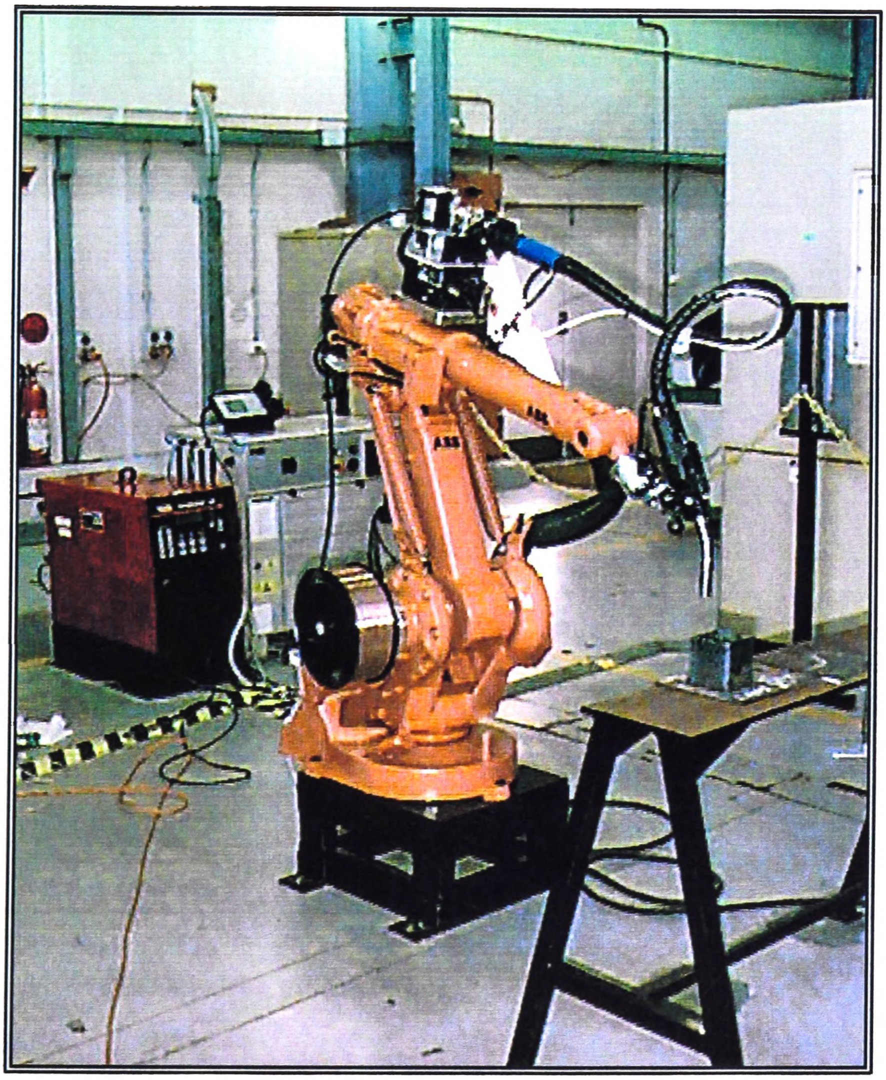

Figure 4.4

The IRB 1400 robot

Figure 4.5

The IRB 1400 controller

4.3 The IRB 1400 Coordinate Systems

The IRB 1400 has several programmable coordinate systems (See figure 4.6). Each of the coordinate systems are summarised below [19]:

- **The world coordinate system:** The world coordinate system defines a reference to the floor and this is the starting point for the other coordinate systems.

- **The base coordinate system:** The base coordinate system is attached to the base-mounting surface of the robot.
- **The tool coordinate system:** The tool coordinate system specifies the tool's centre point and orientation.
- **The user coordinate system:** The user coordinate system specifies the position of a fixture or workpiece manipulator.
- **The object coordinate system:** The object coordinate system specifies how a workpiece is positioned in a fixture or workpiece manipulator.

Tool Centre Point (TCP) is also indicated in figure 4.6. The Tool Centre Point defines the position of the welding given for the experiments carried out in this thesis.

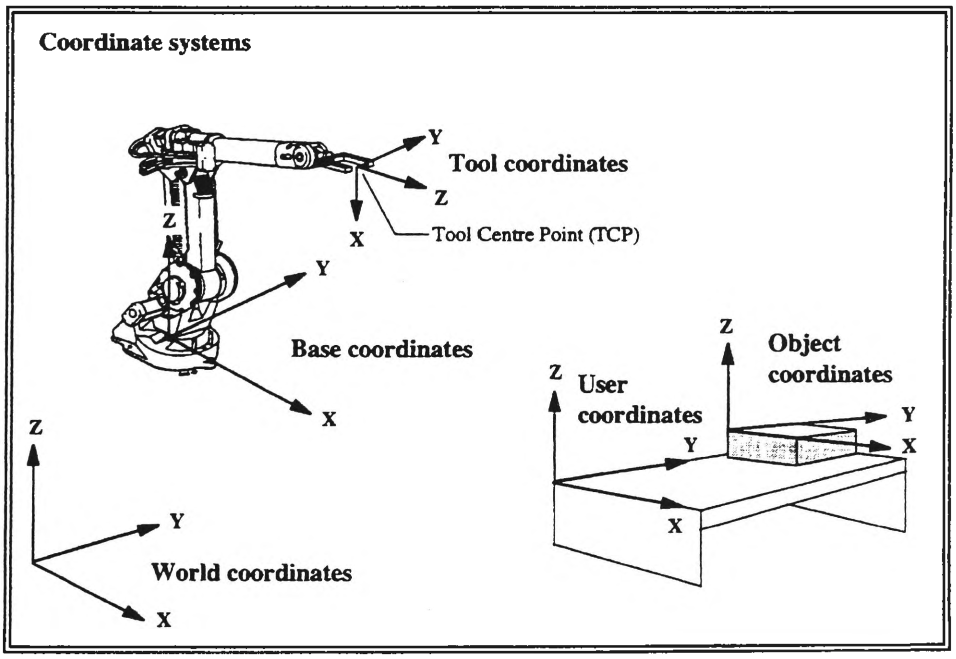

Figure 4.6

The IRB 1400 coordinate systems [19]

4.4 Tool Centre Point

'The point generally is the tip of a tool and it moves along the programmed path at the programmed velocity' [26]. It is important to define where the Tool Centre Point is in a program, so that it is known exactly where the robot will first come into contact with the work piece to avoid any collision between the robot and the surrounding environment. The position of the weld on the work piece is defined with respect to the Tool Centre Point. Therefore, for our application the tool centre point was defined as the tip of the welding torch.

4.5 Teach Pendant

Programming, jogging, teaching positions and many other functions in the IRB1400 can be done by using the teach pendant. The teach pendant of the IRB1400 is user friendly because it enables the user to program the robot in a high level programming language. When several process packages have been added to the system such as ArcWare, SpotWare etc, the teach pendant allows the user to define which package should be used for the program.

The teach pendant also allows the user to test the program by disabling the arc so that before a real-time welding operation is done the user can test-run and ensure all of the steps and positions are correct.

The teach pendant also enables the user to display and tune various events and conditions during the process such as number of loops being performed and the welding conditions (travel speed, wire feed rate and voltage) can be tuned on-line as the robot is welding. The display can accommodate 16 lines and each line can accommodate 40 characters.

The teach pendant can stop and restart the process by just touching a key. An emergency stop button is also available in case the user must stop the process and shuts down all the power in such an emergency situation.

The robot can be jogged in various ways using the joystick (the joystick is also part of the teach pendant). The joystick allows the user to choose whether the robot is jogged along a straight line, aligned with the tool along a coordinate axis, jogged only along a specified axis. The joystick movement can also be specified in continuous or increment motion mode. In the increment mode the user can define how many millimetres per increment the robot moves when the joystick is moved into a certain direction. This mode is very useful when accurate positioning is needed during programming such as determining the distance from the contact tip to the workpiece. The schematic picture of the teach pendant and an overview of the various keys on teach pendant are depicted in figures 4.7 and 4.8 respectively. The picture of the teach pendant is depicted in figure 4.9.

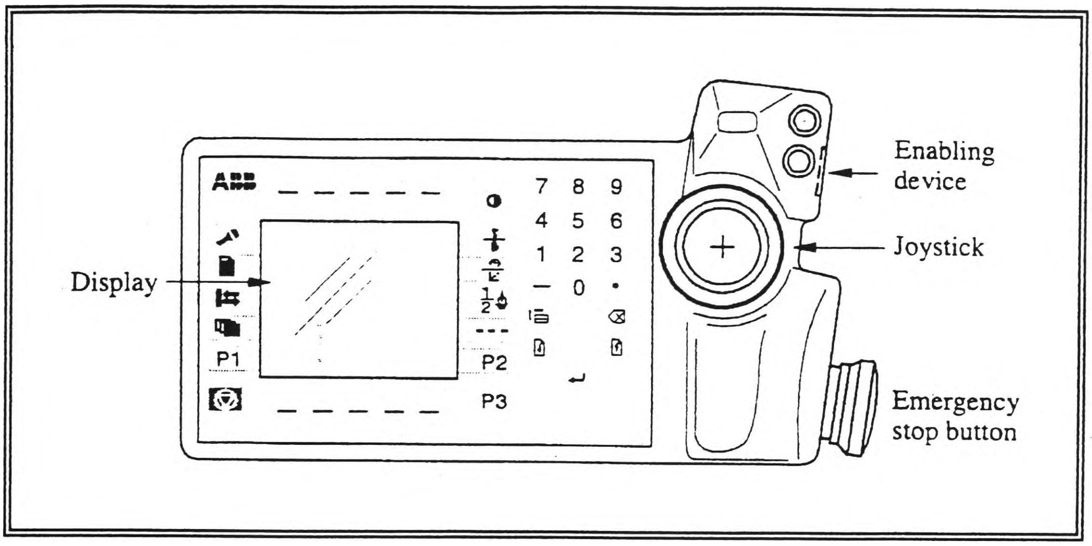

Figure 4.7

IRB1400 teach pendant [26]

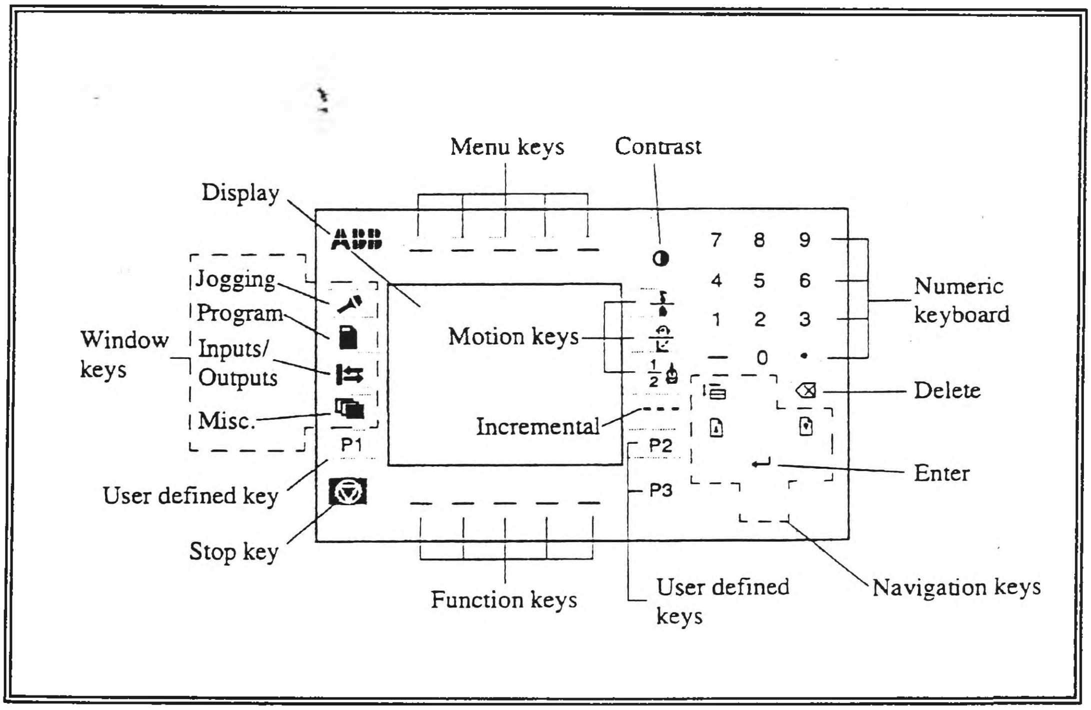

Figure 4.8

Various keys on the teach pendant [26]

Figure 4.9

The IRB 1400 teach pendant

4.6 Programming with ArcWare

The ArcWare function allows the user to perform welding operation. Programming an arc welding instruction basically contains three arguments, ie. seam, weld and weave data, which serves as data for the arc welding process. Each of the data types is used at different stages in the welding operation as described below [26]:

- Seamdata describes how the seam is to be started and ended.
- Welddata describes how the actual welding phase is done.
- Weavedata describes how any weaving is to be carried out.

4.6.1 Seam Data

Seam data has the function to control the start and the end of the welding operation. This includes preparing for welding operation, igniting the arc, heating after the ignition and ending the weld.

There are three major groups included in the seam data, these are:

- Ignition group
- Heat group
- End group

Each one of these groups contains several components. The various components are summarised in the following [27]:

1. **Ignition Component Group:**

- Purge_time: Purge time is the time [seconds] it takes to fill the gas lines and the welding gun with the appropriate gas. This process is also known as "gas purging".
- Preflow_time: Preflow time is the time [seconds] it takes to preflow the weld object with protective gas. This process also known as "gas preflowing".
- Ign_voltage: Ignition voltage is the welding voltage [Volts] during ignition of the arc.
- Ign_wirefeed: Ignition wirefeed is the feed speed [metre/minute] of the weld electrode during ignition of the arc.

- Ign_move_delay: Ignition move delay is the delay [seconds] from the time the arc is considered stable at ignition until the heating phase is started.

2. **Heat Component Group:**
   - Heat_speed: Heat speed [millimetres/second] is the welding speed during heating at the start of the weld phase.
   - Heat_time: Heat time is the heating time [seconds] at the start of the weld phase.
   - Heat_distance: Heat distance is the distance [millimetres] at the start of the weld where heat data must be activated.
   - Heat_voltage: Heat voltage is the welding voltage [Volts] during heating.
   - Heat_wirefeed: Heat wirefeed is the feed speed [metre/minute] of the weld electrode during heating.

3. **End Component Group:**
   - Cool_time: Cool time is the time [seconds] during which the process is closed before other terminating activities (filling) takes place.
   - Fill_time: Fill time is the crater-filling time [seconds] at the end phase of the weld.
   - Bback_time: Burnback time is the time [seconds] during which weld electrode is burnt back after electrode feeding has stopped. The purpose of this is to prevent the wire getting stuck to the hardening weld.
   - Postflow_time: Post flow time is the time [seconds] required for purging with protective gas after the end of a process. The purpose of gas post-

flow is to prevent the weld electrode and the seam from oxidising during cooling.

- Fill_voltage: Crater-filling voltage is the welding voltage [Volts] during crater filling at the end phase of a process.
- Fill_wirefeed: Crater-filling wirefeed is the feed speed of the weld electrode when crater-filling process takes place.

4.6.2 Weld Data

Weld data has the function to control the weld during the weld phase, this implies from when the arc is established until the weld is completed. Weld data enables the welding conditions to vary along the seam so that in one program it is possible to have a variation of welding conditions along one seam.

Weld data takes effect after the fusion has been established (after the heating phase) at the start of the process. 'When the program uses flying start, the arc is not ignited until the designated position of the arc welding instruction with the "\On" argument is reached.

For the experiments in this thesis, the following weld data components were used [27]:

- Weld_speed: Weld speed allows the user to input the required speed [millimetre/second] during the weld phase.
- Weld_voltage: Weld voltage is the welding voltage [Volts] during the weld phase.

- Weld_wirefeed: Weld wirefeed is the feed speed [metre/minute] during the weld phase.
- Org_weld_speed: Original weld speed [metre/minute] is the original weld speed during the weld phase. Note: as previously mentioned, the user can vary the welding conditions on-line during welding operation. This component enables the user to revert back to the original weld speed by just touching a key.
- Org_weld_voltage: Original weld voltage [Volts] is the original voltage during weld phase. Again this component enables the user to revert back to the original voltage.
- Org_weld_wfeed: Original weld wirefeed speed is the original weld wirefeed speed [metre/minute] during the weld phase. This component enables the user to revert back to the original wirefeed speed.

4.6.3 Weave Data

The function of weave data is to define any weaving carried out during arc welding. Generally there are three types of weaving pattern, these are; zig-zag, V-shaped and triangular, see figure 4.10, 4.11 and 4.12 respectively.

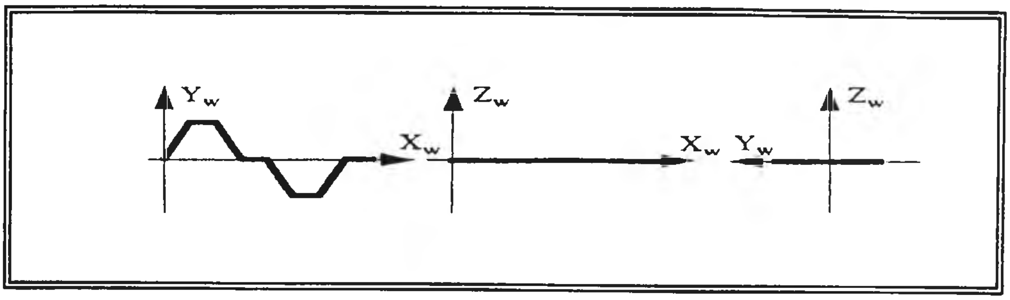

Figure 4.10

Zigzag pattern results in weaving horizontal to the seam [27]

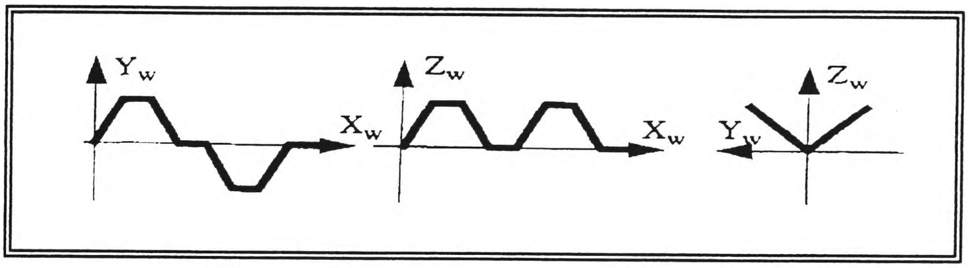

Figure 4.11

V-shape pattern results in weaving in the shape of a "V" vertical to the seam [27]

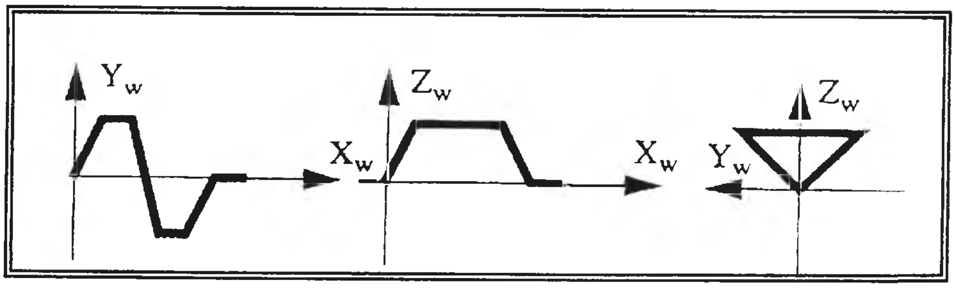

Figure 4.12

Triangular pattern results in a triangular shape vertical to the seam [27]

4.7 The Welding Power Supply Specifications

The welding power supply used for the experiment is the Power Wave™ 450 made by Lincoln Electric. The Invertec Power Wave™ 450 is designed for high performance, it is a digitally controlled inverter welding power source that is capable of complex high-speed waveform control. The Power Wave™ 450 is a three-phase welding power supply and designed to be used as a synergic welding system in conjunction with a wire feeder.

'The word synergic comes from the word synergism which means two or more thing working together to achieve an effect which neither can be achieved individually' [20]. The power supply and the wire feeder operate together as a team. This kind of power supply is equipped with a pre-programmed settings to perform the best range of process settings according to wire type, wire size and gas combination. The Power Wave™ 450 comes with pre-programmed settings for GMAW processes such as pulse, short-circuit and spray mode.

The Power Wave™ 450 provides various options and controls. These include things like multiple process selection, memory storage of procedures, weld from memory operation and dual process capability. The power supply is rated at 500 Amps, 40 Volts at 60% duty cycle on a ten-minute time period. A higher duty cycle can be achieved at lower output currents. In the case of overloading, the thermostat will shut off the output until the machine cools to a reasonable operating temperature. The features of the power supply are listed below [20]:

- Multiple process output ranges from 5-540 Amps

- 2-line LCD display
- Easy access for input connections
- Thermostatically protected
- Electronic over-current protection
- Over-voltage protection
- Digital signal processor and microprocessor control
- RS232 interface for future welding application updates
- Simple and reliable reconnection for various input voltages
- New accessories and wire feeders communicate using a digital current loop to transfer information
- Auto device recognition simplifies accessory cable connections
- Direct support of two wire feeders
- Auto-configurable for both metric or English mode
- Multi-process control for stick; GMAW such as short arc. spray and pulse; flux cored arc welding (FCAW)
- Simple control through overlays that limit access to only those keys required for a given application

The ArcTool software (V1.30 P) is used to interface the power supply with a robot, it is also equipped with touch sensing and arc tracking. In the operator's manual [20], it is mentioned that the interface does not control the wire feed speed and welding voltage independently, but it is always operating in a synergic mode and the welding voltage is programmed as a function of the wire feed speed. The picture of the power supply and the overlay panel are depicted in figure 4.13.

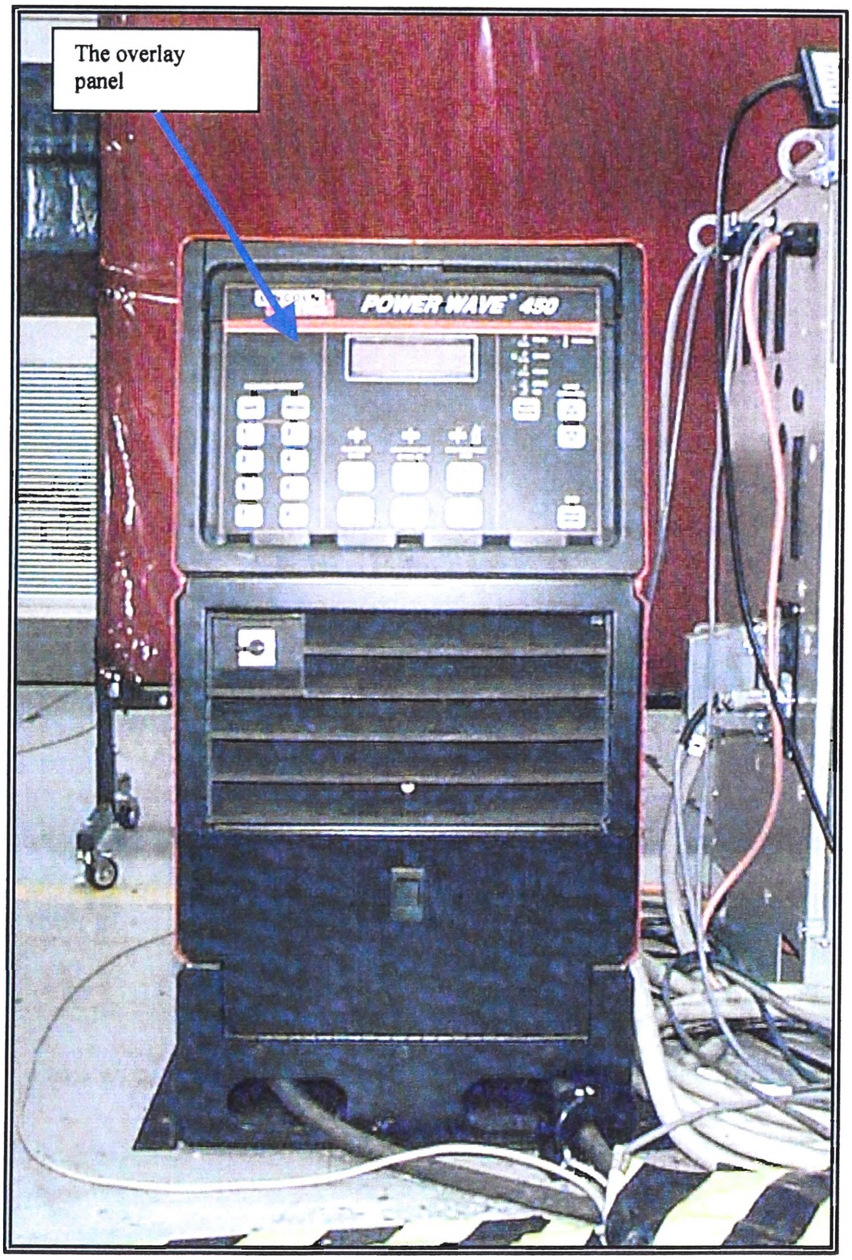

Figure 4.13

Power Wave 450

4.8 Filler Wire and Shielding Gas Specifications

The filler wire used for the experiments are Autocraft LW1 made by CIGWELD and the shielding gas used for the experiments are Argoshield ™ 51 made by CIG. The detailed specifications of the filler wire and the shielding gas were described previously in chapter 3.

4.9 Programming the IRB 1400

There are two types of programs which are used for this thesis, these are:

- A program for manufacturing a thin walled weld metal specimen
- A program for manufacturing a solid weld slab metal specimen

The thin walled weld metal specimen will demonstrate and evaluate the capability of the rapid prototyping technique to create hollow objects. where as the solid weld slab metal specimen will demonstrate and evaluate the capability of Rapid Prototyping technique to create a solid object.

In terms of robot movements, there are five basic principal positions that the robot performs. The different positions of the program are depicted in the illustration below. For more detailed description on how to use these programs will be given in the next two chapters.

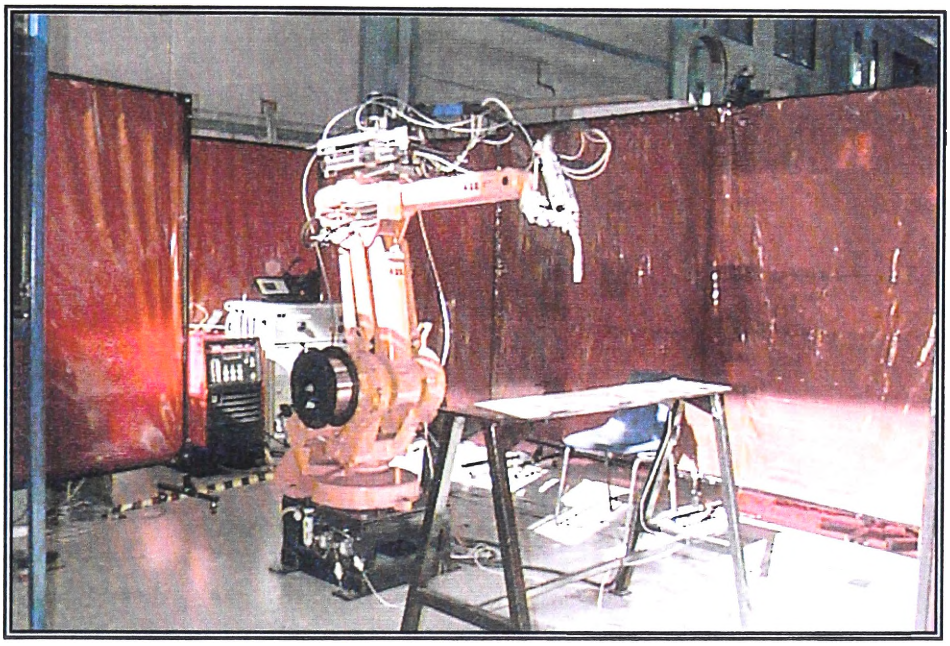

Figure 4.14

The home position of the robot

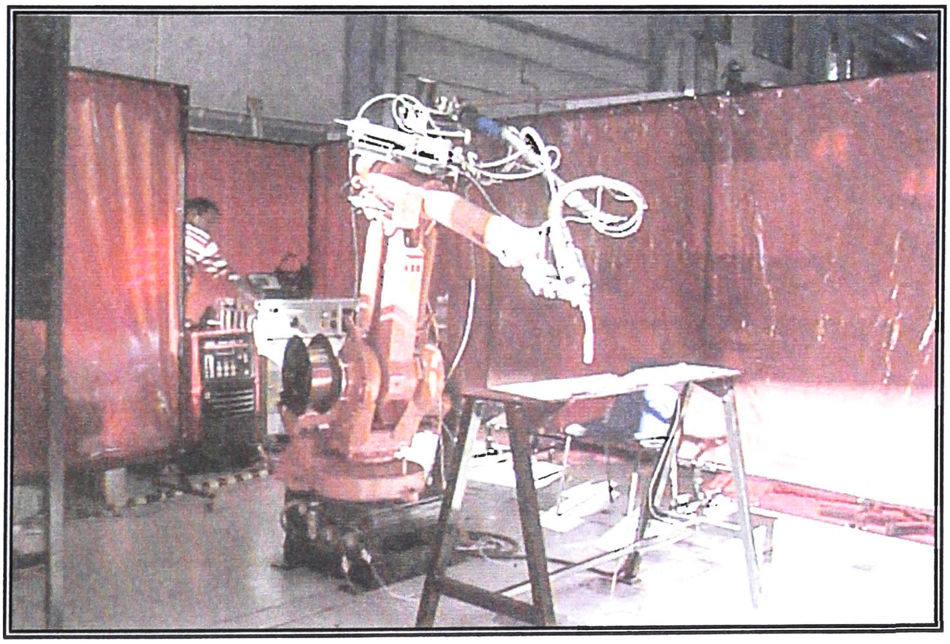

Figure 4.15

The robot moves above the workpiece

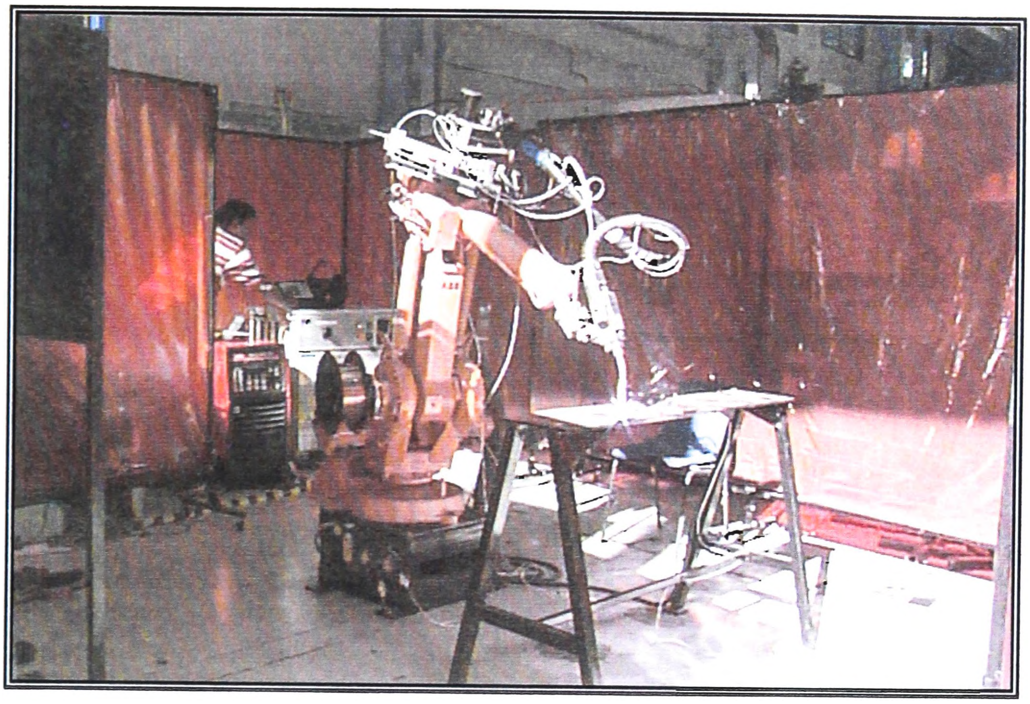

Figure 4.16

The robot moves to start position and starts welding

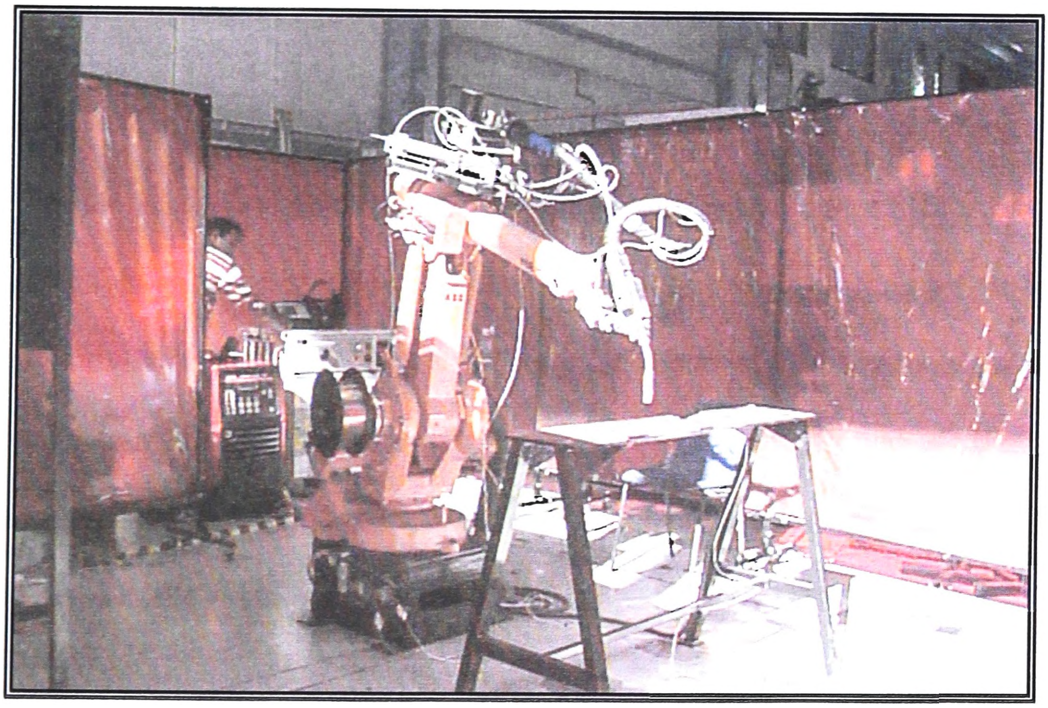

Figure 4.17

The robot returns to position above the workpiece after welding operation finished

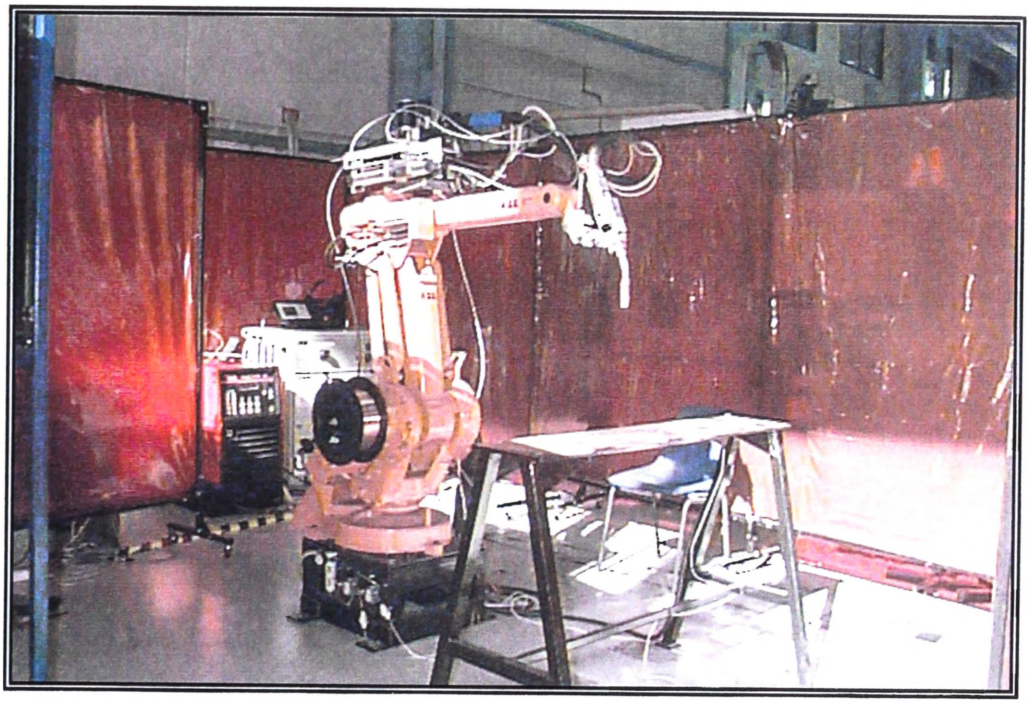

Figure 4.18

The robot returns to the home position

4.10 Description of the ArcWare Settings

Appropriate seam data and weld data were determined as part of the ArcWare conditions. Suitable seam data is required so that the welding operation can start successfully with having as little build-up of metal at the beginning and to perform crater filling at the end of the weld. However weaving was not required for this application, thus all the values for weaving are set to zero. The seam data values used in the experiment are depicted in appendix B.

4.11 The Weld Monitoring System

The monitoring software used for the IRB 1400 is similar to the one used for the preliminary experiment. An additional feature is added so that it is be able to monitor the gas flow.

Four sensors are used by the monitoring system. These are:

- Voltage sensor
- Current sensor
- Wire feed rate sensor
- Gas flow sensor

These sensors enable the acquisition of welding conditions on-line. The instantaneous values of voltage are obtained by connecting the voltage lead to the anode and cathode sides of the welding circuit. The voltage was taken on the welding gun as close as physically possible to the contact tip.

The welding current is measured using a Hall effect sensor connected to the positive terminal of the welding power supply. The wire feed rate was measured by connecting a tachogenerator to the wire electrode near the wire spool. The tachogenerator converts the wire feed rate speed into a proportional average reading. Since the sensor is placed near the spool, it was unable to detect the wire feed rate near the arc, and therefore only gives an indication of the average wire feed rate. The sensor's descriptions and their locations in the welding cell are depicted in figures 4.19, 4.20, 4.21 and 4.22.

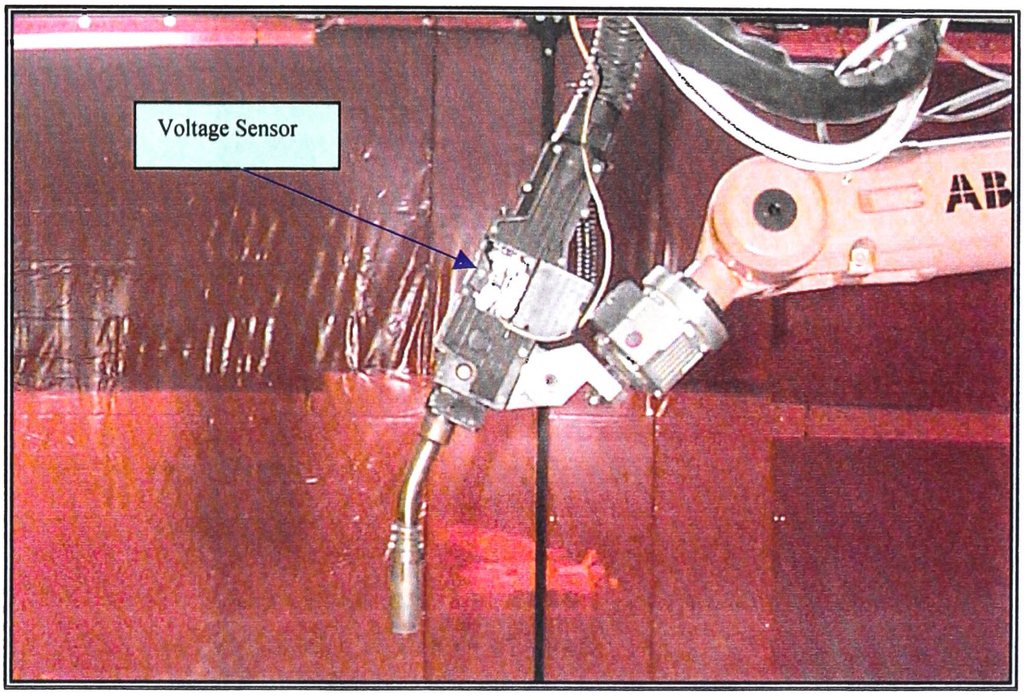

Figure 4.19

Voltage sensor

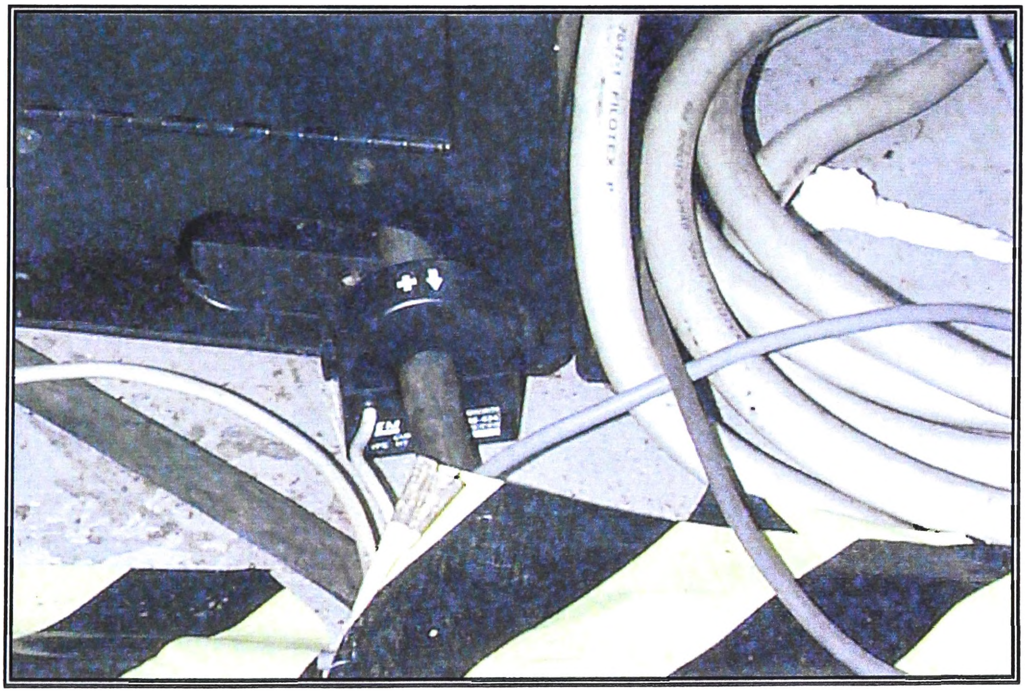

Figure 4.20

Current sensor

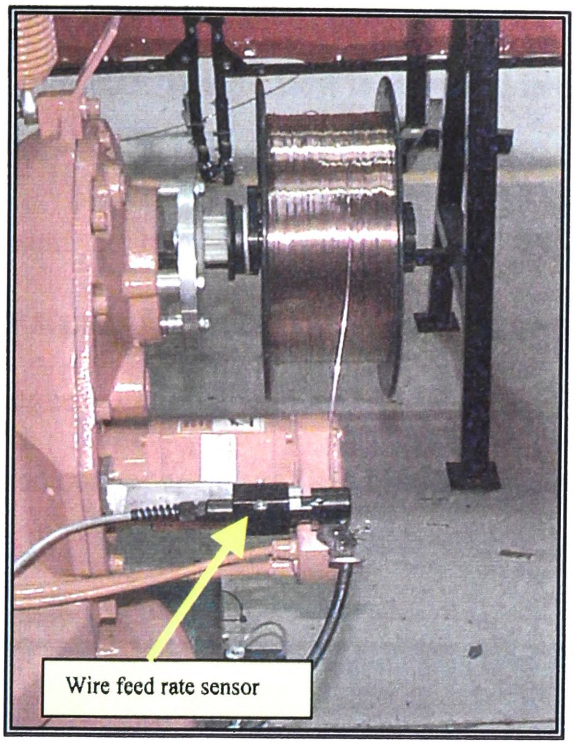

Figure 4.21

Wire feed rate sensor

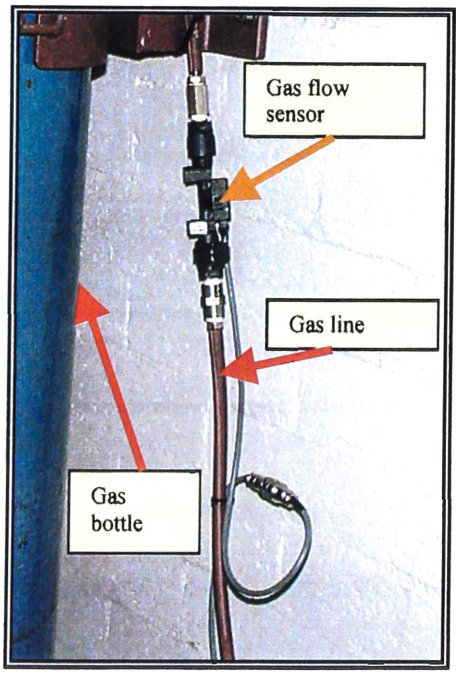

Figure 4.22

Gas flow sensor

The new layout of the monitoring panel with an additional channel for the gas flow is depicted in figure 4.23. The gas flow is measured in litres per minute.

The monitoring system contains signal-conditioning box which isolates and conditions the censor signals for the analogue to digital converter. The PC is also equipped with analogue to digital converter and a monitor. The monitoring welding equipment and computer for the IRB 1400 is depicted in figure 4.24.

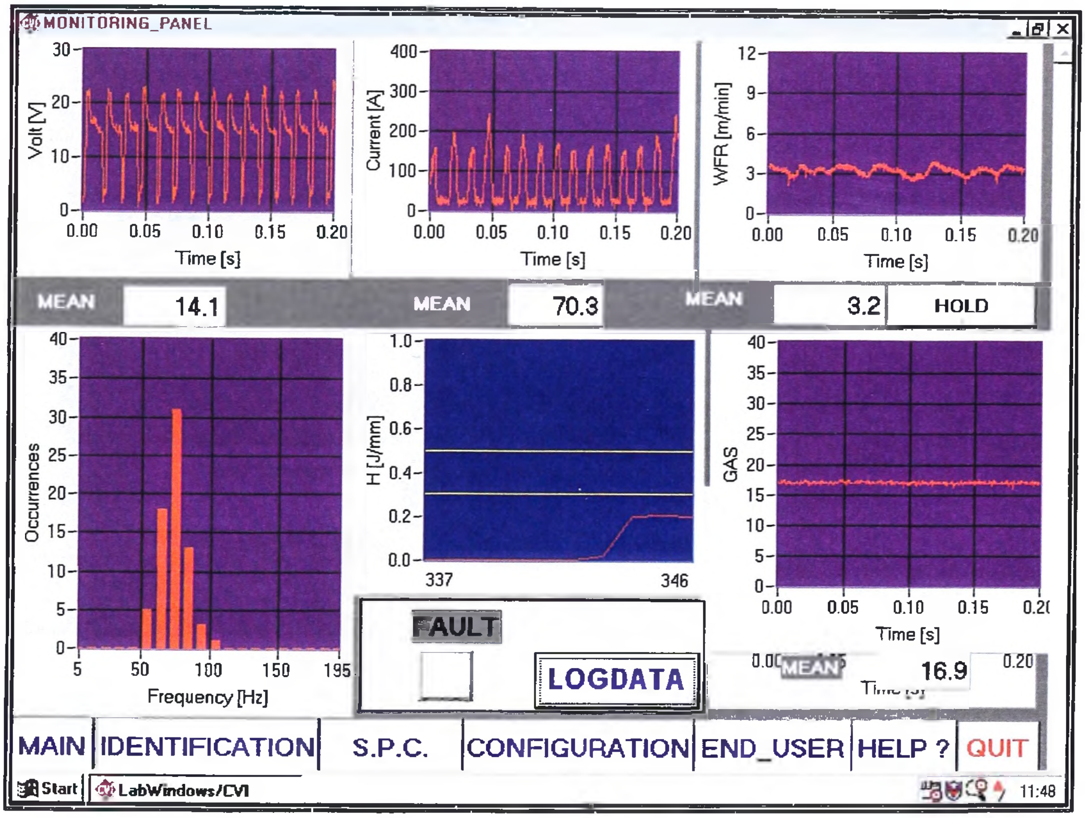

Figure 4.23

The monitoring panel of the IRB 1400

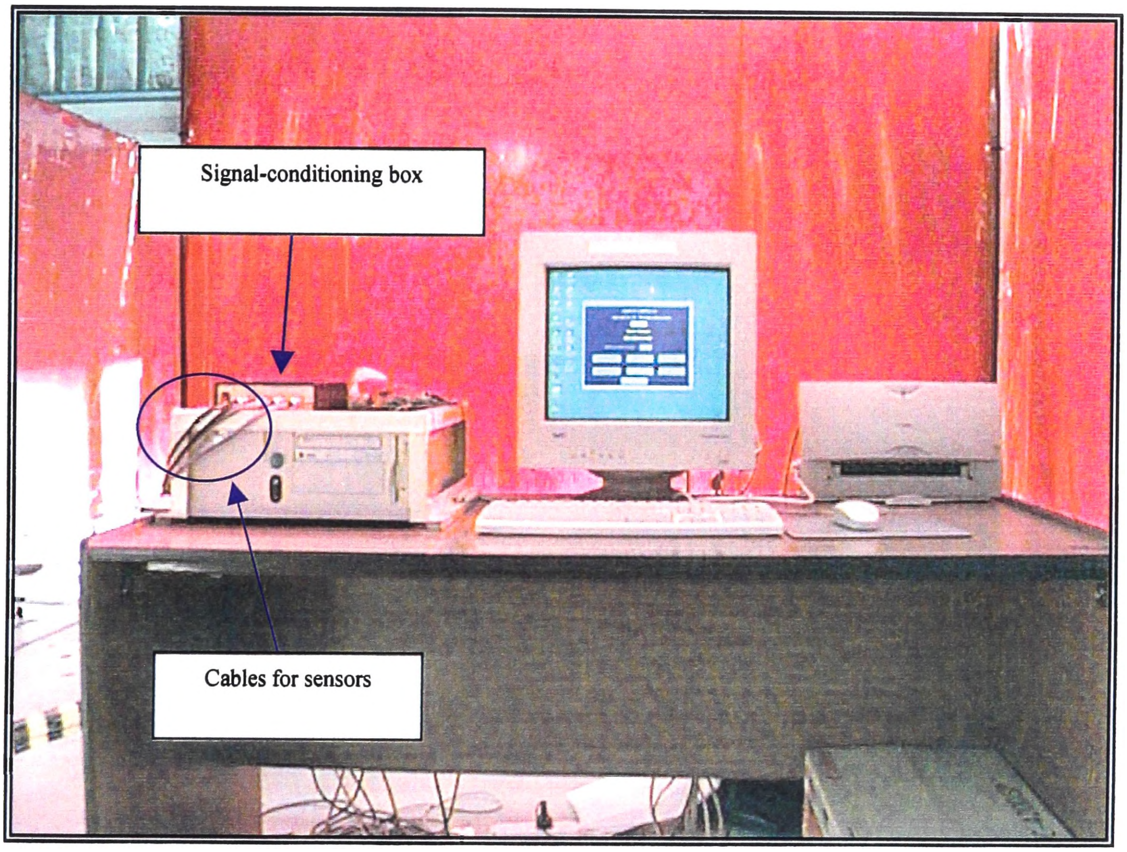

Figure 4.24

The monitoring system equipment of the IRB 1400

Chapter 5

Thin Walled Objects

5.1 Introduction

In this chapter. the experiments of creating a thin walled weld metal specimen will be investigated in more detailed. The IRB 1400 robot and its accessories will be used for these experiments.

Determining the quality of thin walled weld metal specimen includes analysing physical defects such as spatter, porosity. surface irregularity and excess material. Stability of the process can also be determined from the electrical data signal recorded during the experiments. Surface regularity will be investigated and tensile strength will also be investigated. The approximation of the tensile strength can be determined from the hardness property obtained in the experiments. The relationship between the tensile strength and the hardness can be determined by looking at transformation table [30]. Two different travel speeds were also used in the experiments to determine whether it would have a great influence on the weld quality.

5.2 Selection of the Welding Parameters and Conditions

The Power Wave™ 450 has pre-programmed parameters as part of its capability and speciality of being a synergic power supply. However, for a given wire feed rate, the user can deviate from the pre-programmed setting by changing a voltage percentage from 50-150, where 100 corresponds to the initial pre-programmed setting. Therefore the numbers on the teach pendant do not represent actual voltage, but it is related to it by unknown scaling factors.

For each wire feed rate used in the experiments, the original voltage in percentage is converted into more useful measure in volts. This is investigated by doing several single weld runs for wire feed rate ranging from 1 m/min to 9 m/min. For each of these wire feed settings, the voltage displayed on the teach pendant is changed from 50 to 150. By doing so, the actual voltage used by the power supply for each of the wire feed rate can be determined. The actual voltage was determined from the electrical data recorded by the monitoring system. It was then established that the voltage displayed on the front panel of the power supply also represents the actual voltage in volts.

The experiment indicated that the characteristic of the power supply for each wire feed rate used was not the same, but was similar in shape. It should be mentioned that the characteristic of the power supply is dependent on the wire feed rate, but it is not dependent on travel speed. As example the characteristic of the power supply for a wire feed rate of 2 m/min is shown in figure 5.1. The characteristic of the power supply for each of the wire feed rates used is given in Appendix C.

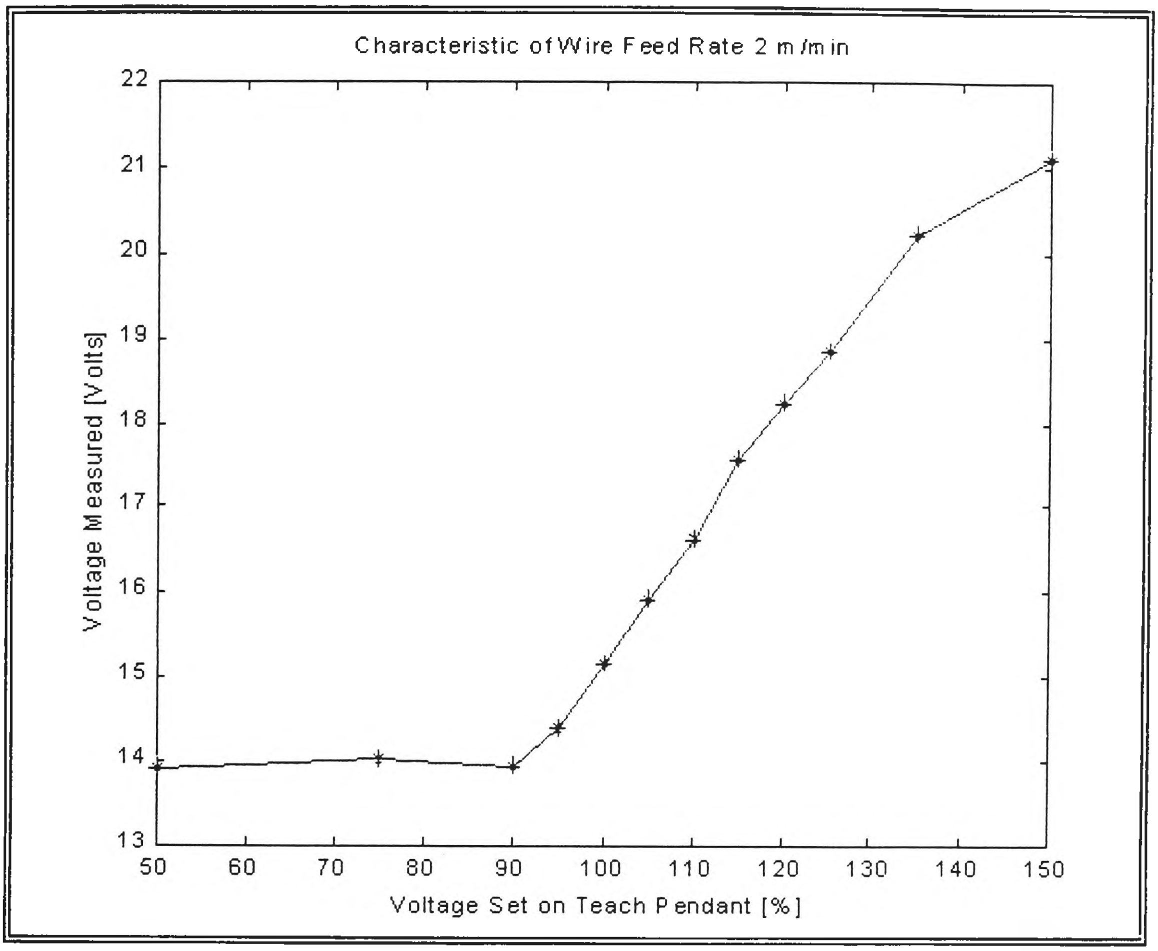

Figure 5.1

Characteristic of the power supply for wire feed rate of 2 m/min

The test object geometry used in the experiment has the same length and shape as the preliminary experiment described in chapter 3, but the programming is done much more accurately by using the IRB 1400 robot where the locations of points are calculated in the program.

As determined in the preliminary experiments, the short-circuit transfer mode is the most suitable for rapid prototyping applications as it has the characteristics of having a low heat input, stability and good control of deposition rate during the process. The synergic power supply is also expected to improve the weld quality because it has a better control over the deposition in comparison with a conventional power supply.

The base plate used in the experiment is identical to the one used in the preliminary experiment described in chapter 3. The temperature measurement is done the same way like it is described in the preliminary experiment. The same temperature measurement probe as the one described in chapter 2 is also used for these experiments.

5.3 Programming a Thin Walled Object with the IRB 1400

The program named F_WALL.prg was made to create a thin walled object. The program creates a weld with length of 150 mm. The layers are created by welding from a start position to an end position, the robot Tool Centre Point then comes back to a start position increments the vertical z axis and creates another weld and so on until the number of layers specified by the user are completed. In terms of the number of points taught, the F_WALL program has several positions, these are:

- home position
- a position above the workpiece
- start position
- end position

After setting the seam data, weld data and weave data, the program is ready to run. When the user runs the program the program will prompt the following:

- Increment [mm]: When the user sees this prompt, he or she is required to enter the increment of the vertical axis. This value determines how many millimetres the robot will move up in z direction after each layer of weld.
- No of layers: When the user sees this prompt, he or she is required to enter the number of layers that he or she would like to have. In the case of the experiment, ten layers of welds were made for each setting as discussed in chapter 3.

The F_WALL.prg is given in Appendix D.

5.4 Angle Compensation

When the F_WALL program was created, the robot coordinate system and tool centre point were still in default as set by the manufacturer. Thus the world coordinate system is located on the robot base and the tool centre point is located on the robot wrist, see chapter 4 for their locations. However, it was not realised that there is a slight elevation difference (about 5°) between the floor where the robot base is mounted and where the workbench is mounted.

As a result, the x,y,z coordinates of the robot base and the workbench are about 5° different. Therefore when the specimens were analysed under the profile projector, it can be seen that the specimen is tilted by about 5°, see figure 5.2. It can be noted that the specimen is not actually 90° in the vertical axis the weld build-up.

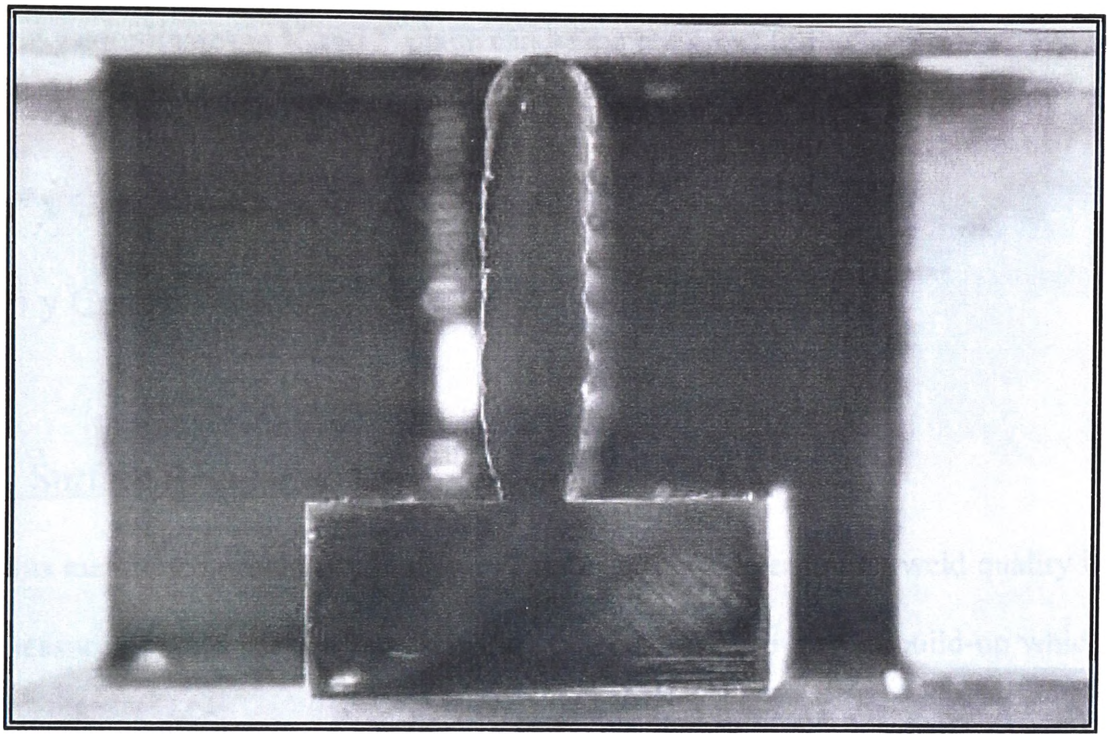

Figure 5.2

Cross-sectional view of sample f2-75-05

To compensate for this error caused by the angle between the two planes, a mathematical formula has been derived. This angle compensation is useful to minimise errors for the surface regularity calculations. The method of approximating the surface regularity will be described further in the next section.

Consider this situation, suppose the plane of the base plate lies on x and y, the plane of the weld lies on X and Y and there is an average angle theta (θ) between the two planes.

The specimen was measured in the x and y plane and it is required to determine what are the corresponding values to the X and Y. Therefore the new values of the x and y coordinates in X and Y plane can be expressed as follow:

$$X = x\,\text{Cos}(\theta) + y\,\text{Sin}(\theta) \qquad (5.1)$$

$$Y = y\,\text{Cos}(\theta) - x\,\text{Sin}(\theta) \qquad (5.2)$$

5.5 Surface Regularity Approximation

It was mentioned previously that one of the criteria of determining weld quality is a measure of weld surface regularity. It is desired to have a weld build-up which has a smooth surface as well as having good mechanical properties.

It was also mentioned in chapter 2 that the surface texture measuring machine could not be used to measure surface regularity of the weld specimens because the surface of the weld specimens is too rough to be measured with this machine. Therefore a profile projector is used in the experiments as an alternative way to give an indication of the surface regularity.

A section of the weld specimen is cut cross-sectionally. By doing this, the cross-sectional view of the weld specimen can be seen. However, just by rough cutting, the surface profile could not be seen clearly. Therefore the cross-section of the specimen had to be smoothen by further grinding so that the surface profile is revealed clearly. This is also needed for the Vickers hardness test so that the indentation can be seen clearly.

Due to the way the specimen is analysed, spatter which sticks on the weld wall could not be detected because the surface regularity measurement is done by taking x and y coordinates points along both sides of the cross-section of the weld specimen. The spatters would fall off during the specimen preparation (grinding). To indicate the trends of surface regularity, for each wire feed rate, several samples were examined. It was not possible to examine all of the samples because the laborious time required for preparing the specimens. The same holds also for the hardness measurements.

Therefore for each wire feed rate setting, one sample from a higher voltage setting and one sample from a lower voltage setting were examined to indicate trends. However for settings with wire feed rate of 2 /m/min with travel speed of 5 mm/s, all of the samples were examined because from the visual inspections, it was suspected that the optimal settings for rapid prototyping and wear replacement applications lie within this region. Also three samples from wire feed rate of 1 m/min and 3 m/min with travel speed of 5 mm/sec were examined to indicate the transition trends. The plot of voltage versus wire feed rate for the various settings which were examined for the hardness and surface regularity are shown in figure 5.3.

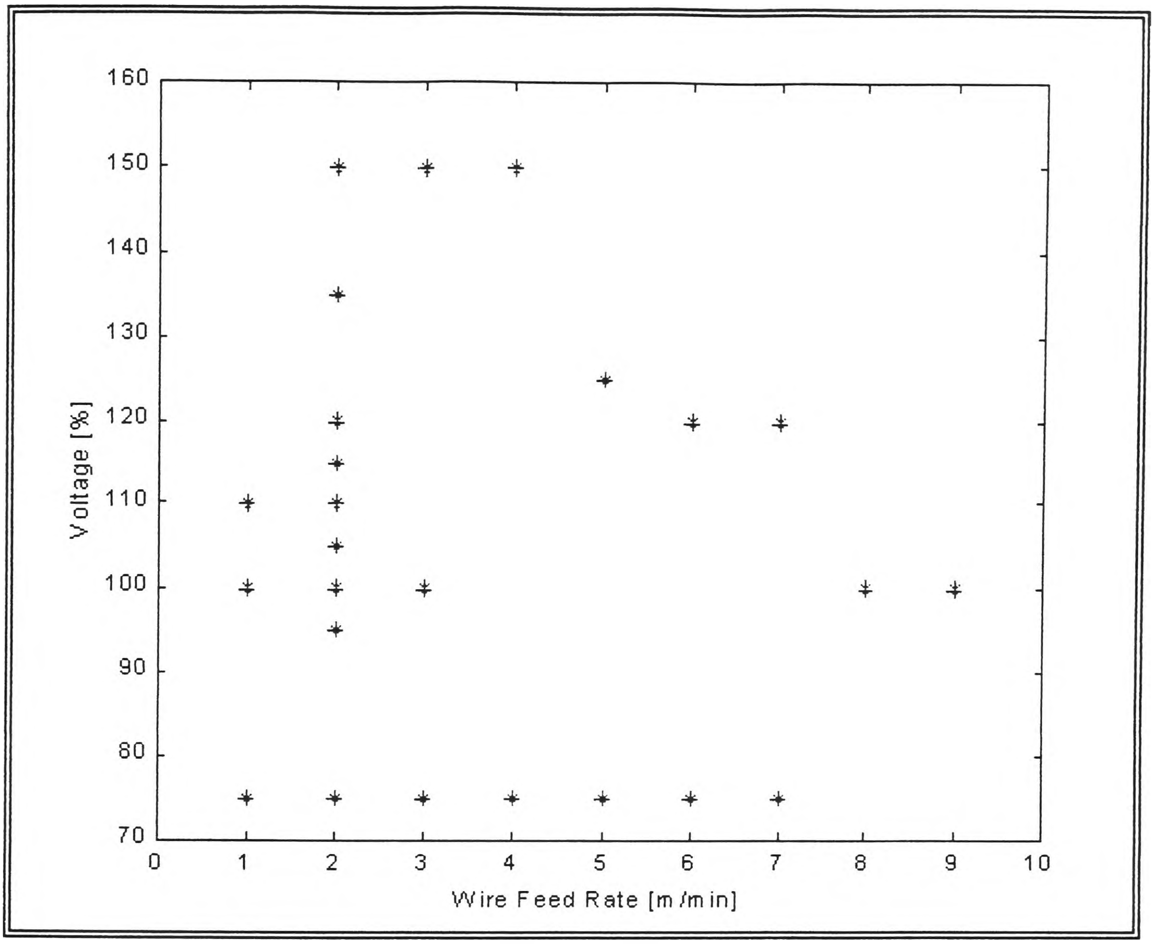

Figure 5.3

The plot of wire feed rate versus voltage for the examined settings

To get an approximation of surface regularity, a number of points along x and y coordinates were taken. By using the same sample of figure 5.2 (f2-75-05), consider figure 5.4.

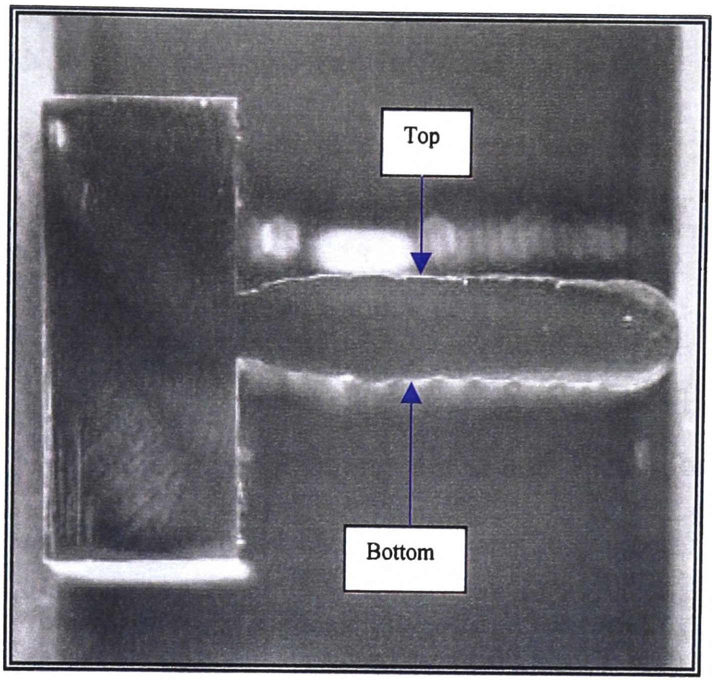

Figure 5.4

Cross-sectional view of sample f2-75-05

Several numbers of x and y coordinates were taken from the top and bottom part of the sample. The surface depicted in figure 5.3 was ground to about 10 microns so that a reasonable profile in the two surfaces can be identified clearly. Also by grinding the surface to about 10 microns, defects such as porosity, inclusions and lack of penetrations can be identified. An approximation of the surface regularity and mathematical calculations were analysed using Matlab Version. 5.2.

The plots of the x and y points obtained from the profile projector are depicted in figure 5.5. The figure 5.5 shows how the original profile looks like in x and y coordinate plane (base plate coordinate), note the slight angle variations. In addition the new profile after being compensated is shown in figure 5.6.

By using a first order polynomial fit, the angle (θ) can be found for the top and bottom surfaces. Note that the angle can be found by inverting tangent of the gradient, ie. θ = atan (gradient), where the gradient can be obtained from the equation of the first order polynomial fit. Then by using the mathematical formula described in previous section, the new X and Y coordinates can be determined.

As it was mentioned previously, obtaining the x and y coordinates using the profile projector was done manually because the profile projector does not have any facility to be interfaced with a PC or any other electronic device. Therefore there was a limitation regarding how many number of points could be recorded within a reasonable time.

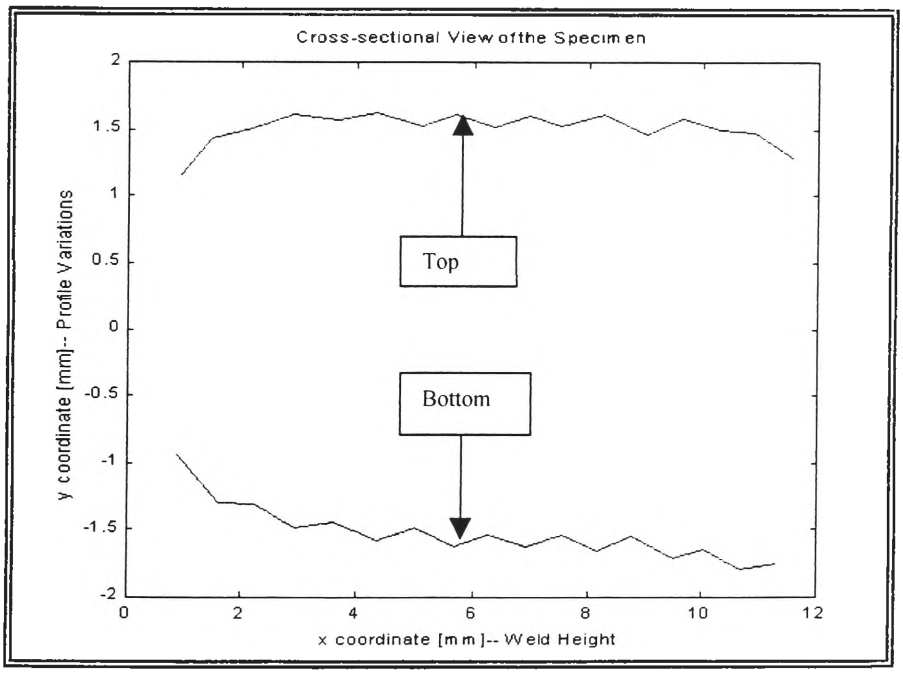

Figure 5.5

Surface regularity of the top and bottom profiles of sample f2-75-05 in x and y coordinates

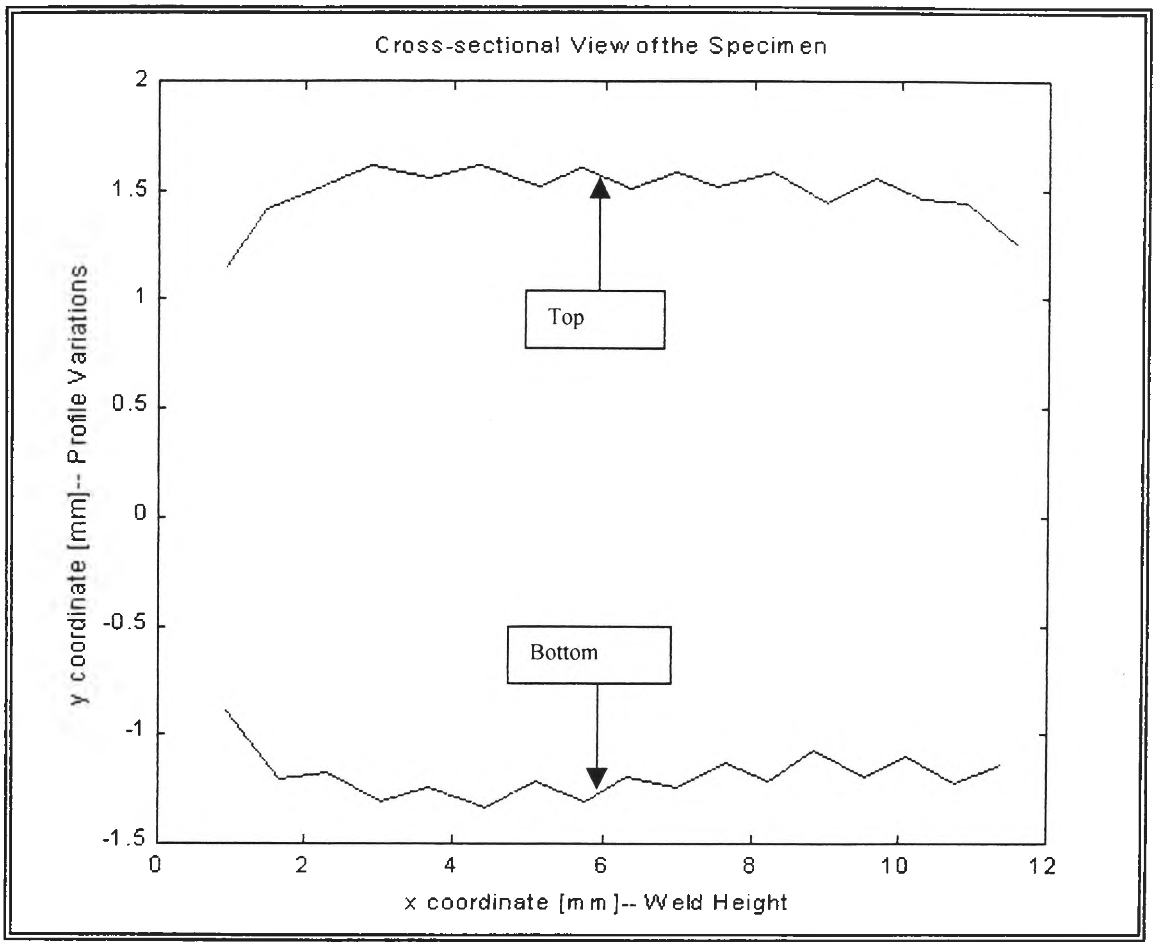

Figure 5.6

Surface regularity of the top and bottom profiles of sample f2-75-05 in X and Y coordinates

The calculation of approximating the surface regularity has been established by assuming that the surface looks like a saw tooth for each layer (See figure 5.7). Three points were taken for each layer, the start, peak and end of the layer. Thus in the case of the experiments, there would be ten layers adjacent to one another. A Matlab program was written to calculate the average of the deviation from the centre line describing the weld surface. The formula used in the calculation in shown in equation 5.3.

Equation 5.3:

$$Surface\ \text{regularity} = \frac{\sum_{i=1}^{N} | di |}{N}$$

Where

di = Distance from centre line to peak (See figure 5.7)

N = Number of measured points. In the case of ten layers, N = 21

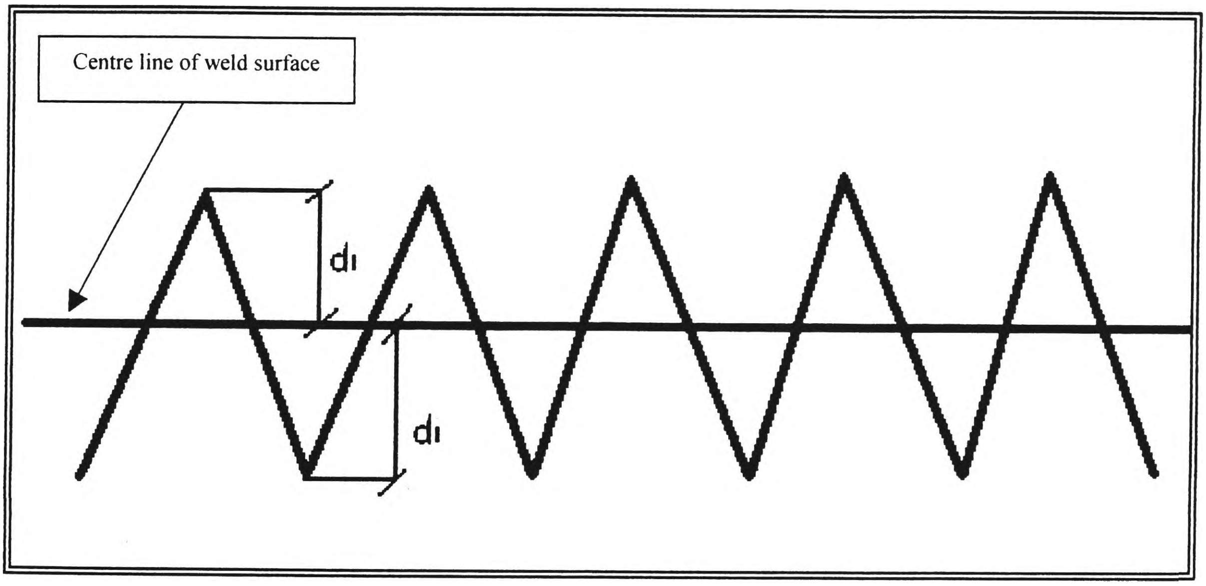

Figure 5.7

Surface regularity approximation

5.6 The Hardness Testing

The hardness testing was done with the 6030LKV Vickers Hardness Testing Machine made by Indentec Hardness Testing Machine Limited. There are four locations where the hardness measurements were taken for the samples. These locations are top section of the weld, middle section of the weld, bottom section of the weld and the base plate.

The top section of the weld reveals the material properties at layer ten. The middle section of the weld represents the material properties from layer two to layer nine. The bottom section of the weld represents the material properties at the start of the process at layer one. Hardness of the base plate was also taken so that the values obtained in the experiments can be compared with the given values from the manufacturer (See table 3.2). Note that the Vickers hardness number can be converted to an equivalent tensile strength by using a specified standard table [30]. The locations where the hardness was taken are described with blue dots in figure 5.8.

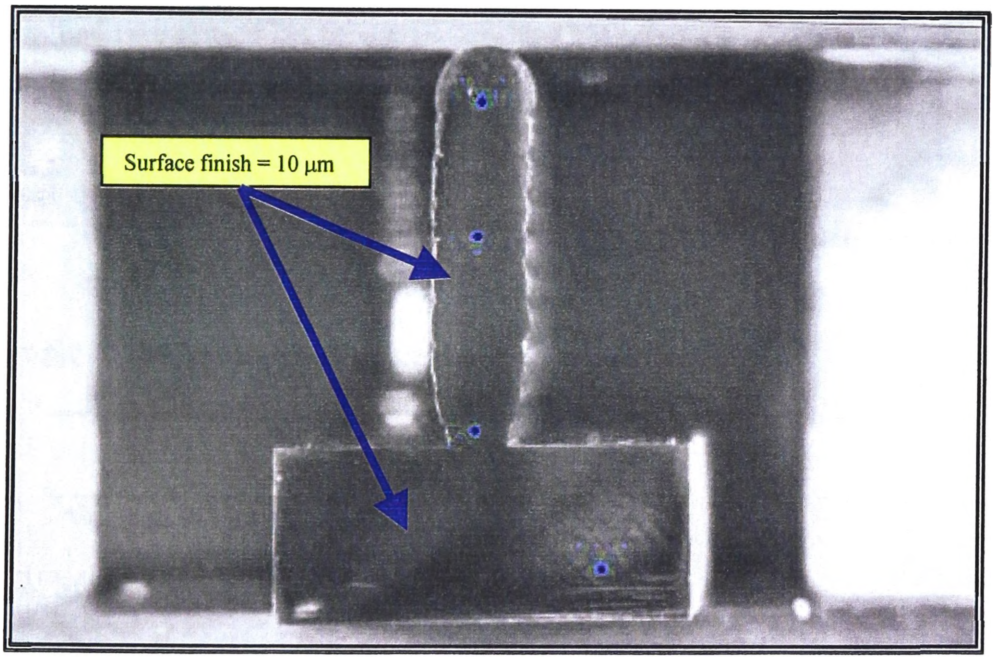

Figure 5.8

The hardness testing locations

5.7 Experimental Results

There were seventy-six samples made in the experiments. Therefore a coding system was established to identify the samples and data plots. The coding format chosen is described below:

fw-vv-zz, where

f	=	Identification of the thin walled objects
w	=	wire feed rate setting on the teach pendant [m/min]
vv	=	voltage setting on the teach pendant [%]
zz	=	travel speed [mm/sec]

The example of the above format is described below:

Consider the case where the coding is f2-75-05. Thus, it means this is a final experiment with the following parameters as described below:

- Wire feed rate setting on the teach pendant = 2 m/min
- Voltage setting on the teach pendant = 75 %
- Travel speed = 5 mm/sec

An example of the layout for the particular setting above is illustrated below.

Set Values	
Voltage [%]	75
Wire feed rate [m/min]	2
Travel speed [mm/sec]	5
Gas flow [l/min]	15

Weld Geometry		Visual Defects and Weld Property	
Weld height [mm]	13.6	Spatters	No
Weld width [mm]	3.6	Porosity	No
Stand-off at layer 1 [mm]	15	Excess material	No
Stand-off at layer 10 [mm]	16	Surface regularity [μm]	40.85
Temperature at layer 10 [deg.C]	177	Average hardness [HV]	166
Number of layers	10		

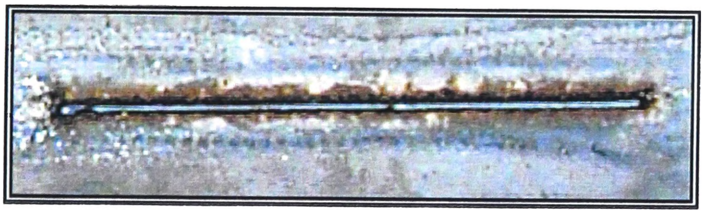

Figure 5.9

Sample f2-75-05 (Top view)

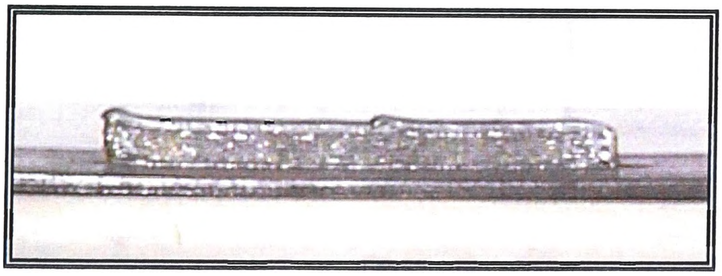

Figure 5.10

Sample f2-75-05 (Front view)

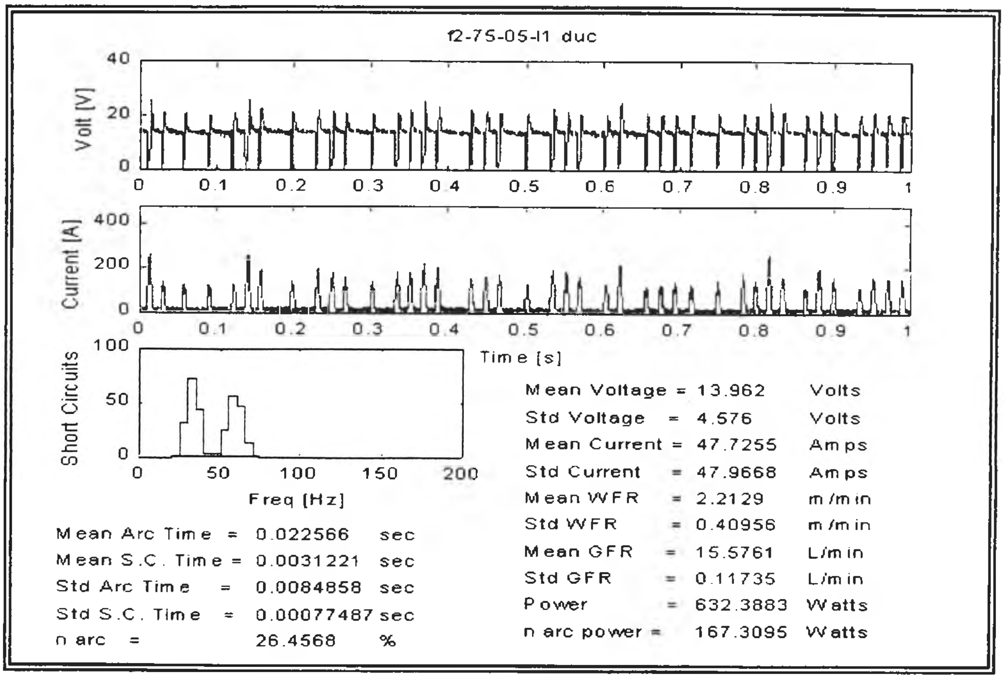

Figure 5.11

Electrical data plot of sample f2-75-05 at layer 1

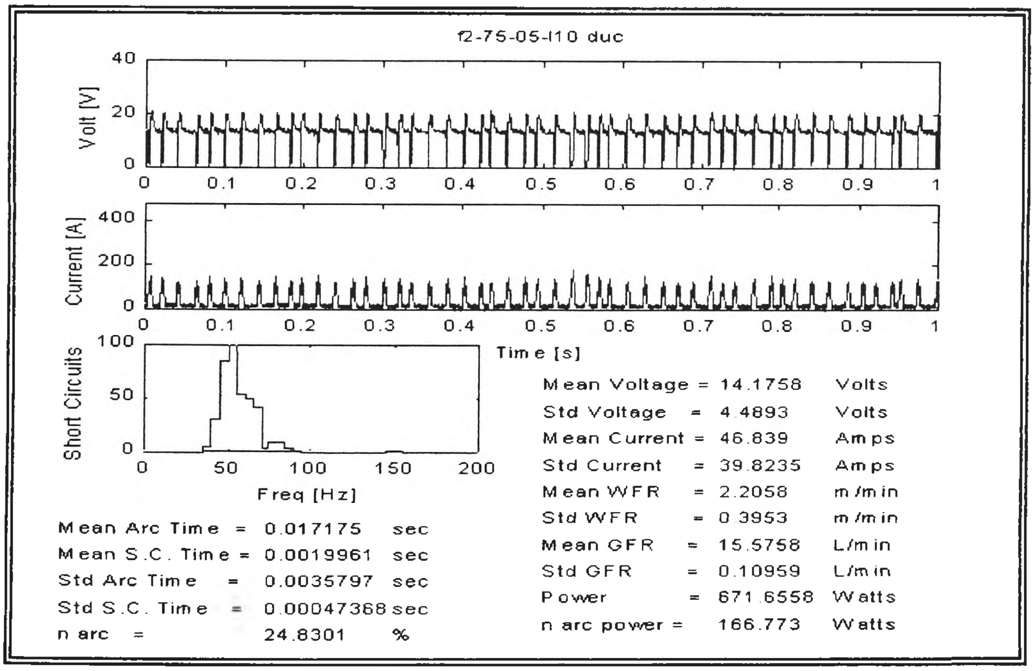

Figure 5.12

Electrical data plot of sample f2-75-05 at layer 10

The pictures of all the weld samples, welding parameters and plots of the electrical data measured during the experiments are given in Appendix F.

In the experiments, the weld quality of the samples was analysed in detail. There are several properties observed during the experiment, these are:

- Physical defects such as spatter, porosity and excess material
- Material properties such as tensile strength, hardness and the surface regularity
- Stability of the process. This can be analysed from electrical signals measured by the sensors during the process such as voltage, current, wire feed rate, short circuit frequency and gas flow rate.
- Temperature reached at the last layer
- Weld geometry such as the weld width and weld height
- Stand-off distance variances

From the experiments, it was found that the heat input is one of the most important parameters in determining the weld quality. Several properties were found to have direct relationship with heat input eg. Surface temperature, weld width, and hardness. Others such as weld height was found to have a link to wire feed rate as well as to heat input.

The surface temperature is directly influenced by heat input. From the results, it was determined that these two parameters seem to have a kind of a linear relationship. It can be said that the higher the heat input will result in the higher surface temperature. The plot of surface temperature versus heat input with travel speed of 5 mm/sec and 10 mm./sec are depicted in figure 5.13 and 5.14 respectively.

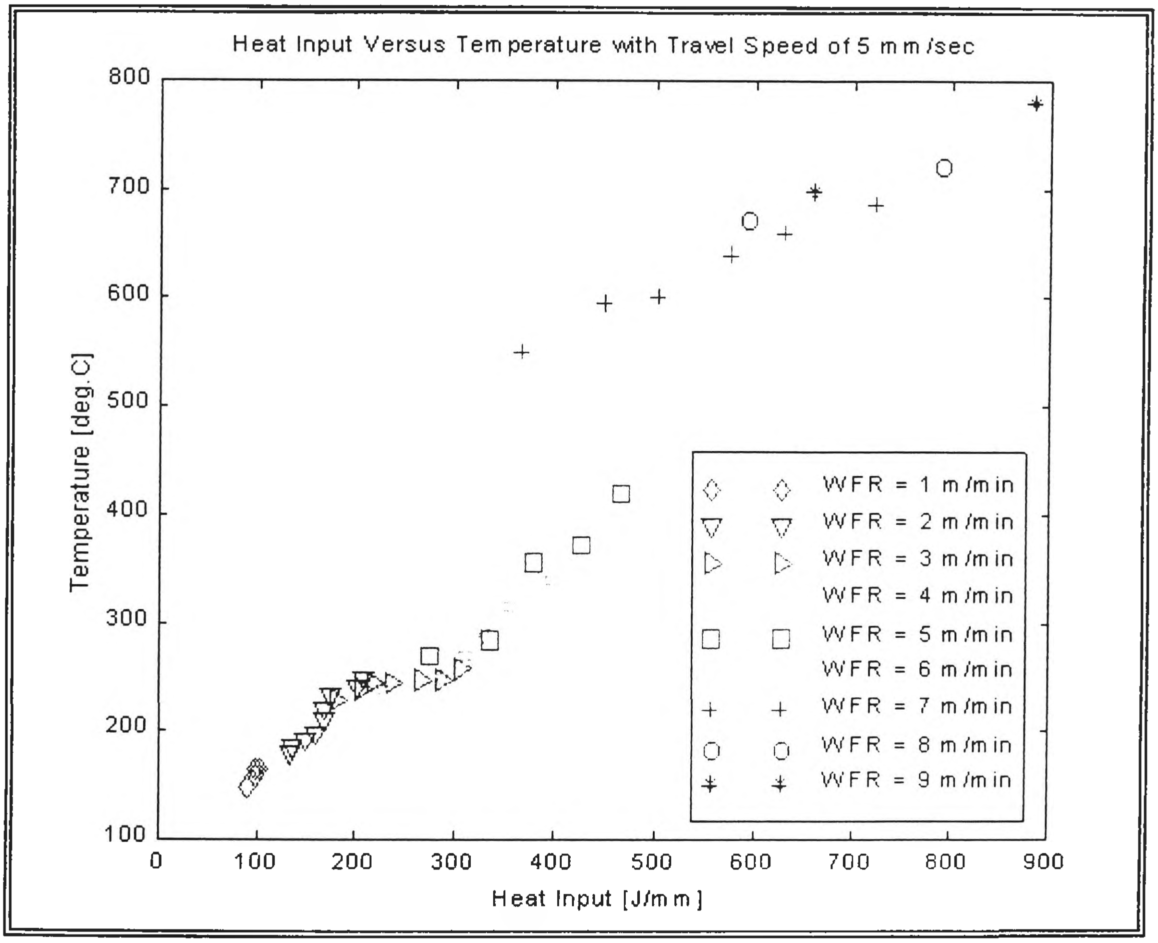

Figure 5.13

Heat input versus surface temperature with travel speed 5 mm/sec

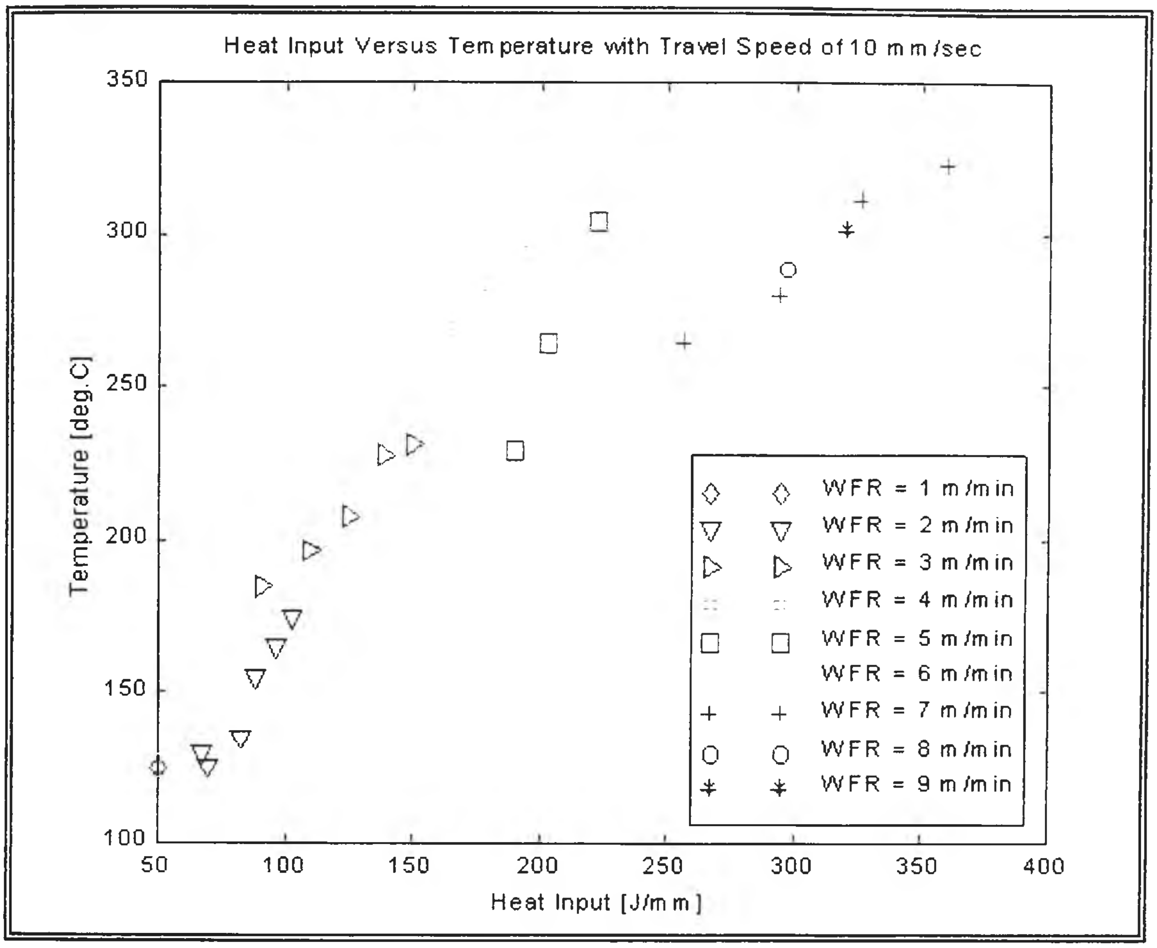

Figure 5.14

Heat input versus surface temperature with travel speed 10 mm/sec

The weld width was also directly influenced by heat input. From the results, it can also be determined that these two parameters seem to have a kind of a linear relationship. It can be said that a higher heat input will result in a larger width of the weld. Another phenomena is also revealed from this result, that is heat input has a direct influence in determining weld pool size, where the physical effect of this can be seen clearly with the change of the weld geometry, ie. change in weld width. The plot of weld width versus heat input with travel speed of 5 mm/sec and 10 mm/sec are depicted in figure 5.15 and 5.16 respectively.

The heat input was also found to have a direct influence to hardness. This can be determined from the results obtained in the experiments. It can be seen that the hardness seems to be higher in the lower heat input region. However these values seem to be lower and have less deviation in the higher heat input region. It should be mentioned that from the hardness value, the tensile strength could also be determined by using conversion table provided in the steel handbook [30]. Thus it can also be said from this phenomena that the heat input has an influence in determining tensile strength of a material in welding process. The results obtained from the experiments using travel speed of 5 mm/sec and 10 mm/sec are depicted in figures 5.17 and 5.18.

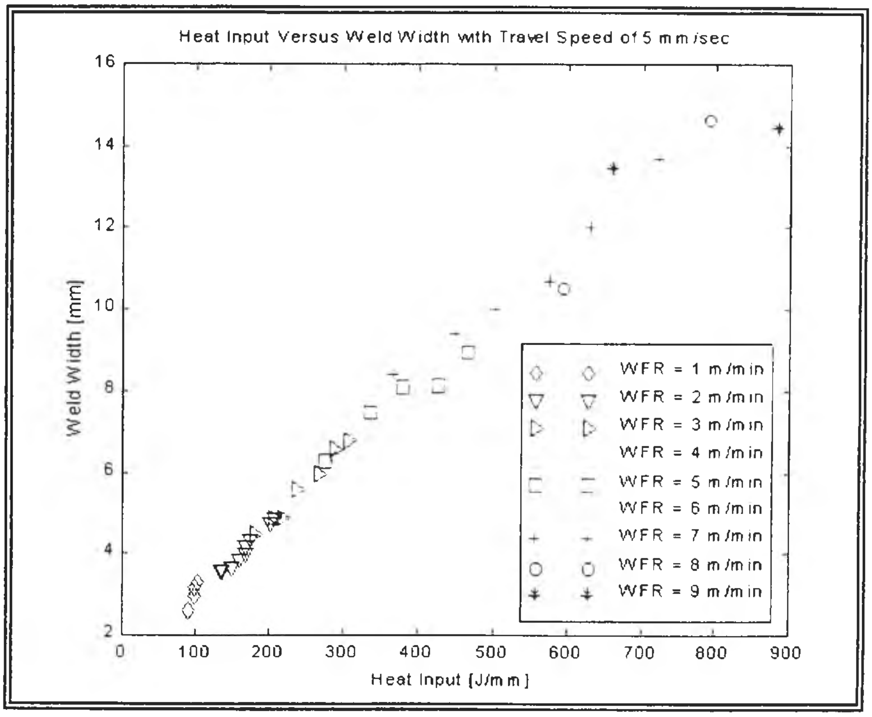

Figure 5.15

Heat input versus weld width with travel speed 5 mm/sec

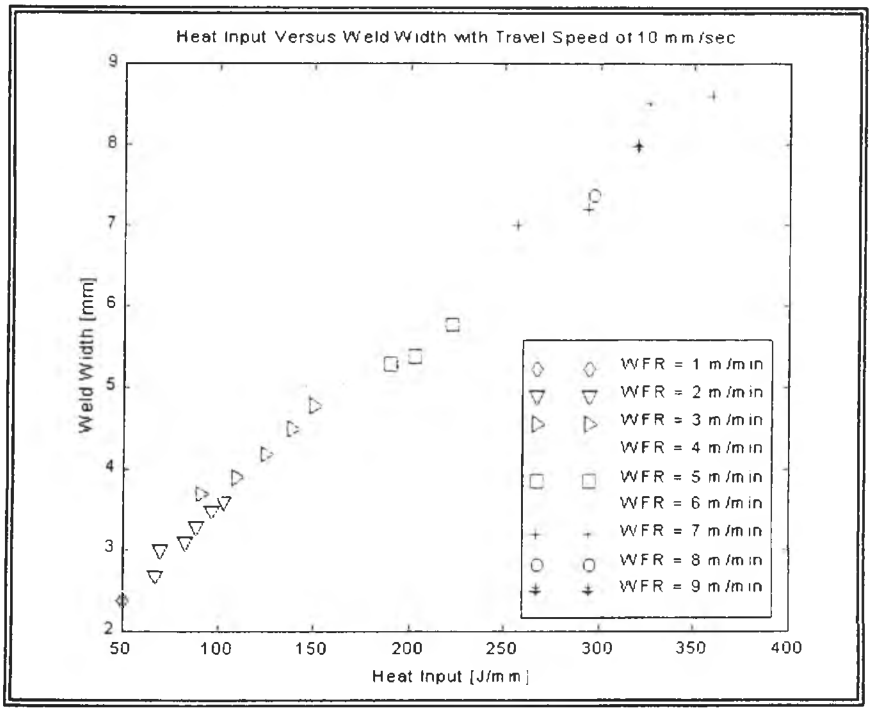

Figure 5.16

Heat input versus weld width with travel speed 10 mm/sec

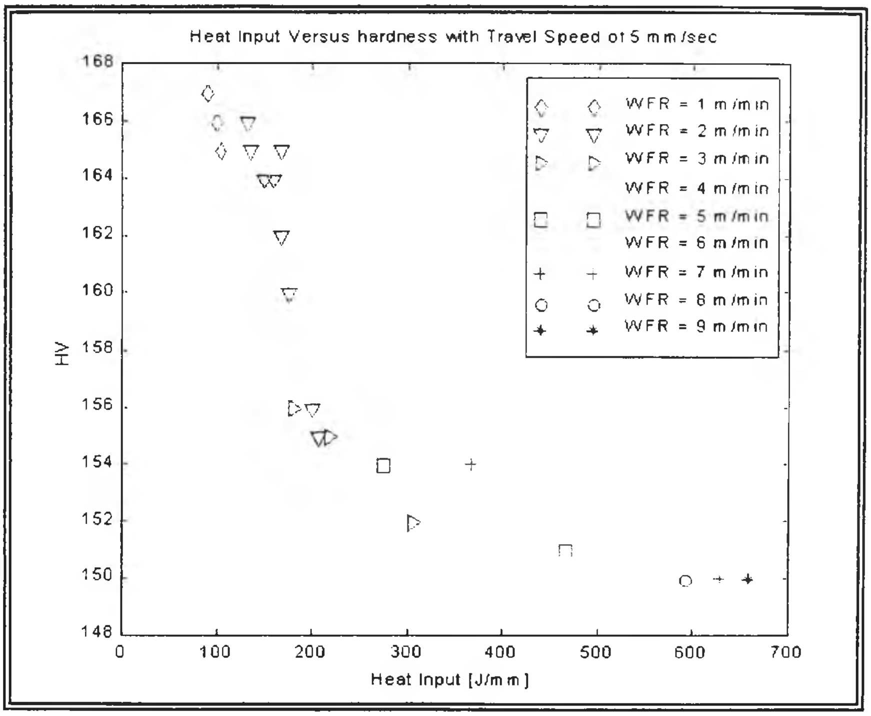

Figure 5.17

Heat input versus hardness with travel speed 5 mm/sec

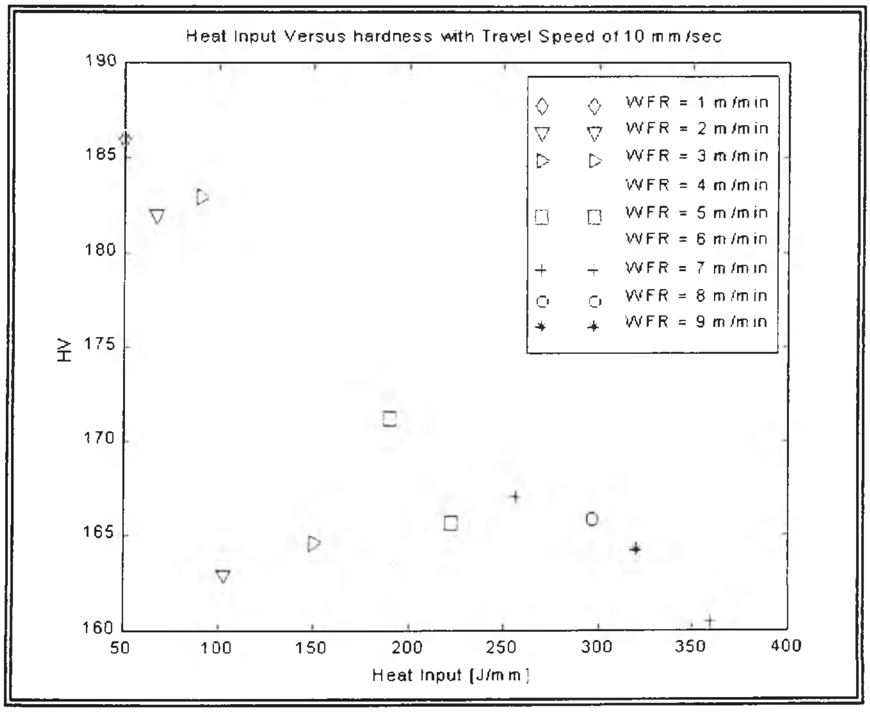

Figure 5.18

Heat input versus hardness with travel speed 10 mm/sec

However in other property such as weld height, it can be seen that apart from heat input, the wire feed rate also has an influence in determining this property.

It can be seen fairly clearly that for a particular wire feed rate, the weld height is getting lesser with an increase of heat input. It seems that the reduction has a linear relationship. The results obtained in the experiments using travel speed of 5 mm/sec and 10 mm/sec are shown in figure 5.19 and 5.20 respectively.

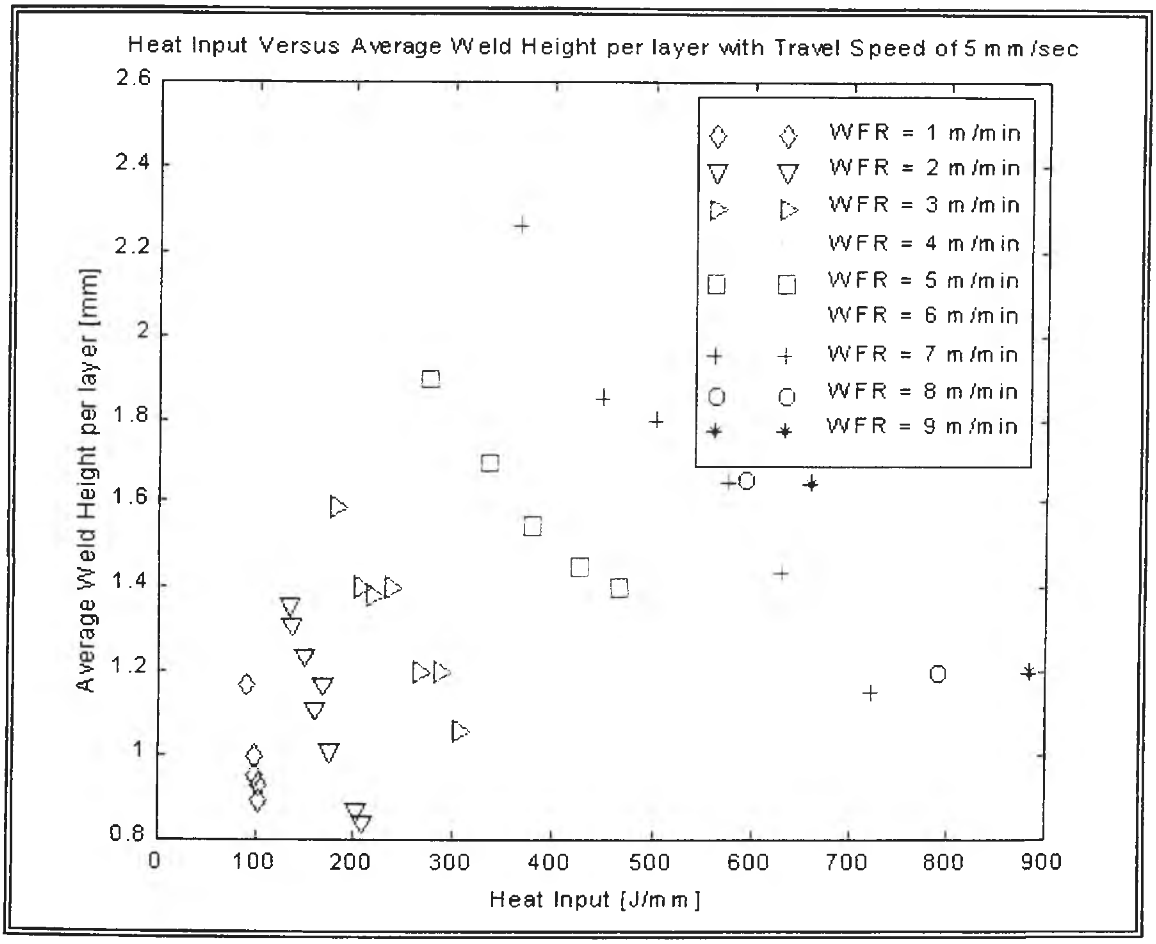

Figure 5.19

Heat input versus weld height with travel speed 5 mm/sec

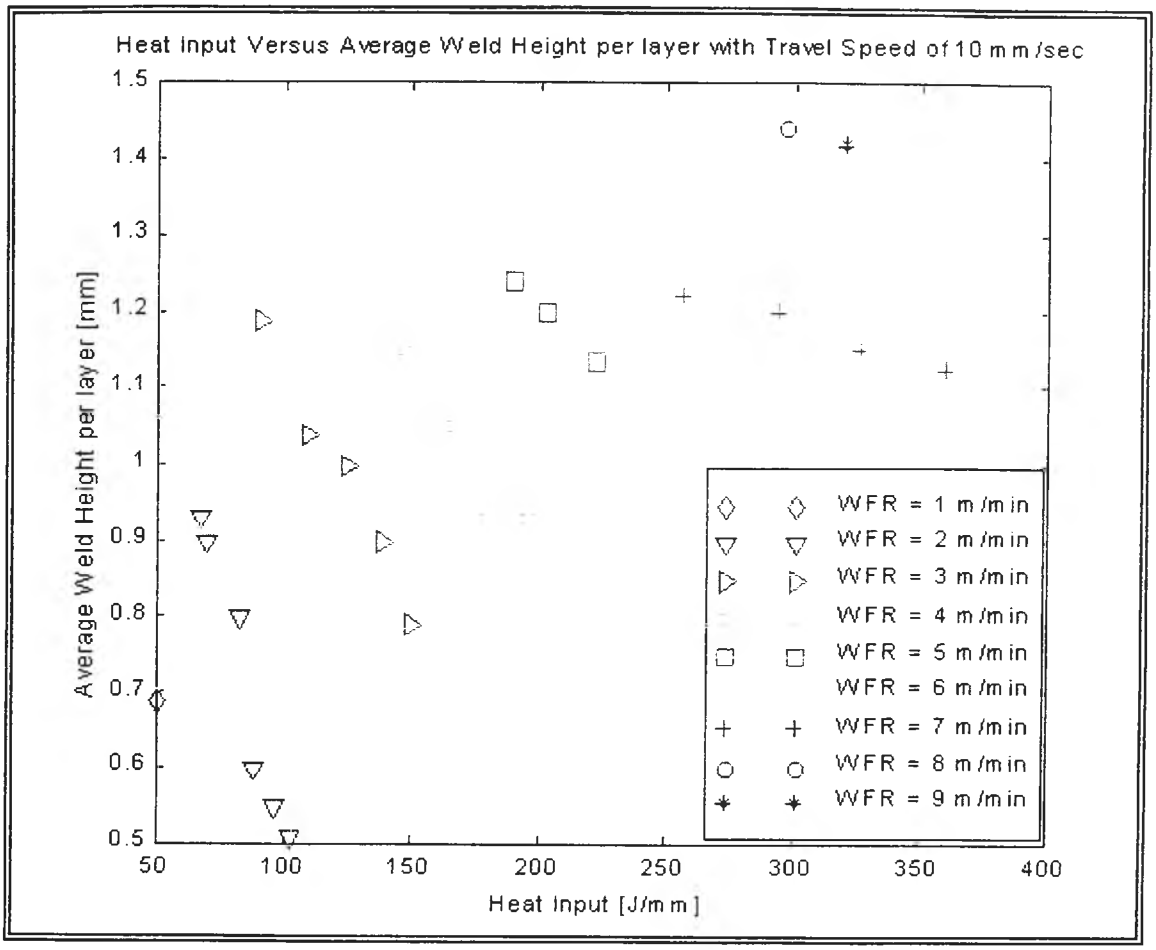

Figure 5.20

Heat input versus weld height with travel speed 10 mm/sec

Furthermore, surface regularity was also investigated in the experiments. The results show the region where the weld surface is reasonably smooth and the region where the weld surface becomes fairly rough. The results obtained in the experiments using travel speed of 5 mm/sec and 10 mm/sec are shown in figure 5.21 and 5.22 respectively. However note that for samples with spatters the number representing the surface regularity is no longer accurate due to the way the surface regularity is approximated as described in section 5.4 and 5.5.

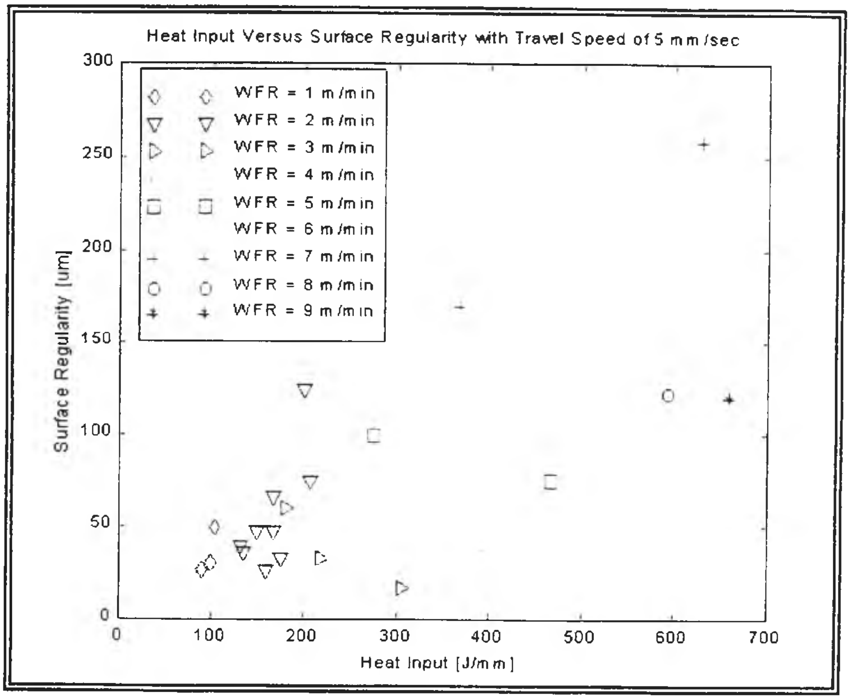

Figure 5.21

Heat input versus surface regularity with travel speed 5 mm/sec

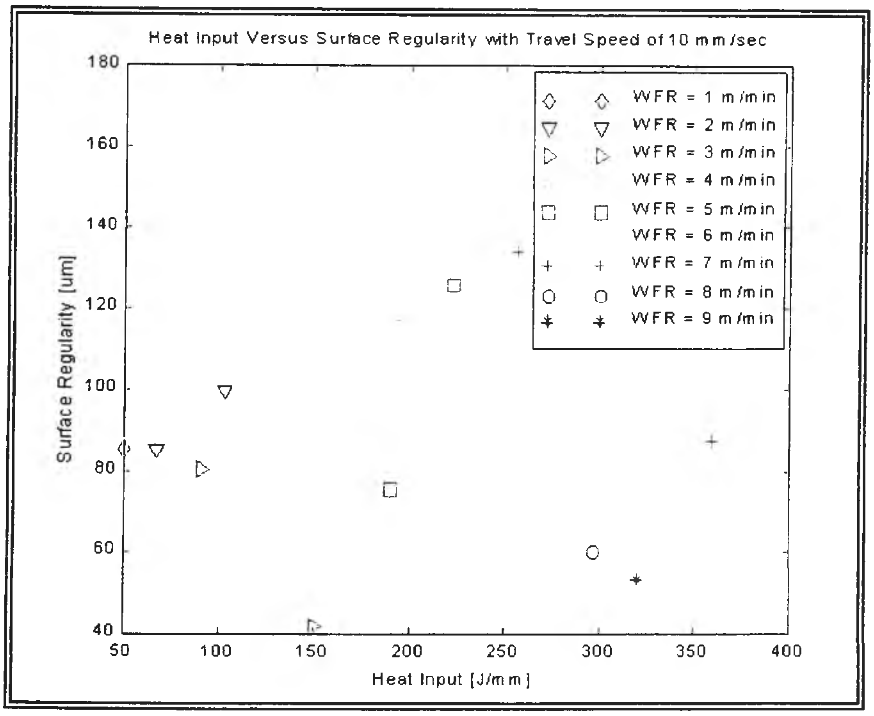

Figure 5.22

Heat input versus surface regularity with travel speed 10 mm/sec

It was also determined in the experiments that a globular transfer was unsuitable for this application because the instability of the process, which created spatters, rough surface and arc failures during welding. Consider a sample f2-150-10 where globular transfer has occurred. From the electrical data plot, it can be seen that the setting has a fairly long arc time and the voltage approximately 21 volts. The sample obtained from the experiment is depicted in figure 5.23 and 5.24. The electrical data plots obtained are shown in figure 5.25 and 5.26.

Figure 5.23

Sample f2-150-10 (Top view)

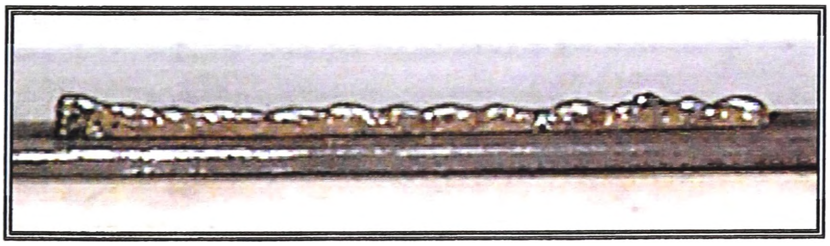

Figure 5.24

Sample f2-150-10 (Front view)

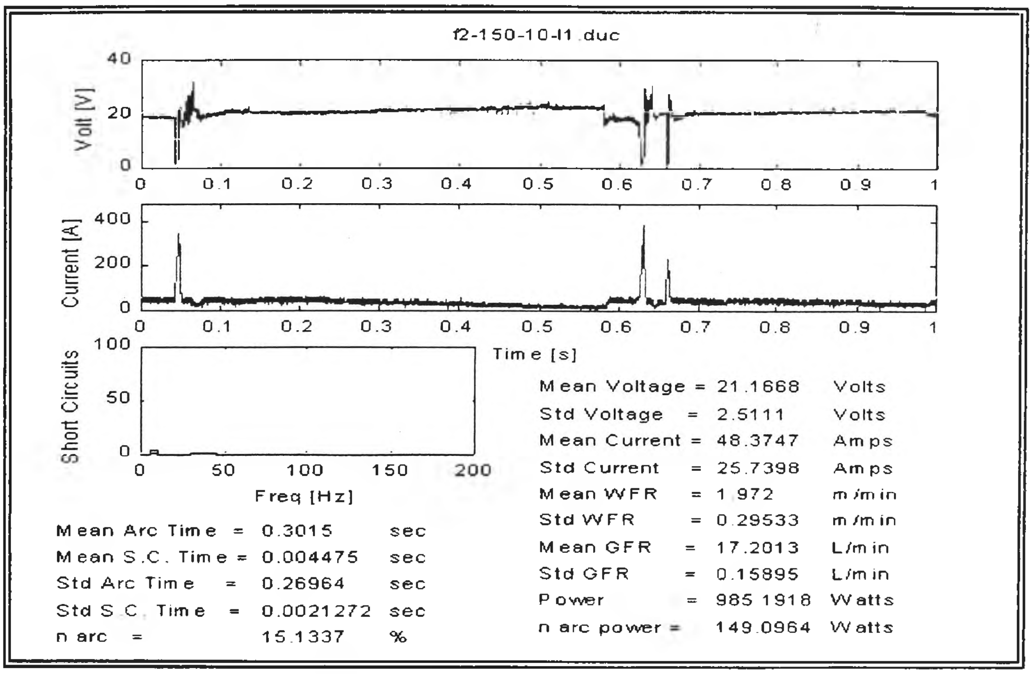

Figure 5.25

Electrical data plot of sample f2-150-10 at layer 1

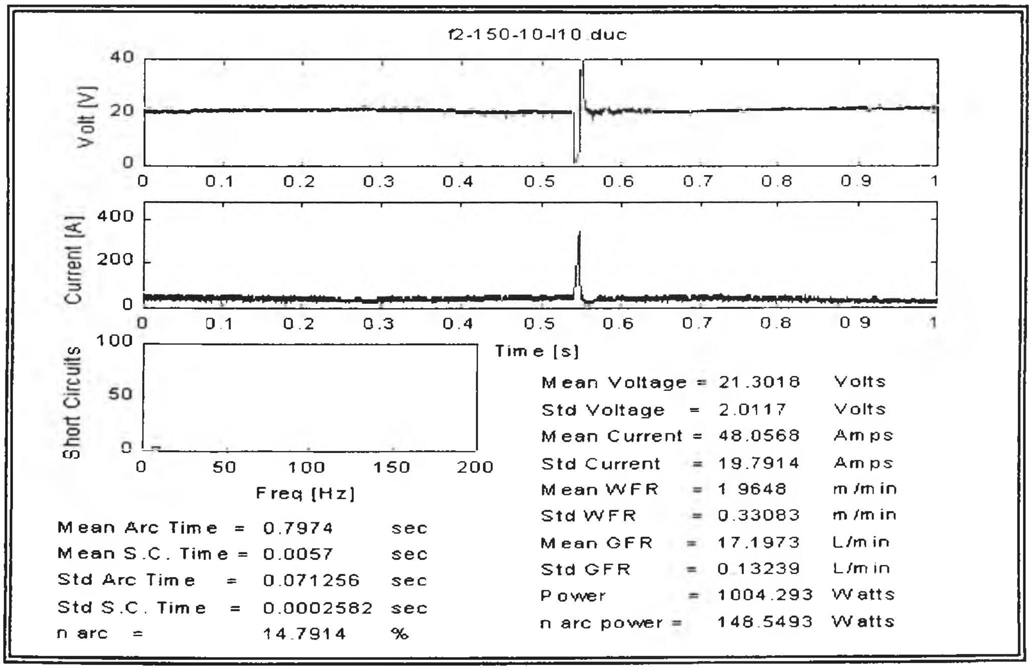

Figure 5.26

Electrical data plot of sample f2-150-10 at layer 10

It was mentioned that there are two travel speeds used in the experiments ie. 5 mm/sec and 10 mm/sec. Many aspects were investigated such as comparing two samples from the two travel speeds which have similar heat input. Consider sample f2-95-05 which has heat input of 135.9 J/mm and sample f3-120-10 which has a heat input of 139.2 J/mm. Although these two samples have similar heat input, qualities obtained from these two samples were fairly different. Sample f2-95-05 is much better in comparison to the sample f3-120-10 in many ways. For sample f2-95-05, spatter was not identified, the surface is much smoother, see figure 5.27 and 5.28. Also the process is much more stable as it can be seen from the electrical data plot shown in figure 5.29 and 5.30.

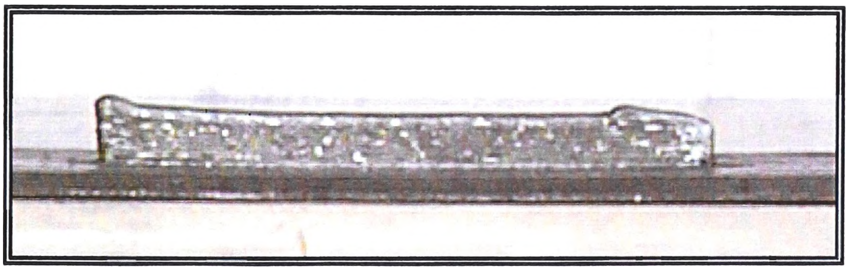

Figure 5.27

Sample f2-95-05 (Front view)

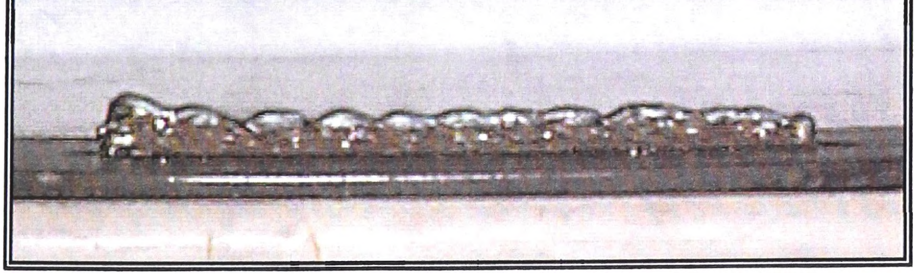

Figure 5.28

Sample f3-120-10 (Front view)

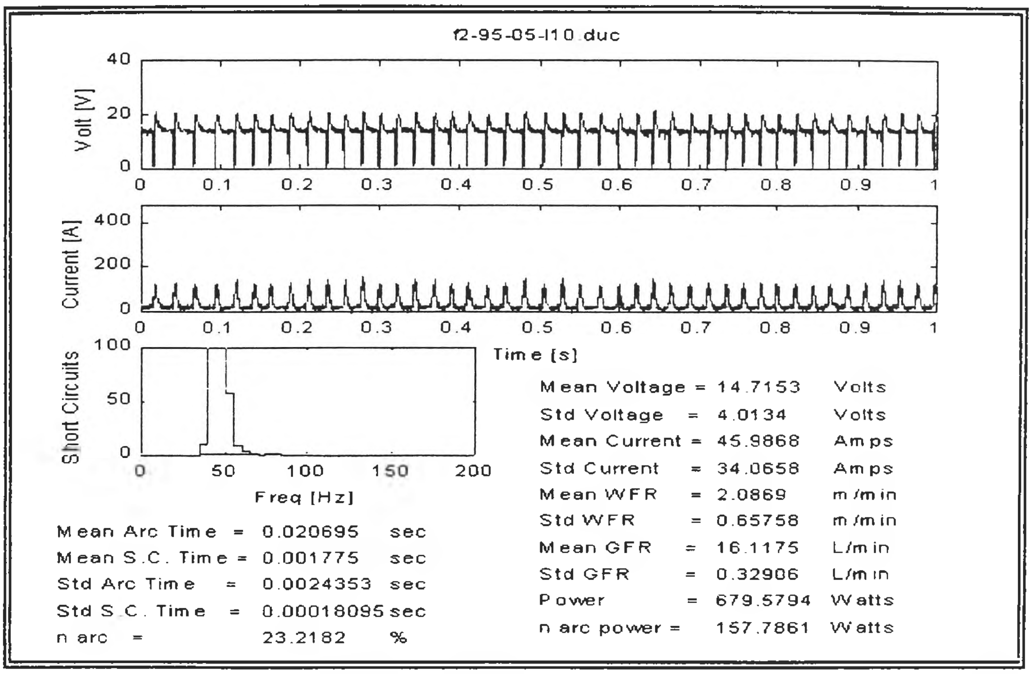

Figure 5.29

Electrical data plot of sample f2-95-05 layer at 10

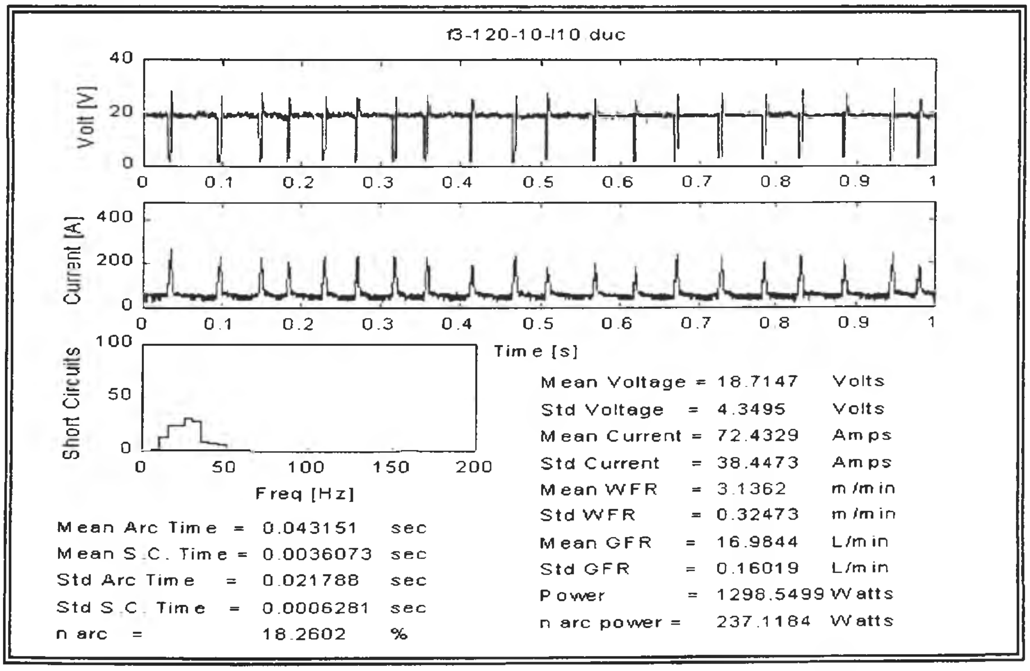

Figure 5.30

Electrical data plot of sample f3-120-10 at layer 10

From the results obtained, it was determined that travel speed has a great influence in determining process stability. This can be seen fairly clearly that the sample and electrical data obtained by using travel speed 10 mm/sec such as the one shown in figure 5.28 and figure 5.30 were not good at all.

During the experiments, it was also found that there are more parameter limitations using travel speed of 10 mm/sec. For example, there is only one voltage setting in wire feed rate 1 m/min can be performed because when other voltage settings were tried, an arc failure was identified. This is suspected because the process is far too unstable so it does not permit the arc to ignite properly. This also happened in other wire feed rate settings where not all of the voltage settings can be performed like the one in travel speed of 5 mm/sec. Thus there are less samples made using travel speed of 10 mm/sec because of this limitation. Furthermore, it was found that there is not one single sample which was found satisfactory with this travel speed. Dominant defects which are determined in conjunction with this travel speed are spatter and surface irregularity. The discussions of the results obtained in the experiments will be discussed further in the next section.

5.8 Discussion of the Results

In the experiments, the relationships of several properties were determined. These are:

- The relationships between heat input and surface temperature
- The relationships between heat input and weld width
- The relationships between heat input and hardness
- The relationships between heat input, wire feed rate and weld height
- The relationships between heat input and surface regularity

From the experimental results, the dominant physical defects were identified. These are defects such as spatter, porosity, excess materials and surface regularity. Generally rapid prototyping requires settings which enables it to create layers of a thin wall to form the desired shape. Hence, the settings would be able to produce a thin wall object without any defect.

Surface Temperature Analysis

From the experiments, it was determined that heat input has a direct influence towards the surface temperature. The correlations show that these two properties have a linear relationship. Another important result that comes out in relations with these two properties is excess materials.

Excess material occurs where the surface temperature reaches about 550 °C. The first evidence of excess material however was found on sample f5-125-05 where the surface temperature on the tenth layer was approximately 420°C. The excess material found was still fairly small (See figure 5.31) compared to what appears on the other samples at higher temperature, see figure 5.32.

In the example shown in figure 5.32, it can be seen that the sample f9-125-05 has a lot of excess materials along the weld wall. It can be said that the weld pool seemed to collapse as the temperature gets too high. For this particular example the weld surface temperature was approximately 782°C. In addition for this particular sample other defects such as porosity and spatters were also identified.

It is predicted that porosity occurred because of the hot air from underneath influenced the gas flow as the weld build-up gets higher. Also the nozzle gets further away from the base plate as more build-up is created which gradually changes the gas flow pattern as the angle of the flow changes.

Furthermore, as the hot air disturbed the gas flow and caused porosity, at the same time it is also causing the process to become unstable. The physical evidence of this can be seen in the form of spatter. Also it should be mentioned that in the case where excess materials were identified, the surface regularity measure is no longer useful because the surface is fairly rough and can be identified with naked eyes and measure with a ruler.

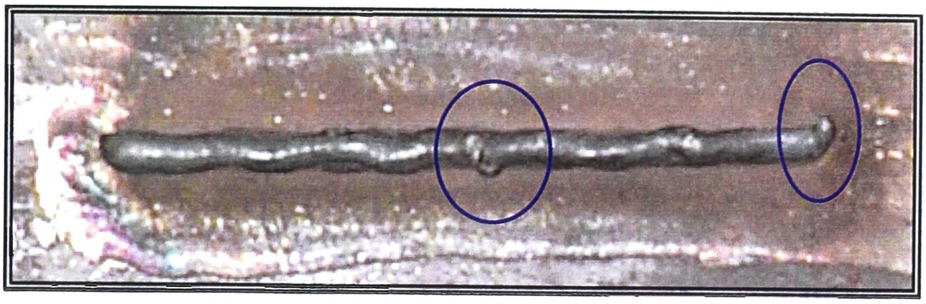

Figure 5.31

Excess materials on sample f5-125-05

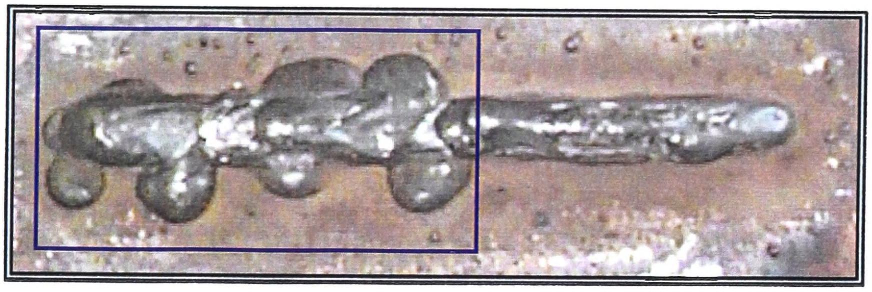

Figure 5.32

Excess materials on sample f9-125-05

Weld Width Analysis

The results also indicated that heat input has also a direct influence on the weld width. From the experiments it can be determined that the weld width becomes wider with an increase of heat input. The results from the two travel speeds used show that these two properties have a linear relationship. It should be mentioned that as heat input becomes higher the surface temperature also become higher as well as the weld width also becomes wider. Therefore there is a limitation how wide the weld width can be before excess materials start to become a problem like the one shown in figure 5.32.

Hardness Analysis

The hardness relationship to heat input was also determined for the experiments. The results show that the samples have higher hardness values in the lower heat input region. Hence at lower wire feed rate and voltage settings. It is also indicated that the hardness becomes lower and has less deviation in a higher heat input region. It is also determined from the results that the hardness stabilises when the heat input reaches around 300 J/mm.

It is also found from the hardness measurement that the average top part of the weld is relatively harder compared to the middle and lower part of the weld. It is because at the top layer the weld cooled much more rapidly compared to the rest of the layers. The more the detailed description regarding the multi-pass welding process and its effects on the mechanical properties will be discussed further in chapter 6.

The hardness value of the base plate was also determined in the experiments. The value found approximately 148 Vickers. As it was mentioned previously that by using conversion table [30] tensile strength could be determined, in this case 148 Vickers is approximately equal to tensile strength of 481 Mpa. Referring to the specification obtained from the steel manufacturer [28], the tensile strength of the base plate is equal to 440 Mpa. Thus it can be said that the measurements are within 90 % accuracy, hence 10 % error. It should be mentioned that it was not possible to obtain hardness values of all the samples due to laborious work of sample polishing preparations. However, the results obtained enable to give a fairly good indication of trends of the hardness. The detailed data of the hardness measurements are tabulated in Appendix G.

Weld Height Analysis

It was determined that the weld height is influence by heat input and wire feed rate. The results shown that for a particular wire feed rate the weld height is becoming lower with an increase of heat input. This is fairly logical because the filler weld seems to transform into width more as the heat input is increasing.

Surface Regularity Analysis

From the experiments, a region of a regular surface was identified. For every wire feed rate settings, the surface regularity was analysed at the lower voltage setting and at the higher voltage setting to indicate the trends, see appendix F for the detail descriptions. However for wire feed rate of 2 m/min with travel speed of 5 mm/sec, the surface regularity was obtained for all of the samples because from visual inspections it was suspected that the optimal settings for rapid prototyping lie in this region.

It should be mentioned that when spatters occur in a particular sample, usually a lot of these spatters stick on the weld surface as well as the base plate. Where there are spatters sticking to the surface of the weld the numbers indicating the surface regularity are no longer accurate measurement because it does not take the spatters into the considerations as the spatters would fall off during surface grinding process. The rough-cut surface then fined ground so that the surface profile can be revealed clearly under the profile projector. Thus this method does not permit to consider spatters sticking to the surface of the weld wall, see section 5.4 and section 5.5 for more detailed.

Note that in many settings which results in spatters, often numbers of the surface regularity gives an impression that the surface is very smooth however actually the surface of the weld is fairly rough because of the presentation of spatters.

Synergic Welding Power Supply and IRB Robot Controller

Unlike the conventional power supply used in the preliminary experiment which failed to give satisfactorily results, the synergic power supply used in the experiment gives satisfactorily results for rapid prototyping application. However, it was found from the experiments that the optimal settings for rapid prototyping are within a narrow range.

The minimum wire feed rate that can be used with the power supply was also determined. When wire feed rate was set to be 1 m/min on the teach pendant, however the power supply automatically performed the welding by using wire feed rate of 1.4 m/min. Thus it can be said that a wire feed rate of 1.4 m/min is the lowest wire feed rate that can be used by the power supply.

The IRB robot controller allows the user to program the robot using its advanced programming language. Unlike the Hitachi controller which is limited to programming by teaching points, the IRB controller allows the user to program by inputting numerical values and perform calculations in the program. Therefore the control of the contact tip distance was improved significantly because the increments of the layers can be inputted numerically.

Suitable and Unsuitable Settings for Rapid Prototyping

From the seventy-six samples analysed in the experiments, there are only eleven samples where no defect were detected. These samples are:

- Sample f1-75-05
- Sample f2-75-05
- Sample f2-95-05
- Sample f2-100-05
- Sample f3-75-05
- Sample f3-95-05
- Sample f3-100-05
- Sample f3-105-05
- Sample f4-100-05
- Sample f4-105-05
- Sample f5-105-05

It can be determined that all of the suitable settings above were found with travel speed of 5 mm/sec. In addition, it was determined that none of the samples with travel speed 10 mm/sec were found to be useless for this application. Spatters and irregular surface are the dominant problems with travel speed 10 mm/sec. An example of an irregular surface where spatters sticking to the weld surface is depicted in figure 5.33.

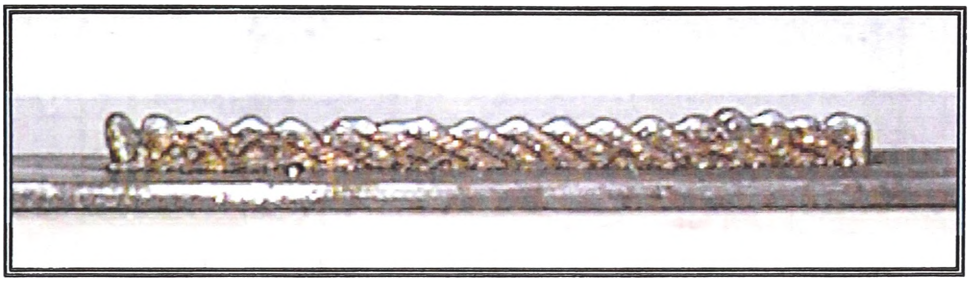

Figure 5.33

An example of an irregular surface with spatter sticking to the weld surface

(Sample f2-75-10)

From the results of the suitable settings, it can be said that the optimal settings for this application lie within a very narrow range. There are several aspects that can be looked into in relation to with the results. These are heat input, surface temperatures, weld width, weld height, hardness, surface regularity and wire feed rate.

It was determined that a suitable wire feed rate for this application is ranging from 1 m/min to 5 m/min with travel speed of 5 mm/sec. From the results obtained, the range of the heat input of these suitable settings can also be determined. It was found that the suitable heat input is ranging from 89.17 J/mm to 378.52 J/mm. Also the surface temperature for the suitable settings is ranging from 150°C to

357°C. The plot of heat input and surface temperature of the suitable settings is depicted in figure 5.34.

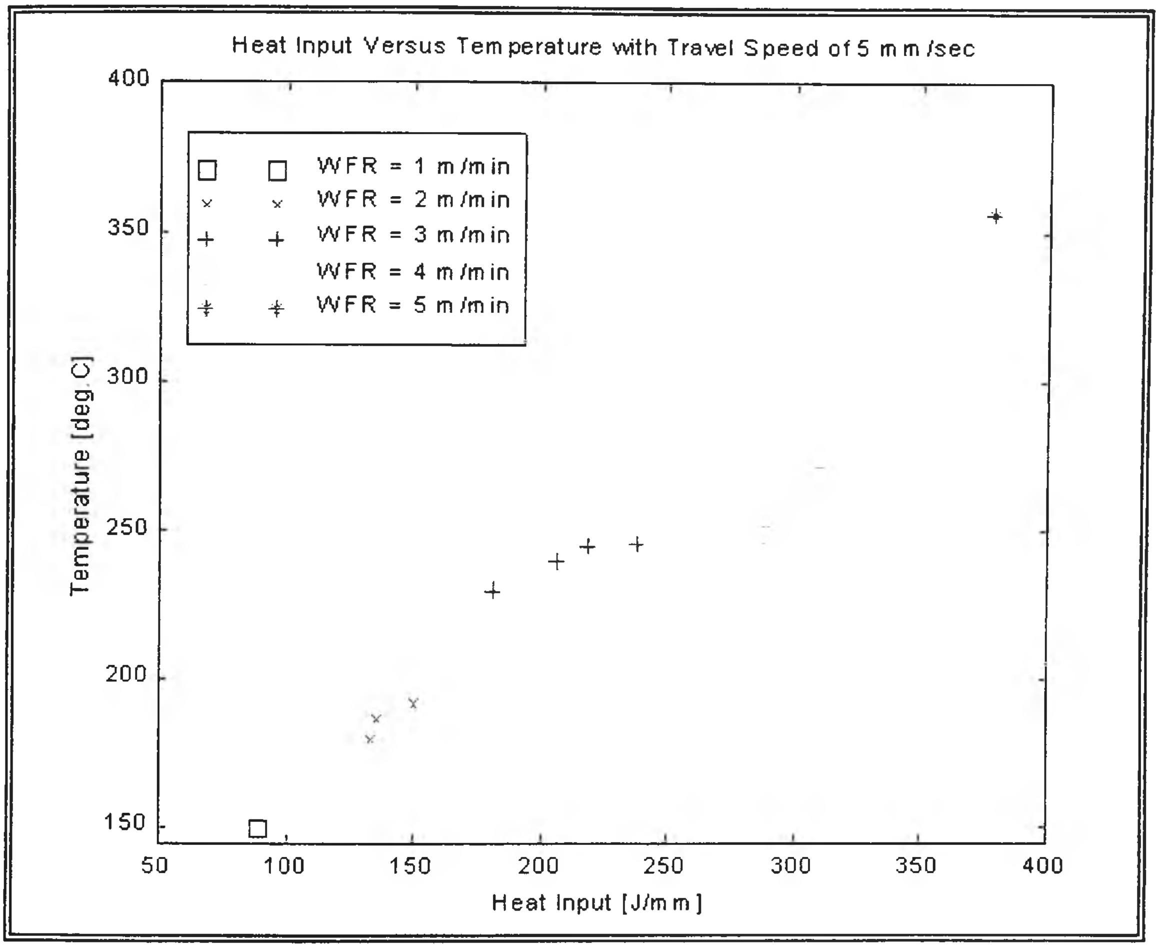

Figure 5.34

Heat input versus surface temperature for suitable settings

Although it was not possible to obtain all of the hardness and surface regularity for all of the samples, the trends in relations with these properties can be identified. In the case of the suitable settings, the hardness is ranging from 155 - 167 Vickers and the surface regularity is ranging from 27.05 microns to 100 microns approximately.

From the conversion table [30] it is found that in terms of ultimate tensile strength the values above are approximately 481 Mpa for 150 Vickers and 530 Mpa for 165 Vickers. In comparison with the data obtained from CIGWELD [23] the electrode wire has an ultimate tensile strength of 520 Mpa. Assuming 10% error tolerance for the hardness measurements the values obtained from the experiments are fairly close to the data obtained from the CIGWELD guide. Therefore from a hardness point of view, the process does not intend to change the tensile strength greatly.

It is also determined that it seems that a wider width of the weld has tendency of obtaining a rougher weld surface. However, depending on the applications, having a very smooth surface may not be the crucial part and necessary for some applications. The plot of a range of weld width versus heat input for the suitable settings is depicted in figure 5.35. The suitable widths are ranging from 2.6 mm to 8.1 mm depending on the wire feed rate.

The arc efficiency for the suitable settings is ranging from 20 to 26 percent. Hence from the results above, it can be said that in the suitable settings, approximately 20 % to 26 % of the total energy is used to melt the wire. The plot of arc efficiency versus heat input of the suitable settings is depicted in figure 5.36.

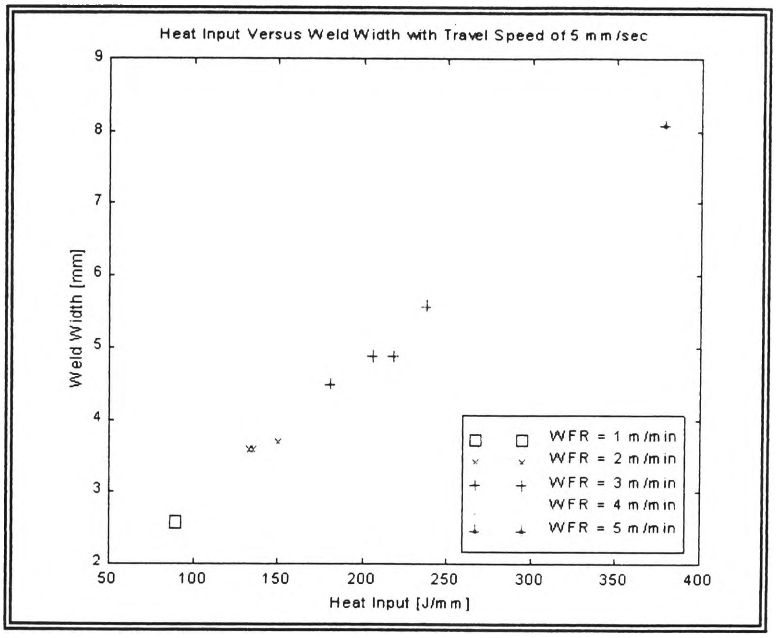

Figure 5.35

Heat input versus weld width for suitable settings

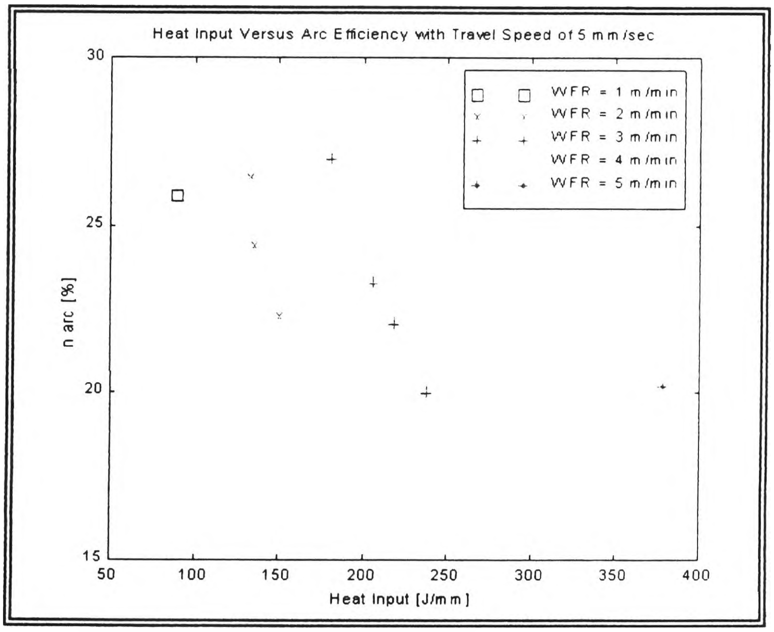

Figure 5.36

Heat input versus arc efficiency for suitable settings

As was mentioned previously, out of the seventy-six samples made, only eleven samples were found to have no defect. However, not all the rest of the samples were found to have all of the defects on them (spatters, porosity, irregular surface and excess materials). Therefore as well as investigating the samples which have no defect, further analysis was also carried out to analyse samples which have all of the defects. From the analysis, it was determined that out of the sixty-five defected samples, only ten of them which have all of the defects. These samples are:

- Sample f5-125-05
- Sample f6-120-05
- Sample f6-130-05
- Sample f7-110-05
- Sample f7-120-05
- Sample f7-130-05
- Sample f8-100-05
- Sample f8-125-05
- Sample f9-100-05
- Sample f9-125-05

From the analysis results obtained from the ten samples above, it was found that these unsuitable settings tend to occur in a higher heat input and surface temperature. It is determined that the heat input for these unsuitable settings is ranging from 465.55 J/mm to 884.37 J/mm and the surface temperature is ranging from 420 °C to 782°C. It is also noted that the defects become worst as the heat input and the surface temperature become higher. The plot of heat input versus surface temperature is depicted in figure 5.37

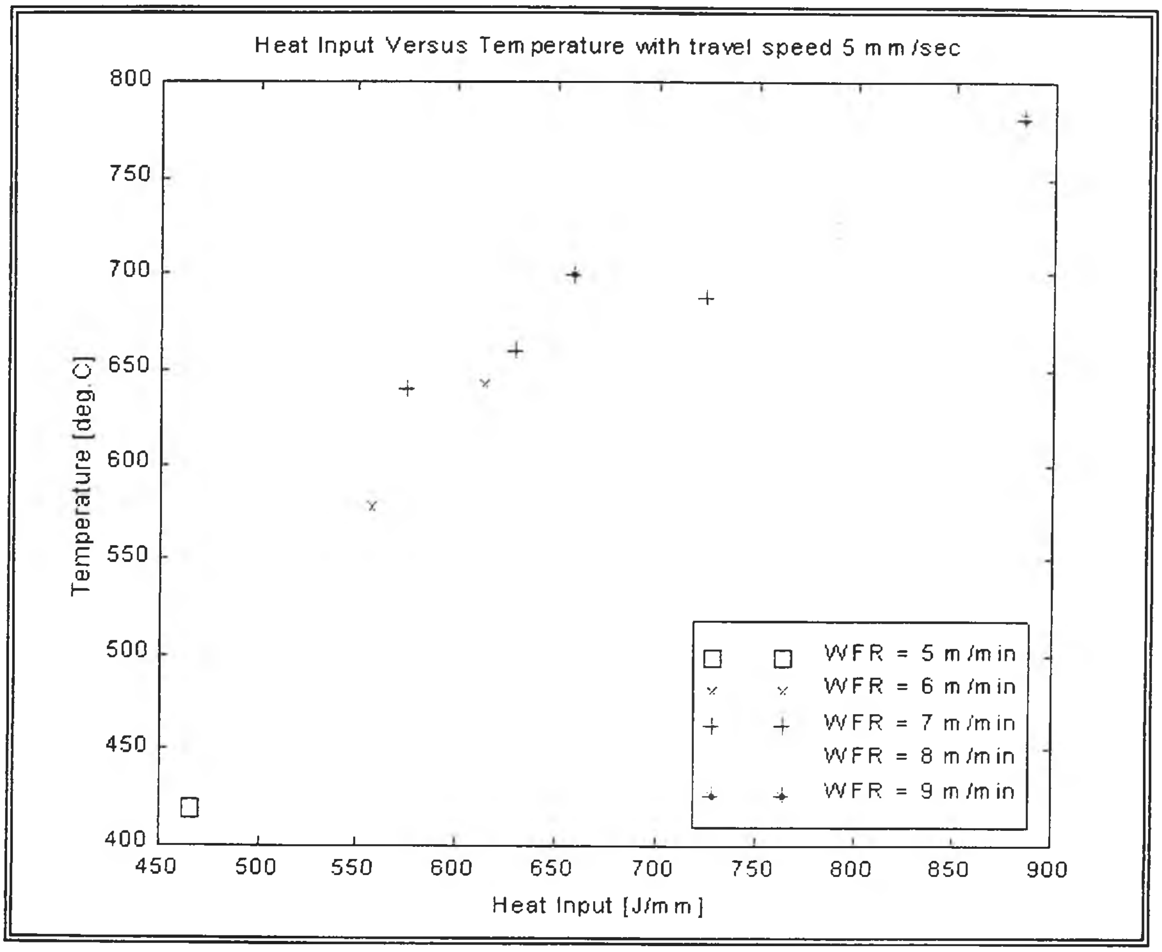

Figure 5.37

Heat input versus surface temperature for unsuitable settings

The hardness and surface regularity of the samples were also determined. It was found that the hardness is ranging from 149 Vickers -152 Vickers. It can be said that the hardness does not vary much in comparison with the values given in table 3.2. Therefore the tensile strength is predicted to be fairly similar (Approximately 520 Mpa).

The surface regularity determined ranges from 75.9 microns to 257.89 microns. However, bear in mind that these values are not too accurate any more as spatters was present in all of the samples.

Apart from heat input, it is also noted that these unsuitable settings intend to occur in the globular transfer mode rather in the short circuit transfer mode. This can be determined from the voltage range (19 volts -25 volts) of the unsuitable settings. This is logical because at a voltage around 20 volts the transfer mode starts changing from short-circuit to globular transfer mode. However, the exact voltage when the transfer mode is changing may vary from one power supply to the other.

Globular transfer mode is known to be an unstable transfer mode in Gas Metal Arc Welding process and is usually an undesirable transfer mode to have where stability is required during the welding process. In the globular transfer mode, the power supply can no longer have good control over metal deposition. The results above proved that stability is an important phenomenon in determining weld quality for rapid prototyping application.

The range of weld width for the unsuitable settings was also determined. It can be noted that the weld width for the unsuitable settings seem to be wider compared to the suitable settings. It is noted that as the heat input gets higher, the surface temperature becomes higher and the weld width also becomes wider. Gradually, due to the excessive heat the weld pool intends to collapse and form excess materials like the one shown previously in figure 5.32. The plot of heat input versus weld width for the unsuitable settings is depicted in figure 5.38.

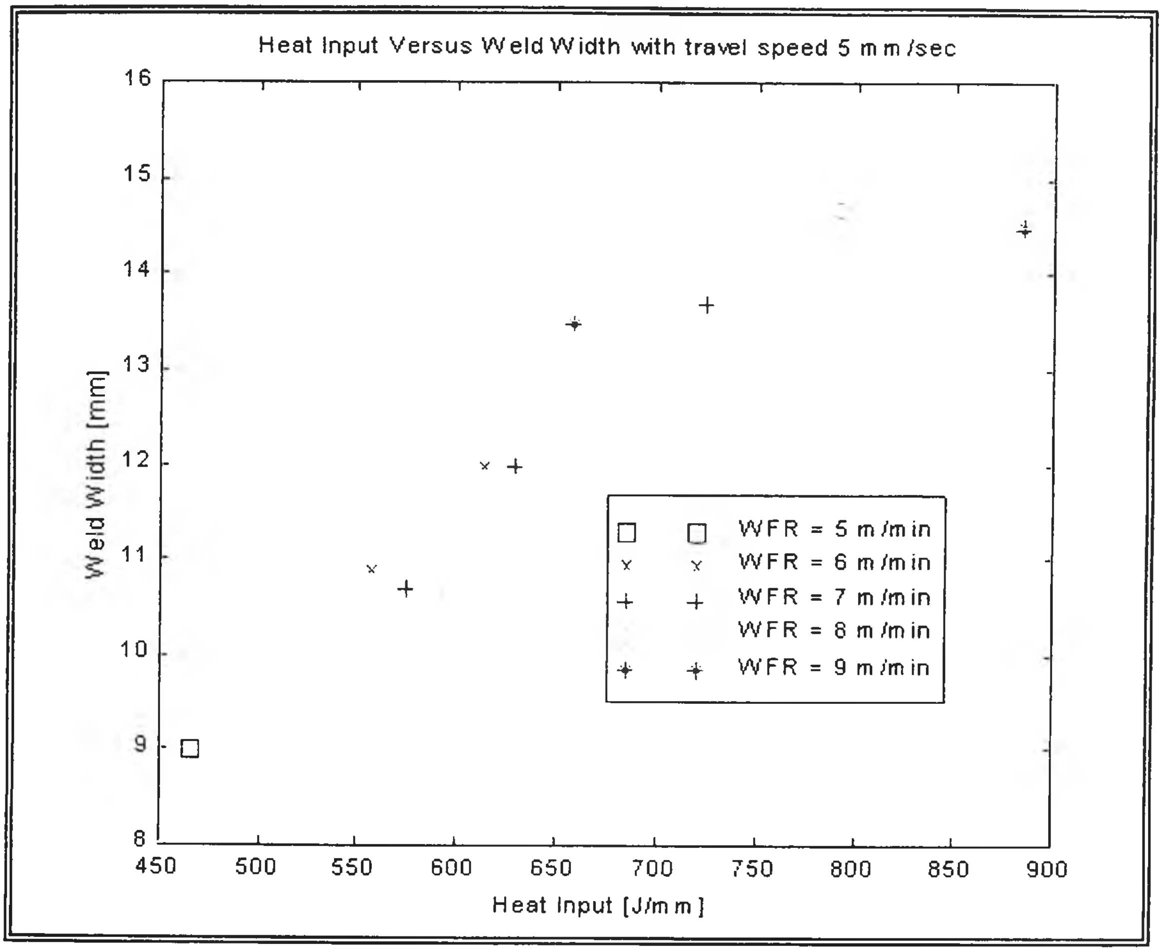

Figure 5.38

Heat input versus weld width for unsuitable settings

5.9 Summary

From the experimental results and observations, it could be concluded that robotic gas metal arc welding for rapid prototyping of thin walled objects application is feasible.

The IRB 1400 robot was proven to have sufficient accuracy and its advanced programming language enabled the user to create a fairly complicated but user friendly program. The standoff distance variation was minimised significantly as the program allows the user to input the increment up to three decimal places in accuracy.

The synergic power supply used was proven to be suitable for rapid prototyping applications. The synergic power supply was proven to be able to weld stably in low heat input (approximately from 89.17 J/mm), where the conventional power supply used in the preliminary experiment failed to perform. The minimum heat input that can be performed by the conventional power supply is 268.6 J/mm.

Travel speed was found to be an important factors in determining weld quality. This can be seen from the results obtained from travel speed 5 mm/sec and 10 mm/sec, where travel speed 5 mm/sec was found to be a suitable travel speed for this application. In the other hand, travel speed 10 mm/sec was found to be an unsuitable travel speed for this application.

Relationships for several welding parameters were found. Some of these parameters such as surface temperature, weld width and hardness were found to have a direct link with heat input. The other parameters such as weld height and arc efficiency were influenced by wire feed rate as well as heat input. A region of smooth and rough surface was also identified.

For practical purposes, suitable and unsuitable surface temperature and weld width regions in conjunction with heat input and wire feed rate was identified. The suitable region is shown in blue and the unsuitable region is shown in red. The plots of surface temperature versus heat input and surface temperature versus wire feed rate are given in figure 5.39 and 5.40 respectively. The plots of weld width versus heat input and weld width versus wire feed rate are given in figure 5.41 and 5.42 respectively.

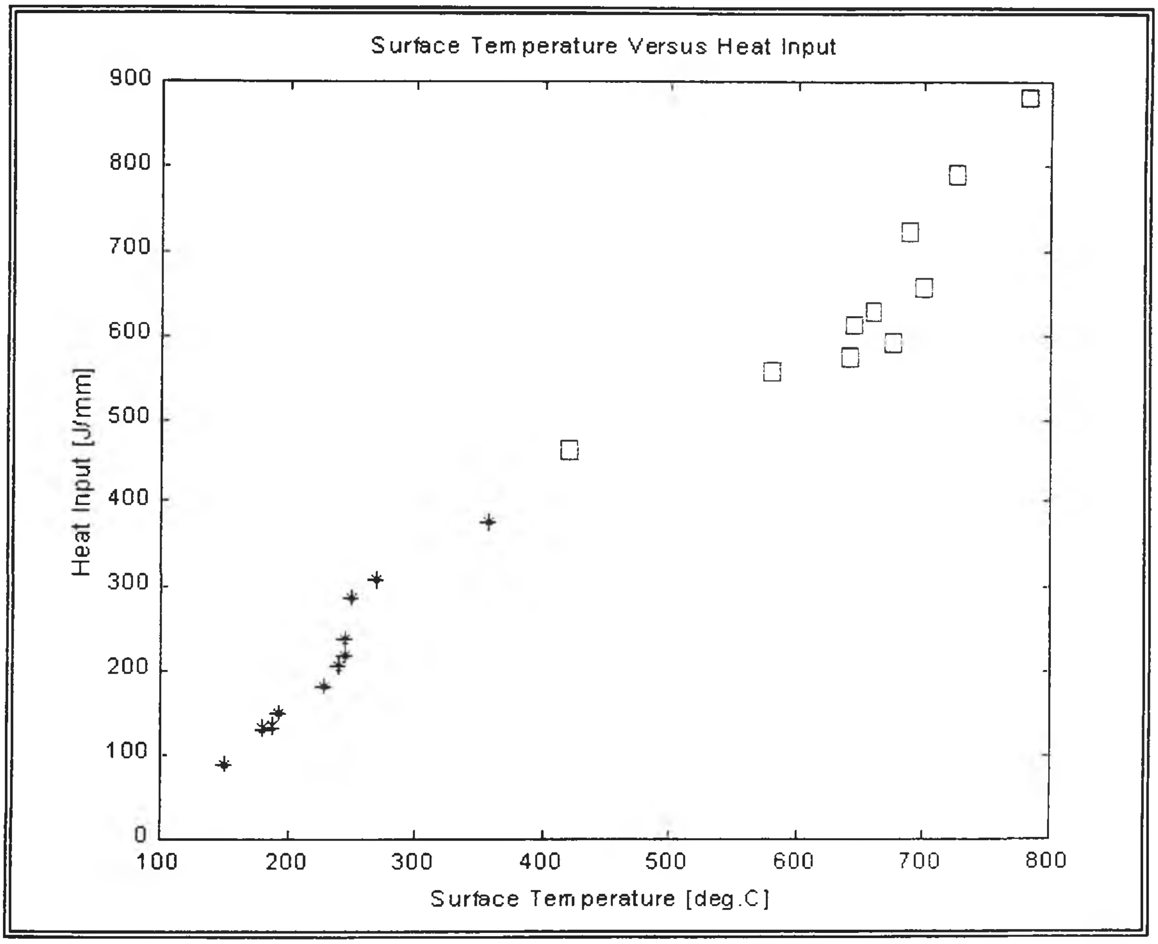

Figure 5.39

Surface temperature versus heat input (Travel speed = 5 mm/sec)

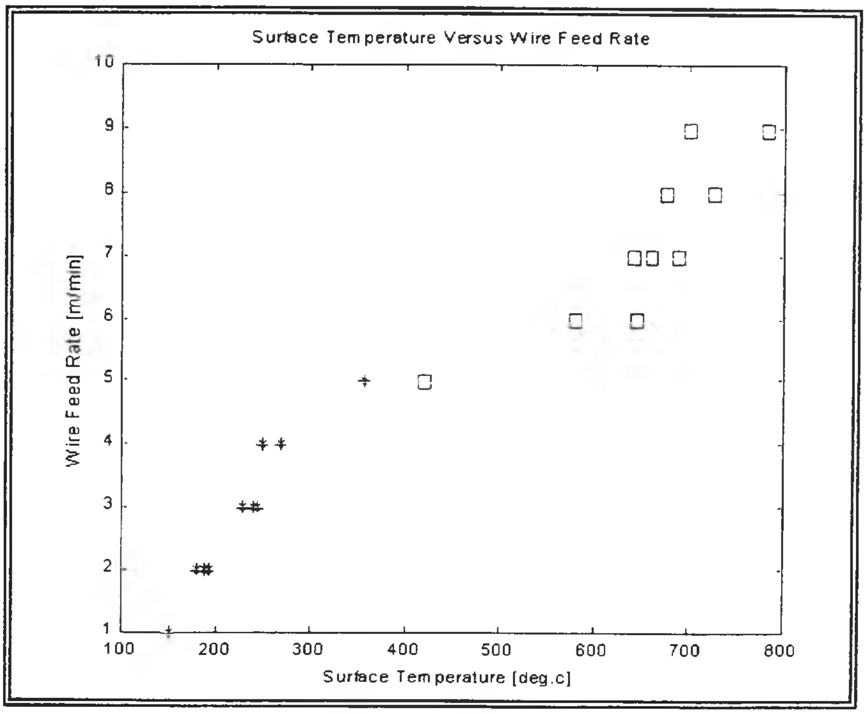

Figure 5.40

Surface temperature versus wire feed rate (Travel speed = 5 mm/sec)

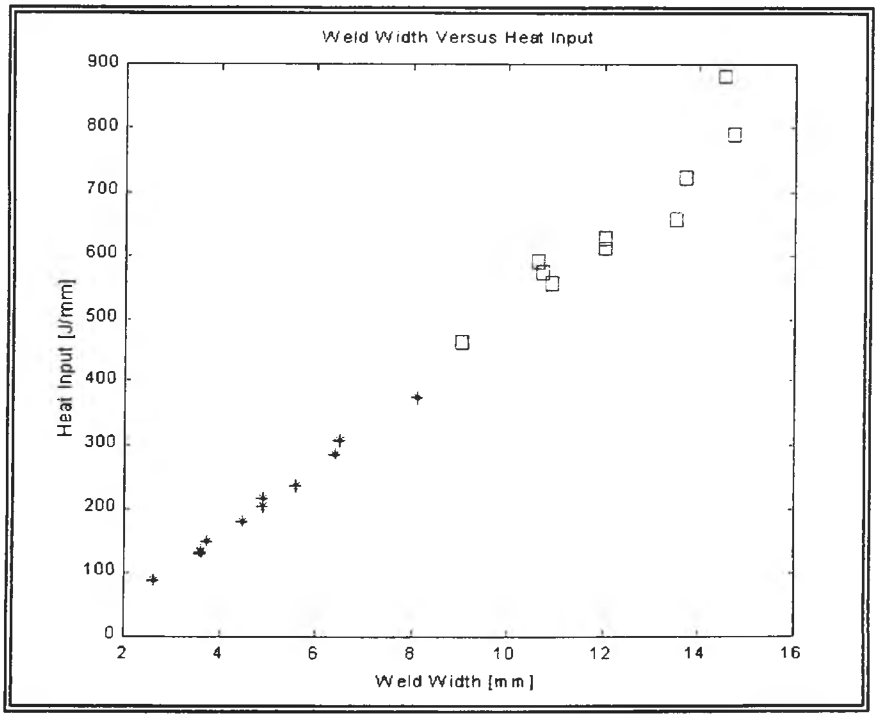

Figure 5.41

Weld width versus heat input (Travel speed = 5 mm/sec)

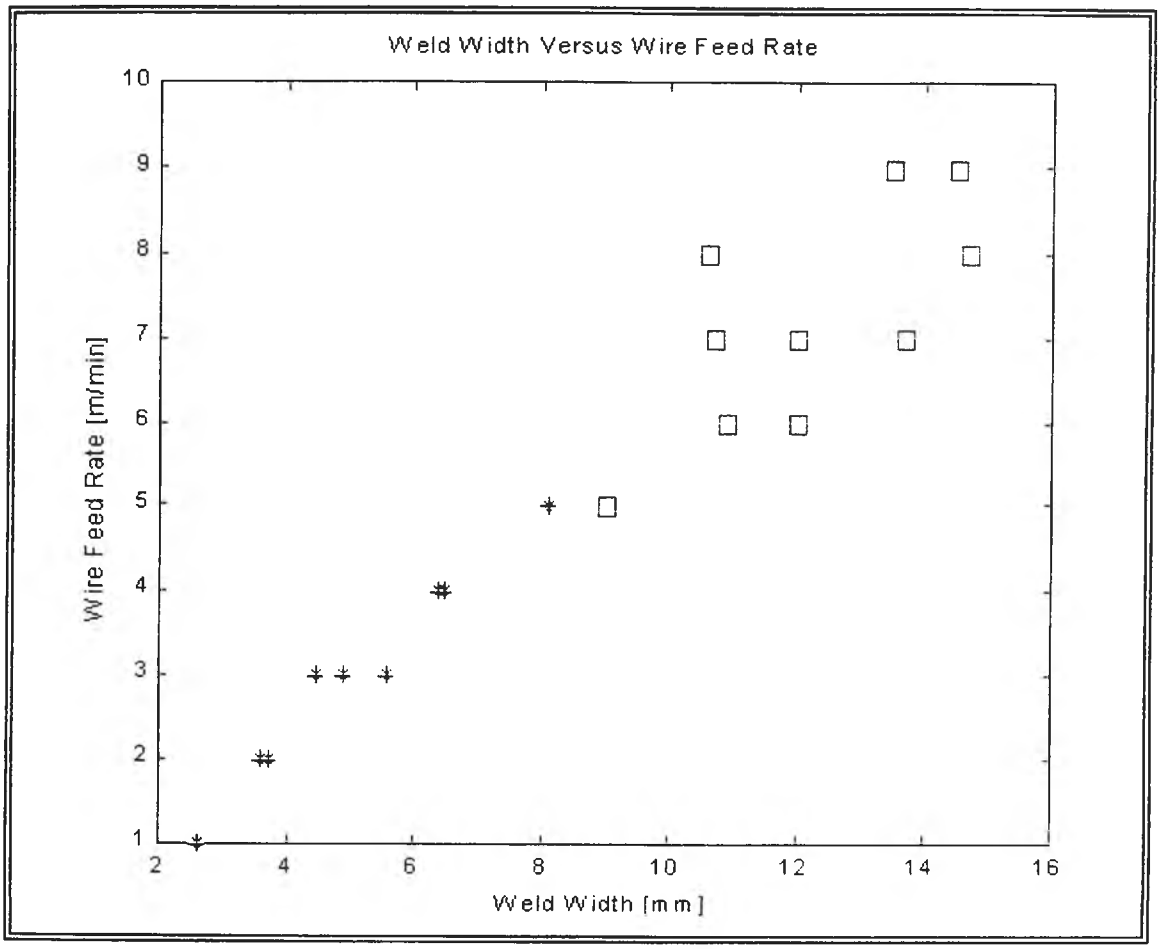

Figure 5.42

Weld width versus wire feed rate (Travel speed = 5 mm/sec)

Chapter 6 Solid Objects

6.1 Introduction

The manufacturing of thin objects using rapid prototyping techniques was investigated in the previous chapter. This chapter will investigate the manufacturing of a solid object build-up. The thin section build-up is generally required for making a prototype of a hollow object. A solid object is generally required to rehabilitate, for example worn objects using wear replacement applications. It is usually a fairly large object such as digging tools. crushers and other consumable parts which are rapidly wearing out when used.

The experiments were carried out into different stages as follow:

- Selecting the geometry of the solid object
- Considering the method of creating the solid object
- Selecting the welding parameters
- Macrographic examinations
- Tensile testing
- Chary-V testing
- Vickers hardness testing

It was decided to make a slab of weld with a length of 150 mm, minimum width of 15 mm and minimum thickness of 15 mm to ensure that there are sufficient build-up materials for making the test specimens. It was not necessary to create a precise width and thickness dimensions of the block because the main aim of this experiment is being able to prove the feasibility of creating a solid object and evaluation of its mechanical property. These slabs of welds were then macroetched and machined to standard tensile and Charpy specimens to obtain their mechanical properties. Hardness measurement was also obtained for these samples. The hardness is useful as a reference to a tensile strength property because the hardness can be converted to an equivalent tensile strength by using a conversion table [30]. Hence it is expected that the conversion will be similar with the results obtained from a tensile test.

The method of creating a solid object and its welding parameter selections will be described in detail in section 6.5 and section 6.6. The macrographic examination of the multi-pass welds and the mechanical testing apparatus will also be described in detail in section 6.2, 6.3 and 6.4.

6.2 Macrographic Examinations of the Weld Specimens

Macrographic examination is also known as macro-etching. Macrographic examination reveals the constituent zone of weld which reveals in different colourations.

Granjon [31] described that the difference in colours reveals the variations in constitution and structure generated by the welding operation. If the chemical etching is strong enough, these variation will be visible by naked eye or under a low magnification. Generally, there are four zones that can be identified from a macrographic examination, these zones are [31]:

- Weld zone: Weld zone is the liquid region during execution of the weld.

- Fusion boundary: Fusion boundary corresponds to the limit up to which the parent metal has been induced to melt.
- Heat affected zone (HAZ): The heat affected zone is the zone in which the welding heat cycle has produced one or more transformations from the initial state to the solid state involved in heating.
- Parent metal: Although the name explained it self, it is important to mention the parent metal as being part of a weld sample for macrographic examination.

The graphical illustration of the zones mentioned above is depicted in figure 6.1.

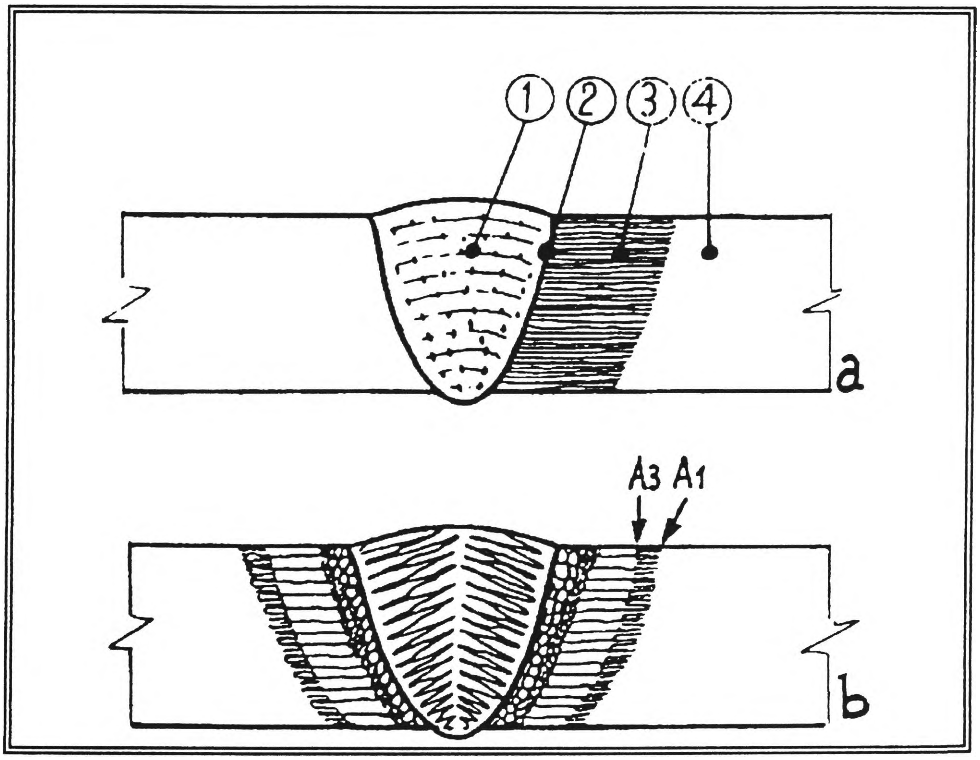

Figure 6.1

Constituent zones of a single pass fusion butt weld [31]

a) General case: 1 weld metal zone, 2 fusion boundary, 3 heat affected zone, 4 parent metal

b) Particular case of steel

The macrographic examination reveals several physical defects on the weld such as porosity, non-metallic inclusions (slag), lack of fusion and cracks. In the experiment the following etching chemical solution was used:

- 100 millilitres of saturated aqueous picric acid
- 10 drops of hydrochloric acid
- 10 drops of teepol detergent

The chemical solution is heated to 60° C and the sample is emersed for ten minutes.

6.3 Multi-pass Welding Cycles

In the experiment of making a solid object, the welding process involved welding in several runs or cycles. Therefore it is required to investigate further what the effects are relating to a multi-pass welding process.

There are four dominant factors influencing the temperature evolutions during multi-pass welding process, these factors are [31]:

- The initial temperature
- The number and arrangement of runs and the conditions in which they are applied
- The time lapse between runs
- The position in relation to the weld of the point at which temperature variation monitored

Lets consider temperature-time curve illustrated in figure 6.2, in the case of a V-butt weld which was made in three runs without preheating. In figure 6.2, the temperature-time-curve is determined at point A. In addition, figure 6.3 illustrate an identical operation except that now the temperature time curve is determined at point B.

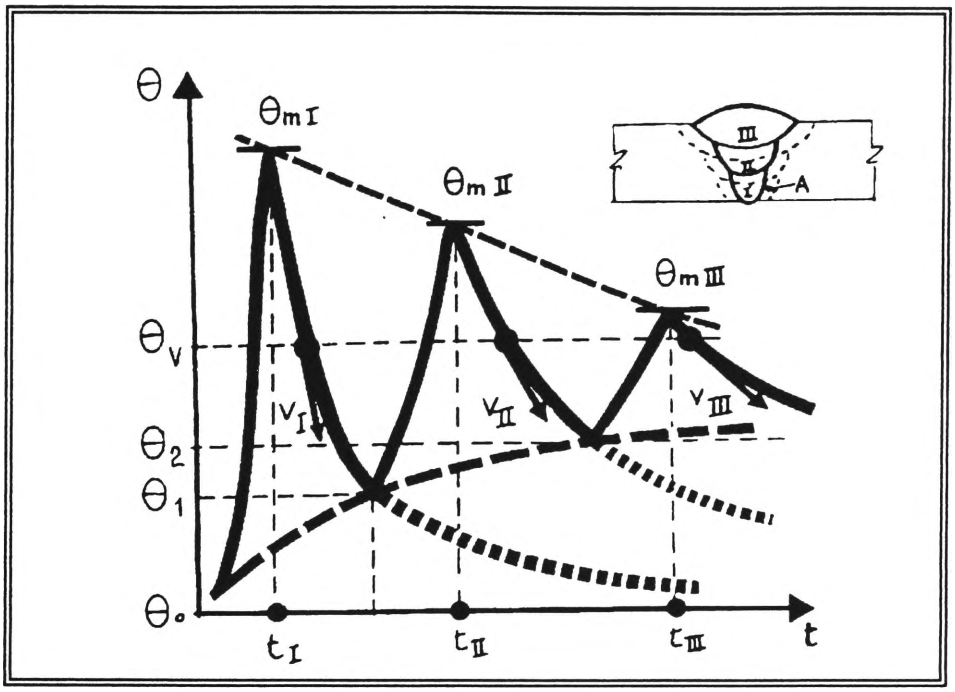

Figure 6.2

Heat cycles in the vicinity of a three-pass butt weld determined from point A [31]

Measurement point close to first pass: the maximum temperature θ_{mI} is the highest as is the cooling speed V_I. Both decreased during the subsequent passes, whilst the initial temperature for each pass from θ_0 (Broken line curve). The maximum temperature reached may exceed by twice or even three times a given value, for example point A_1 of steel. The dotted curves represent the cooling which would follow each pass if the next pass was not made. Hence the importance of the time gap between passes.

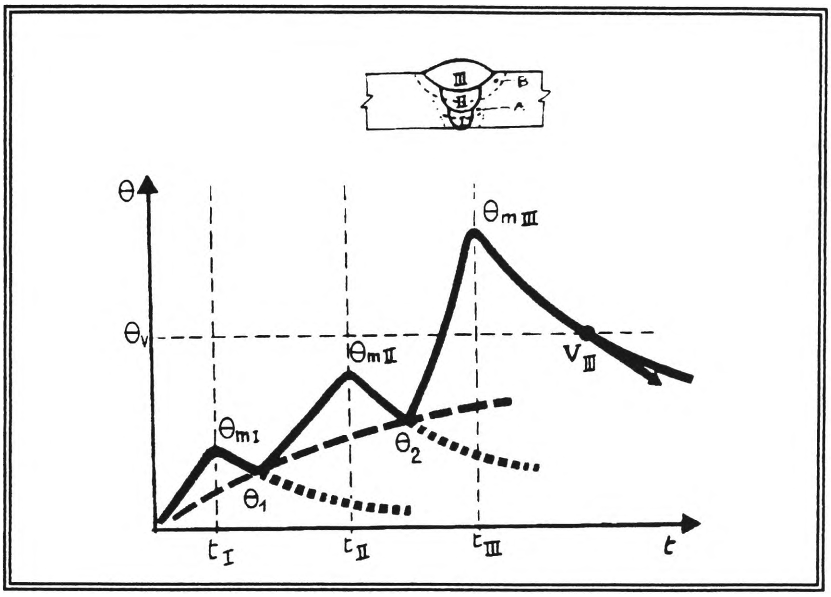

Figure 6.3

Heat cycles in the vicinity of a three-pass butt weld determined from point B [31]
Measurement point close to the third pass: the maximum temperatures are increasing and may exceed a given value only once

When point A is considered in an illustration depicted in figure 6.2, 'the first run results in an initial temperature rise to maximum value θ_{mI}, followed by cooling which, characterised by speed V_I until temperature θ_v, continues until the initial temperature if the second run is carried out after some delay' [31]. However, this is not generally the case in the multi-pass welding operation because usually the second run is performed before the temperature at point A has returned to initial temperature θ_0. Thus $\theta_1 > \theta_0$ when the a heat cycle commences as result of the second run. This cycle on the second run is being characterised by a maximum temperature θ_{mII} and the cooling speed V_{II} at temperature θ_V. However this second cycle differs from the first cycle in the following condition that the θ_{mII} is less than θ_{mI}, the reason being is because the distance of measurement point A in relation to the second run is greater. The V_{II} is less than V_I for the same reason as described above and also the heat cycle of the second run is influenced by an effect that is similar like preheating as the cycle starts from $\theta_1 > \theta_0$. The same effect also applies to the third pass.

In comparison, now consider figure 6.3 where the measurement is considered from point B, ie. The point that is close to the third pass. When the measurement is taken from this point it is clearly determined that the heat shock due to the first two runs is relatively weak. The maximum temperature is reached on the third run while cooling speed is moderate by the preheating effect like described in the last paragraph.

In the experiments, the fusion is made in several passes and the corresponding heat cycle causes re-austenitisation in all or part of the weld metal that already deposited and transformed. The re-austenitisation also occurred in the heat affected zone in every layer. The re-austenitisation can occur one or more times at a given point depending on the arrangement and size of the passes until temperature A_3 (complete austenitisation) is no longer reached, see figure 6.1 for location of A_3 in steel. Consider the situation of three-pass-pipe-line type weld (See figure 6.4), where the second pass may totally re-austenitise the weld metal and the zone affected by the first pass. In the other hand the third pass affects only a part of the weld metal of the second pass.

'If the steel and the welding condition permit, each of the re-austenitisation due to a pass gives rise to structural regeneration which results in refinement of the ferrite and pearlite grains resulting from the previous pass' [31]. Thus, multi-pass welding process has considerable effect in changing grain structure and size.

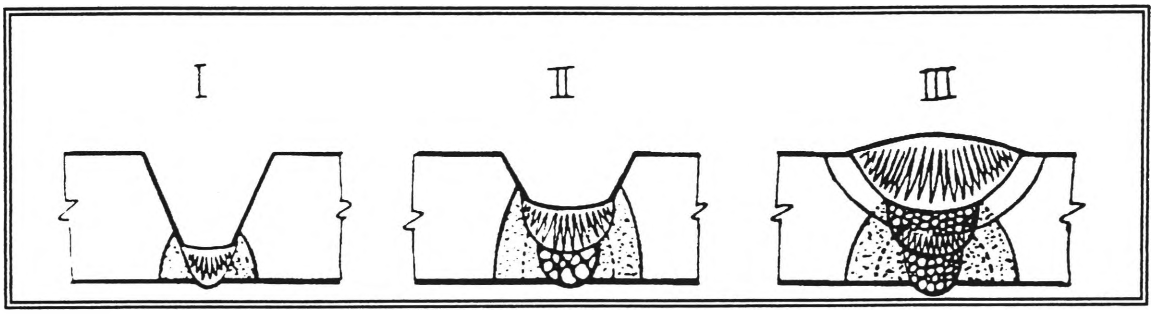

Figure 6.4

Structural evolution of the metal during a three-pass weld on steel [31]

6.4 Mechanical Testing of the Weld Specimens

Due to the heating and cooling effect resulting from the multi-pass welding process, it is expected that due to the particular conditions of solidification and the resulting structures, metal zone of fusion welds would present particular features from its mechanical properties point of view.

For that reason, mechanical properties of the samples made in the experiment will be investigated. As mentioned in chapter 2, this includes tensile testing, hardness testing and Charpy V-notch testing. The testings of the samples are carried out according to the Australian Standard described previously in chapter 2.

In the multi-pass welding process, each process would have some particular grain structures depending on how the weld is made [31]. The grain orientation in successive runs would create directionality of mechanical property which results in different grain performance depending whether they are stressed in their direction of growth or in the perpendicular direction. The experiment indicated that a higher ductility was indicated in the grain growth direction rather in the transverse direction [31].

The more detailed description regarding the mechanical testing and their apparatus carried out in the experiment will be discussed further in the next following sections.

6.4.1 Tensile Testing

The tensile testing machine INSTRON 1341 was used for the experiments. As it is mentioned previously in chapter 2 that the tensile testing is carried out according to the Australian Standard 2205.2.2-1997 (All Weld Metal Tensile Test methods for destructive testing). For the experiment, a standard size of diameter of 5 mm is chosen for the tensile testing of the weld sample. The detailed specifications of the standard specimen are given in table 2.1.

The experiments were carried out at a room temperature. At the end of the test the machine determines at what load that the sample failed and what is the elongation of the sample.

The technical data regarding the tensile property of the welding wire used in the experiment is depicted in table 3.2. In the table 3.2, it is depicted that the tensile strength is 520 Mpa and the elongation is 30 %. The tensile properties of the weld specimens obtained from the experiment will be described in detailed in the next several sections. The tensile specimen is depicted in figure 6.5. The tensile testing machine used in the experiment is depicted in figure 6.6.

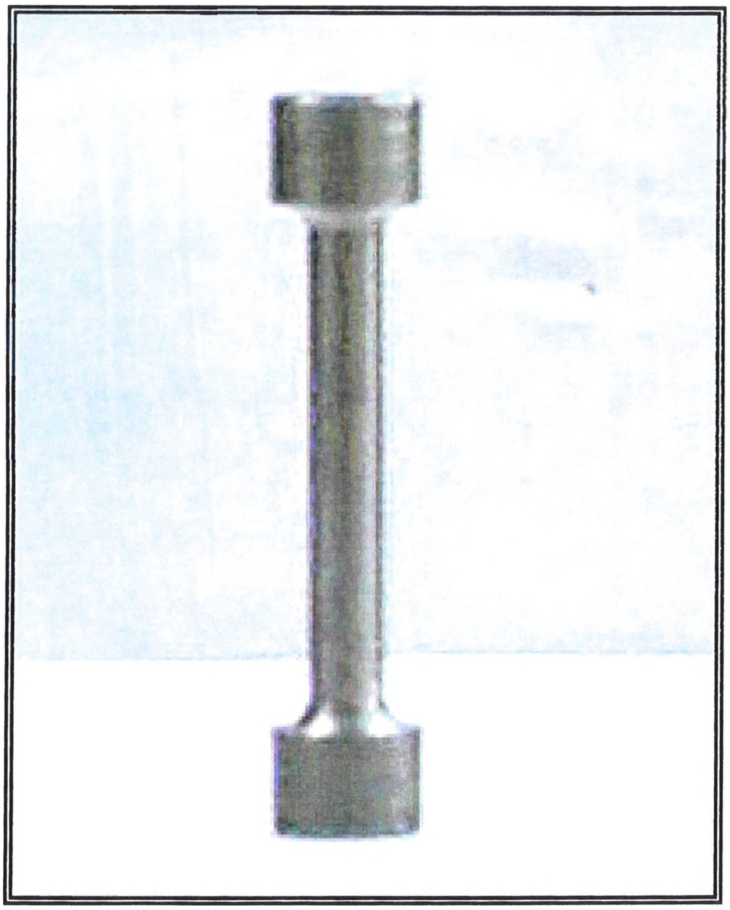

Figure 6.5

The tensile specimen

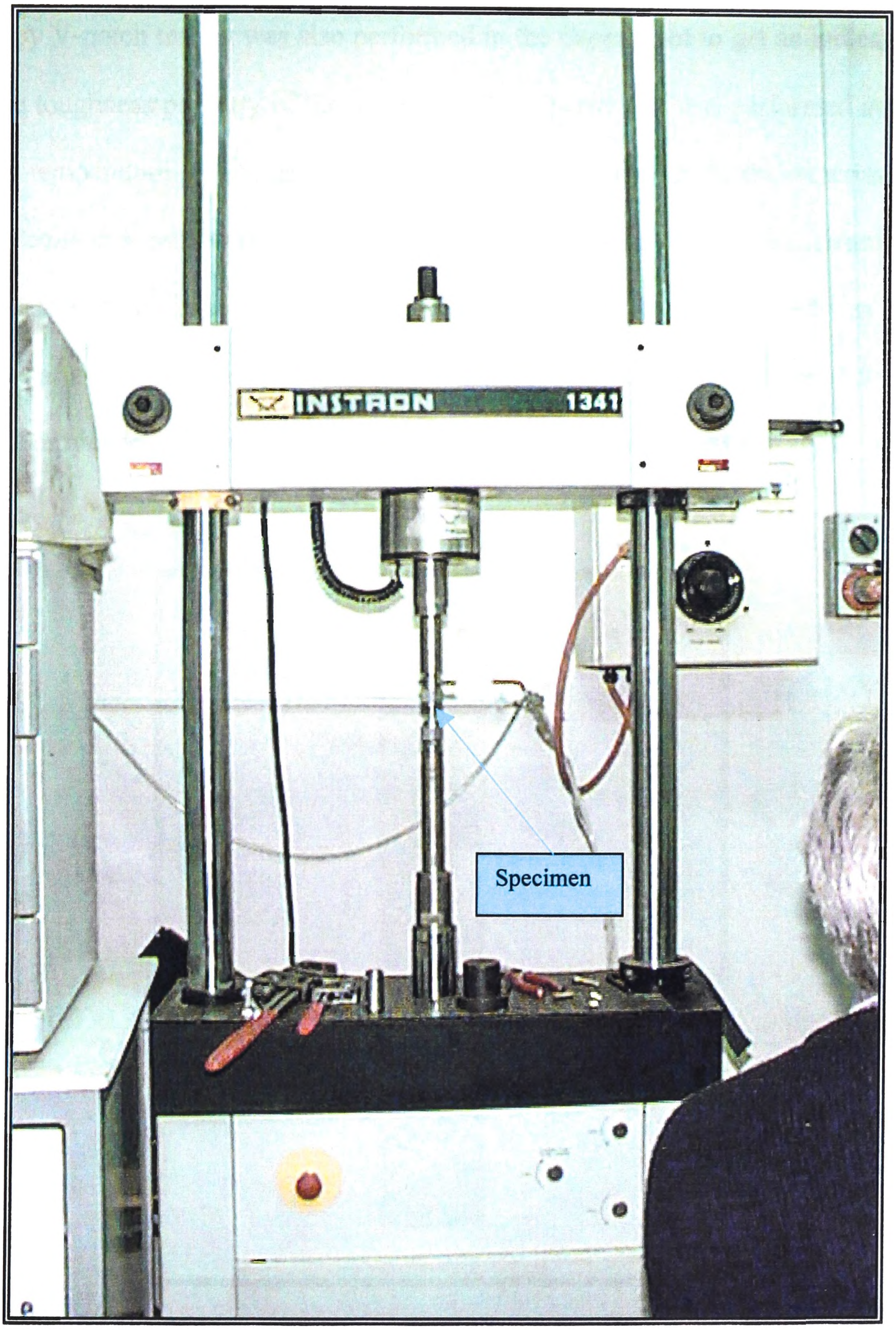

Figure 6.6

The Instron 1341

6.4.2 Charpy V-notch Testing

Charpy V-notch testing was also performed in the experiment to get an indication of the toughness property of the materials. The Charpy test was performed at the room temperature. A standard Charpy test piece was chosen in the experiment. The detailed specification of the standard test piece according to the Australian Standard is given in table 2.2. In the experiments, breaking energy used was 300 Joules at a speed of 5 m/s. The standard test piece is illustrated in figure 6.7 and the Charpy machine used in the experiment is depicted in figure 6.8.

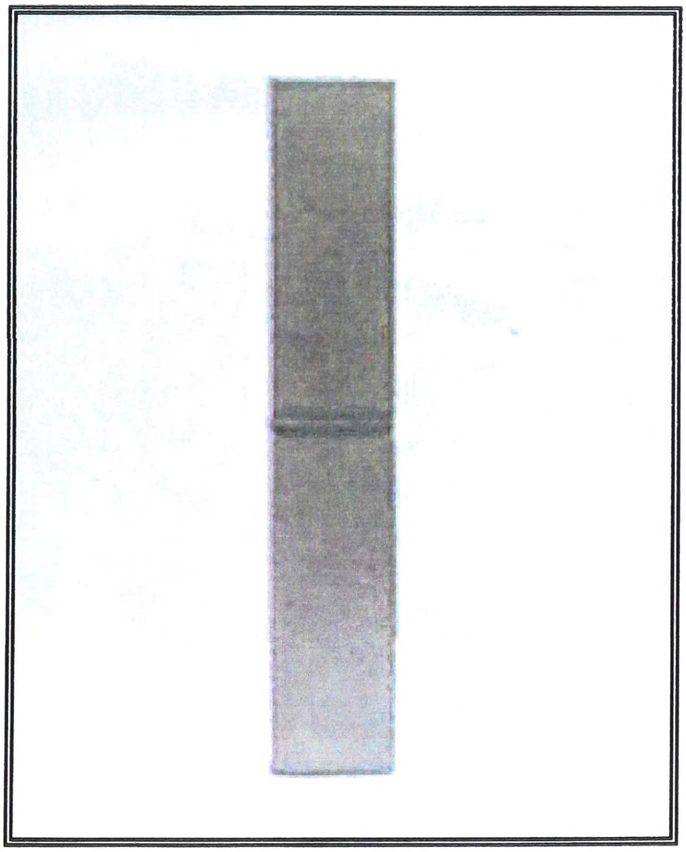

Figure 6.7

The standard Charpy specimen

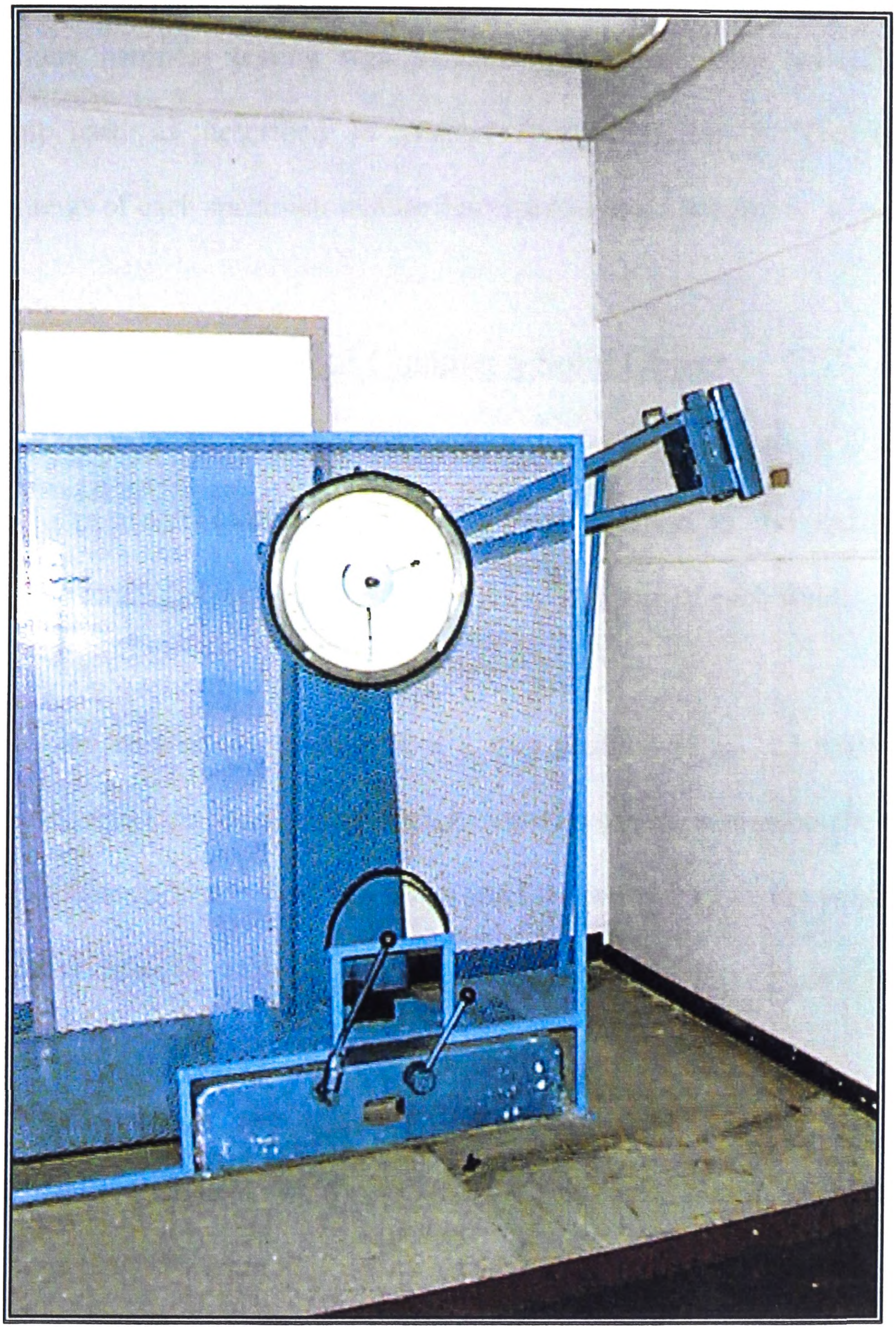

Figure 6.8

The Charpy machine

6.4.3 Vickers Hardness Testing

The Vickers hardness testing was performed with the same procedure and equipment used as described in chapter 2 and chapter 5. The hardness measurements of each specimen will be described in more detailed in Appendix I.

6.5 Non Boundary Method of Creating a Solid Object

A program named F_BLOCK.prg was made to create a solid object. It is made so that the robot welds continuously from a start position to the end position consisting several adjacent welds with a length of 150 mm of each weld.

The layers are created by welding from a start position to an end position, the robot Tool Centre Point then comes back to a start position increments the vertical z axis and creates another weld and so on until the number of layers specified by the user are completed.

To run the program, the user must specify the distance between these weld runs. The distance between these weld runs is dependent on the size of the weld bead. Bear in mind that it is required to create a solid object, therefore a gap between the adjacent welds is not desirable. For example if the weld bead size were 2 mm, the distance specified between the weld runs would be less than 2 mm. As a general rule of thumb the reasonable distance is approximately between 0.5 to 0.75 times the weld bead size. In the case of the weld bead size of 2 mm, the distance between the welds can be anywhere from 1 mm to 1.5 mm. As it was mentioned previously that it was required to acquire a minimum width of 15 mm to have enough build-up for making the test specimen. Therefore with using 1.5 mm distance between the welds it would be required to have ten adjacent welds. However, to ensure the minimum width is acquired, an extra weld would be added so that the numbers of adjacent welds become eleven in this case. Trials were made to investigate an appropriate distance required for each setting used in the experiment. A trial and error method was used to determine the height of each layer for the different settings so that this could be used for the robot program. The illustration of the welding process is described in figure 6.9.

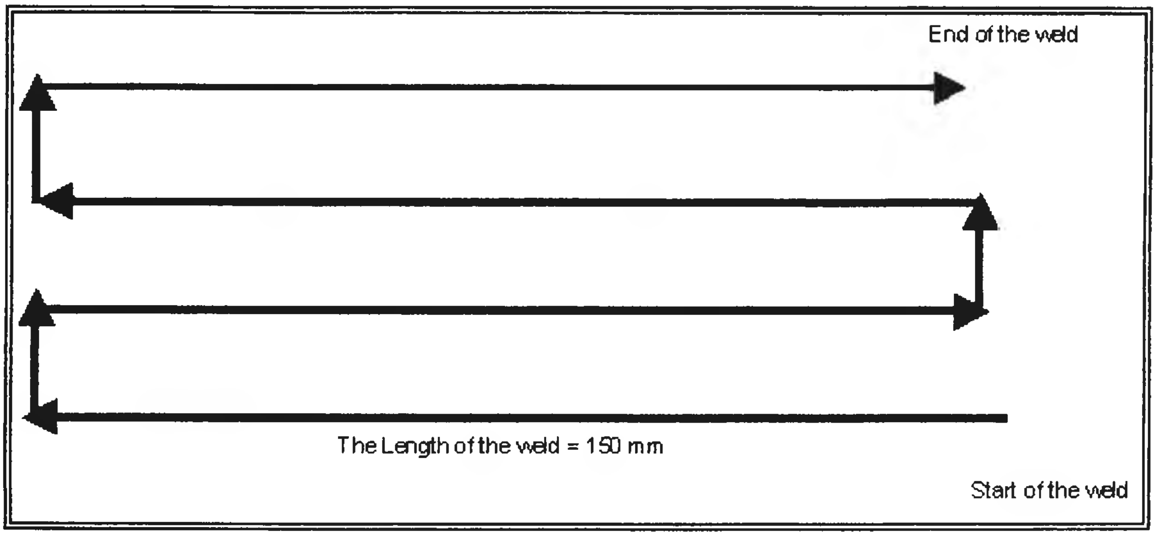

Figure 6.9

Process diagram of a non-boundary method

After setting all of the seam data, weld data and weave data, the program is ready to run. When the user runs the program the program will prompt the following:

- Number of vertical layers: When the user sees this prompt, he or she is required to enter the number of layers.

- Number of horizontal welds: When the user sees this prompt, he or she is required to enter the number of adjacent welds.
- Vertical Increments [mm]: When the user sees this prompt, he or she is required to enter the vertical increment values. This value determines how many millimetres the robot will move up in z axis after each layer of weld.
- Horizontal increment [mm]: When the user sees this prompt, he or she is required to enter the distance between the adjacent welds. Predicting of the correct increment value is important to ensure that there is no gap between the adjacent welds.

The program F_BLOCK.prg is depicted in Appendix H.

6.5.1 The Experimental Results

There are six samples made in the experiment, these samples are:

- Sample s2-75-05
- Sample s2-100-05
- Sample s3-75-05
- Sample s3-100-05
- Sample s4-75-05
- Sample s4-100-05

The six samples chosen above are a reasonably stable settings in the short-circuit transfer mode. In addition, some of the settings were the optimal settings for a thin walled objects.

The chosen format is described below:

sw-vv-zz, where

s	=	solid
w	=	wire feed rate setting on the teach pendant [m/min]
vv	=	voltage setting on the teach pendant [%]
zz	=	travel speed [mm/sec]

The example of the above format is described below:

Consider the case where the coding is s2-75-05. Thus, it means this is a solid object experiment with the following parameters as described below:

- Wire feed rate setting on the teach pendant = 2 m/min
- Voltage setting on the teach pendant = 75 [%]
- Travel speed = 5 mm/sec

The experimental results obtained for each sample will be described in the next sections.

6.5.1.1 Sample s2-75-05

Although this sample inherited good weld geometry (See figure 6.10 and figure 6.11) as would be expected being one of the suitable settings for thin walled objects, it had a significant lack of fusion. In addition, slag was also found inside of the porosity. It is also noted that there are some parts of the weld that were not properly fused with the parent metal as well as between the layers.

The locations of the porosity are mainly in between the weld beads. This is caused by slag on weld, if the temperature during welding of next layer is not high enough, these contaminants will not be burnt which causes lack of fusion. This can be determined from the macrographic examination picture of the sample's cross-section.

From the picture of the macrographic examination, the heat affected zone (HAZ) can been identified very clearly (Darker greyish) at each layer of the weld, see figure 6.12. From the hardness testing obtained, it was found that the hardness is similar between the heat affected zone and other part of the weld. It is also found that the hardness of the first and last layers is the highest compared to the other layers. The sample has a tensile strength of 461 Mpa, hardness of 181.5 Vickers and Charpy V-notch of 159 J. The detailed description of the sample is depicted in Appendix I1.

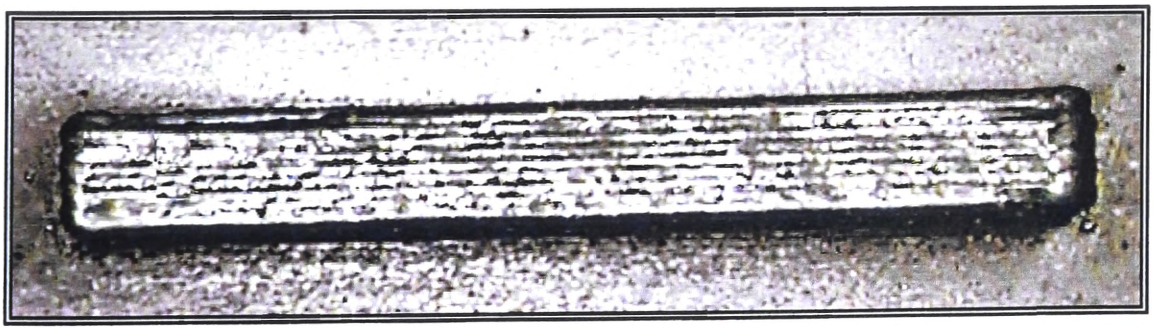

Figure 6.10

Sample s2-75-05 (Top view)

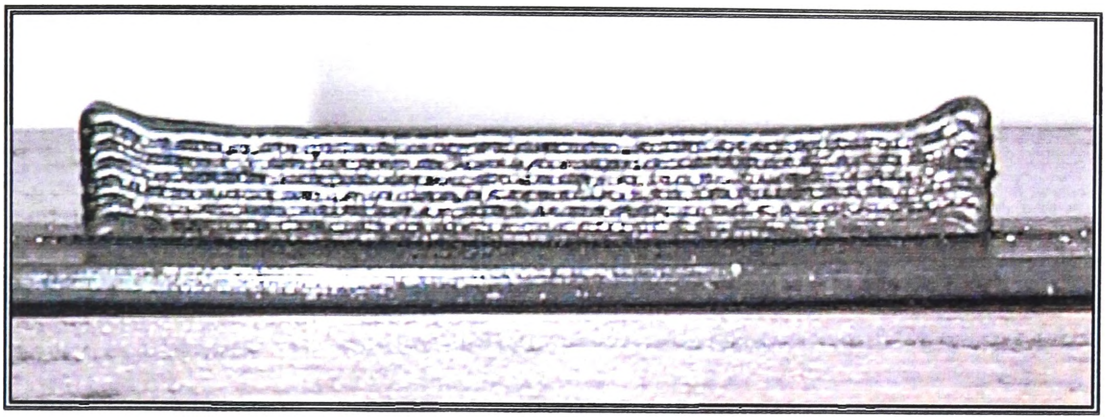

Figure 6.11

Sample s2-75-05 (Front view)

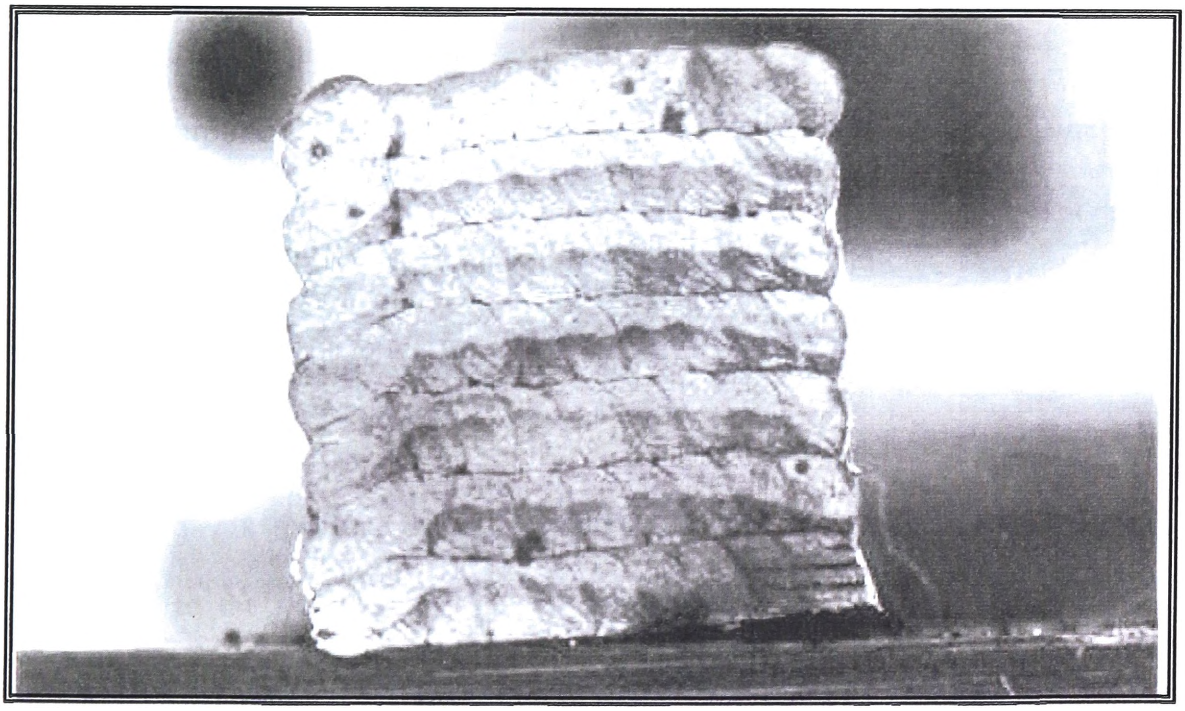

Figure 6.12

Cross-sectional macrograph of sample s2-75-05

6.5.1.2 Sample s2-100-05

As well as loosing its shape, this sample has problems with spatters sticking to the parent metal and the weld surface, and a lack of fusion (See figure 6.13 and figure 6.14). In addition, slags were also found inside of the porosity. It is noted that the weld and parent metal is fused better in this sample in comparison with the previous sample with the lower voltage. The fusion between the layers also improved.

The locations of the porosity are mainly in between the weld beads. This is caused by slag on weld, if the temperature during welding of next layer is not high enough, these contaminants will not be burnt which causes lack of fusion. This can be determined from the macrographic examination picture of the sample's cross-section.

From the picture of macrographic examination, the heat affected zone (HAZ) is identified like the one in the previous sample, see figure 6.15. It is also found in the experiments that the hardness of the first and last layers is the highest compared to the other layers. The sample has a tensile strength of 481 Mpa, hardness of 180.4 Vickers and Charpy V-notch of 160 J. The detailed description of the sample is depicted in Appendix I2.

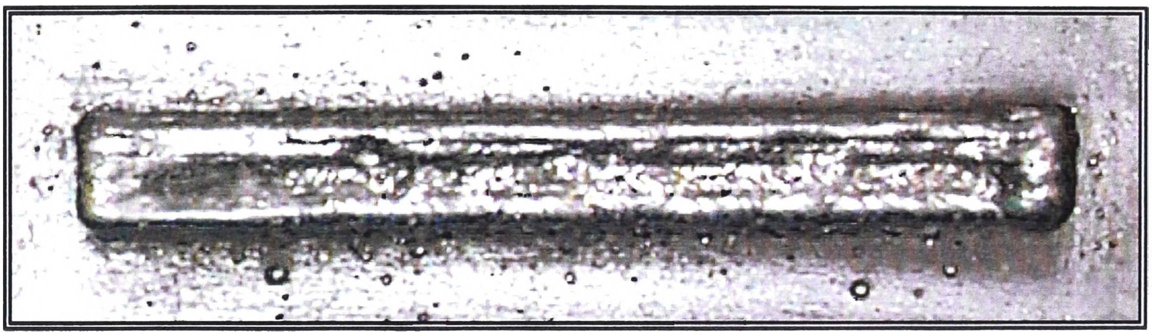

Figure 6.13

Sample s2-100-05 (Top view)

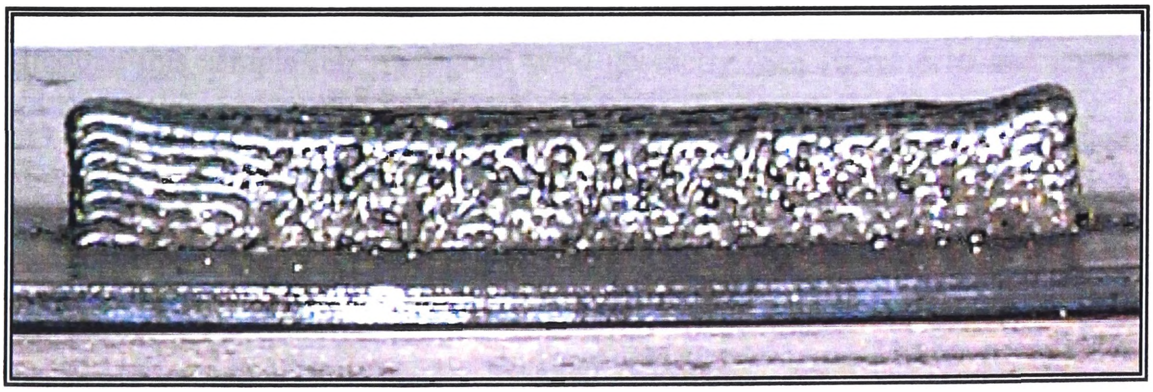

Figure 6.14

Sample s2-100-05 (Front view)

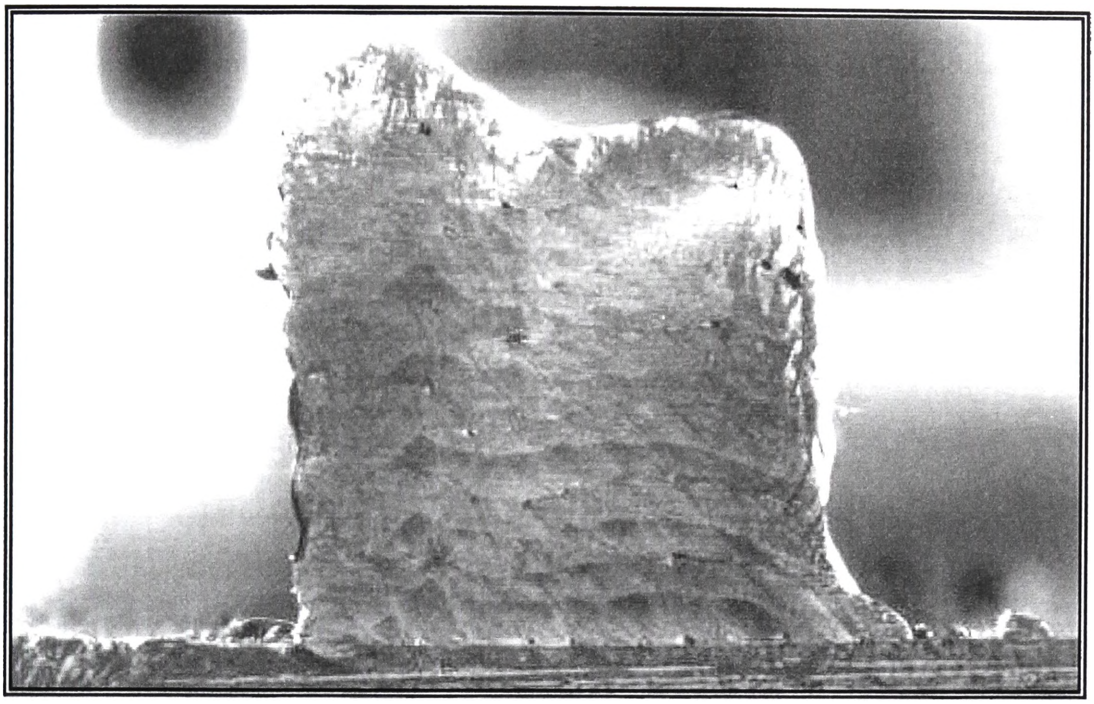

Figure 6.15

Cross-sectional macrograph of sample s2-100-05

6.5.1.3 Sample s3-75-05

Although this sample inherited good weld geometry (See figure 6.16 and figure 6.17) as would be expected being one of the suitable settings for a thin walled object, it has a problem with a lack of fusion. In addition, slags were also found inside of the porosity. It is also noted that there are some parts of the weld that does not properly fuse with the parent metal as well as between the layers.

This is caused by slag on weld, if the temperature during welding of next layer is not high enough, these contaminants will not be burnt which causes lack of fusion. This can be determined from the macrographic examination picture of the sample's cross-section.

It is also found again that the hardness of the first and last layers is the highest compared to the other layers. The sample has a tensile strength of 528 Mpa, hardness of 168.8 Vickers and Charpy V-notch of 160 J. The detailed description of the sample is depicted in Appendix I3.

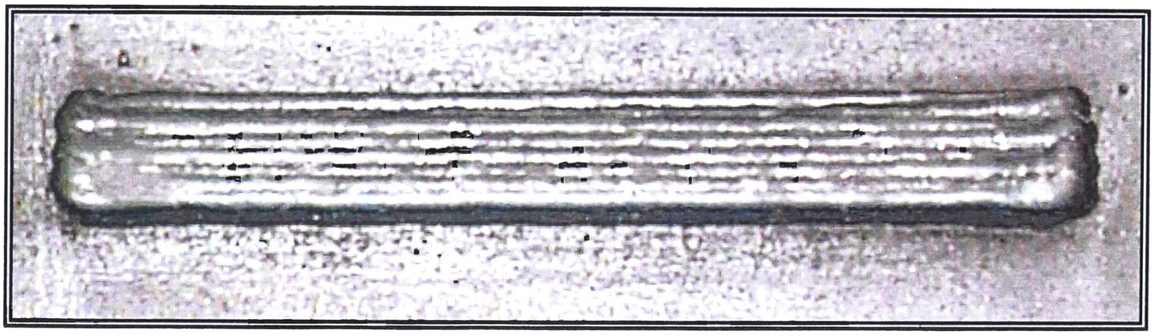

Figure 6.16

Sample s3-75-05 (Top view)

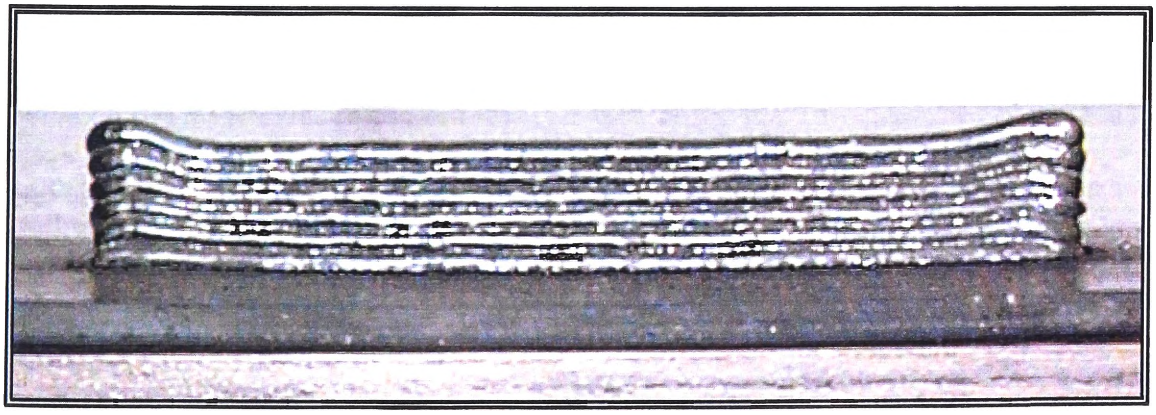

Figure 6.17

Sample s3-75-05 (Front view)

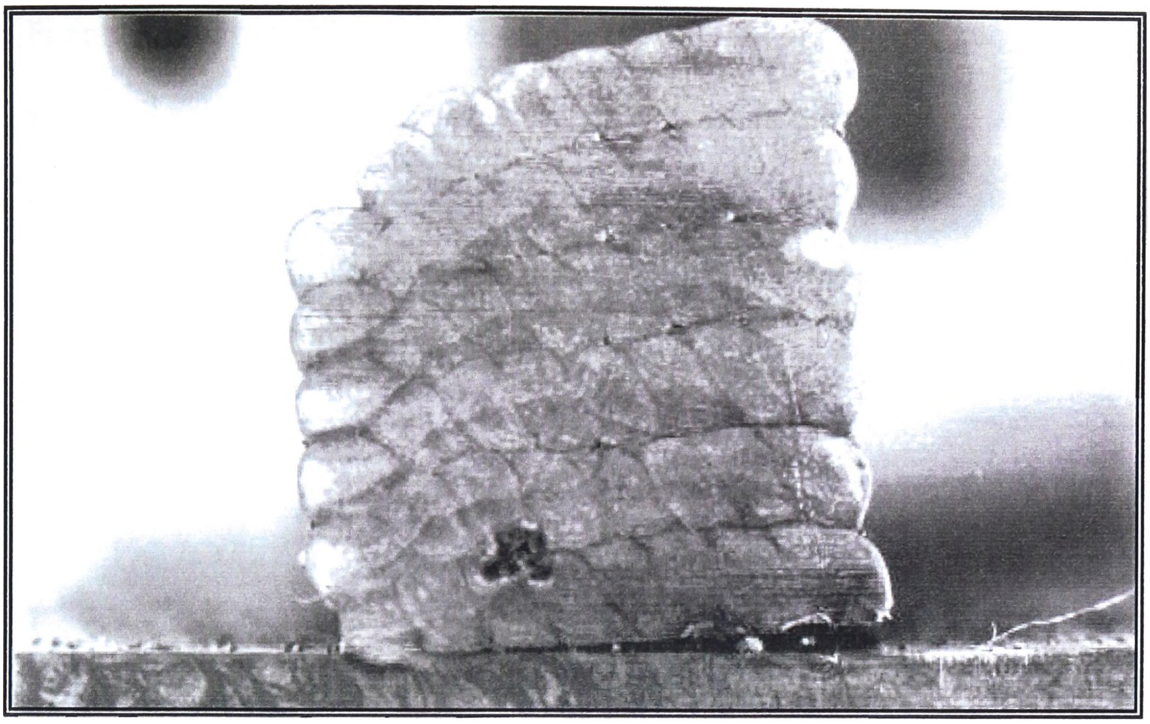

Figure 6.18

Cross-sectional macrograph of sample s3-75-05

6.5.1.4 Sample s3-100-05

This sample has problems with spatters as well as a lack of fusion (See figure 6.19 and figure 6.20). In addition, slags were also found inside of the porosity. However, it is noted that the weld and parent metal is properly fused. The fusion between the layers was improved and it is also noted that the quantities of porosity and slag are less compared to the previous samples.

This is caused by slag on weld, if the temperature during welding of next layer is not high enough, this contaminants will not be burnt which causes lack of fusion. This can be determined from the macrographic examination picture of the sample's cross-section.

From the macrographic examination, the heat affected zone (HAZ) was identified similar like the one identified in other samples, see figure 6.21. The sample has a tensile strength of 517 Mpa, hardness of 162 Vickers and Charpy V-notch of 212 J. The detailed description of the sample is depicted in Appendix I4.

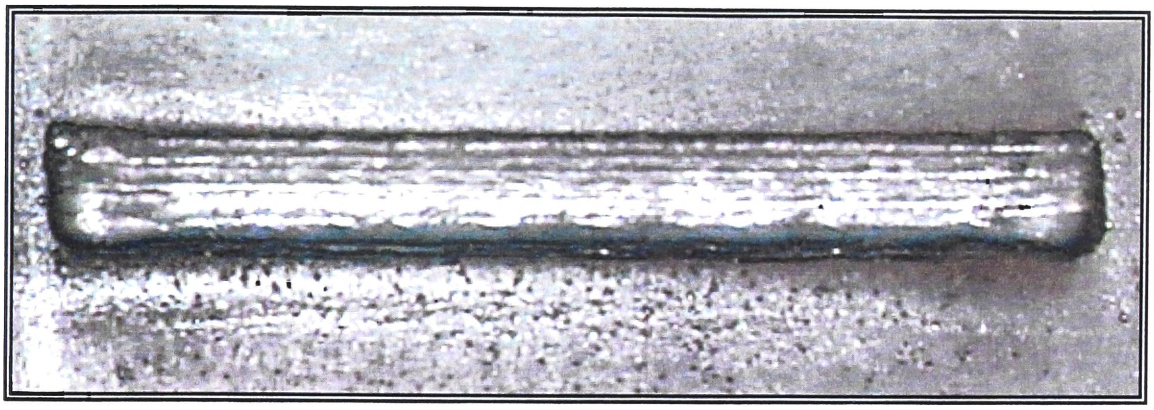

Figure 6.19

Sample s3-100-05 (Top view)

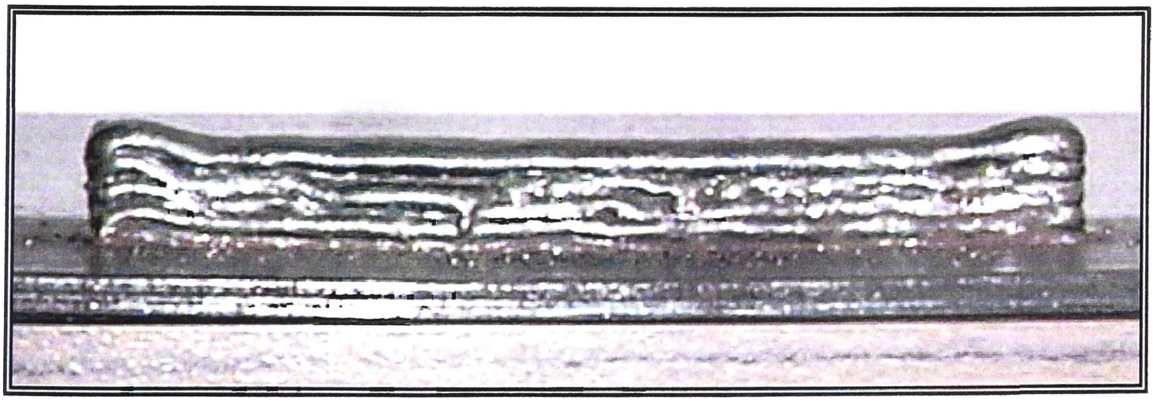

Figure 6.20

Sample s3-100-05 (Front view)

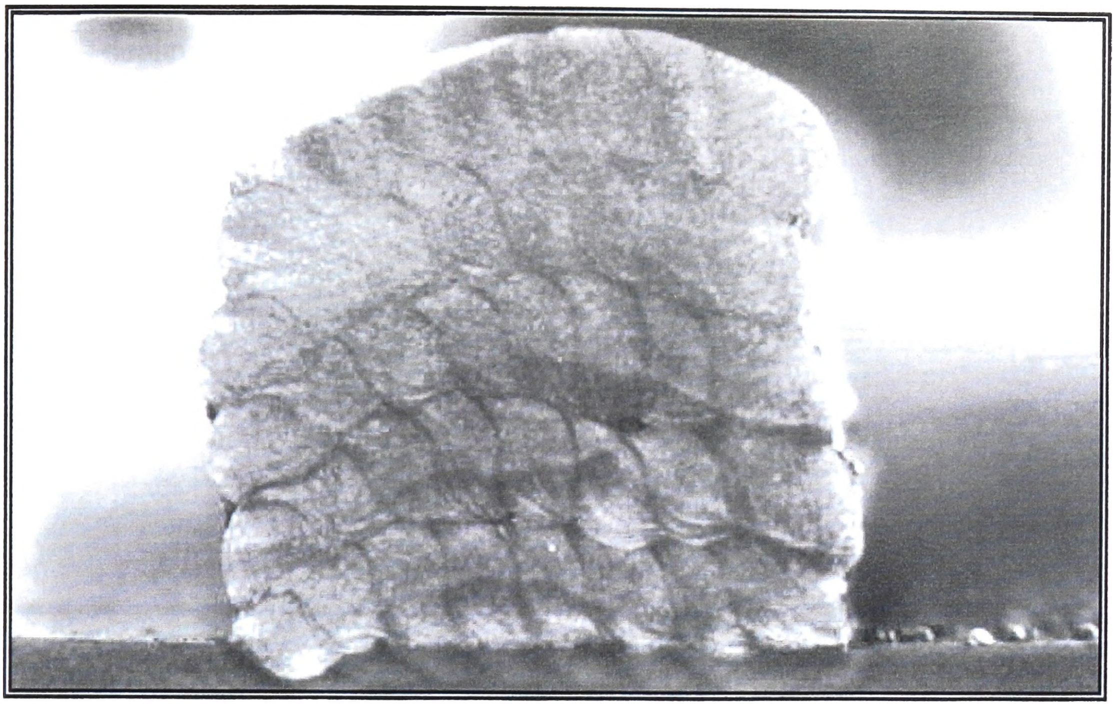

Figure 6.21

Cross-sectional macrograph of sample s3-100-05

6.5.1.5 Sample s4-75-05

Although this sample has good weld geometry (See figure 6.22 and figure 6.23), it has a problem with a lack of fusion. In addition, slags were also found inside of the porosity. It is also noted that there are some parts of the weld that do not properly fuse with the parent metal as well as between the layers.

This is caused by slag on weld, if the temperature during welding of next layer is not high enough, these contaminants will not be burnt which causes lack of fusion. This can be determined from the macrographic examination picture of the sample's cross-section. The sample has a tensile strength of 522 Mpa, hardness of

152.4 Vickers and Charpy V-notch of 215 J. The detailed description of the sample is depicted in Appendix I5.

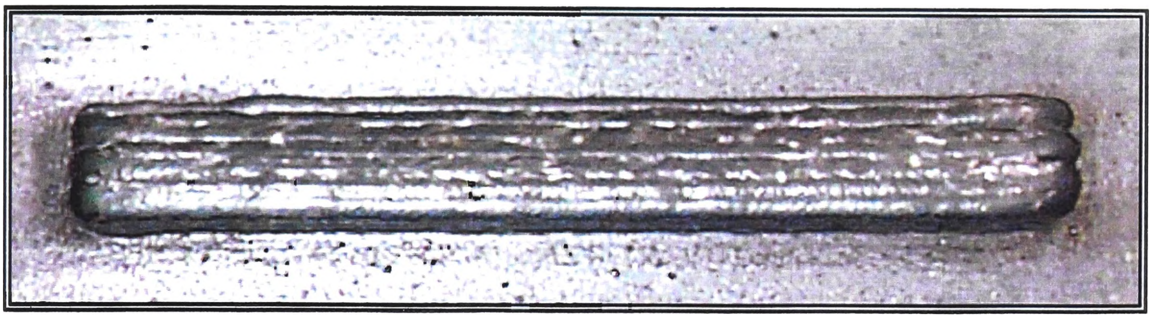

Figure 6.22

Sample s4-75-05 (Top view)

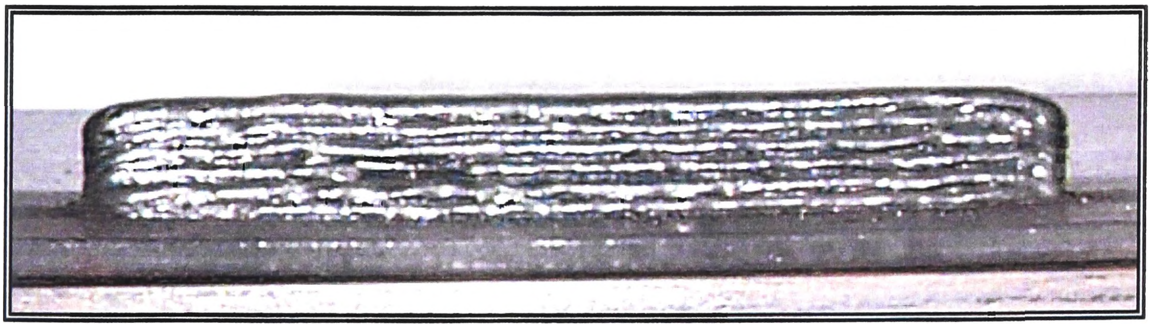

Figure 6.23

Sample s4-75-05 (Front view)

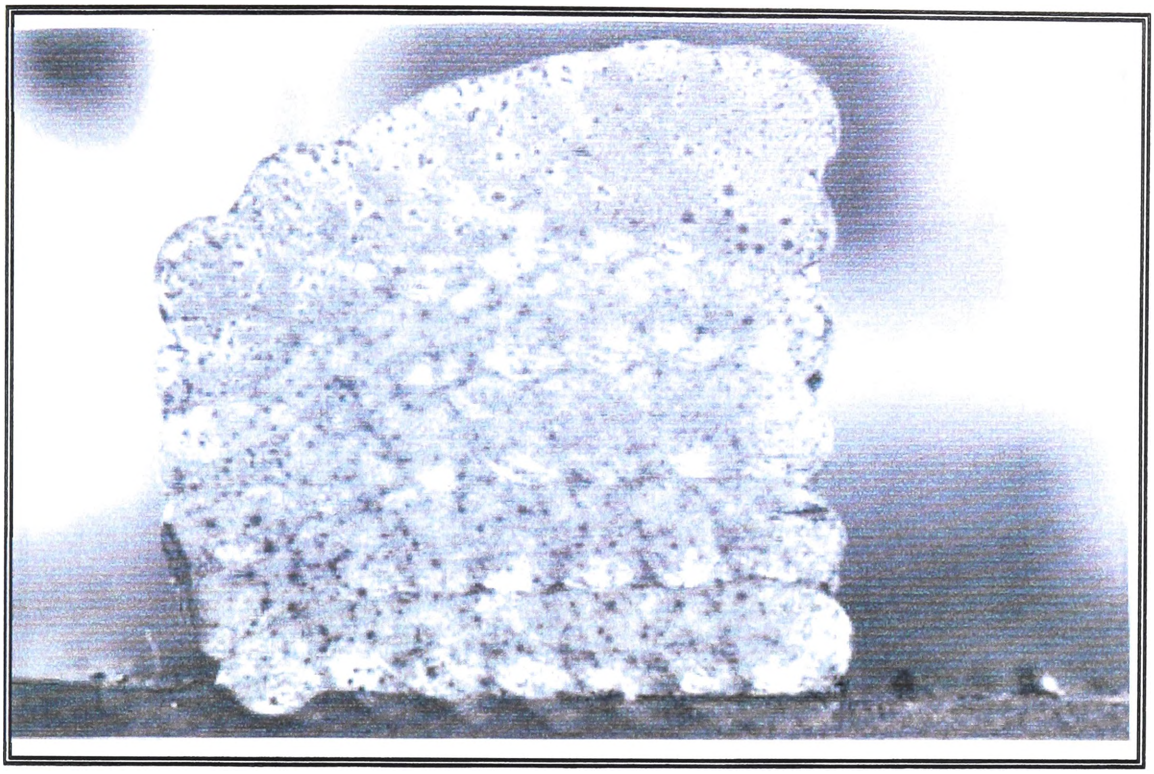

Figure 6.24

Cross-sectional macrograph of sample s4-75-05

6.5.1.6 Sample s4-100-05

Unlike the other samples, this sample indicates no physical defects such as spatters, porosity, slag and lack of fusion. This can be seen from the macrographic examination of the sample's cross-section, see figure 6.25. However, it is noted in figure 6.25 that as the heat input is increased, the weld cross-section becoming less rectangular ie. it starts losing its shape. The picture of the sample s4-100-05 is depicted in figure 6.26 and figure 6.27. The sample has a tensile strength of 486 Mpa, hardness of 150.1 Vickers and Charpy V-notch of 206 J. The detailed description of the sample is depicted in Appendix I6.

Figure 6.25

Cross-sectional macrograph of sample s4-100-05

Figure 6.26

Sample s4-100-05 (Top view)

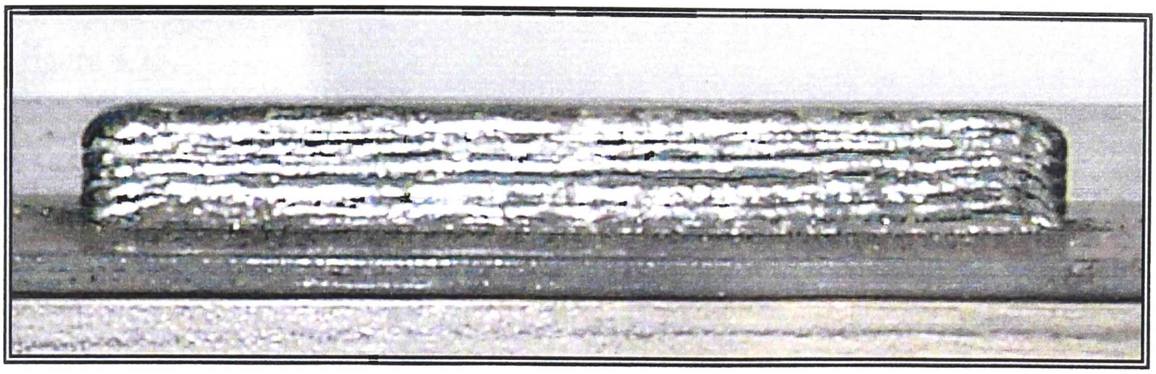

Figure 6.27

Sample s4-100-05 (Front view)

6.5.2 Discussions of the results

From the experimental results it was determined that lack of penetration or lack of fusion was a dominant problem for building-up a solid object. In addition, it is noted when the voltage is increased to have a better fusion, the solid object starts to lose its shape as well as spatter was becoming a problem in some of the samples. This can be noted in the cross-sectional view of the macrographic pictures of the solid object.

The problem of a lack of fusion in this case is because the settings used had low heat input. Nevertheless, lack of penetration and the other defects revealed for building-up a solid object did not occur for building-up a thin walled object. For example, a sample f2-75-05 (from a thin section object) was taken for a macrographic examination because it is noted that lack of penetration, porosity and slag were detected in sample s2-75-05. Note that the welding parameters of the two samples are identical. A character *'s'* is used to identify a solid from a thin section. The macrographic examination picture of the sample f2-75-05 is depicted in figure 6.28.

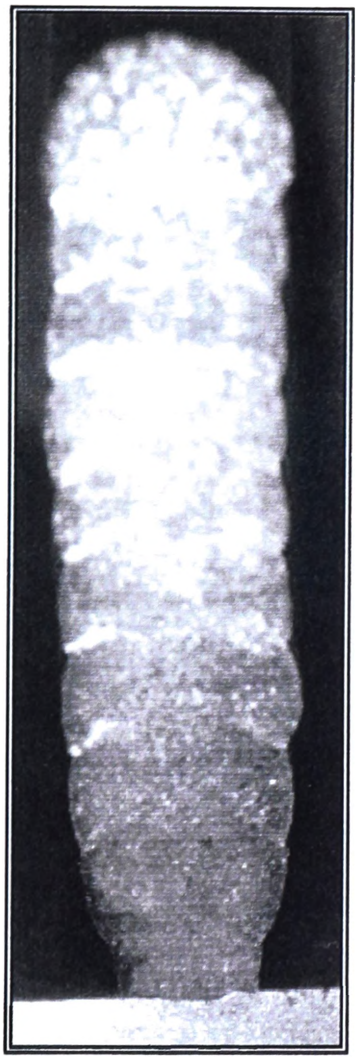

Figure 6.28

Macrographic picture cross-sectional view of sample f2-75-05

From the macrographic picture depicted in figure 6.28, it can be determined that the sample does not have defects such as lack of penetration, porosity and slag like the one determined for making a solid block (Figure 6.12). In addition, the defects could already be seen with a naked eye when the samples of the solid object were polished. However, it is noted in figure 6.28 that the first layer requires more heat input to have a better fusion with the parent metal. This would not be a problem as a setting with a higher heat input can be used for the first layer. It is also noted that when the macrographic picture of a sample s2-75-05 (See figure 6.12) was analysed, the defect does not occur at the first weld run; ie. the first weld beads column on the left of the macrographic examination picture.

The lack of fusion is predicted because the process is using low heat input. It is suspected that when the adjacent weld runs partly weld on top of the previous adjacent weld as well as to the parent metal, the part that is welding to the previous adjacent weld does not have enough heat to fuse properly with the parent metal. This can be seen from the cross-sectional view that some the bottom of the solid does not actually stick to the parent metal at all. Also internal stress and plate buckling are other factors which should be taken into considerations.

A trend was also identified from the experimental result that by increasing the heat input, apparently the lack of penetration seemed to be overcome. However, it is also noted on the other hand that as the heat input is increased the solid tends to lose its shape.

Another problem was also identified during the experiment. It was noted that there are some higher build-up is at the both ends of the solid. This can be seen clearly from the front view of samples s2-75-05, s2-100-05, s3-75-05 and s3-100-05. This problem was investigated and solved by increasing the travel speed slightly to 6 mm/sec when the robot about 5 mm from the end of the weld length of the speed is maintained until 5 mm after the new weld run. Thus a new program was made to overcome the problem. In the new program, the user can specify the suitable speed and distance. The improved program called F_BLOCKEC.PRG is depicted in Appendix H. It can be seen that by increasing the speed slightly it seemed to overcome the higher build-up at the both ends. The improvements can be seen for the samples s4-75-05 and s4-100-05.

Hardness Results

It is noted that the hardness property of several samples such as sample s2-75-05, s2-100-05, s3-75-05 was harder at the top and first layers. However, at the higher heat input settings such sample s3-100-05, s4-75-05 and s4-100-05 it is noted the hardness property is more uniform across the layers and the hardness is lower compared to the hardness at the lower heat input settings. Note that this property behaves similarly for the thin walled objects. The average hardness of the samples is given in figure 6.29.

Cleaning and Maintenance during Welding

The robot was stopped at the end of every layer for nozzle cleaning, this is to avoid blocking the gas flow. The electrode wire was also trimmed during this time to avoid arc failure at the beginning of the next layer. However, this would not be a problem in an automated robotic welding cell because there is an automatic nozzle cleaner and wire trimmer are available on the market and should be incorporated in a welding cell for this application. The coordinate system is compensated for the 5° difference between the base and the workpiece.

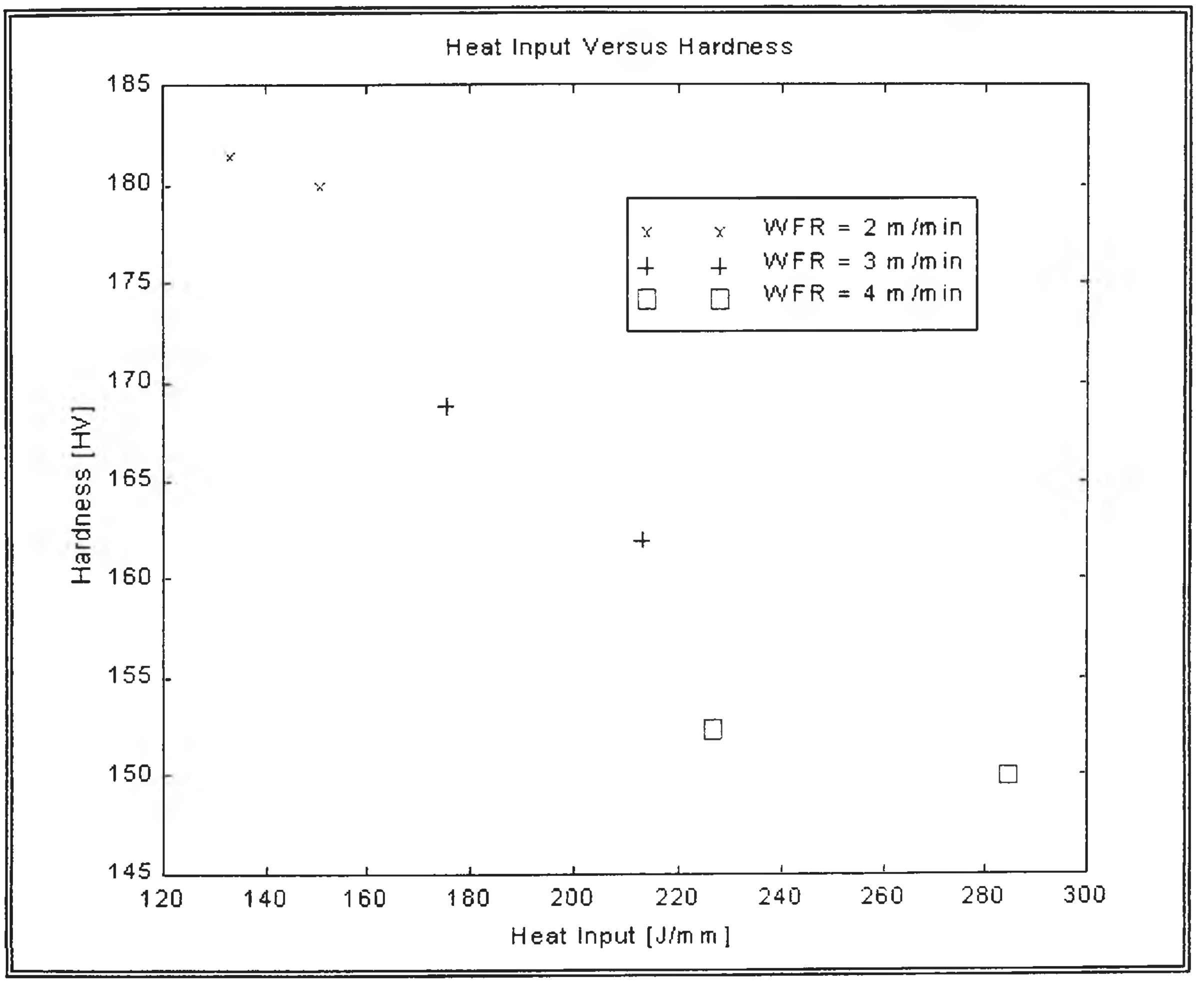

Figure 6.29

Heat input versus hardness

Tensile and Charpy V-notch Results

As it was mentioned previously that as well as taking the hardness property of the weld samples, tensile and Charpy V-notch test were also taken into considerations. The weld samples were machined to the specified dimensions for tensile and Charpy specimens according to the Australian Standard, see chapter 2.

From the tensile and Charpy results, it was determined that the weld samples are ductile. The tensile strength [Mpa], elongation [%] and energy [J] results obtained from the experiment are depicted in figure 6.30, 6.31 and 6.32 respectively. Trends could also be seen as the quality of the sample is improved, hence less defects, the tensile strength is greater, capacity of absorbing the impact is greater and the elongation also tends to increase. From the CIG weld [23] filler metal specifications, it is determined that the tensile strength is 520 Mpa, elongation is 30% and Charpy V-notch impact value is 110 Joules. However it is noted that the Charpy was performed at -20° C, however the experiment was performed at the room temperature as stated in the Australian Standard [15]. It is also noted that the tensile strength seemed to get closer to the values obtained from the CIG weld [23] as the sample quality improved with the higher heat input. It is noted that the elongation in several samples exceeded the specified values from the CIG weld [23]. Hence it can be said that the weld samples are seemed to be more ductile than what is expected to be. Although the impact values obtained seemed to be higher in comparison with the specified value in the CIG weld [23], it is important to note that the temperature where the samples were tested were also different. Therefore it is predicted the temperature much likely causes the difference in impact value. Nevertheless, the samples are expected to be tougher than the specified values as it is found to be more ductile than expected it. This can be determined from the higher elongation values obtained.

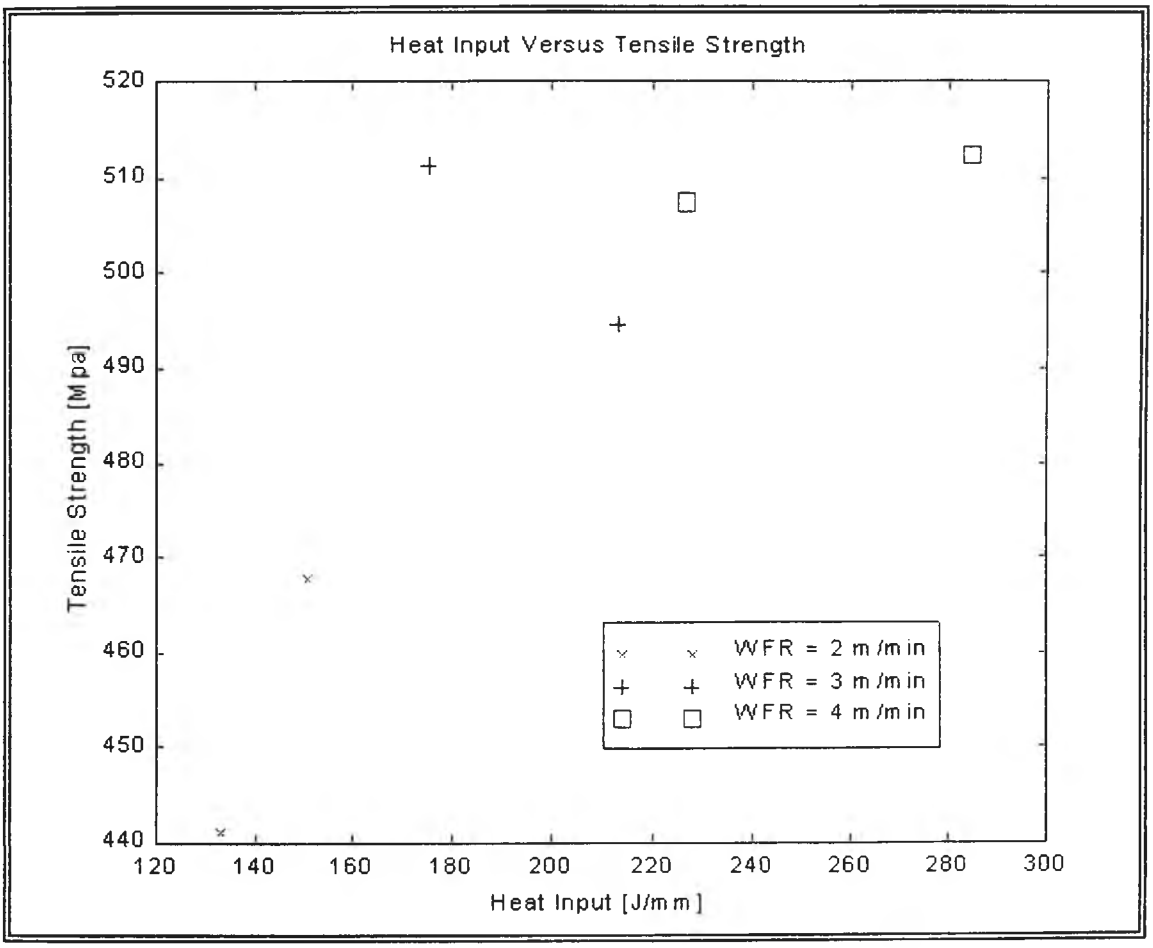

Figure 6.30

Heat input versus tensile strength

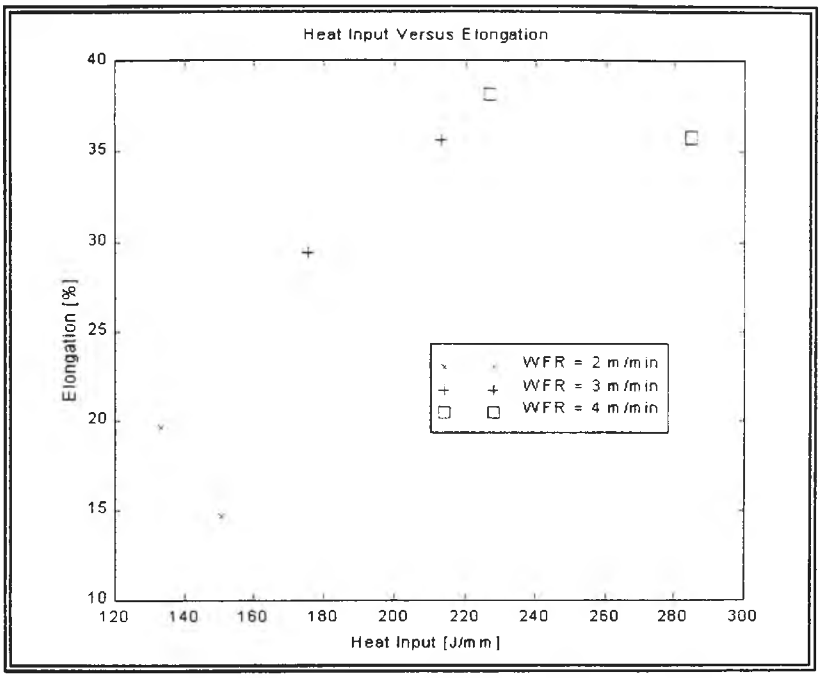

Figure 6.31

Heat input versus elongation

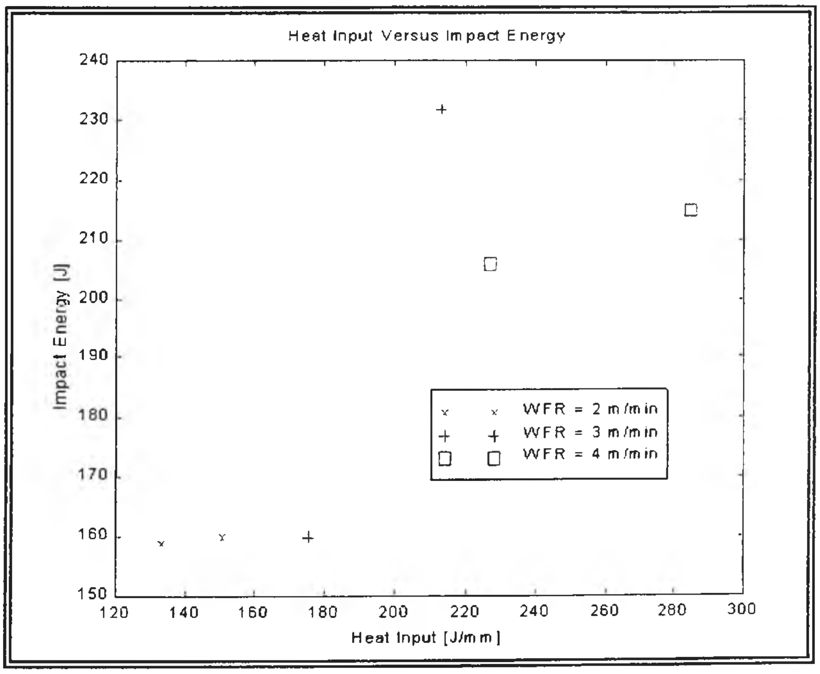

Figure 6.32

Heat input versus impact energy

6.5.3 Summary

It was determined from the experiment that a solid object requires different welding parameters from thin walled object. It is also determined that the defects mainly relate to insufficient of heat input. This is can be seen from the lack of fusion between the layers and the parent metal, and non-metallic inclusions (slag).

It is also determined that by increasing the heat input, it seemed to overcome the problems mentioned above, however it is noted that at the same time the solid seemed to failed to maintain its shape.

Therefore a better method of creating a solid must be considered. This can be achieved by using two different sets of welding parameters for the wall and the filler of the solid. The detailed description of this new method will be described further in the next section of this chapter.

6.6 Boundary Method of Creating a Solid Object

In the previous section. it was shown that a higher heat input is required to overcome the problem of lack of penetration or fusion for manufacturing solid objects. However. it was also determined that by increasing the heat input. there was a tendency of losing the shape of the solid. This is also undesirable because it is required to create a solid with a good mechanical property. free of defect which has approximately the desired shape.

Therefore another method of creating a solid object was developed to achieve the goals mentioned above. A similar program was made to create the solid, however with this program, the solid will be made with two different set of welding parameters.

The two welding parameters have different functions in the process. one set of parameters creates the outer wall and the other set of parameters fills the area inside the wall. The outer wall is created before the robot performs the filling so that the solid produced will have a good shape, as the outer wall will stop the molten weld from into forming an undesirable shape. The new program will still create the same dimensions and shape of solid as the previous method.

The methodology of the process is depicted in figure 6.33. The outer wall is drawn in red colour and the filling area is drawn in black colour (See figure 6.33).

The number of adjacent welds inside the wall area depends on the welding parameters used. Hence the wider the width of the weld, the less number of adjacent welds is required. The arrow in figure 6.33 indicates the weld direction.

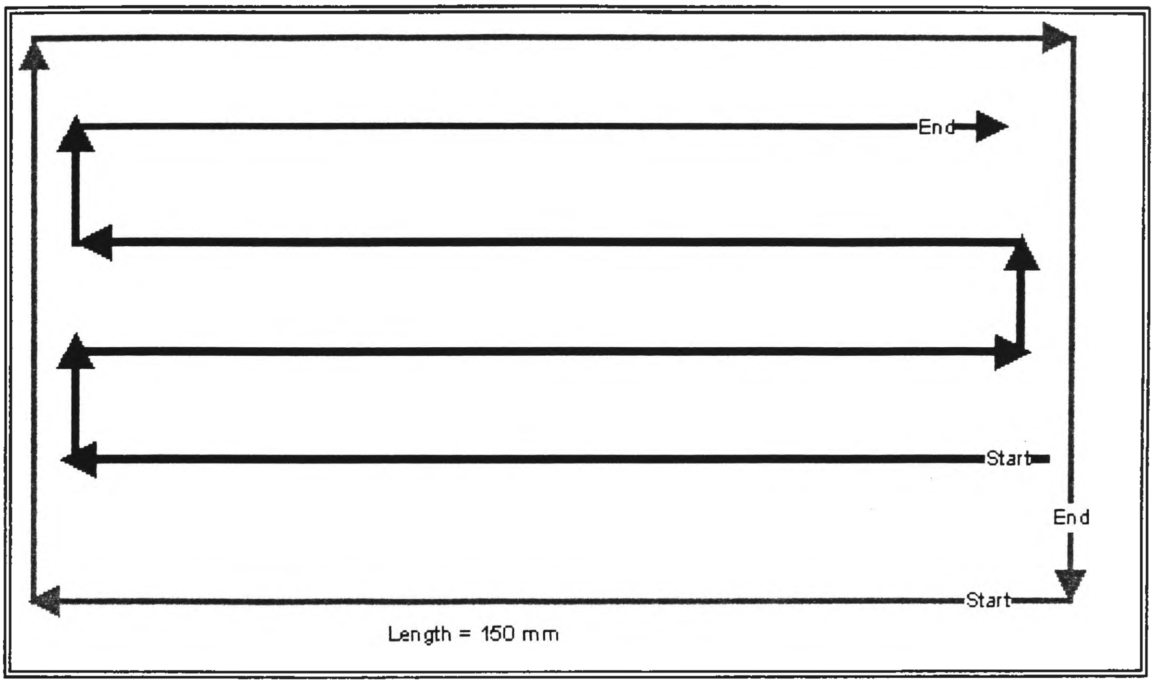

Figure 6.33

Process diagram of boundary method

The program named F_BLOIO2.PRG was made to create a solid object using this method. The program creates a preset weld length of 150 mm. Firstly, the robot creates the outer boundary wall (outer wall), and then it performs the filling inside the bounded area. The process keeps looping until the number of layers specified by the operator are completed. The layers ratio between the boundary wall and the filling area depends on the welding parameters used. For example, for particular settings, it might be required to create two layers of the boundary wall and one layer of the filling, where as in other setting it might be the opposite. The number of adjacent welds and layers for filling varies and is also dependent on the settings. Trial error was applied to investigate the right ratio for the settings used in the experiment.

After setting all of the seam data, weld data and weave data, the program is ready to run. When the user runs the program the program will prompt the following:

- Number of consecutive outer layers: When the user sees this prompt, he or she is required to enter the number of layers for the boundary wall.
- The outer layer vertical increment [mm]: When the user sees this prompt, he or she is required to enter the vertical increment. This value determines how many millimetres the robot will move up in z axis after each layer of weld is completed.
- Number of consecutive inner layers: When the user sees this prompt, he or she required to enter how many layers require for the filling area.
- Inner layer vertical increment [mm]: When the user sees this prompt, he or she is required to enter the vertical increment for the filling area. This value determines how many millimetres the robot will move up in the z axis after each layer of weld is completed.
- Width of block [mm]: When the user sees this prompt, he or she is required to enter the width for the block.
- Outer pre/post corner distance [mm]: When the user sees this prompt, he or she is required to enter the distance before and after at each end of the weld length where the robot will slightly speed up. This is to prevent a higher built-up at the both end of weld.

- Number of inner filler passes: When the user sees this prompt, he or she is required to enter how many adjacent welds inside the filling area.
- Inner start/end to wall gap [mm]: This distance specifies how far the inner weld will start and end from the weld wall. It is undesirable to start filling the area at exactly the same start position and end position as the boundary wall because it would melt the boundary wall. Having the distance too far is also undesirable because it would create a gap between the filling area and the weld wall.
- Inner pre/post corner distance [mm]: This is the same as the outer pre/post corner distance except it is now for the filling area instead of the boundary wall.
- Do you want to continue welding more layers?: After the program satisfied the conditions above, it will prompt the user if he or she wishes to continue welding more layers. In the case of 'YES', the program would prompt the above statement again. However, it remembers its last positions, so that it would keeps on building up the thickness. In the case of 'NO' the robot would go back to the home position.

The program F_BLOIO2.prg is depicted in Appendix H.

6.6.1 The Experimental Results

There are three samples observed in the experiment, these samples are:

- Sample s2-75-05/s4-100-05
- Sample s2-100-05/s5-100-05
- Sample s4-100-05/s8-150-05

The first set of coding represent the outer wall parameters and the second set of coding represent the filling parameters. The experimental results obtained for each sample will be described in the next sections.

6.6.1.1 Sample s2-75-05/s4-100-05

This sample has a good weld geometry, however some porosity with inclusions are still detected in a particular area of the solid, ie. the last adjacent weld runs where inner filler meets the boundary wall. This can be seen clearly from the macrographic picture depicted in figure 6.34. The picture of the top and front view of the solid block is depicted in figure 6.35 and 6.36. For this sample, it was required to have two layers of outer wall to have the same thickness of one layer of the inner filler in every consecutive run. The sample has a tensile strength of 509 Mpa, hardness of 152 Vickers and Charpy V-notch of 216 J.

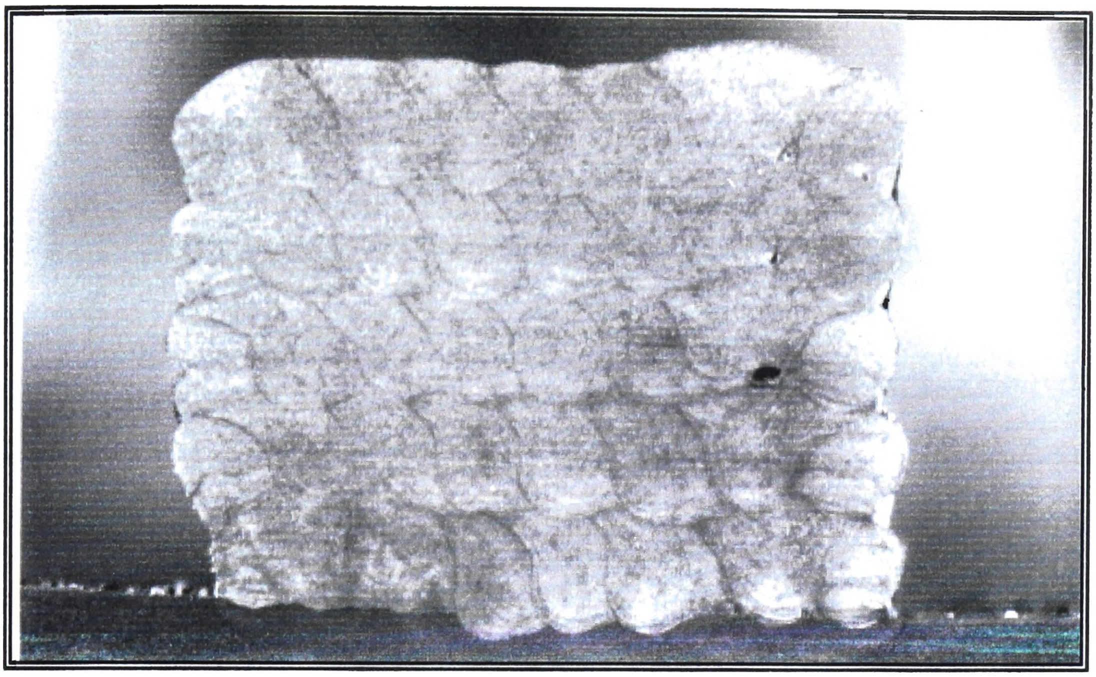

Figure 6.34

Cross-sectional macrograph of sample s2-75-05/s4-100-05

Figure 6.35

Sample s2-75-05/s4-100-05 (Top view)

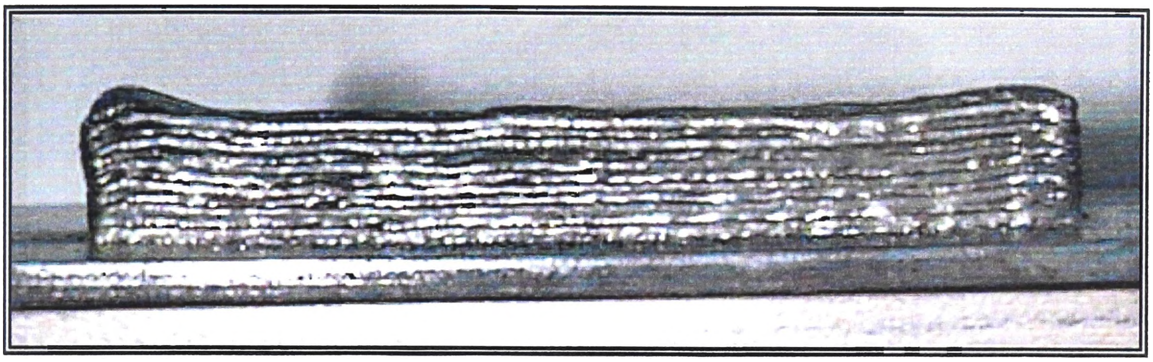

Figure 6.36

Sample s2-75-05/s4-100-05 (Front view)

6.6.1.2 Sample s2-75-05/s5-100-05

This sample still has a reasonably good weld geometry, however some porosity with inclusions are still detected in a particular area of the solid, ie. the last adjacent weld runs where inner filler meets the boundary wall. Note that the defects occurred approximately in the same area as the previous sample. This can be seen clearly from the macrographic picture depicted in figure 6.37. The picture of the top and front view of the solid block is depicted in figure 6.38 and 6.39. For this sample, it was required to have two layers of outer wall to have the same thickness of one layer of the inner filler in every consecutive run. The sample has a tensile strength of 500 Mpa, hardness of 151.4 Vickers and Charpy V-notch of 218 J.

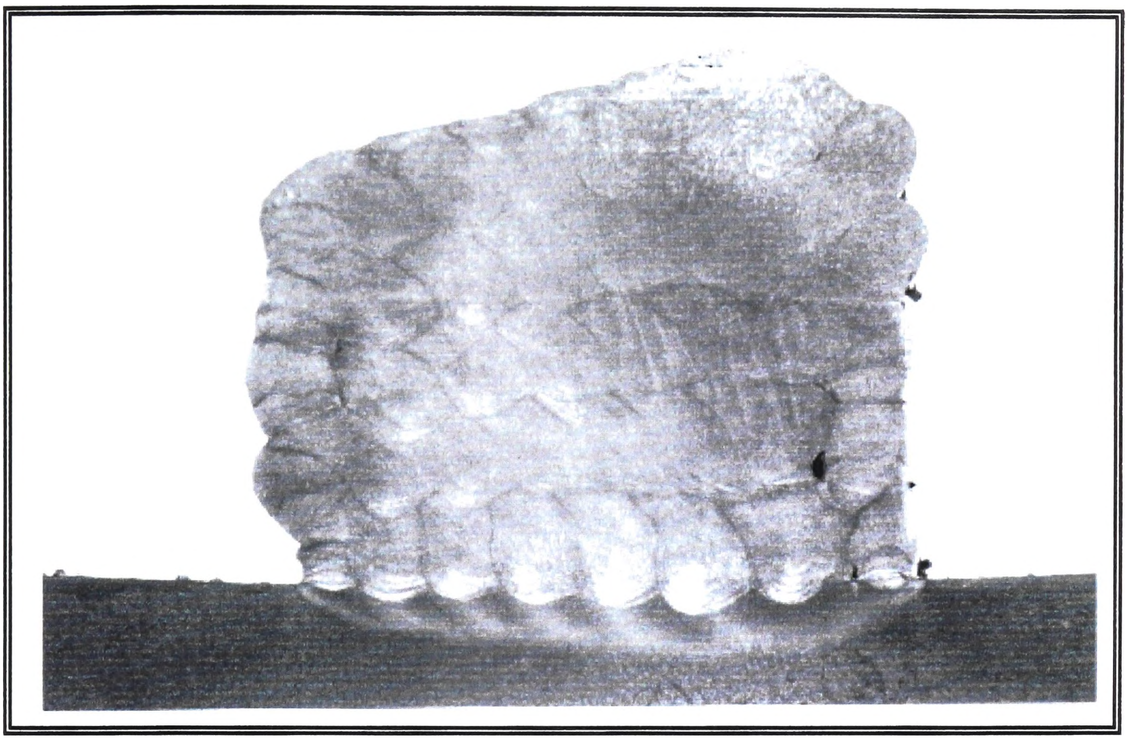

Figure 6.37

Cross-sectional macrograph of the sample s2-75-05/s5-100-05

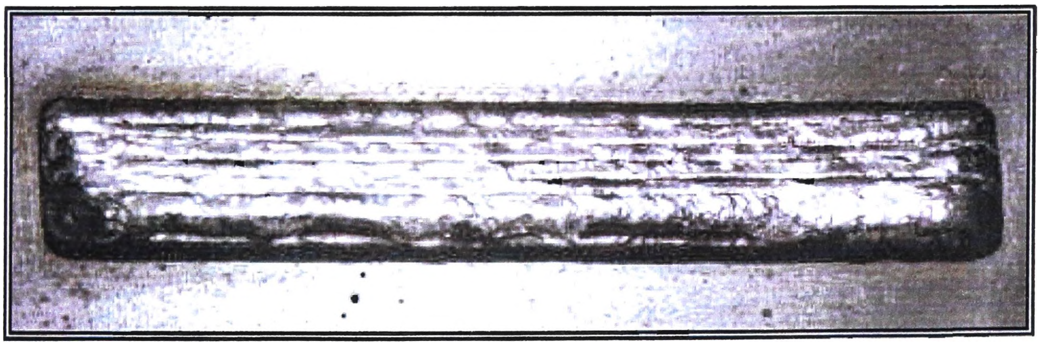

Figure 6.38

Sample s2-75-05/s5-100-05 (Top view)

Figure 6.39

Sample s2-75-05/s5-100-05 (Front view)

6.6.1.3 Sample s4-100-05/s8-150-05

This sample has good weld geometry and no defect was identified. This can be seen clearly from the macrographic picture depicted in figure 6.40. The filler setting used for this sample is no longer in a short-circuit mode as the previous sample but it is in the spray transfer mode. Thus a much higher heat input is used for the filler setting. The picture of the top and front view of the solid block is depicted in figures 6.41 and 6.42. For this sample, it was required to have one layer of outer wall to have the same thickness of one layer of the inner filler in every consecutive run. The sample has a tensile strength of 514 Mpa, hardness of 150.8 Vickers and Charpy V-notch of 214 J.

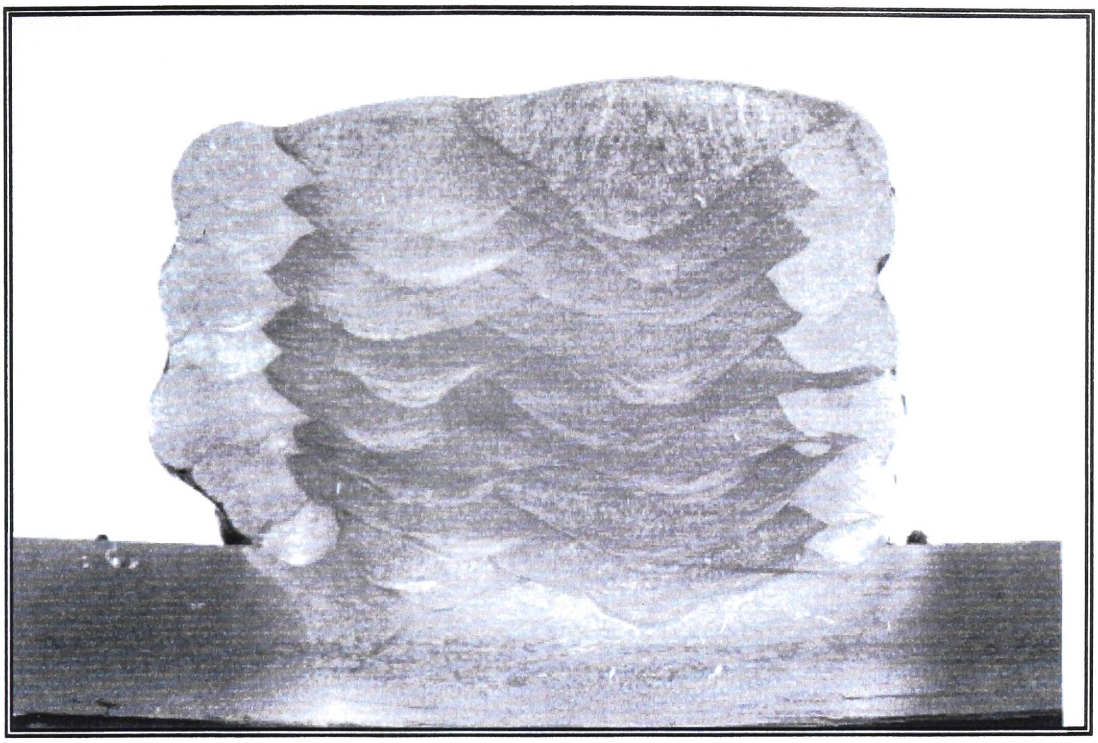

Figure 6.40

Cross-sectional macrograph of the sample s4-100-05/s8-150-05

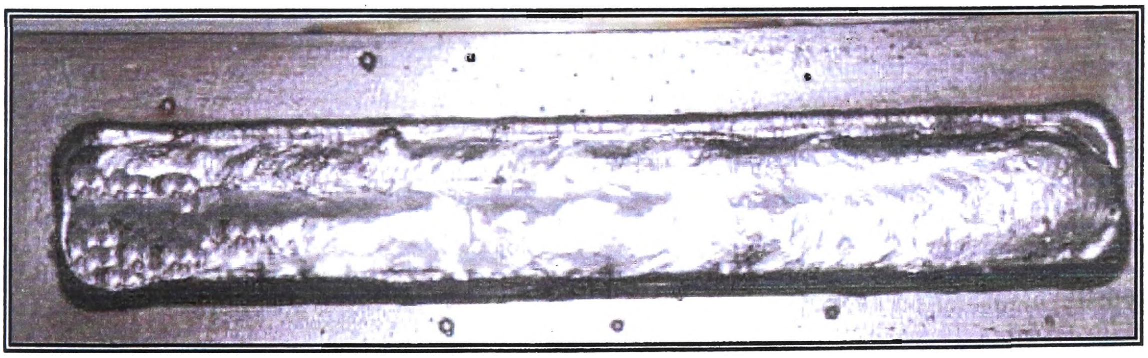

Figure 6.41

Sample s4-100-05/s8-150-05 (Top view)

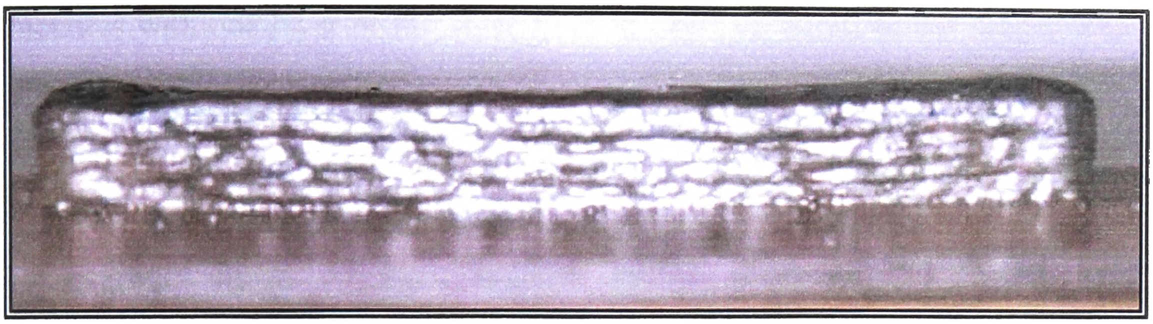

Figure 6.42

Sample s4-100-05/s8-150-05 (Front view)

6.6.2 Discussions of the results

From the previous method (Non-boundary method), it was determined that a higher heat input was required to eliminate lack of fusion or penetration problem. However, it was also determined that by increasing the heat input seemed to jeopardise the shape, ie. It is no longer maintaining its rectangular shape, this can be noted from the macrographic picture of the cross-sectional view of the sample. There are three samples made using the boundary method (See paragraphs below) and travel speed of 5 mm/sec was used through out the experiments.

Sample s2-75-05/s4-100-05 and Sample s2-75-05/s5-100-05

For sample s2-75-05/s4-100-05, the outer layer was made by using setting s2-75-05 to create the boundary wall and the inner filler setting used was s4-100-05. The two settings above were selected because s2-75-05 is one of the suitable settings for a thin wall and s4-100-05 was a setting found from the non-boundary method which was free of defect. Two outer layers are required obtaining an equal thickness with one layer of the inner filler in every consecutive run. There were five consecutives runs performed to obtain the thickness required.

The solid shape obtained from these settings was quite good. however unfortunately there is still porosity with inclusions detected as is shown in the figure 6.34. It is noted that the porosity occurred in a particular area of the solid, where the last weld run of the inner filler meets the outer wall. It is predicted that this is because all the contaminants from the previous runs accumulate in this area as they have no where else to go. However at the last weld run of the filler, there was no sufficient heat to burn these contaminants, thus resulting in a form of porosity with non-metallic inclusions inside the porosity.

Therefore, it was decided to increase the inner filler setting slightly using setting s5-100-05 with the same outer setting (s2-75-05). From the experimental results it is noted that the solid shape is not as rectangular as the previous setting and also porosity with non-metallic inclusions were still detected. This result gives a fairly good indication that it is required to have a much higher heat input for the filler setting to overcome this problem.

<u>Sample s4-100-05/s8-150-05</u>

The heat input for the filler settings is increased significantly in comparison to the previous two samples. This is achieved by increasing the filler setting with the wire feed rate to 8 m/min and a voltage of 30 volts, results in a setting s8-150-05.

From the result, it was found that the problem of porosity with inclusions was eliminated. This can be seen clearly from the macrographic picture of the sample depicted in figure 6.40.

It was found that the spray transfer is more suitable to be used for the filler as it is fairly stable and has sufficient heat input to burn the contaminants as well as having good penetration. Also the weld bead was a lot wider so that it was only required to have two adjacent weld runs to cover the same area.

It is also noted from the experiment that in conjunction with using spray transfer mode for the filler, it is required to have a sufficient outer wall thickness to absorb the heat. Trials were made by using lower settings for the outer wall like one used in the previous samples and it was found that the outer wall was completely melted.

Cleaning and Maintenance during Welding

It was also required to stop the robot from welding at the end of every consecutive layer for cleaning of the nozzle to avoid gas blockage. The electrode wire was also trimmed during this time to avoid arc failure at the beginning of the next layer. In addition, extra cooling time of approximately two minutes was required when spray mode was used for the filler as it is noted that the surface of the weld was red hot (Approximately 880 °C) at the end of every consecutive run. However, bear in mind that in the experiments, a fairly small solid object was made and also the thickness of the base plate is only 6 mm. For industrial applications, wear replacement is used for repairing larger objects. In this case the heat would be absorbed quickly by the large part. Therefore a high surface temperature would not be a problem for these applications.

Hardness results

The hardness was measured along the cross-sectional surface of the weld. From the hardness measurement, it was determined that the hardness of the samples is fairly uniform across the surface. Also the hardness obtained for each of the samples is fairly similar too. The results obtained is given below:

- Sample s2-75-05/s4-100-05 = 152 HV
- Sample s2-75-05/s5-100-05 = 151.4 HV
- Sample s4-100-05/s8-150-05 = 150.8 HV

From the conversion table [30] it is determined that 150 HV is approximately equal to the tensile strength of 481 Mpa and it is known that the filler metal [23] has tensile strength of 520 Mpa. Consider some factors of experimental errors, this result is within 10% error.

Tensile and Charpy V-notch Results

The tensile and Charpy V-notch tests were also performed with the same apparatus and procedures as the previous samples. Tensile strength obtained from the experiment of each of the samples is shown in the following below:

- Sample s2-75-05/s4-100-05 = 509 Mpa
- Sample s2-75-05/s5-100-05 = 500 Mpa
- Sample s4-100-05/s8-150-05 = 514 Mpa

Elongation obtained from the experiment of each of the samples is shown in the following below:

- Sample s2-75-05/s4-100-05 = 43.3 %
- Sample s2-75-05/s5-100-05 = 36.1 %
- Sample s4-100-05/s8-150-05 = 36.7 %

These results show that the values of the tensile strength obtained is similar to the one specified in the CIG weld [23]. It is specified the tensile strength of the electrode wire is 520 Mpa. From the results obtained in the experiment and considering some experimental errors, it can be said that the tensile strength property does not change greatly during the process.

It is also found that the elongation values obtained from the experiment are also similar to the one specified in the CIG weld [23]. The property of elongation of the electrode wire specified is 30 %. In the experiment the three samples above indicate that the values obtained were slightly higher than 30 %. Thus it can be determined that this property also does not change greatly during the process.

The Charpy results obtained from the experiment of each of the samples is shown in the following below:

- Sample s2-75-05/s4-100-05 = 216 Joules
- Sample s2-75-05/s5-100-05 = 218 Joules
- Sample s4-100-05/s8-150-05 = 215 Joules

It can also be determined from the Charpy results that the three samples above have similar toughness. Although it seems these results are a lot higher from the specified value (110 Joules), comparison cannot be made as the experiment was conducted in different temperature. In the experiment the Charpy test was done at the room temperature, whereas in the CIG weld [23], the Charpy test was done at -20 °C.

From the tensile and Charpy tests, it can be determined that the samples were very ductile. Also the impact values obtained from the Charpy V-notch test indicated that the samples were quite tough as it could absorb a lot of energy.

Therefore according to the experimental results obtained, it can be determined that mechanical property of the electrode wire does not change greatly during the welding process. Thus it can be said that assuming the solid block does not have defects, its mechanical property would be similar to the mechanical property of the electrode wire. Also from the experiment, the building-up of solid object for wear replacement application was proven to be feasible.

6.6.3 Summary

The boundary method was found to be a better method to use for building-up a solid object because this method allows the solid to be made using two different set of welding parameters. One of the parameters is to create the outer wall (boundary wall) and the other parameter is to fill the bounded area. It is also found that by increasing the heat input the lack of penetration and porosity with non-metallic inclusions were eliminated. Thus using this method had successfully made a solid with a good shape without any physical defect.

It was also found that a suitable setting of the thin walled objects could be used for the outer wall to give smooth surface finish as well as maintaining a good shape of the solid. It was also found that spray transfer is a more suitable setting to be used for the filling area. The reason is because in spray transfer mode, the process is fairly stable, has sufficient heat input to burn the contaminants as well as having good penetration and has a much wider weld bead so that less weld runs are required to fill the area.

Chapter 7

Conclusions and Further Research

7.1 Conclusions

In this thesis, it has been established that robotic GMAW can be used for rapid prototyping and wear replacement applications. Also, it is proven that the IRB 1400 robot and its accessories were capable of achieving a good quality weld for these applications.

The synergic power supply used in the experiment proved to be suitable welding power supply for the rapid prototyping and wear replacement applications. The weld quality obtained from the synergic welding power supply is better than the weld quality obtained from the conventional power supply. In addition, it can be said that a conventional power supply failed to produce a good quality weld required for the applications.

A Thin Walled Object

In this thesis, the range of suitable settings for building-up thin walled objects were determined. These parameters were found to be within a narrow range. It was also determined that the suitable settings are in the short-circuit transfer mode. Globular transfer mode was found to be unsuitable for rapid prototyping applications because many of defects occur in this mode. In addition, it is also found that when the surface temperature reached approximately 550° C and above, defects such as spatter, excess material and porosity are likely to occur.

A Solid Object Build-up

The method of making a solid object, for example for wear replacement applications, has been established in this thesis by using the boundary method. The boundary method was found to be a suitable method for this application. This method is using two sets of welding parameters, one for the outer wall and one for the filling area. It was found that the suitable settings established for a thin section object can be used for the outer wall of the solid object. It was also shown that the filling area required a setting in the spray transfer mode to overcome the lack of penetration and porosity with non-metallic inclusions.

7.2 Further Research

Further research of this thesis can be expanded into the following areas:

- Further research in finding more suitable settings for building-up a solid object should be investigated, especially suitable settings for spray transfer mode for the fill.
- Further research for finding more productive settings for building-up a thin walled object with a faster travel speed should be investigated.
- A range of materials such as aluminium, stainless steel and other commonly used materials should be investigated for their suitability for rapid prototyping process.
- Further experiments with other shapes with sharp corners should be investigated to overcome the problem of weld build-up on the corner.

7.3 Recommendation of Modification of Experiment Facility

- An automatic cleaning station for the nozzle cleaner and wire trimmer should be purchased to have a fully automatic process.
- A modification of cooling system of the existing welding gun should be investigated as the nozzle tends to overheat in a spray transfer mode.

References

[1] Norrish John. "Advanced Welding Processes ", IOP Publishing Ltd 1992, pp. 1-17

[2] MATL 407 Introduction to Materials Welding and Joining Lecture Notes 1997, pp. 1-1 - 1-27

[3] Cary Howard B. "Modern Welding Technology", Prentice Hall, Inc 1979, pp. 1-13, 102-192

[4] Gourd L.M. "Principles of Welding Technology", Edward Arnold Ltd 1986, pp. 8-37

[5] Houldroft P.T. "Welding Process Technology", Cambridge University Press 1977, pp. 229-230

[6] Kearns W.H. (editor), "Welding Handbook Seventh Edition Volume Two", American Welding Society 1978, pp.113-152

[7] Fuller James L, "Robotics Introduction, Programming, and Projects", Macmillan Publishing Company, a division of Macmillan, Inc. 1991, pp.1-77

[8] Klafter, "Robotic Engineering an Integrated Approach", Prentice Hall Inc. 1989

[9] Besel Michael N., "Microsoft Encarta 96 Encyclopedia", Microsoft 1996

[10] Wohlers Terry T, "What is Rapid Prototyping?", 1995, [Online, accessed 12/02/1998]. URL: http://lamar.colostate.edu/~wohlers/rp.html

[11] American Welding Society 1989 Welding Handbook (vol 1 Welding Technology) 8th edition

[12] Jamesion Ron and Herbert Hacker, "Direct Slicing of CAD Models for Rapid Prototyping, 1995 [Online, accessed 12/02/1998]. URL: http://www.mcb.co.sevices/conferen/dec95/rapidpd/jamieson/jamieson.htm

[13] Ribeiro F and Norrish J, "Rapid Prototyping using robotic welding - slicing system development", 1996, [Online, accessed 15/02/1998]. URL: http://www.dei.uminho.pt/~fernando/eps/pm-guima.zip

[14] Ribeiro F, "Simulation Figure", 1997, [Online, accessed 15/02/1998]. URL: http://www.dei.uminho.pt/~fernando/gifs/rp/tese-fim.gif

[15] AS 1544.2-1989, "Australian Standard Methods for impact tests on metals Part 2: Charpy V-notch", Standards Association of Australia 1989, pp.7-9

[16] AS 1391-1991, " Australian Standard Methods for tensile testing of metals", Standards Association of Australia 1991, pp. 7-9

[17] Fenner, A.J, "Mechanical Testing of Materials", William Clowes and Sons Limited London 1965, pp. 4-5, pp. 26-29, pp. 101-103

[18] AS 1817-1991, "Metallic Materials-Vickers Hardness Test", Standards Association of Australia 1991, pp.4-7

[19] ABB Flexible Automation, "Product Manual IRB 1400", ABB Robotics Products ABB AB S-721 68 Vasteras Sweden, Chapter 2, pp.3-30

[20] Lincoln Electric, "Invertec Power Wave™ 450 Robotic Operator's Manual", Lincoln Electric 22801 St. Clair Ave. Cleveland, Ohio 44117-1199 USA, pp.B-3, pp. C-1

[21] Sabo Richard S, "The Procedure Handbook of Arc Welding", The Lincoln Electric Company 13th Edition December 1994, pp. 1.2-1

[22] CIGWELD, "Pocket Guide Welding Consumables Reference", Comweld Group Pty.Ltd. 1997, pp. 116-117, 307-309

[23] CIGWELD, "Technical Product Manual", Comweld Group Pty.Ltd. 1997

[24] Hitachi M6060II manual, pp 2 - 10

[25] The Lincoln Electric Company, Ohio, USA. July 1986. "IDEAL ARC® DC-400 product manual", Lincoln® Welders, pp.4

[26] ABB Flexible Automation, "User's Guide IRB 1400", ABB Robotics Products ABB AB S-721 68 Vasteras Sweden, pp.4-10 - 4-11, 15-6 - 15-7

[27] ABB Flexible Automation, "Rapid Reference Manual IRB 1400", ABB Robotics Products ABB AB S-721 68 Vasteras Sweden, pp.13-seamdata-1 - 13-seamdata-9, 13-weavedata-1 - 13-weavedata-7, 13-welddaata-1 - 13-welddata-8

[28] BHP Hot Rolled and Structural Steel Products 98 edition

[29] Lam Yim Ming, "Parameter Prediction for Rapid Prototyping and Wear Replacement by Robotic GMAW", Honours Bachelor of Engineering Thesis, Department of Mechanical Engineering University of Wollongong 1998

[30] British Steel, "Iron and Steel Specifications 7th edition", pp.344

[31] Granjon H, " Fundamentals of Welding Metallurgy", Woodhead Publishing Ltd, 1991, pp.

[32] British Standards Institution 1983 BS 499: Part 1 (Welding Terms and Symbols, Glossary of Welding, Brazing and Thermal Cutting)

[33] Do Khac Duc, "Adaptive Control of Robotic Gas Metal Arc Welding Process", Honours Masters of Engineering Thesis, Department of Mechanical Engineering University of Wollongong 1998

Appendix A

Preliminary Experimental Results

A1 Wire Feed Rate of 3 metre/minute

A2 Wire Feed Rate of 4 metre/minute

A3 Wire Feed Rate of 5 metre/minute

A4 Wire Feed Rate of 6 metre/minute

A5 Wire Feed Rate of 7 metre/minute

A6 Wire Feed Rate of 8 metre/minute

A7 Wire Feed Rate of 9 metre/minute

A8 Table Data

A1 Wire Feed Rate of 3 metre/minute

Sample p-17-03-05-4

Data:

Voltage [V]	17	Weld width [mm]	7.2
Wire feed rate [m/min]	3	Stand-off at layer 1 [mm]	15
Travel speed [mm/sec]	5	Stand-off at layer 10 [mm]	17
Number of layers	10	Temperature at layer 10 [deg.C]	230
Weld height [mm]	15	Pinch setting	4

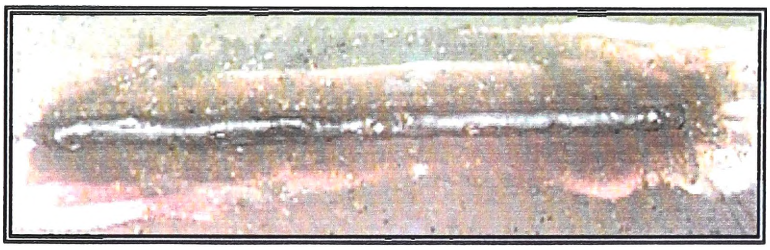

Figure A1-1

Sample p-17-03-05-4 (Top view)

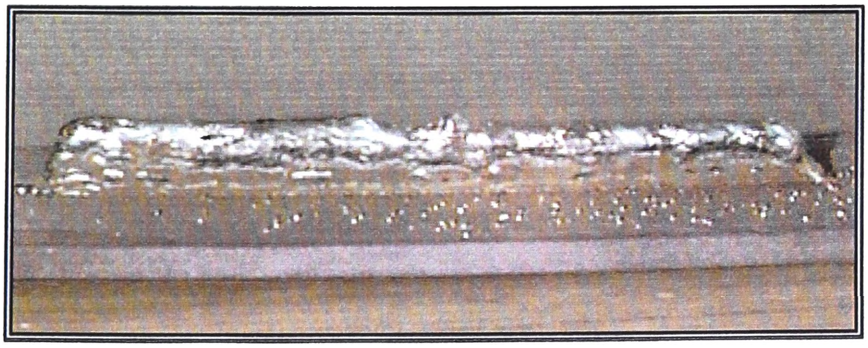

Figure A1-2

Sample p-17-03-05-4 (Front view)

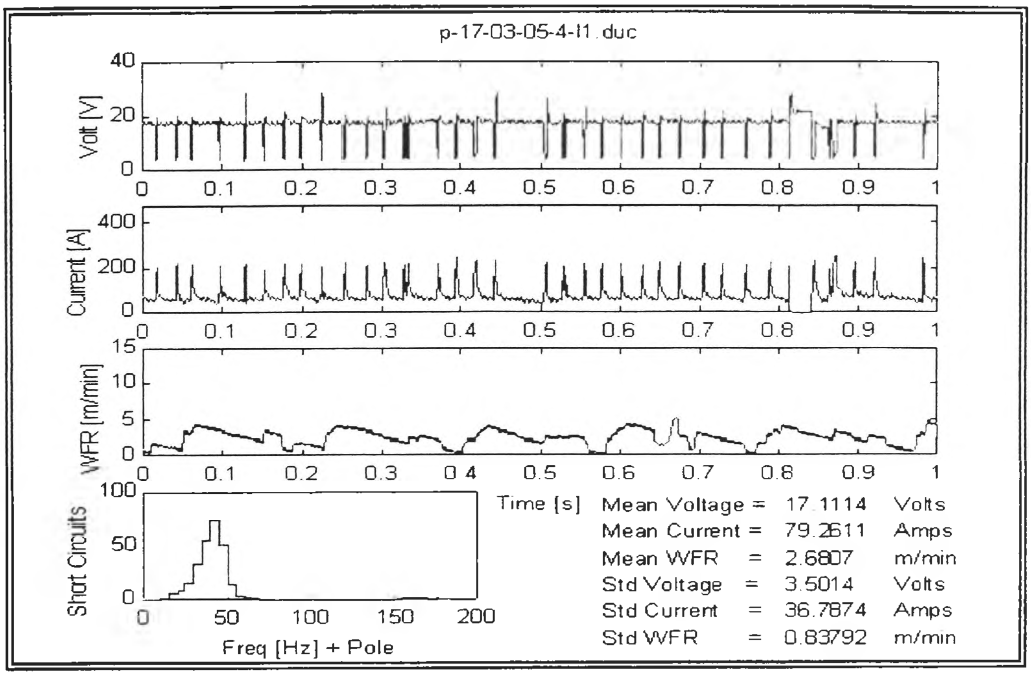

Plot A1-1

Sample p-17-03-05-4-layer 1

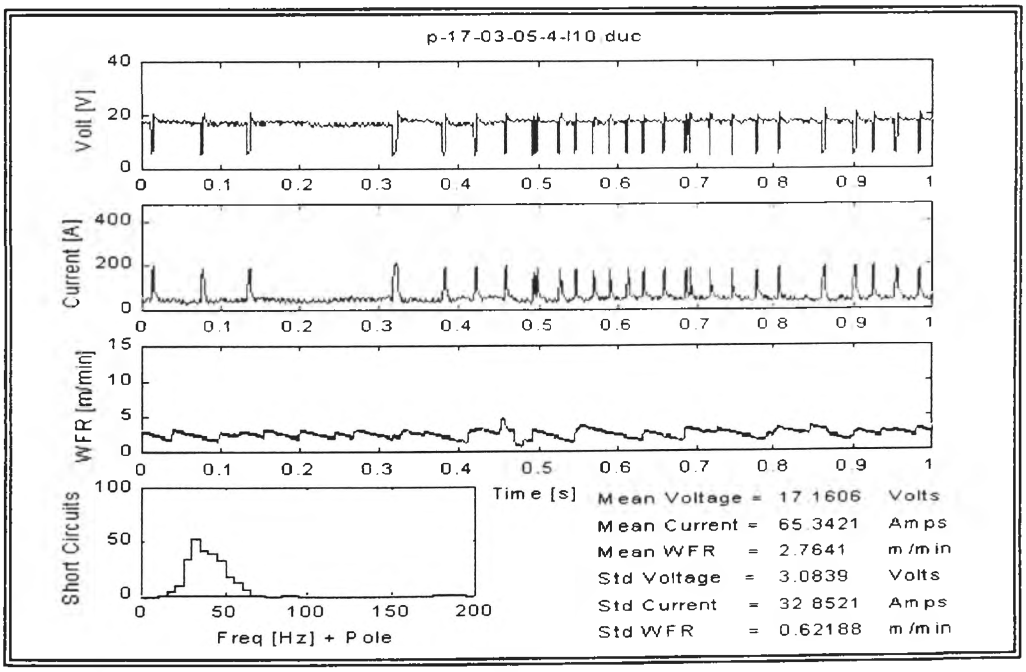

Plot A1-2

Sample p-17-03-05-4-layer 10

Sample p-18-03-05-4

Data:			
Voltage [V]	18	Weld width [mm]	6.8
Wire feed rate [m/min]	3	Stand-off at layer 1 [mm]	15
Travel speed [mm/sec]	5	Stand-off at layer 10 [mm]	20.5
Number of layers	10	Temperature at layer 10 [deg.C]	273
Weld height [mm]	14.5	Pinch setting	4

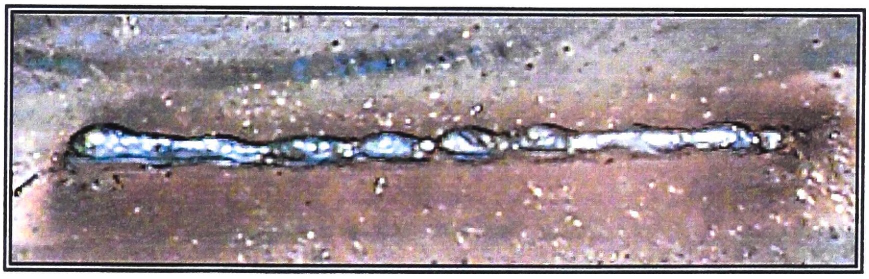

Figure A1-3

Sample p-18-03-05-4 (Top view)

Figure A1-4

Sample p-18-03-05-4 (Front view)

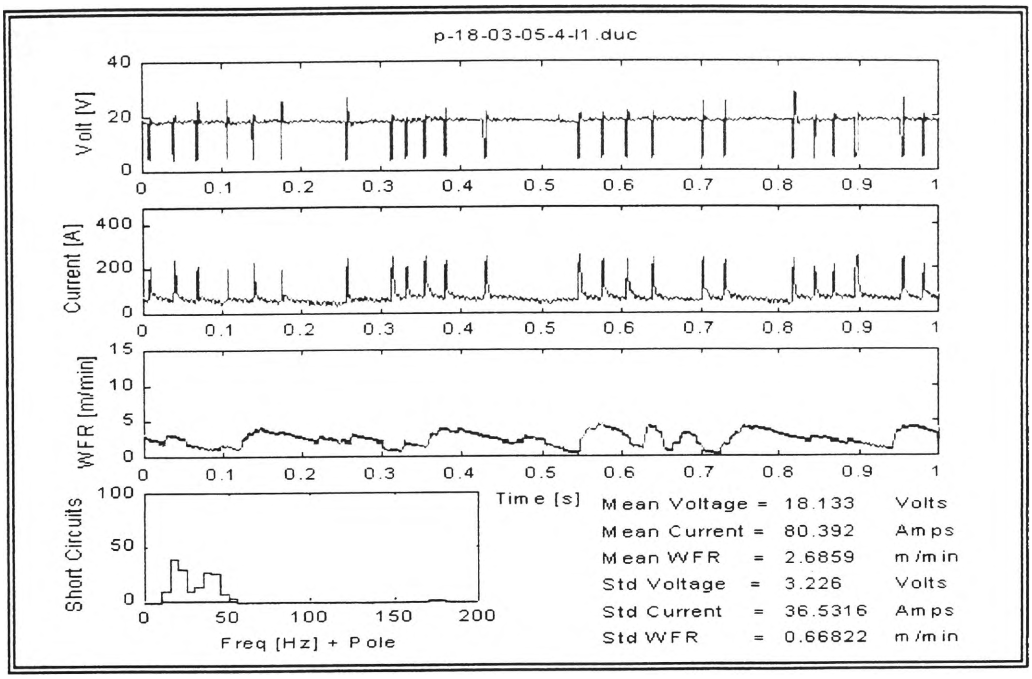

Plot A1-3

Sample p-18-03-05-4-layer 1

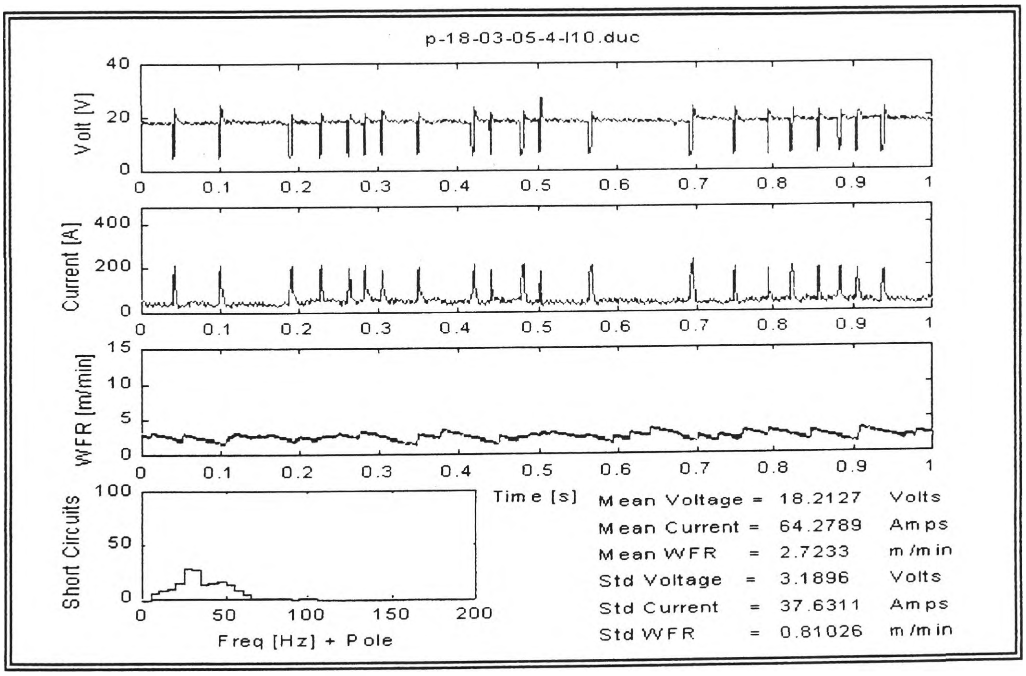

Plot A1-4

Sample p-18-03-05-4-layer 10

Sample p-19-03-05-4

Data:			
Voltage [V]	19	Weld width [mm]	6.8
Wire feed rate [m/min]	3	Stand-off at layer 1 [mm]	15
Travel speed [mm/sec]	5	Stand-off at layer 10 [mm]	21
Number of layers	10	Temperature at layer 10 [deg.C]	350
Weld height [mm]	14.4	Pinch setting	4

Figure A1-5

Sample p-19-03-05-4 (Top view)

Figure A1-6

Sample p-19-03-05-4 (Front view)

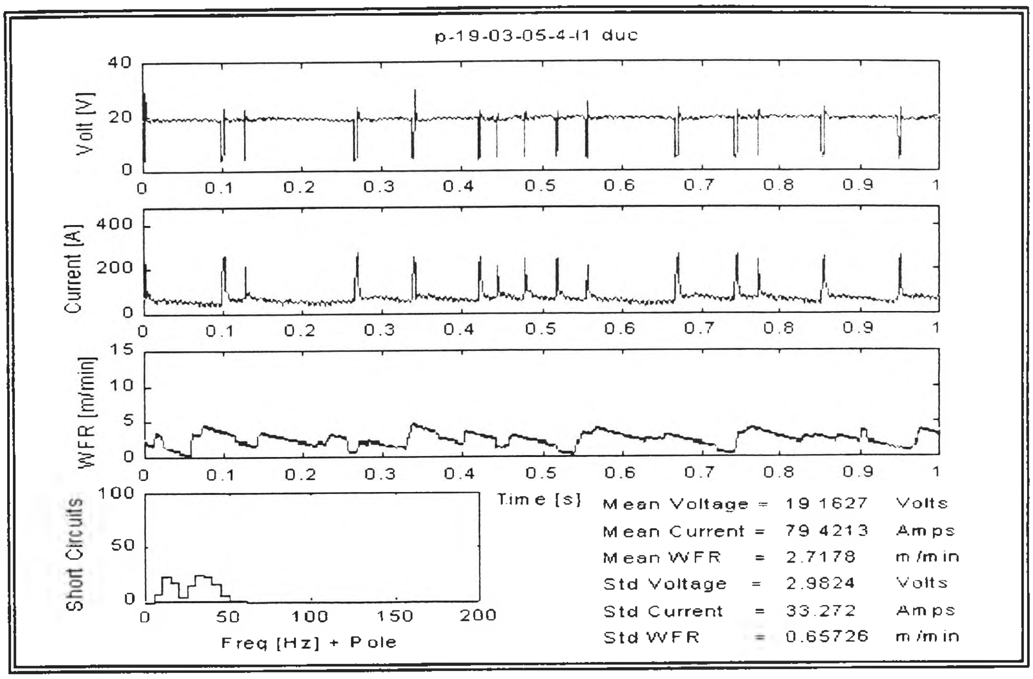

Plot A1-5

Sample p-19-03-05-4-layer 1

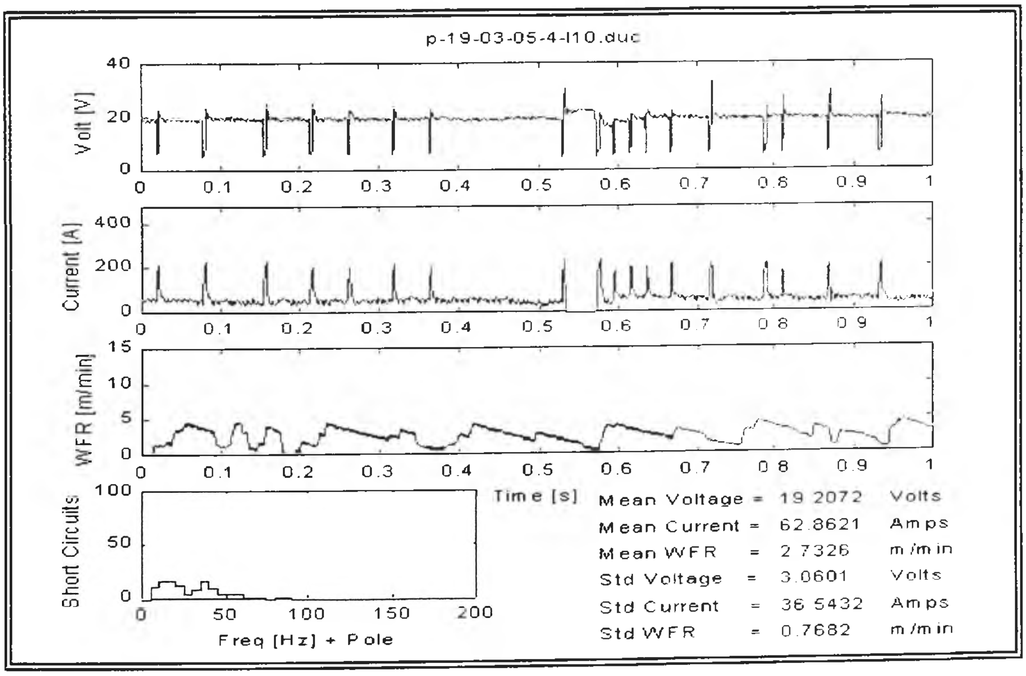

Plot A1-6

Sample p-19-03-05-4-layer 10

A2 Wire Feed Rate of 4 metre/minute

Sample p-17-04-05-4

Data:			
Voltage [V]	17	Weld width [mm]	7.26
Wire feed rate [m/min]	4	Stand-off at layer 1 [mm]	15
Travel speed [mm/sec]	5	Stand-off at layer 10 [mm]	18.5
Number of layers	10	Temperature at layer 10 [deg.C]	419
Weld height [mm]	16.5	Pinch setting	4

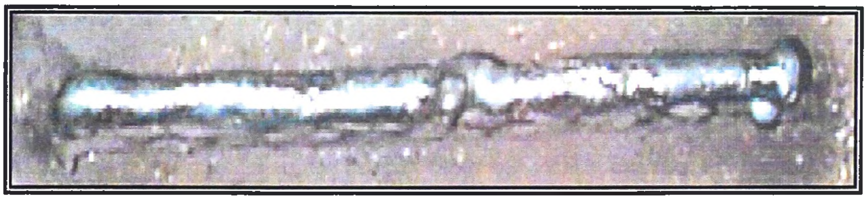

Figure A2-1

Sample p-17-04-05-4 (Top view)

Figure A2-2

Sample p-17-04-05-4 (Front view)

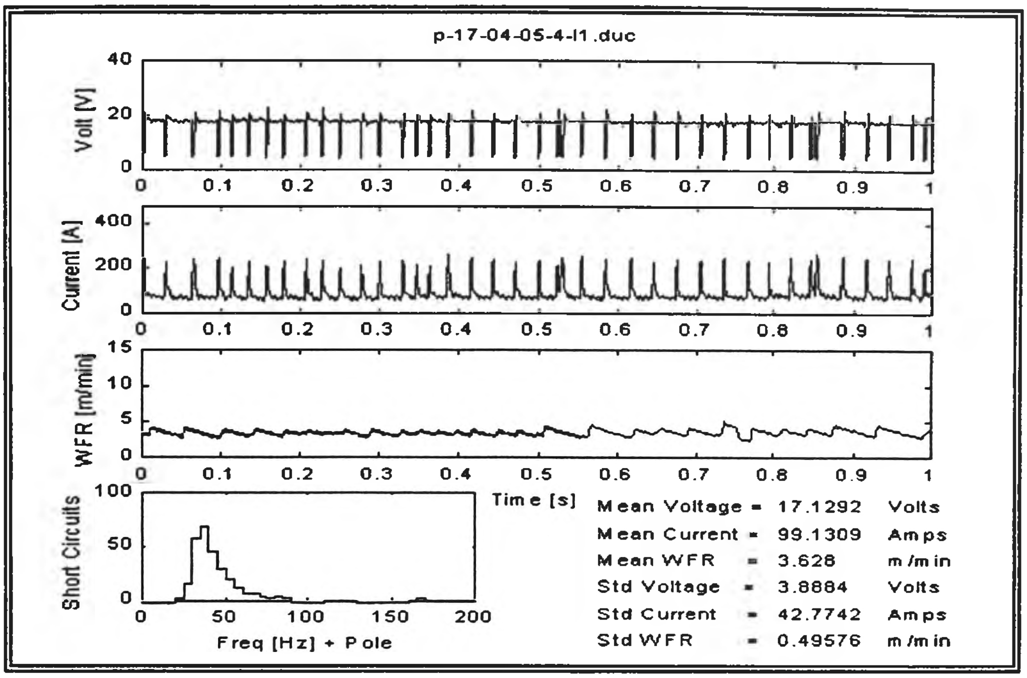

Plot A2-1

Sample p-17-04-05-4-layer 1

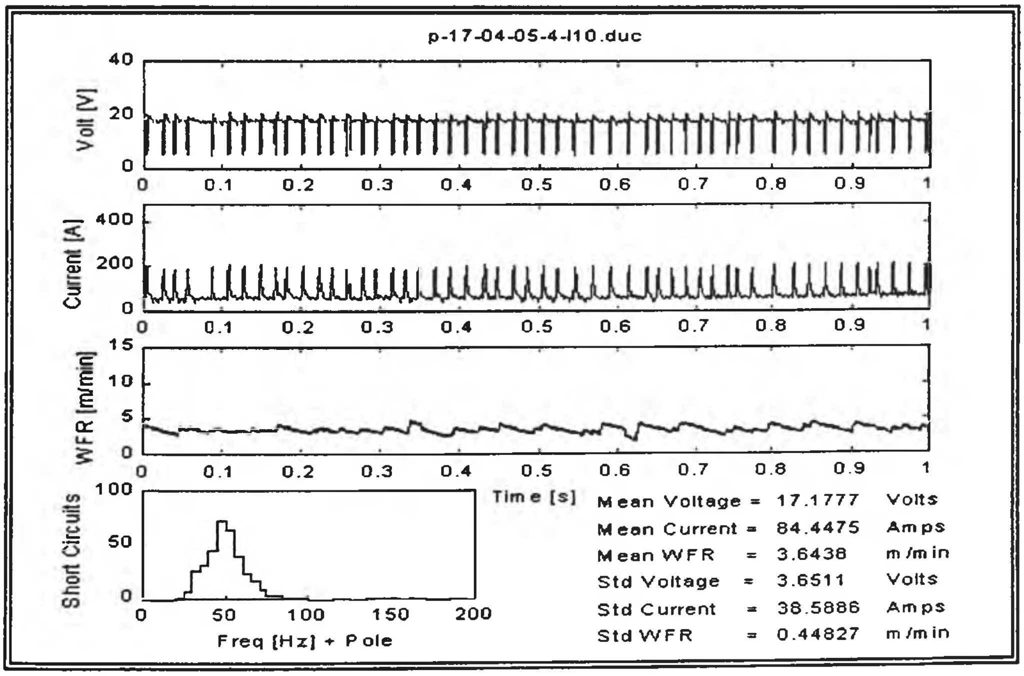

Plot A2-2

Sample p-17-04-05-4-layer 10

Sample p-18-04-05-4

Data:			
Voltage [V]	18	Weld width [mm]	8.64
Wire feed rate [m/min]	4	Stand-off at layer 1 [mm]	15
Travel speed [mm/sec]	5	Stand-off at layer 10 [mm]	18.5
Number of layers	10	Temperature at layer 10 [deg.C]	437
Weld height [mm]	14	Pinch setting	4

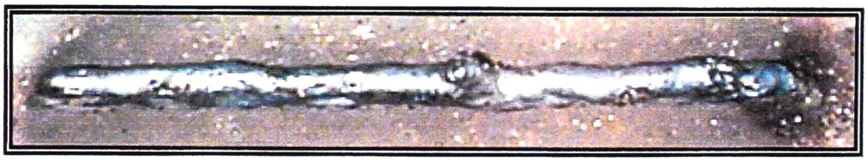

Figure A2-3

Sample p-18-04-05-4 (Top view)

Figure A2-4

Sample p-18-04-05-4 (Front view)

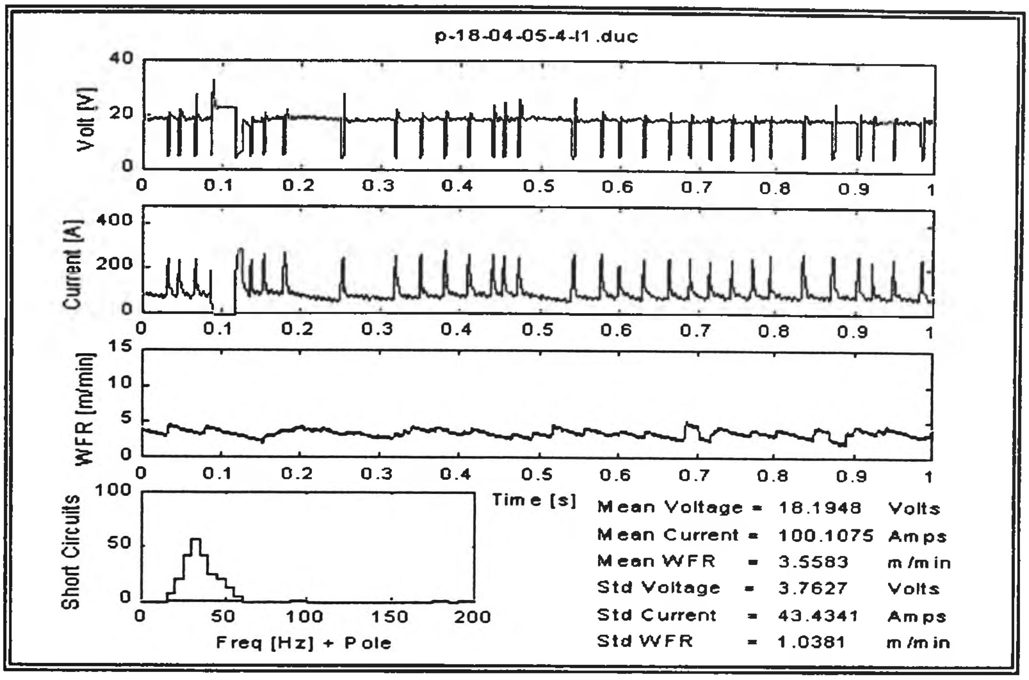

Plot A2-3

Sample p-18-04-05-4-layer 1

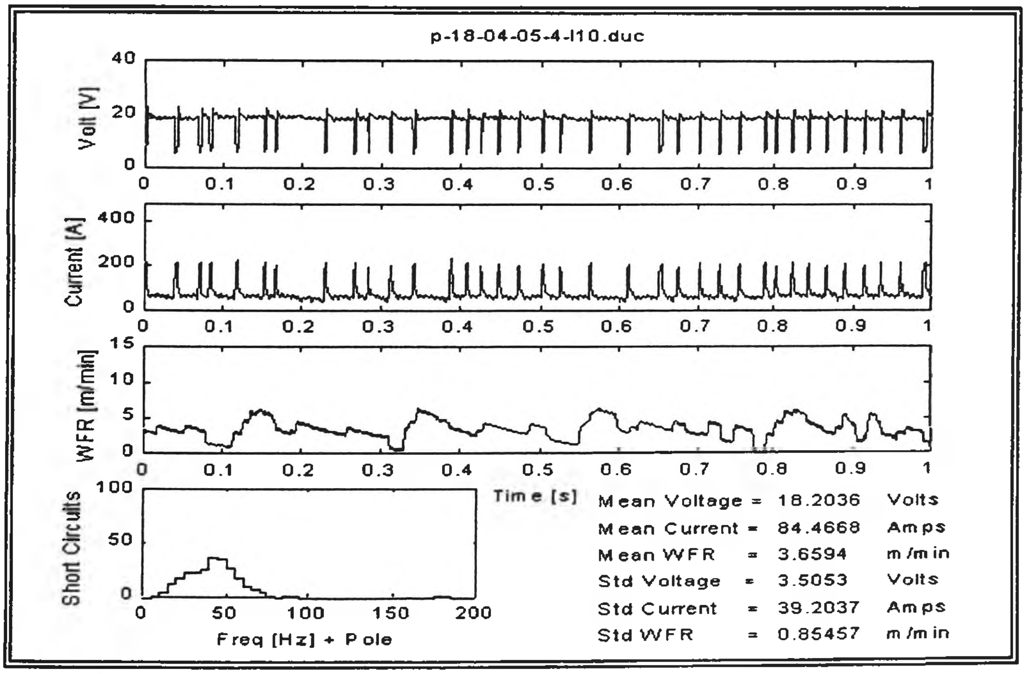

Plot A2-4

Sample p-18-04-05-4-layer 10

Sample p-19-04-05-4

Data:

Voltage [V]	19	Weld width [mm]	8.2
Wire feed rate [m/min]	4	Stand-off at layer 1 [mm]	15
Travel speed [mm/sec]	5	Stand-off at layer 10 [mm]	19.5
Number of layers	10	Temperature at layer 10 [deg.C]	461
Weld height [mm]	14	Pinch setting	4

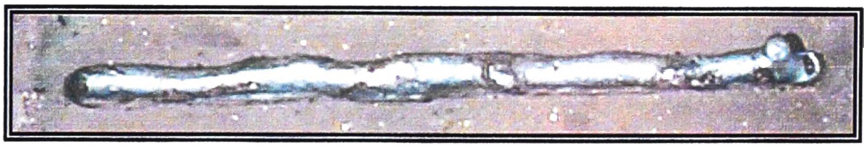

Figure A2-5

Sample p-19-04-05-4 (Top view)

Figure A2-6

Sample p-19-04-05-4 (Front view)

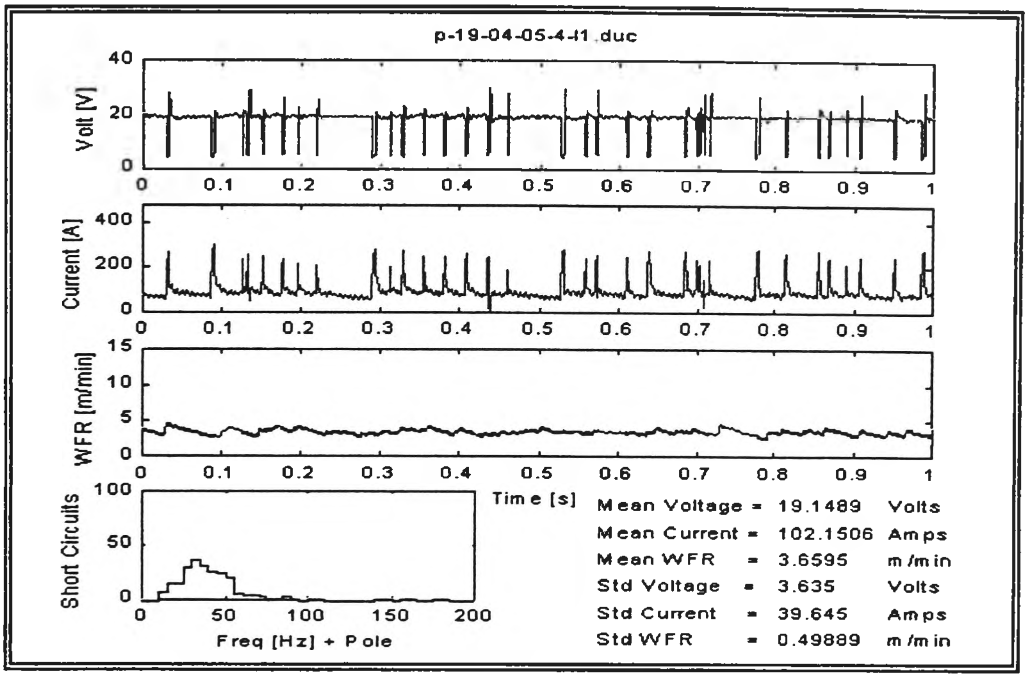

Plot A2-5

Sample p-19-04-05-4-layer 1

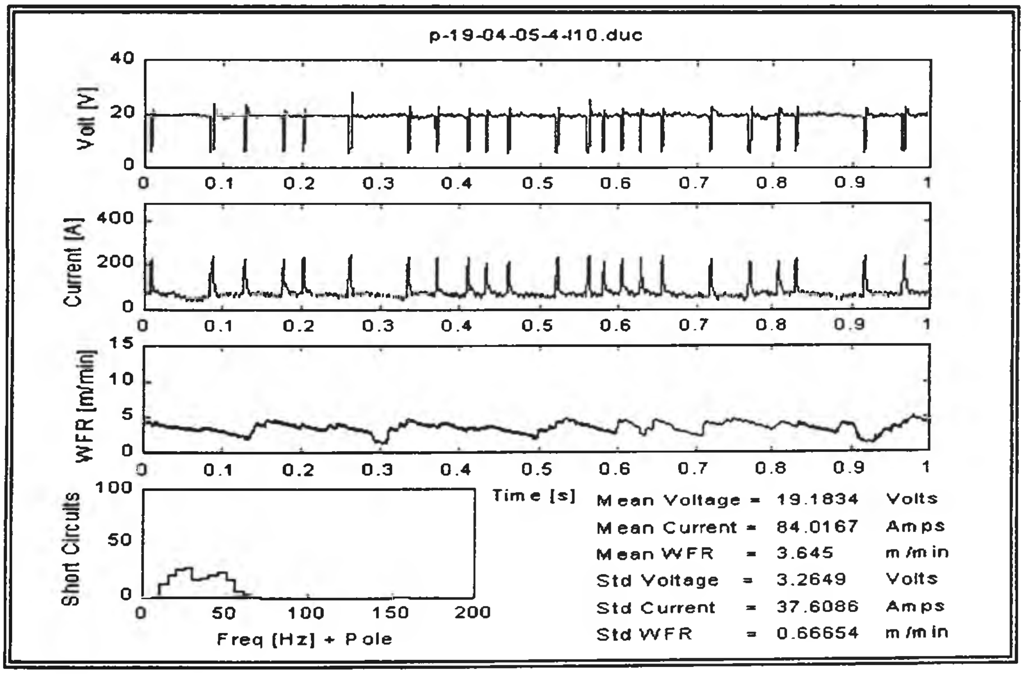

Plot A2-6

Sample p-19-04-05-4-layer 10

A3 Wire Feed Rate of 5 metre/minute

Sample p-17-05-05-4

Data:

Voltage [V]	17	Weld width [mm]	9.3
Wire feed rate [m/min]	5	Stand-off at layer 1 [mm]	15
Travel speed [mm/sec]	5	Stand-off at layer 10 [mm]	17.5
Number of layers	10	Temperature at layer 10 [deg.C]	365
Weld height [mm]	18	Pinch setting	4

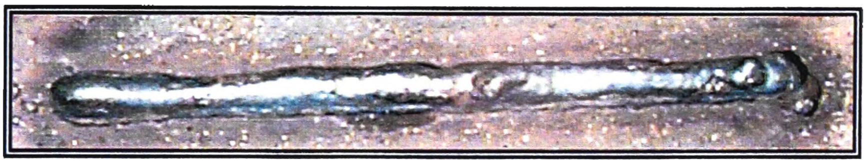

Figure A3-1

Sample p-17-05-05-4 (Top view)

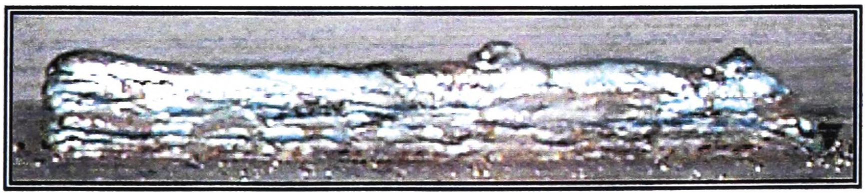

Figure A3-2

Sample p-17-05-05-4 (Front view)

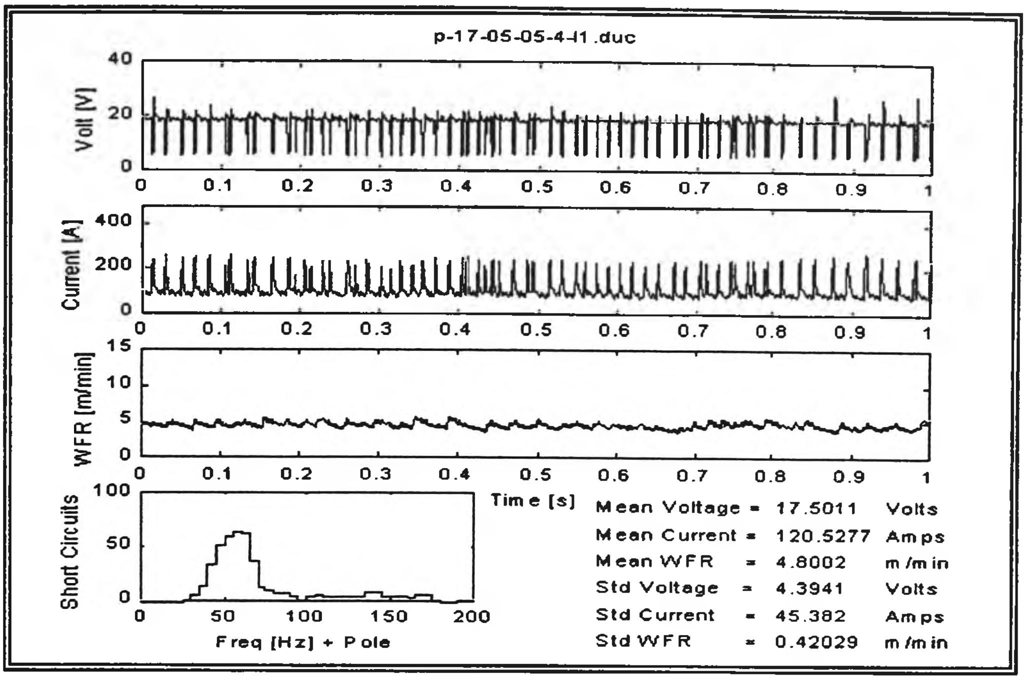

Plot A3-1

Sample p-17-05-05-4 layer 1

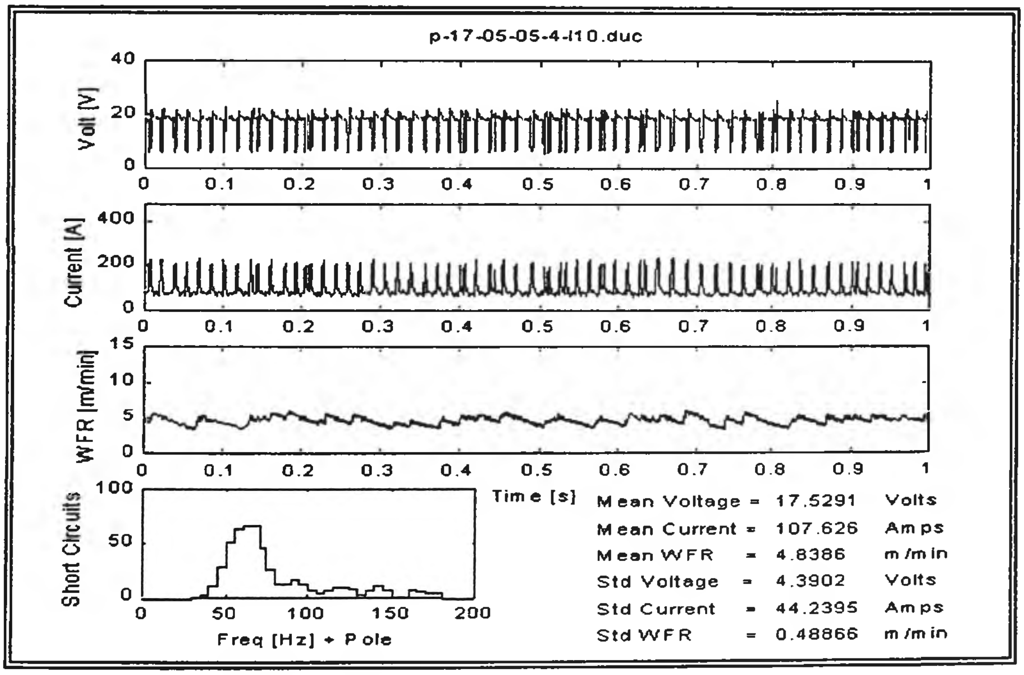

Plot A3-2

Sample p-17-05-05-4 layer 10

Sample p-18-05-05-4

Data:			
Voltage [V]	18	Weld width [mm]	9.2
Wire feed rate [m/min]	5	Stand-off at layer 1 [mm]	15
Travel speed [mm/sec]	5	Stand-off at layer 10 [mm]	
Number of layers	10	Temperature at layer 10 [deg.C]	406
Weld height [mm]	18	Pinch setting	4

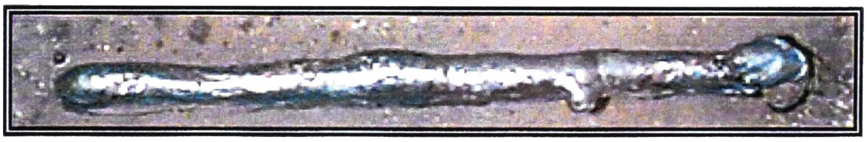

Figure A3-3

Sample p-18-05-05-4 (Top view)

Figure A3-4

Sample p-18-05-05-4 (Front view)

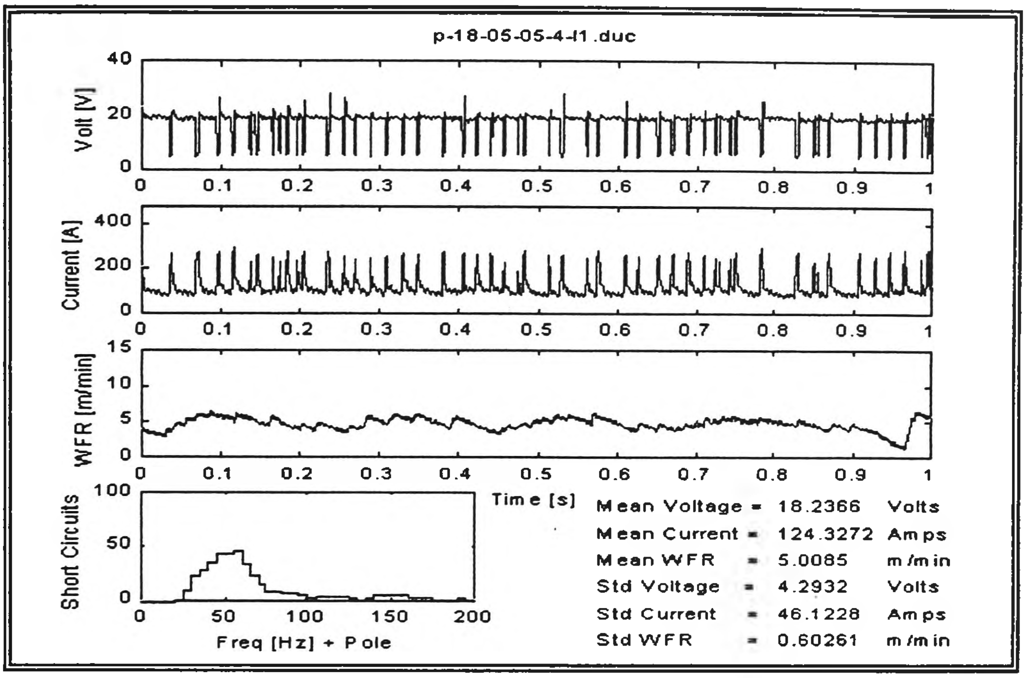

Plot A3-3

Sample p-18-05-05-4-layer 1

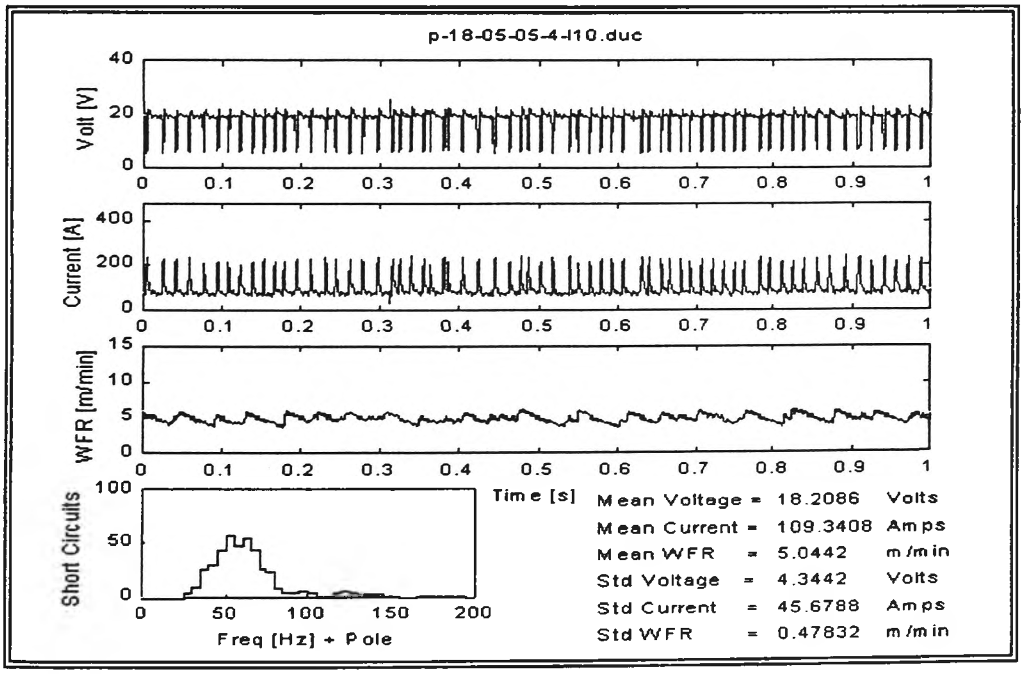

Plot A3-4

Sample p-18-05-05-4-layer 10

Sample p-19-05-05-4

Data:			
Voltage [V]	19	Weld width [mm]	8.62
Wire feed rate [m/min]	5	Stand-off at layer 1 [mm]	15
Travel speed [mm/sec]	5	Stand-off at layer 10 [mm]	17.5
Number of layers	10	Temperature at layer 10 [deg.C]	501
Weld height [mm]	17	Pinch setting	4

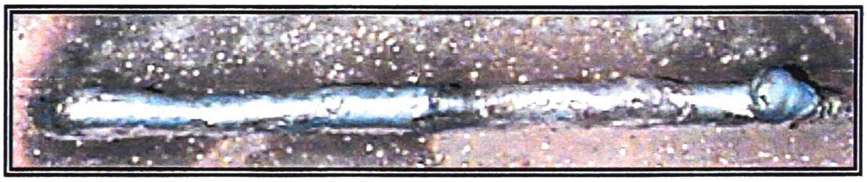

Figure A3-5

Sample p-19-05-05-4 (Top view)

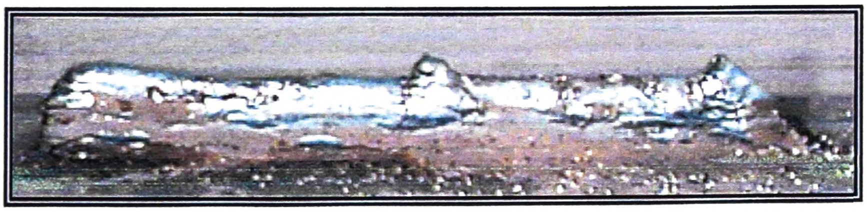

Figure A3-6

Sample p-19-05-05-4 (Front view)

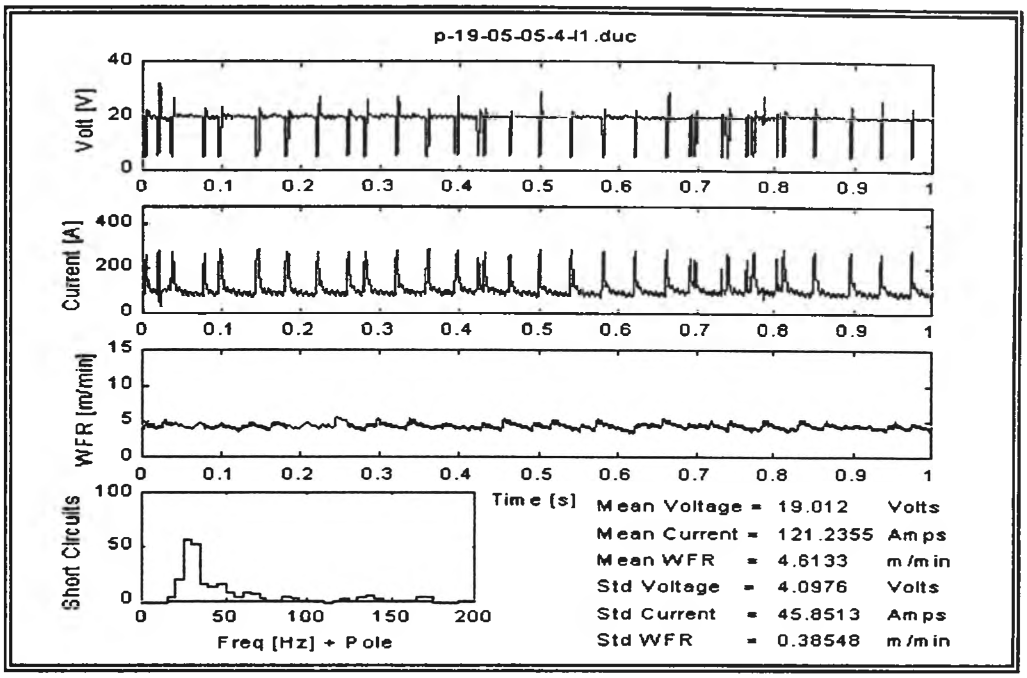

Plot A3-5

Sample p-19-05-05-4-layer 1

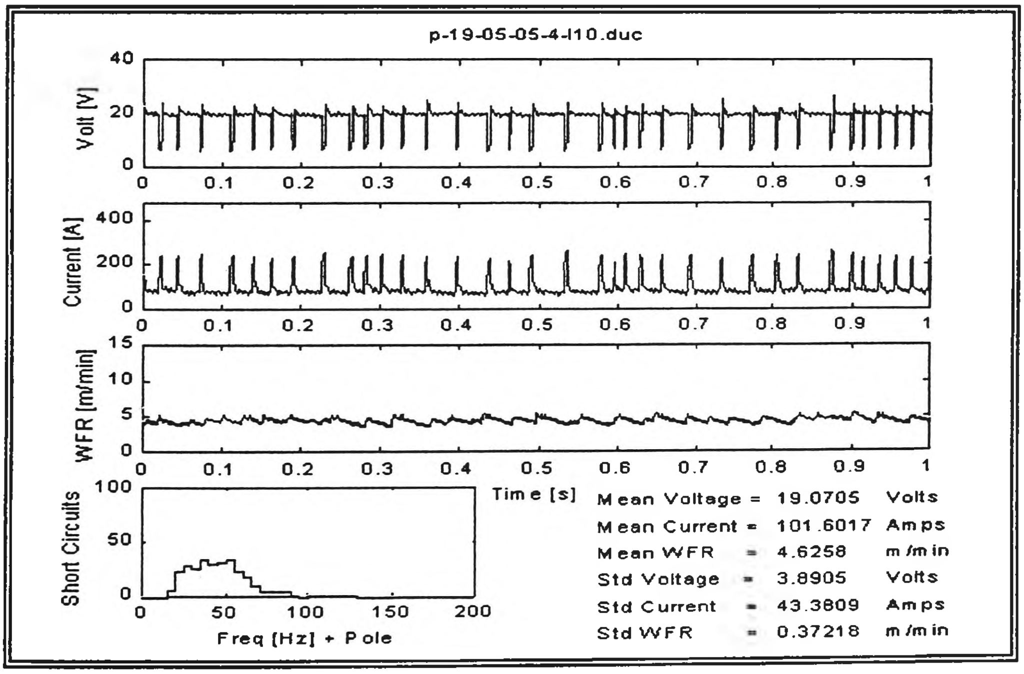

Plot A3-6

Sample p-19-05-05-4-layer 10

A4 Wire Feed Rate of 6 metre/minute

Sample p-17-06-05-4

Data:			
Voltage [V]	17	Weld width [mm]	8.64
Wire feed rate [m/min]	6	Stand-off at layer 1 [mm]	15
Travel speed [mm/sec]	5	Stand-off at layer 10 [mm]	16
Number of layers	10	Temperature at layer 10 [deg.C]	444
Weld height [mm]	19	Pinch setting	4

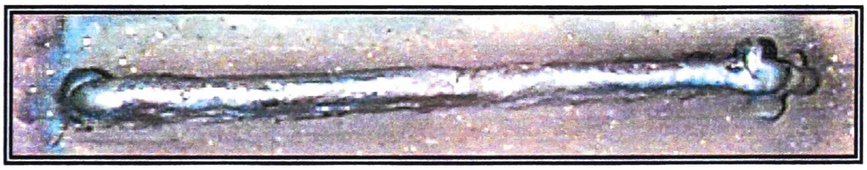

Figure A4-1

Sample p-17-06-05-4 (Top view)

Figure A4-2

Sample p-17-06-05-4 (Front view)

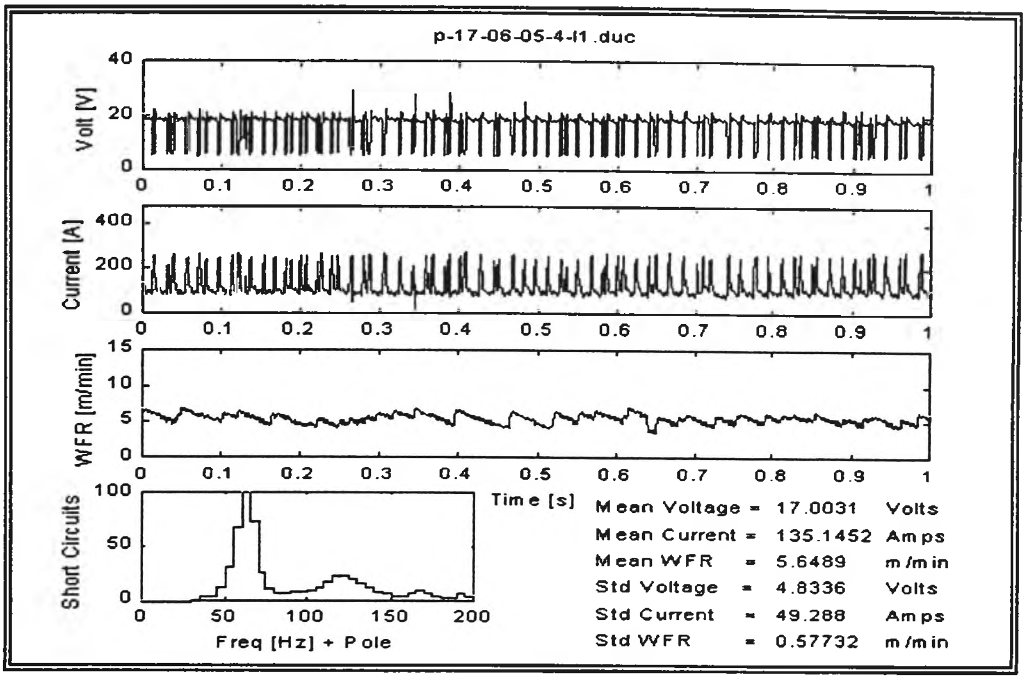

Plot A4-1

Sample p-17-06-05-4-layer1

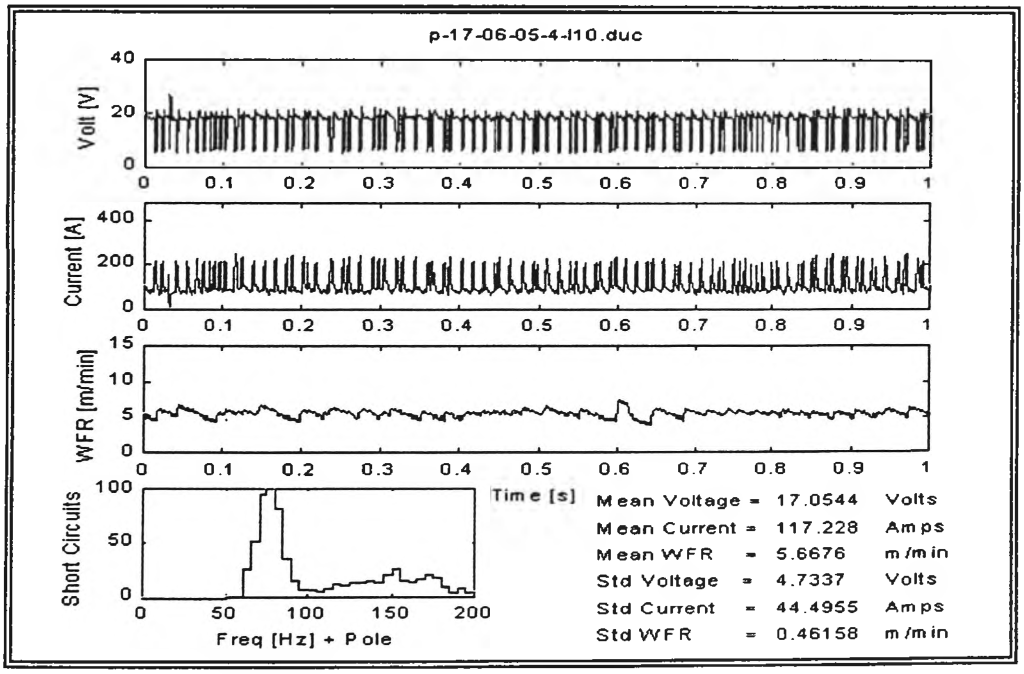

Plot A4-2

Sample p-17-06-05-4-layer10

Sample p-18-06-05-4

Data:			
Voltage [V]	18	Weld width [mm]	8.94
Wire feed rate [m/min]	6	Stand-off at layer 1 [mm]	15
Travel speed [mm/sec]	5	Stand-off at layer 10 [mm]	17.5
Number of layers	10	Temperature at layer 10 [deg.C]	465
Weld height [mm]	18	Pinch setting	4

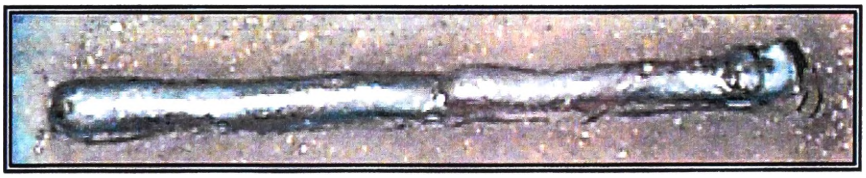

Figure A4-3

Sample p-18-06-05-4 (Top View)

Figure A4-4

Sample p-18-06-05-4 (Front View)

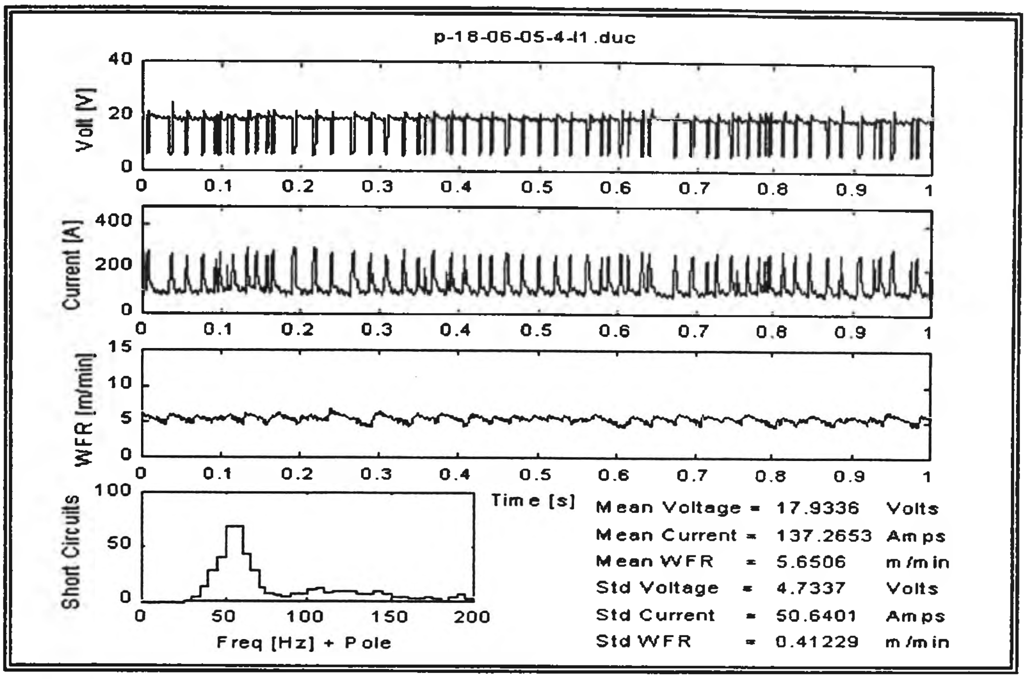

Plot A4-3

Sample p-18-06-05-4-layer1

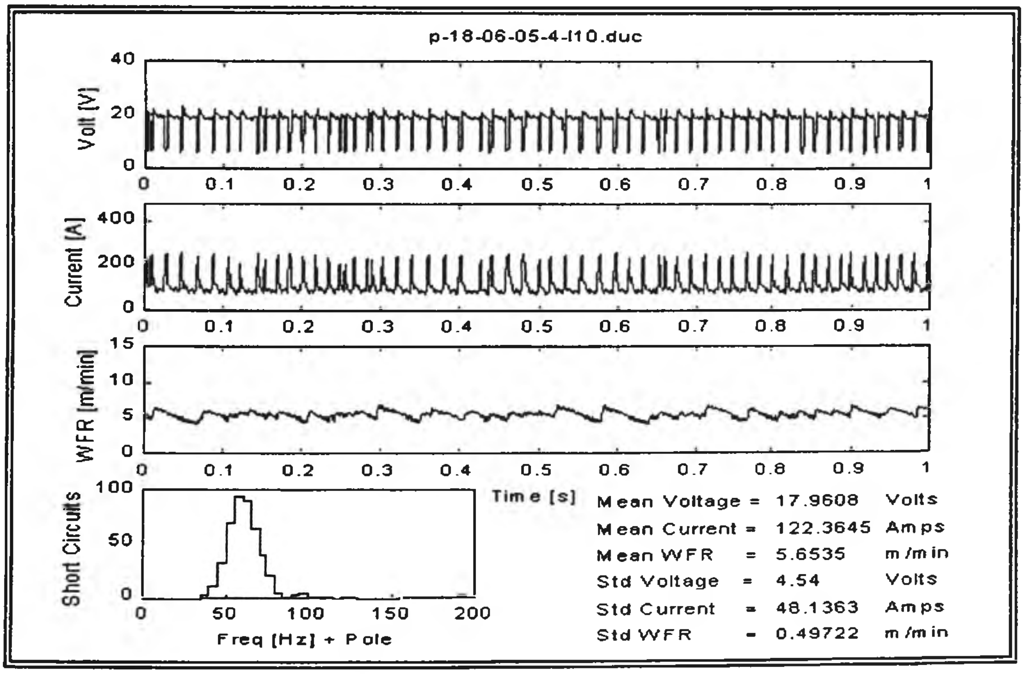

Plot A4-4

Sample p-18-06-05-4-layer10

Sample p-19-06-05-4

Data:			
Voltage [V]	19	Weld width [mm]	18.8
Wire feed rate [m/min]	6	Stand-off at layer 1 [mm]	15
Travel speed [mm/sec]	5	Stand-off at layer 10 [mm]	15
Number of layers	10	Temperature at layer 10 [deg.C]	473
Weld height [mm]	18	Pinch setting	4

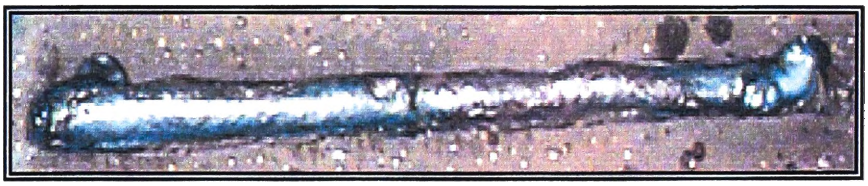

Figure A4-5

Sample p-19-06-05-4 (Top view)

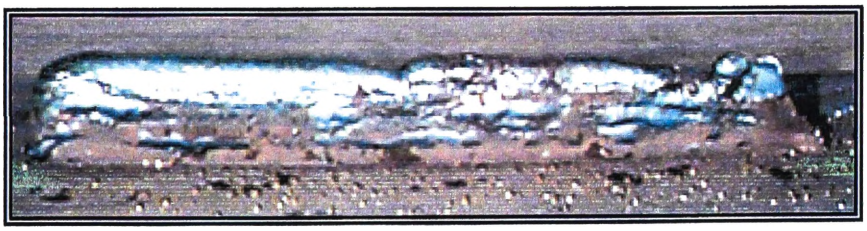

Figure A4-6

Sample p-19-06-05-4 (Front view)

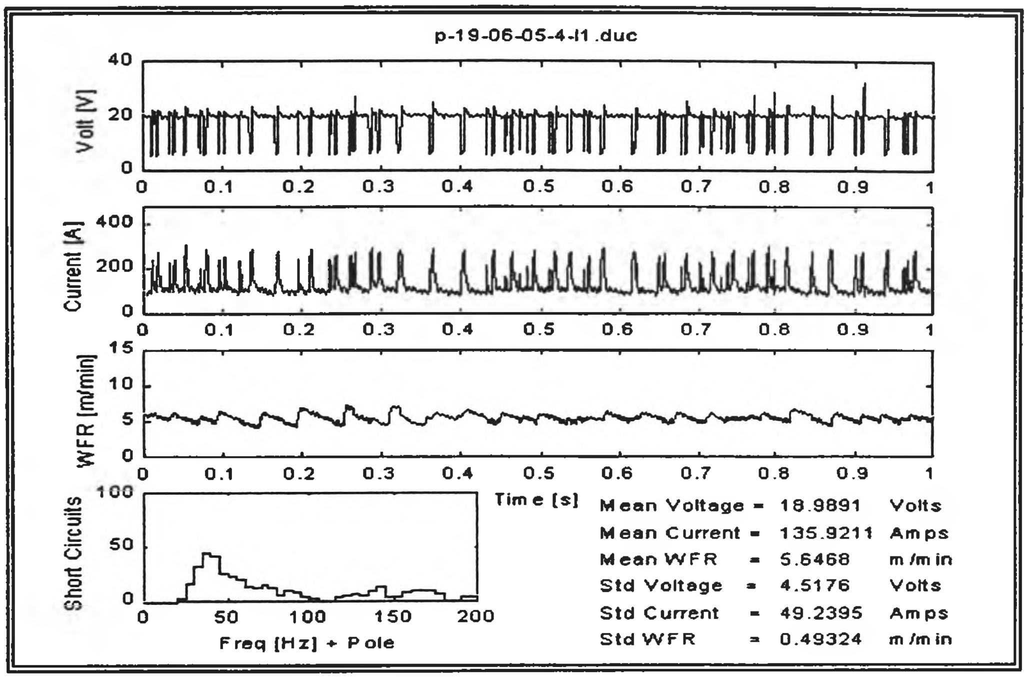

Plot A4-5

Sample p-19-06-05-4-layer1

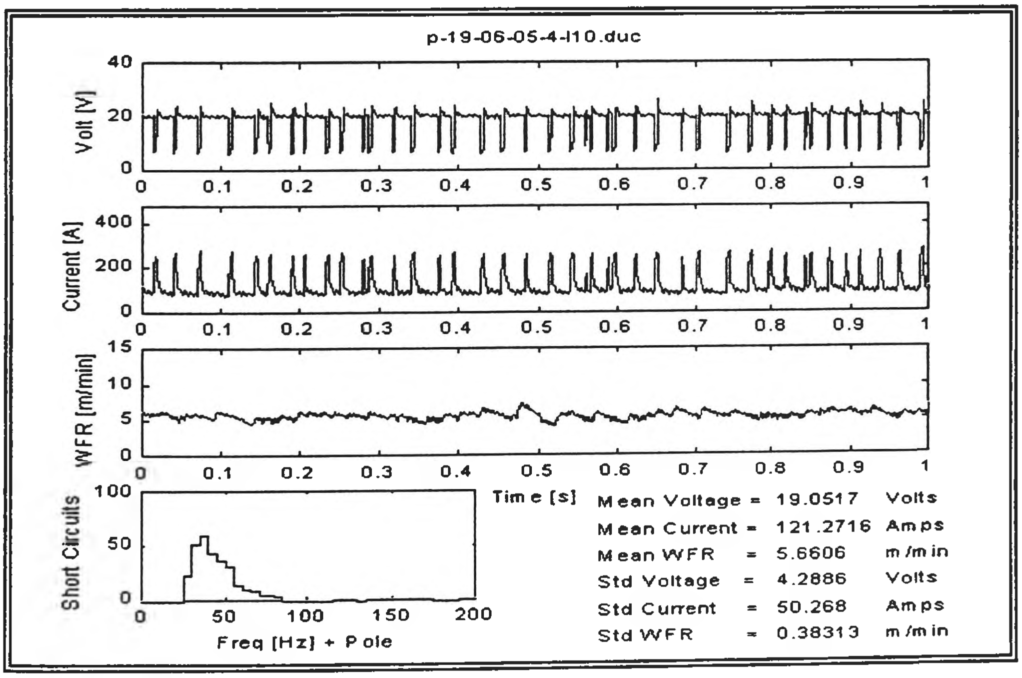

Plot A4-6

Sample p-19-06-05-4-layer10

A5 Wire Feed Rate of 7 metre/minute

Sample p-17-07-05-4

Data:

Voltage [V]	17	Weld width [mm]	10.1
Wire feed rate [m/min]	7	Stand-off at layer 1 [mm]	15
Travel speed [mm/sec]	5	Stand-off at layer 10 [mm]	15
Number of layers	10	Temperature at layer 10 [deg.C]	537
Weld height [mm]	20	Pinch setting	4

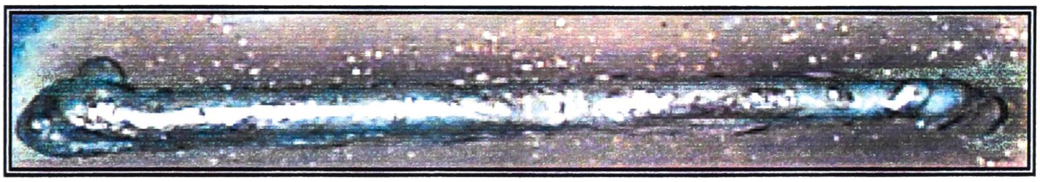

Figure A5-1

Sample p-17-07-05-4 (Top view)

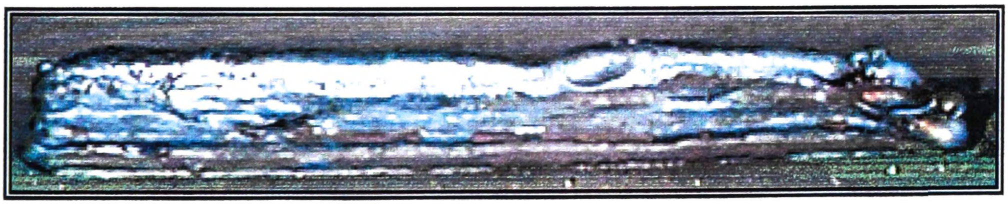

Figure A5-2

Sample p-17-07-05-4 (Front view)

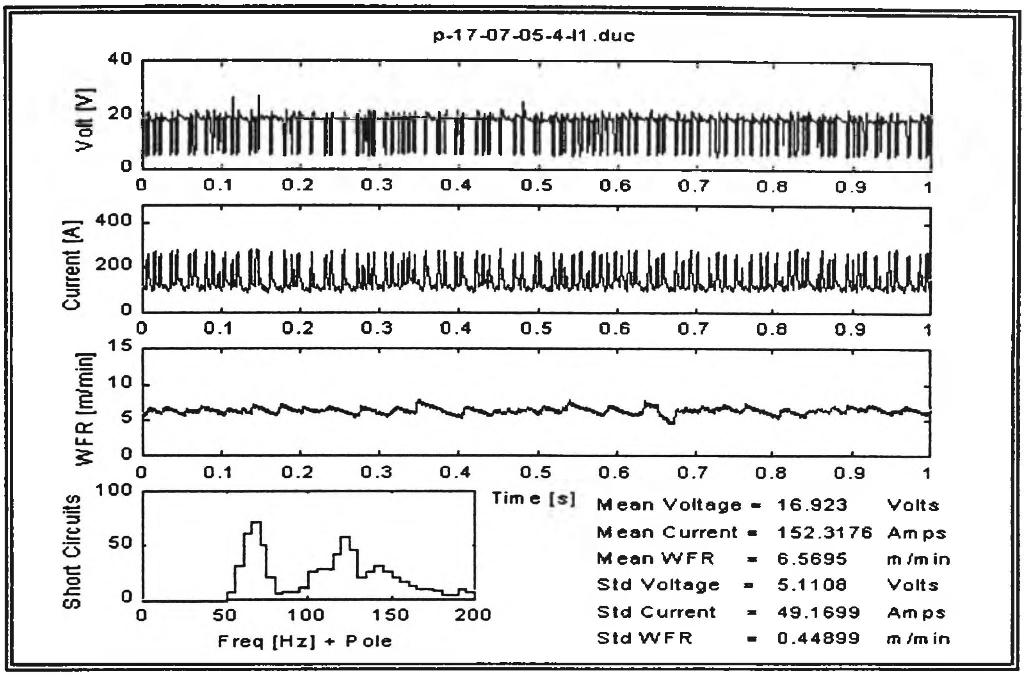

Plot A5-1

Sample p-17-07-05-4-layer1

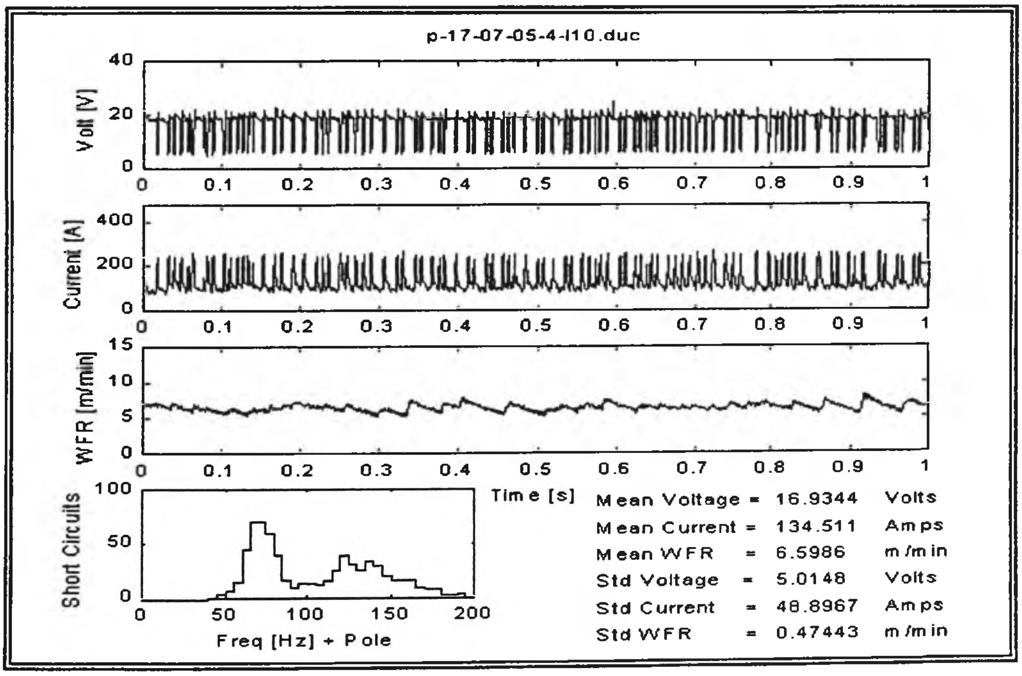

Plot A5-2

Sample p-17-07-05-layer10

Sample p-18-07-05-4

Data:

Voltage [V]	18	Weld width [mm]	9.92
Wire feed rate [m/min]		Stand-off at layer 1 [mm]	15
Travel speed [mm/sec]	5	Stand-off at layer 10 [mm]	15
Number of layers	10	Temperature at layer 10 [deg.C]	602
Weld height [mm]	19	Pinch setting	4

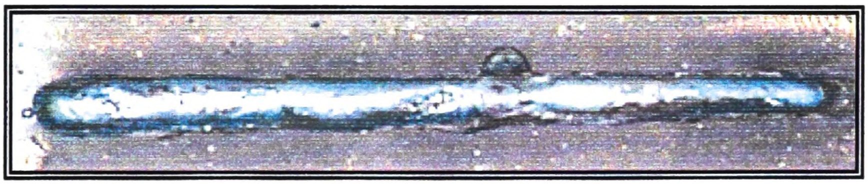

Figure A5-3

Sample p-18-07-05-4 (Top view)

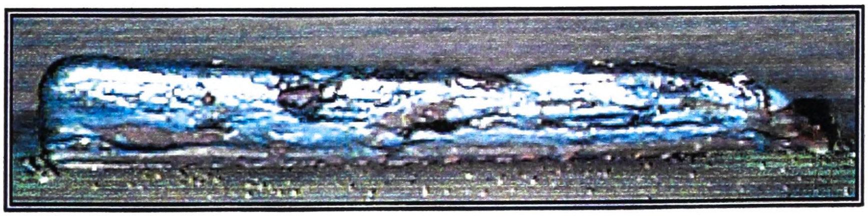

Figure A5-4

Sample p-18-07-05-4 (Front view)

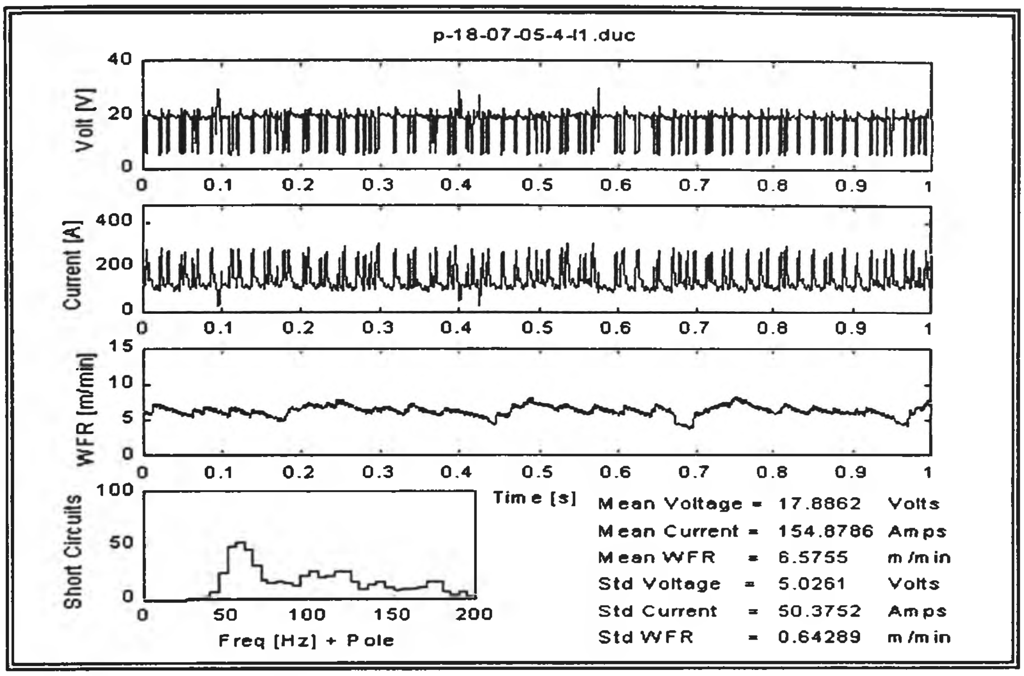

Plot A5-3

Sample p-18-07-05-4-layer1

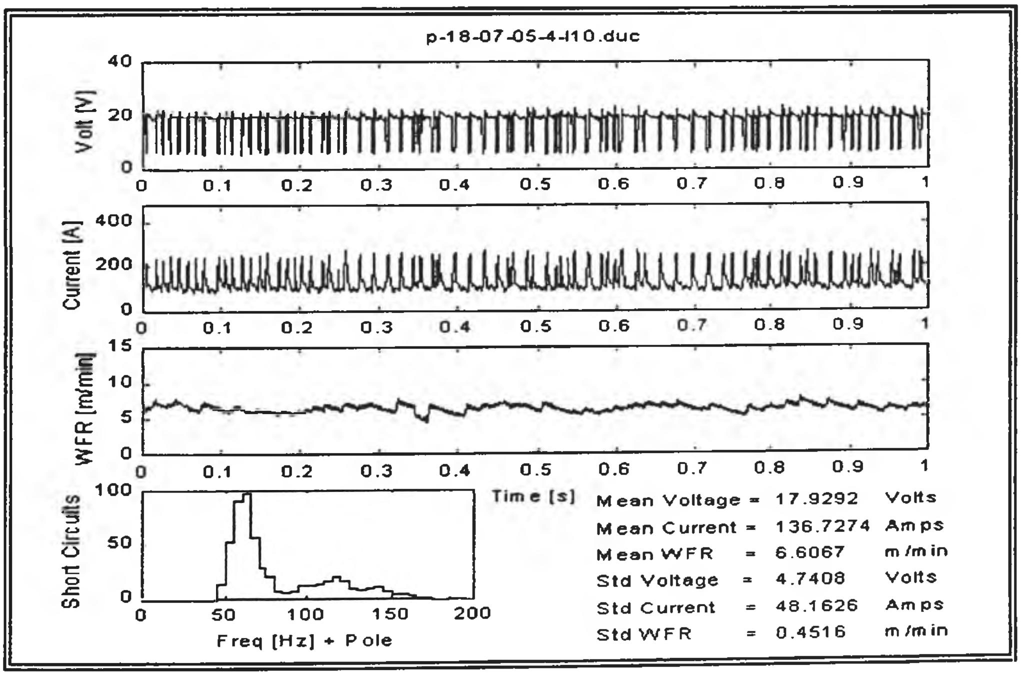

Plot A5-4

Sample p-18-07-05-4-layer10

Sample p-19-07-05-4

Data:			
Voltage [V]	19	Weld width [mm]	10.2
Wire feed rate [m/min]	7	Stand-off at layer 1 [mm]	15
Travel speed [mm/sec]	5	Stand-off at layer 10 [mm]	16.5
Number of layers	10	Temperature at layer 10 [deg.C]	595
Weld height [mm]	18	Pinch setting	4

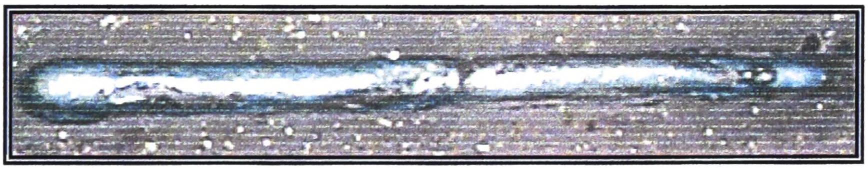

Figure A5-5

Sample p-19-07-05-4 (Top view)

Figure A5-6

Sample p-19-07-05-4 (Front view)

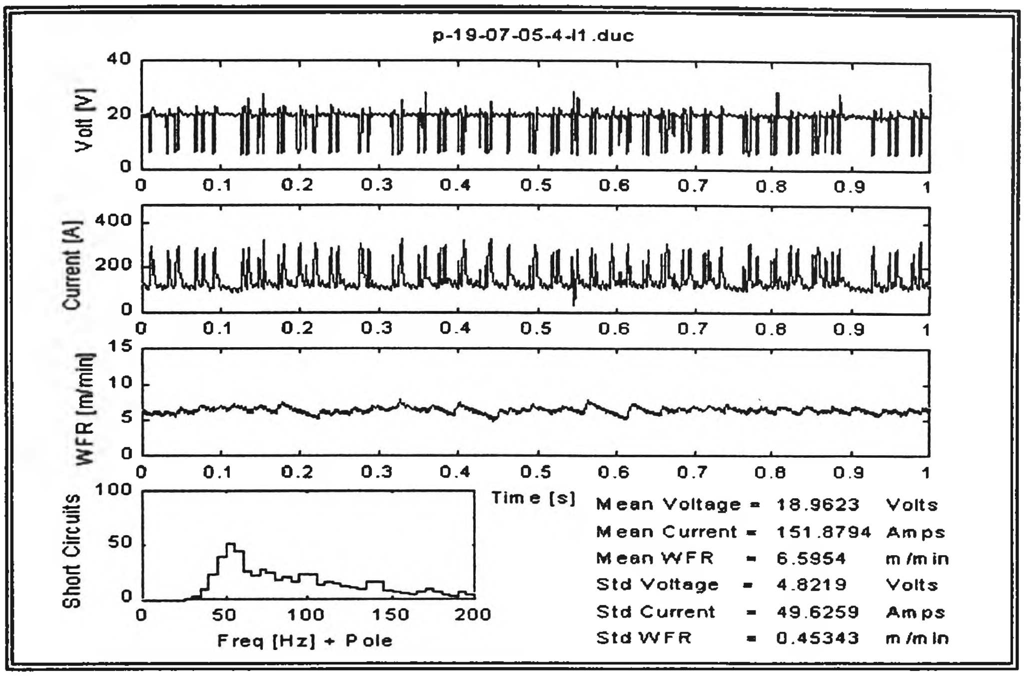

Plot A5-5

Sample p-19-07-05-4-layer1

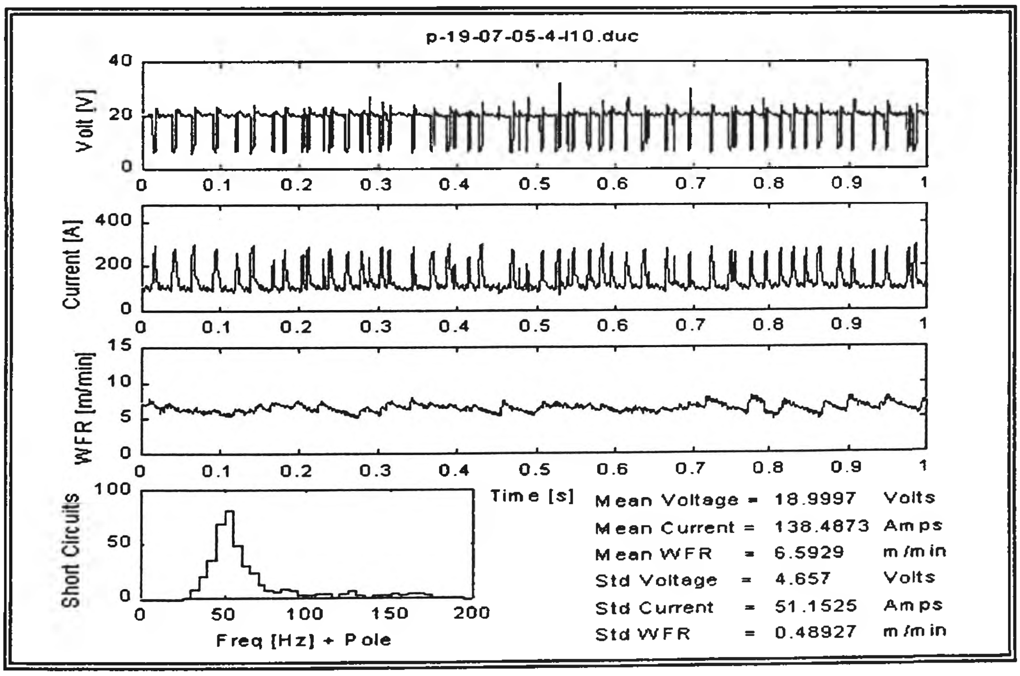

Plot A5-6

Sample p-19-07-05-4-layer10

A6 Wire Feed Rate of 8 metre/minute

Sample p-17-08-05-4

Data:			
Voltage [V]	17	Weld width [mm]	9.64
Wire feed rate [m/min]	8	Stand-off at layer 1 [mm]	15
Travel speed [mm/sec]	5	Stand-off at layer 10 [mm]	14
Number of layers	10	Temperature at layer 10 [deg.C]	599
Weld height [mm]	22.5	Pinch setting	4

Figure A6-1

Sample p-17-08-05-4 (Top view)

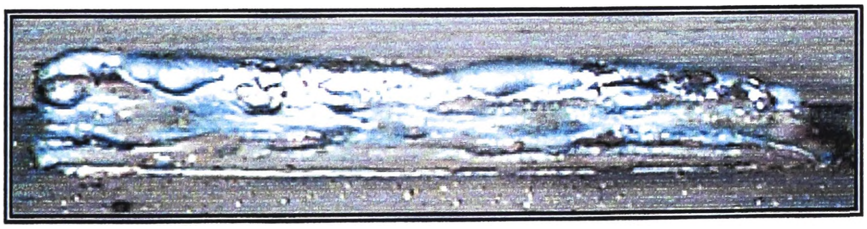

Figure A6-2

Sample p-17-08-05-4 (Front view)

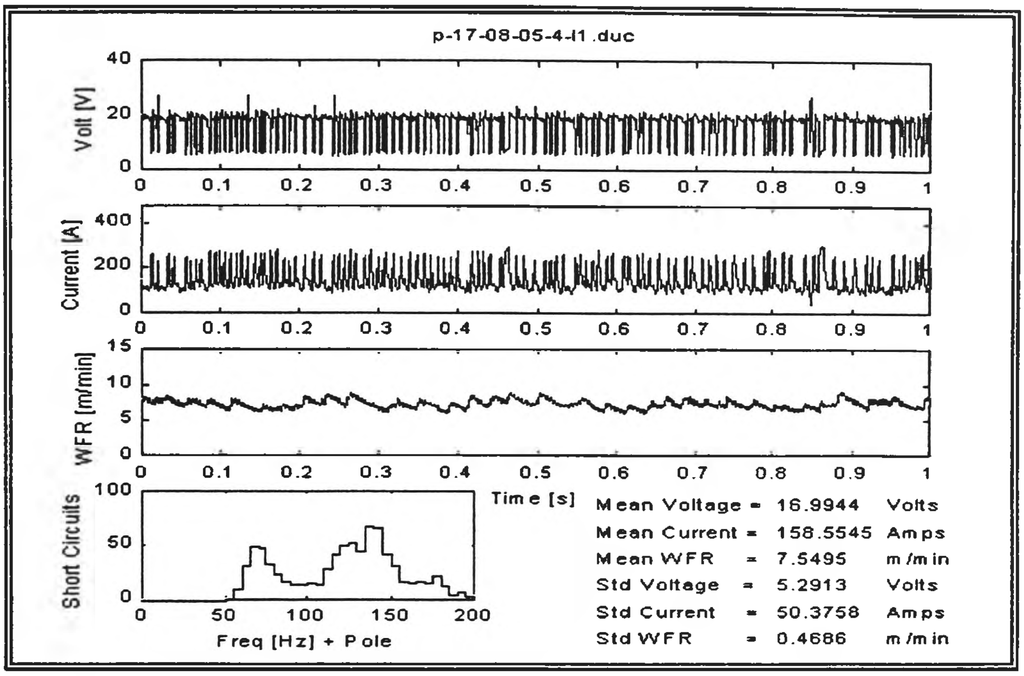

Plot A6-1

Sample p-17-08-05-4-layer1

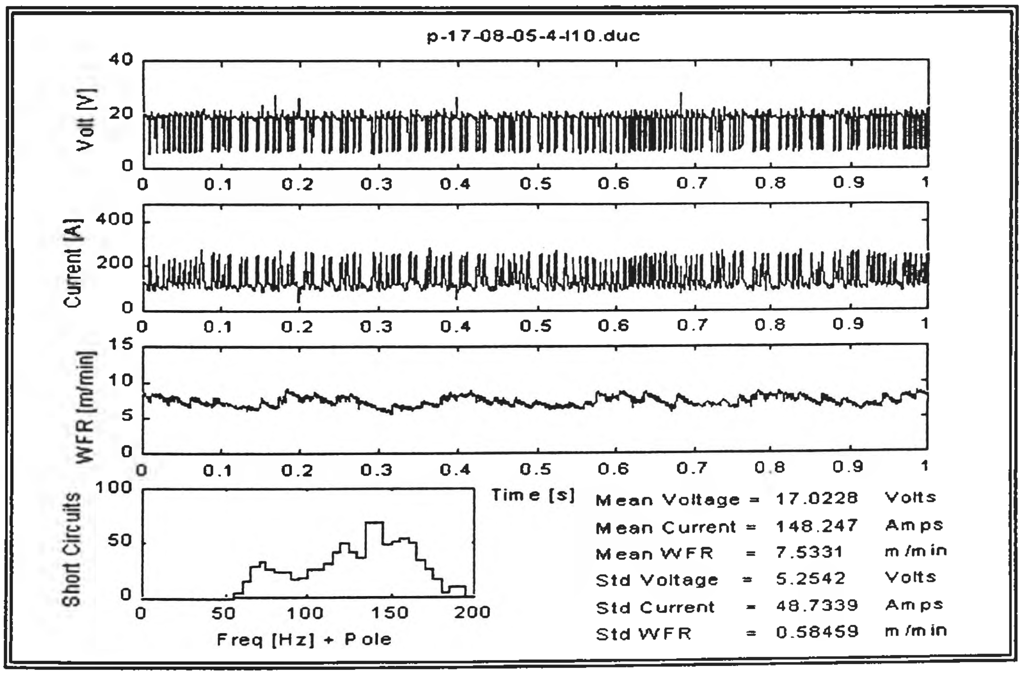

Plot A6-2

Sample p-17-08-05-4-layer 10

4.5.6.2 Sample p-18-08-05-4

Data:			
Voltage [V]	18	Weld width [mm]	10.5
Wire feed rate [m/min]	8	Stand-off at layer 1 [mm]	15
Travel speed [mm/sec]	5	Stand-off at layer 10 [mm]	15
Number of layers	10	Temperature at layer 10 [deg.C]	627
Weld height [mm]	20.5	Pinch setting	4

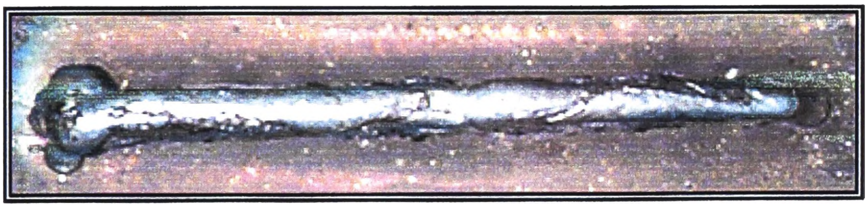

Figure A6-3

Sample p-18-08-05-4 (Top view)

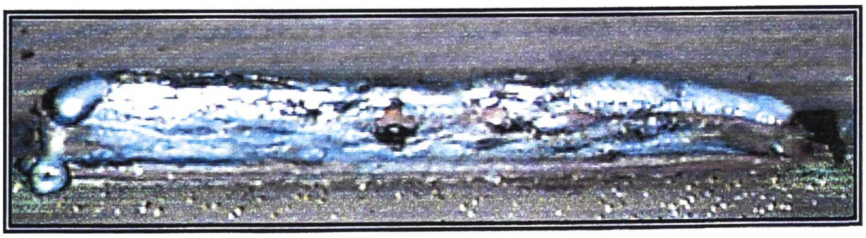

Figure A6-4

Sample p-18-08-05-4 (Front view)

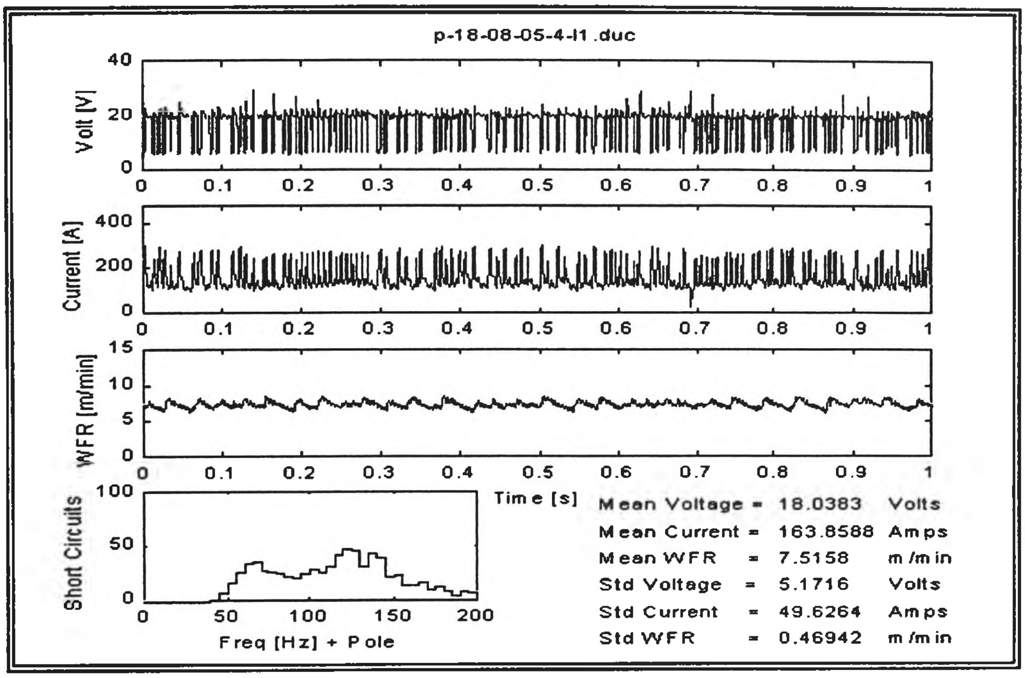

Plot A6-3

Sample p-18-08-05-4-layer 1

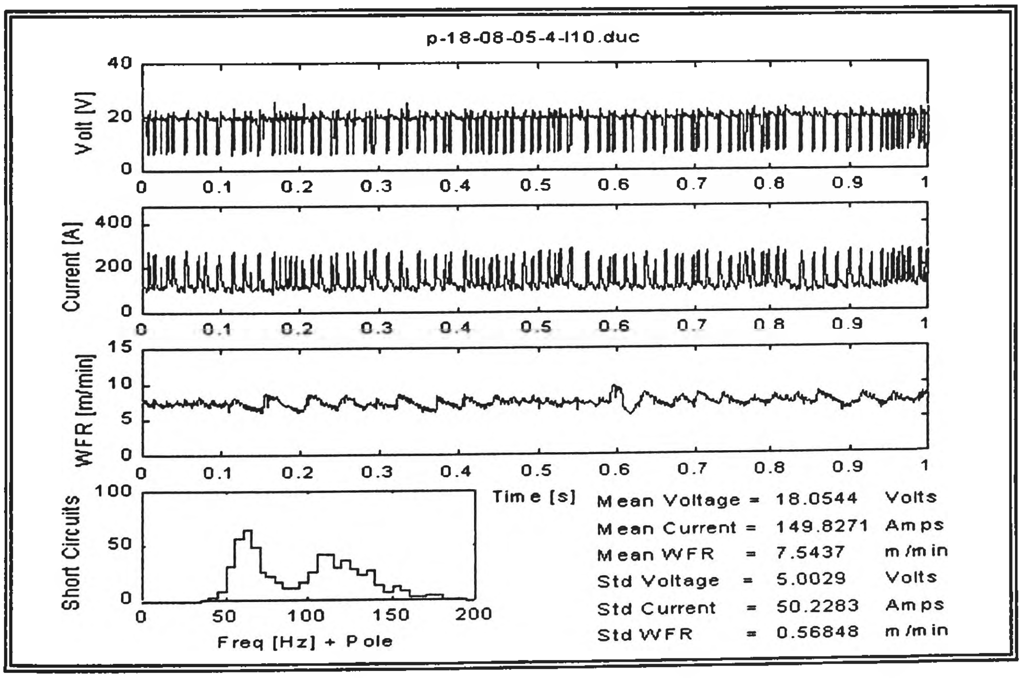

Plot A6-4

Sample p-18-08-05-4-layer 10

Sample p-19-08-05-4

Data:			
Voltage [V]	19	Weld width [mm]	12
Wire feed rate [m/min]	8	Stand-off at layer 1 [mm]	15
Travel speed [mm/sec]	5	Stand-off at layer 10 [mm]	15.5
Number of layers	10	Temperature at layer 10 [deg.C]	572
Weld height [mm]	19	Pinch setting	4

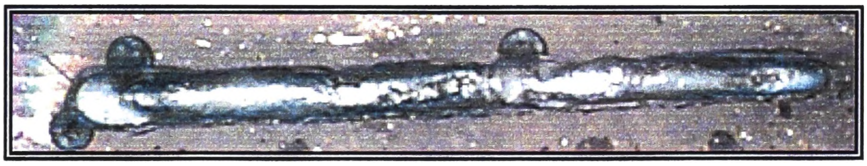

Figure A6-5

Sample p-19-08-05-4 (Top view)

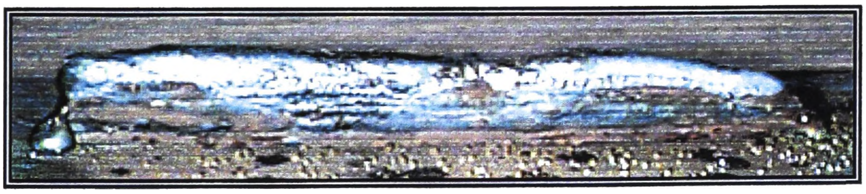

Figure A6-6

Sample p-19-08-05-4 (Front view)

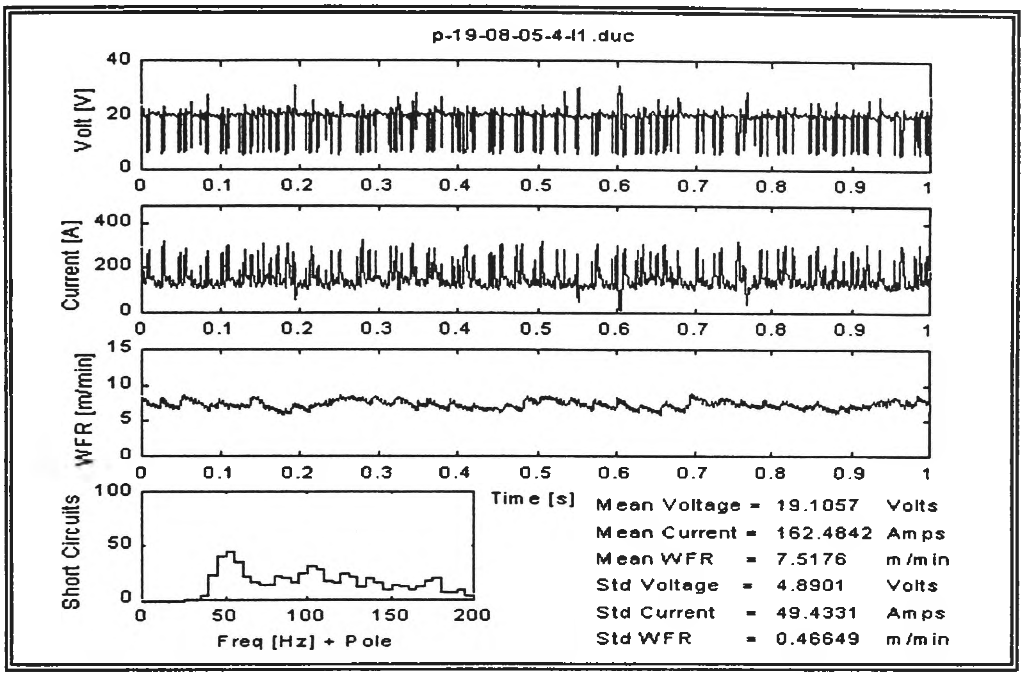

Plot A6-5

Sample p-19-08-05-4-layer 1

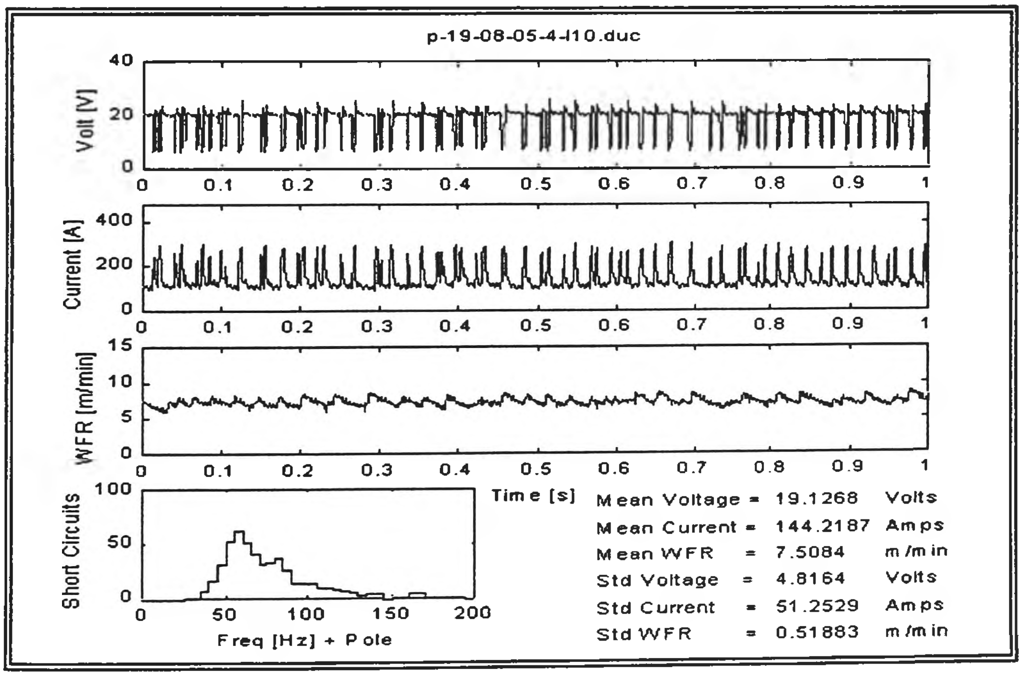

Plot A6-6

Sample p-19-08-05-4-layer 10

A7 Wire Feed Rate of 9 metre/minute

Sample p-17-09-05-4

Data:

Voltage [V]	17	Weld width [mm]	11.2
Wire feed rate [m/min]	9	Stand-off at layer 1 [mm]	15
Travel speed [mm/sec]	5	Stand-off at layer 10 [mm]	12
Number of layers	10	Temperature at layer 10 [deg.C]	590
Weld height [mm]	23.5	Pinch setting	4

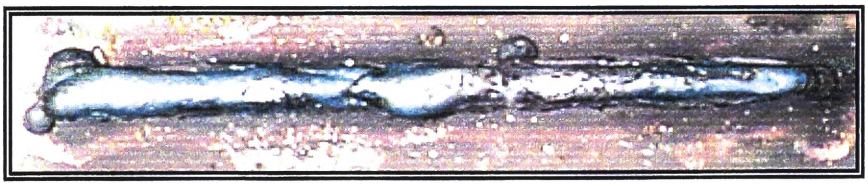

Figure A7-1

Sample p-17-09-05-4 (Top view)

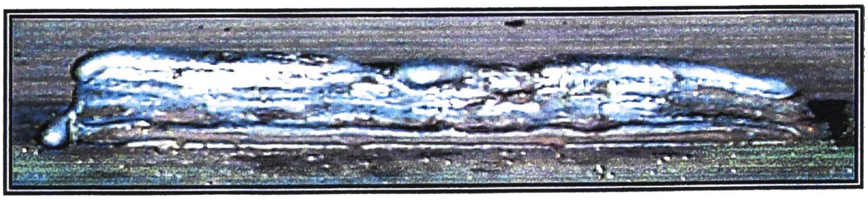

Figure A7-2

Sample p-17-09-05-4 (Front view)

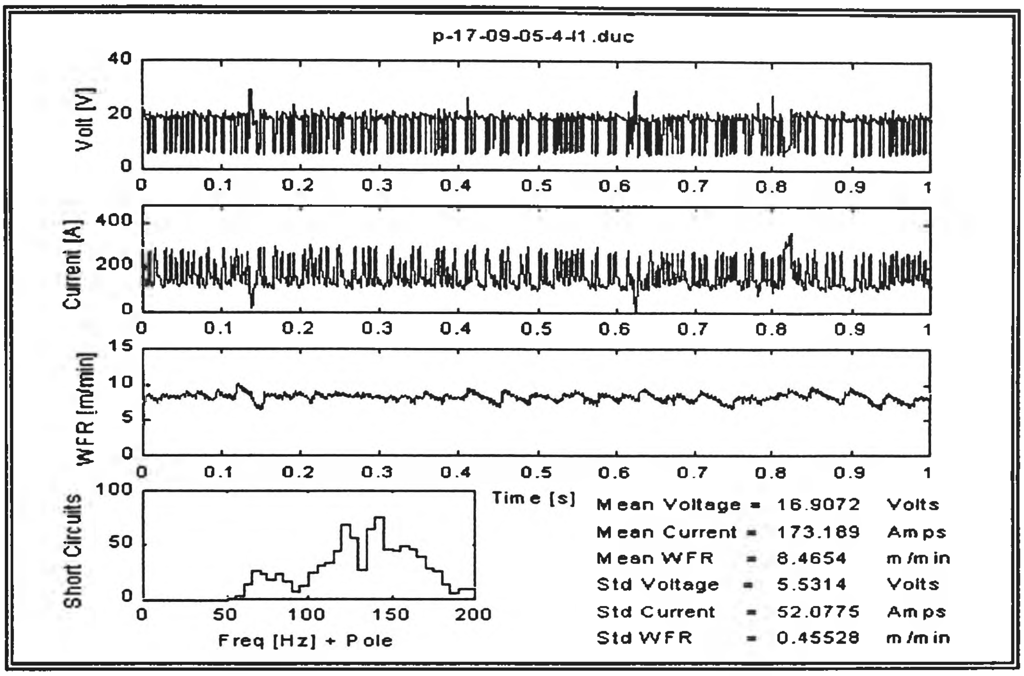

Plot A7-1

Sample p-17-09-05-4-layer 1

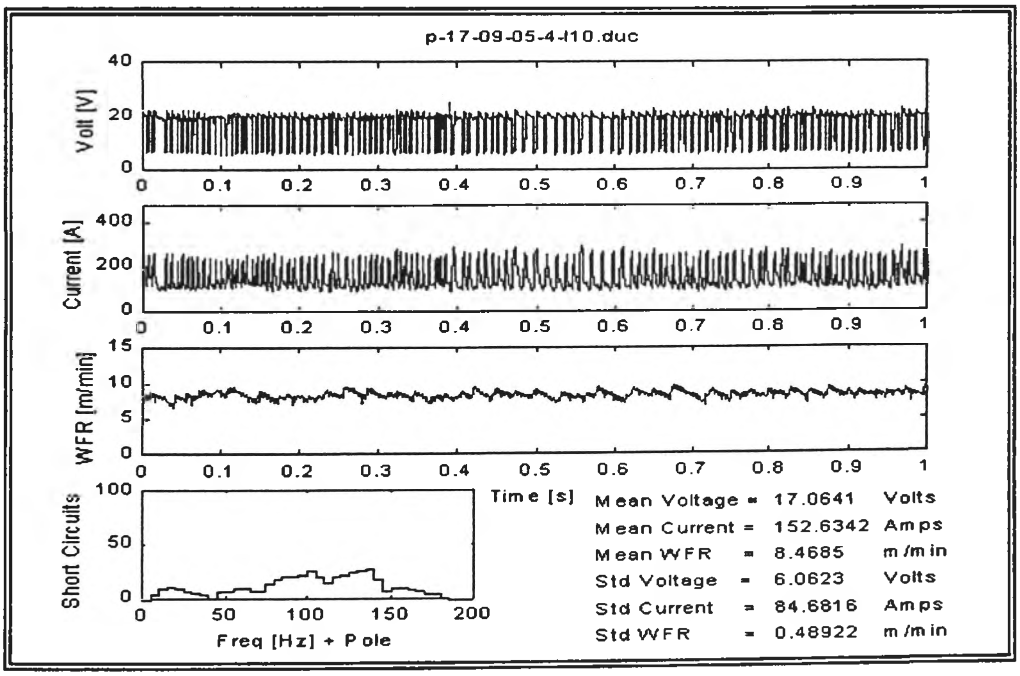

Plot A7-2

Sample p-17-09-05-4 layer 10

Sample p-18-09-05-4

Data:			
Voltage [V]	18	Weld width [mm]	12.9
Wire feed rate [m/min]	9	Stand-off at layer 1 [mm]	15
Travel speed [mm/sec]	5	Stand-off at layer 10 [mm]	15
Number of layers	10	Temperature at layer 10 [deg.C]	638
Weld height [mm]	22.5	Pinch setting	4

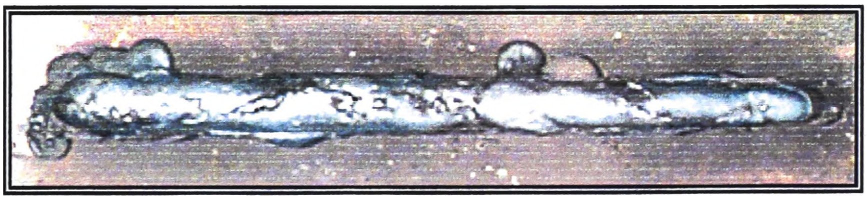

Figure A7-3

Sample p-18-09-05-4 (Top view)

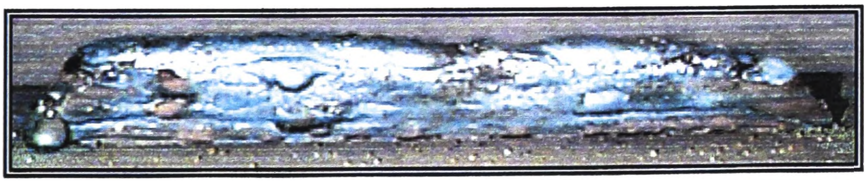

Figure A7-4

Sample p-18-09-05-4 (Front view)

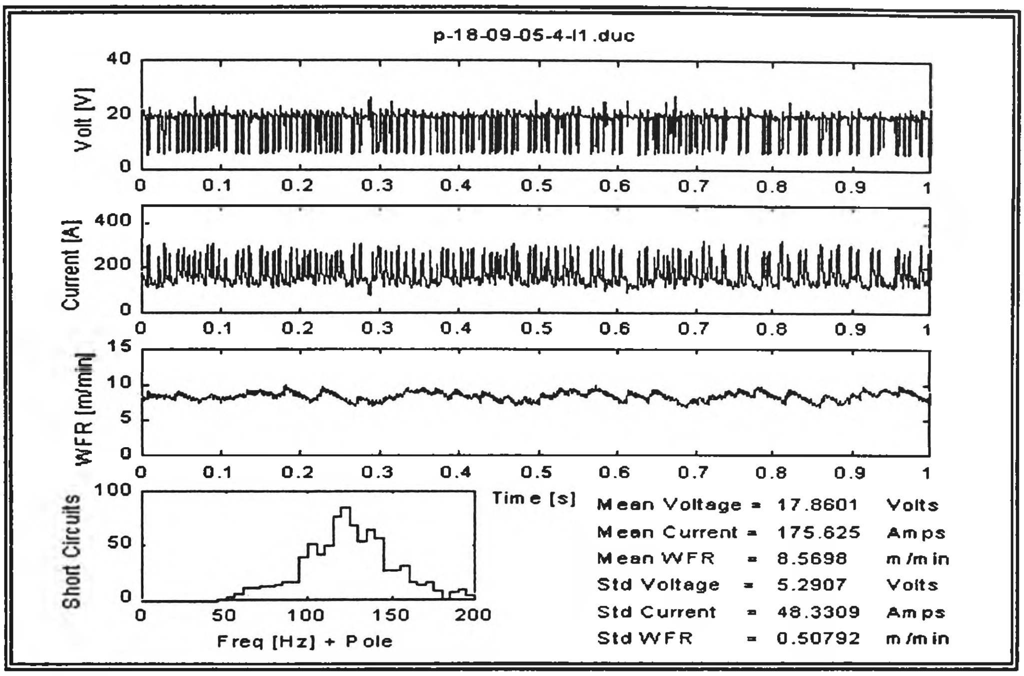

Plot A7-3

Sample p-18-09-08-4-layer 1

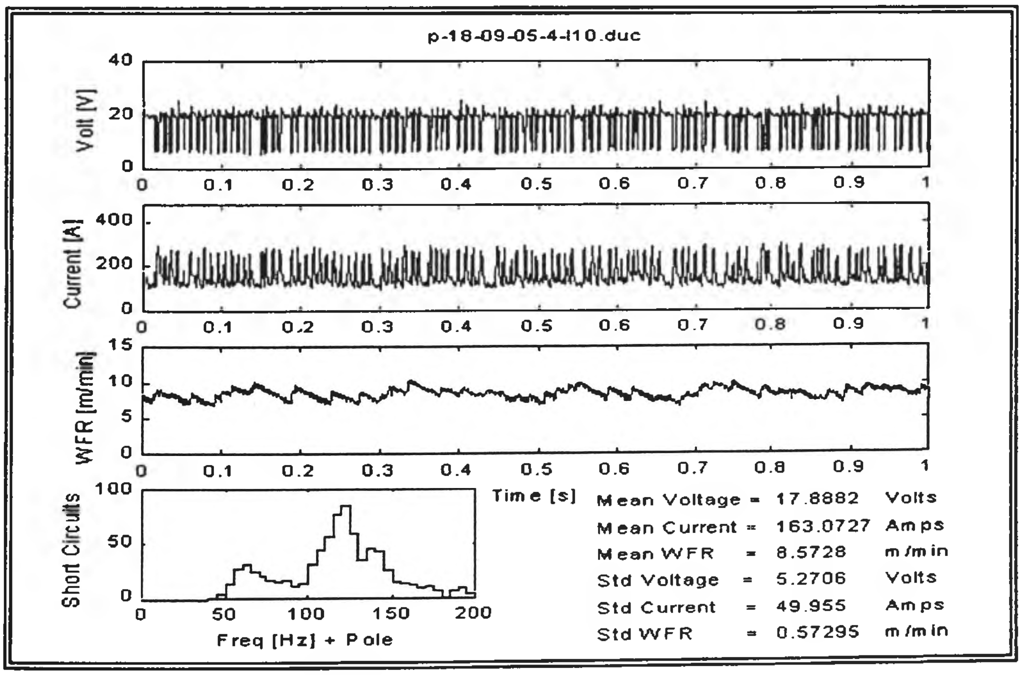

Plot A7-4

Sample p-18-09-08-4-layer 10

Sample p-19-09-05-4

Data:			
Voltage [V]	19	Weld width [mm]	13.2
Wire feed rate [m/min]	9	Stand-off at layer 1 [mm]	15
Travel speed [mm/sec]	5	Stand-off at layer 10 [mm]	15
Number of layers	10	Temperature at layer 10 [deg.C]	682
Weld height [mm]	20	Pinch setting	4

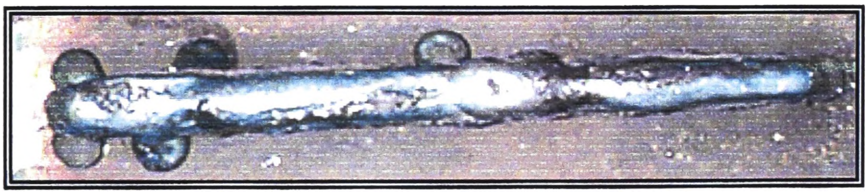

Figure A7-5

Sample p-19-09-05-4 (Top view)

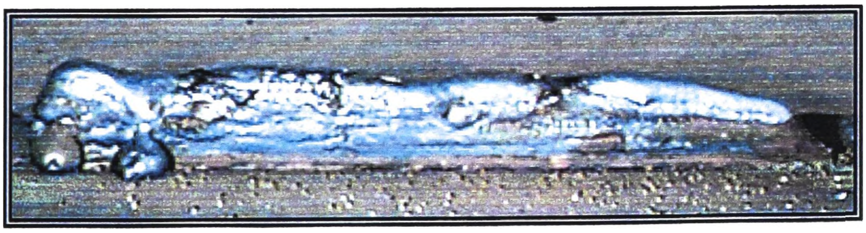

Figure A7-6

Sample p-19-09-05-4 (Front view)

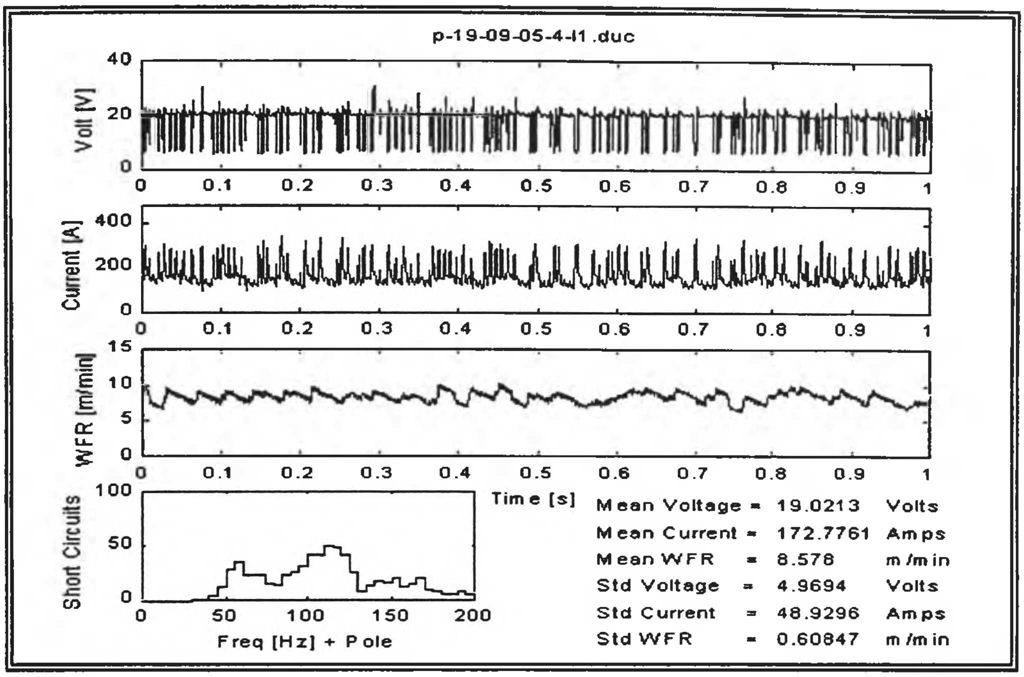

Plot A7-5

Sample p-19-09-05-4-layer 1

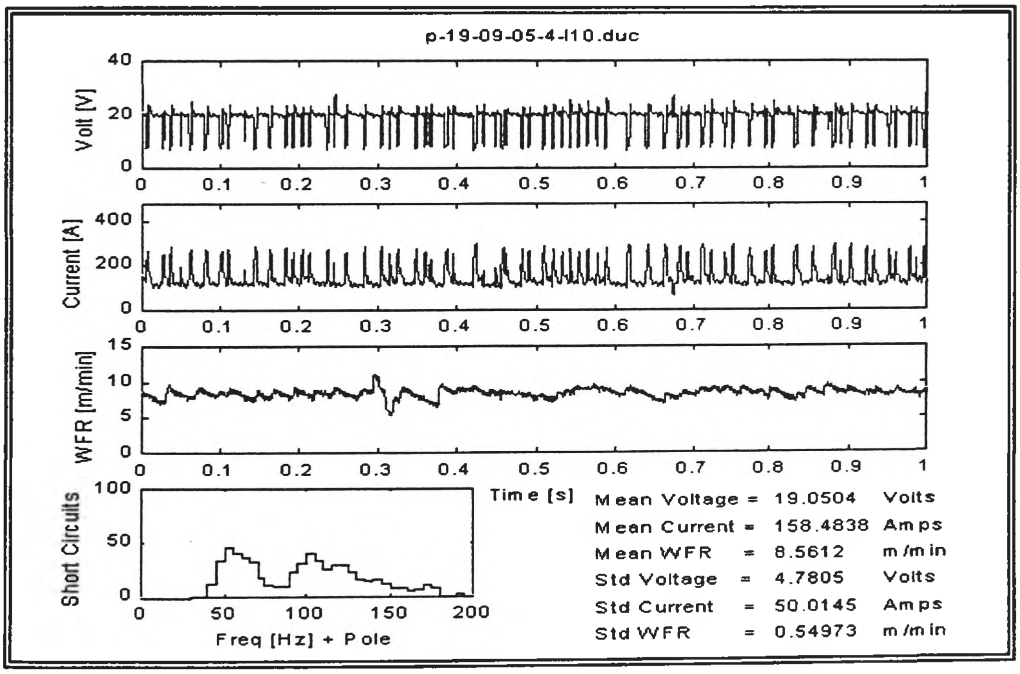

Plot A7-6

Sample p-19-09-05-4-layer 10

Table A8

Workpiece Code	Voltage [V]	Current [V]	WFR [m/min]	Travel Speed [mm/sec]	Heat Input [J/mm]	Gas Flow [l/min]	Temp at start [C]	Temp at layer 10 [C]	Number of Layers	Stand-off at start [mm]	Stand-off at layer 10 [mm]	Weld height [mm]	Weld width [mm]
p-17-03-05-4	17	79	3	5	268.6	15	20	230	10	15	17.5	15	7.2
p-18-03-05-4	18	80	3	5	288.0	15	21	273	10	15	21.0	14.5	6.8
p-19-03-05-4	19	79	3	5	300.2	15	25	350	10	15	21.5	14.4	6.8
p-17-04-05-4	17	99.1	4	5	336.9	15	20	419	10	15	19.0	16.5	7.26
p-18-04-05-4	18	100.1	4	5	360.4	15	27	437	10	15	19.0	14	8.64
p-19-04-05-4	19	102.2	4	5	388.4	15	24	461	10	15	20.0	14	8.2
p-17-05-05-4	17	120.5	5	5	409.7	15	22	365	10	15	18.0	18	9.3
p-18-05-05-4	18	124.32	5	5	447.6	15	26	406	10	15	18.0	18	9.2
p-19-05-05-4	19	121.24	5	5	460.7	15	20	501	10	15	18.0	17	8.62
p-17-06-05-4	17	135.14	6	5	459.5	15	24	444	10	15	17.0	19	8.64
p-18-06-05-4	18	137.27	6	5	494.2	15	23	465	10	15	18.0	18	8.94
p-19-06-05-4	19	135.92	6	5	516.5	15	22	473	10	15	15.0	18	8.8
p-17-07-05-4	17	152.32	7	5	517.9	15	24	537	10	15	15.0	20	10.1
p-18-07-05-4	18	154.88	7	5	557.6	15	26	602	10	15	15.0	19	9.92
p-19-07-05-4	19	151.88	7	5	577.1	15	24	595	10	15	17.0	18	10.2
p-17-08-05-4	17	158.56	8	5	539.1	15	20	599	10	15	14.0	22.5	9.64
p-18-08-05-4	18	163.86	8	5	589.9	15	20	627	10	15	14.5	20.5	10.5
p-19-08-05-4	19	162.48	8	5	617.4	15	22	572	10	15	15.5	19	12
p-17-09-05-4	17	173.2	9	5	588.9	15	28	590	10	15	12.0	23.5	11.2
p-18-09-05-4	18	175.6	9	5	632.2	15	24	638	10	15	14.5	22.54	12.9
p-19-09-05-4	19	172.78	9	5	656.6	15	26	682	10	15	14.5	20	13.2

Appendix B

Seam Data Settings

Travel Speed = 5 mm/sec

WFR Set [m/min]	Voltage set [%]	Purge Time [sec]	Pre Flow Time [sec]	Ign Voltage [%]	Ign WFR [m/min]	Ign Move Delay [sec]	Heat Speed [mm/sec]	Heat Time [sec]	Heat Distance [mm]	Heat Voltage [%]	Heat WFR [m/min]	Cool Time [sec]	Fill Time [sec]	b_back Time [sec]	Post_Flow time [sec]	Fill Voltage [%]	Fill WFR [m/min]
1	75	0.1	0.1	125	0.01	0	5	5	25	75	1	0	0	0.5	1	100	0
2	75	0.1	0.1	125	0.5	0	5	5	25	75	2	0	0	0.5	1	100	0
3	75	0.1	0.1	125	0.5	0	5	5	25	75	3	0	1	0.5	1	100	1.5
4	75	0.1	0.1	125	0.5	0	5	5	25	75	4	0	1	0.5	1	100	2
5	75	0.1	0.1	125	0.5	0	5	5	25	75	5	0	1	0.5	1	100	2.5
6	75	0.1	0.1	125	0.5	0	5	5	25	75	6	0	1	0.5	1	100	3
7	100	0.1	0.1	125	1	0	5	5	25	100	7	0	1	0.5	1	100	3.5
8	100	0.1	0.1	125	1	0	5	5	25	100	8	0	1	0.5	1	100	4
9	100	0.1	0.1	125	1	0	5	5	25	100	9	0	1	0.5	1	100	4.5
10	100	0.1	0.1	125	1	0	5	5	25	100	10	0	1	0.5	1	100	5

Travel Speed = 10 mm/sec

WFR Set [m/min]	Voltage set [%]	Purge Time [sec]	Pre Flow Time [sec]	Ign Voltage [%]	Ign WFR [m/min]	Ign Move Delay [sec]	Heat Speed [mm/sec]	Heat Time [sec]	Heat Distance [mm]	Heat Voltage [%]	Heat WFR [m/min]	Cool Time [sec]	Fill Time [sec]	b_back Time [sec]	Post_Flow time [sec]	Fill Voltage [%]	Fill WFR [m/min]
1	75	0.1	0.1	125	0.5	0	10	2	20	75	1	0	0	0.5	1	100	0
2	75	0.1	0.1	125	0.5	0	10	2	20	75	2	0	0	0.5	1	100	0
3	75	0.1	0.1	125	0.5	0	10	2	20	75	3	0	1	0.5	1	100	1.5
4	75	0.1	0.1	125	0.5	0	10	2	20	75	4	0	1	0.5	1	100	2
5	75	0.1	0.1	125	0.5	0	10	2	20	75	5	0	1	0.5	1	100	2.5
6	75	0.1	0.1	125	0.5	0	10	2	20	75	6	0	1	0.5	1	100	3
7	100	0.1	0.1	125	1	0	10	2	20	100	7	0	1	0.5	1	100	3.5
8	100	0.1	0.1	125	1	0	10	2	20	100	8	0	1	0.5	1	100	4
9	100	0.1	0.1	125	1	0	10	2	20	100	9	0	1	0.5	1	100	4.5
10	100	0.1	0.1	125	1	0	10	2	20	100	10	0	1	0.5	1	100	5

Appendix C

C1 Characteristic of Wire Feed Rate 1 m/min

C2 Characteristic of Wire Feed Rate 2 m/min

C3 Characteristic of Wire Feed Rate 3 m/min

C4 Characteristic of Wire Feed Rate 4 m/min

C5 Characteristic of Wire Feed Rate 5 m/min

C6 Characteristic of Wire Feed Rate 6 m.min

C7 Characteristic of Wire Feed Rate 7 m/min

C8 Characteristic of Wire Feed Rate 8 m/min

C9 Characteristic of Wire Feed Rate 9 m/min

C1 Characteristic of Wire Feed Rate 1 m/min

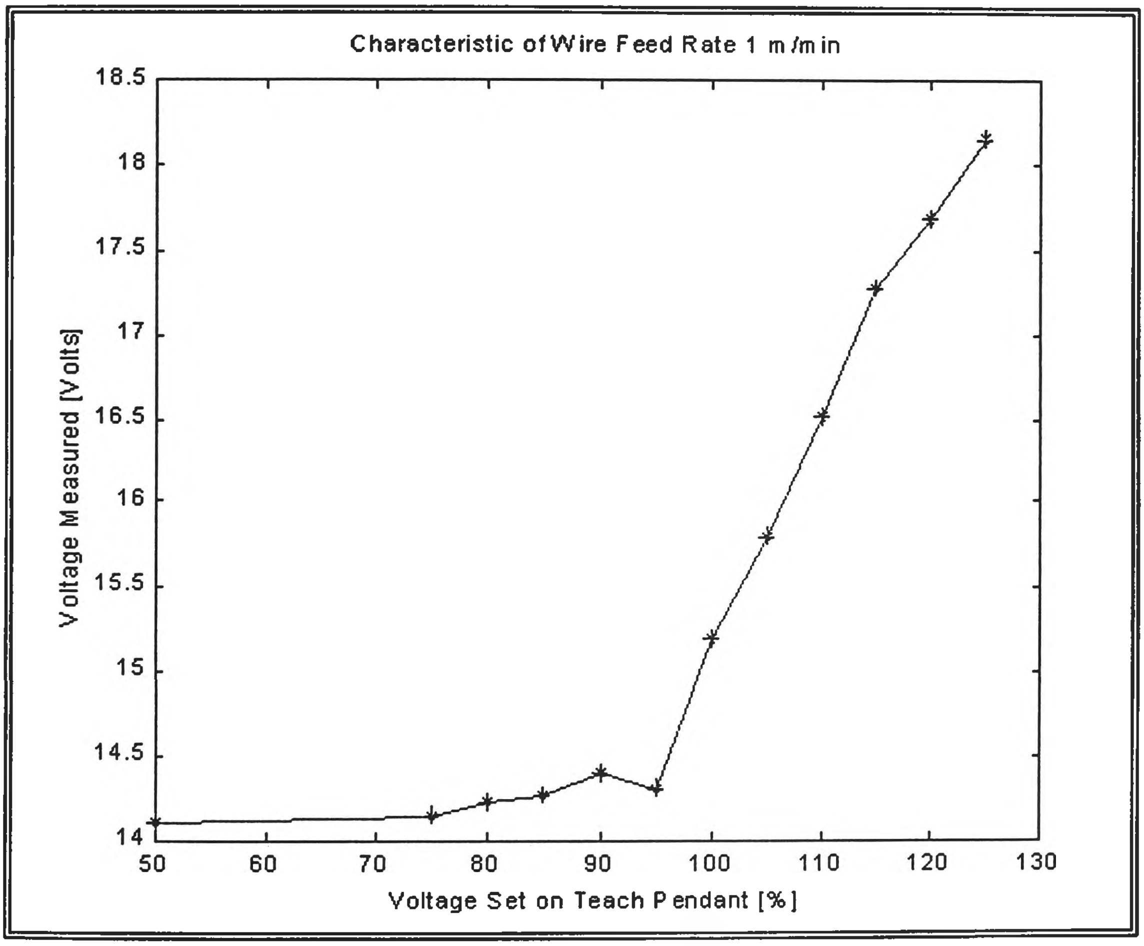

<u>C2 Characteristic of Wire Feed Rate 2 m/min</u>

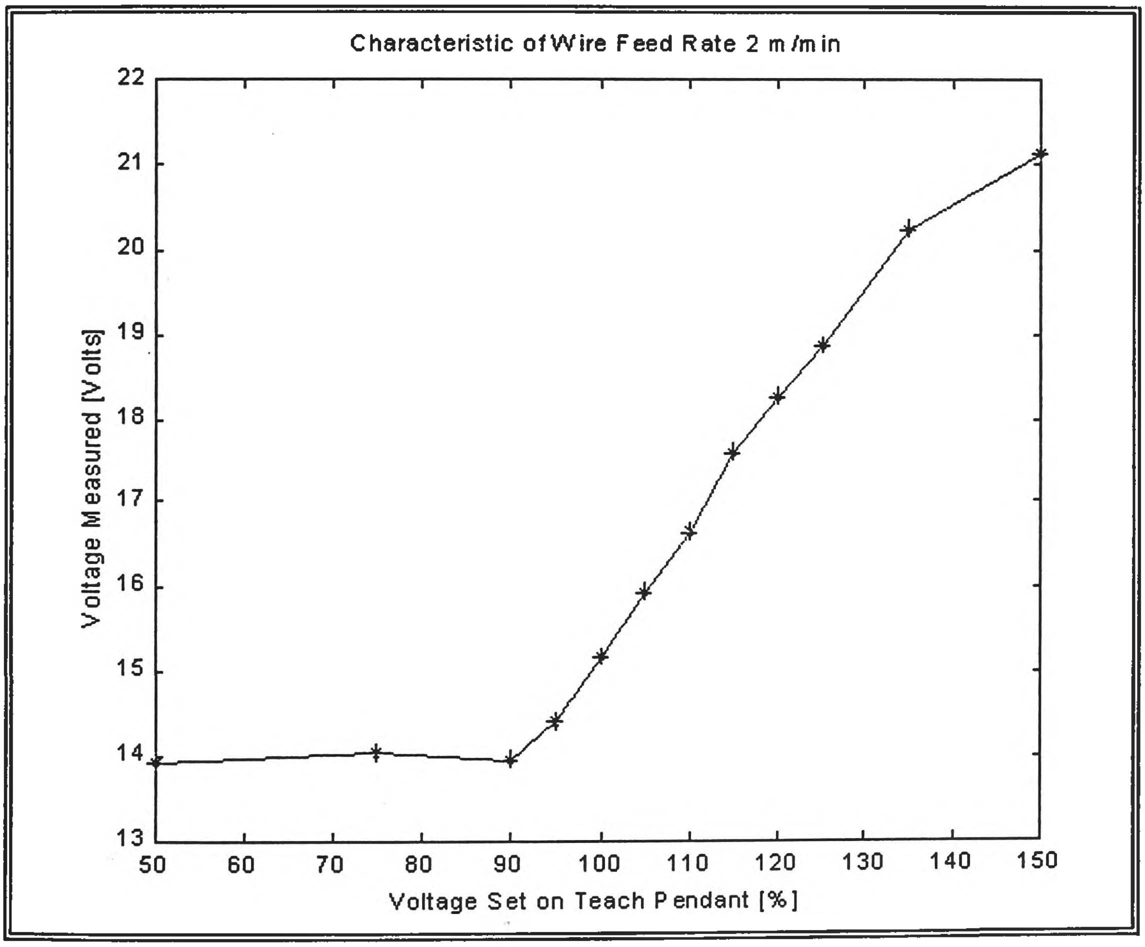

C3 Characteristic of Wire Feed Rate 3 m/min

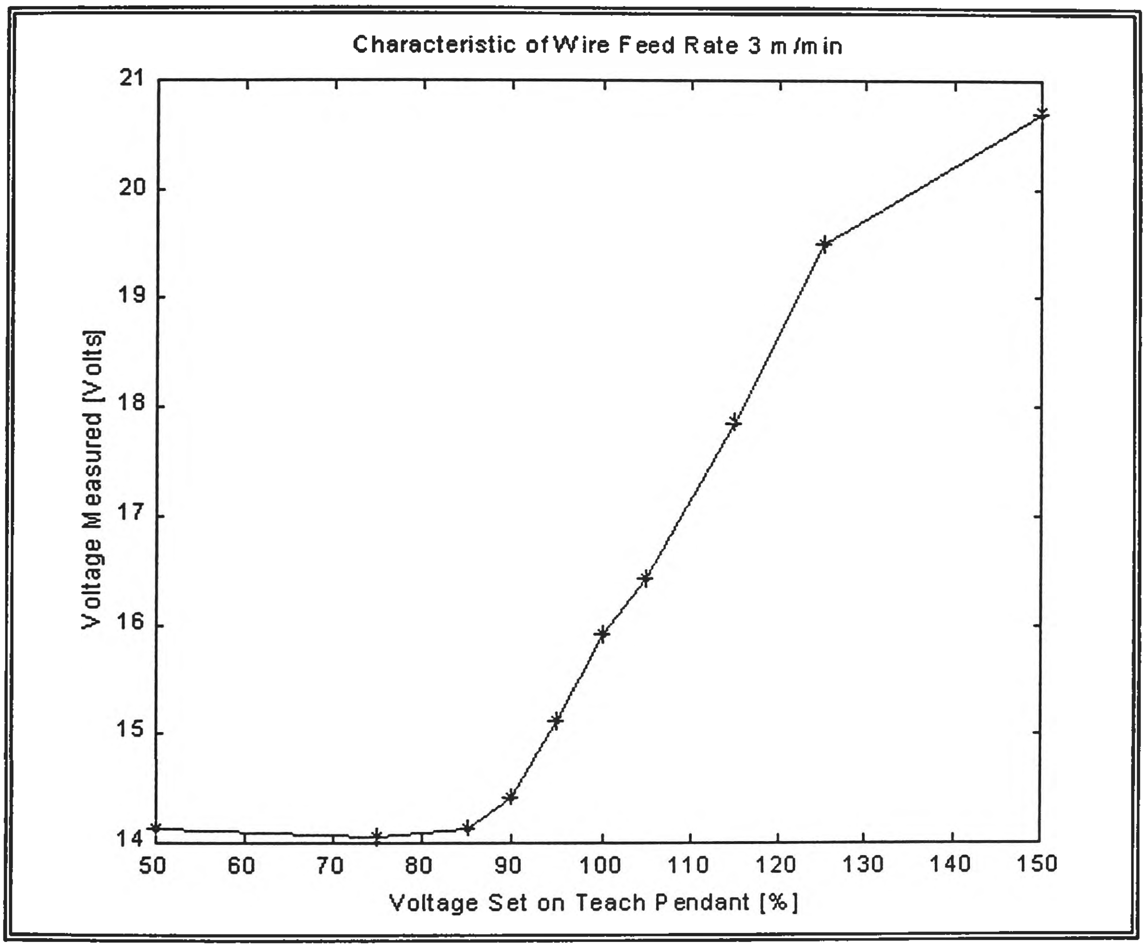

C4 Characteristic of Wire Feed Rate 4 m/min

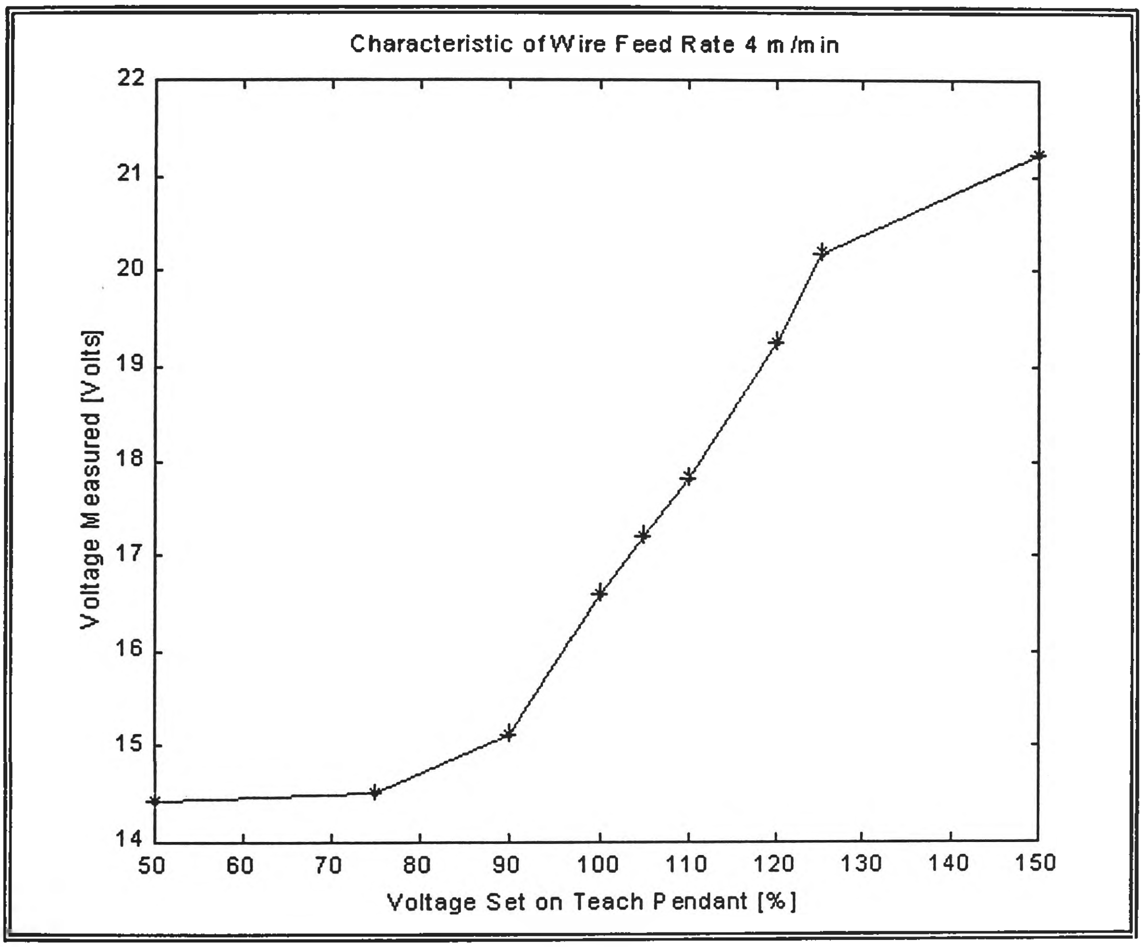

C5 Characteristic of Wire Feed Rate 5 m/min

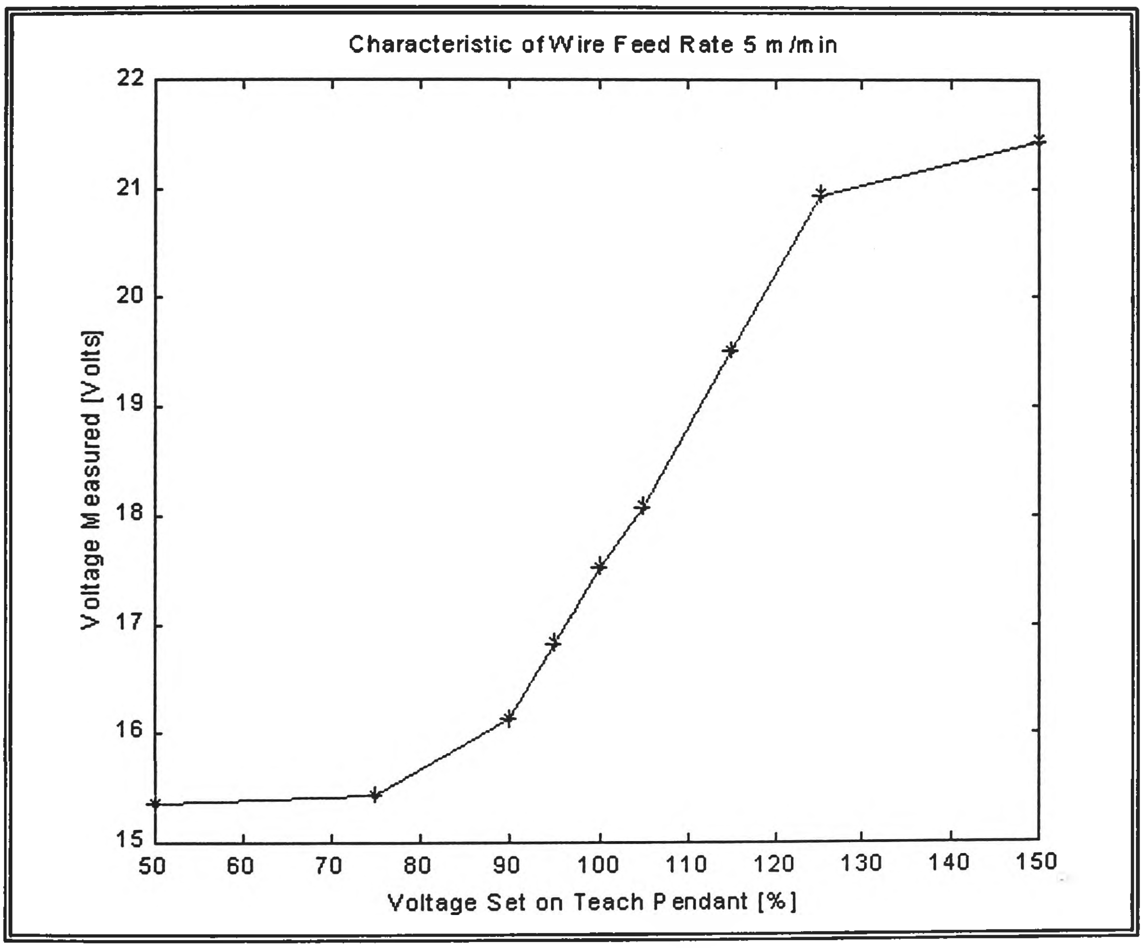

C6 Characteristic of Wire Feed Rate 6 m/min

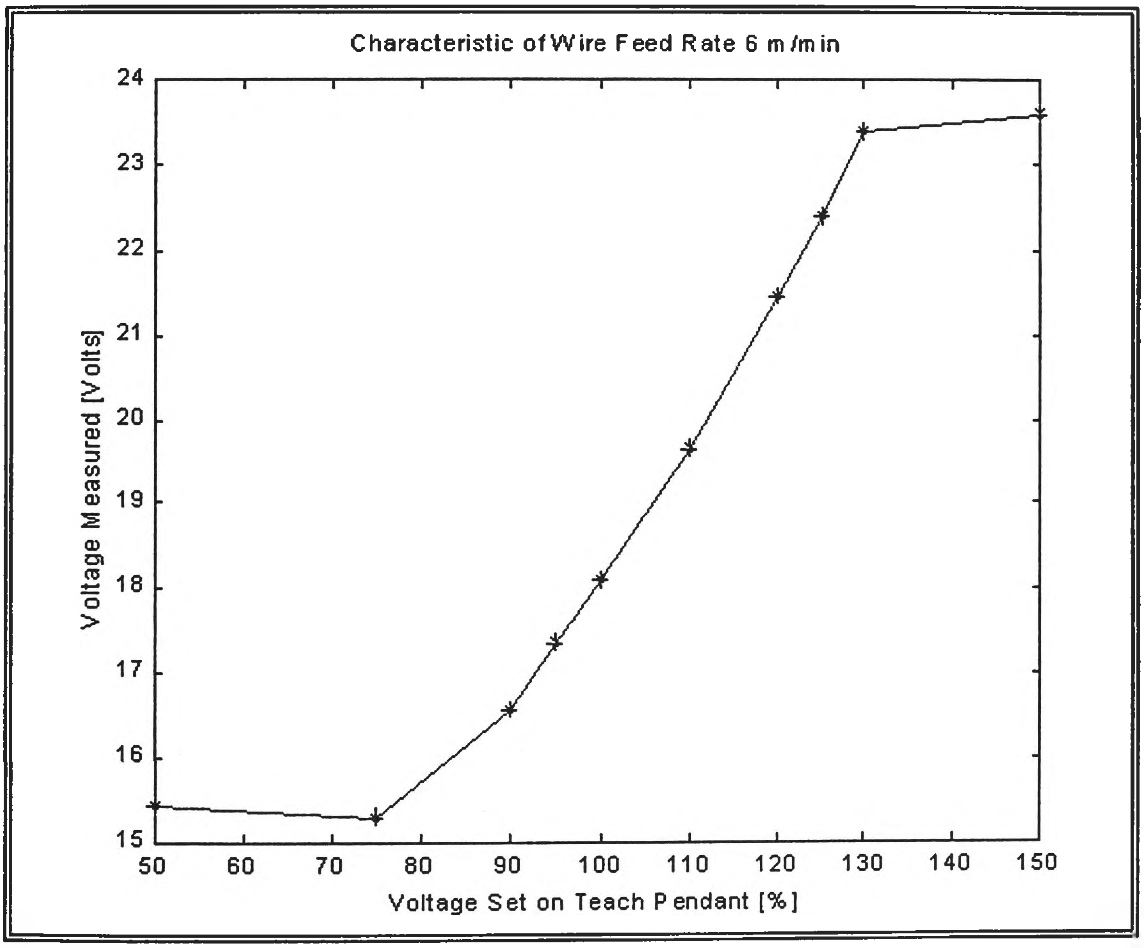

C7 Characteristic of Wire Feed Rate 7 m/min

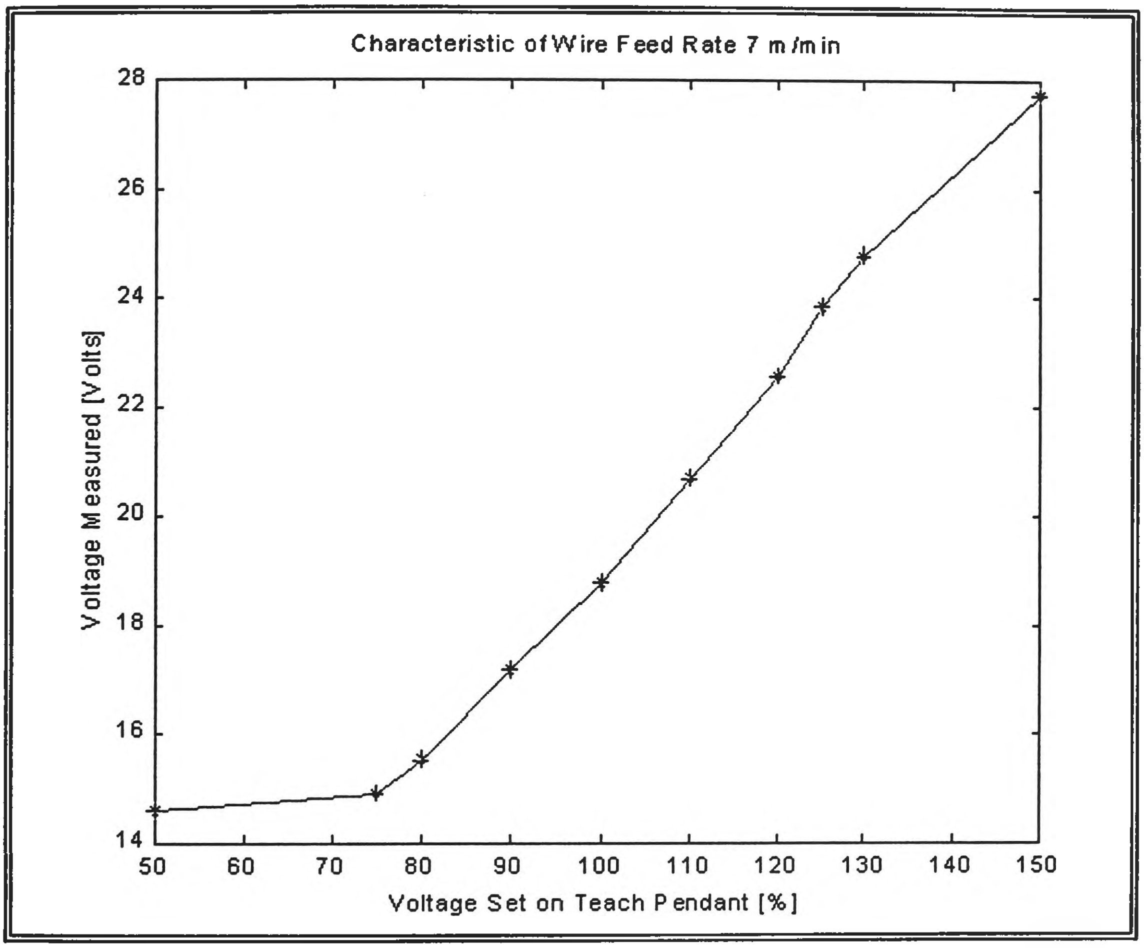

C8 Characteristic of Wire Feed Rate 8 m/min

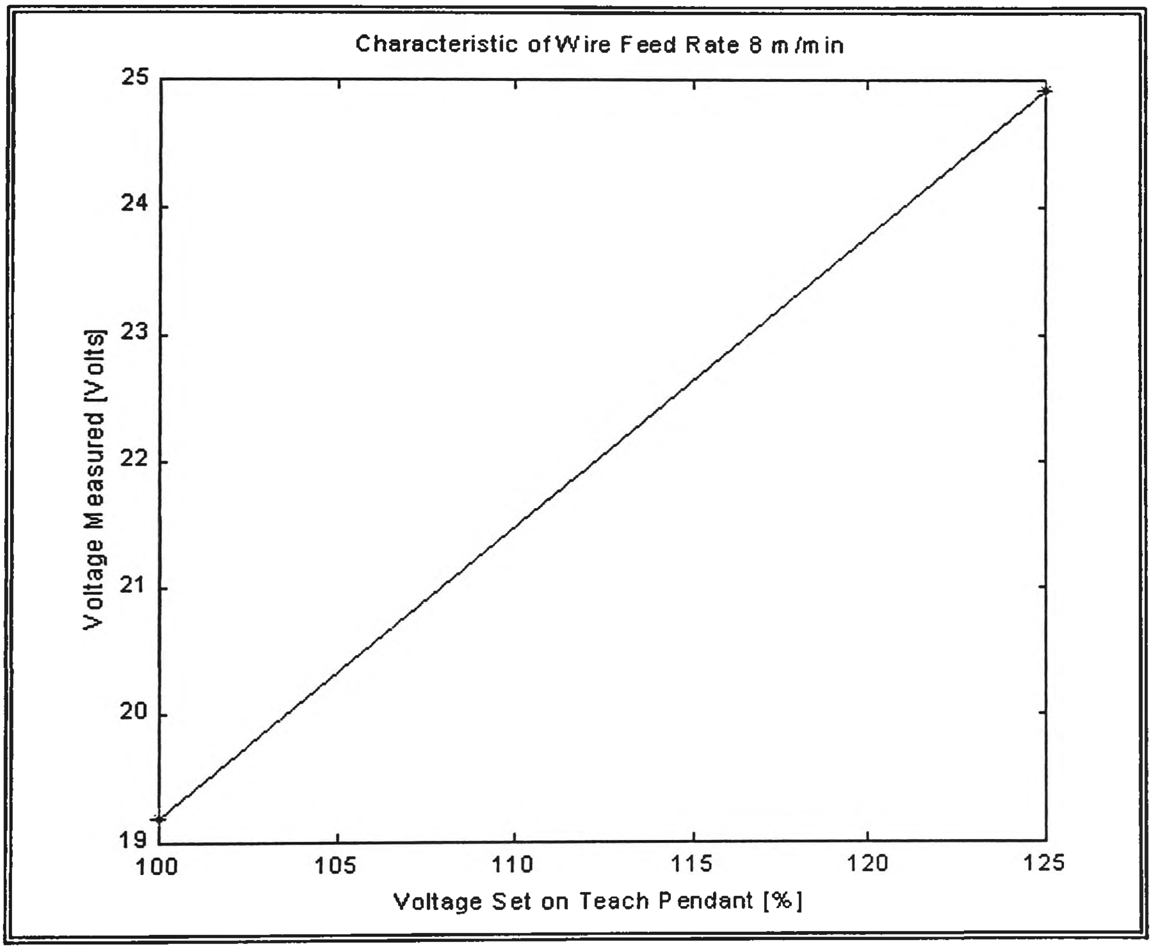

C9 Characteristic of Wire Feed Rate 9 m/min

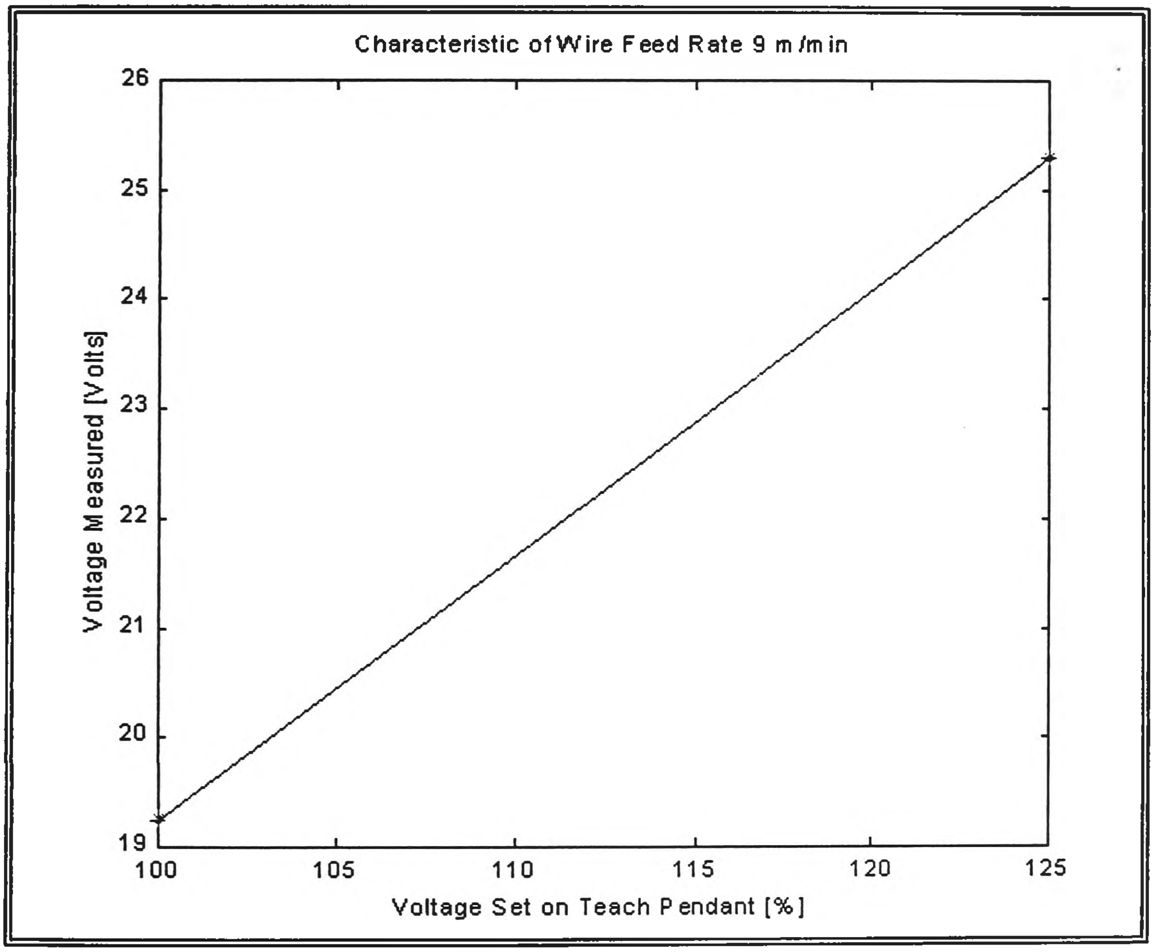

Appendix D

Thin Wall Program

F_WALL.PRG

```
%%%
  VERSION:1
  LANGUAGE:ENGLISH
%%%

MODULE F_WALL
  CONST string string2:="";
  CONST string string1:="";
  VAR robtarget pwt:=[[1029.55,-61.12,867.66],[0.364574,0.045856,0.929915,-
0.015569],[-1,-1,0,0],[9E+09,9E+09,9E+09,9E+09,9E+09,9E+09]];
  CONST robtarget p40:=[[1029.54,-61.12,867.65],[0.364561,0.045847,0.92992,-
0.015573],[-1,-1,0,0],[9E+09,9E+09,9E+09,9E+09,9E+09,9E+09]];
  CONST robtarget p30:=[[1038.27,-
98.69,818.64],[0.364146,0.045626,0.930088,-0.015872],[-
1,0,0,0],[9E+09,9E+09,9E+09,9E+09,9E+09,9E+09]];
  CONST robtarget p20:=[[1003.28,-74.15,912.09],[0.364029,0.04567,0.930133,-
0.015835],[-1,-1,0,0],[9E+09,9E+09,9E+09,9E+09,9E+09,9E+09]];
  CONST robtarget p10:=[[602.84,57.42,989.53],[0.364006,0.045642,0.930144,-
0.015763],[0,-1,0,0],[9E+09,9E+09,9E+09,9E+09,9E+09,9E+09]];
```

```
CONST robtarget pw4:=[[951.61,51.67,858.63],[0.358874,0.054668,0.931657,-
0.015375],[0,-1,0,0],[9E+09,9E+09,9E+09,9E+09,9E+09,9E+09]];
CONST robtarget pw3:=[[896.83,-
215.45,824.98],[0.373866,0.086186,0.923469,0.001078],[-1,0,-
1,0],[9E+09,9E+09,9E+09,9E+09,9E+09,9E+09]];
VAR robtarget pw2:=[[536.82,-57.04,1121.5],[0.351149,0.028061,0.935513,-
0.026891],[-1,-1,-1,0],[9E+09,9E+09,9E+09,9E+09,9E+09,9E+09]];
VAR robtarget pw1:=[[536.83,-57.03,1121.5],[0.351157,0.028078,0.93551,-
0.026874],[-1,-1,-1,0],[9E+09,9E+09,9E+09,9E+09,9E+09,9E+09]];

PROC wall()
  FOR i FROM 1 TO reg2 DO
    TPWrite "layer no.:"\Num:=i;
    ArcL\On,pw1,v100,sd6_frank,wd_frank,wvd_mike,fine,tool0;
    ArcL\Off,pw2,v100,sd6_frank,wd_frank,wvd_mike,fine,tool0;
    MoveL pwt,v500,z10,tool0;
    pw1.trans.z:=pw1.trans.z+reg1;
    pw2.trans.z:=pw2.trans.z+reg1;
    pwt.trans.z:=pwt.trans.z+reg1;
  ENDFOR
ENDPROC

! PERS weavedata wv1:=[0,0,0,0,0,0,0,0,0,0,0,0,0,0,0];
! PERS welddata wd2:=[5,22,50,0,0,0];
```

```
! PERS welddata wd1:=[0,0,0,0,0,0];

! PERS seamdata sm1:=[0.5,0.5,0.5,1,0.2,0,35,72];

PROC main()

  pw1:=[[1029.56,-61.11,817.51],[0.364551,0.045732,0.929928,-0.015642],[-1,-1,0,0],[9E+09,9E+09,9E+09,9E+09,9E+09,9E+09]];

  pw2:=[[1032.49,93.72,816.36],[0.364432,0.045731,0.929974,-0.015723],[0,-1,0,0],[9E+09,9E+09,9E+09,9E+09,9E+09,9E+09]];

  pwt:=[[1029.55,-61.12,867.65],[0.364571,0.045856,0.929916,-0.015569],[-1,-1,0,0],[9E+09,9E+09,9E+09,9E+09,9E+09,9E+09]];

  TPReadNum reg1,"increment (mm) =";

  TPReadNum reg2,"no. layers =";

  MoveJ p10,v1000,z200,tool0;

  MoveL pwt,v500,z10,tool0;

  wall;

  MoveJ p10,v1000,z200,tool0;

ENDPROC

ENDMODULE
```

Appendix E

Surface Regularity Approximation

Profile.m

```
clear

clf

(Enter the file name for x and y coordinate)


start=3;

xt=xt(start:length(xt));

xb=xb(start:length(xb));

yt=yt(start:length(yt));

yb=yb(start:length(yb));


ym=mean([yt' yb']);

yt=ym-yt;

yb=ym-yb;


%Top side

pt=polyfit(xt,yt,1);

theta_t=atan(pt(1));

xtt=xt*cos(theta_t)+yt*sin(theta_t);

ytt=yt*cos(theta_t)-xt*sin(theta_t);
```

```
%fit a polynomial curve
pt1=polyfit(xtt,ytt,1);
Yt=polyval(pt1,xtt);

%Bottom side
pb=polyfit(xb,yb,1);
theta_b=atan(pb(1));
xbb=xb*cos(theta_b)+yb*sin(theta_b);
ybb=yb*cos(theta_b)-xb*sin(theta_b);

pb1=polyfit(xbb,ybb,1);
Yb=polyval(pb1,xbb);



%Average_Roughness_Top
RT = sum(abs(ytt-Yt))/(2*length(xtt))
%Average_Roughness_bottom
RB = sum(abs(ybb-Yb))/(2*length(xbb))
%Average_witdh
%W= mean(ytt)-mean(ybb)
Angle_1= theta_t*180/pi
Angle_2= theta_b*180/pi
%Weld_height= 16.90-5.20
```

```
figure(1);

plot(xt,yt,xb,yb)

title('Cross-sectional View of the Specimen')

xlabel('x coordinate [mm]-- Weld Height');

ylabel('y coordinate [mm]-- Profile Variations')


figure(2);

plot(xtt,ytt,xbb,ybb)

title('Cross-sectional View of the Specimen')

xlabel('x coordinate [mm]-- Weld Height');

ylabel('y coordinate [mm]-- Profile Variations')


figure(3);

plot(xtt,ytt,xtt,Yt)

title('Side 1')

xlabel('x coordinate [mm]-- Weld Height');

ylabel('y coordinate [mm]-- Profile Variations')


figure(4);

plot(xbb,ybb,xbb,Yb)

title('Side 2')

xlabel('x coordinate [mm]-- Weld Height');

ylabel('y coordinate [mm]-- Profile Variations')
```

Appendix F

Thin Walled Object Results

Travel Speed = 5 mm/sec

F1 Wire Feed Rate of 1 m/min

F2 Wire Feed Rate of 2 m/min

F3 Wire Feed Rate of 3 m/min

F4 Wire Feed Rate of 4 m/min

F5 Wire Feed Rate of 5 m/min

F6 Wire Feed Rate of 6 m/min

F7 Wire Feed Rate of 7 m/min

F8 Wire Feed Rate of 8 m/min

F9 Wire Feed Rate of 9 m/min

Travel Speed = 10 mm/sec

F10 Wire Feed Rate of 1 m/min

F11 Wire Feed Rate of 2 m/min

F12 Wire Feed Rate of 3 m/min

F13 Wire Feed Rate of 4 m/min

F14 Wire Feed Rate of 5 m/min

F15 Wire Feed Rate of 6 m/min

F16 Wire Feed Rate of 7 m/min

F17 Wire Feed Rate of 8 m/min

F18 Wire Feed Rate of 9 m/min

F19 Table Data

Travel Speed = 5 mm/sec

F1 Wire Feed Rate of 1 m/min

Sample f1-75-05

Set Values	
Voltage [%]	75
Wire feed rate [m/min]	1
Travel speed [mm/sec]	5
Gas flow [l/min]	15

Weld Geometry		Visual Defects and Weld Property	
Weld height [mm]	11.7	Spatters	No
Weld width [mm]	2.6	Porosity	No
Stand-off at layer 1 [mm]	15	Excess material	No
Stand-off at layer 10 [mm]	16.5	Surface regularity [µm]	27.1
Temperature at layer 10 [deg.C]	150	Average hardness [HV]	167
Number of layers	10		

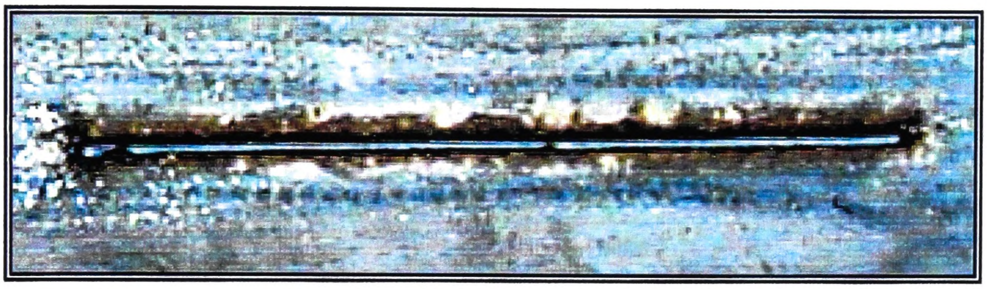

Figure F1-1

Sample f1-75-05 (top view)

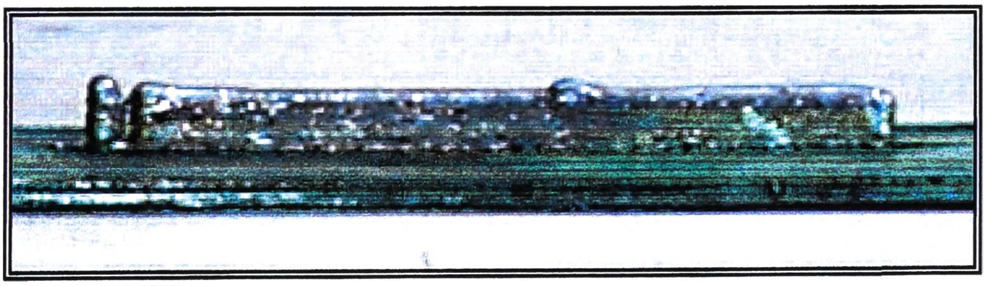

Figure F1-2

Sample f1-75-05 (front view)

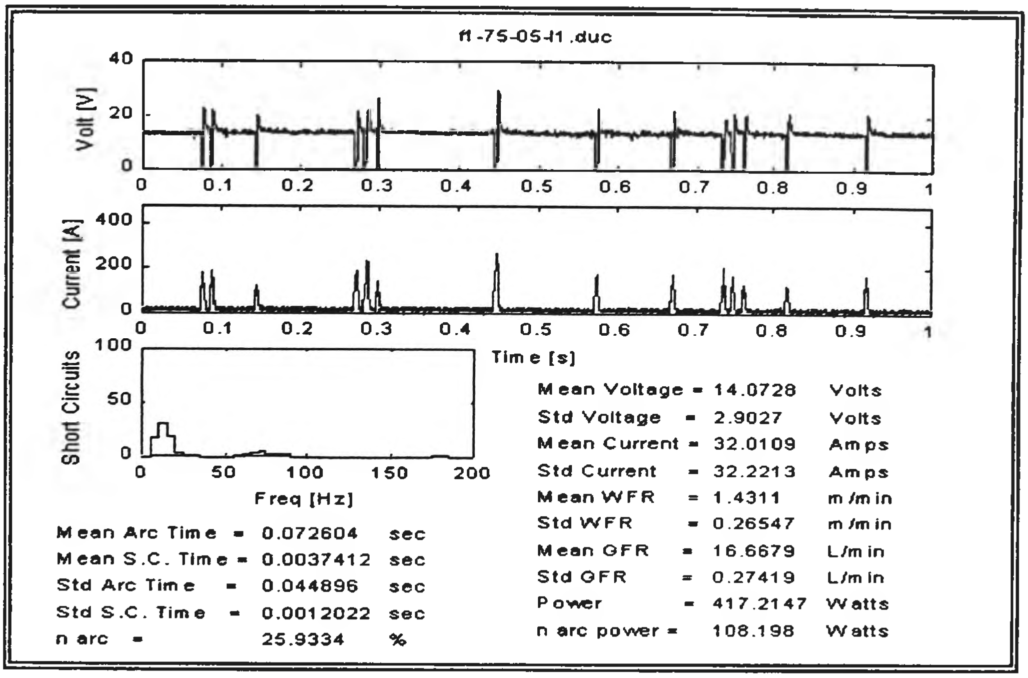

Plot F1-1

Sample f1-75-05-layer 1

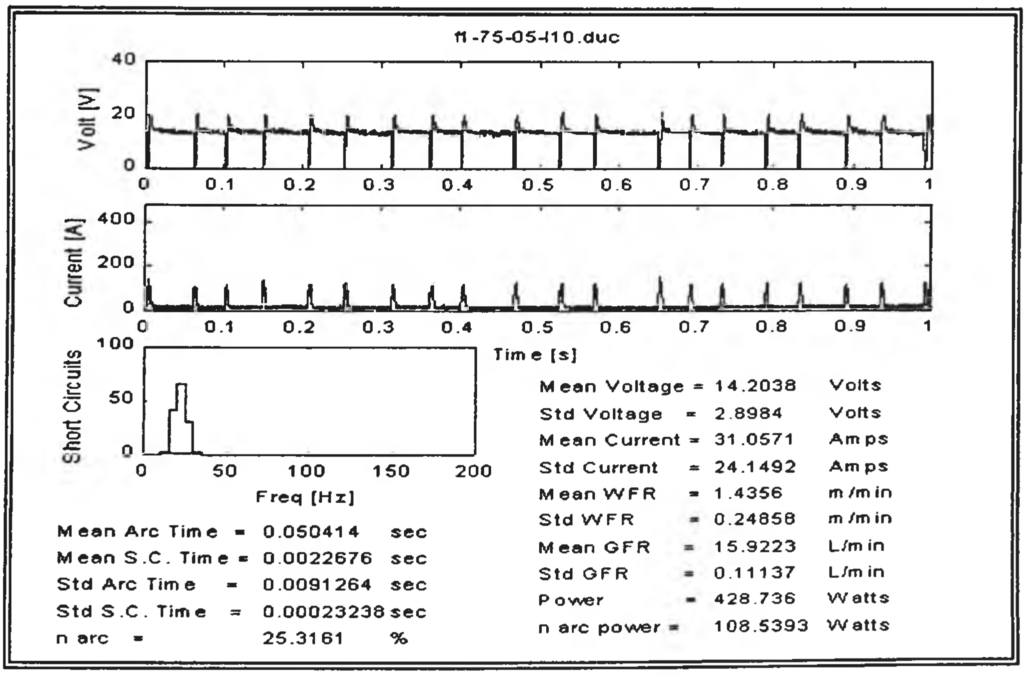

Plot F1-2

Sample f1-75-05-layer 10

Sample f1-95-05

Set Values	
Voltage [%]	95
Wire feed rate [m/min]	1
Travel speed [mm/sec]	5
Gas flow [l/min]	15

Weld Geometry		Visual Defects and Weld Property	
Weld height [mm]	10	Spatters	Yes
Weld width [mm]	3	Porosity	No
Stand-off at layer 1 [mm]	15	Excess material	No
Stand-off at layer 10 [mm]	16.5	Surface regularity [μm]	N/a
Temperature at layer 10 [deg.C]	160	Average hardness [HV]	N/a
Number of layers	10		

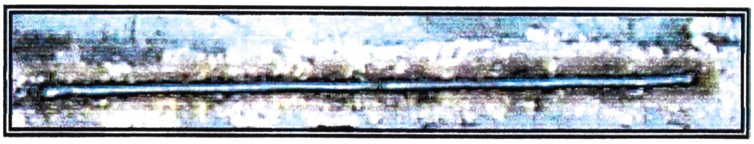

Figure F1-3

Sample f1-95-05 (top view)

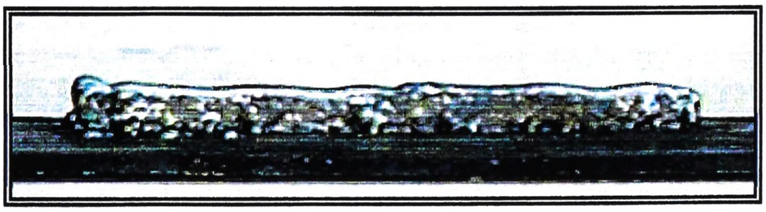

Figure F1-4

Sample f1-95-05 (front view)

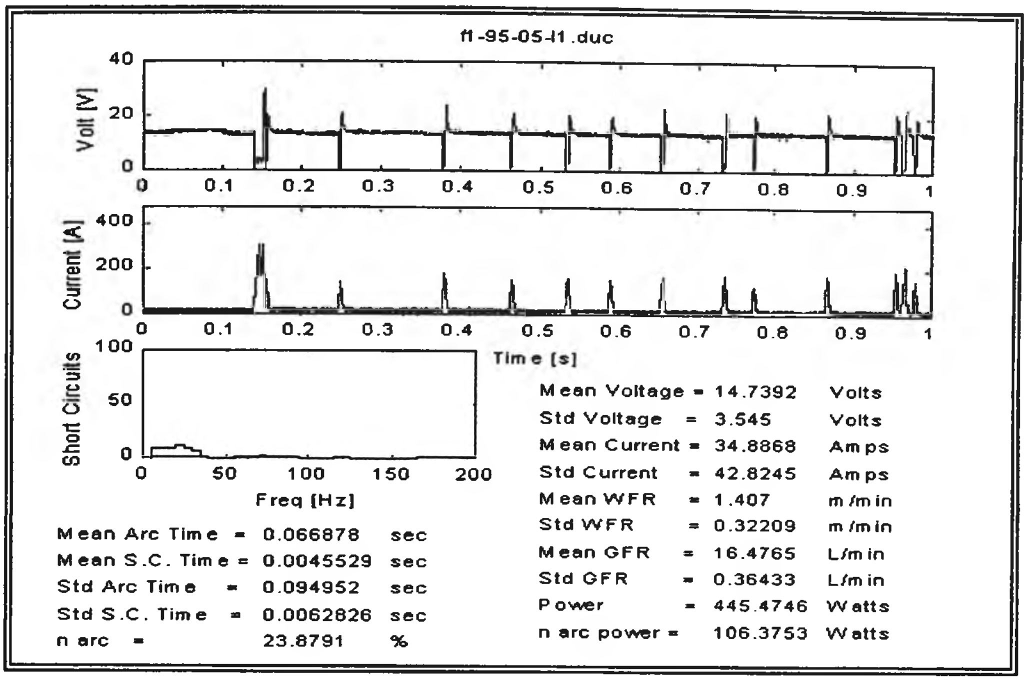

Plot F1-3

Sample f1-95-05-layer 1

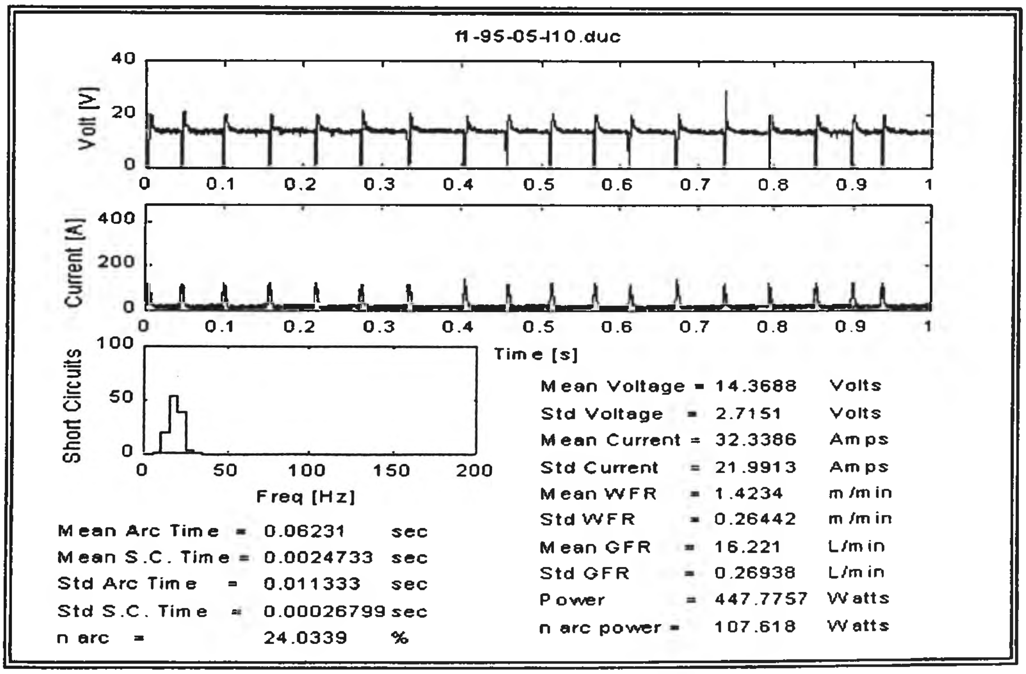

Plot F1-4

Sample f1-75-05-layer 10

Sample f1-100-05

Set Values	
Voltage [%]	100
Wire feed rate [m/min]	1
Travel speed [mm/sec]	5
Gas flow [l/min]	15

Weld Geometry		Visual Defects and Weld Property	
Weld height [mm]	9.5	Spatters	Yes
Weld width [mm]	3.2	Porosity	No
Stand-off at layer 1 [mm]	15	Excess material	No
Stand-off at layer 10 [mm]	18	Surface regularity [μm]	30.65
Temperature at layer 10 [deg.C]	165	Average hardness [HV]	164
Number of layers	10		

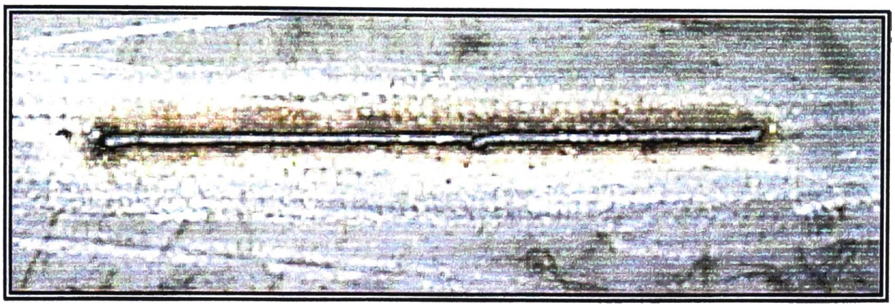

Figure F1-5

Sample f1-100-05 (top view)

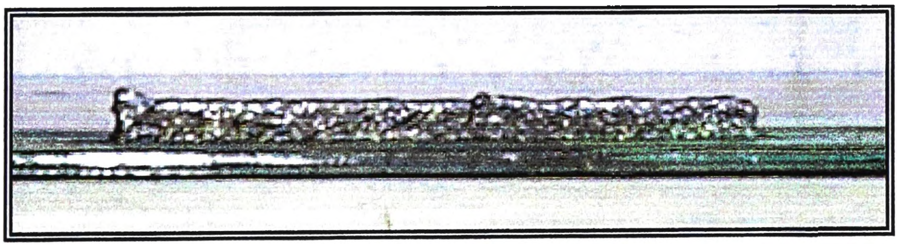

Figure F1-6

Sample f1-100-05 (front view)

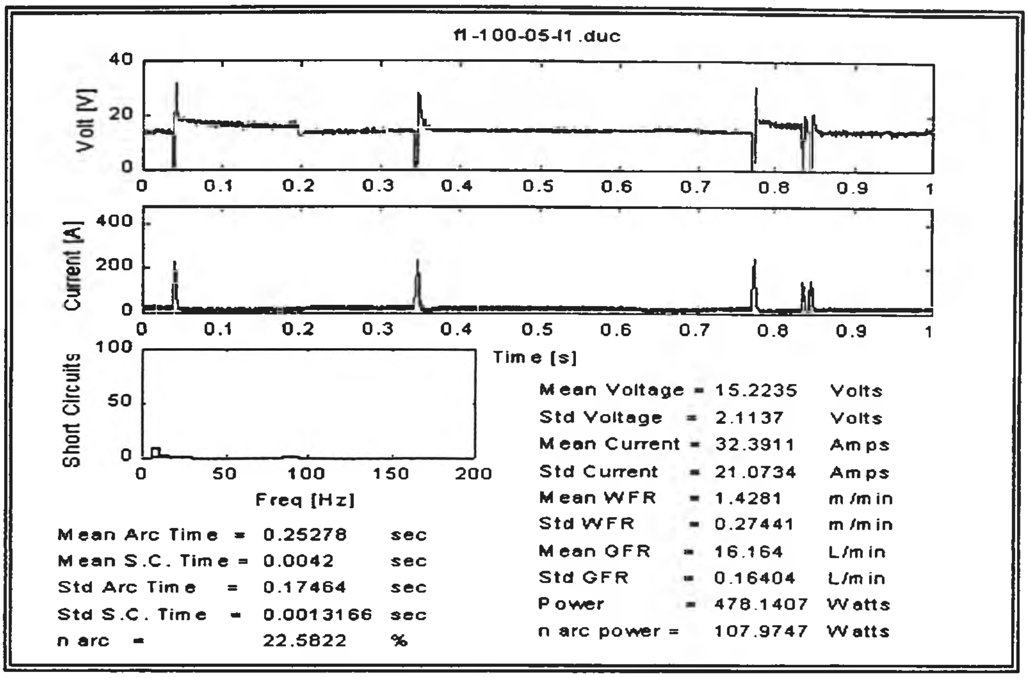

Plot F1-5

Sample f1-100-05-layer 1

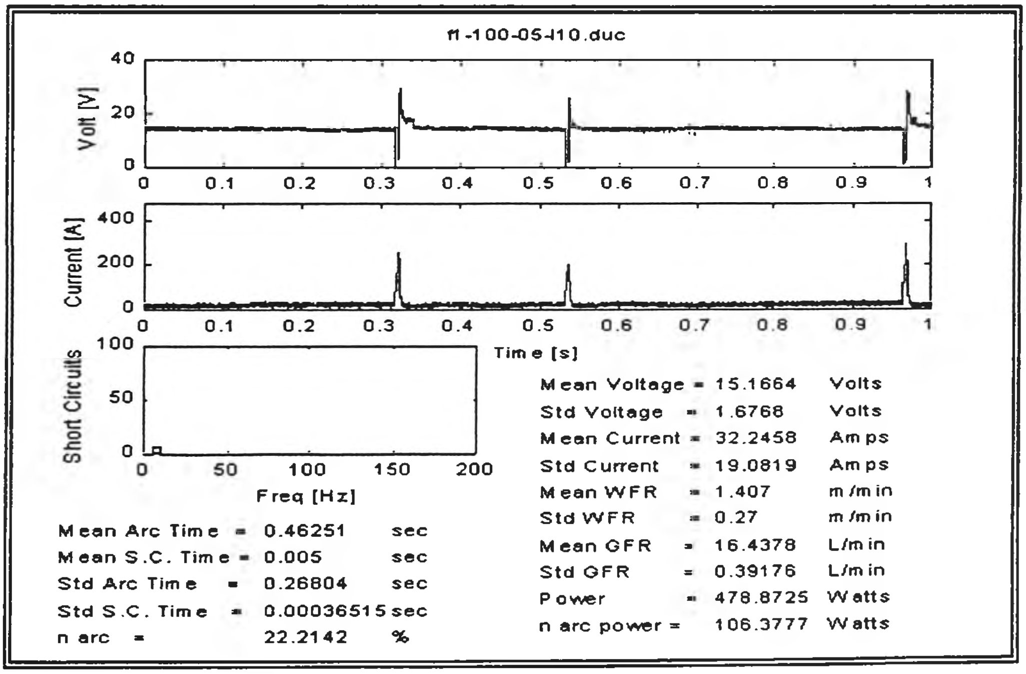

Plot F1-6

Sample f1-100-05-layer 10

Sample fl-105-05

Set Values	
Voltage [%]	105
Wire feed rate [m/min]	1
Travel speed [mm/sec]	5
Gas flow [l/min]	15

Weld Geometry		Visual Defects and Weld Property	
Weld height [mm]	9.3	Spatters	Yes
Weld width [mm]	3.3	Porosity	No
Stand-off at layer 1 [mm]	15	Excess material	No
Stand-off at layer 10 [mm]	18	Surface regularity [μm]	N/A
Temperature at layer 10 [deg.C]	166	Average hardness [HV]	N/A
Number of layers	10		

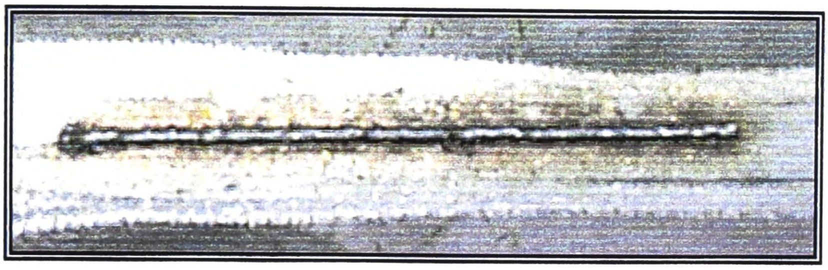

Figure F1-7

Sample f1-100-05 (top view)

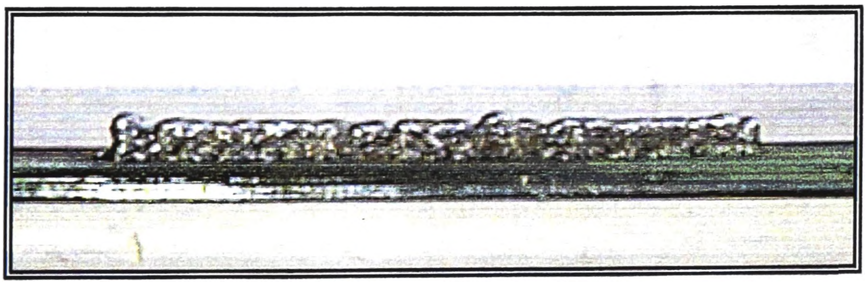

Figure F1-8

Sample f1-100-05 (front view)

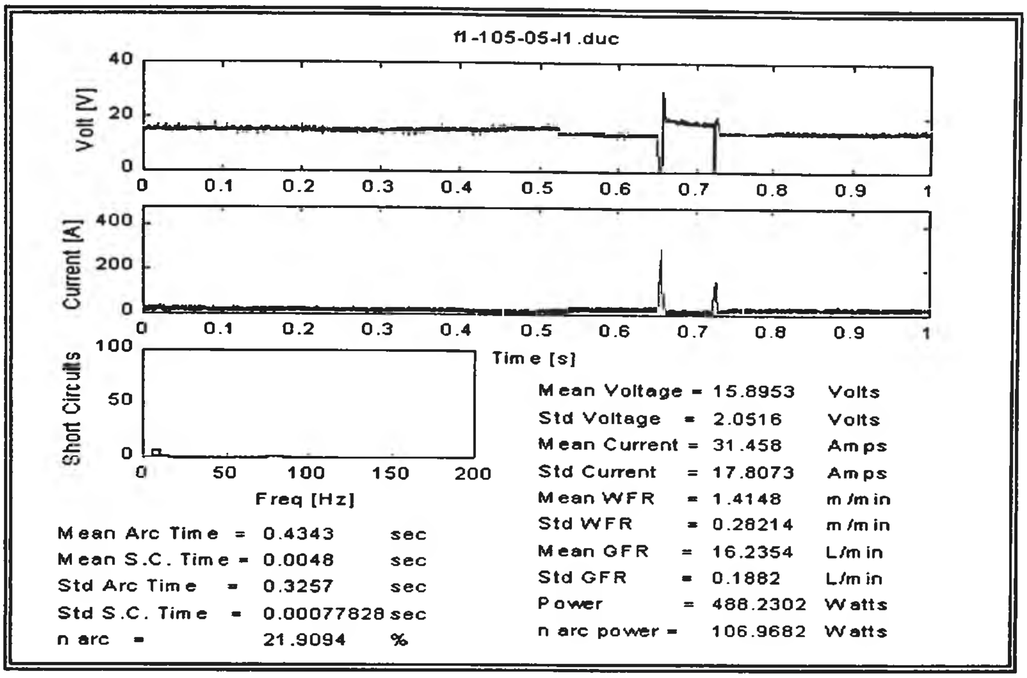

Plot F1-7

Sample f1-105-05-layer 1

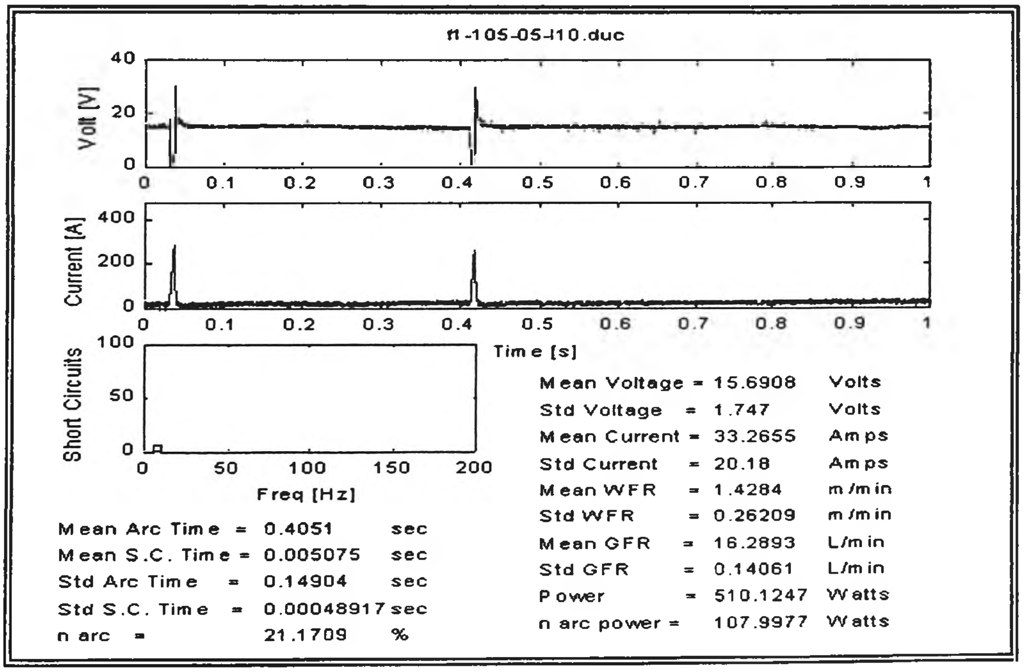

Plot F1-8

Sample f1-105-05-layer 10

Sample f1-110-05

Set Values	
Voltage [%]	110
Wire feed rate [m/min]	1
Travel speed [mm/sec]	5
Gas flow [l/min]	15

Weld Geometry		Visual Defects and Weld Property	
Weld height [mm]	9.0	Spatters	Yes
Weld width [mm]	3.3	Porosity	No
Stand-off at layer 1 [mm]	15	Excess material	No
Stand-off at layer 10 [mm]	18	Surface regularity [μm]	50.3
Temperature at layer 10 [deg.C]	165	Average hardness [HV]	157
Number of layers	10		

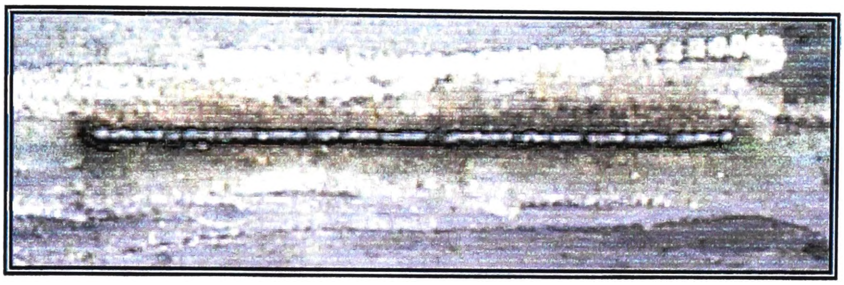

Figure F1-9

Sample f1-110-05 (top view)

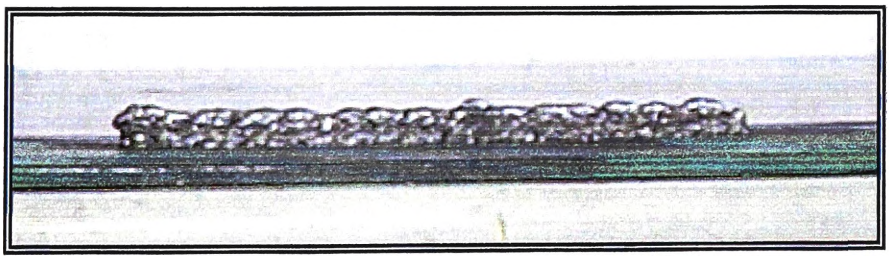

Figure F1-10

Sample f1-110-05 (front view)

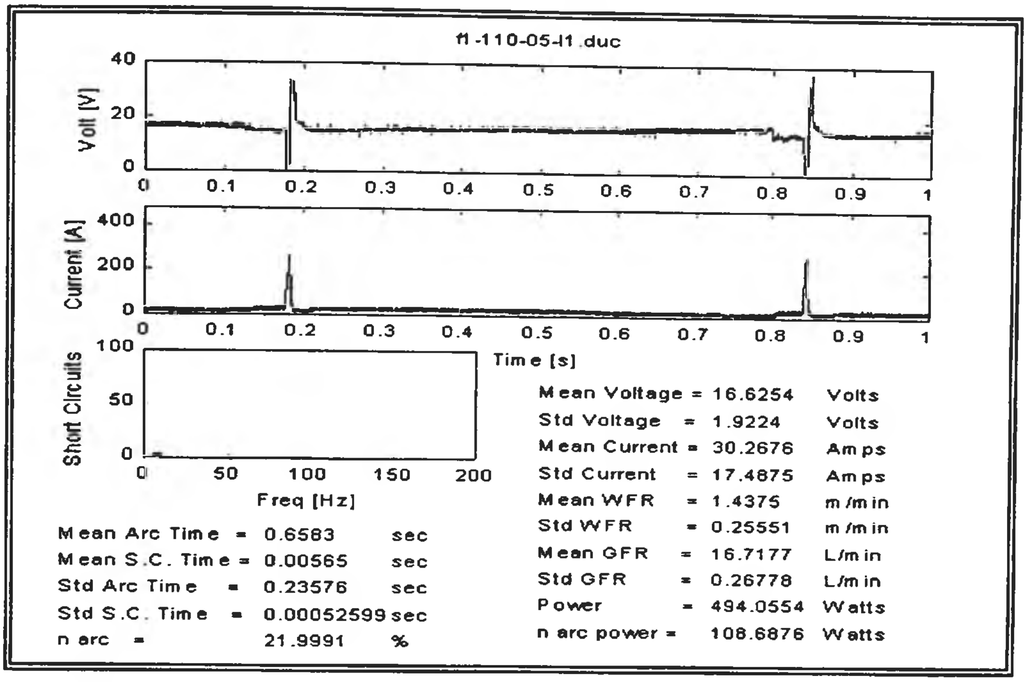

Plot F1-9

Sample f1-110-05-layer 1

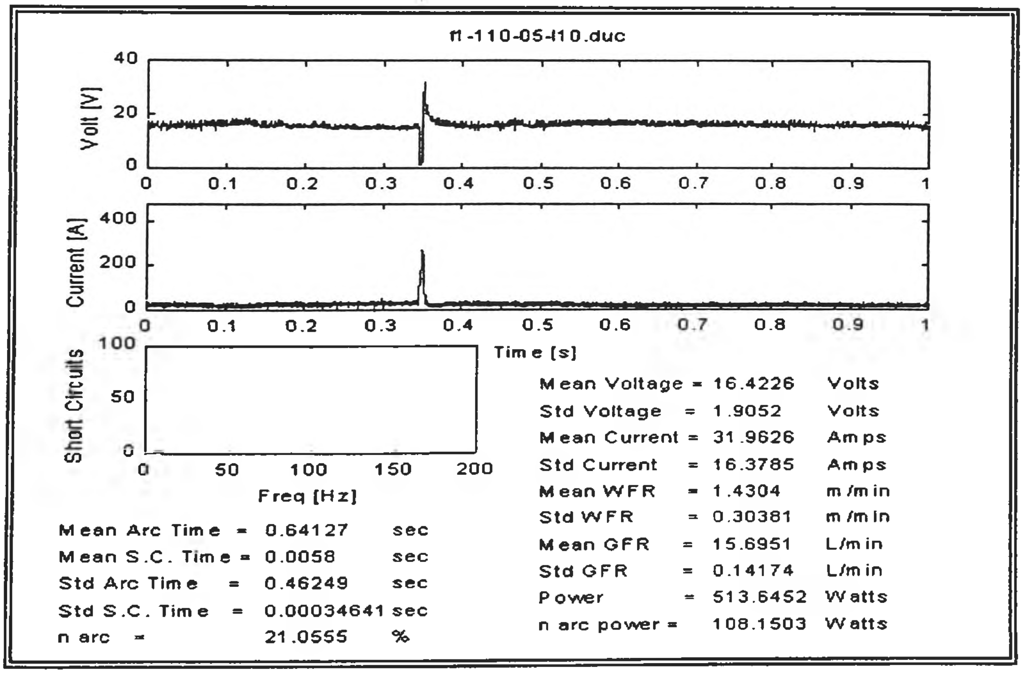

Figure F1-10

Sample f1-110-05-layer 10

F2 Wire Feed Rate of 2 m/min

Sample f2-75-05

Set Values	
Voltage [%]	75
Wire feed rate [m/min]	2
Travel speed [mm/sec]	5
Gas flow [l/min]	15

Weld Geometry		Visual Defects and Weld Property	
Weld height [mm]	13.6	Spatters	No
Weld width [mm]	3.6	Porosity	No
Stand-off at layer 1 [mm]	15	Excess material	No
Stand-off at layer 10 [mm]	16	Surface regularity [μm]	40.85
Temperature at layer 10 [deg.C]	180	Average hardness [HV]	166
Number of layers	10		

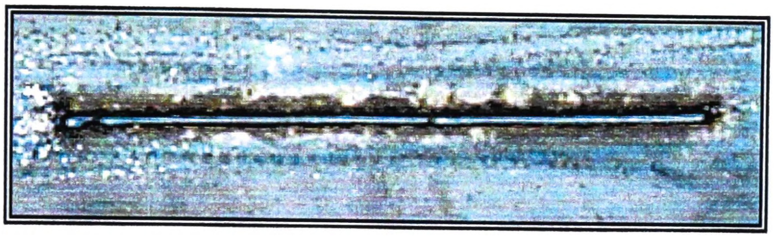

Figure F2-1

Sample f2-75-05 (top view)

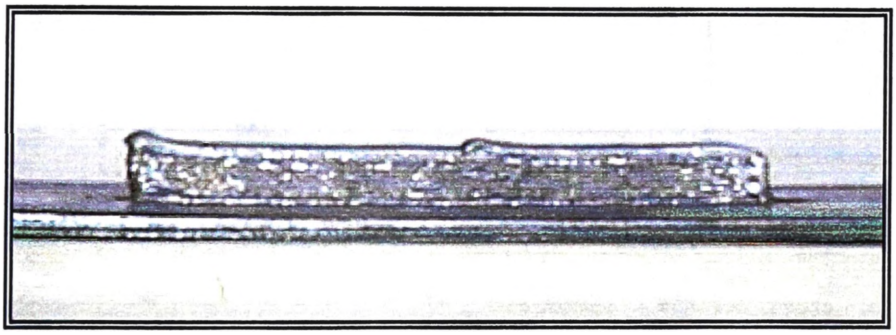

Sample F2-2

Sample f2-75-05 (front view)

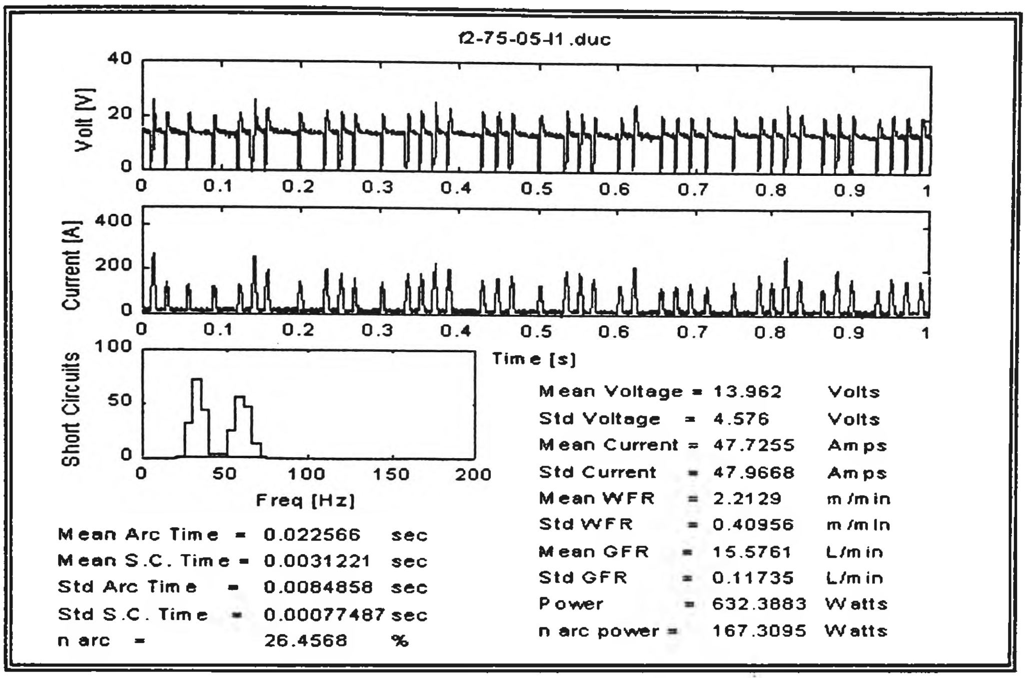

Plot F2-1

Sample f2-75-05-layer 1

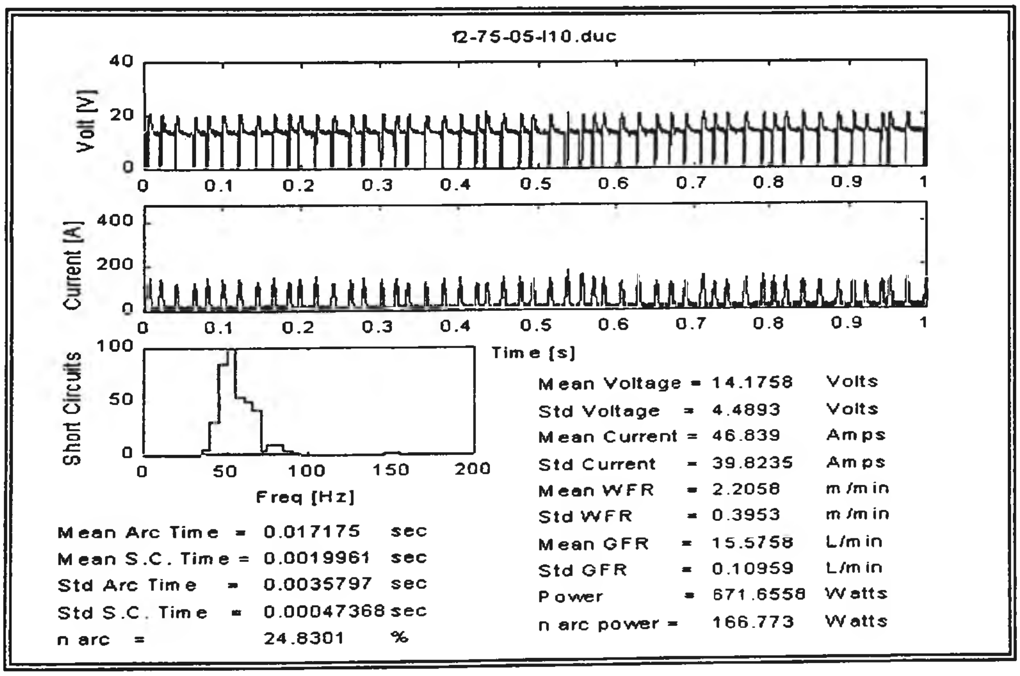

Plot F2-2

Sample f2-75-05-layer 10

Sample f2-95-05

Set Values	
Voltage [%]	95
Wire feed rate [m/min]	2
Travel speed [mm/sec]	5
Gas flow [l/min]	15

Weld Geometry		Visual Defects and Weld Property	
Weld height [mm]	13.1	Spatters	No
Weld width [mm]	3.6	Porosity	No
Stand-off at layer 1 [mm]	15	Excess material	No
Stand-off at layer 10 [mm]	15.5	Surface regularity [μm]	37
Temperature at layer 10 [deg.C]	187	Average hardness [HV]	165
Number of layers	10		

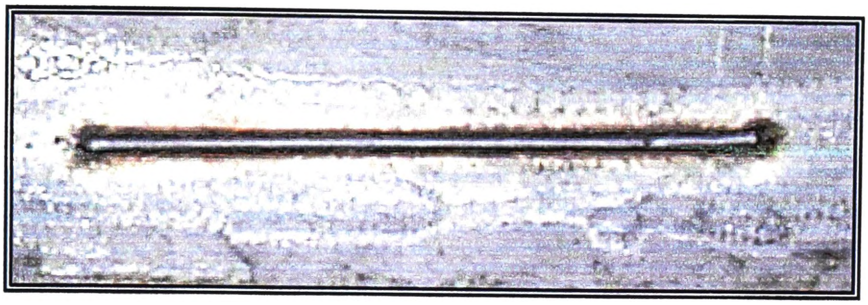

Figure F2-3

Sample f2-95-05 (top view)

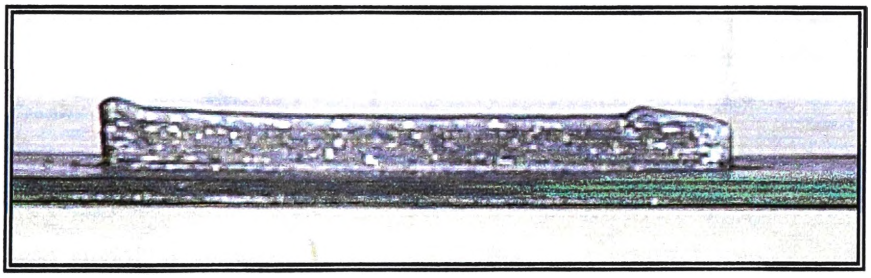

Figure F2-4

Sample f2-95-05 (front view)

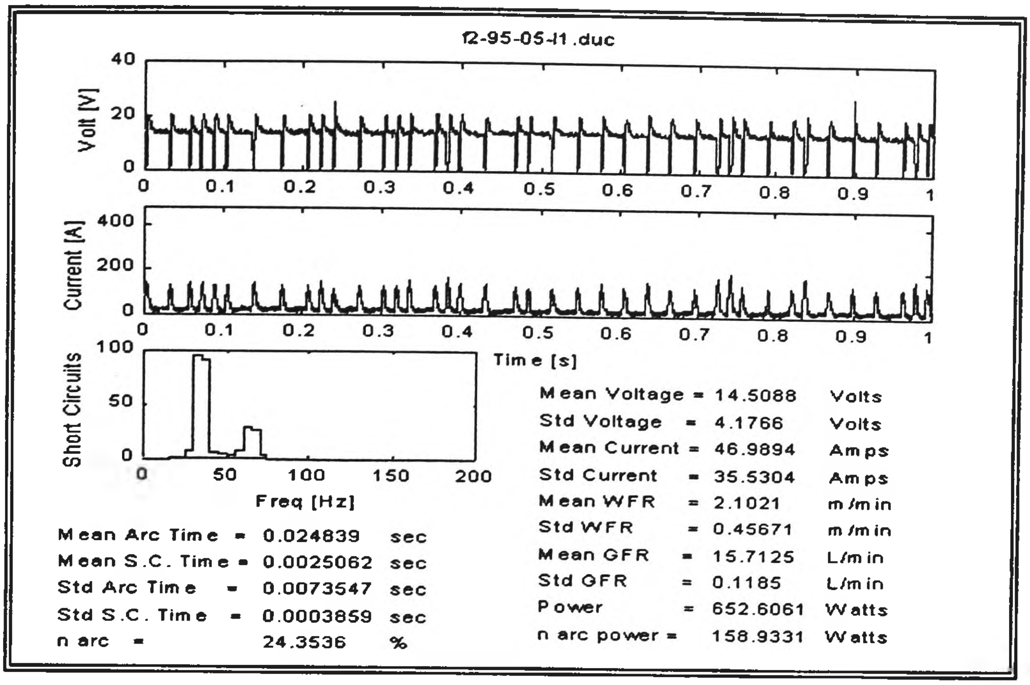

Plot F2-3

Sample f2-95-05-layer 1

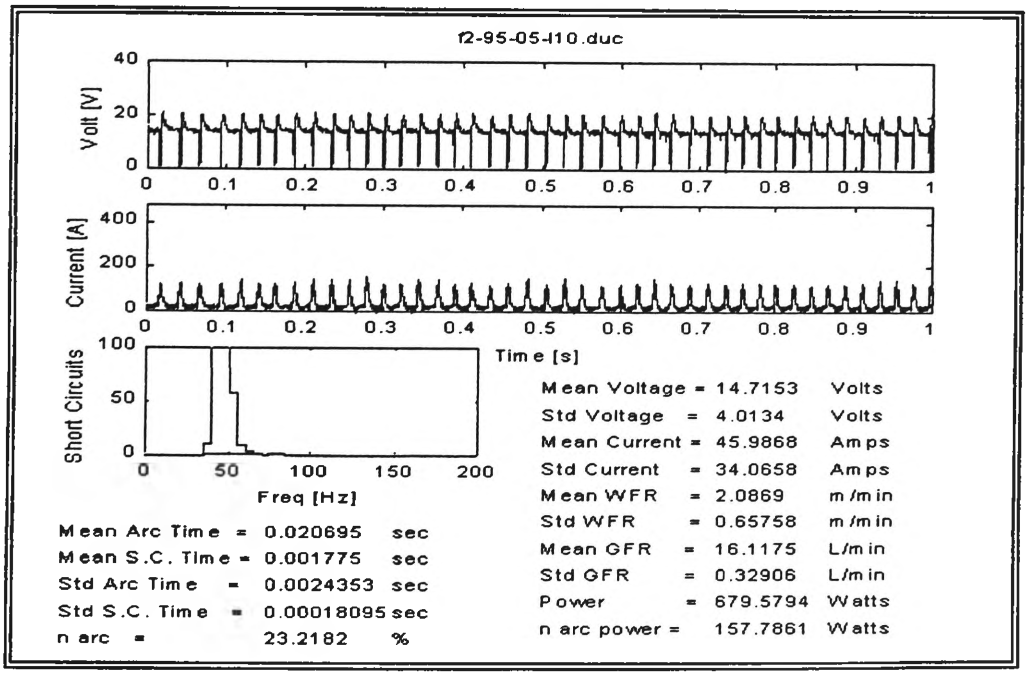

Plot F2-4

Sample f2-95-05-layer 10

Sample f2-100-05

Set Values	
Voltage [%]	100
Wire feed rate [m/min]	2
Travel speed [mm/sec]	5
Gas flow [l/min]	15

Weld Geometry		**Visual Defects and Weld Property**	
Weld height [mm]	12.4	Spatters	No
Weld width [mm]	3.7	Porosity	No
Stand-off at layer 1 [mm]	15	Excess material	No
Stand-off at layer 10 [mm]	16	Surface regularity [μm]	48
Temperature at layer 10 [deg.C]	192	Average hardness [HV]	164
Number of layers	10		

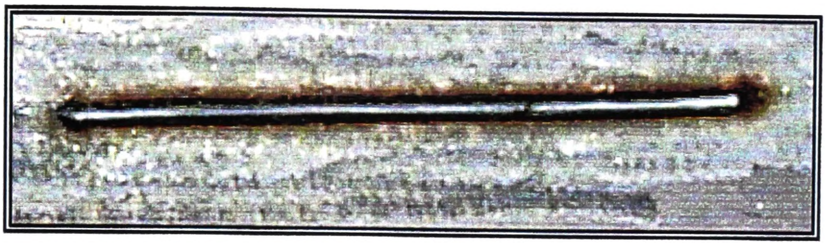

Figure F2-5

Sample f2-100-05 (top view)

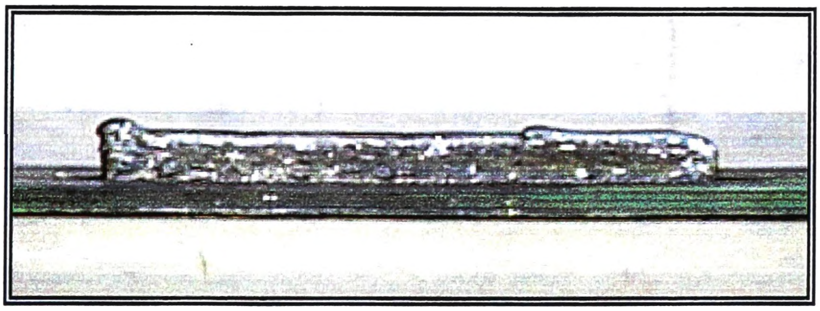

Figure F2-6

Sample f2-100-05 (front view)

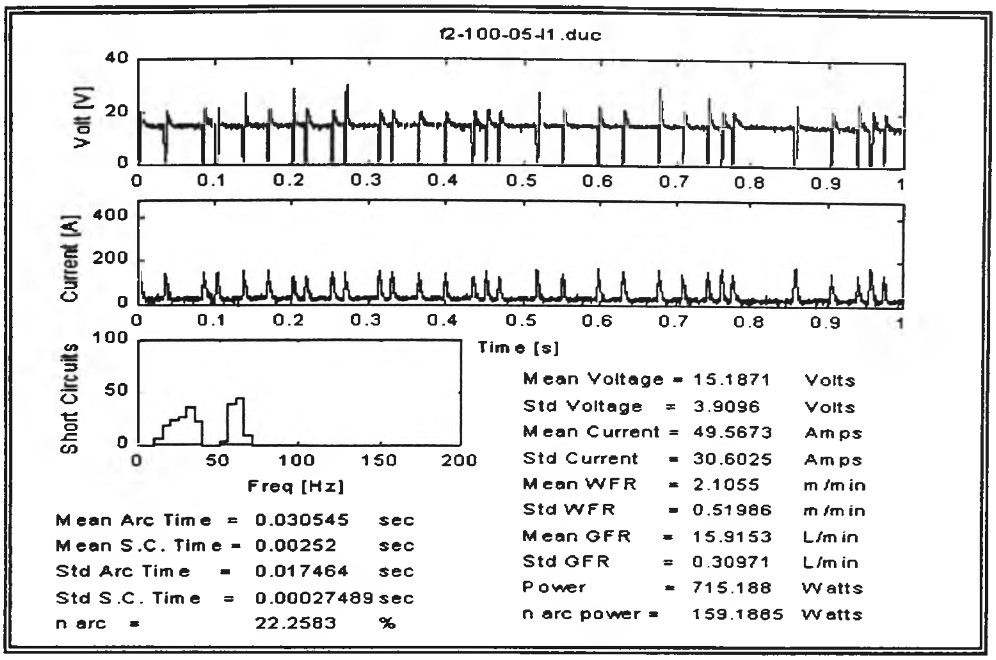

Plot F2-5

Sample f2-100-05-layer 1

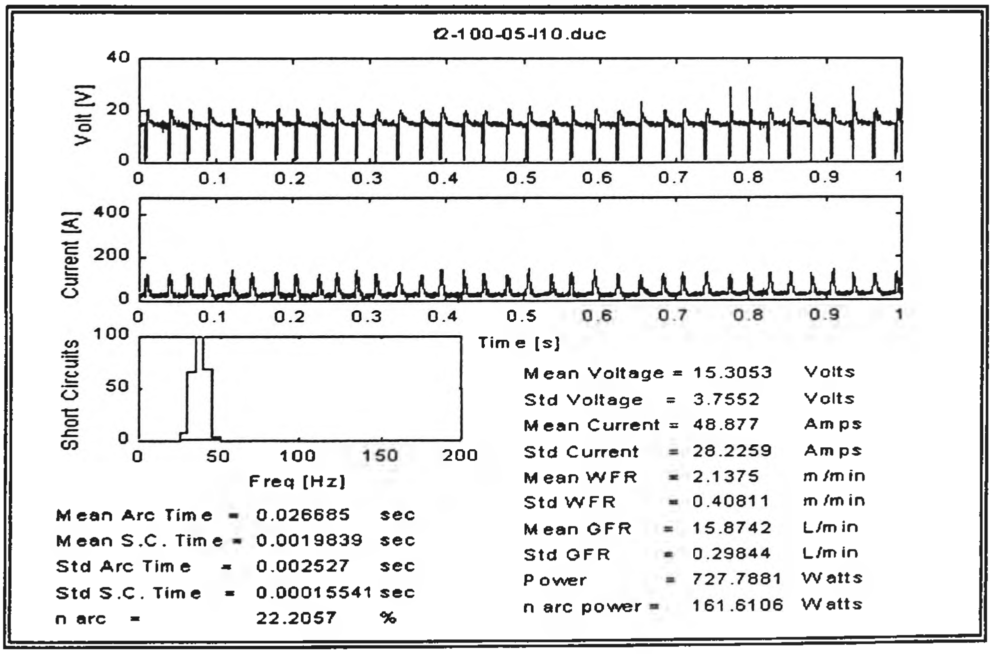

Plot F2-6

Sample f2-100-05-layer 10

Sample f2-105-05

Set Values	
Voltage [%]	105
Wire feed rate [m/min]	2
Travel speed [mm/sec]	5
Gas flow [l/min]	15

Weld Geometry		Visual Defects and Weld Property	
Weld height [mm]	11.1	Spatters	Yes
Weld width [mm]	3.9	Porosity	No
Stand-off at layer 1 [mm]	15	Excess material	No
Stand-off at layer 10 [mm]	17	Surface regularity [μm]	27
Temperature at layer 10 [deg.C]	198	Average hardness [HV]	164
Number of layers	10		

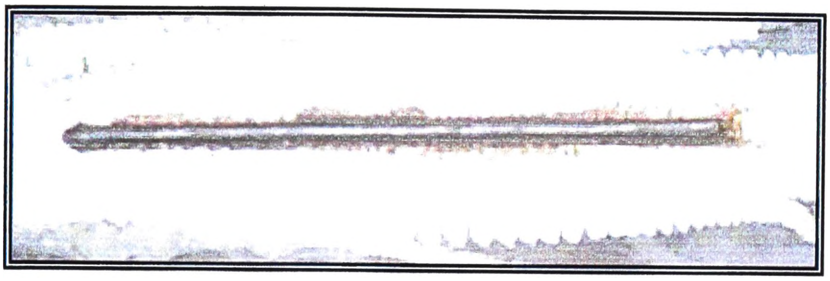

Figure F2-7

Sample f2-105-05 (top view)

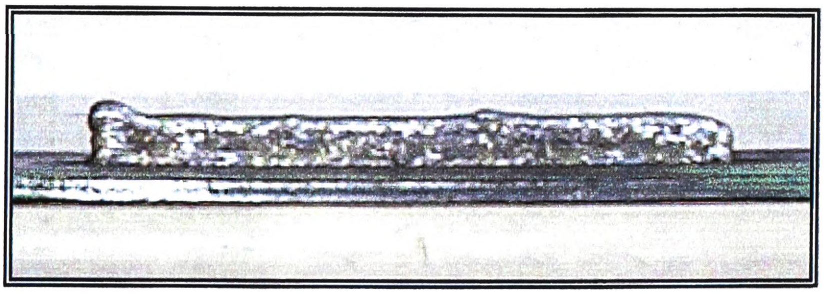

Figure F2-8

Sample f2-105-05 (front view)

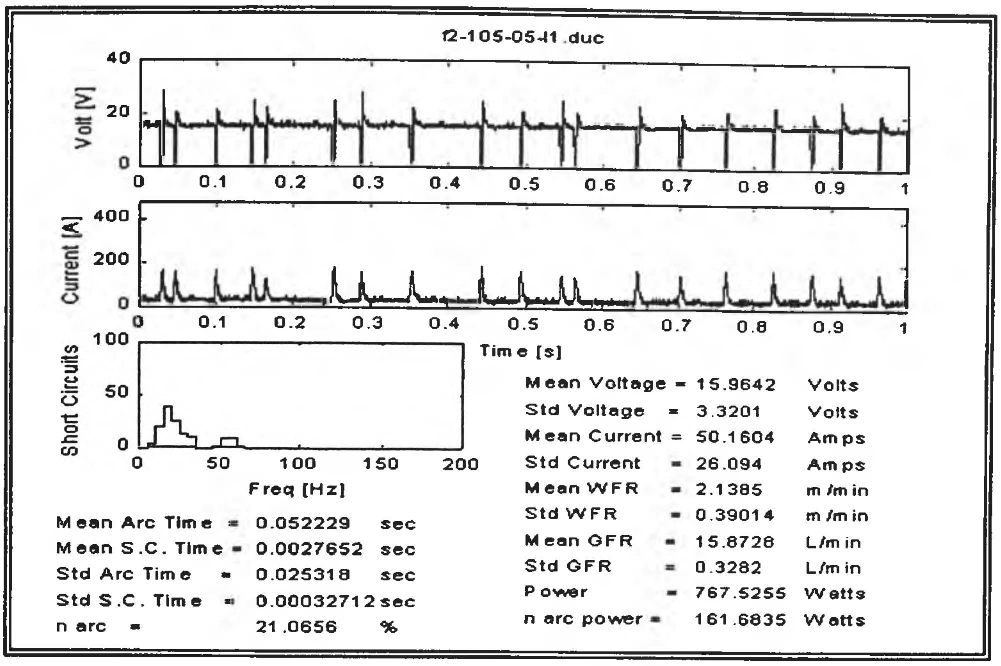

Plot F2-7

Sample f2-105-05-layer 1

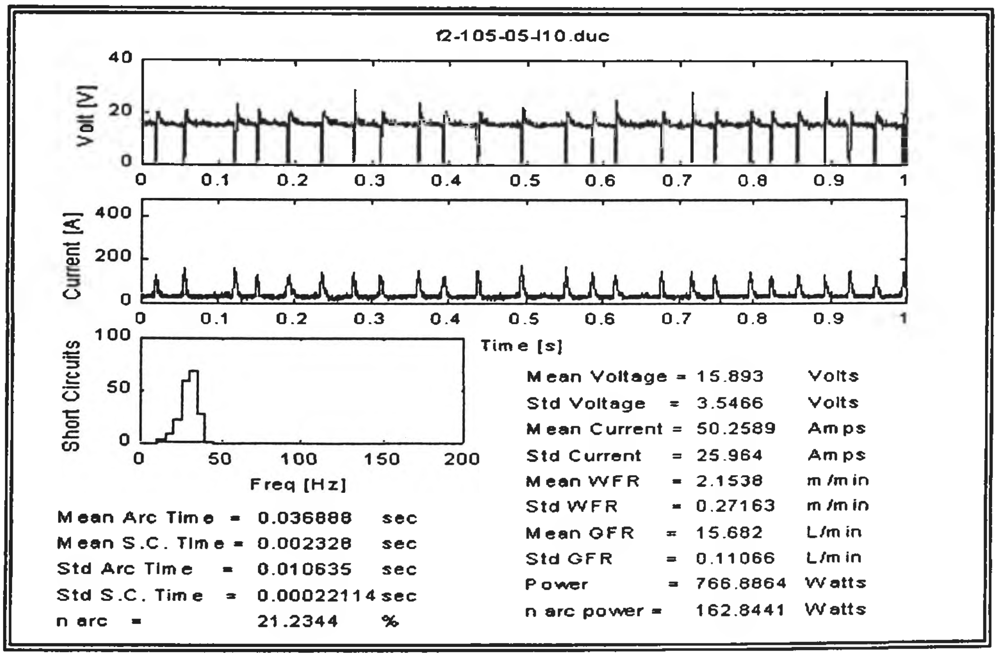

Plot F2-8

Sample f2-105-05-layer 10

Sample f2-110-05

Set Values	
Voltage [%]	110
Wire feed rate [m/min]	2
Travel speed [mm/sec]	5
Gas flow [l/min]	15

Weld Geometry		Visual Defects and Weld Property	
Weld height [mm]	11.7	Spatters	Yes
Weld width [mm]	4.0	Porosity	No
Stand-off at layer 1 [mm]	15	Excess material	No
Stand-off at layer 10 [mm]	16	Surface regularity [μm]	48.6
Temperature at layer 10 [deg.C]	210	Average hardness [HV]	165
Number of layers	10		

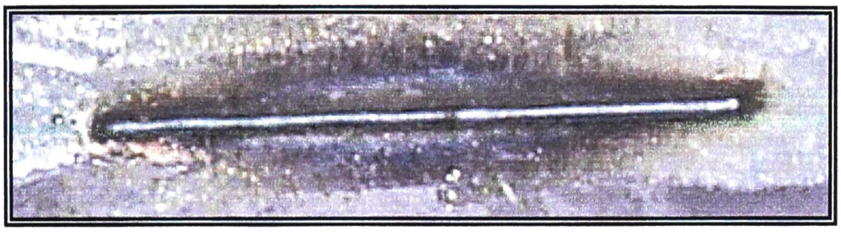

Figure F2-9

Sample f2-110-05 (top view)

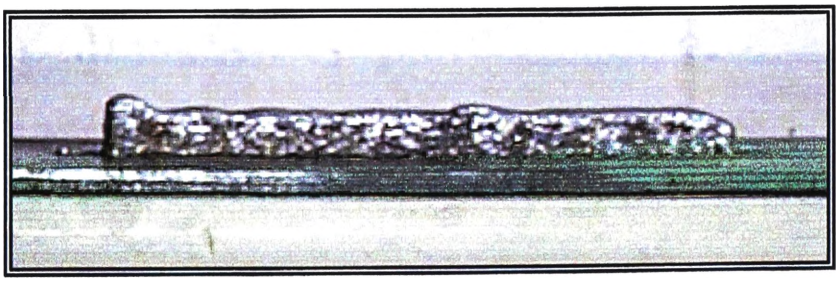

Figure F2-10

Sample f2-110-05 (front view)

Sample f2-115-05

Set Values	
Voltage [%]	115
Wire feed rate [m/min]	2
Travel speed [mm/sec]	5
Gas flow [l/min]	15

Weld Geometry		**Visual Defects and Weld Property**	
Weld height [mm]	11.7	Spatters	Yes
Weld width [mm]	4.2	Porosity	No
Stand-off at layer 1 [mm]	15	Excess material	No
Stand-off at layer 10 [mm]	17	Surface regularity [μm]	66.6
Temperature at layer 10 [deg.C]	222	Average hardness [HV]	162
Number of layers	10		

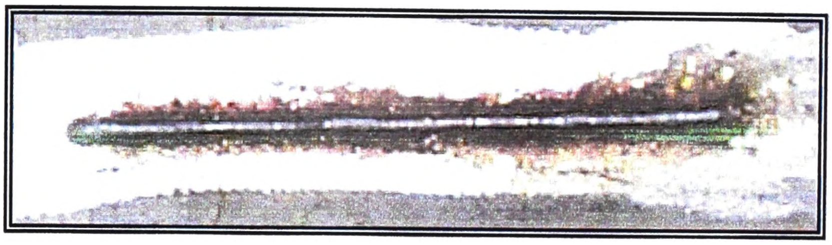

Figure F2-11

Sample f2-115-05 (top view)

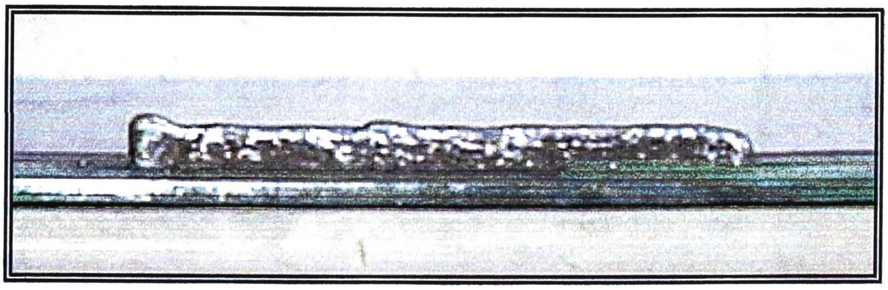

Figure F2-12

Sample f2-115-05 (front view)

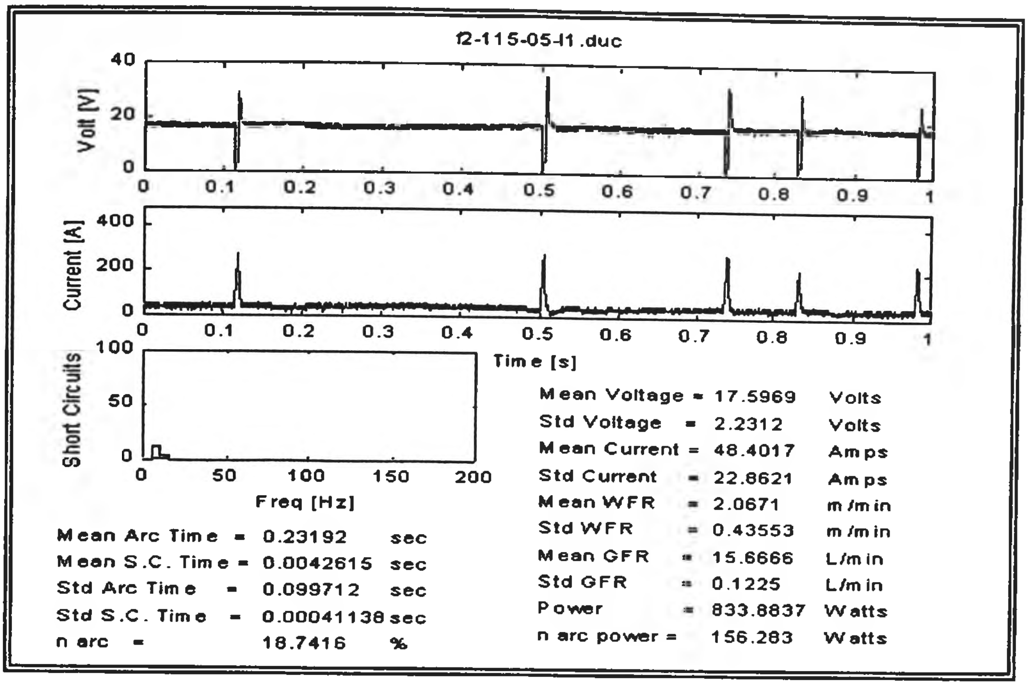

Plot F2-11

Sample f2-115-05-layer 1

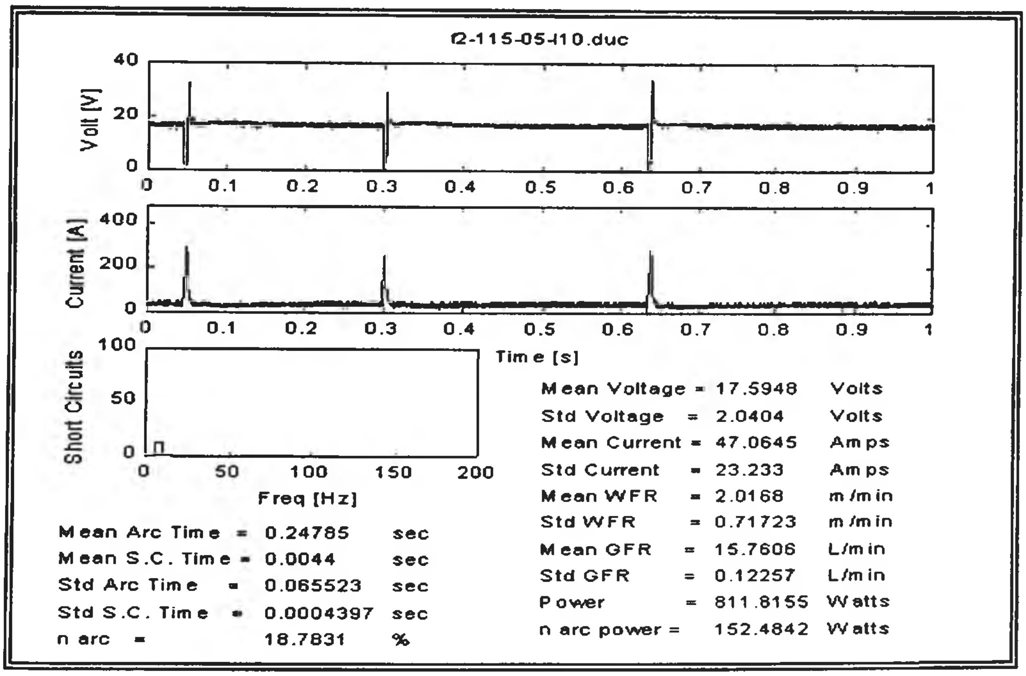

Plot F2-12

Sample f2-115-05-layer 10

Sample f2-120-05

Set Values	
Voltage [%]	120
Wire feed rate [m/min]	2
Travel speed [mm/sec]	5
Gas flow [l/min]	15

Weld Geometry		Visual Defects and Weld Property	
Weld height [mm]	10.1	Spatters	Yes
Weld width [mm]	4.4	Porosity	No
Stand-off at layer 1 [mm]	15	Excess material	No
Stand-off at layer 10 [mm]	17	Surface regularity [µm]	33.5
Temperature at layer 10 [deg.C]	234	Average hardness [HV]	160
Number of layers	10		

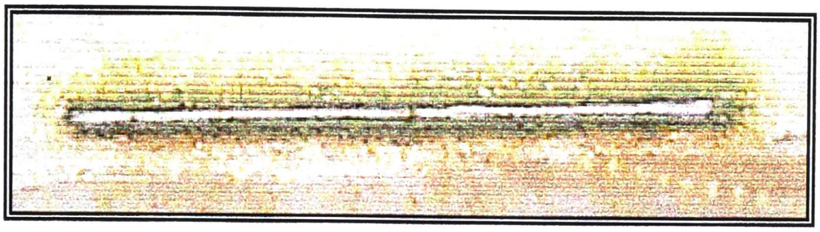

Figure F2-13

Sample f2-120-05 (top view)

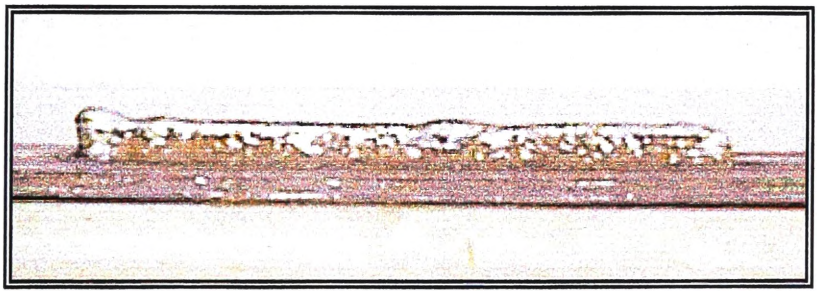

Figure F2-14

Sample f2-120-05 (front view)

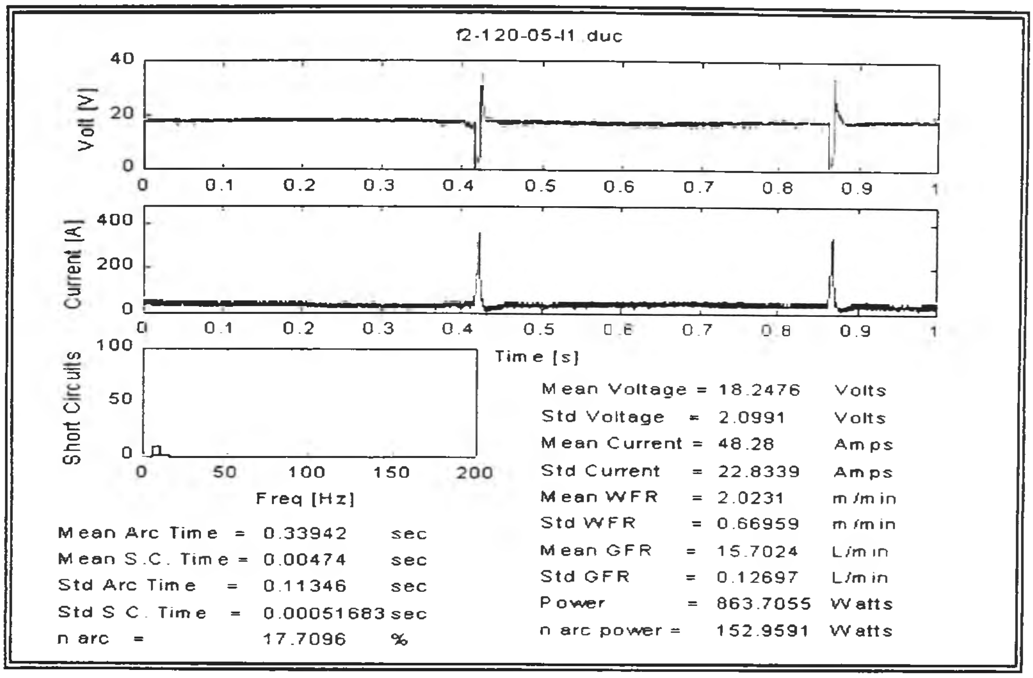

Plot F2-13

Sample f2-120-05-layer 1

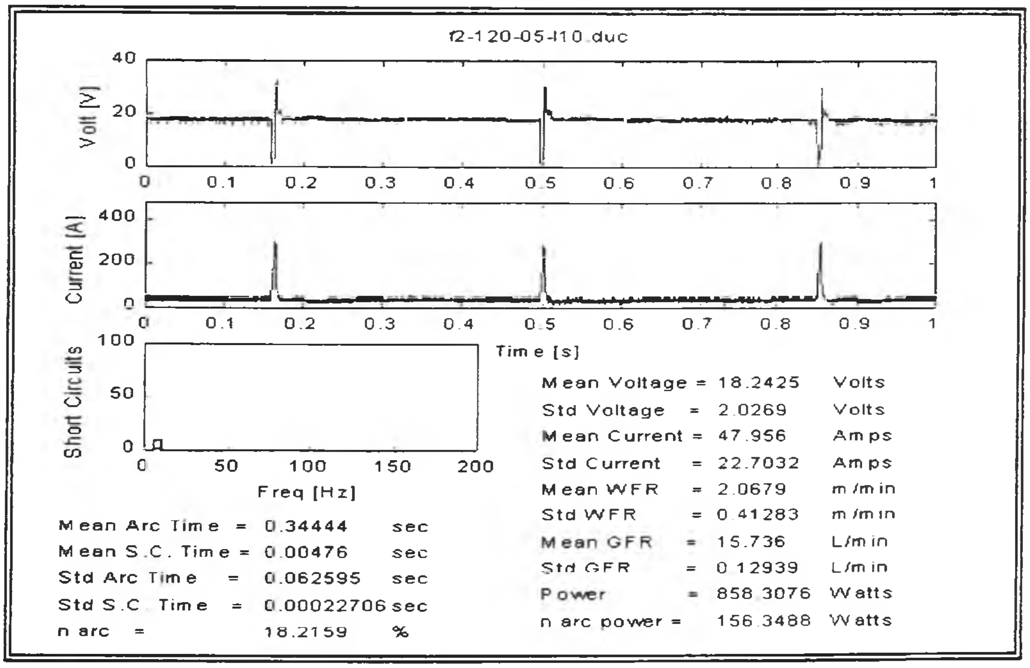

Plot F2-14

Sample f2-120-05-layer 10

Sample f2-135-05

Set Values	
Voltage [%]	135
Wire feed rate [m/min]	2
Travel speed [mm/sec]	5
Gas flow [l/min]	15

Weld Geometry		Visual Defects and Weld Property	
Weld height [mm]	8.7	Spatters	Yes
Weld width [mm]	4.8	Porosity	No
Stand-off at layer 1 [mm]	15	Excess material	No
Stand-off at layer 10 [mm]	16.5	Surface regularity [μm]	125.2
Temperature at layer 10 [deg.C]	241	Average hardness [HV]	156
Number of layers	10		

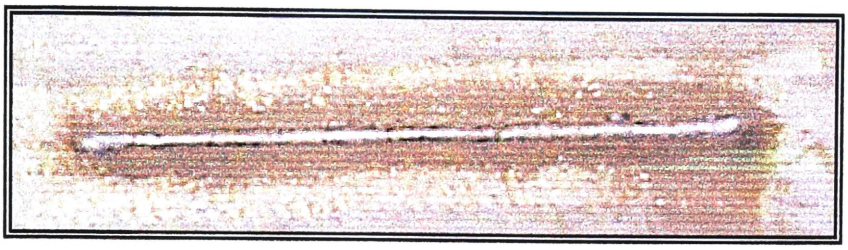

Figure F2-15

Sample f2-135-05 (top view)

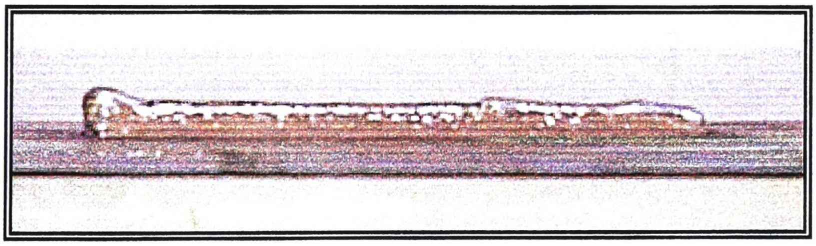

Figure F2-16

Sample f2-135-05 (front view)

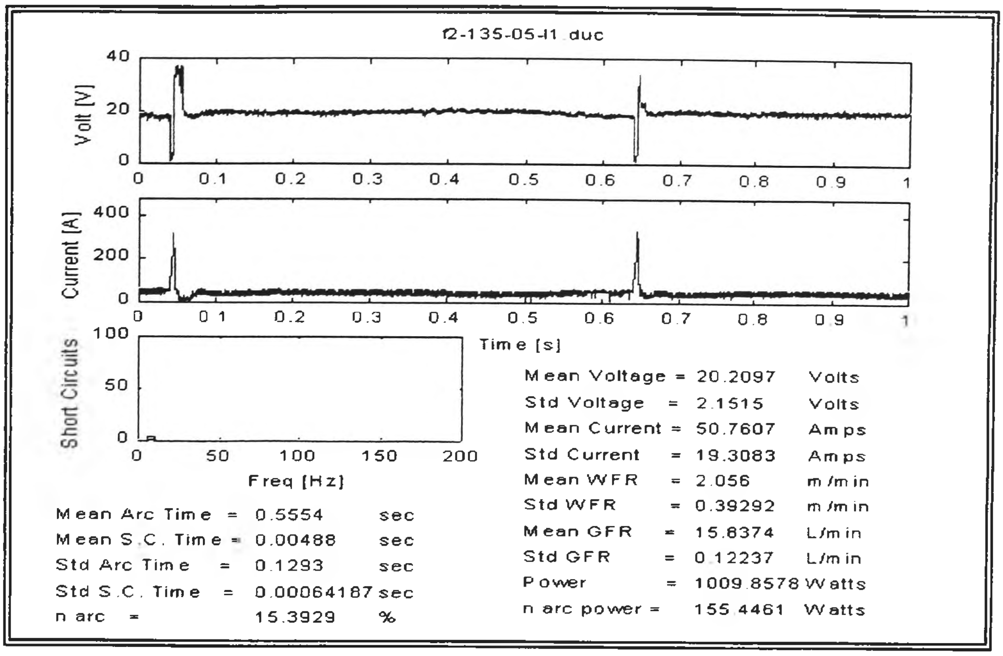

Plot F2-15

Sample f2-135-05-layer 1

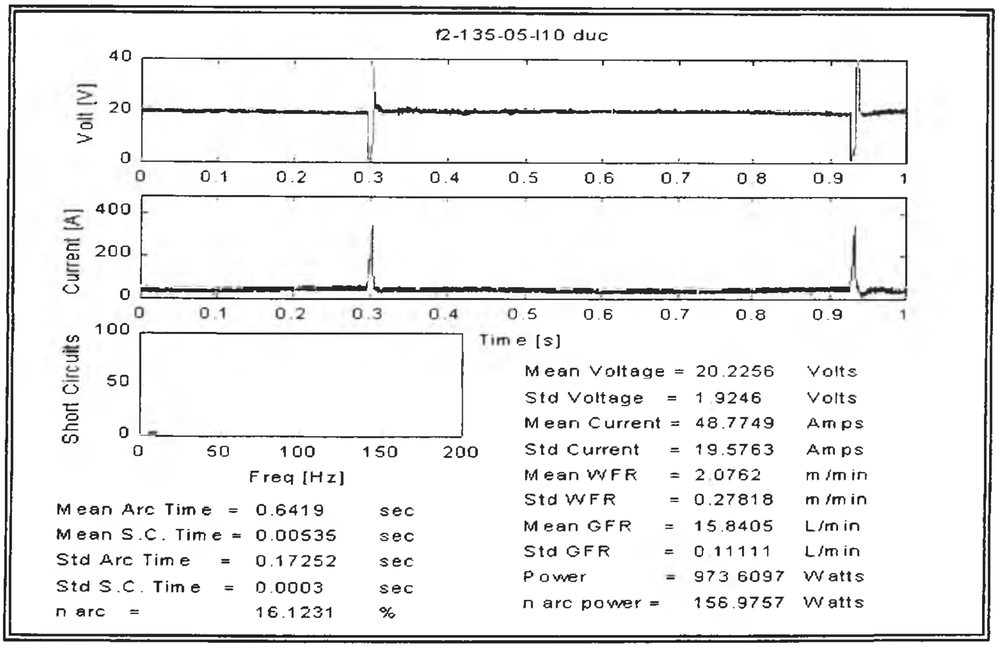

Plot F2-16

Sample f2-135-05-layer 10

Sample f2-150-05

Set Values	
Voltage [%]	150
Wire feed rate [m/min]	2
Travel speed [mm/sec]	5
Gas flow [l/min]	15

Weld Geometry		**Visual Defects and Weld Property**	
Weld height [mm]	8.7	Spatters	Yes
Weld width [mm]	4.8	Porosity	No
Stand-off at layer 1 [mm]	15	Excess material	No
Stand-off at layer 10 [mm]	16.5	Surface regularity [μm]	75.7
Temperature at layer 10 [deg.C]	250	Average hardness [HV]	149
Number of layers	10		

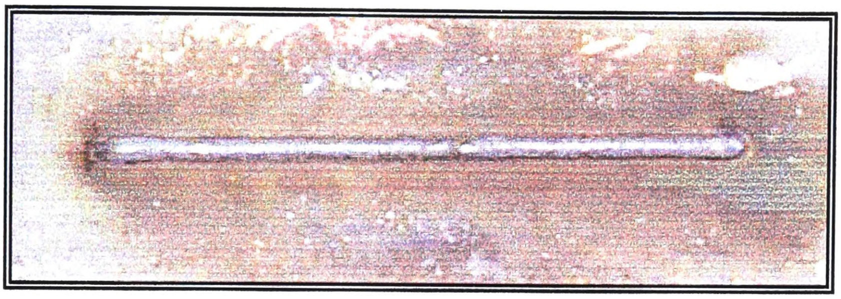

Figure 17

Sample f2-150-05 (top view)

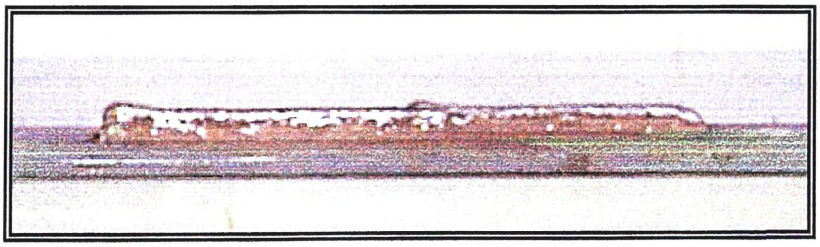

Figure 18

Sample f2-150-05 (front view)

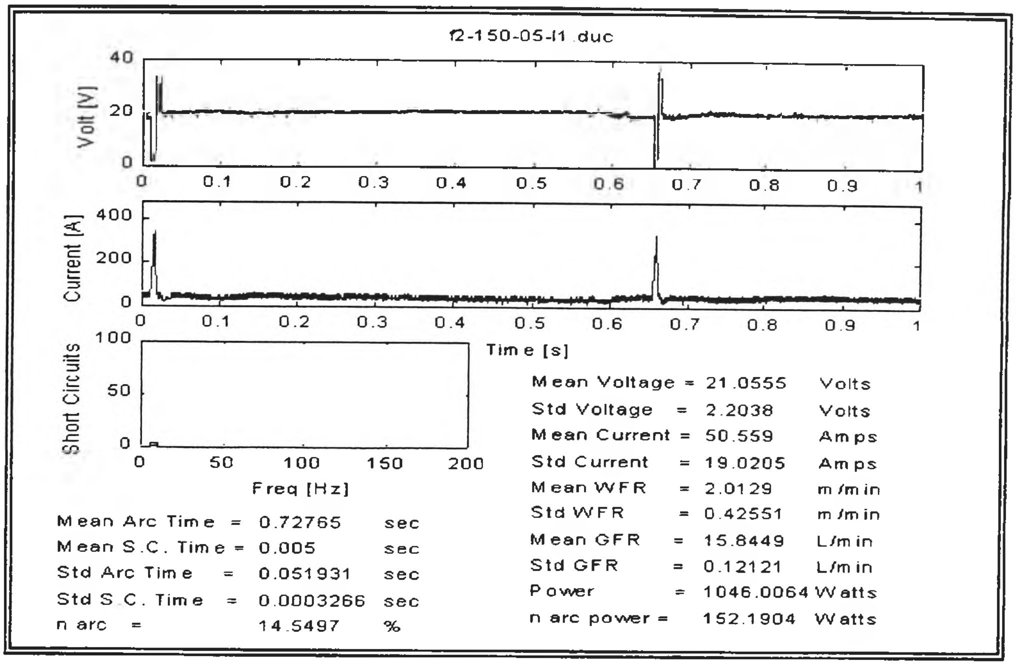

Plot 17

Sample f2-150-05-layer 1

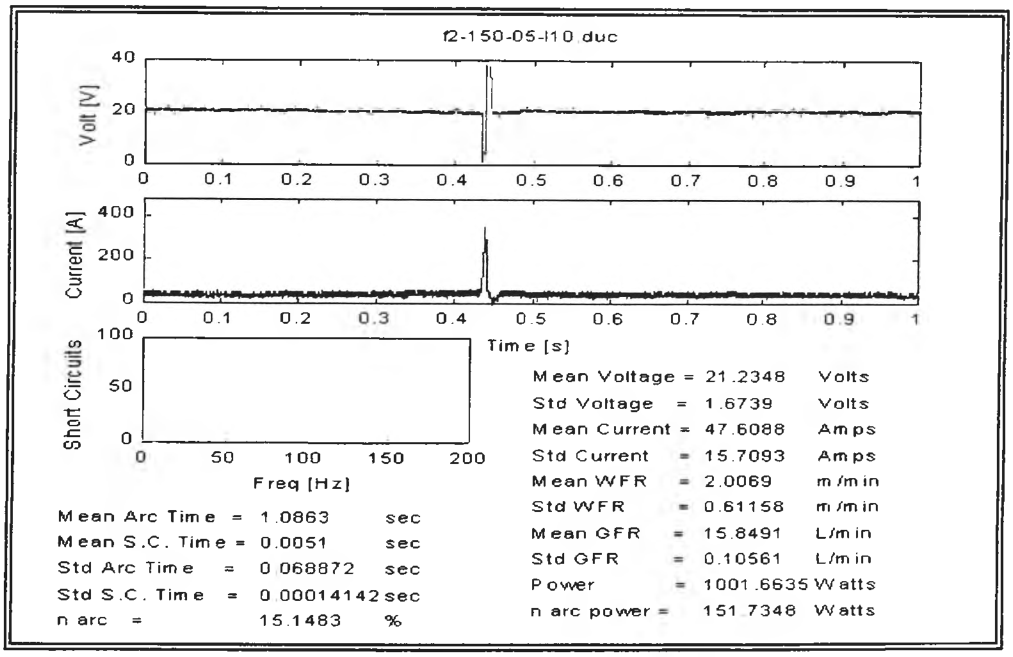

Plot 18

Sample f2-150-05-layer 10

F3 Wire Feed Rate of 3 m/min

Sample f3-75-05

Set Values	
Voltage [%]	75
Wire feed rate [m/min]	3
Travel speed [mm/sec]	5
Gas flow [l/min]	15

Weld Geometry		Visual Defects and Weld Property	
Weld height [mm]	15.9	Spatters	No
Weld width [mm]	4.5	Porosity	No
Stand-off at layer 1 [mm]	15	Excess material	No
Stand-off at layer 10 [mm]	15.5	Surface regularity [μm]	60.35
Temperature at layer 10 [deg.C]	230	Average hardness [HV]	156
Number of layers	10		

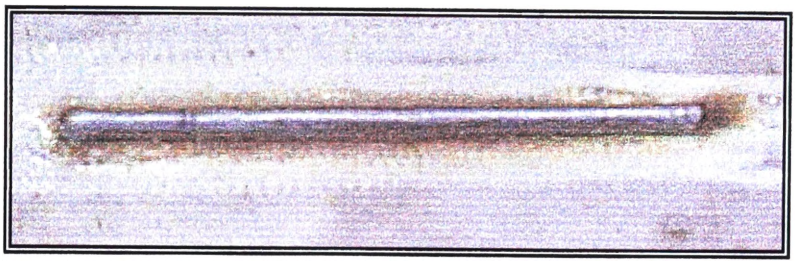

Figure F3-1

Sample f3-75-05 (top view)

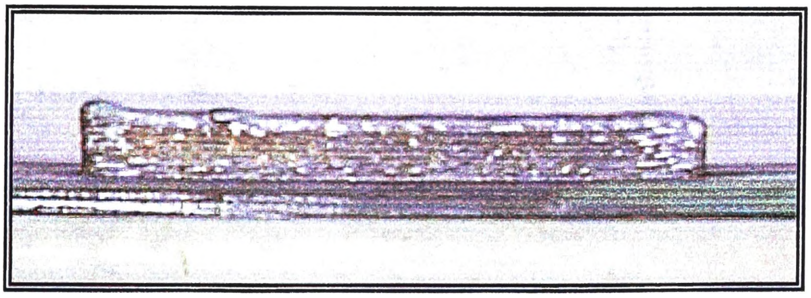

Figure F3-2

Sample f3-75-05 (front view)

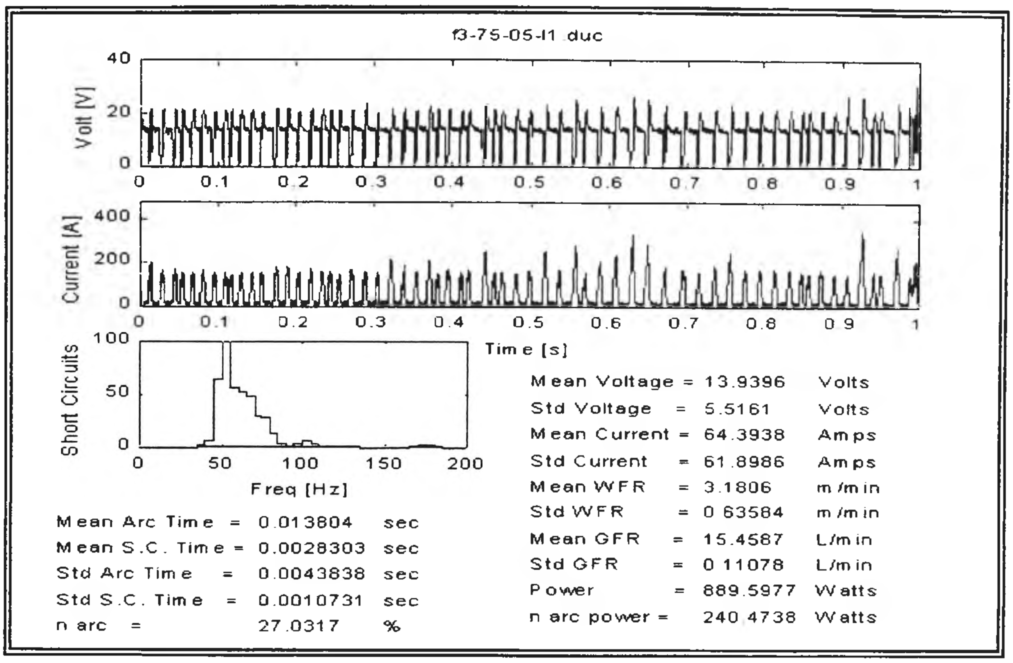

Plot F3-1

Sample f3-75-05-layer 1

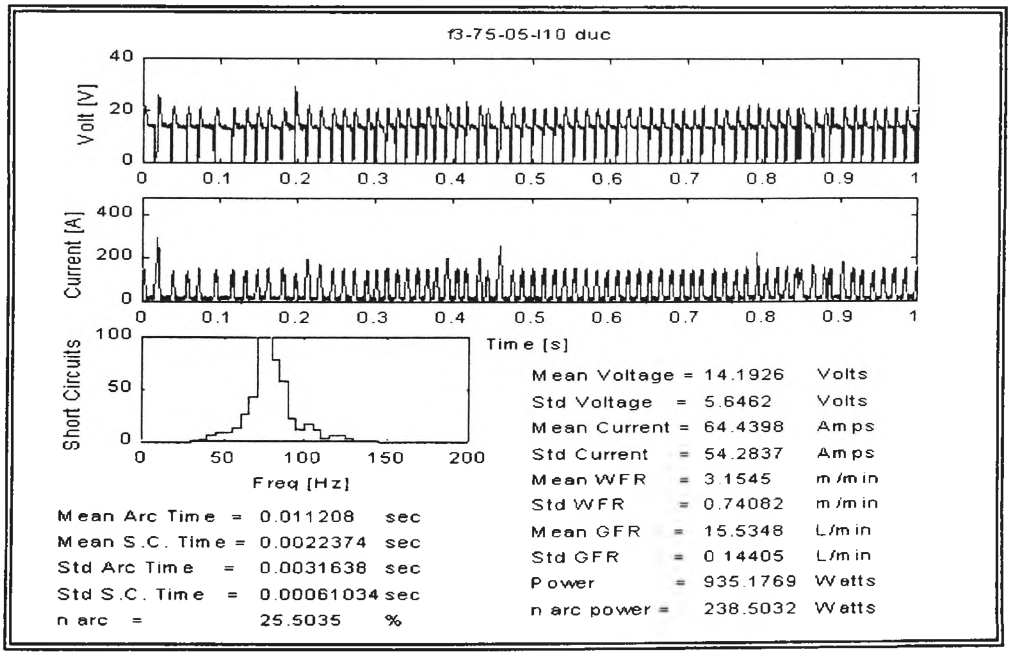

Plot F3-2

Sample f3-75-05-layer 10

Sample f3-95-05

Set Values	
Voltage [%]	95
Wire feed rate [m/min]	3
Travel speed [mm/sec]	5
Gas flow [l/min]	15

Weld Geometry		Visual Defects and Weld Property	
Weld height [mm]	14	Spatters	No
Weld width [mm]	4.9	Porosity	No
Stand-off at layer 1 [mm]	15	Excess material	No
Stand-off at layer 10 [mm]	16	Surface regularity [μm]	N/A
Temperature at layer 10 [deg.C]	240	Average hardness [HV]	N/A
Number of layers	10		

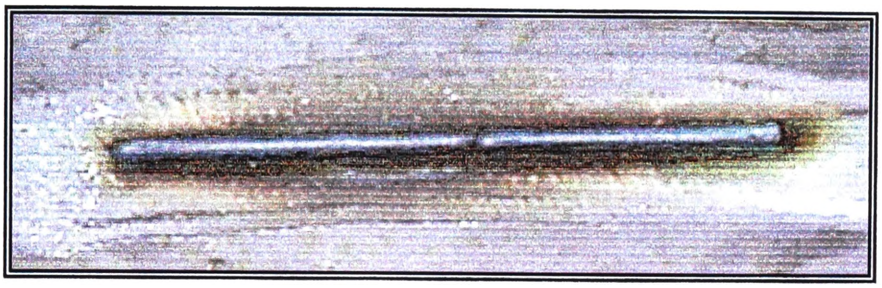

Figure F3-3

Sample f3-95-05 (top view)

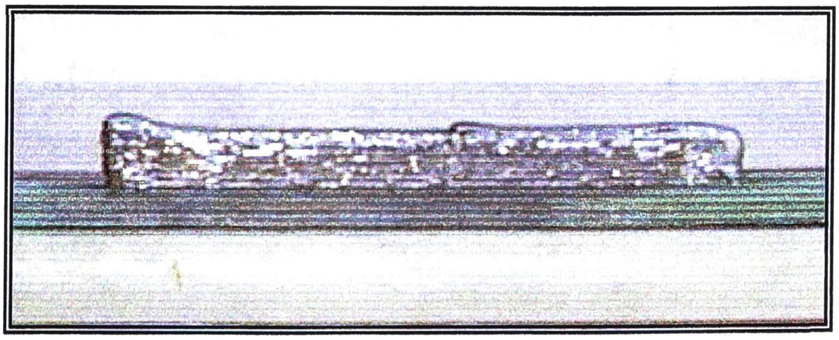

Figure F3-4

Sample f3-95-05 (front view)

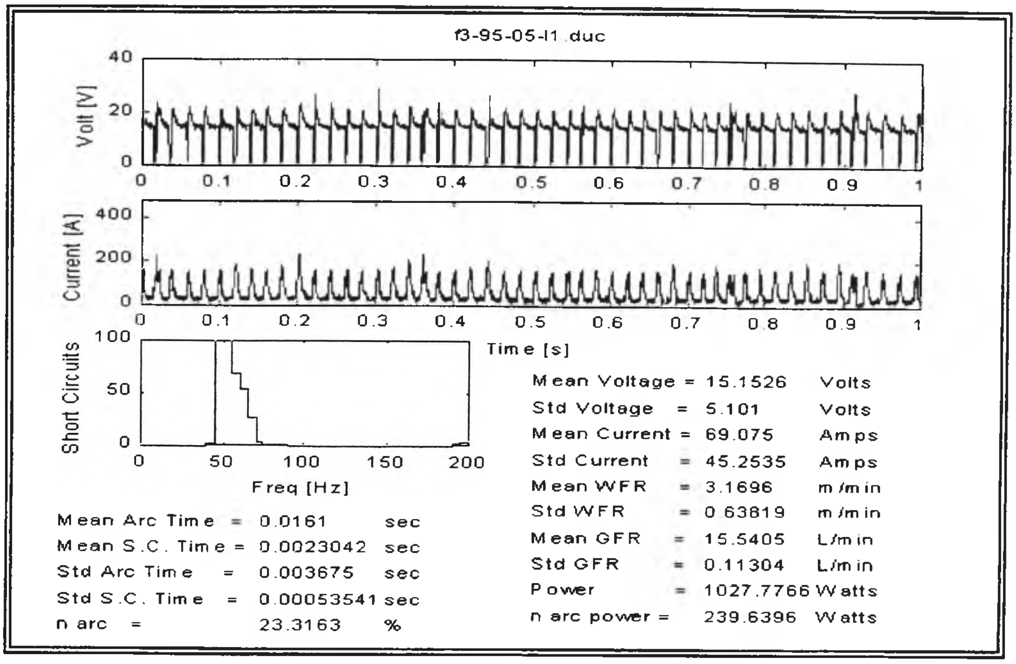

Plot F3-3

Sample f3-95-05-layer 1

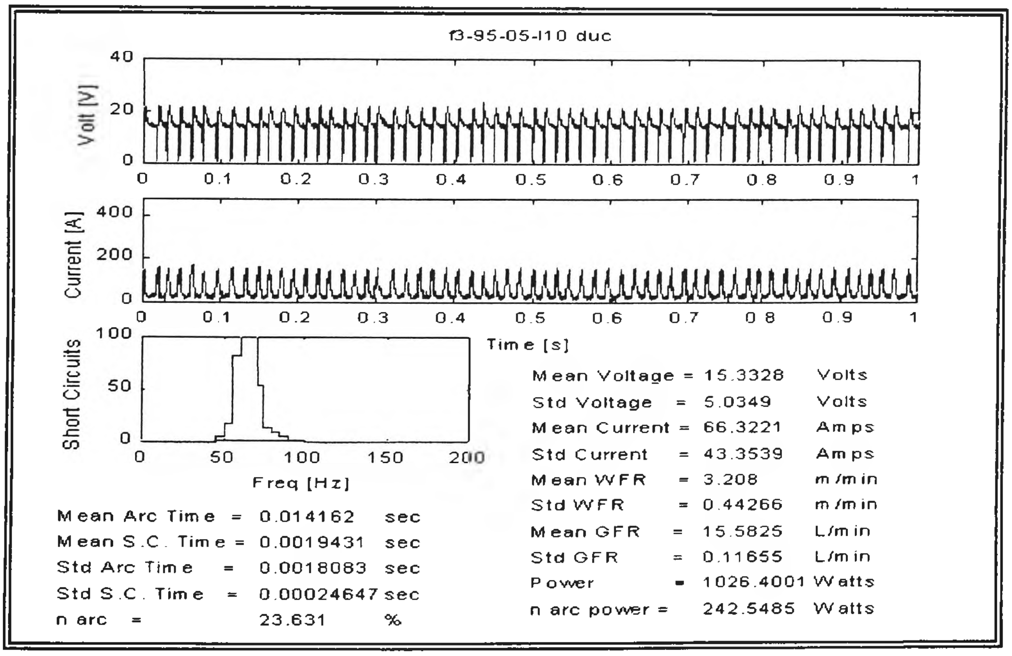

Plot F3-4

Sample f3-95-05-layer 10

Sample f3-100-05

Set Values	
Voltage [%]	100
Wire feed rate [m/min]	3
Travel speed [mm/sec]	5
Gas flow [l/min]	15

Weld Geometry		Visual Defects and Weld Property	
Weld height [mm]	13.8	Spatters	No
Weld width [mm]	4.9	Porosity	No
Stand-off at layer 1 [mm]	15	Excess material	No
Stand-off at layer 10 [mm]	17	Surface regularity [μm]	33.75
Temperature at layer 10 [deg.C]	245	Average hardness [HV]	155
Number of layers	10		

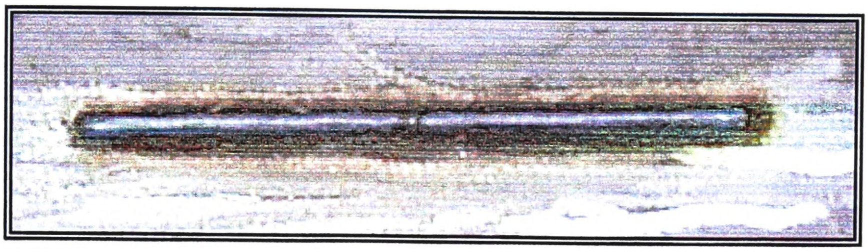

Figure F3-5

Sample f3-100-05 (top view)

Figure F3-6

Sample f3-100-05 (front view)

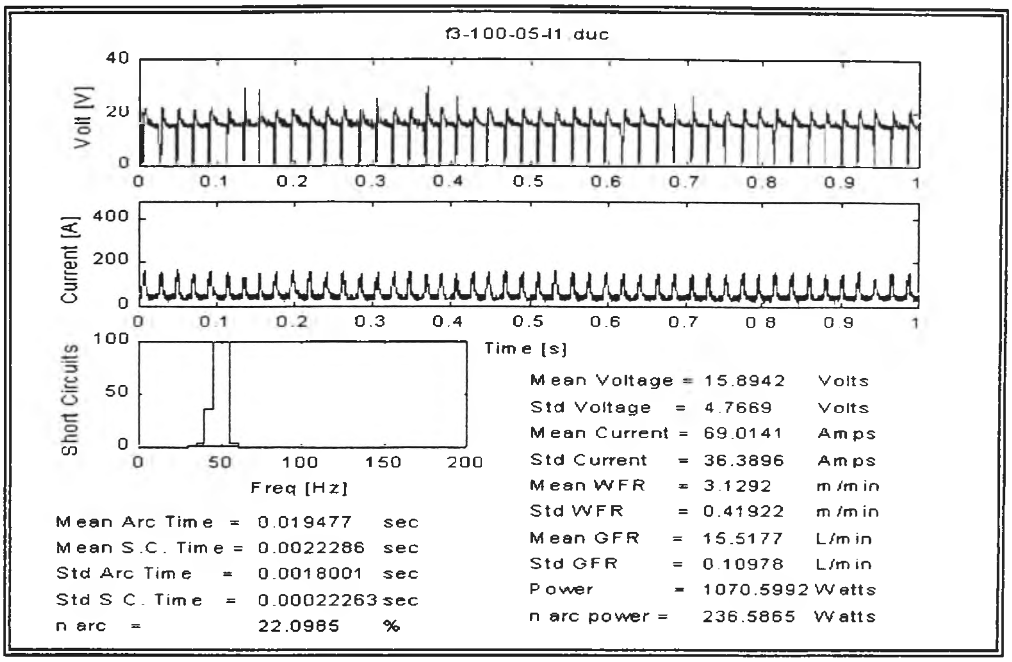

Plot F3-5

Sample f3-100-05-layer 1

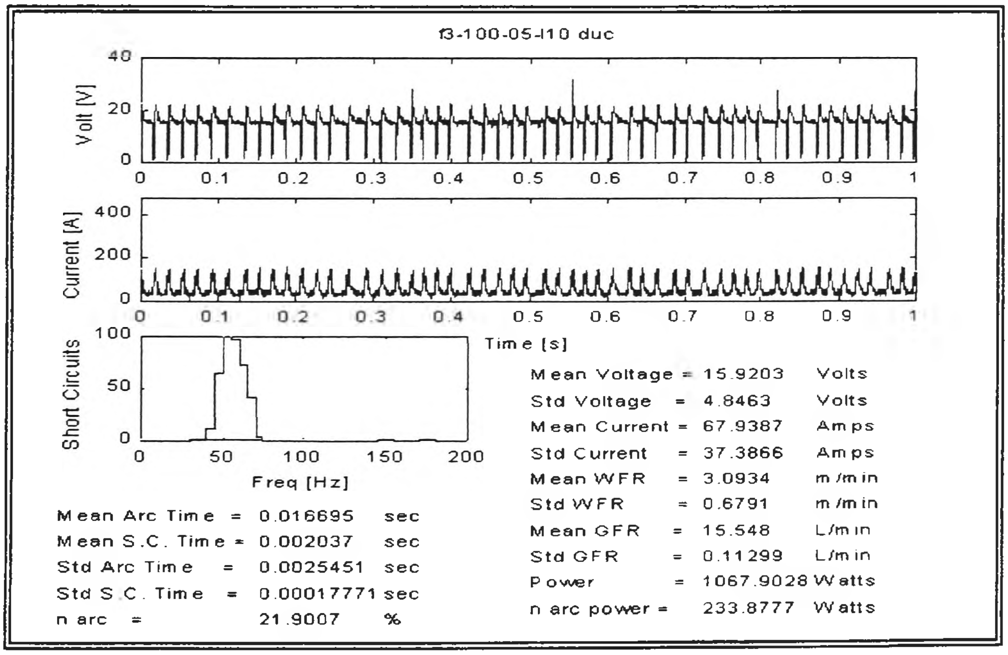

Plot F3-6

Sample f3-100-05-layer 10

Sample f3-105-05

Set Values	
Voltage [%]	105
Wire feed rate [m/min]	3
Travel speed [mm/sec]	5
Gas flow [l/min]	15

Weld Geometry		Visual Defects and Weld Property	
Weld height [mm]	14	Spatters	No
Weld width [mm]	5.6	Porosity	No
Stand-off at layer 1 [mm]	15	Excess material	No
Stand-off at layer 10 [mm]	17	Surface regularity [μm]	N/A
Temperature at layer 10 [deg.C]	246	Average hardness [HV]	N/A
Number of layers	10		

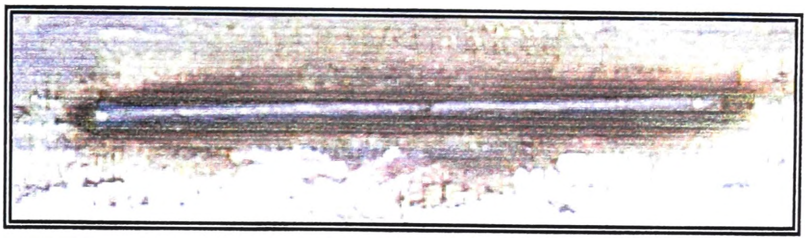

Figure F3-7

Sample f3-105-05 (top view)

Figure F3-8

Sample f3-105-05 (front view)

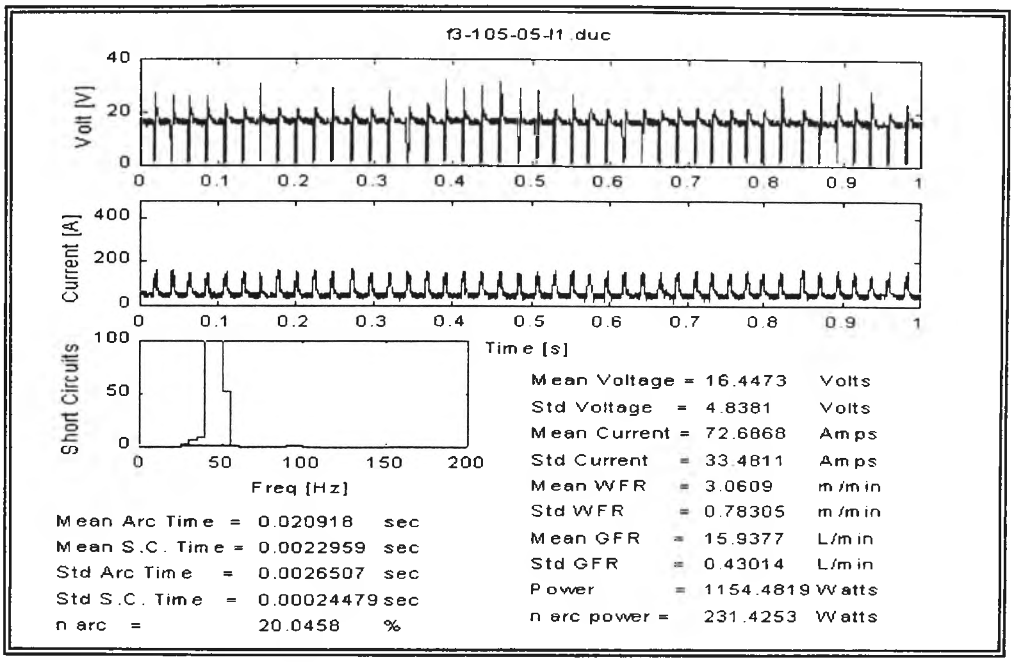

Plot F3-7

Sample f3-105-05-layer 1

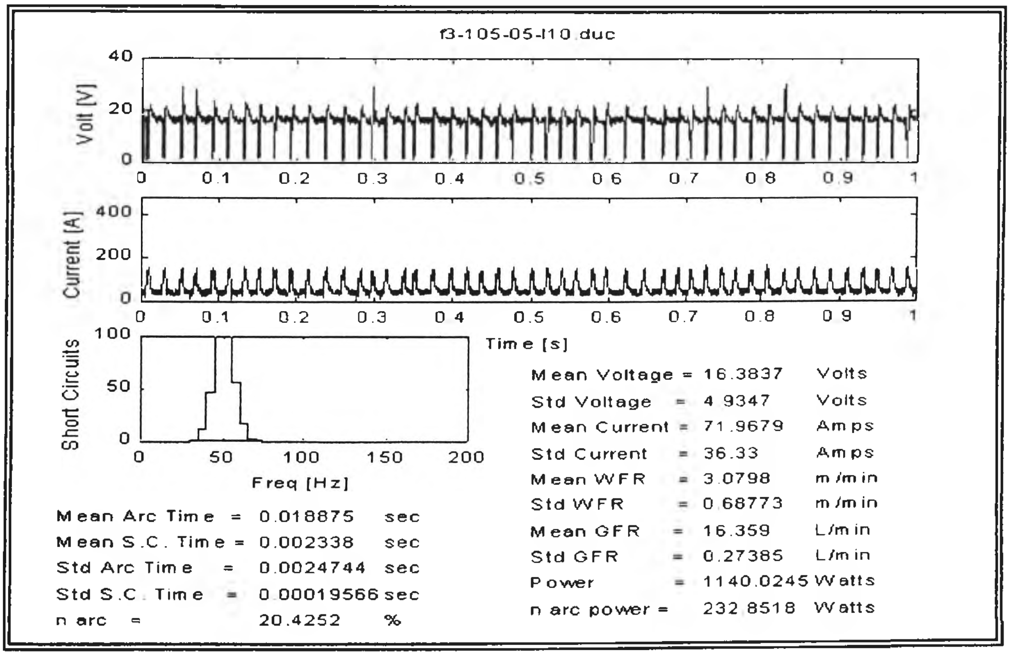

Plot F3-8

Sample f3-105-05-layer 10

Sample f3-115-05

Set Values	
Voltage [%]	115
Wire feed rate [m/min]	3
Travel speed [mm/sec]	5
Gas flow [l/min]	15

Weld Geometry		Visual Defects and Weld Property	
Weld height [mm]	12	Spatters	Yes
Weld width [mm]	6	Porosity	No
Stand-off at layer 1 [mm]	15	Excess material	No
Stand-off at layer 10 [mm]	16	Surface regularity [μm]	N/A
Temperature at layer 10 [deg.C]	247	Average hardness [HV]	N/A
Number of layers	10		

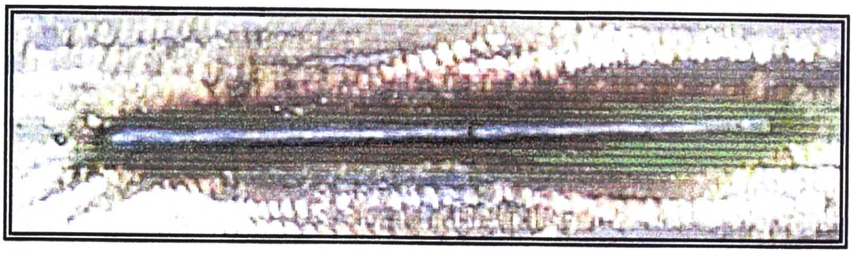

Figure F3-9

Sample f3-115-05 (top view)

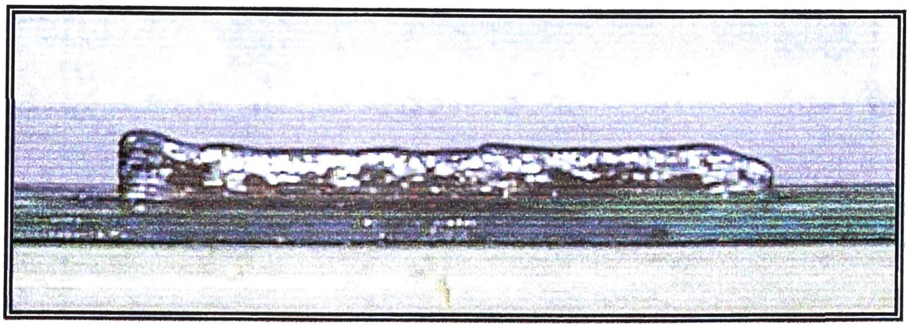

Figure F3-10

Sample f3-115-05 (front view)

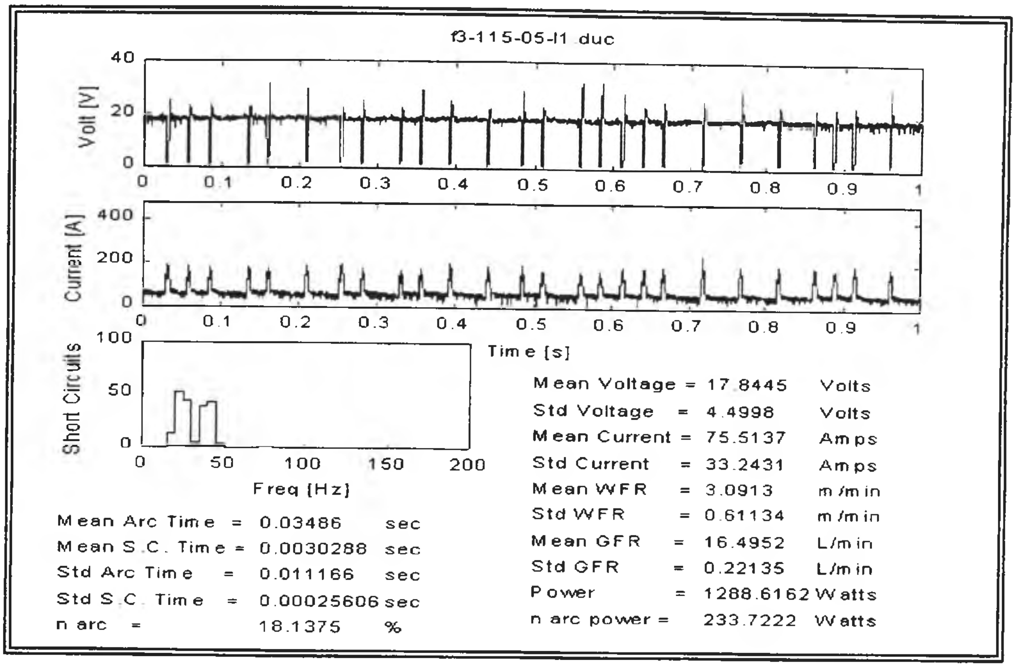

Plot F3-9

Sample f3-115-05-layer 1

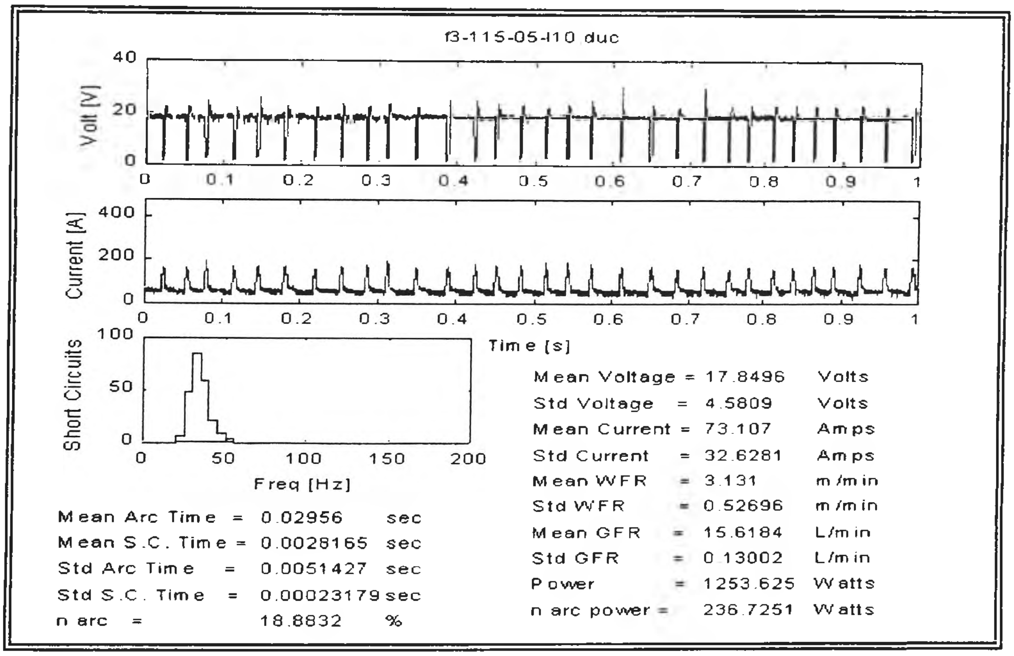

Plot F3-10

Sample f3-115-05-layer 10

Sample f3-125-05

Set Values	
Voltage [%]	125
Wire feed rate [m/min]	3
Travel speed [mm/sec]	5
Gas flow [l/min]	15

Weld Geometry		Visual Defects and Weld Property	
Weld height [mm]	12	Spatters	Yes
Weld width [mm]	6.6	Porosity	No
Stand-off at layer 1 [mm]	15	Excess material	No
Stand-off at layer 10 [mm]	17.5	Surface regularity [μm]	N/A
Temperature at layer 10 [deg.C]	248	Average hardness [HV]	N/A
Number of layers	10		

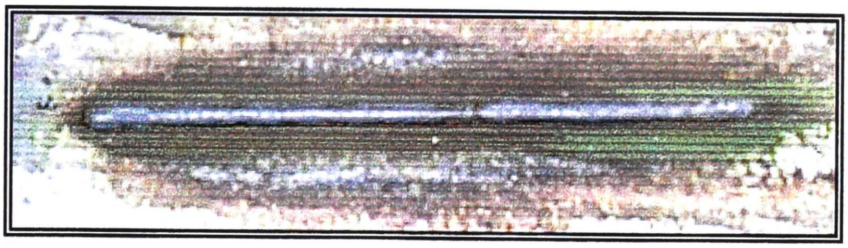

Figure F3-11

Sample f3-125-05 (top view)

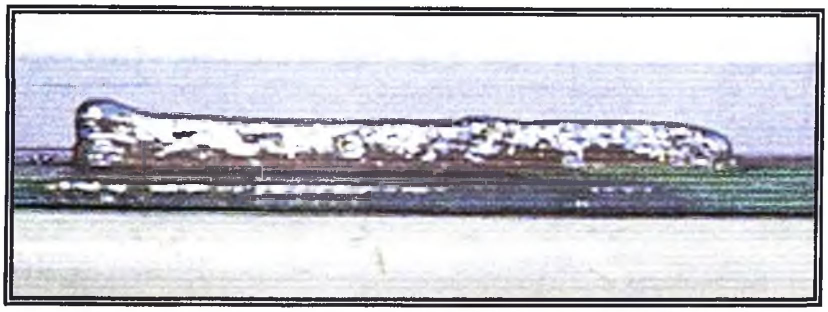

Figure F3-12

Sample f3-125-05 (front view)

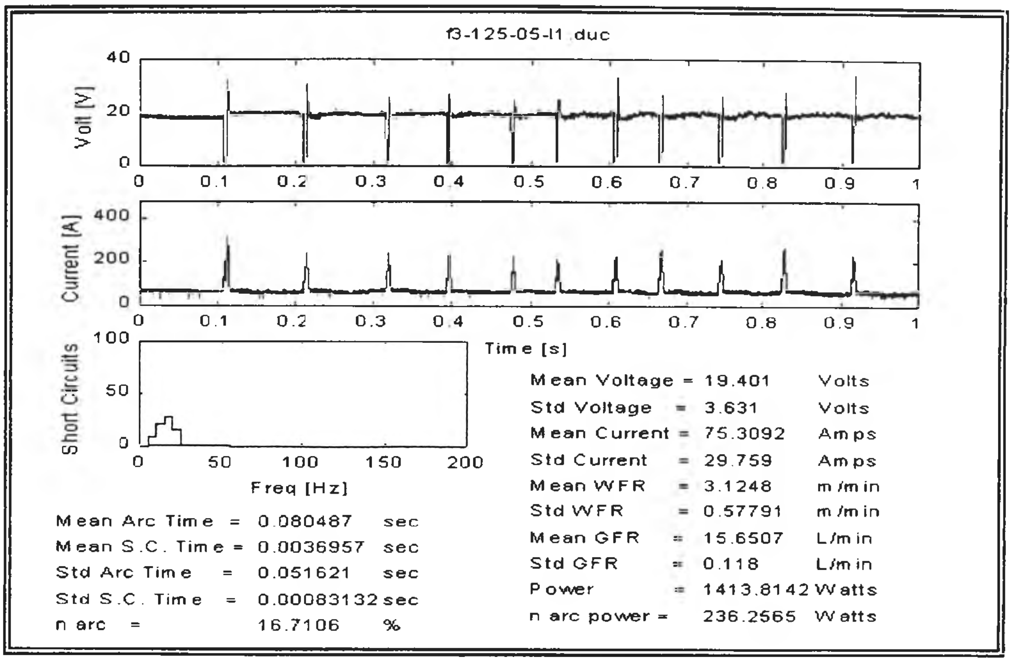

Plot F3-11

Sample f3-125-05-layer 1

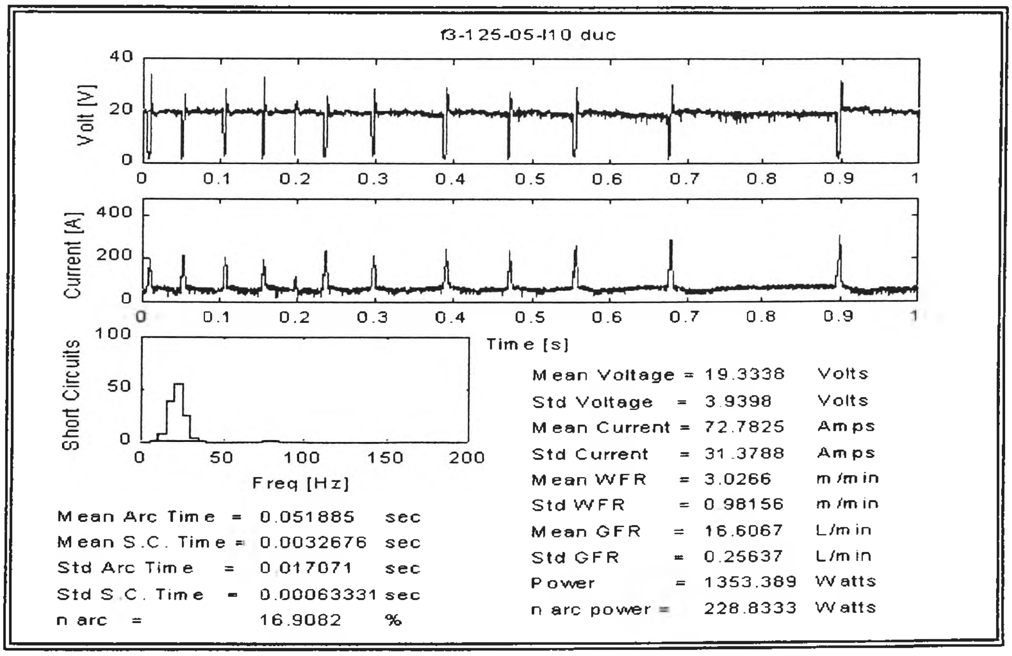

Plot F3-12

Sample f3-125-05-layer 10

Sample f3-150-05

Set Values	
Voltage [%]	150
Wire feed rate [m/min]	3
Travel speed [mm/sec]	5
Gas flow [l/min]	15

Weld Geometry		Visual Defects and Weld Property	
Weld height [mm]	10.6	Spatters	Yes
Weld width [mm]	6.8	Porosity	No
Stand-off at layer 1 [mm]	15	Excess material	No
Stand-off at layer 10 [mm]	19	Surface regularity [µm]	17.5
Temperature at layer 10 [deg.C]	259	Average hardness [HV]	152
Number of layers	10		

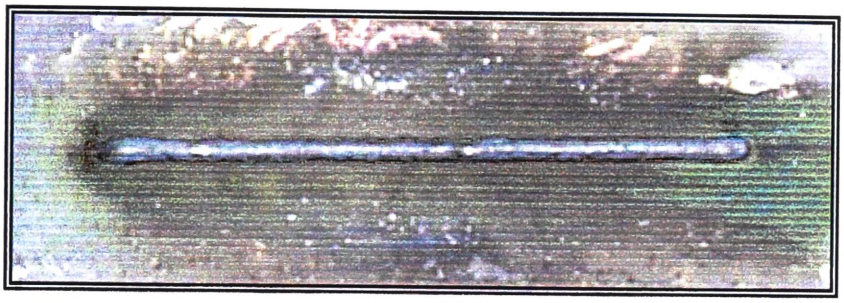

Figure F3-13

Sample f3-150-05 (top view)

Figure F3-14

Sample f3-150-05 (front view)

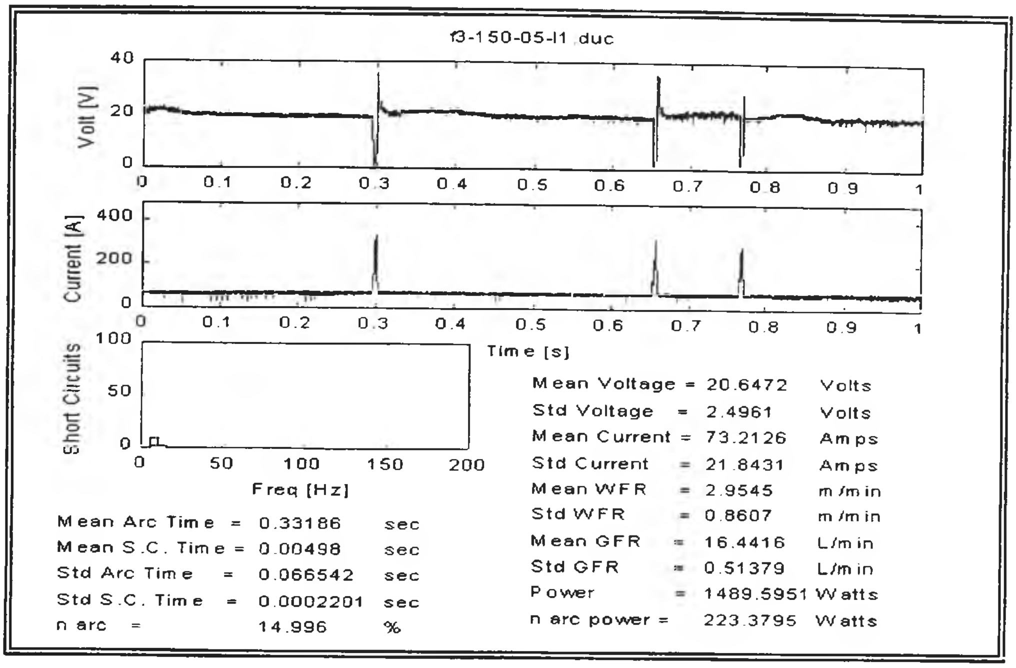

Plot F3-13

Sample f3-150-05-layer 1

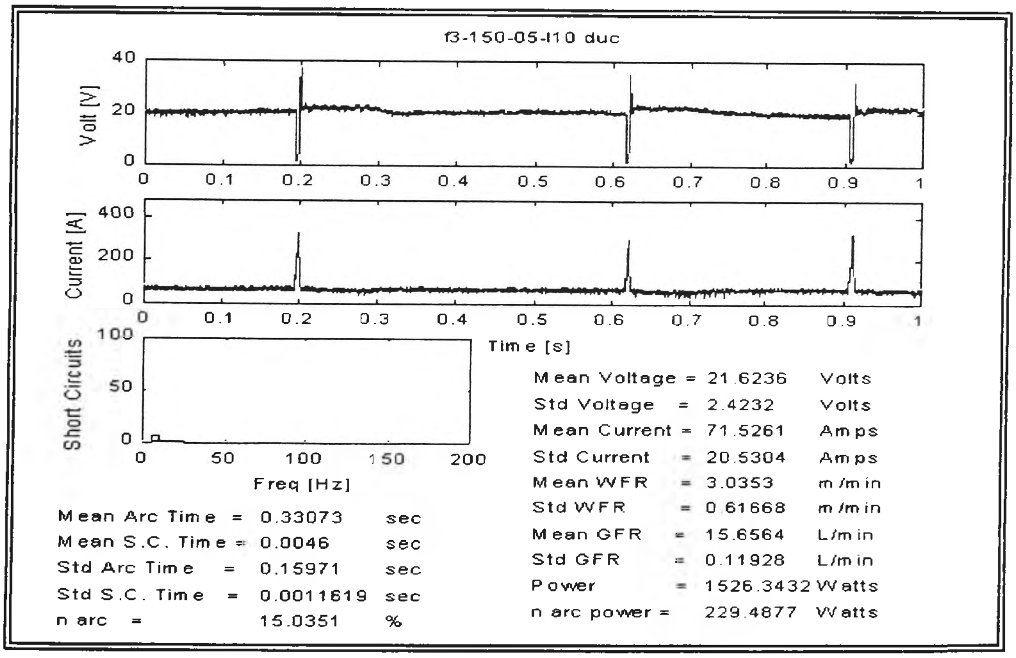

Plot F3-14

Sample f3-150-05-layer 10

F4 Wire Feed Rate of 4 m/min

Sample f4-75-05

Set Values	
Voltage [%]	75
Wire feed rate [m/min]	4
Travel speed [mm/sec]	5
Gas flow [l/min]	15

Weld Geometry		Visual Defects and Weld Property	
Weld height [mm]	17.5	Spatters	Yes
Weld width [mm]	6.1	Porosity	No
Stand-off at layer 1 [mm]	15	Excess material	No
Stand-off at layer 10 [mm]	16	Surface regularity [μm]	62.15
Temperature at layer 10 [deg.C]	240	Average hardness [HV]	153
Number of layers	10		

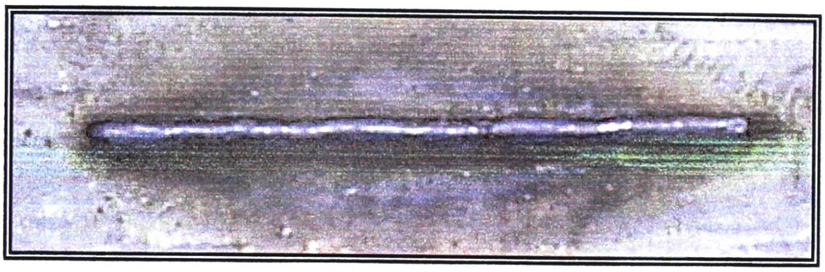

Figure F4-1

Sample f4-75-05 (top view)

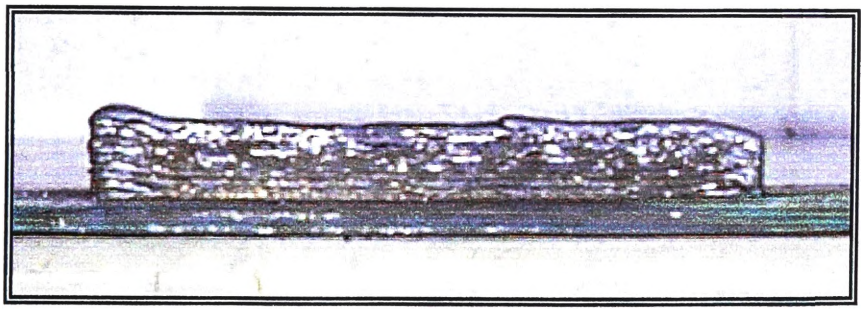

Figure F4-2

Sample f4-75-05 (front view)

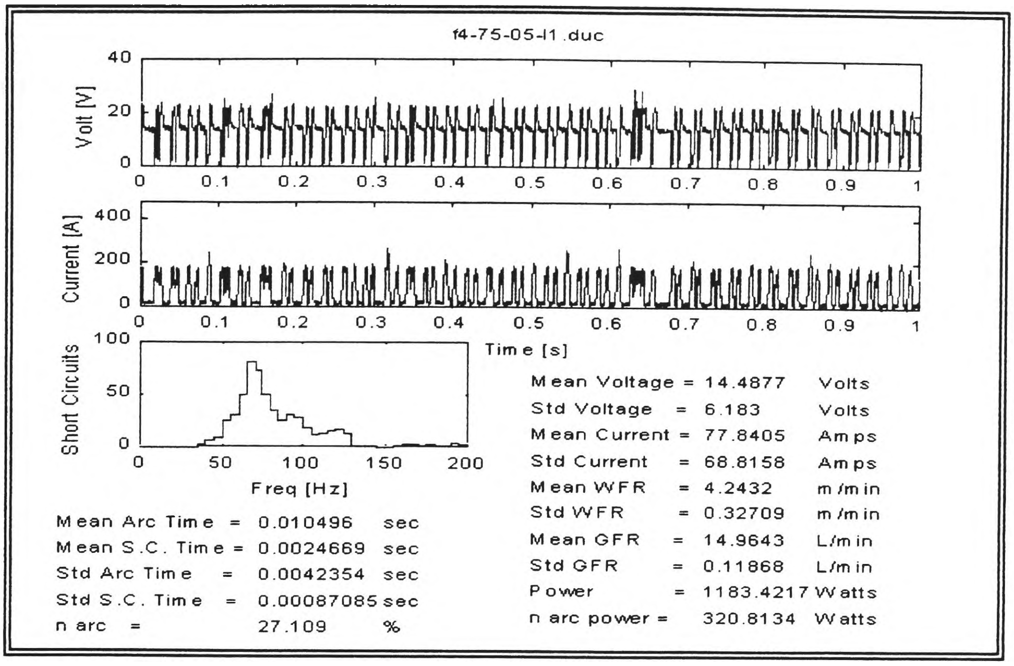

Plot F4-1

Sample f4-75-05-layer 1

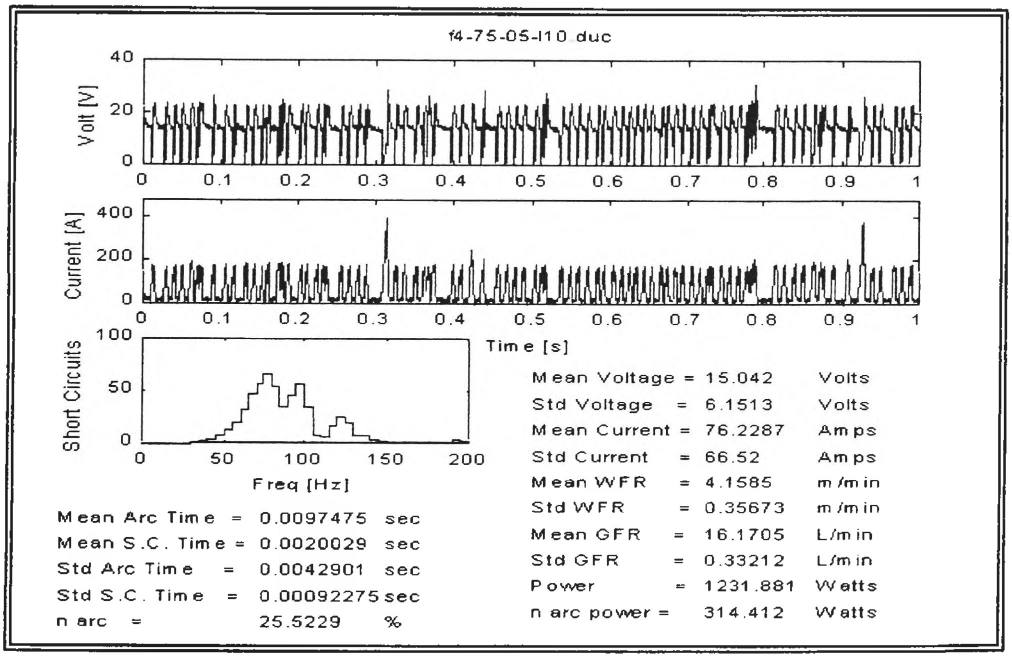

Plot F4-2

Sample f4-75-05-layer 10

Sample f4-100-05

Set Values	
Voltage [%]	100
Wire feed rate [m/min]	4
Travel speed [mm/sec]	5
Gas flow [l/min]	15

Weld Geometry		Visual Defects and Weld Property	
Weld height [mm]	15	Spatters	No
Weld width [mm]	6.4	Porosity	No
Stand-off at layer 1 [mm]	15	Excess material	No
Stand-off at layer 10 [mm]	17	Surface regularity [μm]	N/A
Temperature at layer 10 [deg.C]	250	Average hardness [HV]	N/A
Number of layers	10		

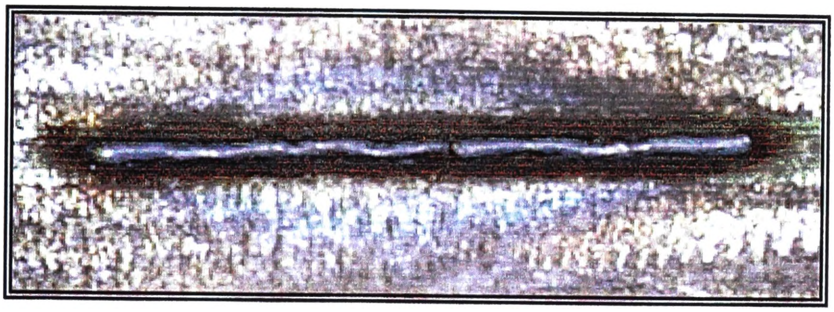

Figure F4-3

Sample f4-100-05 (top view)

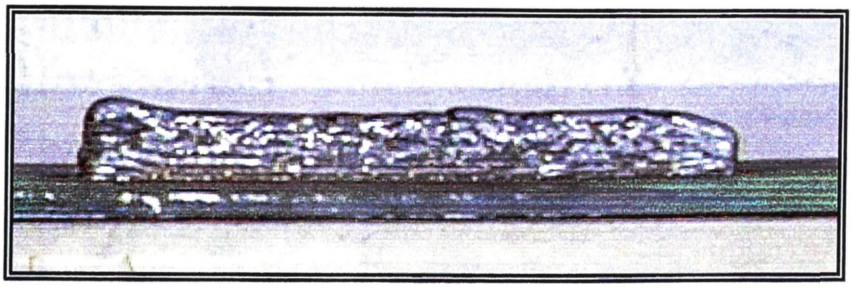

Figure F4-4

Sample f4-100-05 (front view)

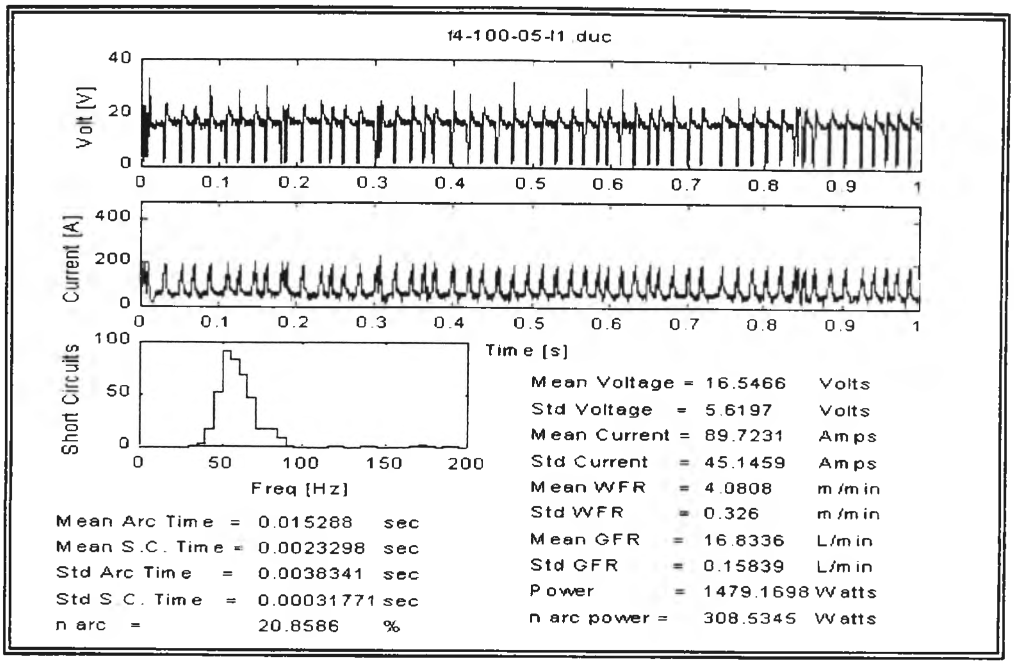

Plot F4-3

Sample f4-100-05-layer 1

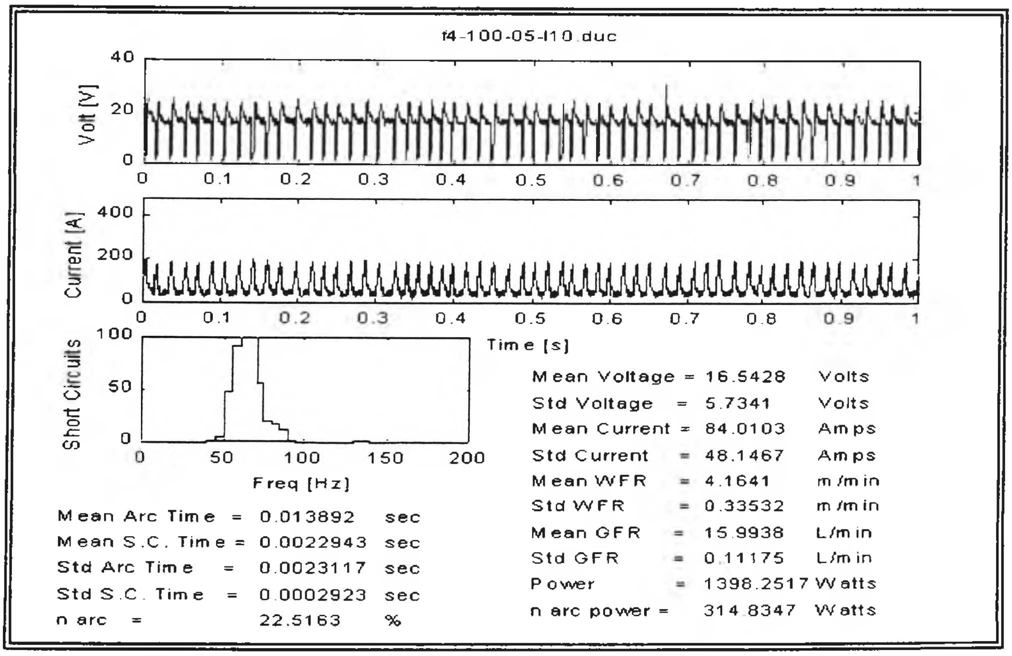

Plot F4-4

Sample f4-100-05-layer 10

Sample f4-105-05

Set Values	
Voltage [%]	105
Wire feed rate [m/min]	4
Travel speed [mm/sec]	5
Gas flow [l/min]	15

Weld Geometry		Visual Defects and Weld Property	
Weld height [mm]	15	Spatters	No
Weld width [mm]	6.5	Porosity	No
Stand-off at layer 1 [mm]	15	Excess material	No
Stand-off at layer 10 [mm]	17.5	Surface regularity [μm]	N/A
Temperature at layer 10 [deg.C]	270	Average hardness [HV]	N/A
Number of layers	10		

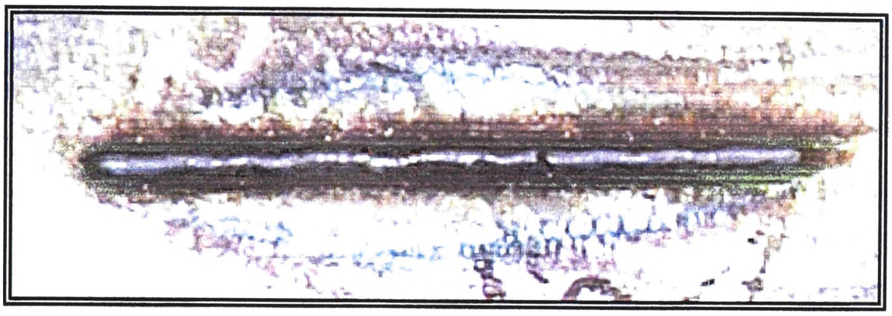

Figure F4-5

Sample f4-105-05 (top view)

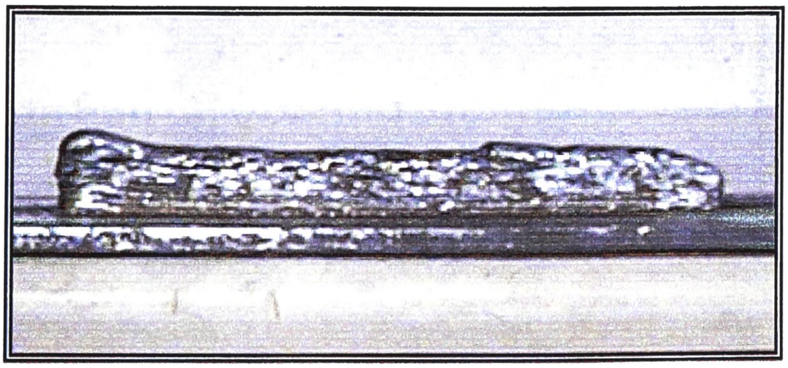

Figure F4-6

Sample f4-105-05 (front view)

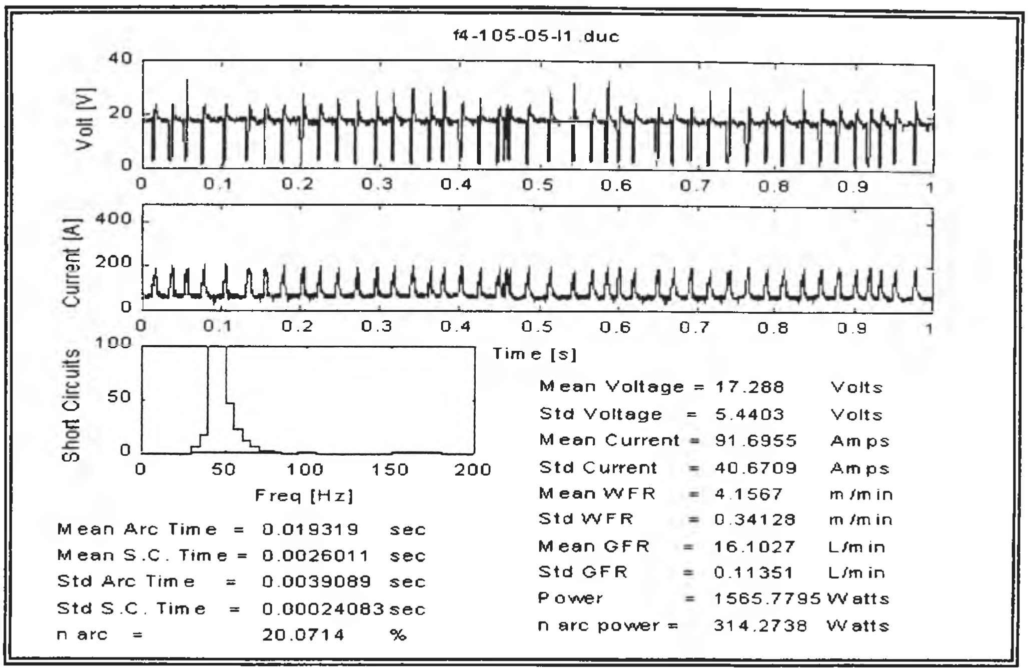

Plot F4-5

Sample f4-105-05-layer 1

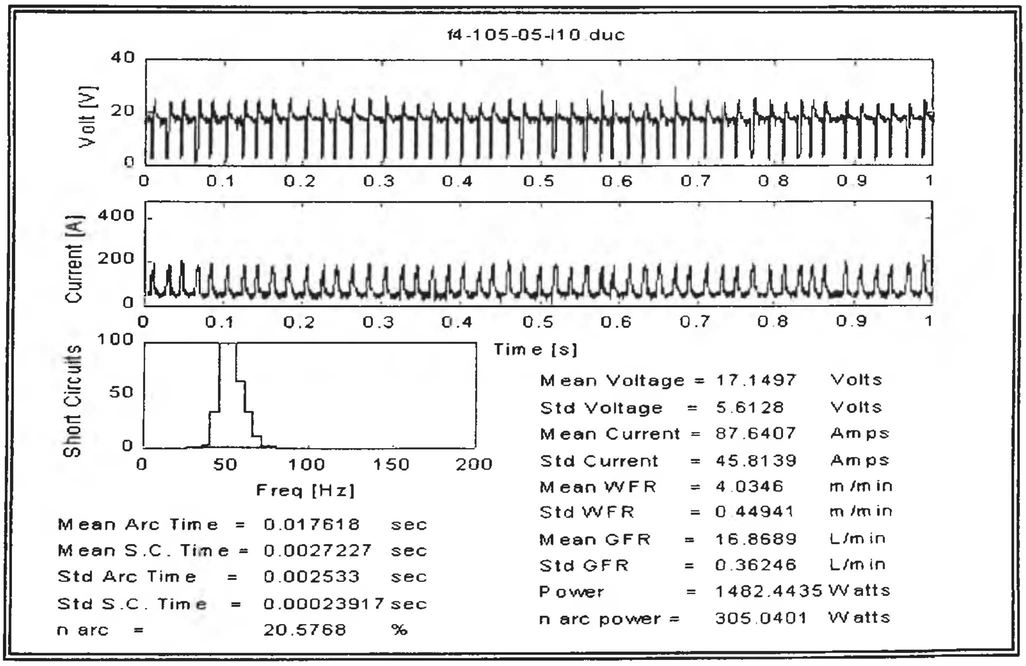

Plot F4-6

Sample f4-105-05-layer 10

Sample f4-110-05

Set Values	
Voltage [%]	110
Wire feed rate [m/min]	4
Travel speed [mm/sec]	5
Gas flow [l/min]	15

Weld Geometry		Visual Defects and Weld Property	
Weld height [mm]	13.5	Spatters	Yes
Weld width [mm]	6.7	Porosity	No
Stand-off at layer 1 [mm]	15	Excess material	No
Stand-off at layer 10 [mm]	15.5	Surface regularity [μm]	N/A
Temperature at layer 10 [deg.C]	290	Average hardness [HV]	N/A
Number of layers	10		

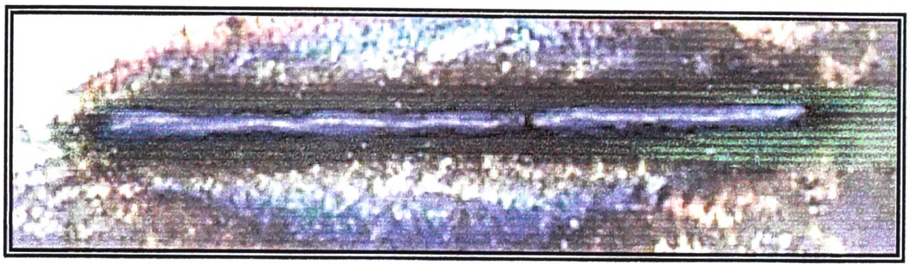

Figure F4-7

Sample f4-110-05 (top view)

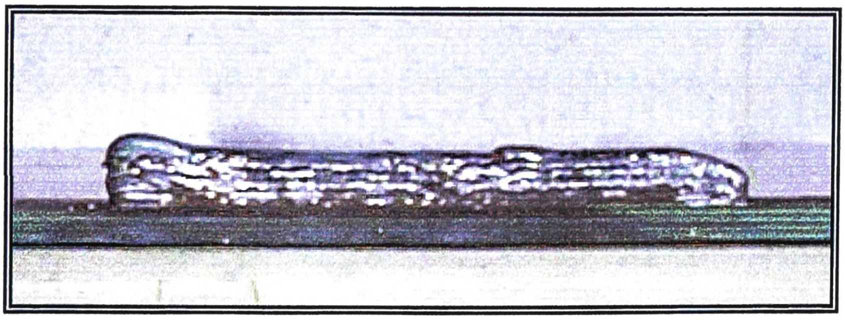

Figure F4-8

Sample f4-110-05- (front view)

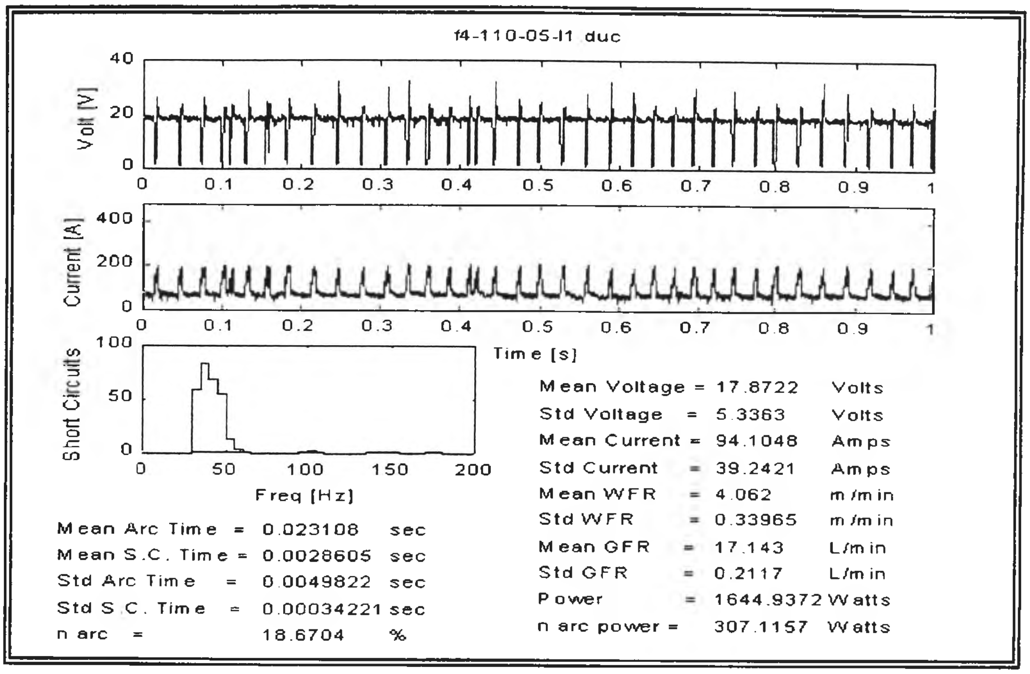

Plot F4-7

Sample f4-110-05-layer 1

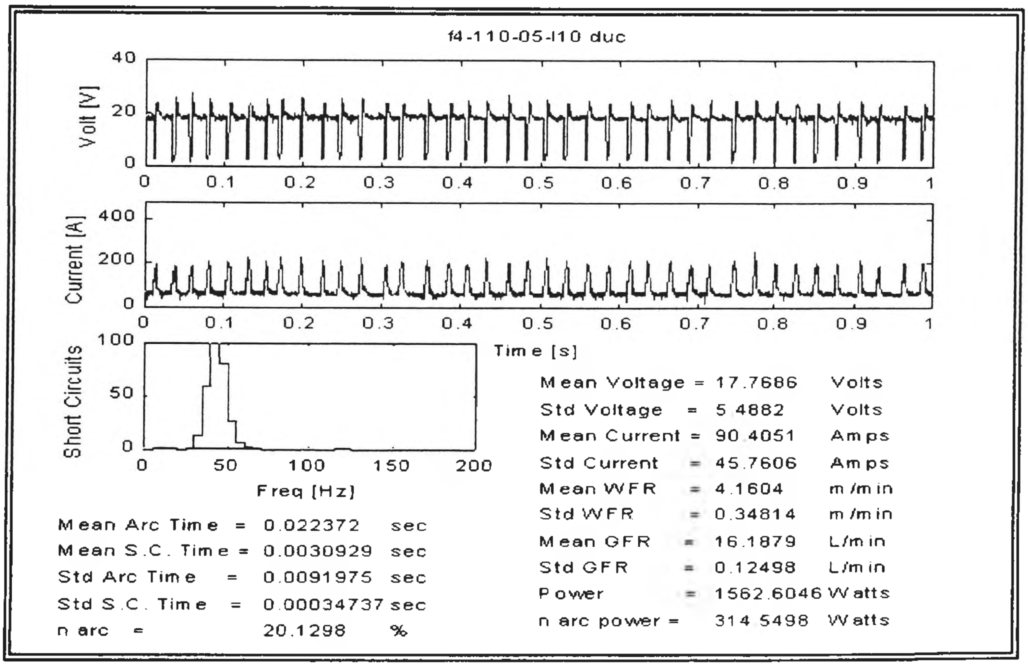

Plot F4-8

Sample f4-110-05-layer 10

Sample f4-120-05

Set Values	
Voltage [%]	120
Wire feed rate [m/min]	4
Travel speed [mm/sec]	5
Gas flow [l/min]	15

Weld Geometry		**Visual Defects and Weld Property**	
Weld height [mm]	13.5	Spatters	Yes
Weld width [mm]	7.2	Porosity	No
Stand-off at layer 1 [mm]	15	Excess material	No
Stand-off at layer 10 [mm]	16.5	Surface regularity [μm]	N/A
Temperature at layer 10 [deg.C]	315	Average hardness [HV]	N/A
Number of layers	10		

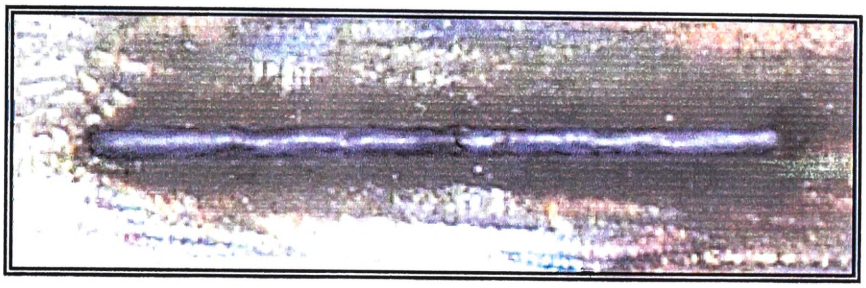

Figure F4-9

Sample f4-120-05 (top view)

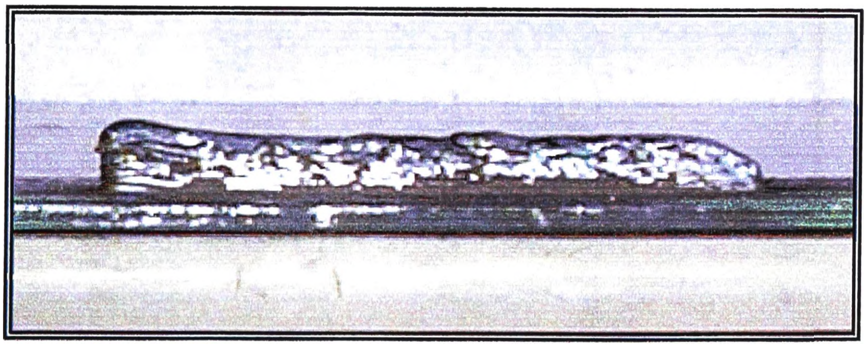

Figure F4-10

Sample f4-120-05 (front view)

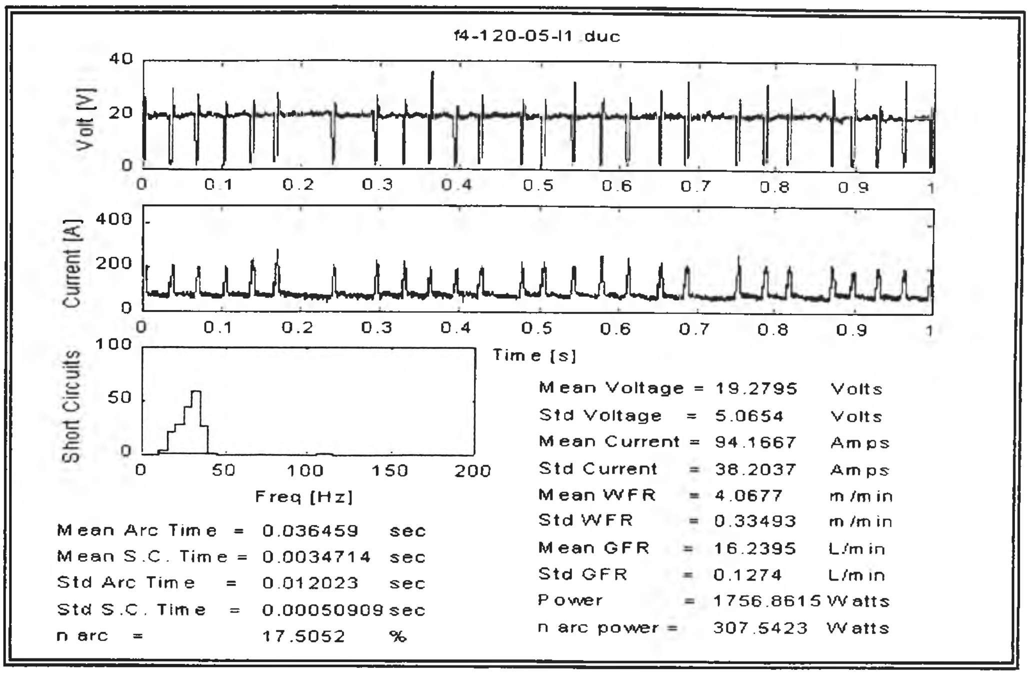

Plot F4-9

Sample f4-120-05-layer 1

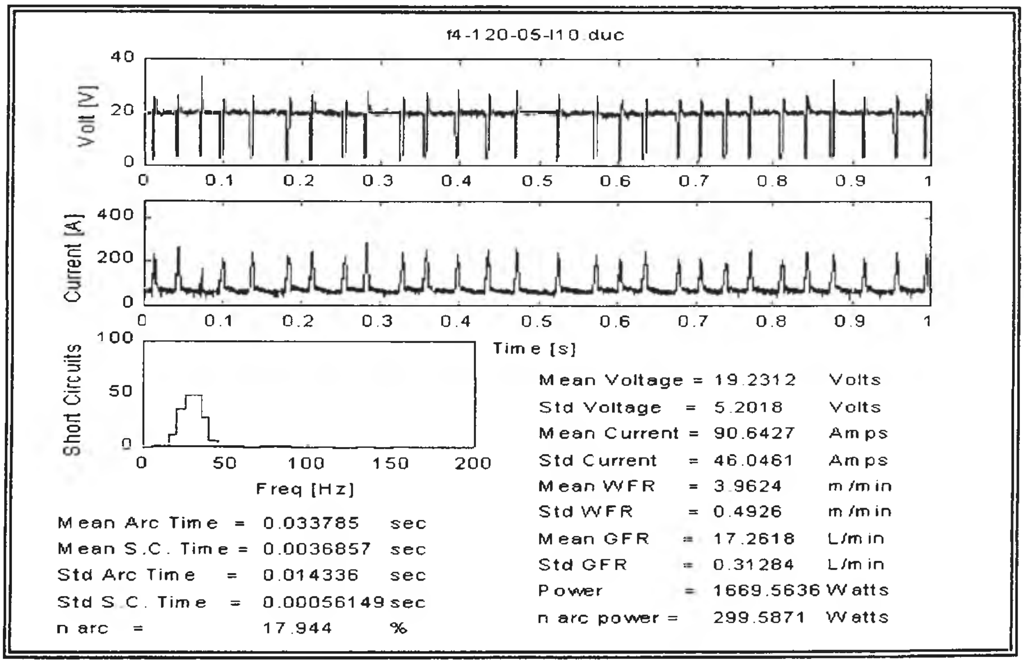

Plot F4-10

Sample f4-120-05-layer 10

Sample f4-150-05

Set Values	
Voltage [%]	150
Wire feed rate [m/min]	4
Travel speed [mm/sec]	5
Gas flow [l/min]	15

Weld Geometry		Visual Defects and Weld Property	
Weld height [mm]	12.5	Spatters	Yes
Weld width [mm]	8	Porosity	No
Stand-off at layer 1 [mm]	15	Excess material	No
Stand-off at layer 10 [mm]	17	Surface regularity [μm]	36.75
Temperature at layer 10 [deg.C]	340	Average hardness [HV]	151
Number of layers	10		

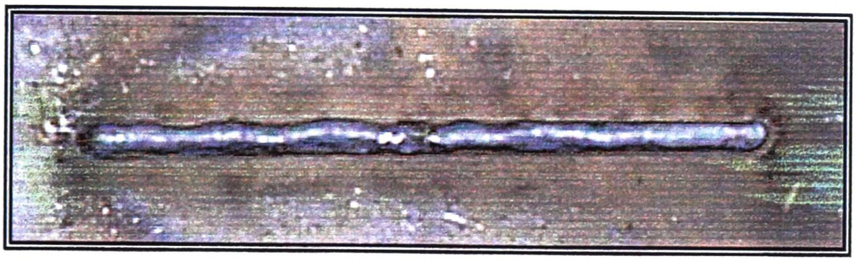

Figure F4-11

Sample f4-150-05 (top view)

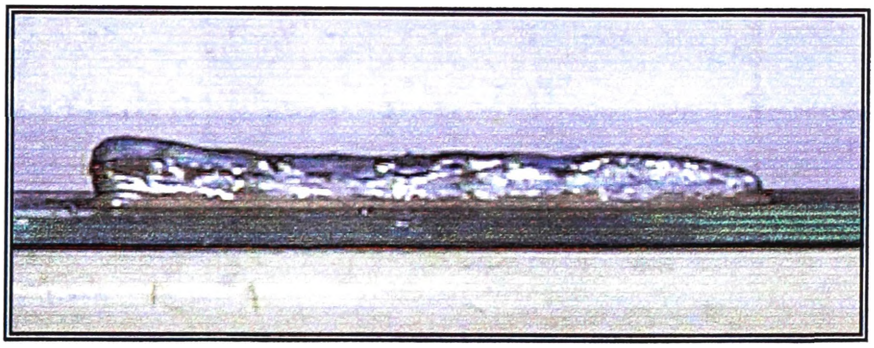

Figure F4-12

Sample f4-150-05 (front view)

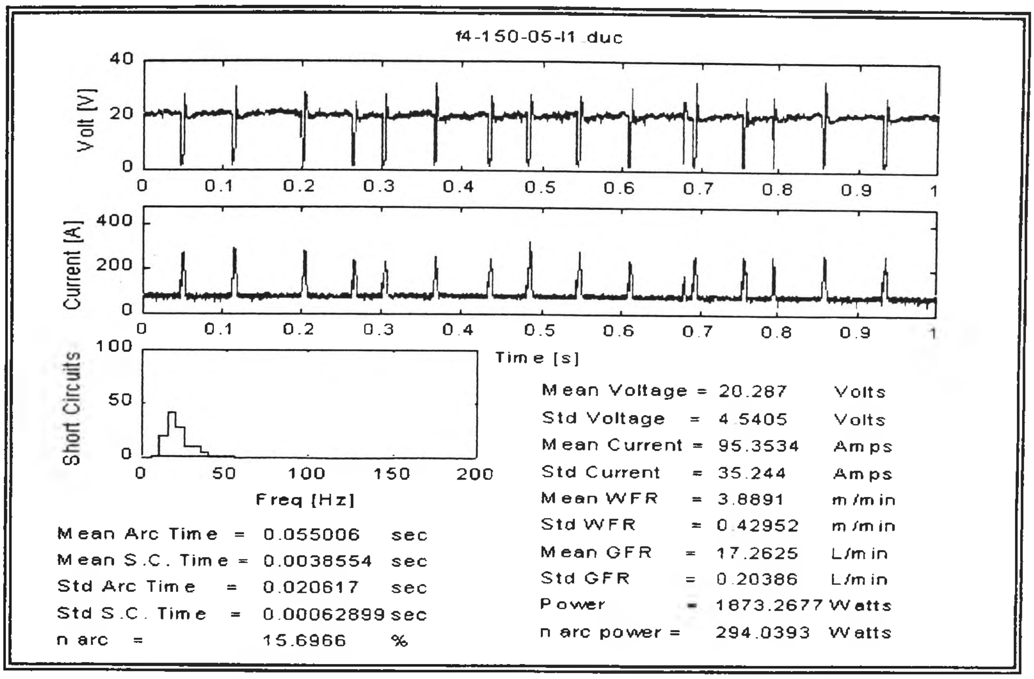

Plot F4-11

Sample F4-150-05-layer 1

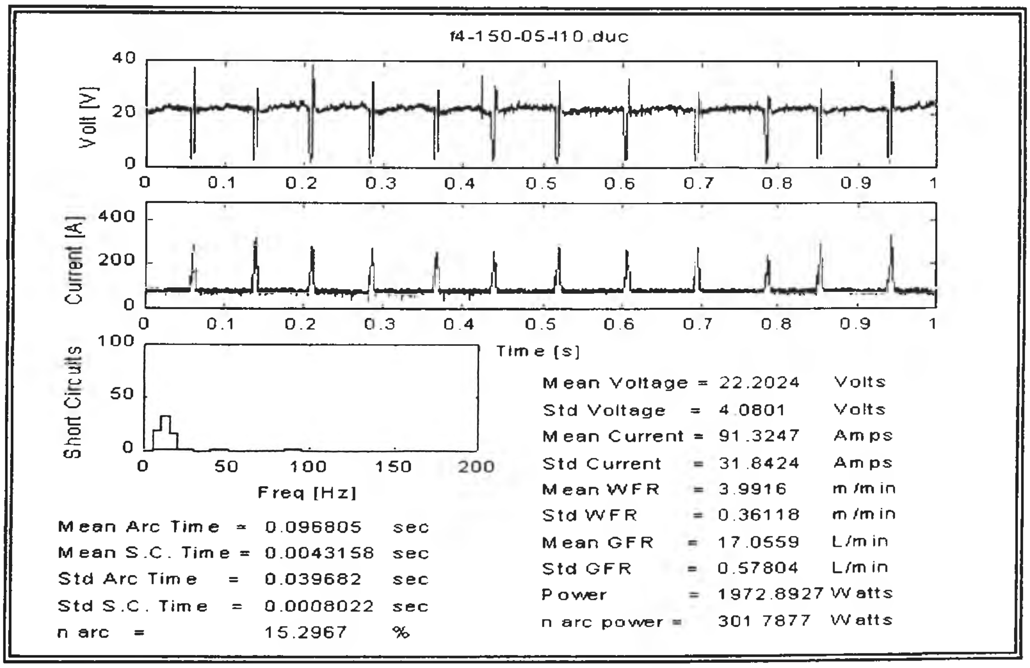

Plot F4-12

Sample F4-150-05-layer 10

F5 Wire Feed Rate of 5 m/min

Sample f5-75-05

Set Values	
Voltage [%]	75
Wire feed rate [m/min]	5
Travel speed [mm/sec]	5
Gas flow [l/min]	15

Weld Geometry		**Visual Defects and Weld Property**	
Weld height [mm]	19	Spatters	Yes
Weld width [mm]	6.3	Porosity	No
Stand-off at layer 1 [mm]	15	Excess material	No
Stand-off at layer 10 [mm]	17.5	Surface regularity [μm]	100.45
Temperature at layer 10 [deg.C]	270	Average hardness [HV]	154
Number of layers	10		

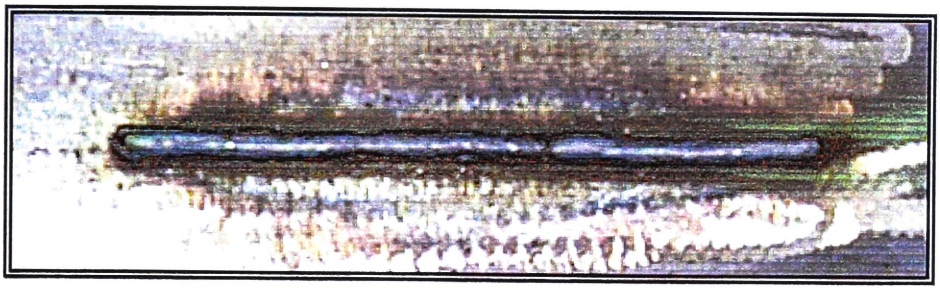

Figure F5-1

Sample f5-75-05 (top view)

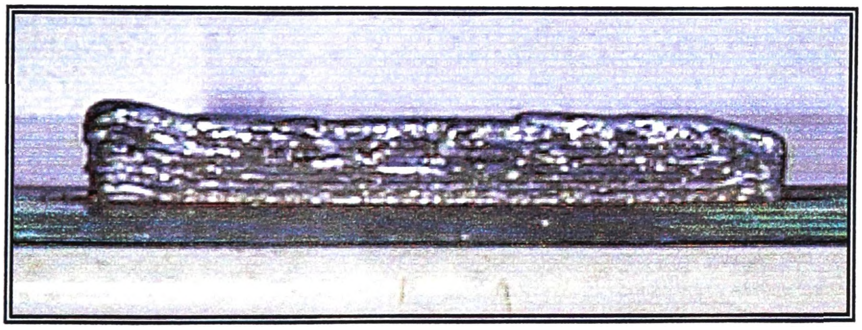

Figure F5-2

Sample f5-75-05 (front view)

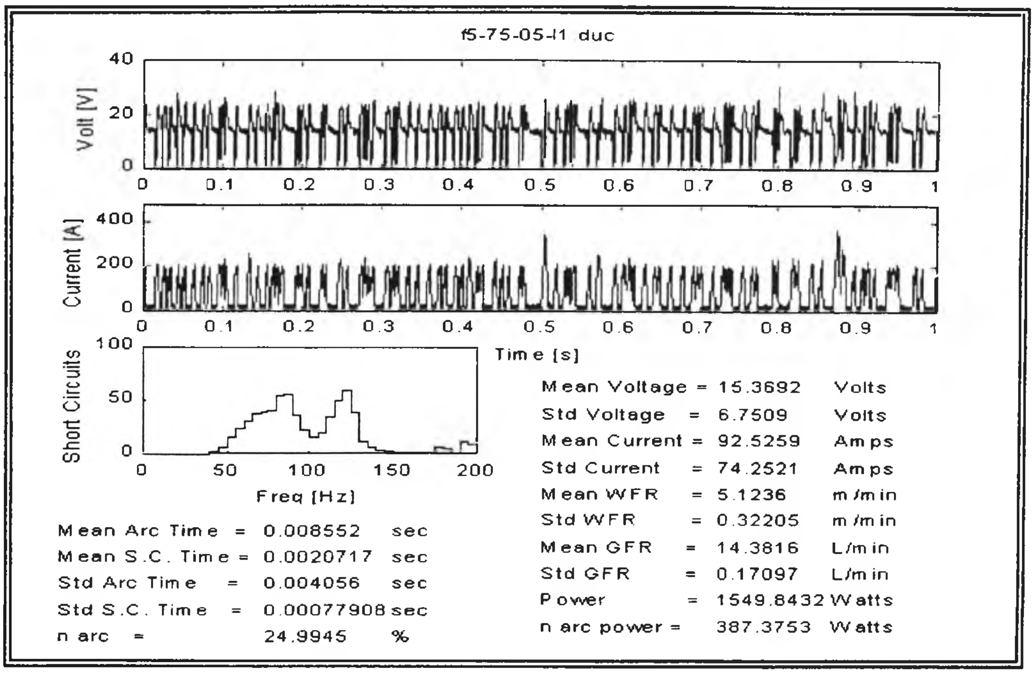

Plot F5-1

Sample f5-75-05-layer 1

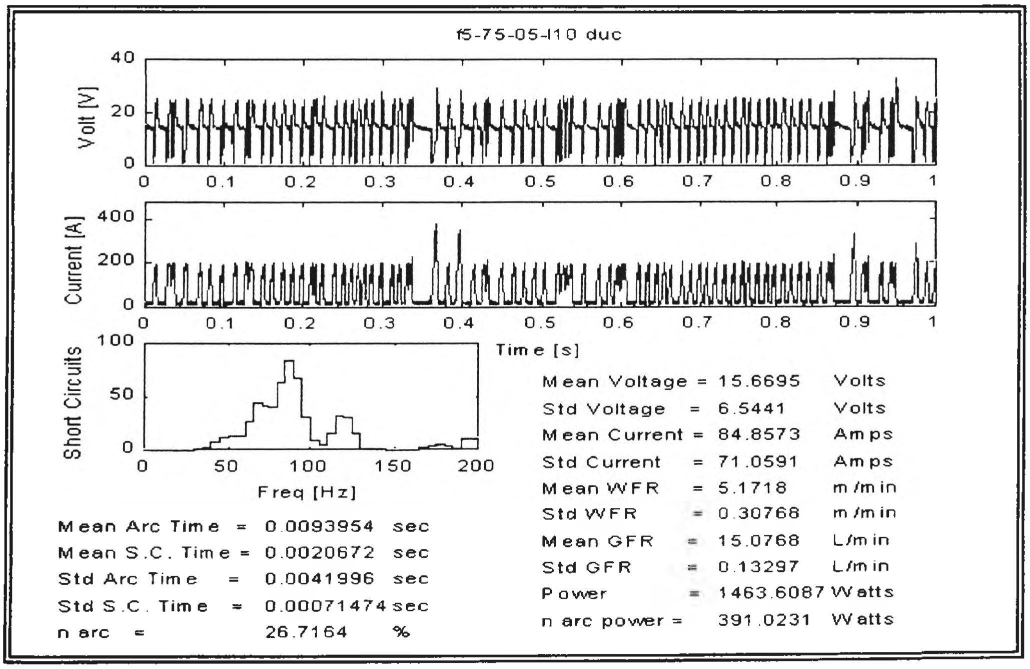

Plot F5-2

Sample f5-75-05-layer 10

Sample f5-95-05

Set Values	
Voltage [%]	95
Wire feed rate [m/min]	5
Travel speed [mm/sec]	5
Gas flow [l/min]	15

Weld Geometry		Visual Defects and Weld Property	
Weld height [mm]	17	Spatters	No
Weld width [mm]	7.5	Porosity	No
Stand-off at layer 1 [mm]	15	Excess material	No
Stand-off at layer 10 [mm]	15	Surface regularity [μm]	N/A
Temperature at layer 10 [deg.C]	285	Average hardness [HV]	N/A
Number of layers	10		

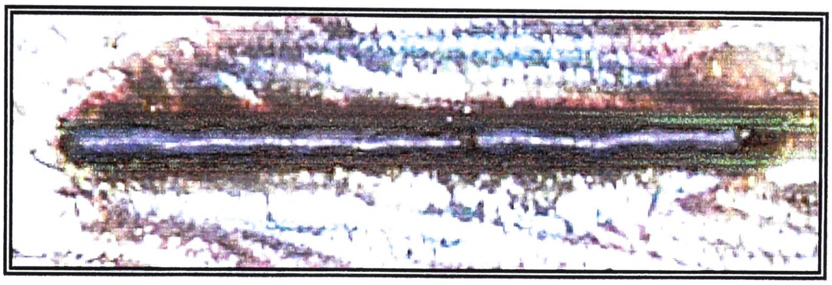

Figure F5-3

Sample f5-95-05 (top view)

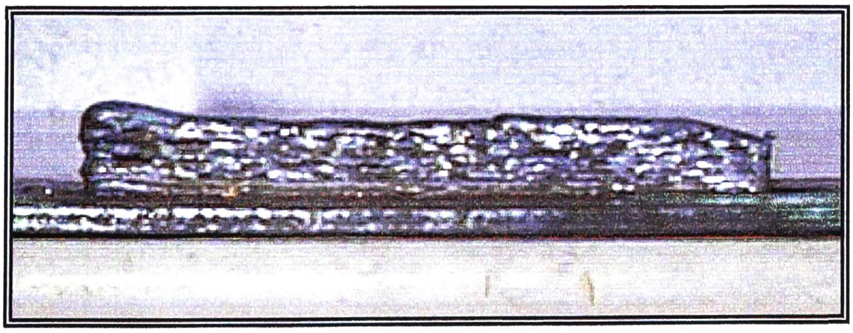

Figure F5-4

Sample f5-95-05 (front view)

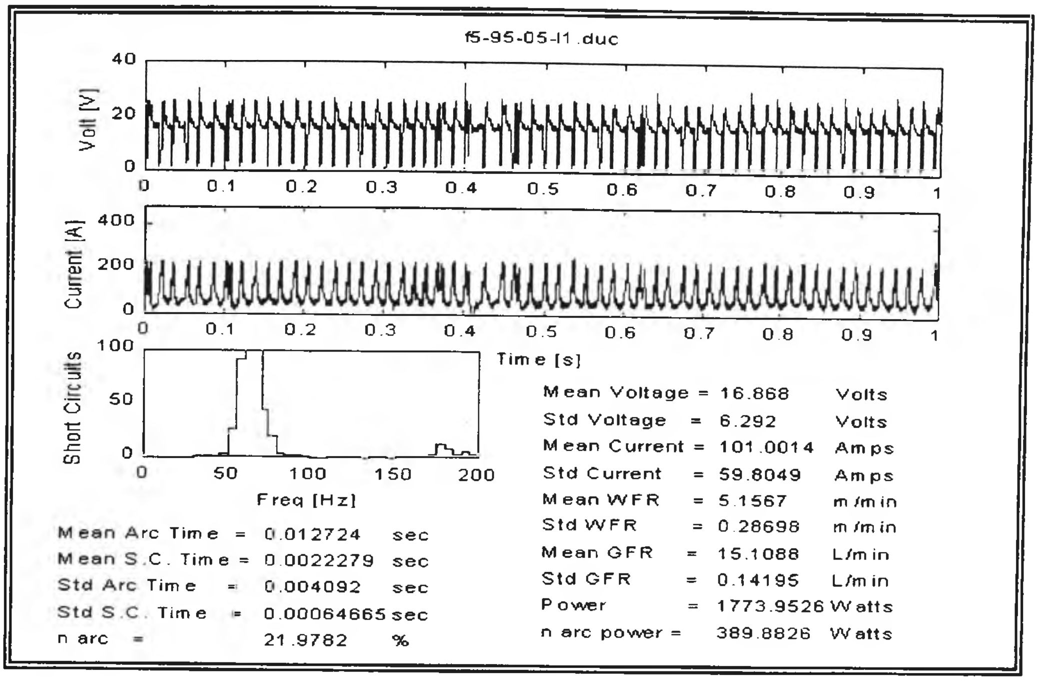

Plot F5-3

Sample f5-95-05-layer 1

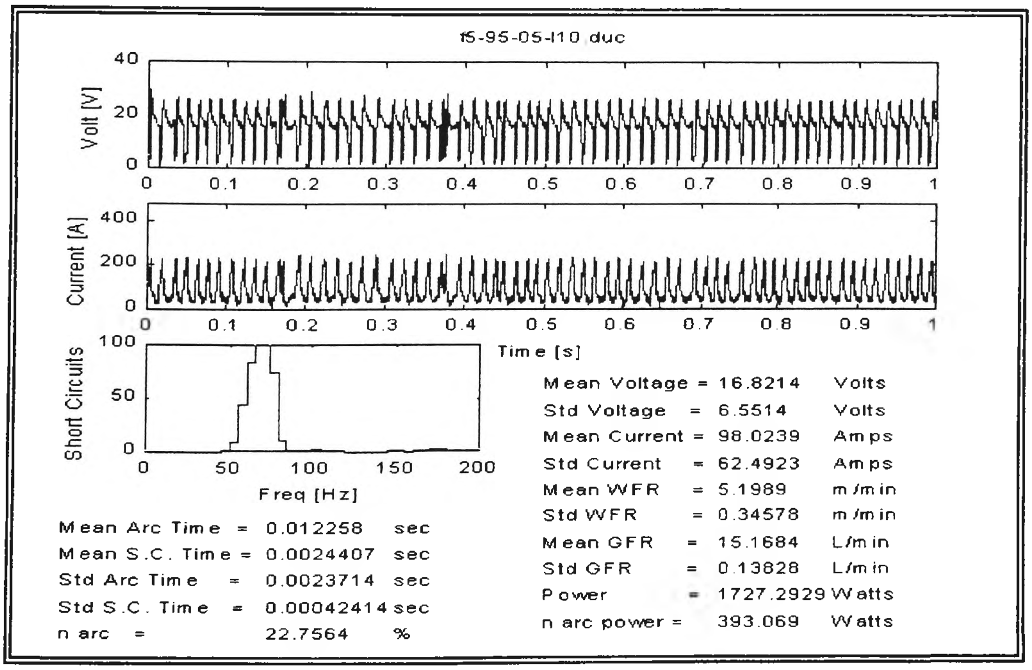

Plot F5-4

Sample f5-95-05-layer 10

Sample f5-105-05

Set Values	
Voltage [%]	105
Wire feed rate [m/min]	5
Travel speed [mm/sec]	5
Gas flow [l/min]	15

Weld Geometry		Visual Defects and Weld Property	
Weld height [mm]	15.5	Spatters	Yes
Weld width [mm]	8.1	Porosity	Yes
Stand-off at layer 1 [mm]	15	Excess material	No
Stand-off at layer 10 [mm]	15.5	Surface regularity [μm]	N/A
Temperature at layer 10 [deg.C]	357	Average hardness [HV]	N/A
Number of layers	10		

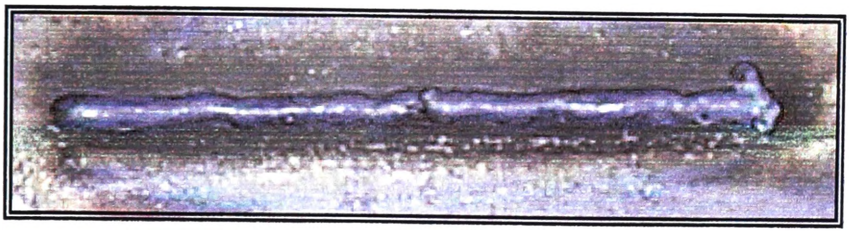

Figure F5-5

Sample f5-105-05 (top view)

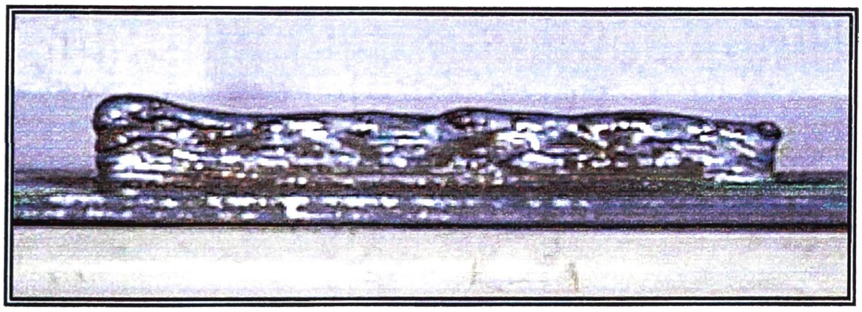

Figure F5-6

Sample f5-105-05 (front view)

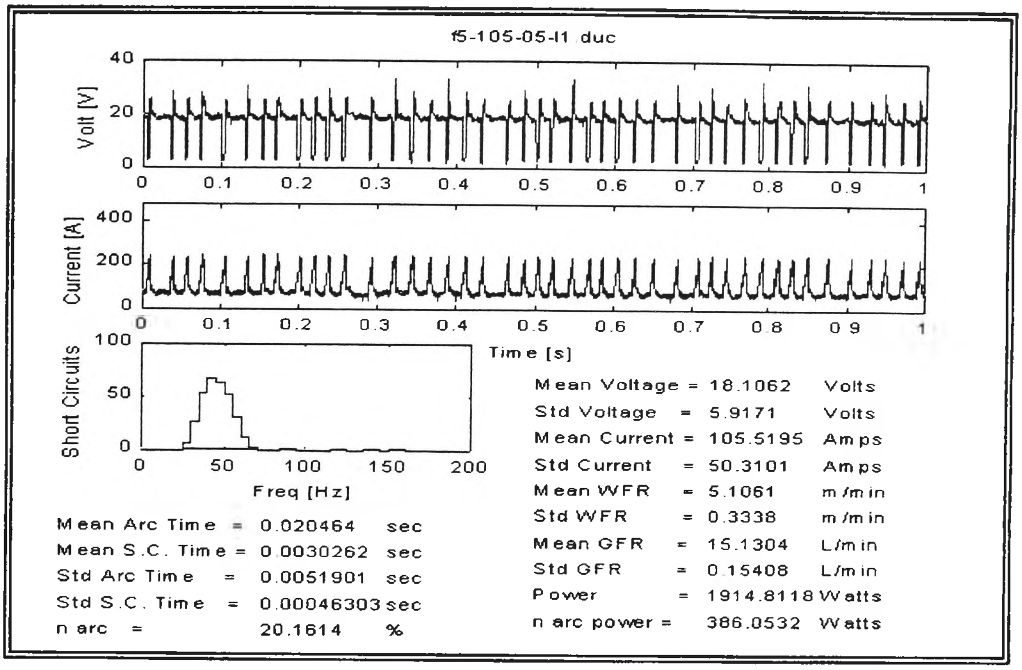

Plot F5-5

Sample f5-105-05-layer 1

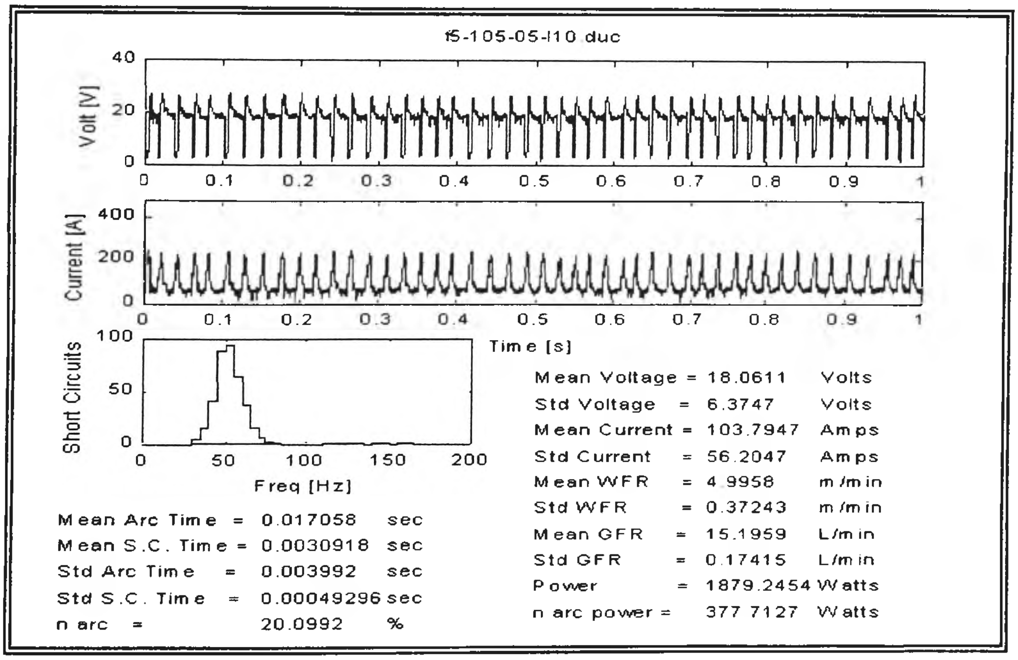

Plot F5-6

Sample f5-105-05-layer 10

Sample f5-115-05

Set Values	
Voltage [%]	115
Wire feed rate [m/min]	5
Travel speed [mm/sec]	5
Gas flow [l/min]	15

Weld Geometry		Visual Defects and Weld Property	
Weld height [mm]	14.5	Spatters	Yes
Weld width [mm]	8.2	Porosity	No
Stand-off at layer 1 [mm]	15	Excess material	No
Stand-off at layer 10 [mm]	16.5	Surface regularity [μm]	N/A
Temperature at layer 10 [deg.C]	372	Average hardness [HV]	N/A
Number of layers	10		

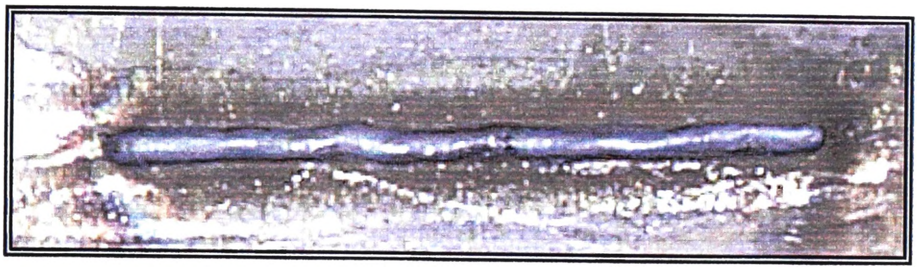

Figure F5-7

Sample f5-115-05 (top view)

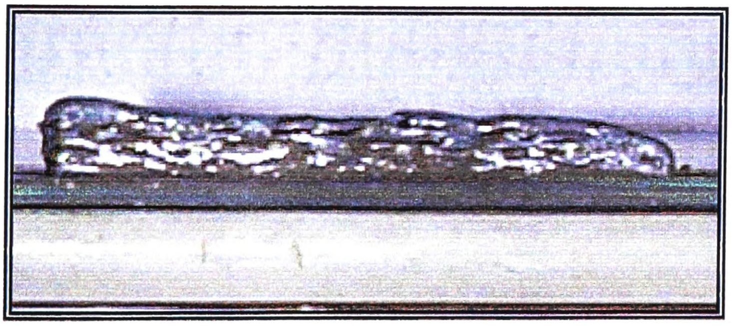

Figure F5-8

Sample f5-115-05 (front view)

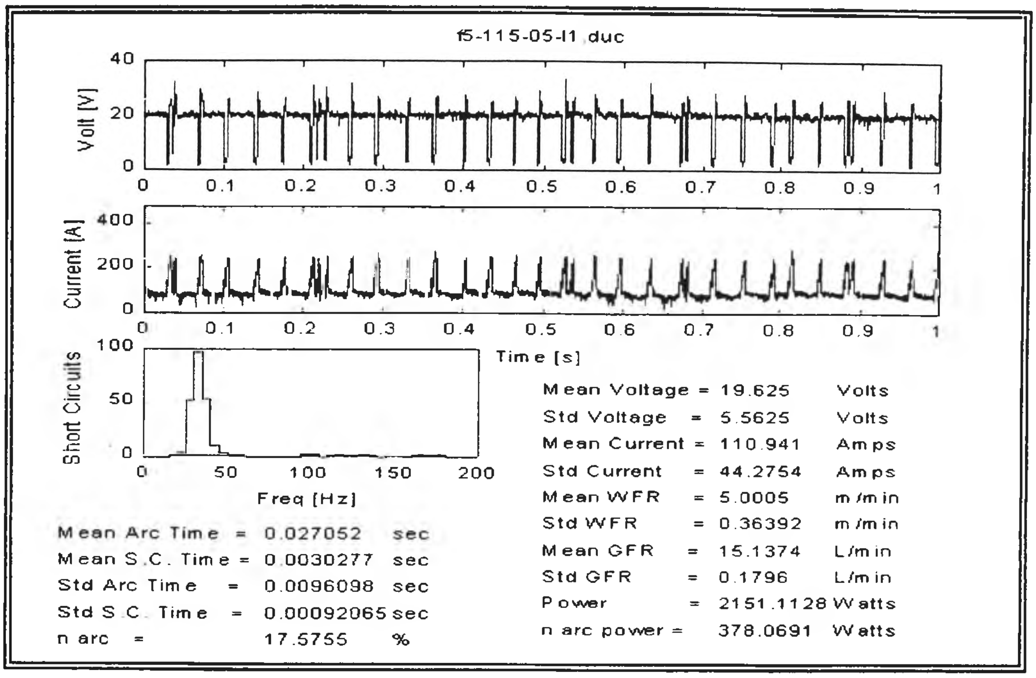

Plot F5-7

Sample f5-115-05-layer 1

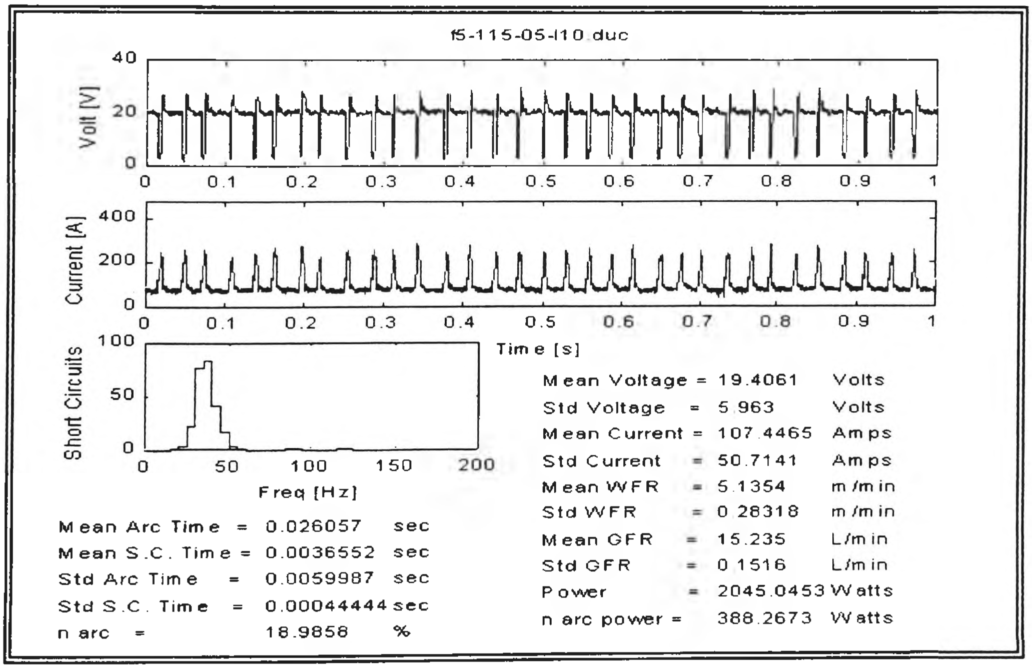

Plot F5-8

Sample f5-115-05-layer 10

Sample f5-125-05

Set Values	
Voltage [%]	125
Wire feed rate [m/min]	5
Travel speed [mm/sec]	5
Gas flow [l/min]	15

Weld Geometry		Visual Defects and Weld Property	
Weld height [mm]	14.9	Spatters	Yes
Weld width [mm]	9	Porosity	Yes
Stand-off at layer 1 [mm]	15	Excess material	Yes
Stand-off at layer 10 [mm]	16	Surface regularity [μm]	75.9
Temperature at layer 10 [deg.C]	420	Average hardness [HV]	151
Number of layers	10		

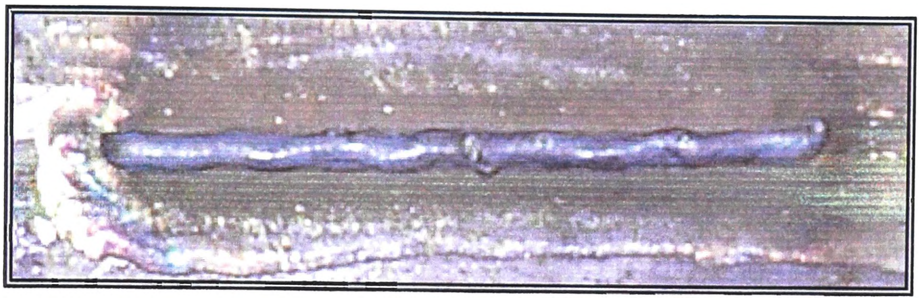

Figure F5-9

Sample f5-125-05 (top view)

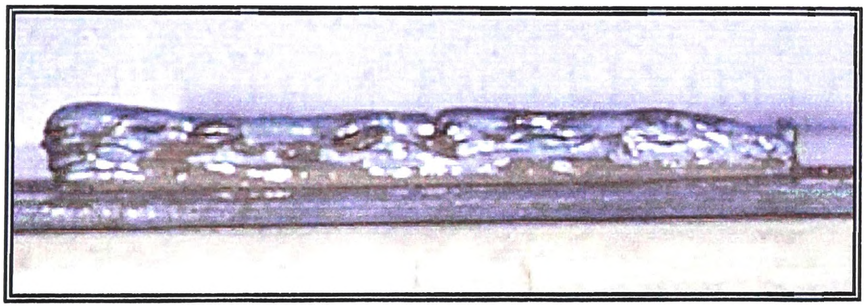

Figure F5-10

Sample f5-125-05 (front view)

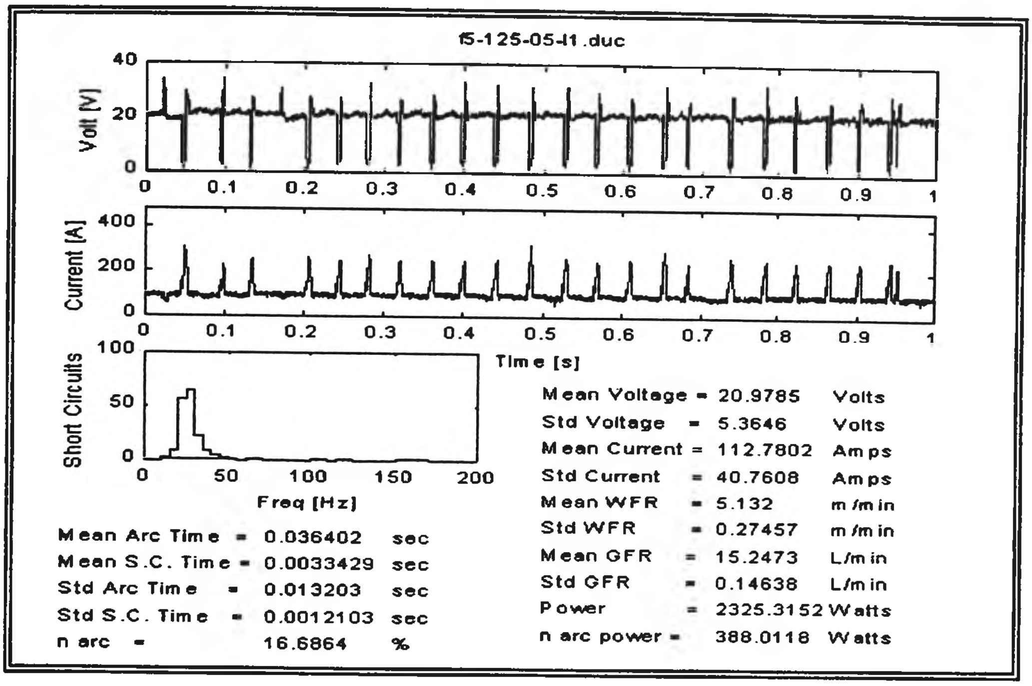

Plot F5-9

Sample f5-125-05-layer 1

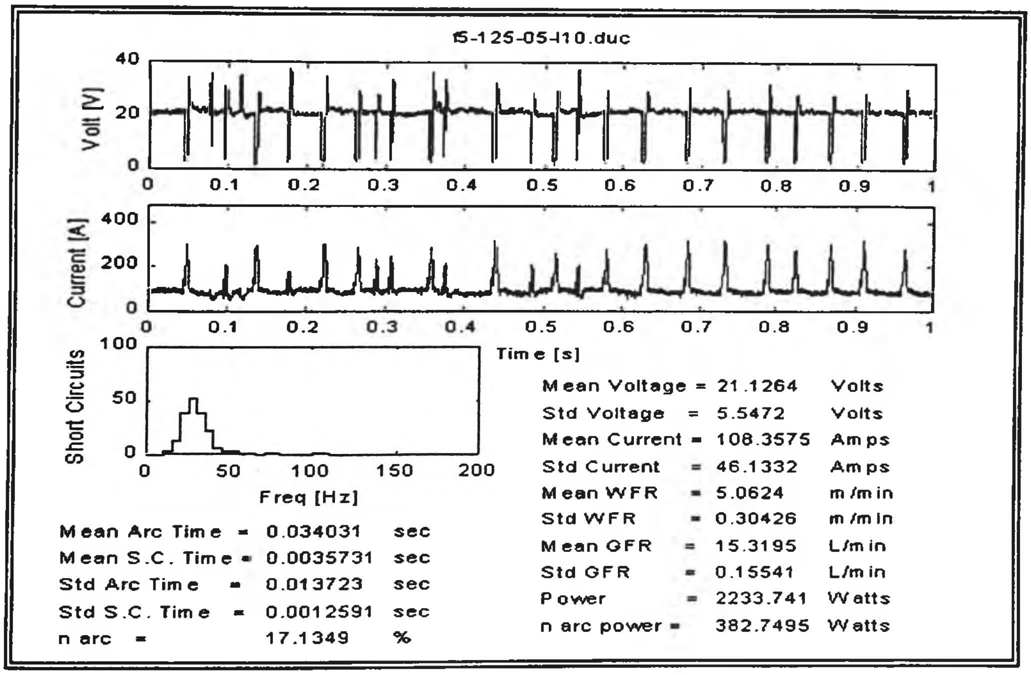

Plot F5-10

Sample f5-125-05-layer 10

F6 Wire Feed Rate of 6 m/min

Sample f6-75-05

Set Values	
Voltage [%]	75
Wire feed rate [m/min]	6
Travel speed [mm/sec]	5
Gas flow [l/min]	15

Weld Geometry		**Visual Defects and Weld Property**	
Weld height [mm]	22	Spatters	Yes
Weld width [mm]	6.9	Porosity	No
Stand-off at layer 1 [mm]	15	Excess material	No
Stand-off at layer 10 [mm]	16.5	Surface regularity [μm]	110.2
Temperature at layer 10 [deg.C]	420	Average hardness [HV]	153
Number of layers	10		

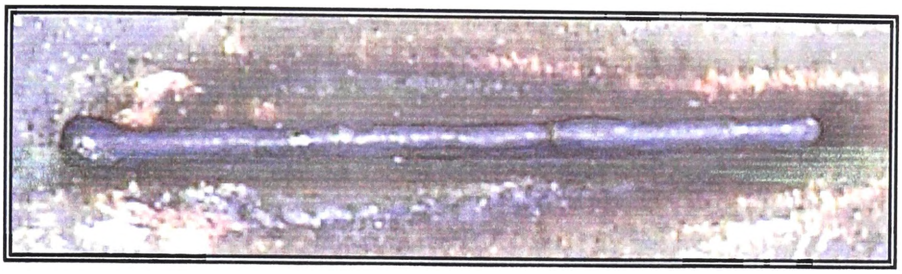

Figure F6-1

Sample f6-75-05 (top view)

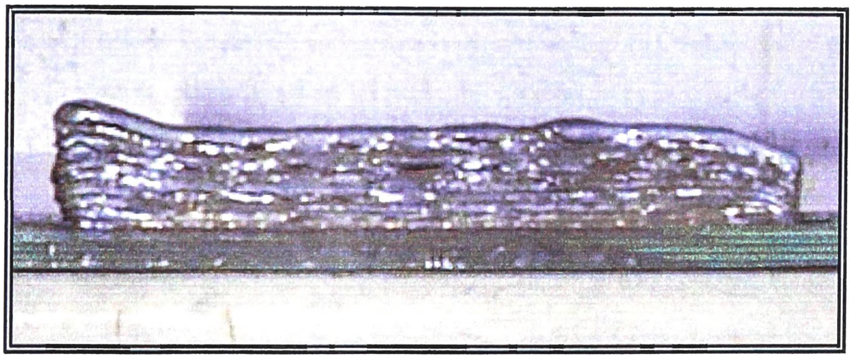

Figure F6-2

Sample f6-75-05 (front view)

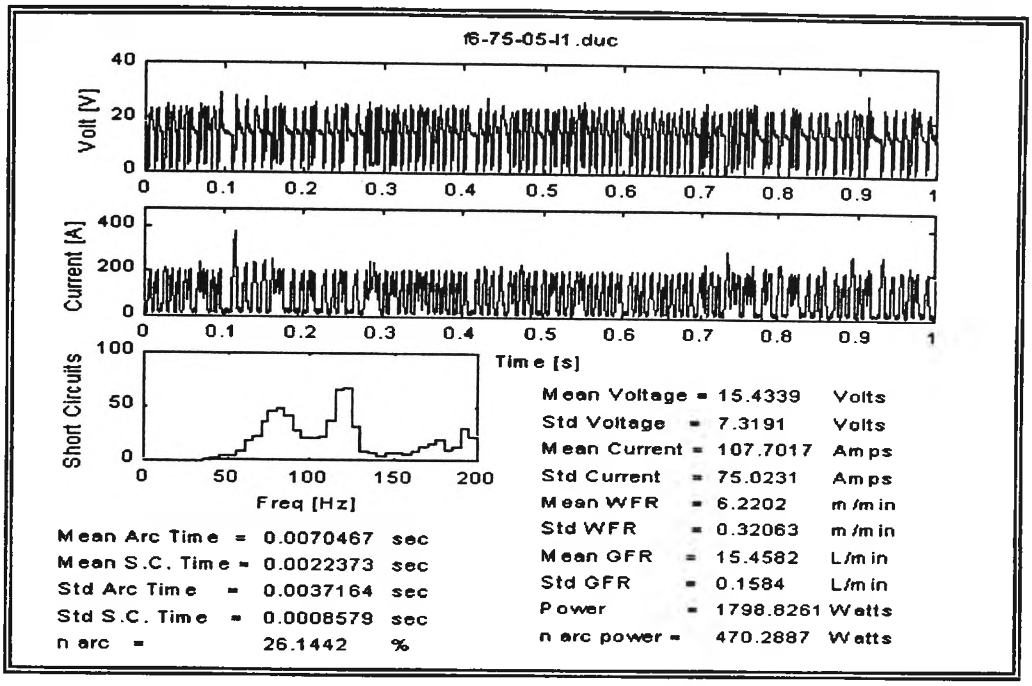

Plot F6-1

Sample f6-75-05-layer 1

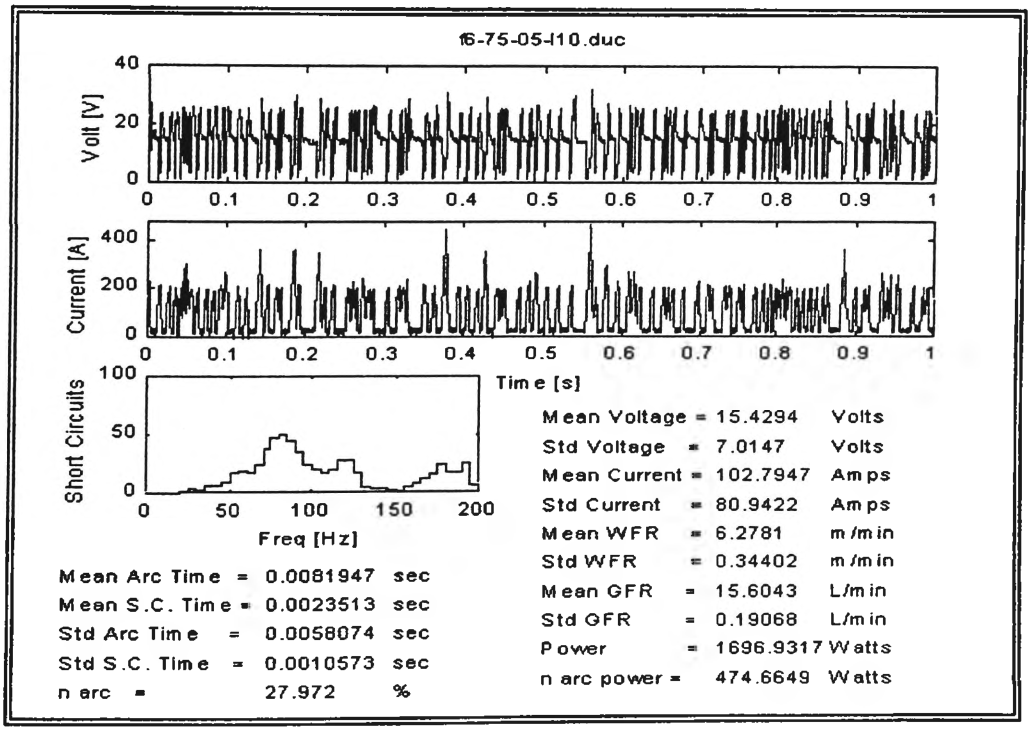

Plot F6-2

Sample f6-75-05-layer 10

Sample f6-90-05

Set Values	
Voltage [%]	90
Wire feed rate [m/min]	6
Travel speed [mm/sec]	5
Gas flow [l/min]	15

Weld Geometry		Visual Defects and Weld Property	
Weld height [mm]	18.5	Spatters	Yes
Weld width [mm]	8.4	Porosity	No
Stand-off at layer 1 [mm]	15	Excess material	No
Stand-off at layer 10 [mm]	15	Surface regularity [µm]	N/A
Temperature at layer 10 [deg.C]	436	Average hardness [HV]	N/A
Number of layers	10		

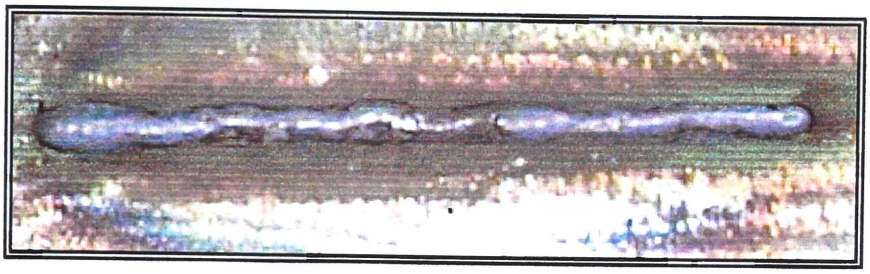

Figure F6-3

Sample f6-90-05 (top view)

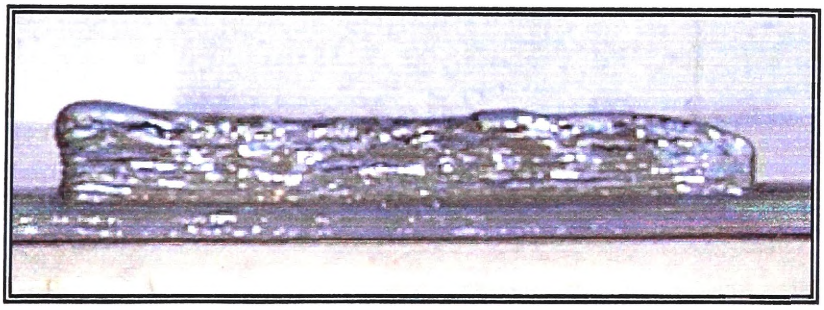

Figure F6-4

Sample f6-90-05 (front view)

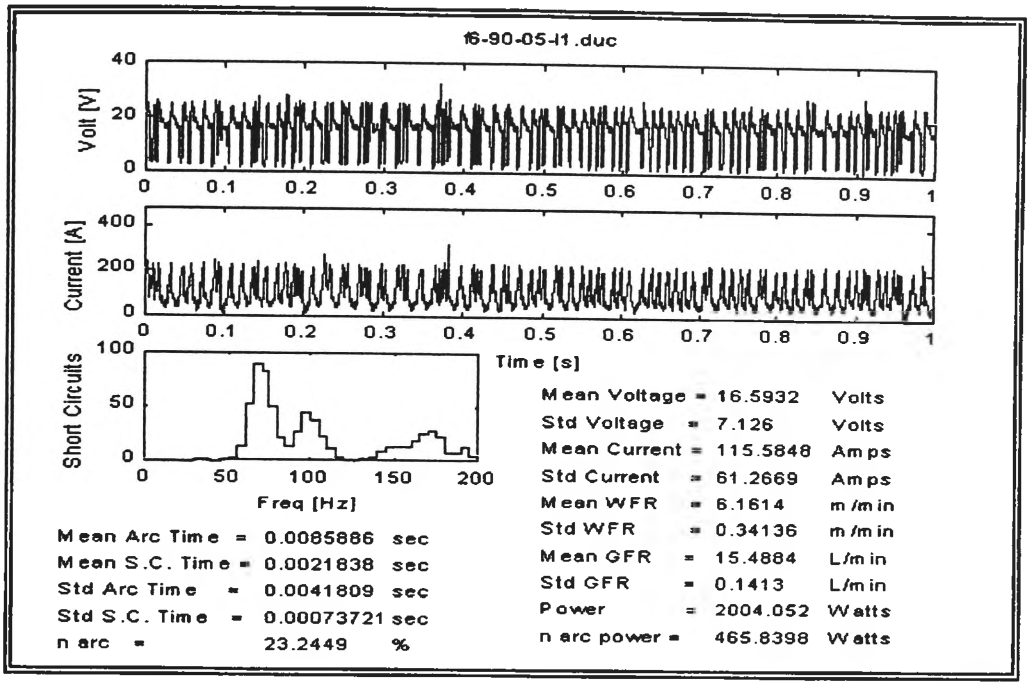

Plot F6-3

Sample f6-90-05-layer 1

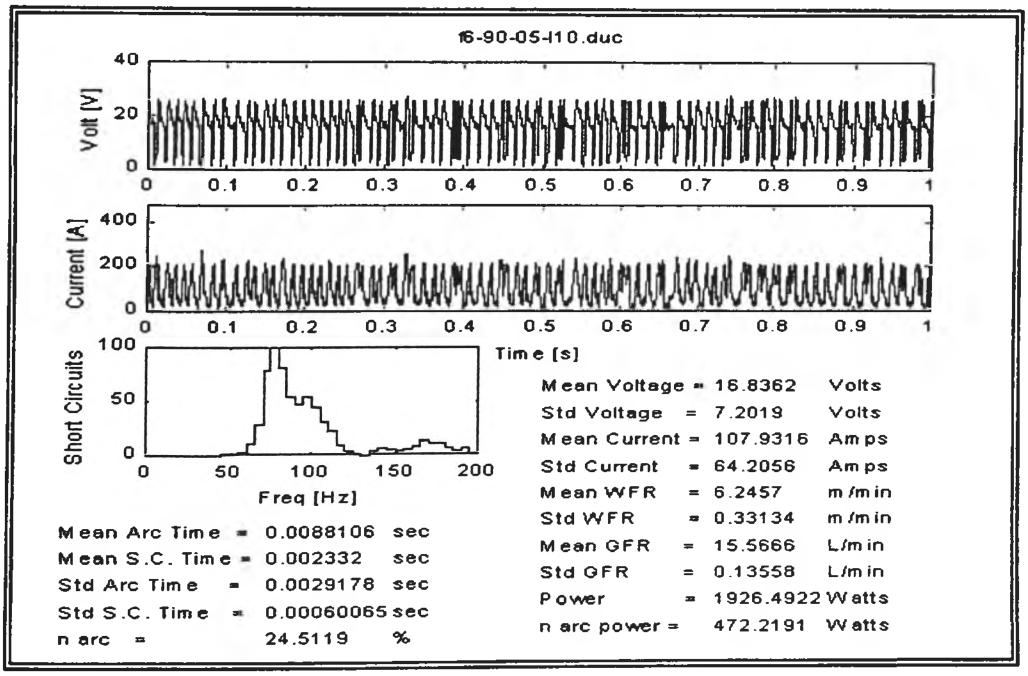

Plot F6-4

Sample f6-90-05-layer 10

Sample f6-100-05

Set Values	
Voltage [%]	100
Wire feed rate [m/min]	6
Travel speed [mm/sec]	5
Gas flow [l/min]	15

Weld Geometry		**Visual Defects and Weld Property**	
Weld height [mm]	18.5	Spatters	Yes
Weld width [mm]	8.5	Porosity	Yes
Stand-off at layer 1 [mm]	15	Excess material	No
Stand-off at layer 10 [mm]	17	Surface regularity [μm]	N/A
Temperature at layer 10 [deg.C]	476	Average hardness [HV]	N/A
Number of layers	10		

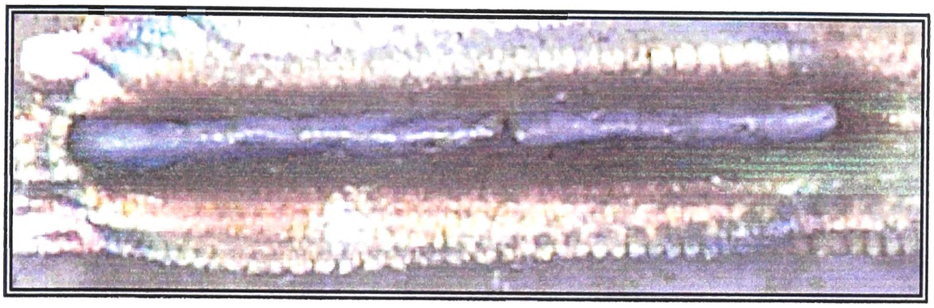

Figure F6-5

Sample f6-100-05 (top view)

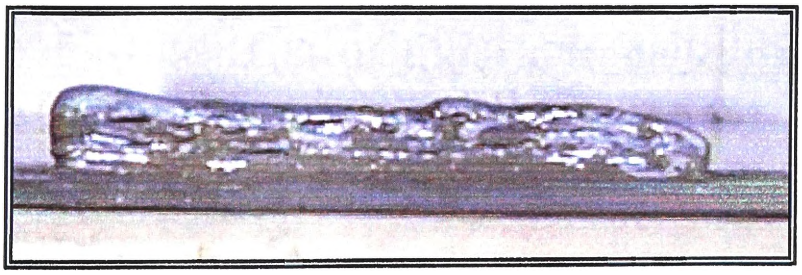

Figure F6-6

Sample f6-100-05 (front view)

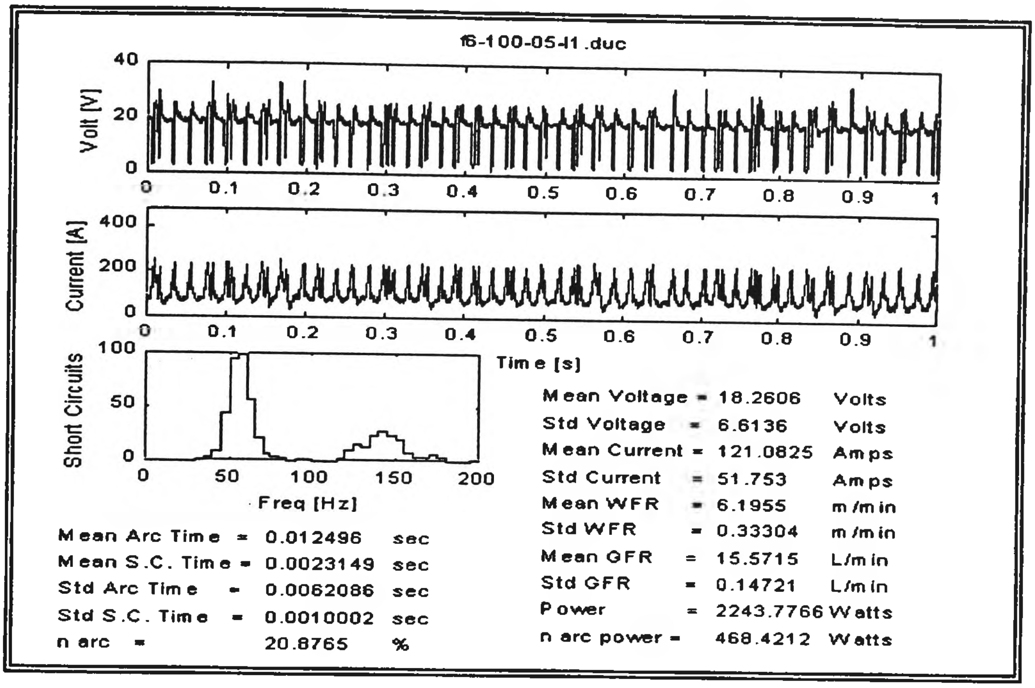

Plot F6-5

Sample f6-100-05-layer 1

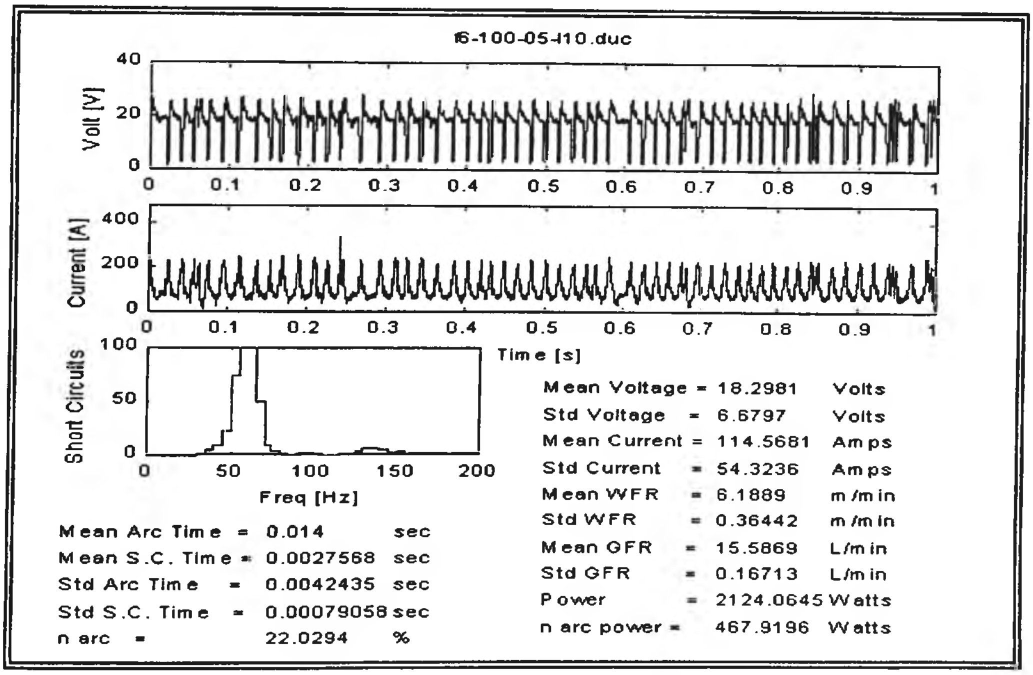

Plot F6-6

Sample f6-100-05-layer 10

Sample f6-110-05

Set Values	
Voltage [%]	110
Wire feed rate [m/min]	6
Travel speed [mm/sec]	5
Gas flow [l/min]	15

Weld Geometry		Visual Defects and Weld Property	
Weld height [mm]	17	Spatters	Yes
Weld width [mm]	8.9	Porosity	Yes
Stand-off at layer 1 [mm]	15	Excess material	No
Stand-off at layer 10 [mm]	16	Surface regularity [μm]	N/A
Temperature at layer 10 [deg.C]	530	Average hardness [HV]	N/A
Number of layers	10		

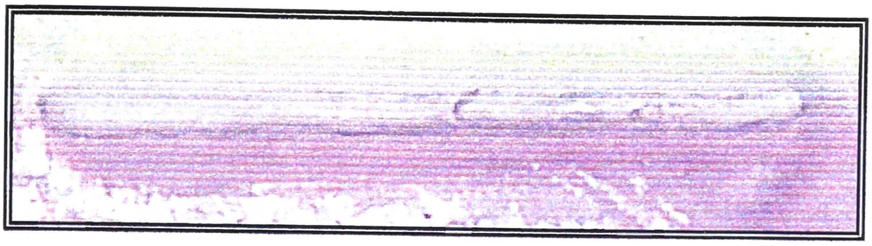

Figure F6-7

Sample f6-110-05 (top view)

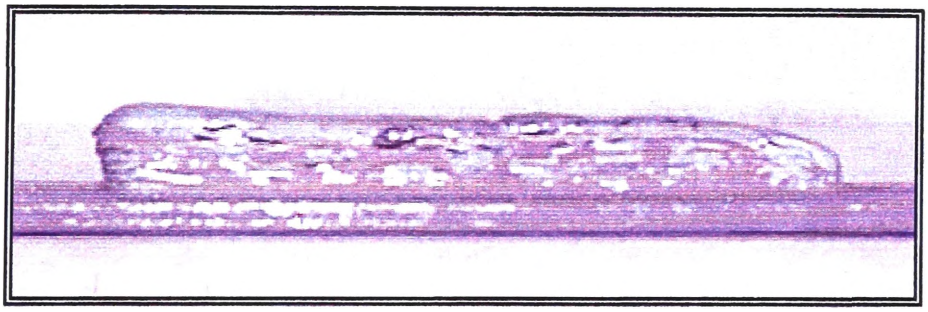

Figure F6-8

Sample f6-110-05 (front view)

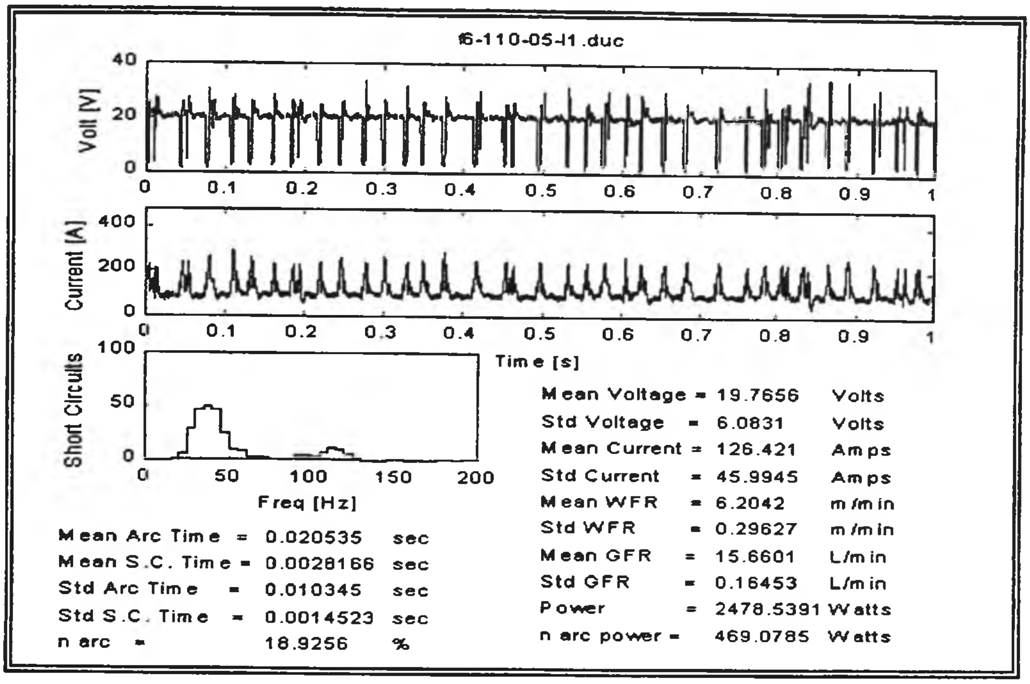

Plot F6-7

Sample f6-110-05-layer 1

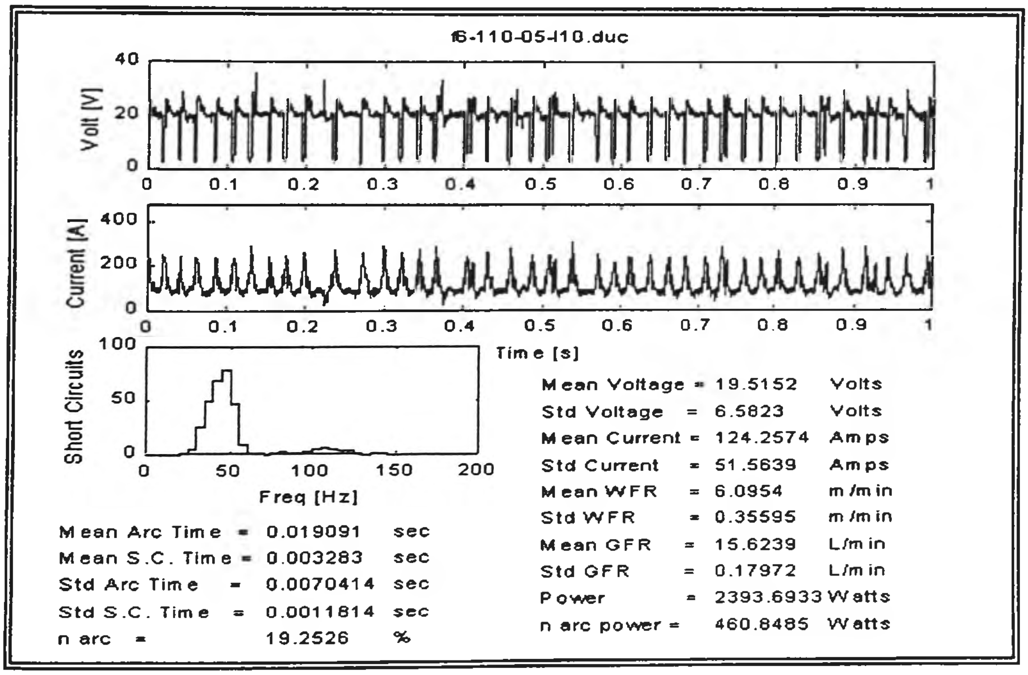

Plot F6-8

Sample f6-110-05-layer 10

Sample f6-120-05

Set Values	
Voltage [%]	120
Wire feed rate [m/min]	6
Travel speed [mm/sec]	5
Gas flow [l/min]	15

Weld Geometry		Visual Defects and Weld Property	
Weld height [mm]	13.4	Spatters	Yes
Weld width [mm]	10.9	Porosity	Yes
Stand-off at layer 1 [mm]	15	Excess material	Yes
Stand-off at layer 10 [mm]	15.5	Surface regularity [μm]	204.1
Temperature at layer 10 [deg.C]	578	Average hardness [HV]	150
Number of layers	10		

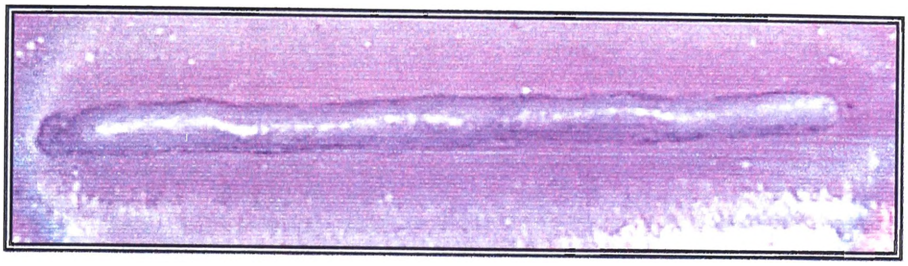

Figure F6-9

Sample F6-120-05 (top view)

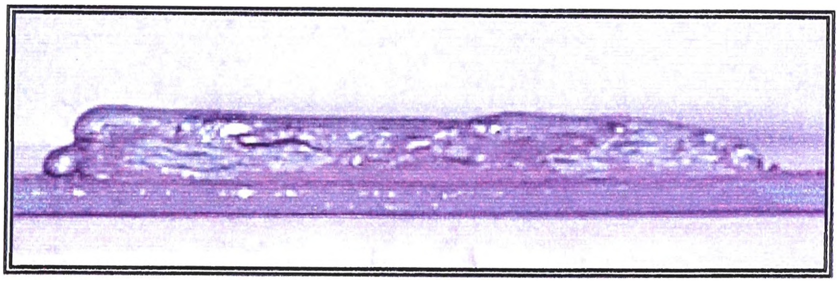

Figure F6-10

Sample F6-120-05 (front view)

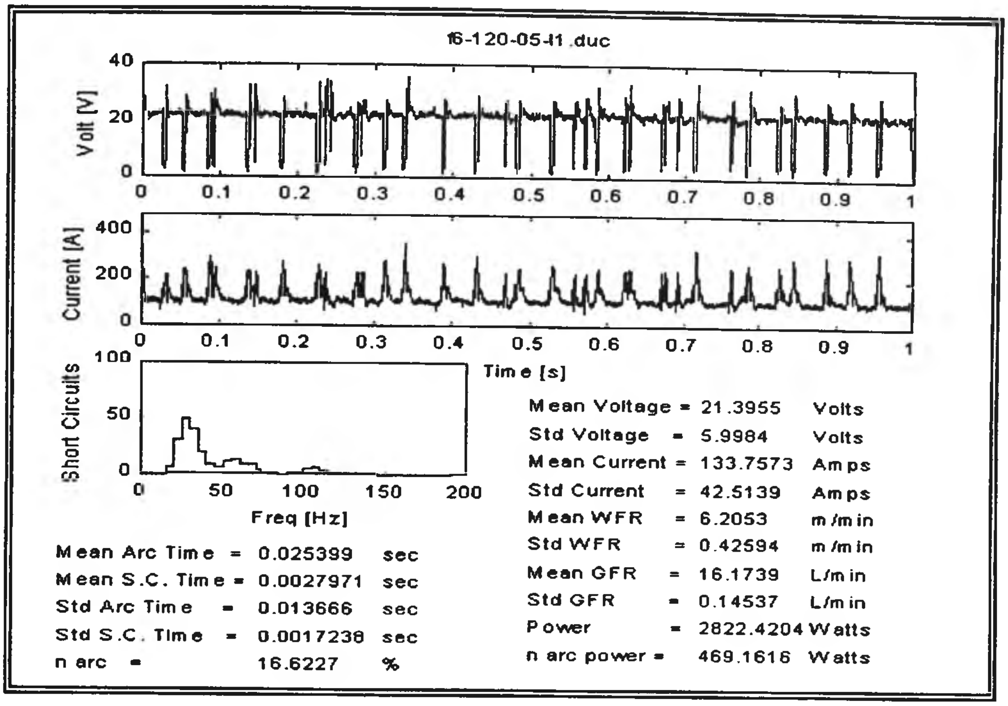

Plot F6-9

Sample f6-120-05-layer 1

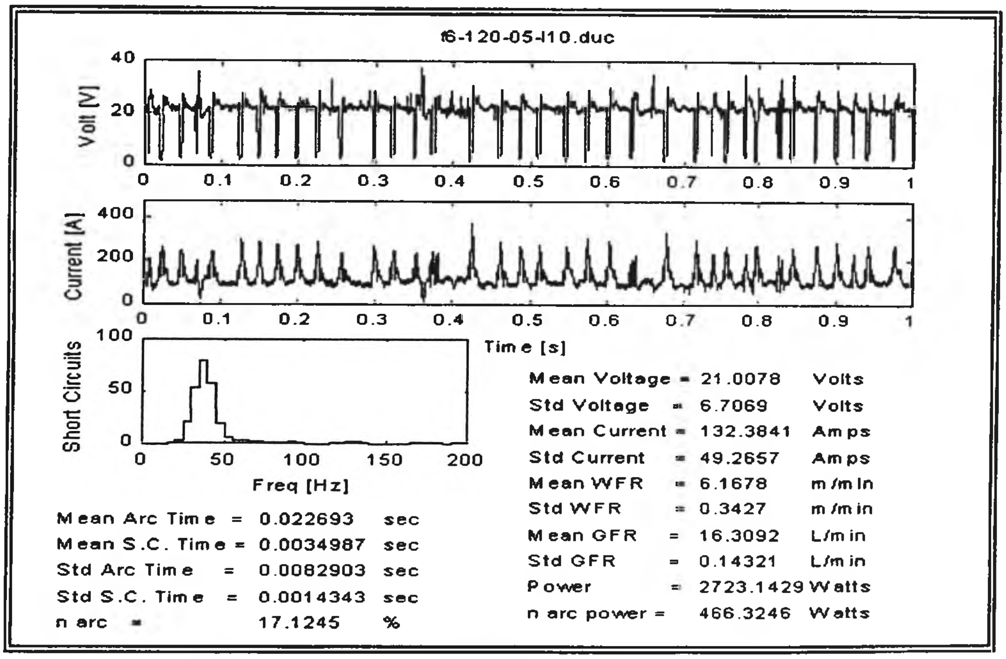

Plot F6-10

Sample f6-120-05-layer 10

Sample f6-130-05

Set Values	
Voltage [%]	130
Wire feed rate [m/min]	6
Travel speed [mm/sec]	5
Gas flow [l/min]	15

Weld Geometry		Visual Defects and Weld Property	
Weld height [mm]	9.5	Spatters	Yes
Weld width [mm]	12	Porosity	Yes
Stand-off at layer 1 [mm]	15	Excess material	Yes
Stand-off at layer 10 [mm]	15	Surface regularity [µm]	
Temperature at layer 10 [deg.C]	643	Average hardness [HV]	N/A
Number of layers	10		

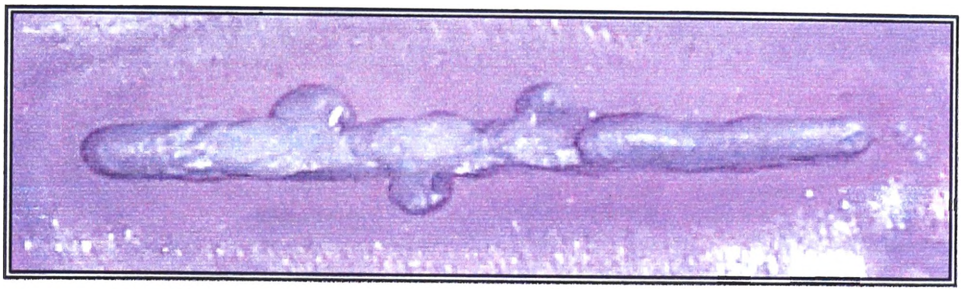

Figure F6-11

Plot f6-130-05 (top view)

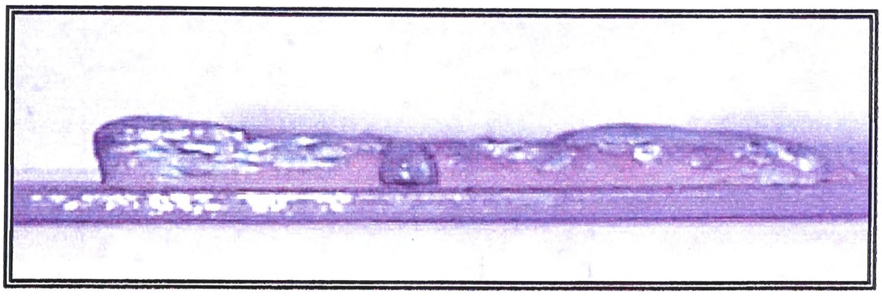

Figure F6-12

Plot f6-130-05 (front view)

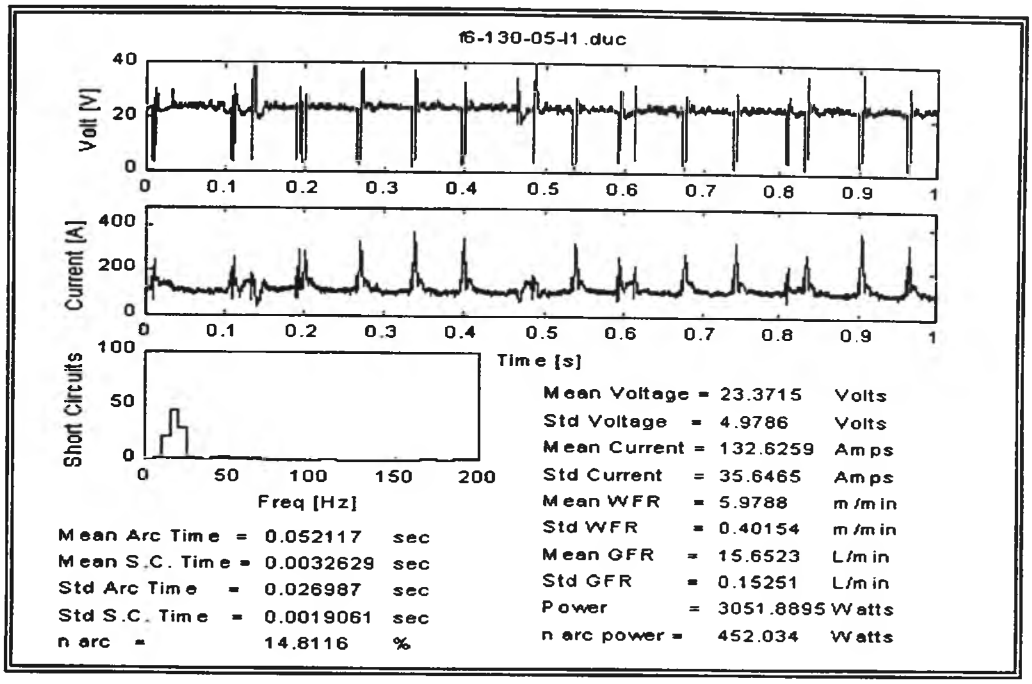

Plot F6-11

Sample f6-130-05-layer 1

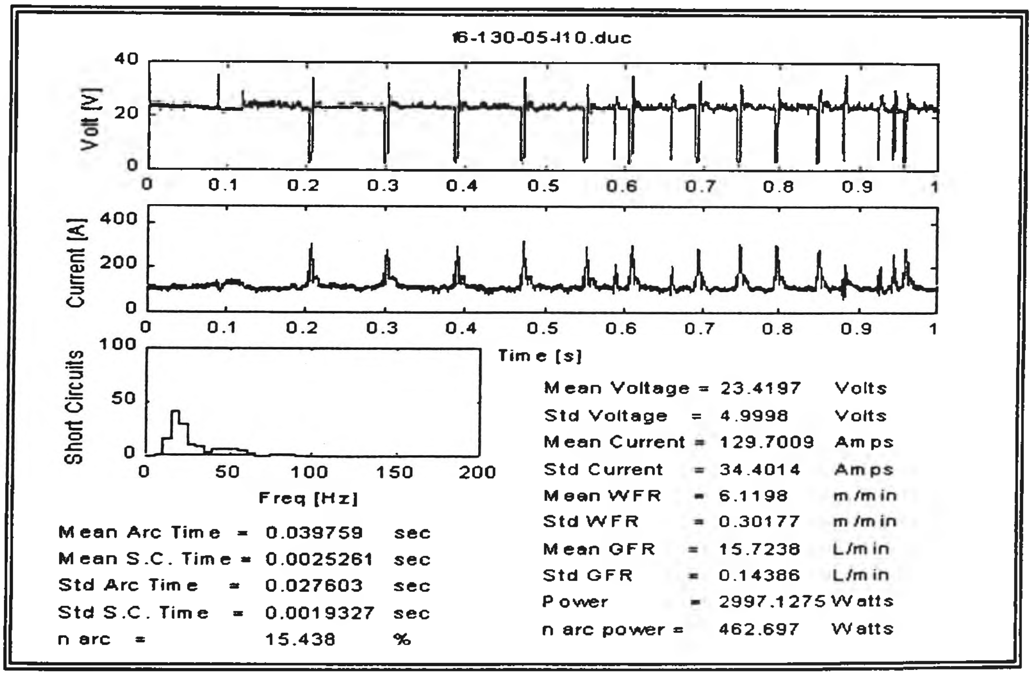

Plot f6-12

Sample f6-130-05-layer 10

F7 Wire Feed Rate of 7 m/min

Sample f7-75-05

Set Values	
Voltage [%]	75
Wire feed rate [m/min]	7
Travel speed [mm/sec]	5
Gas flow [l/min]	15

Weld Geometry		Visual Defects and Weld Property	
Weld height [mm]	22.6	Spatters	Yes
Weld width [mm]	8.4	Porosity	No
Stand-off at layer 1 [mm]	15	Excess material	No
Stand-off at layer 10 [mm]	13	Surface regularity [μm]	168.55
Temperature at layer 10 [deg.C]	550	Average hardness [HV]	154
Number of layers	10		

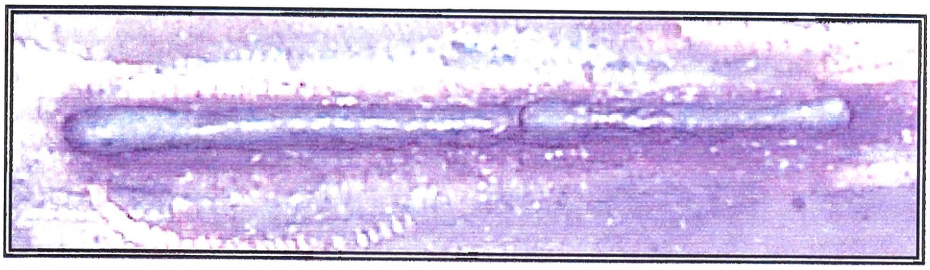

Figure F7-1

Sample f7-75-05 (top view)

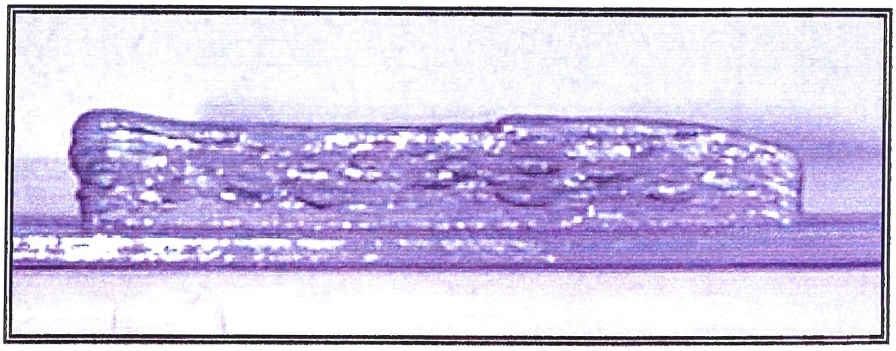

Figure F7-2

Sample f7-75-05 (front view)

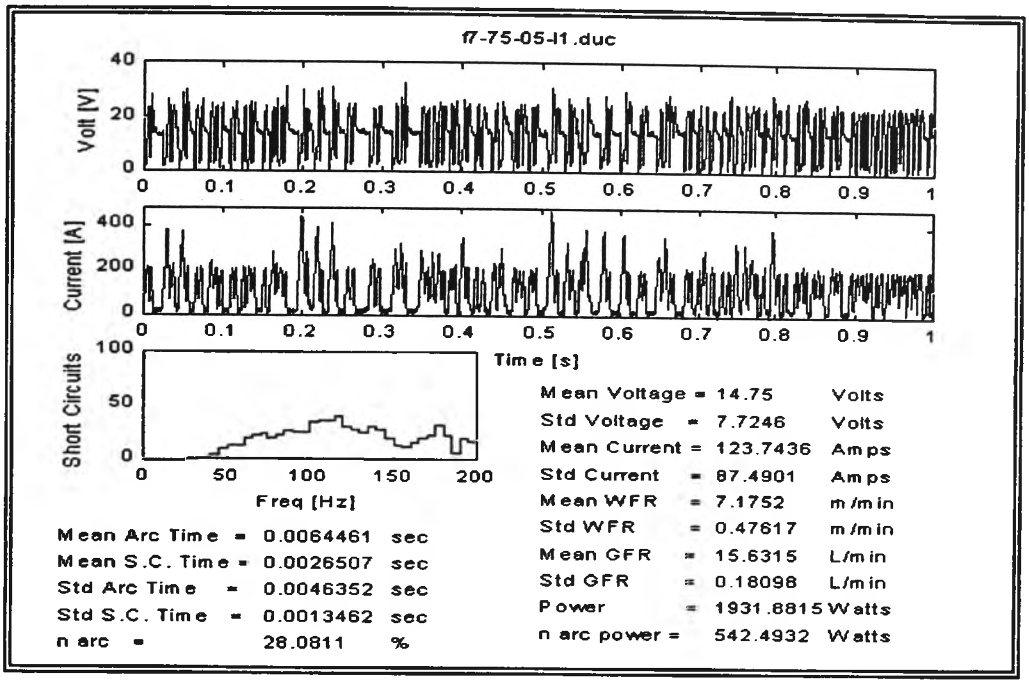

Plot F7-1

Sample f7-75-05-layer 1

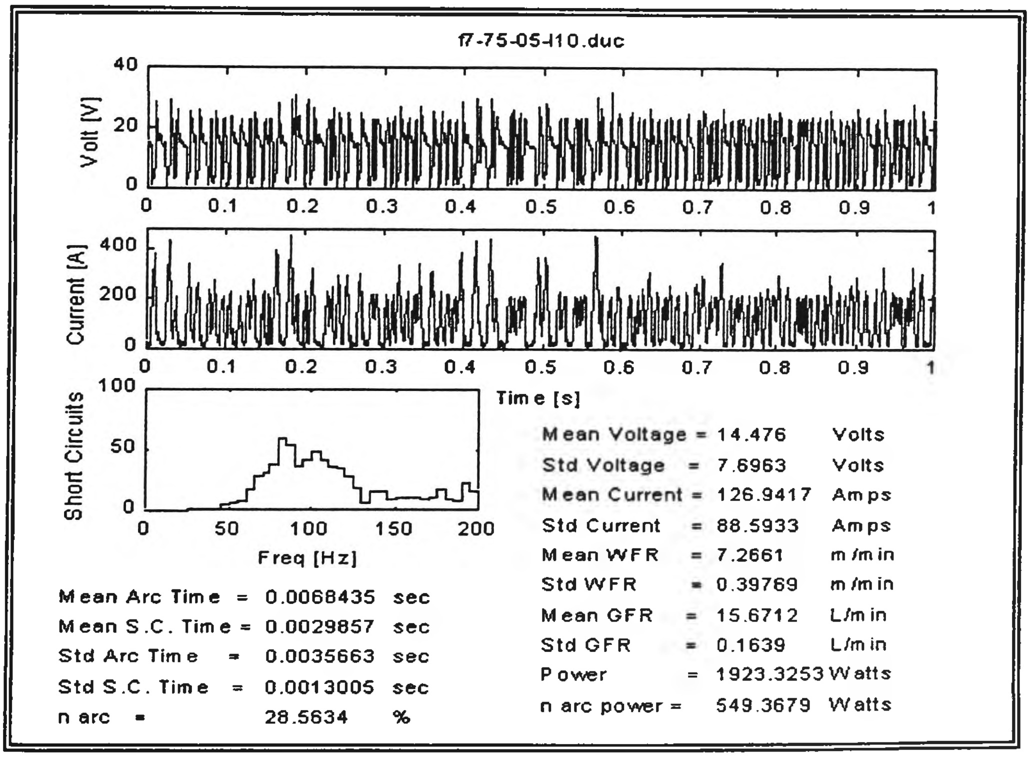

Plot F7-2

Sample f7-75-05-layer 10

Sample f7-90-05

Set Values	
Voltage [%]	90
Wire feed rate [m/min]	7
Travel speed [mm/sec]	5
Gas flow [l/min]	15

Weld Geometry		**Visual Defects and Weld Property**	
Weld height [mm]	18.5	Spatters	Yes
Weld width [mm]	9.4	Porosity	No
Stand-off at layer 1 [mm]	15	Excess material	No
Stand-off at layer 10 [mm]	17	Surface regularity [μm]	N/A
Temperature at layer 10 [deg.C]	595	Average hardness [HV]	N/A
Number of layers	10		

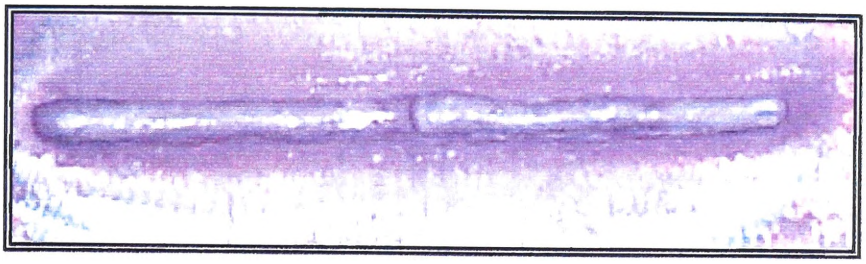

Figure F7-3

Sample f7-90-05 (top view)

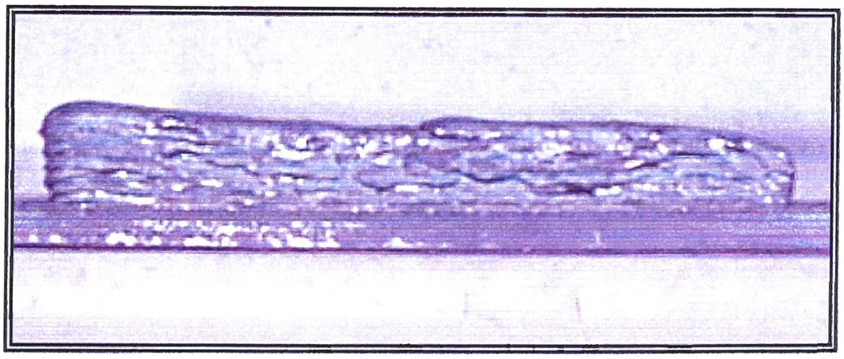

Figure F7-4

Sample f7-90-05 (front view)

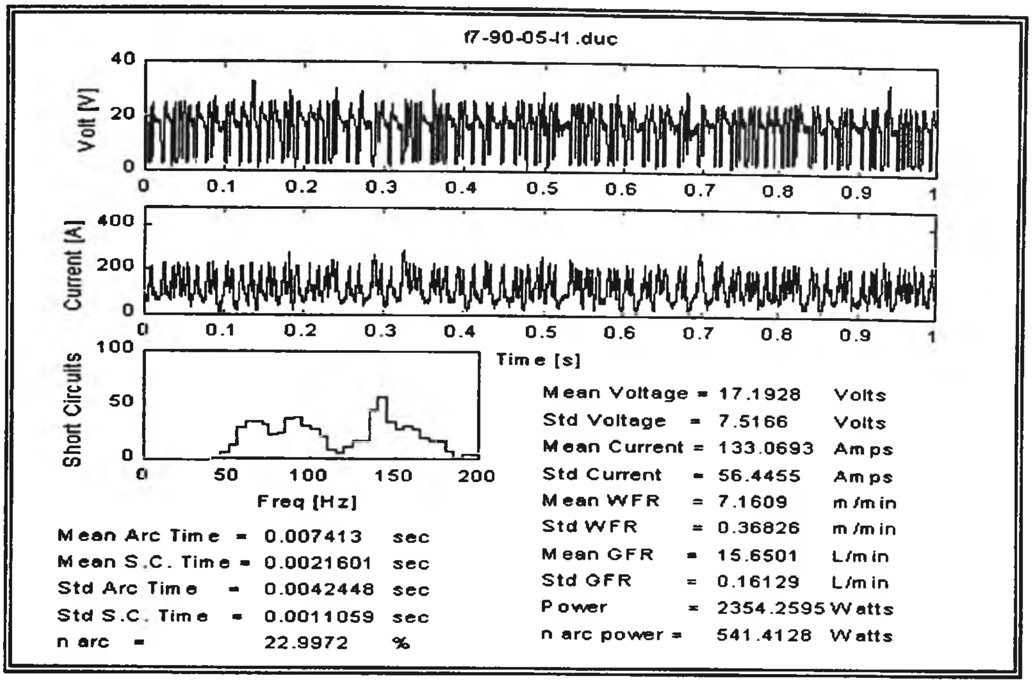

Plot F7-3

Sample f7-90-05-layer 1

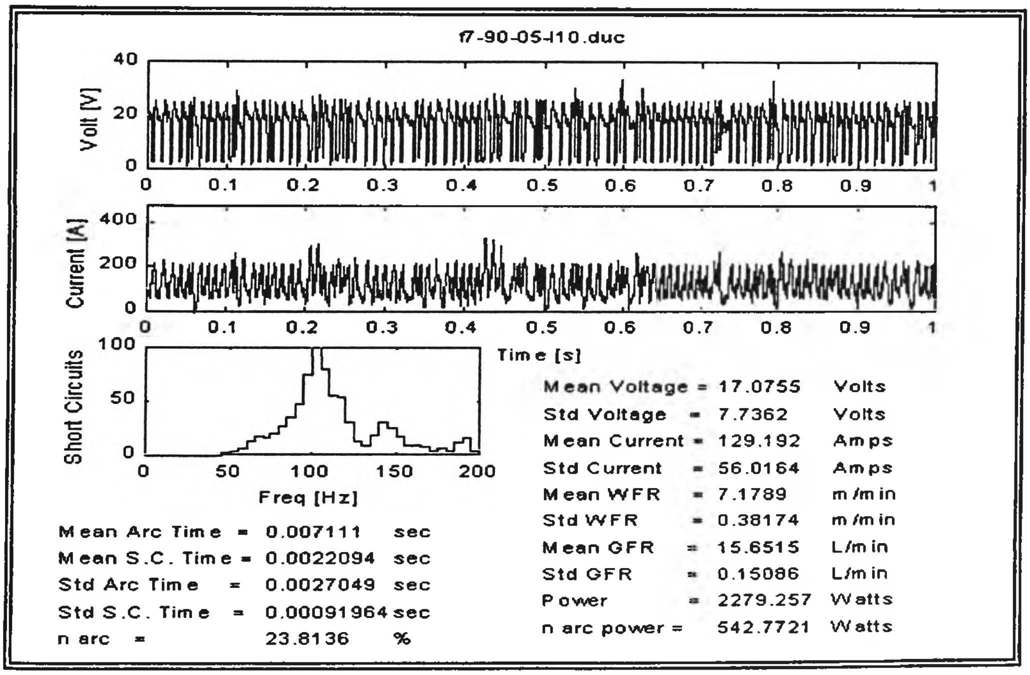

Plot F7-4

Sample f7-90-05-layer 10

Sample f7-100-05

Set Values	
Voltage [%]	100
Wire feed rate [m/min]	7
Travel speed [mm/sec]	5
Gas flow [l/min]	15

Weld Geometry		Visual Defects and Weld Property	
Weld height [mm]	18	Spatters	Yes
Weld width [mm]	10	Porosity	Yes
Stand-off at layer 1 [mm]	15	Excess material	No
Stand-off at layer 10 [mm]	17	Surface regularity [μm]	N/A
Temperature at layer 10 [deg.C]	600	Average hardness [HV]	N/A
Number of layers	10		

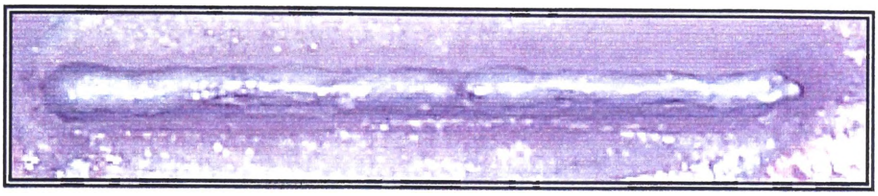

Figure F7-5

Sample f7-100-05 (top view)

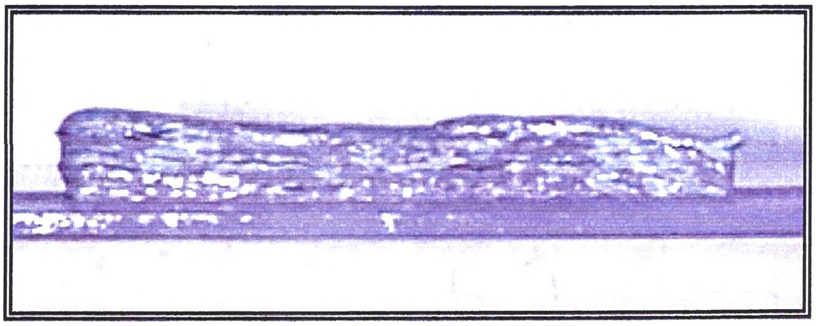

Figure F7-6

Sample f7-100-05 (front view)

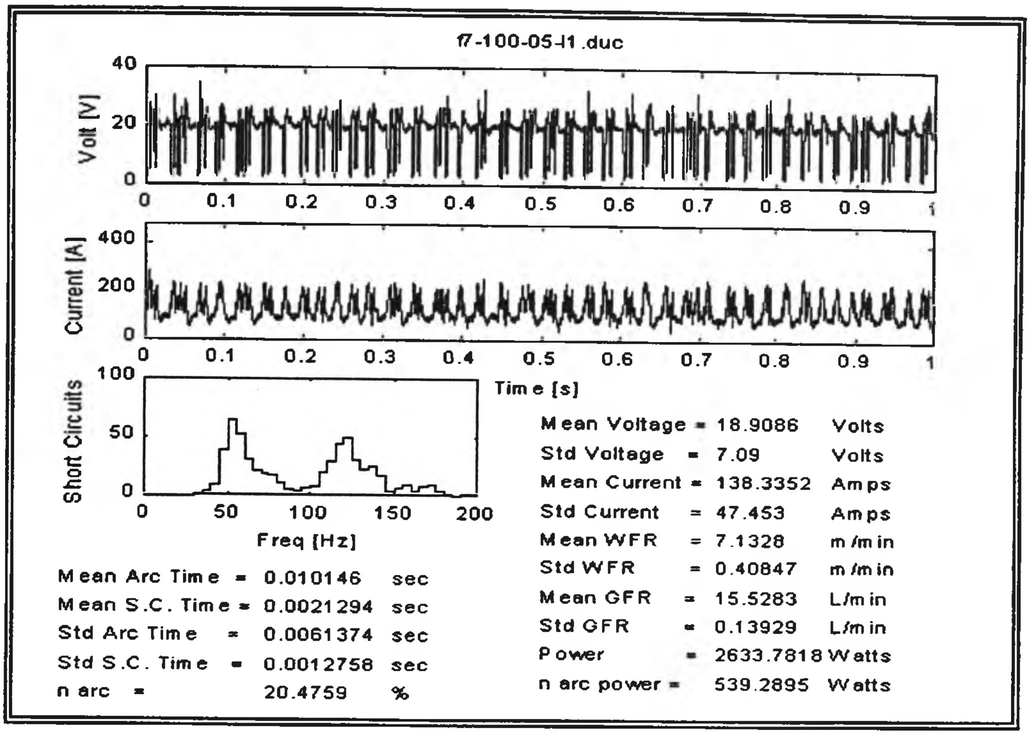

Plot F7-5

Sample f7-100-05-layer 1

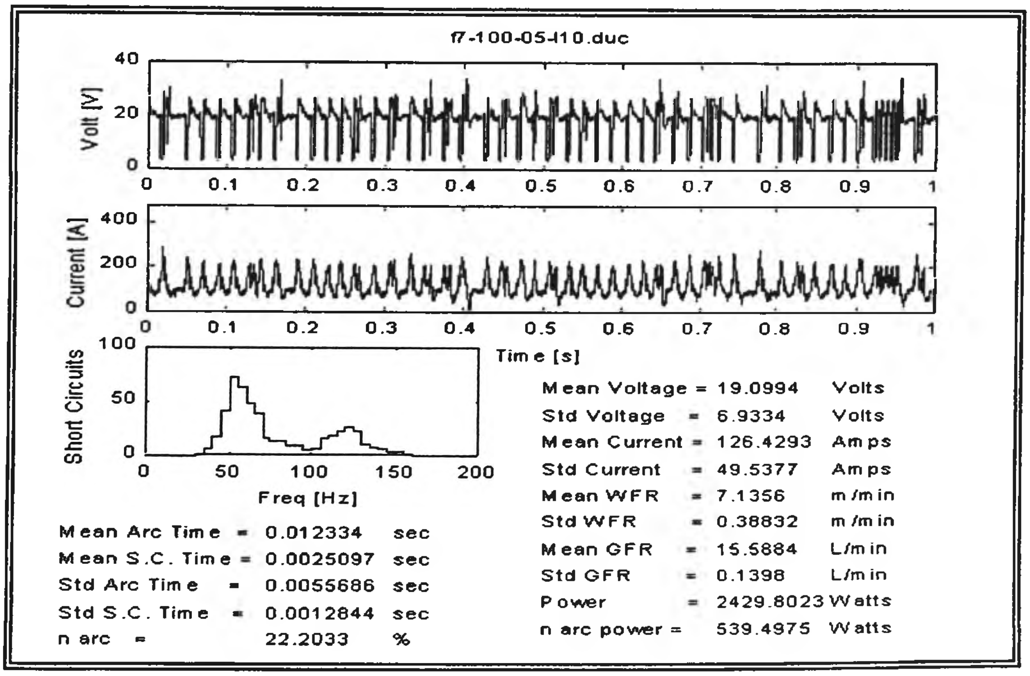

Plot F7-6

Sample f7-100-05-layer 10

Sample f7-110-05

Set Values	
Voltage [%]	110
Wire feed rate [m/min]	7
Travel speed [mm/sec]	5
Gas flow [l/min]	15

Weld Geometry		Visual Defects and Weld Property	
Weld height [mm]	16.5	Spatters	Yes
Weld width [mm]	10.7	Porosity	Yes
Stand-off at layer 1 [mm]	15	Excess material	Yes
Stand-off at layer 10 [mm]	15	Surface regularity [μm]	N/A
Temperature at layer 10 [deg.C]	640	Average hardness [HV]	N/A
Number of layers	10		

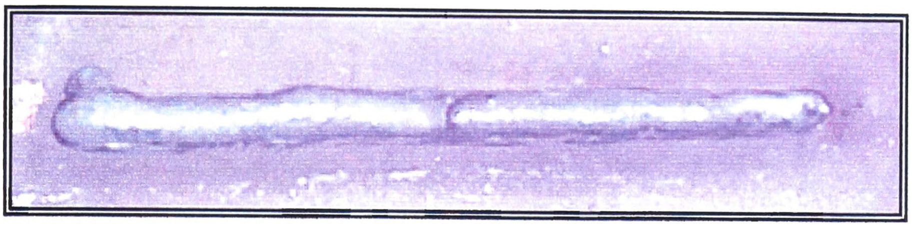

Figure F7-7

F7-110-05 (top view)

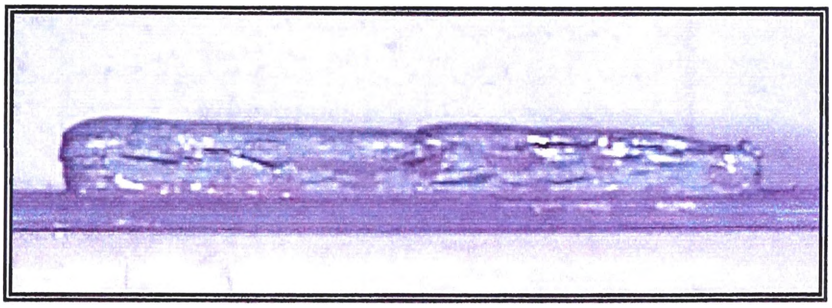

Figure F7-8

F7-110-05 (front view)

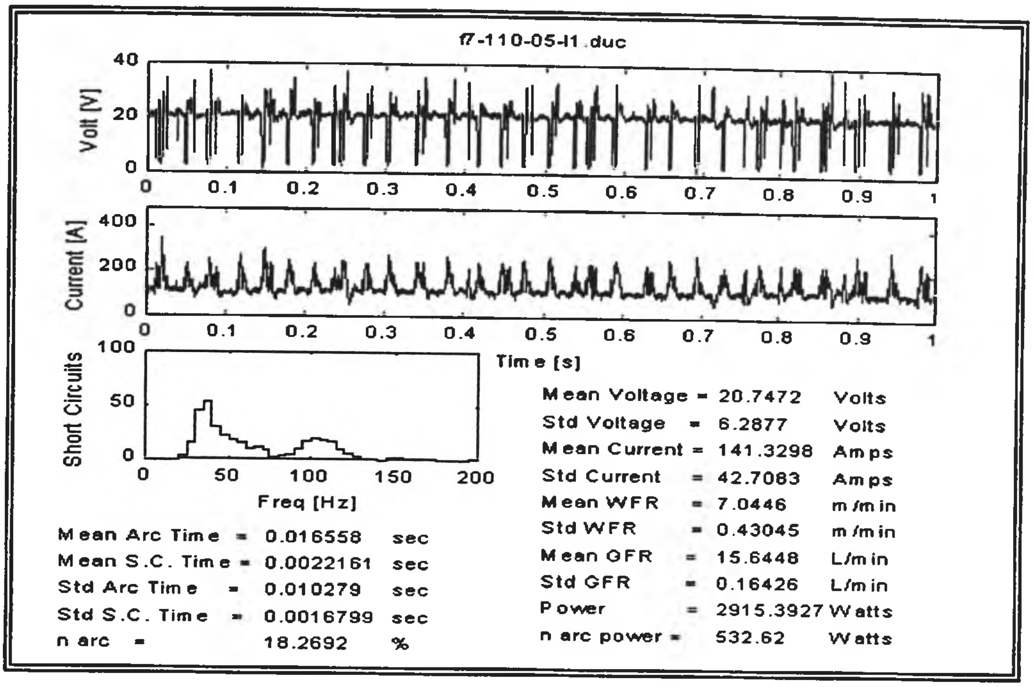

Plot F7-7

Sample f7-110-05-layer 1

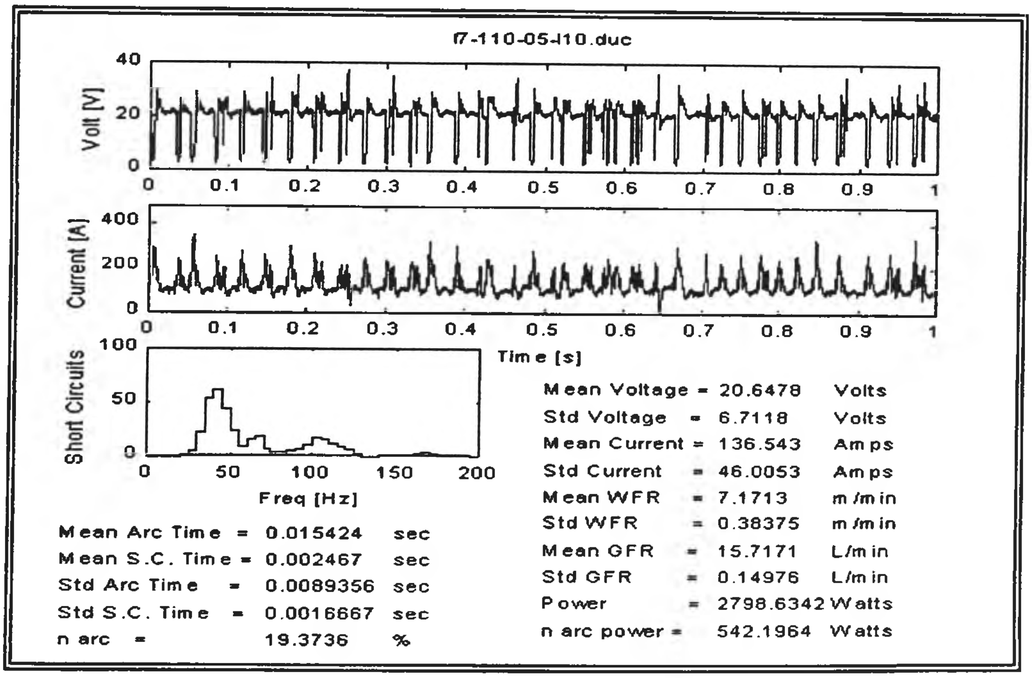

Plot F7-8

Sample f7-110-05-layer 10

Sample f7-120-05

Set Values	
Voltage [%]	120
Wire feed rate [m/min]	7
Travel speed [mm/sec]	5
Gas flow [l/min]	15

Weld Geometry		Visual Defects and Weld Property	
Weld height [mm]	14.4	Spatters	Yes
Weld width [mm]	12	Porosity	Yes
Stand-off at layer 1 [mm]	15	Excess material	Yes
Stand-off at layer 10 [mm]	16	Surface regularity [µm]	204.1
Temperature at layer 10 [deg.C]	660	Average hardness [HV]	150
Number of layers	10		

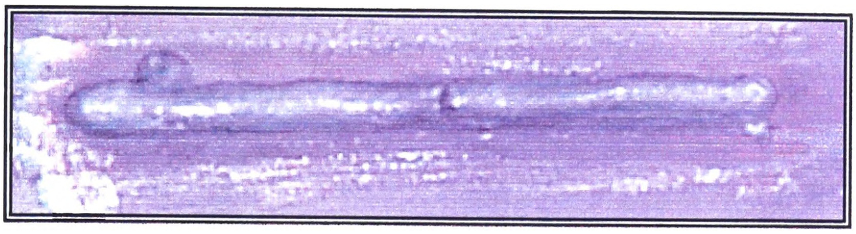

Figure F7-9

Sample f7-120-05 (top view)

Figure F7-10

Sample f7-120-05 (front view)

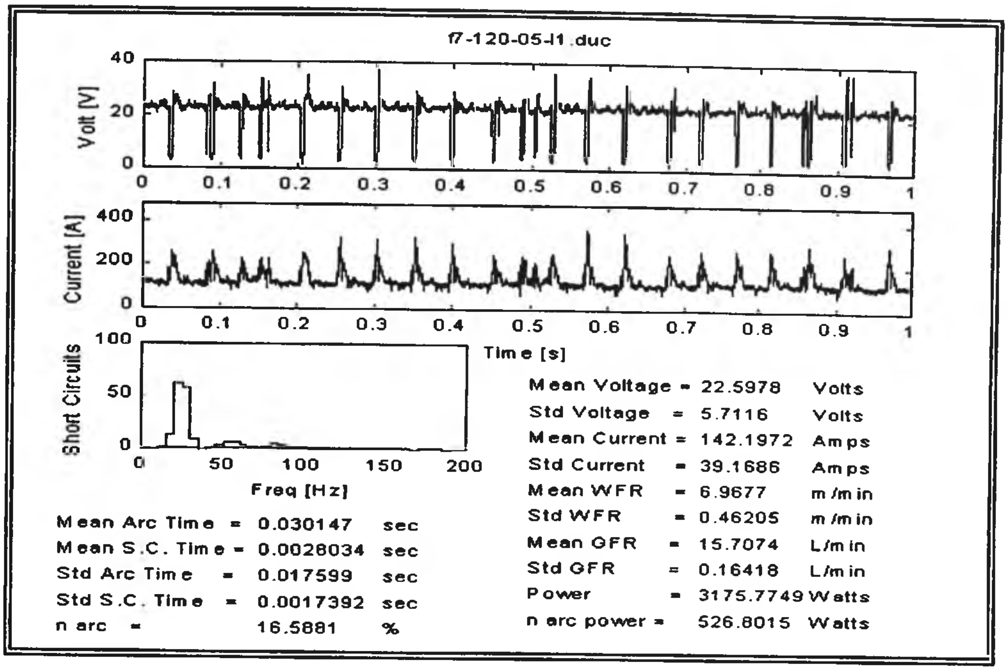

Plot F7-9

Sample f7-120-05-layer 1

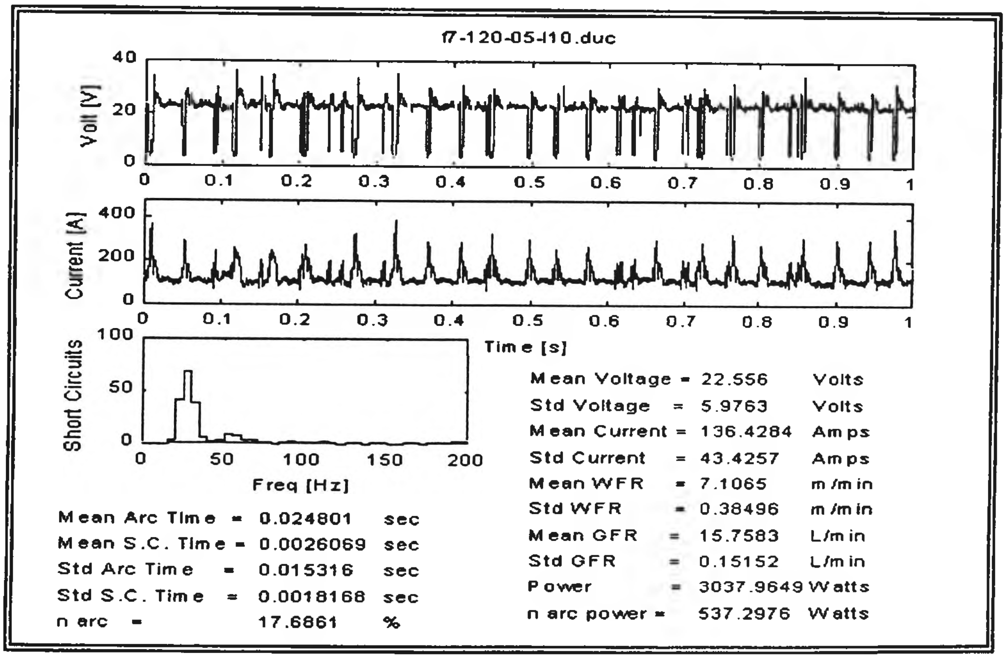

Plot F7-10

Sample f7-120-05-layer 10

Sample f7-130-05

Set Values	
Voltage [%]	130
Wire feed rate [m/min]	7
Travel speed [mm/sec]	5
Gas flow [l/min]	15

Weld Geometry		Visual Defects and Weld Property	
Weld height [mm]	11.5	Spatters	Yes
Weld width [mm]	13.7	Porosity	Yes
Stand-off at layer 1 [mm]	15	Excess material	Yes
Stand-off at layer 10 [mm]	16	Surface regularity [μm]	N/A
Temperature at layer 10 [deg.C]	688	Average hardness [HV]	N/A
Number of layers	10		

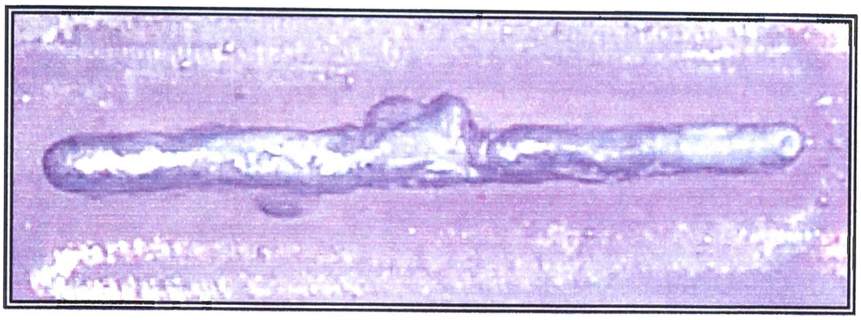

Figure F7-11

Sample f7-130-05 (top view)

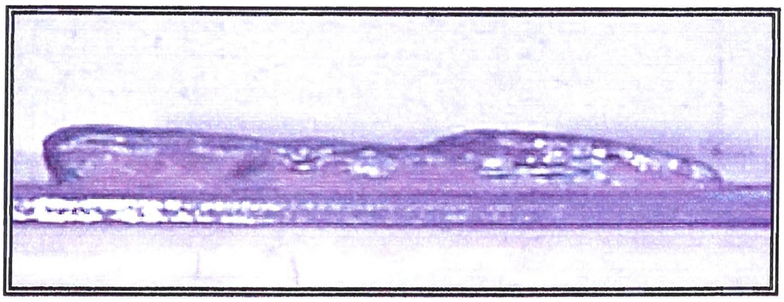

Figure F7 12

Sample f7-130-05 (front view)

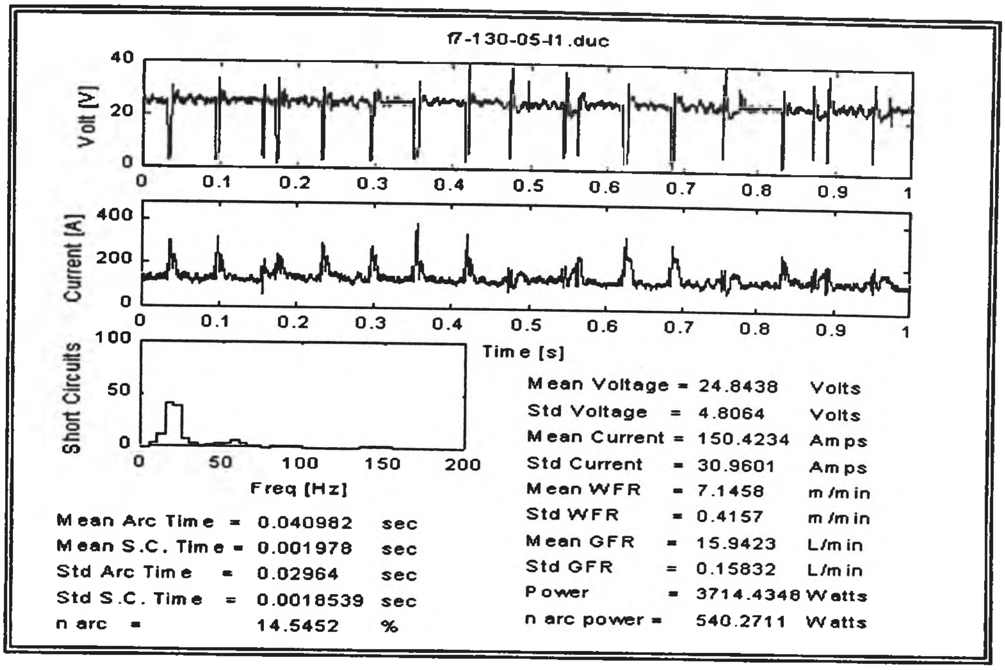

Plot F7-11

Sample f7-130-05-layer 1

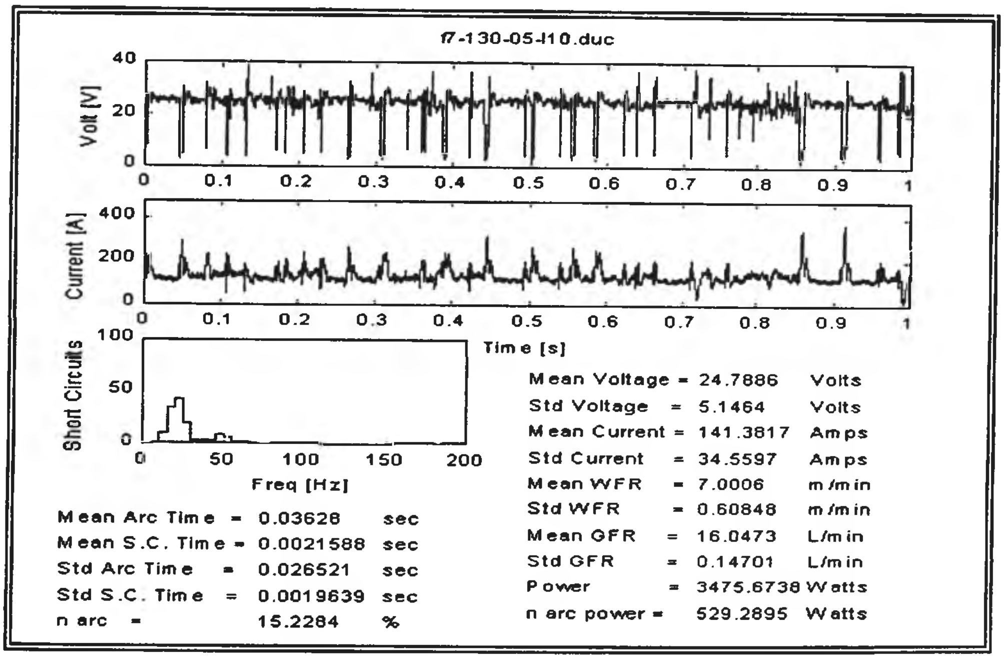

Plot F7-12

Sample f7-130-05-layer 10

F8 Wire Feed Rate of 8 m/min

Sample f8-100-05

Set Values	
Voltage [%]	100
Wire feed rate [m/min]	8
Travel speed [mm/sec]	5
Gas flow [l/min]	15

Weld Geometry		Visual Defects and Weld Property	
Weld height [mm]	16.6	Spatters	Yes
Weld width [mm]	10.6	Porosity	Yes
Stand-off at layer 1 [mm]	15	Excess material	Yes
Stand-off at layer 10 [mm]	17	Surface regularity [μm]	122.8
Temperature at layer 10 [deg.C]	675	Average hardness [HV]	152
Number of layers	10		

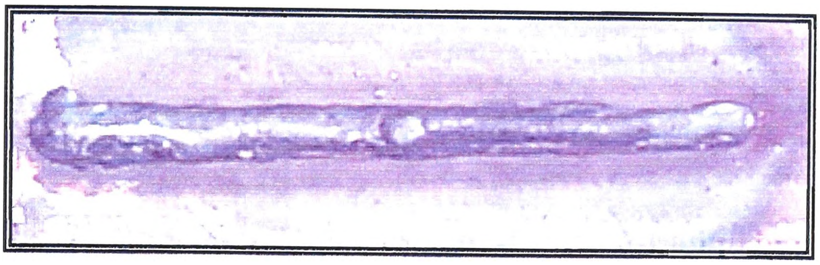

Figure F8-1

Sample f8-100-05 (top view)

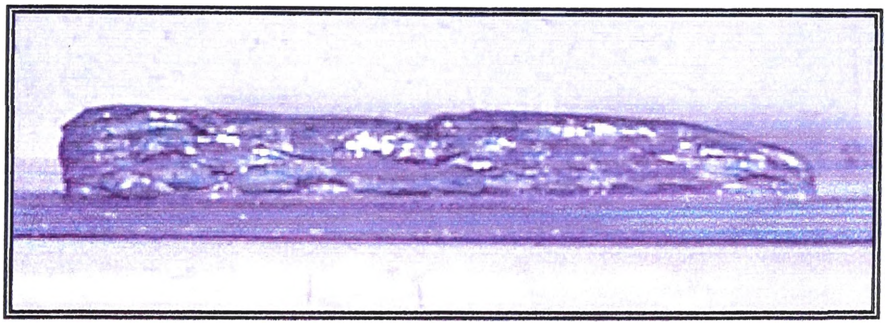

Figure F8-2

Sample f8-100-05 (front view)

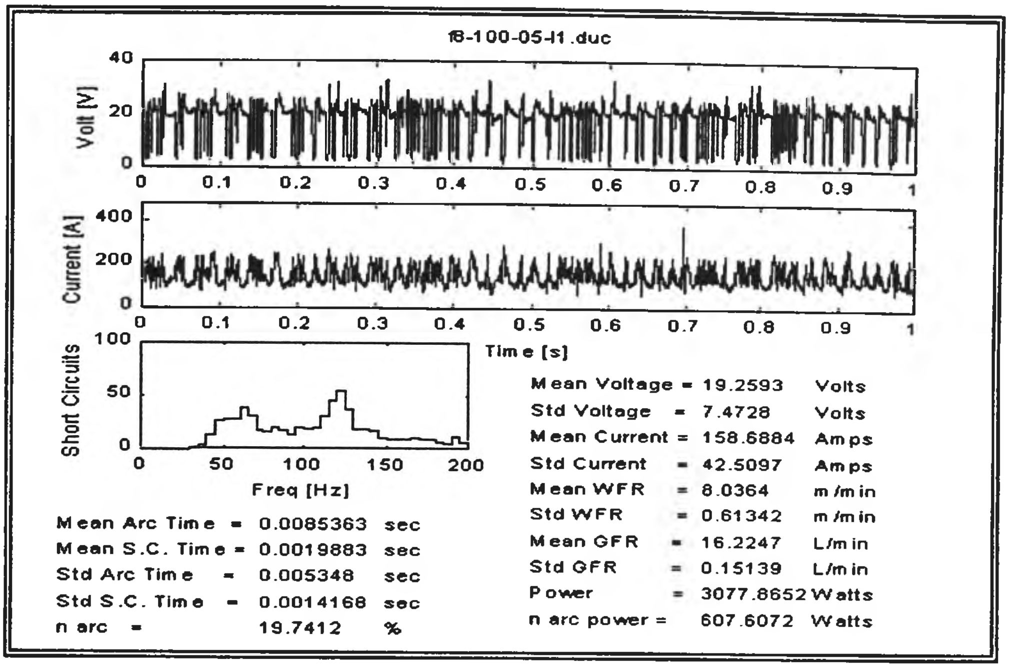

Plot F8-1

Sample f8-100-05-layer 1

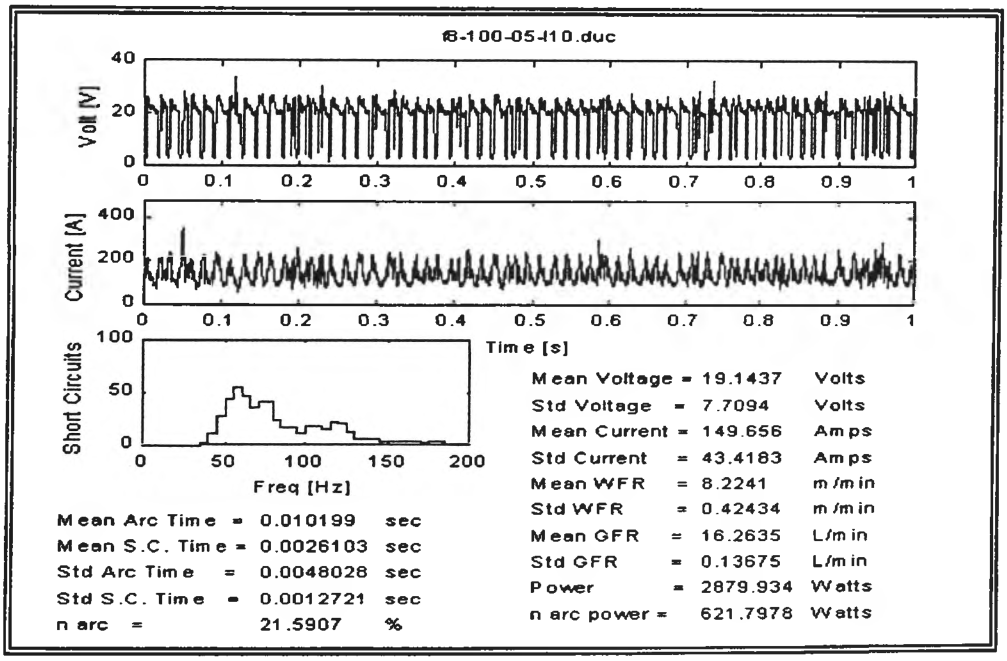

Plot F8-2

Sample f8-100-05-layer 10

Sample f8-125-05

Set Values	
Voltage [%]	125
Wire feed rate [m/min]	8
Travel speed [mm/sec]	5
Gas flow [l/min]	15

Weld Geometry		Visual Defects and Weld Property	
Weld height [mm]	12	Spatters	Yes
Weld width [mm]	14.7	Porosity	Yes
Stand-off at layer 1 [mm]	15	Excess material	Yes
Stand-off at layer 10 [mm]	18	Surface regularity [μm]	N/A
Temperature at layer 10 [deg.C]	725	Average hardness [HV]	N/A
Number of layers	10		

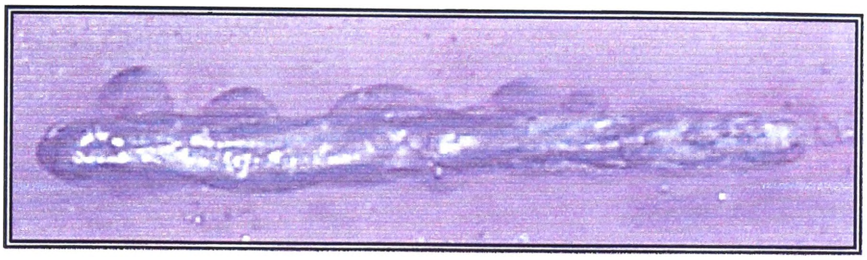

Figure F8-3

Sample f8-125-05 (top view)

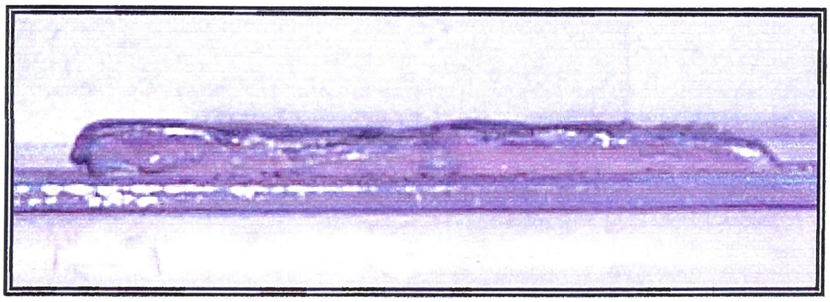

Figure F8-4

Sample f8-125-05 (front view)

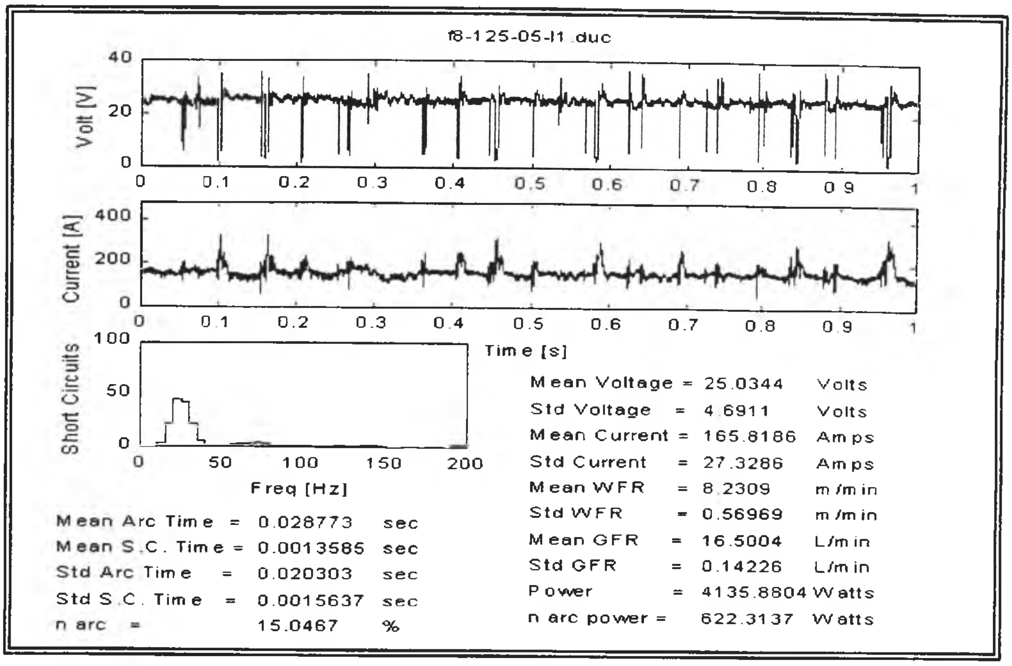

Plot F8-3

Sample f8-125-05-layer 1

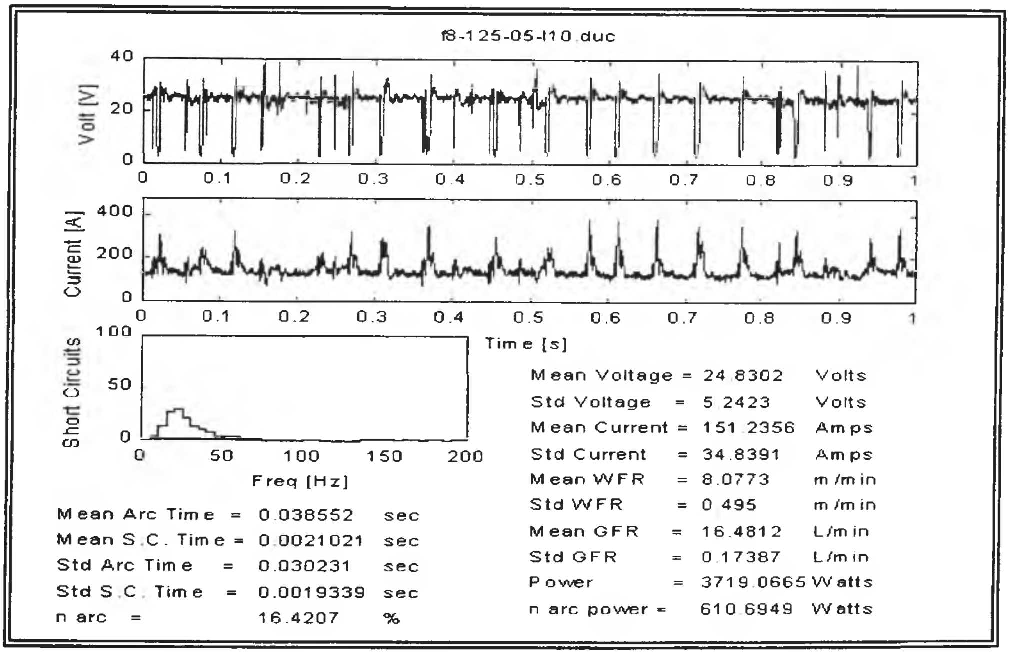

Plot F8-4

Sample f8-125-05-layer 10

F9 Wire Feed Rate of 9 m/min

Sample f9-100-05

Set Values	
Voltage [%]	100
Wire feed rate [m/min]	9
Travel speed [mm/sec]	5
Gas flow [l/min]	15

Weld Geometry		Visual Defects and Weld Property	
Weld height [mm]	16.5	Spatters	Yes
Weld width [mm]	13.5	Porosity	Yes
Stand-off at layer 1 [mm]	15	Excess material	Yes
Stand-off at layer 10 [mm]	15	Surface regularity [μm]	120.3
Temperature at layer 10 [deg.C]	700	Average hardness [HV]	149
Number of layers	10		

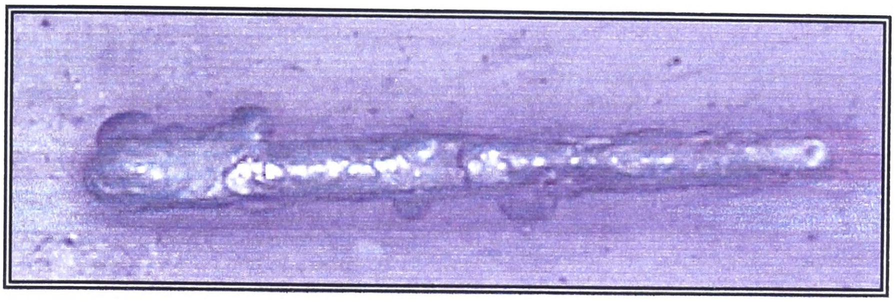

Figure F9-1

Sample f9-100-05 (top view)

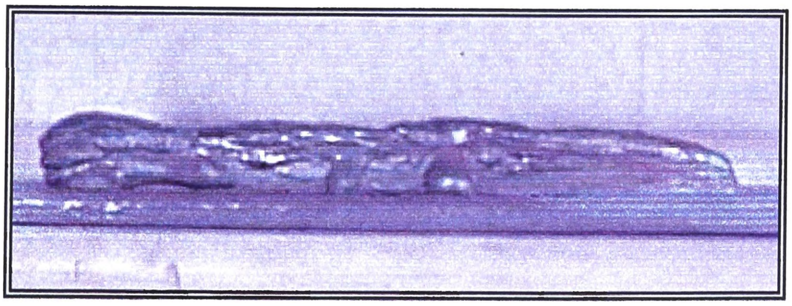

Figure F9-2

Sample f9-100-05 (front view)

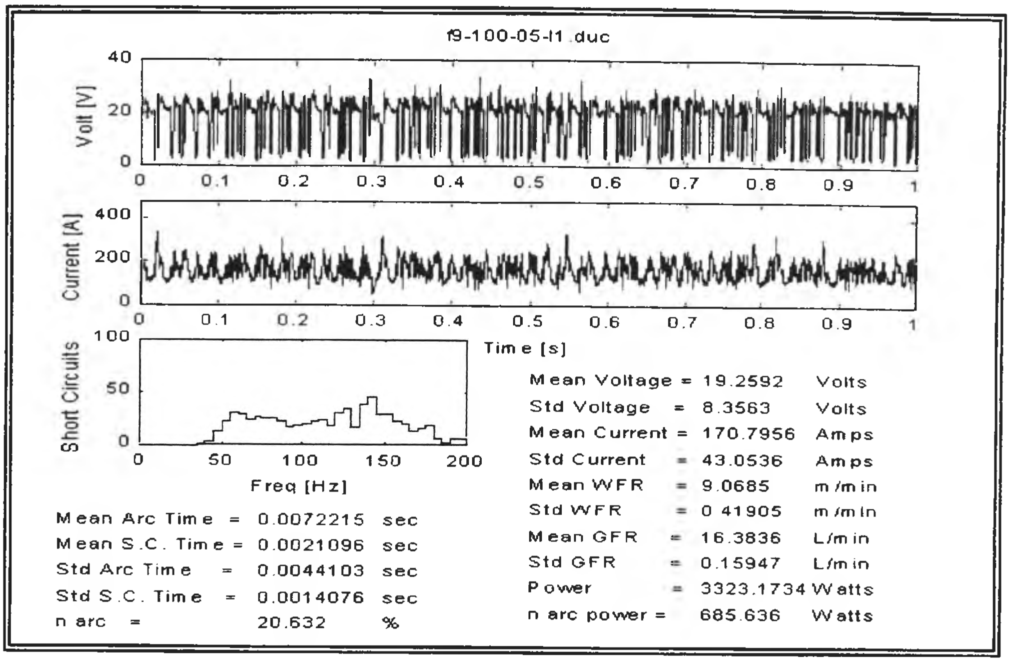

Plot F9-1

Sample f9-100-05-layer 1

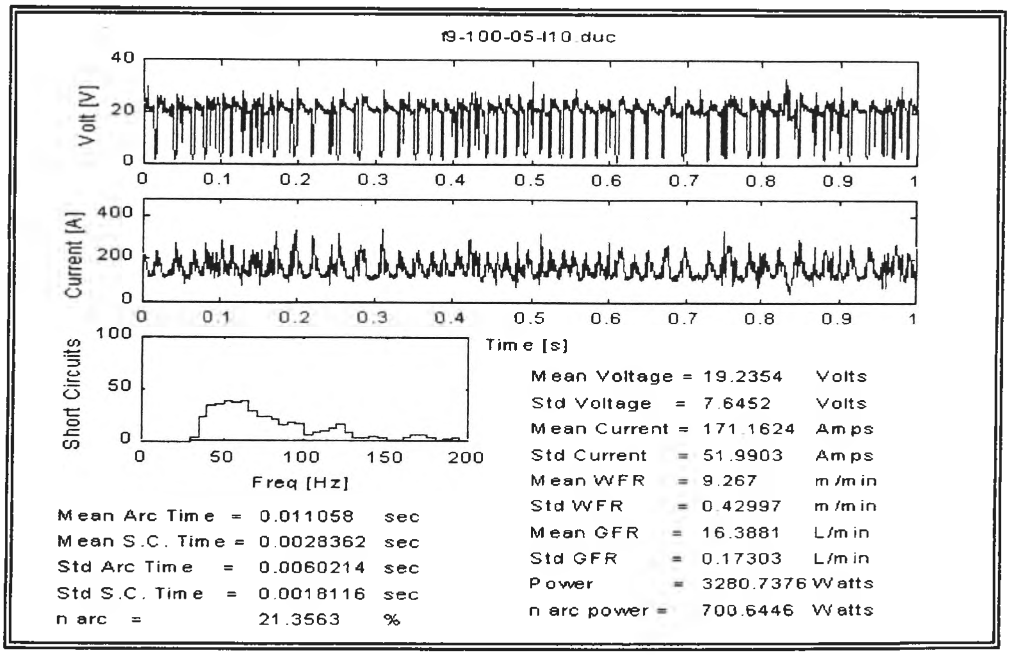

Plot F9-2

Sample f9-100-05-layer 10

Sample f9-125-05

Set Values	
Voltage [%]	125
Wire feed rate [m/min]	9
Travel speed [mm/sec]	5
Gas flow [l/min]	15

Weld Geometry		Visual Defects and Weld Property	
Weld height [mm]	12	Spatters	Yes
Weld width [mm]	14.5	Porosity	Yes
Stand-off at layer 1 [mm]	15	Excess material	Yes
Stand-off at layer 10 [mm]	15	Surface regularity [μm]	N/A
Temperature at layer 10 [deg.C]	782	Average hardness [HV]	N/A
Number of layers	10		

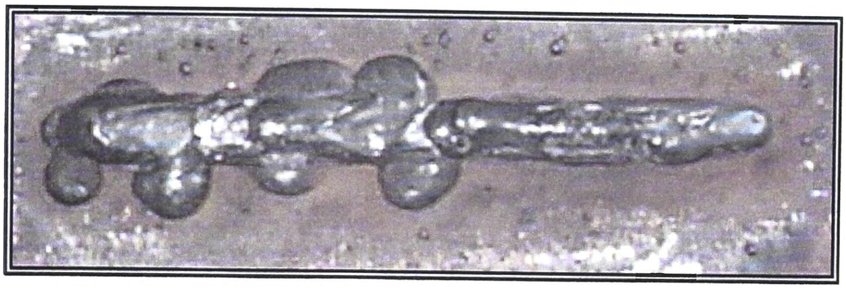

Figure F9-3

Sample f9-125-05 (top view)

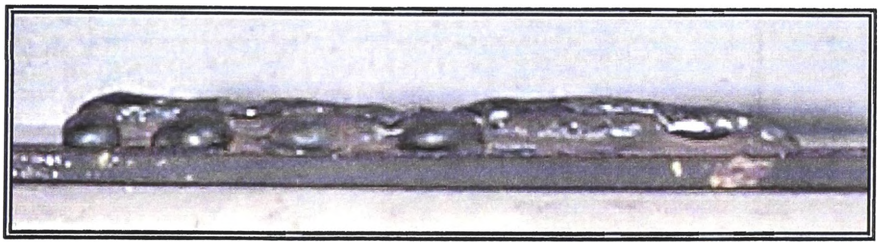

Figure F9-4

Sample f9-125-05

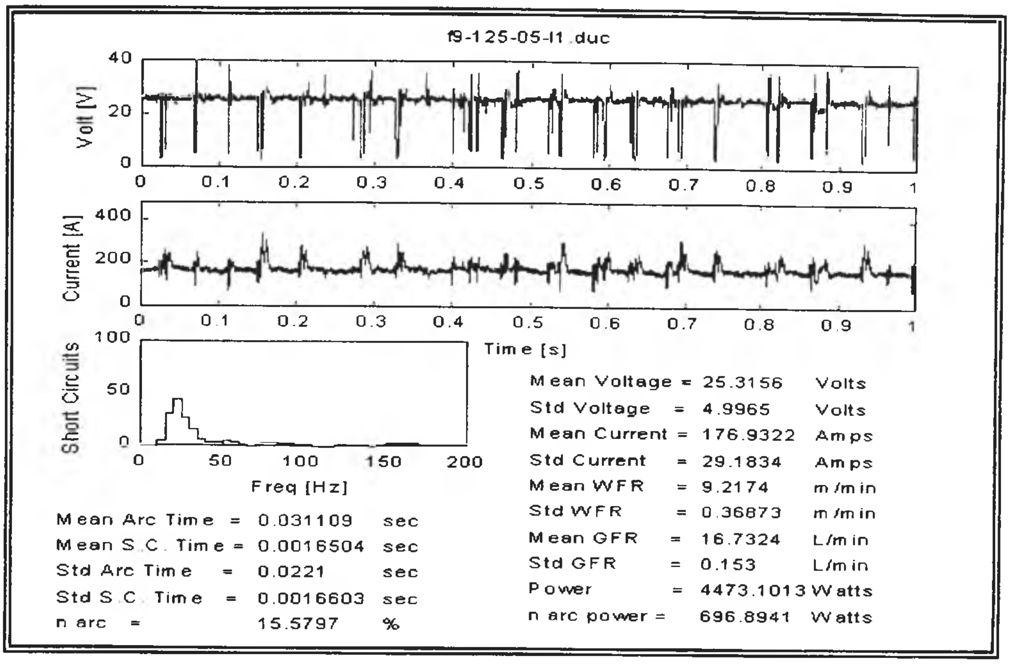

Plot F9-3

Sample f9-125-05-layer 1

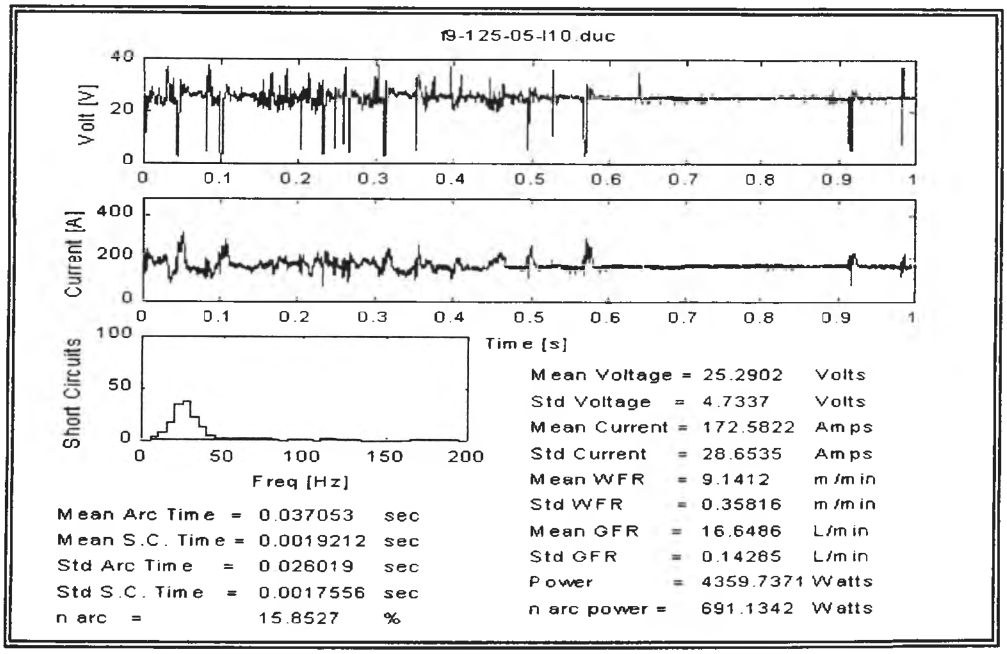

Plot F9-4

Sample f9-125-05-layer 10

Travel Speed = 10 mm/sec

F10 Wire Feed Rate of 1 m/min

Sample f1-100-10

Set Values	
Voltage [%]	100
Wire feed rate [m/min]	1
Travel speed [mm/sec]	10
Gas flow [l/min]	15

Weld Geometry		Visual Defects and Weld Property	
Weld height [mm]	6.87	Spatters	Yes
Weld width [mm]	2.4	Porosity	No
Stand-off at layer 1 [mm]	15	Excess material	No
Stand-off at layer 10 [mm]	17	Surface regularity [μm]	85.7
Temperature at layer 10 [deg.C]	125	Average hardness [HV]	186
Number of layers	10		

Figure F10-1

Sample f1-100-10 (top view)

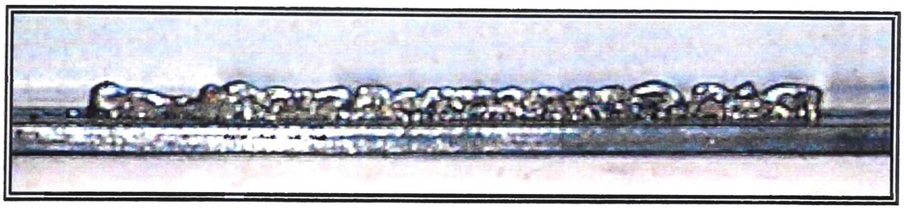

Figure F10-2

Sample f1-100-10 (front view)

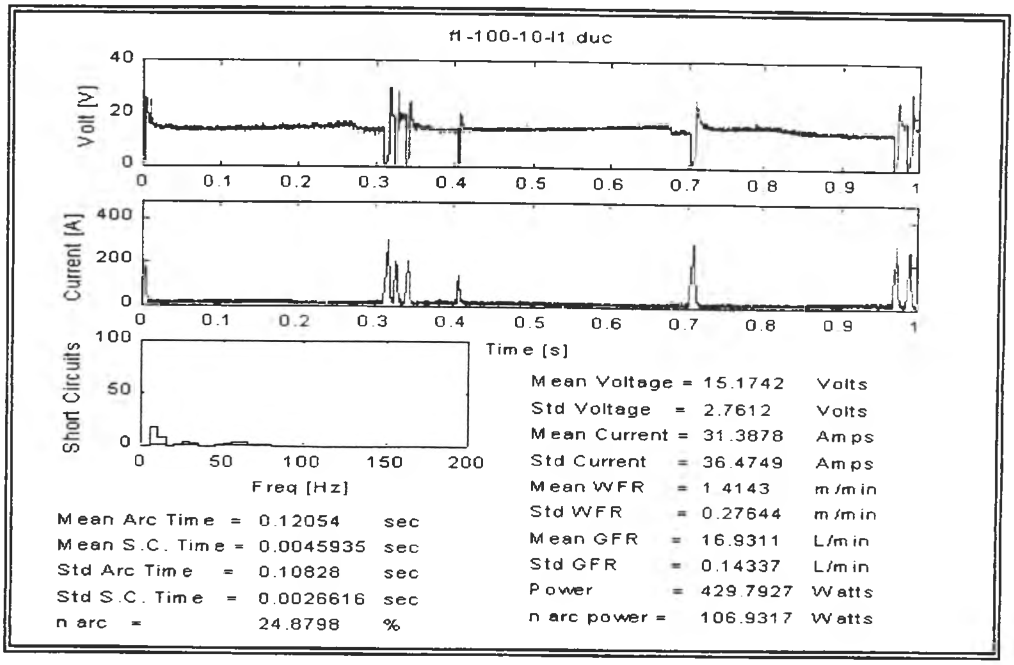

Plot F10-1

Sample f1-100-10-layer 1

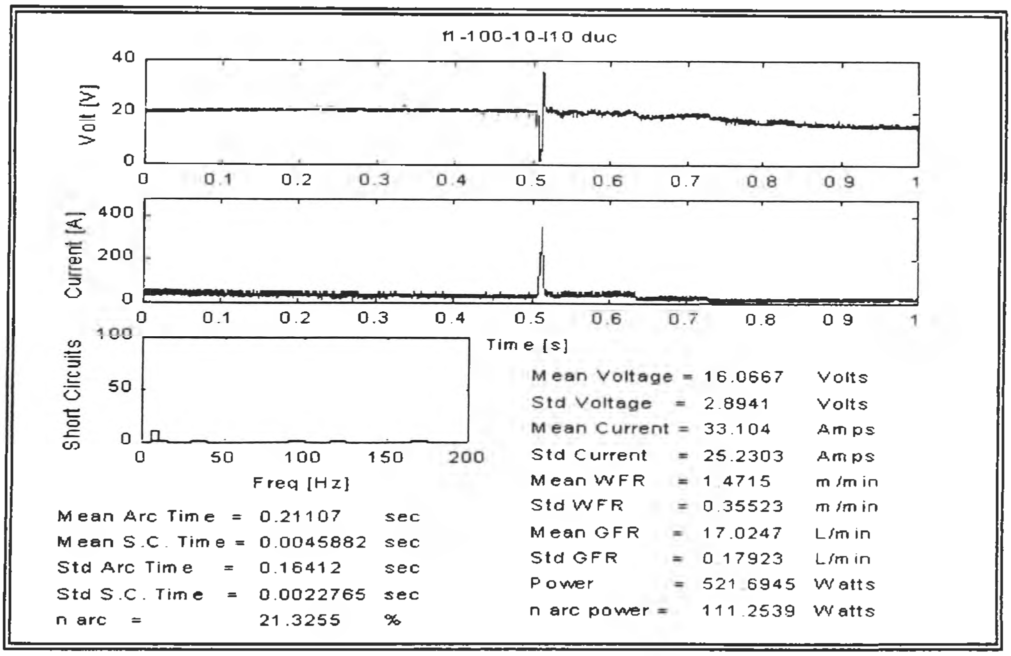

Plot F10-2

Sample f1-100-10-layer 10

F11 Wire Feed Rate of 2 m/min

Sample f2-75-10

Set Values	
Voltage [%]	75
Wire feed rate [m/min]	2
Travel speed [mm/sec]	10
Gas flow [l/min]	15

Weld Geometry		Visual Defects and Weld Property	
Weld height [mm]	8.96	Spatters	Yes
Weld width [mm]	2.7	Porosity	No
Stand-off at layer 1 [mm]	15	Excess material	No
Stand-off at layer 10 [mm]	15	Surface regularity [μm]	100
Temperature at layer 10 [deg.C]	130	Average hardness [HV]	182
Number of layers	10		

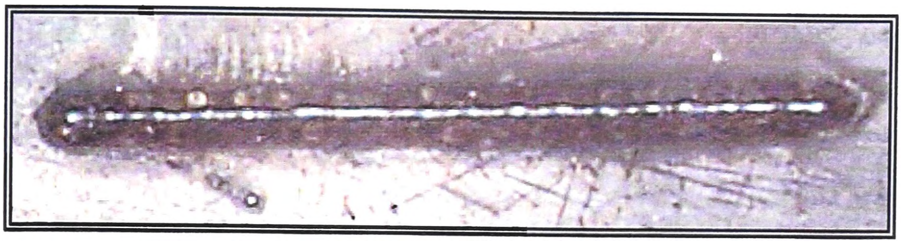

Figure F11-1

Sample f2-75-10 (top view)

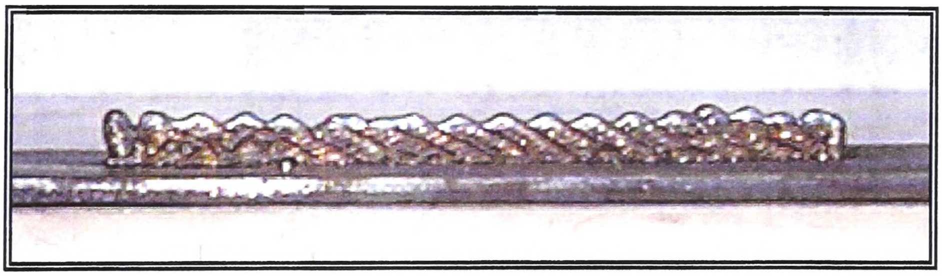

Figure F11-2

Sample f2-75-10 (front view)

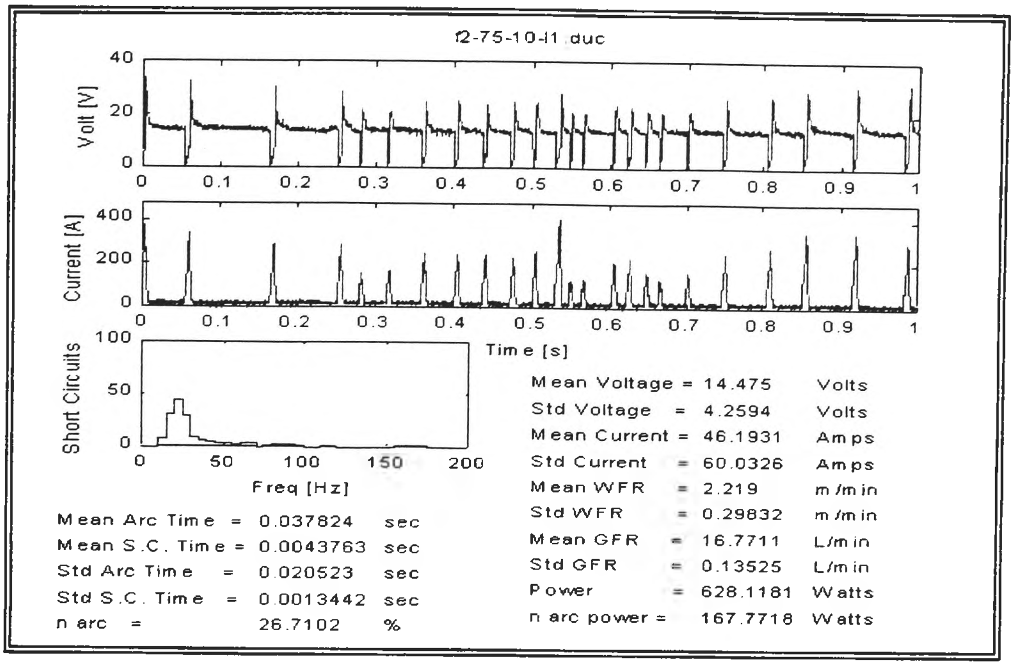

Plot F11-1

Sample f2-75-10-layer 1

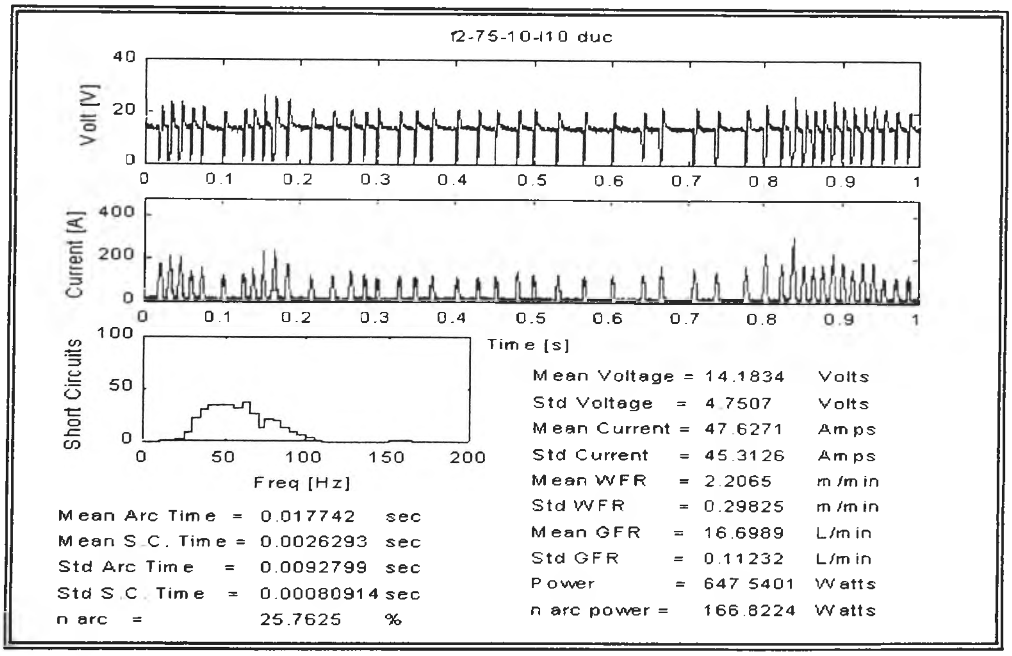

Plot F11-2

Sample f2-75-10-layer 10

Sample f2-100-10

Set Values	
Voltage [%]	100
Wire feed rate [m/min]	2
Travel speed [mm/sec]	10
Gas flow [l/min]	15

Weld Geometry		**Visual Defects and Weld Property**	
Weld height [mm]	9	Spatters	Yes
Weld width [mm]	3	Porosity	No
Stand-off at layer 1 [mm]	15	Excess material	No
Stand-off at layer 10 [mm]	15.5	Surface regularity [μm]	N/A
Temperature at layer 10 [deg.C]	126	Average hardness [HV]	N/A
Number of layers	10		

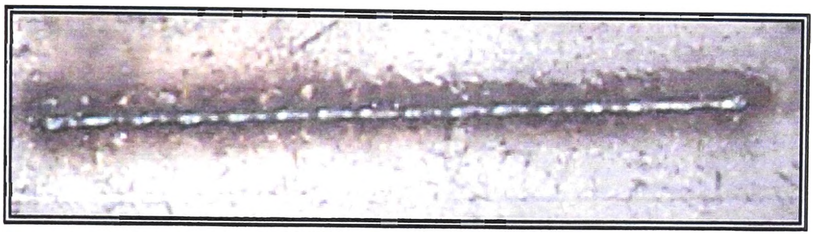

Figure F11-3

Sample f2-100-05 (top view)

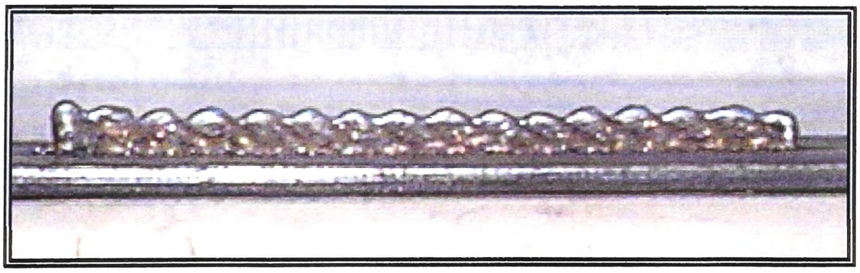

Figure F11-4

Sample f2-100-05 (front view)

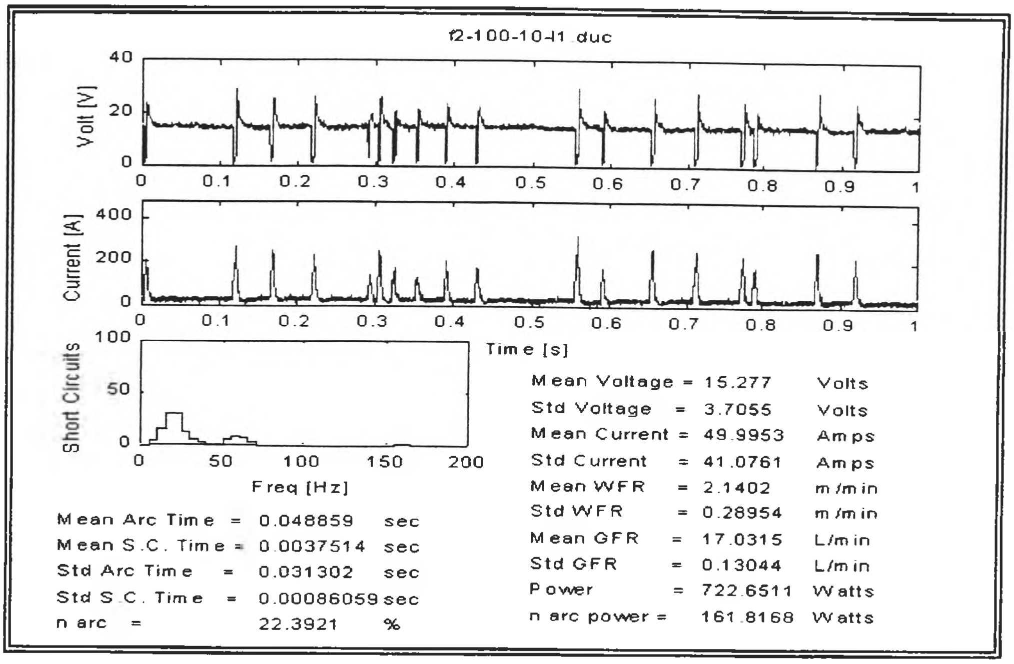

Plot F11-3

Sample f2-100-05-layer 1

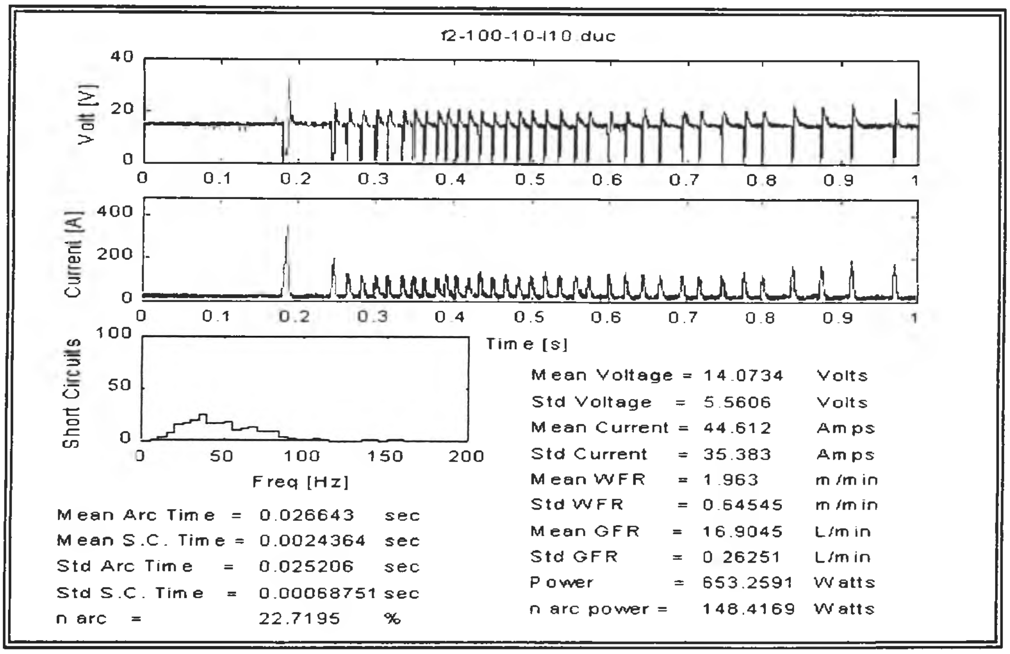

Plot F11-4

Sample f2-100-05-layer 10

Sample f2-110-10

Set Values	
Voltage [%]	110
Wire feed rate [m/min]	2
Travel speed [mm/sec]	10
Gas flow [l/min]	15

Weld Geometry		Visual Defects and Weld Property	
Weld height [mm]	8	Spatters	Yes
Weld width [mm]	3.1	Porosity	No
Stand-off at layer 1 [mm]	15	Excess material	No
Stand-off at layer 10 [mm]	16	Surface regularity [μm]	N/A
Temperature at layer 10 [deg.C]	135	Average hardness [HV]	N/A
Number of layers	10		

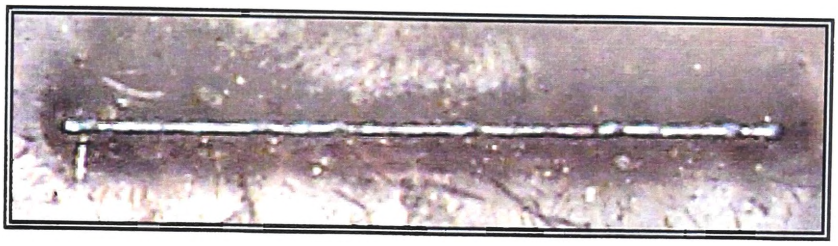

Figure F11-5

Sample f2-110-10 (top view)

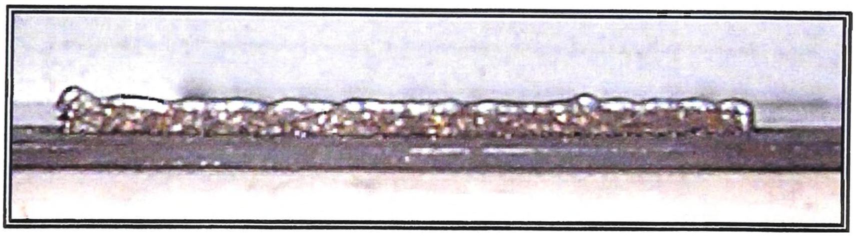

Figure F11-6

Sample f2-110-10 (front view)

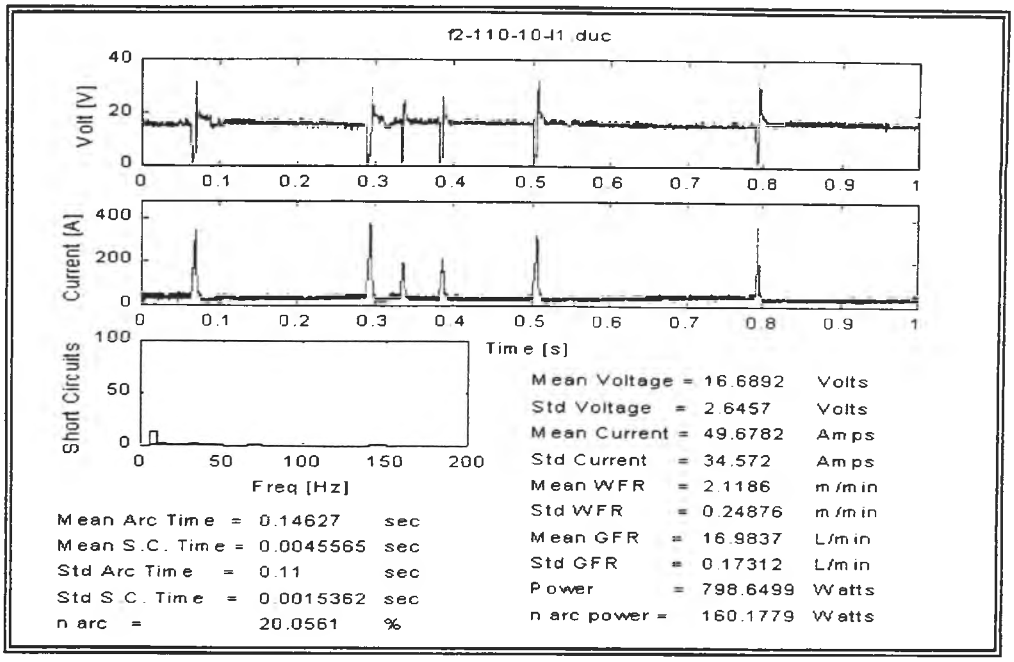

Plot F11-5

Sample f2-110-05-layer 1

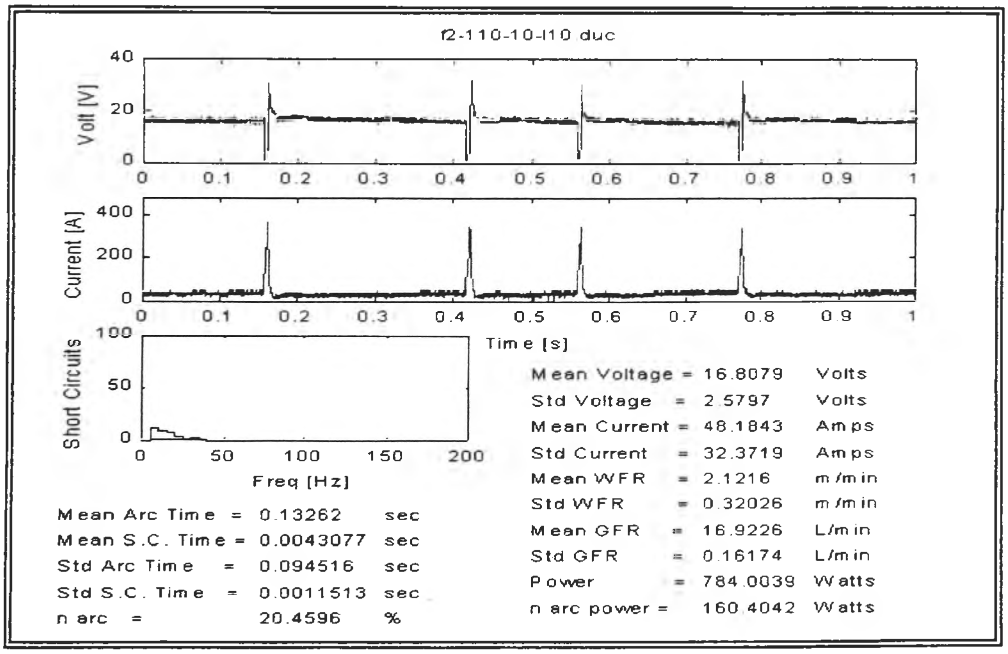

Plot F11-6

Sample f2-110-05-layer 10

Sample f2-120-10

Set Values	
Voltage [%]	120
Wire feed rate [m/min]	2
Travel speed [mm/sec]	10
Gas flow [l/min]	15

Weld Geometry		Visual Defects and Weld Property	
Weld height [mm]	6	Spatters	Yes
Weld width [mm]	3.3	Porosity	No
Stand-off at layer 1 [mm]	15	Excess material	No
Stand-off at layer 10 [mm]	17.5	Surface regularity [μm]	N/A
Temperature at layer 10 [deg.C]	155	Average hardness [HV]	N/A
Number of layers	10		

Figure F11-7

Sample f2-120-10 (top view)

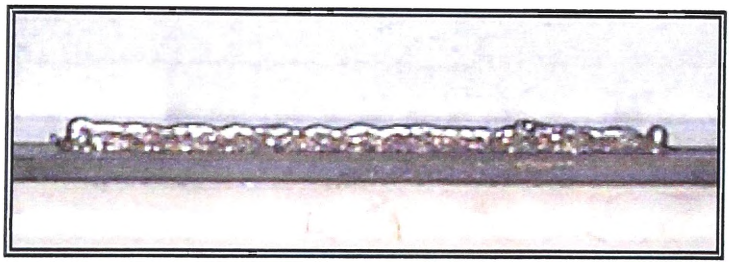

Figure F11-8

Sample f2-120-10 (front view)

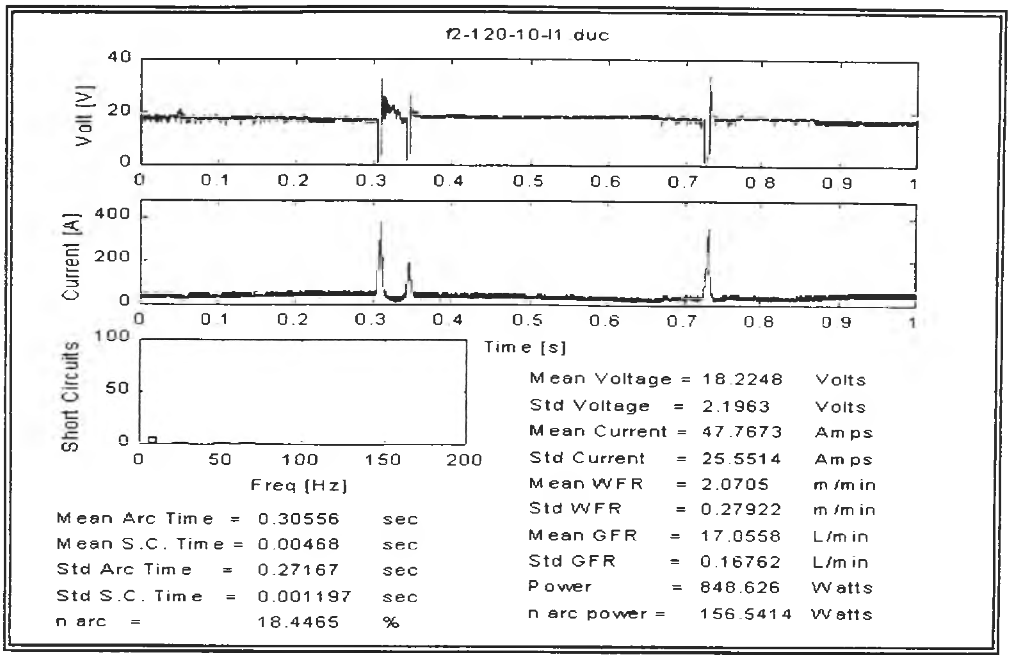

Plot F11-7

Sample f2-120-10-layer 1

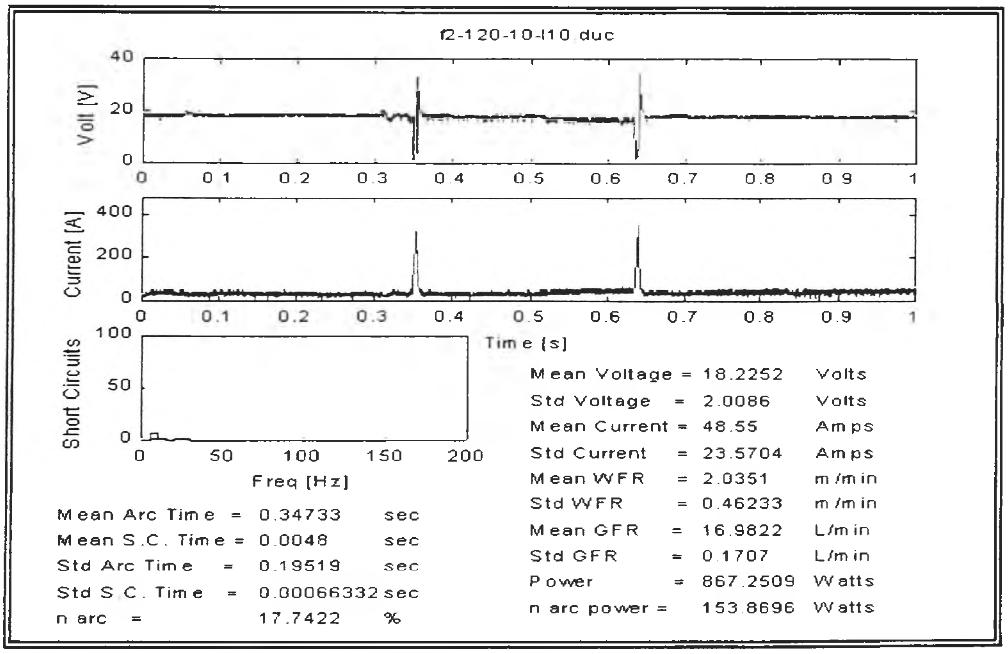

Plot F11-8

Sample f2-120-10-layer 10

Sample f2-130-10

Set Values	
Voltage [%]	130
Wire feed rate [m/min]	2
Travel speed [mm/sec]	10
Gas flow [l/min]	15

Weld Geometry		Visual Defects and Weld Property	
Weld height [mm]	5.5	Spatters	Yes
Weld width [mm]	3.5	Porosity	No
Stand-off at layer 1 [mm]	15	Excess material	No
Stand-off at layer 10 [mm]	15.5	Surface regularity [μm]	N/A
Temperature at layer 10 [deg.C]	165	Average hardness [HV]	N/A
Number of layers	10		

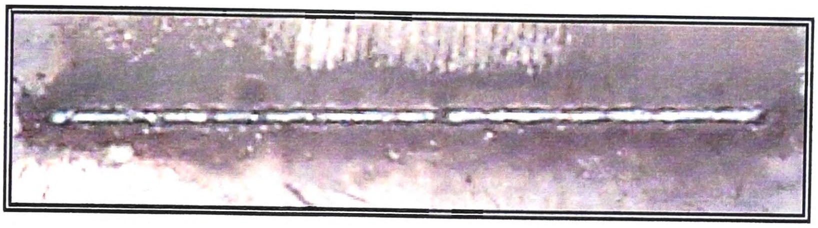

Figure F11-9

Sample f2-130-10 (top view)

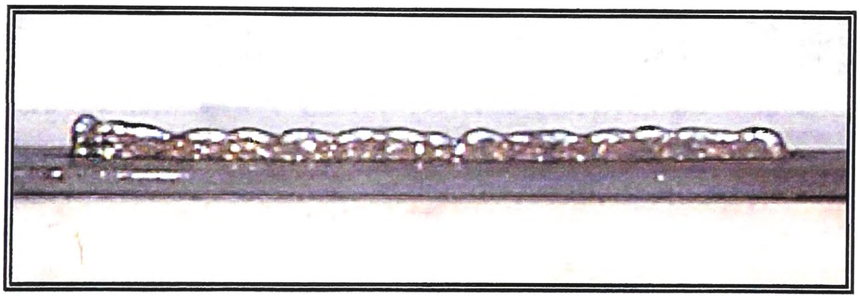

Figure F11-10

Sample f2-130-10 (front view)

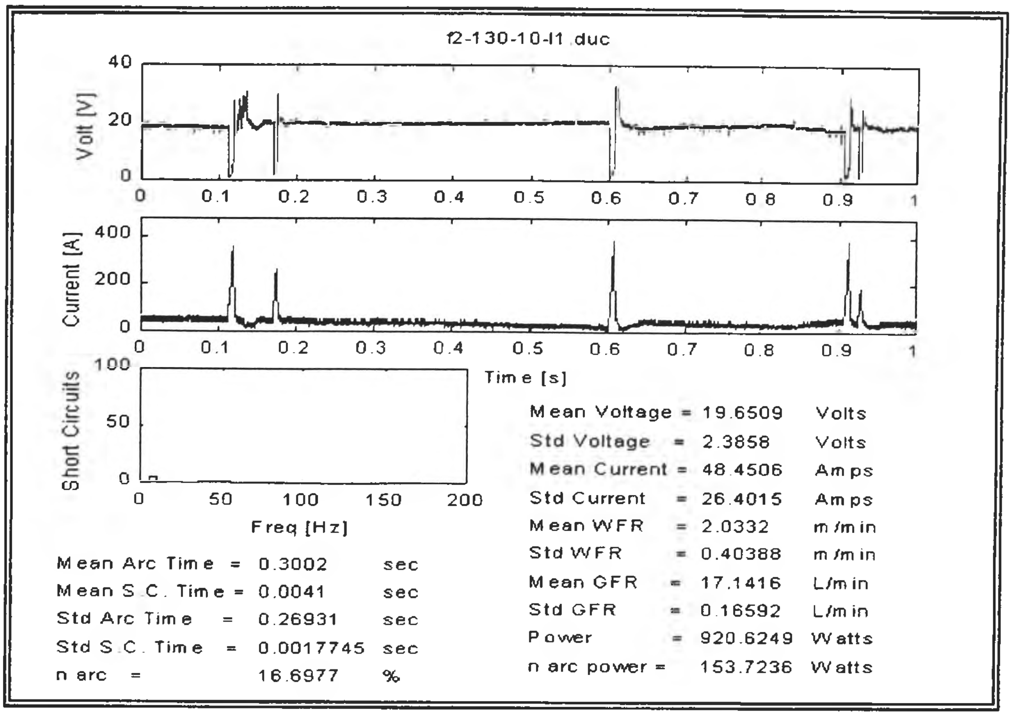

Plot F11-9

Sample f2-130-10-layer 1

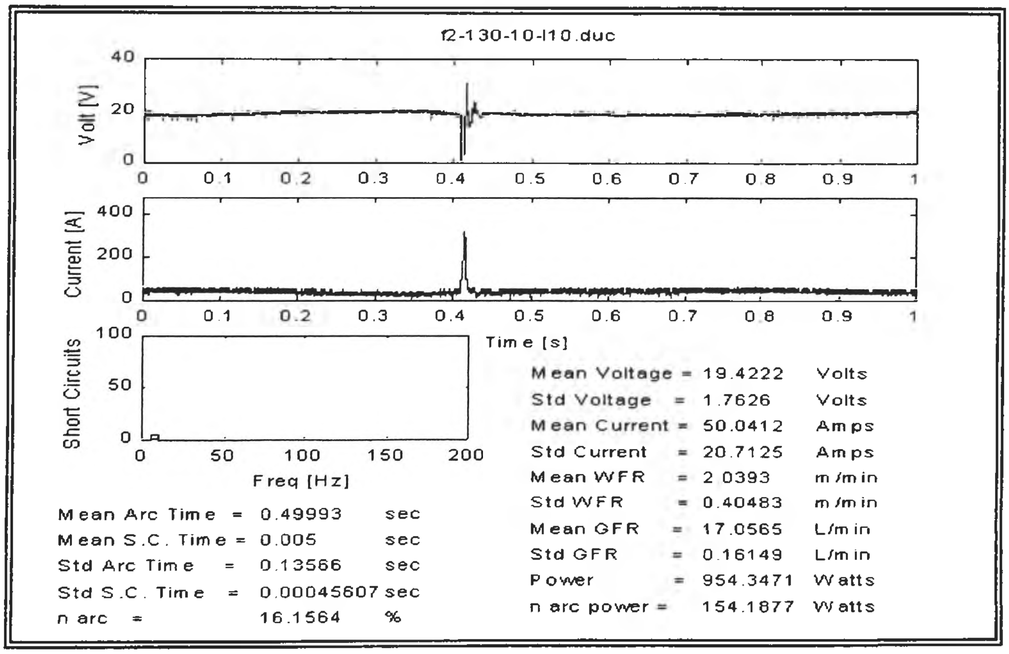

Plot F11-10

Sample f2-130-10-layer 10

Sample f2-150-10

Set Values	
Voltage [%]	150
Wire feed rate [m/min]	2
Travel speed [mm/sec]	10
Gas flow [l/min]	15

Weld Geometry		Visual Defects and Weld Property	
Weld height [mm]	5.09	Spatters	Yes
Weld width [mm]	3.6	Porosity	No
Stand-off at layer 1 [mm]	15	Excess material	No
Stand-off at layer 10 [mm]	14	Surface regularity [μm]	61.55
Temperature at layer 10 [deg.C]	175	Average hardness [HV]	163.7
Number of layers	10		

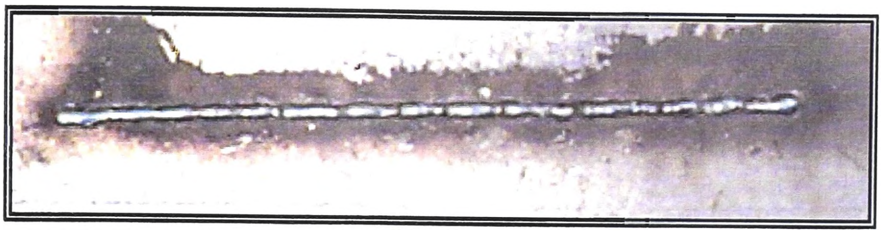

Figure F11-11

Sample f2-150-10 (top view)

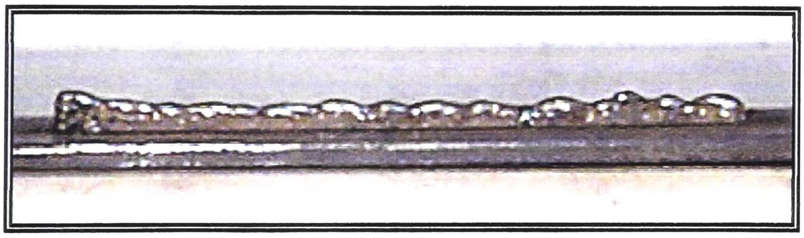

Figure F11-12

Sample f2-150-10 (front view)

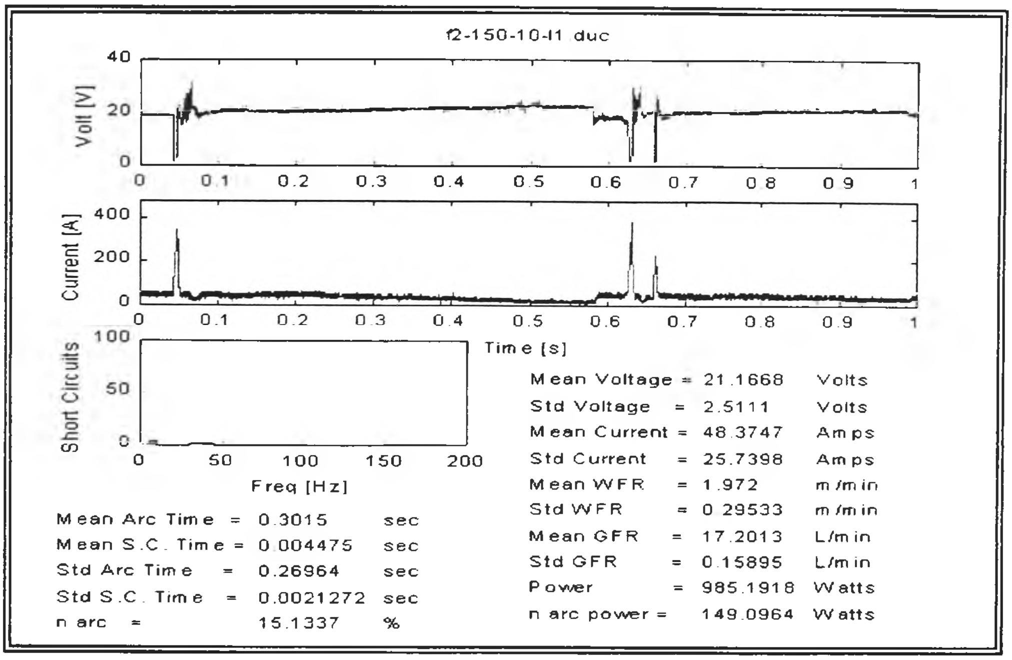

Plot F11-11

Sample f2-150-10-layer 1

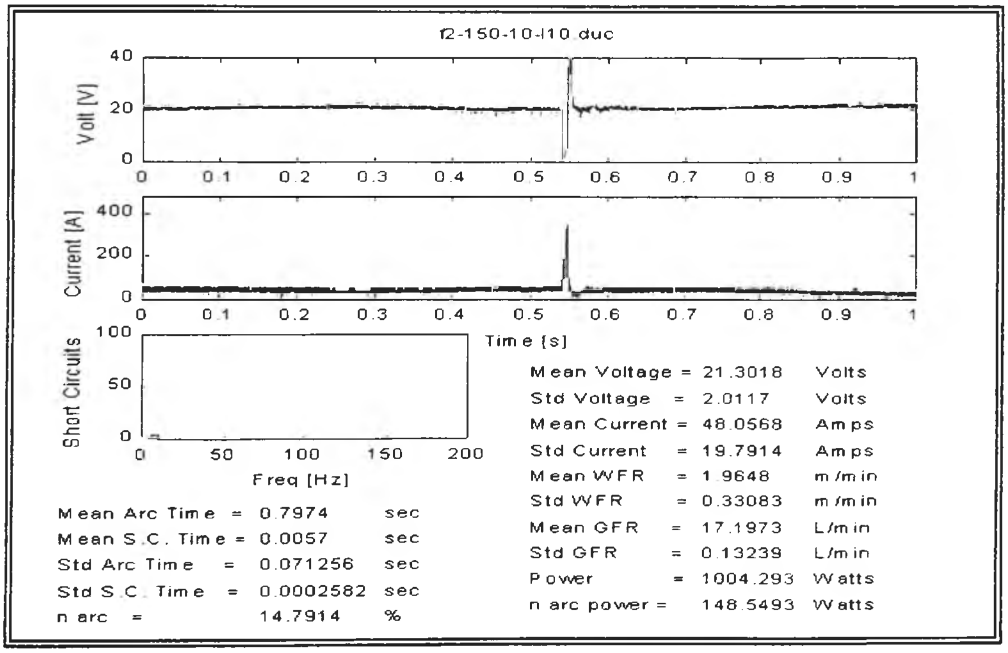

Plot F11-12

Sample f2-150-10-layer 10

F12 Wire Feed Rate of 3 m/min

Sample f3-75-10

Set Values	
Voltage [%]	75
Wire feed rate [m/min]	3
Travel speed [mm/sec]	10
Gas flow [l/min]	15

Weld Geometry		Visual Defects and Weld Property	
Weld height [mm]	11.87	Spatters	Yes
Weld width [mm]	3.7	Porosity	No
Stand-off at layer 1 [mm]	15	Excess material	No
Stand-off at layer 10 [mm]	14.5	Surface regularity [μm]	80.45
Temperature at layer 10 [deg.C]	185	Average hardness [HV]	182.7
Number of layers	10		

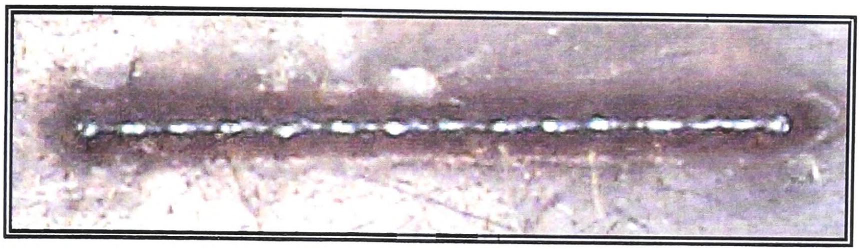

Figure F12-1

Sample f3-75-05 (top view)

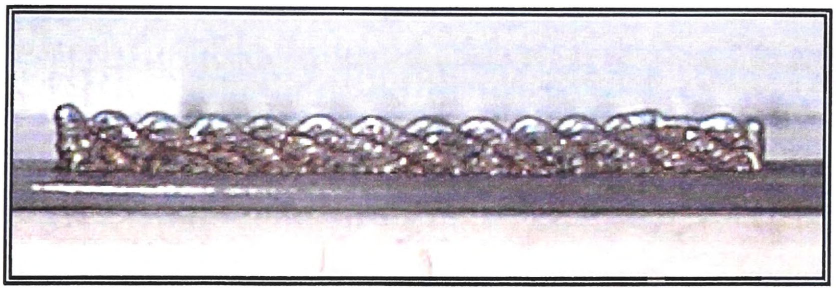

Figure F12-2

Sample f3-75-05 (front view)

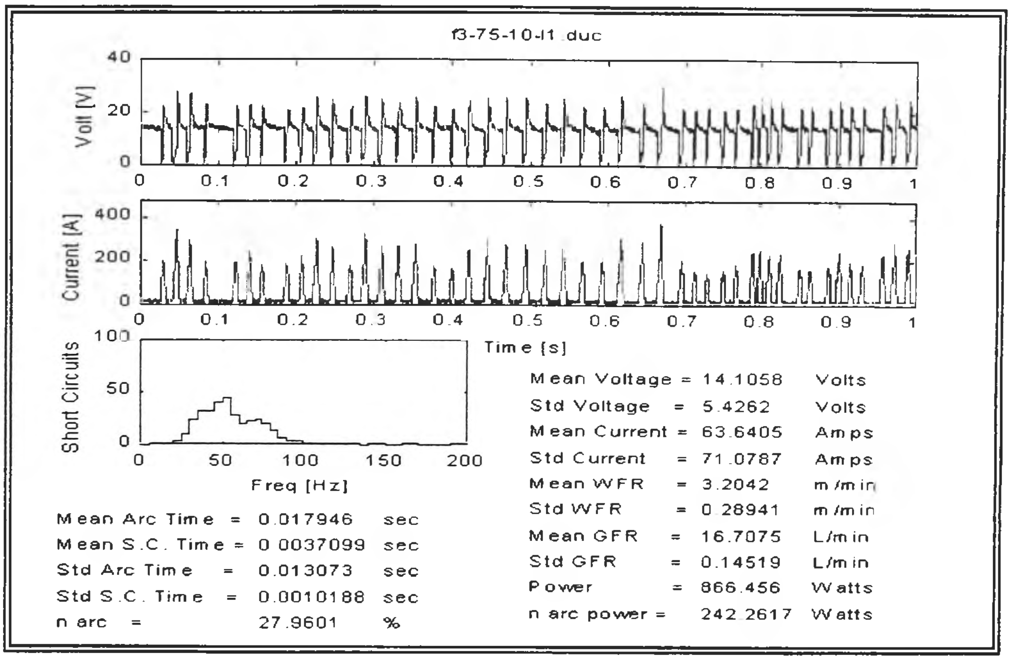

Plot F12-1

Sample f3-75-10-layer 1

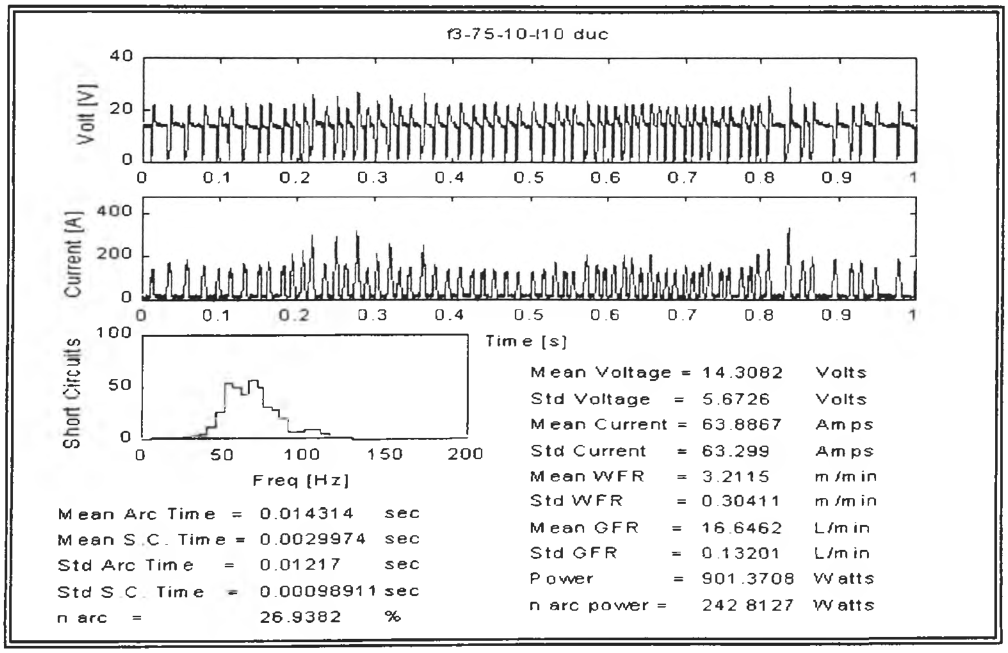

Plot F12-2

Sample f3-75-10-layer 10

Sample f3-100-10

Set Values	
Voltage [%]	100
Wire feed rate [m/min]	3
Travel speed [mm/sec]	10
Gas flow [l/min]	15

Weld Geometry		**Visual Defects and Weld Property**	
Weld height [mm]	10	Spatters	Yes
Weld width [mm]	4.2	Porosity	No
Stand-off at layer 1 [mm]	15	Excess material	No
Stand-off at layer 10 [mm]	16	Surface regularity [μm]	N/A
Temperature at layer 10 [deg.C]	197	Average hardness [HV]	N/A
Number of layers	10		

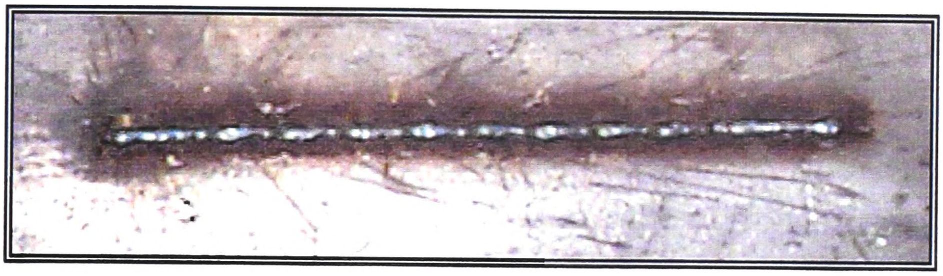

Figure F12-3

Sample f3-100-10 (top view)

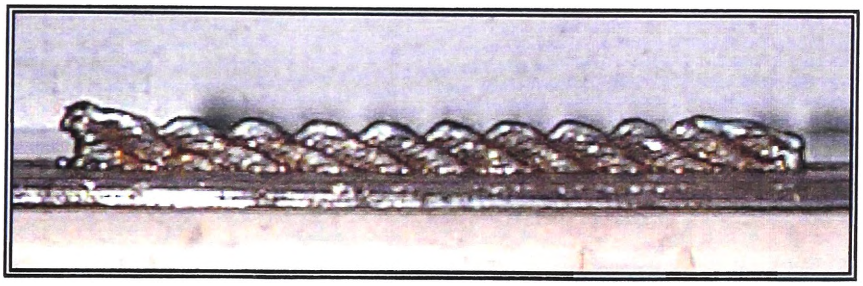

Figure F12-4

Sample f3-100-10 (front view)

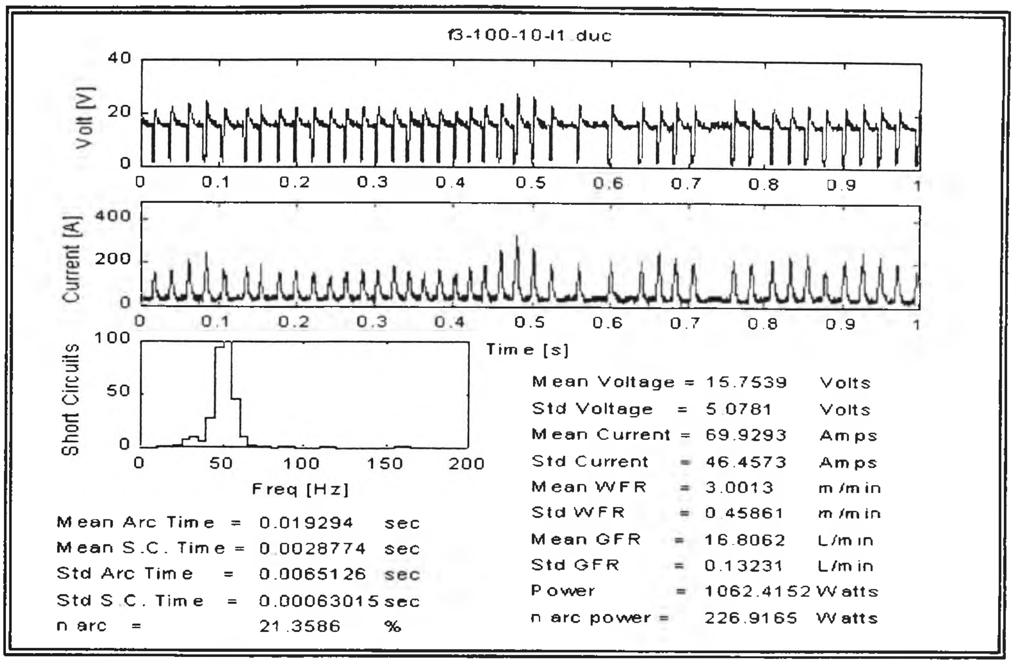

Plot F12-3

Sample f3-100-10-layer 1

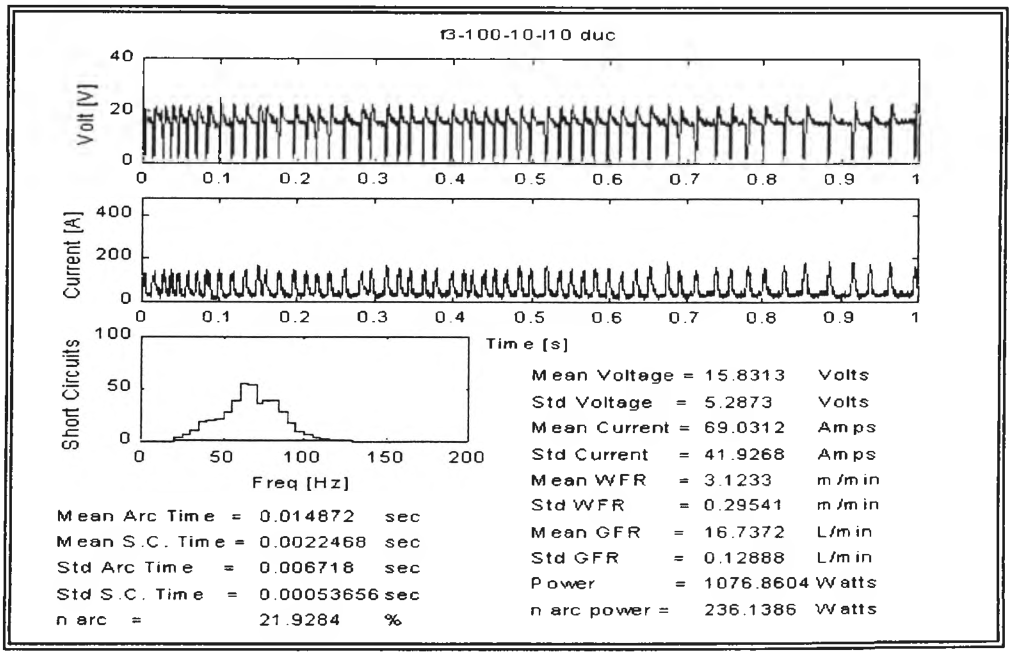

Plot F12-4

Sample f3-100-10-layer 10

Sample f3-110-10

Set Values	
Voltage [%]	110
Wire feed rate [m/min]	3
Travel speed [mm/sec]	10
Gas flow [l/min]	15

Weld Geometry		Visual Defects and Weld Property	
Weld height [mm]	10	Spatters	Yes
Weld width [mm]	4.2	Porosity	No
Stand-off at layer 1 [mm]	15	Excess material	No
Stand-off at layer 10 [mm]	17	Surface regularity [μm]	N/A
Temperature at layer 10 [deg.C]	208	Average hardness [HV]	N/A
Number of layers	10		

Figure F12-5

Sample f3-110-05 (top view)

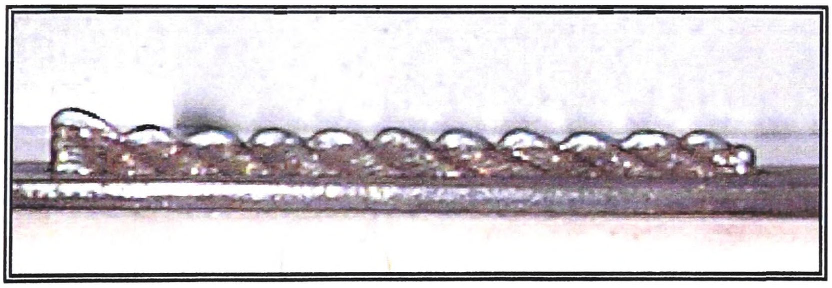

Figure F12-6

Sample f3-110-10- (front view)

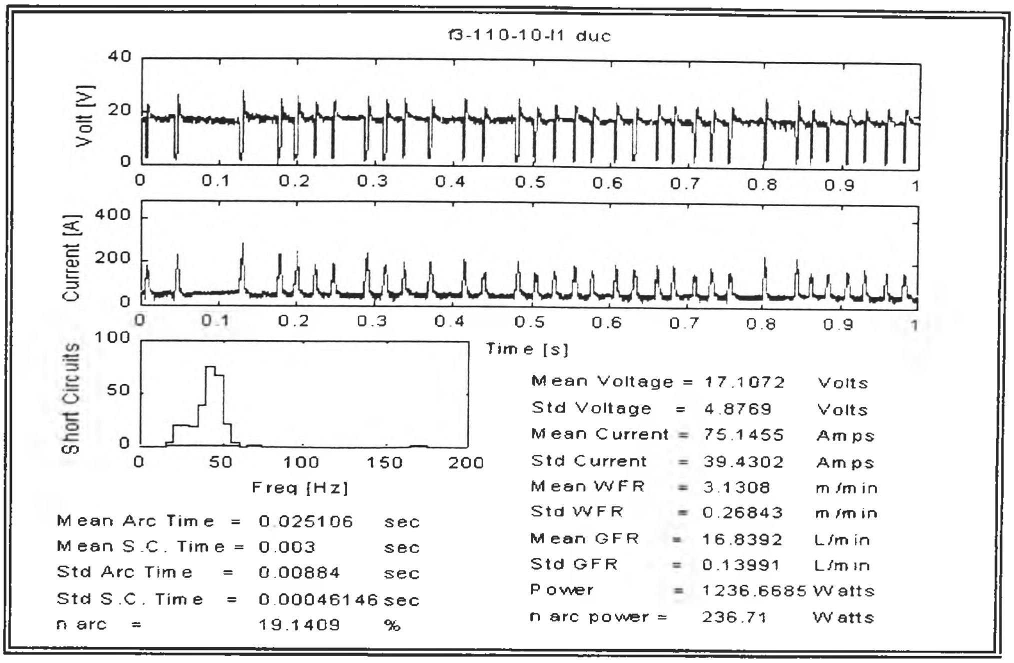

Plot F12-5

Sample f3-110-10-layer 1

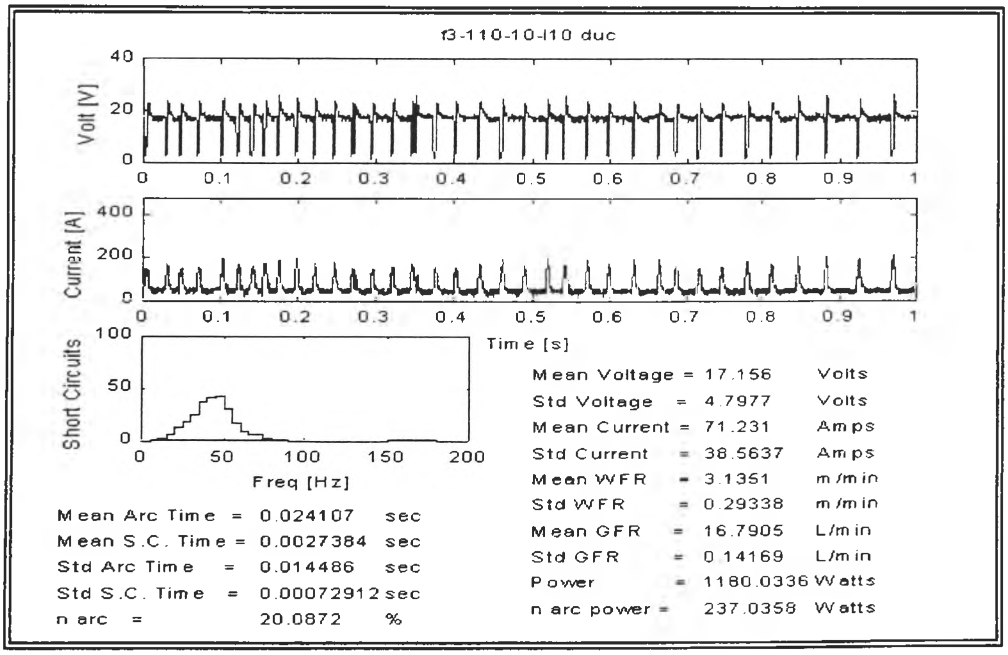

Plot F12-6

Sample f3-110-10-layer 10

Sample f3-120-10

Set Values	
Voltage [%]	120
Wire feed rate [m/min]	3
Travel speed [mm/sec]	10
Gas flow [l/min]	15

Weld Geometry		**Visual Defects and Weld Property**	
Weld height [mm]	9	Spatters	Yes
Weld width [mm]	4.3	Porosity	No
Stand-off at layer 1 [mm]	15	Excess material	No
Stand-off at layer 10 [mm]	15	Surface regularity [μm]	N/A
Temperature at layer 10 [deg.C]	228	Average hardness [HV]	N/A
Number of layers	10		

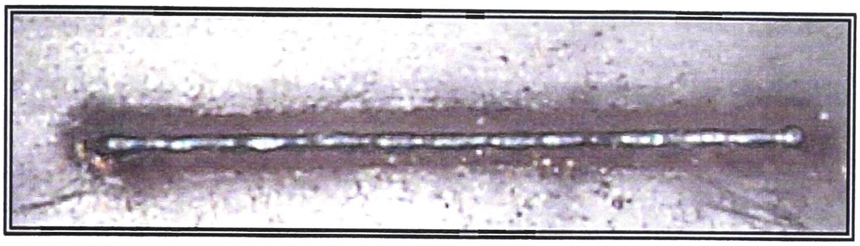

Figure F12-7

Sample f3-120-10 (top view)

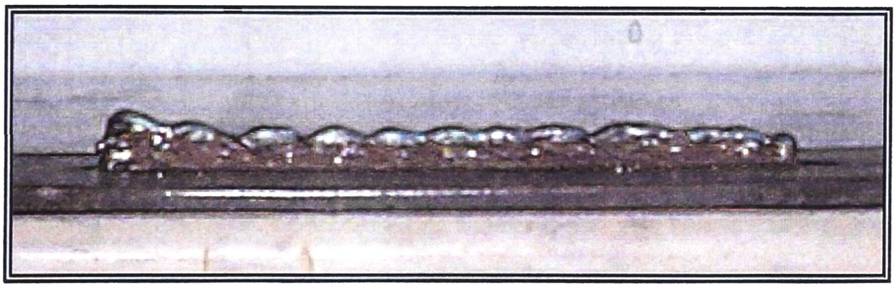

Figure F12-8

Sample f3-120-10 (front view)

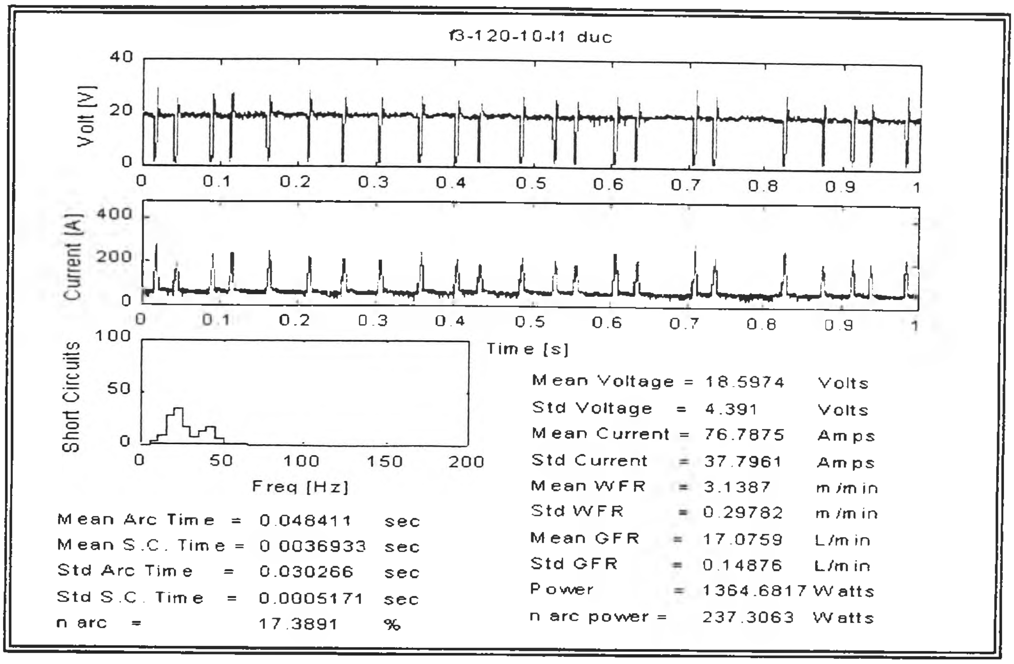

Plot F12-7

Sample f3-120-10-layer 1

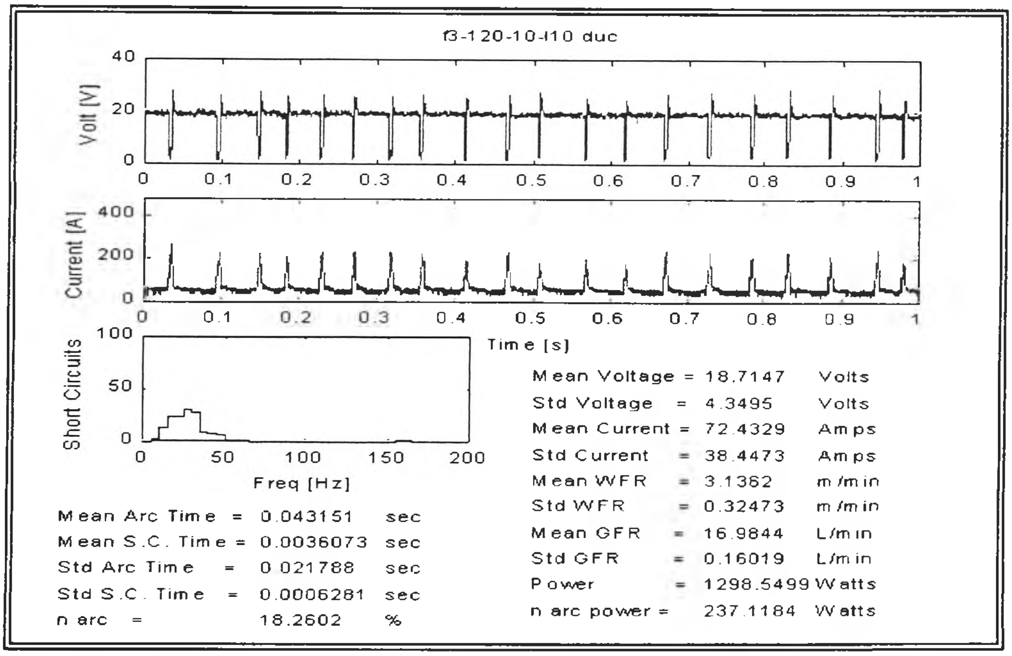

Plot F12-8

Sample F3-120-10-layer 10

Sample f3-150-10

Set Values	
Voltage [%]	150
Wire feed rate [m/min]	3
Travel speed [mm/sec]	10
Gas flow [l/min]	15

Weld Geometry		Visual Defects and Weld Property	
Weld height [mm]	7.9	Spatters	Yes
Weld width [mm]	4.2	Porosity	No
Stand-off at layer 1 [mm]	15	Excess material	No
Stand-off at layer 10 [mm]	17	Surface regularity [μm]	42.05
Temperature at layer 10 [deg.C]	232	Average hardness [HV]	164.7
Number of layers	10		

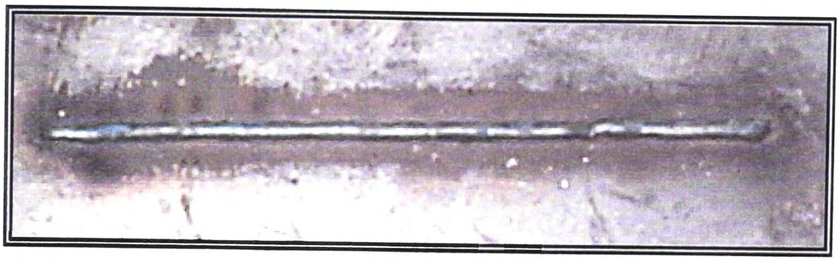

Figure F12-9

Sample f3-150-10 (top view)

Figure F12-10

Sample f3-150-10 (front view)

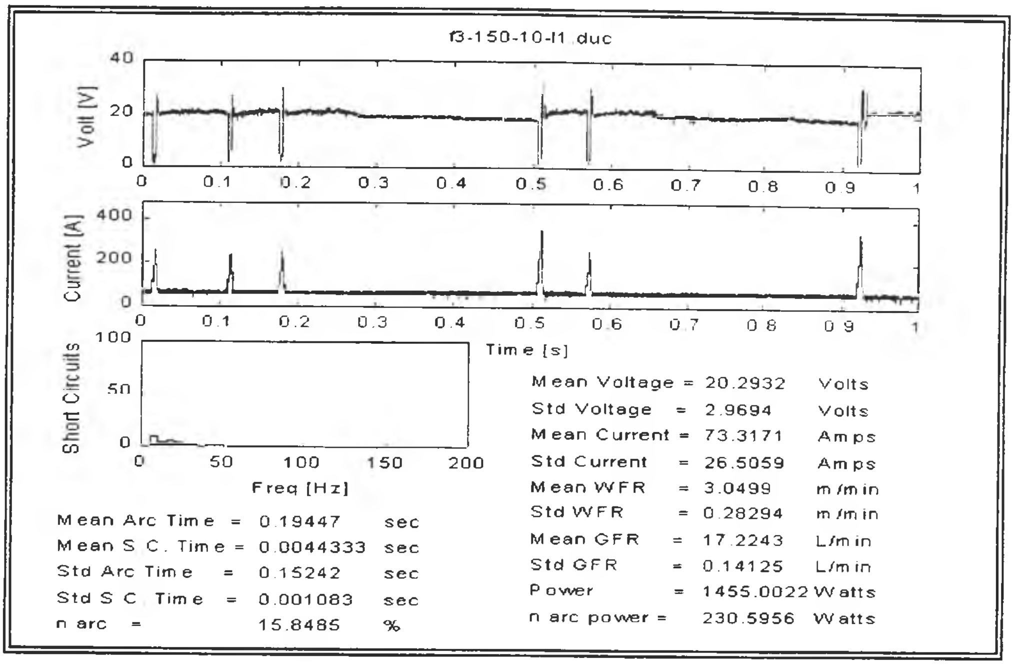

Plot F12-9

Sample f3-150-10-layer 1

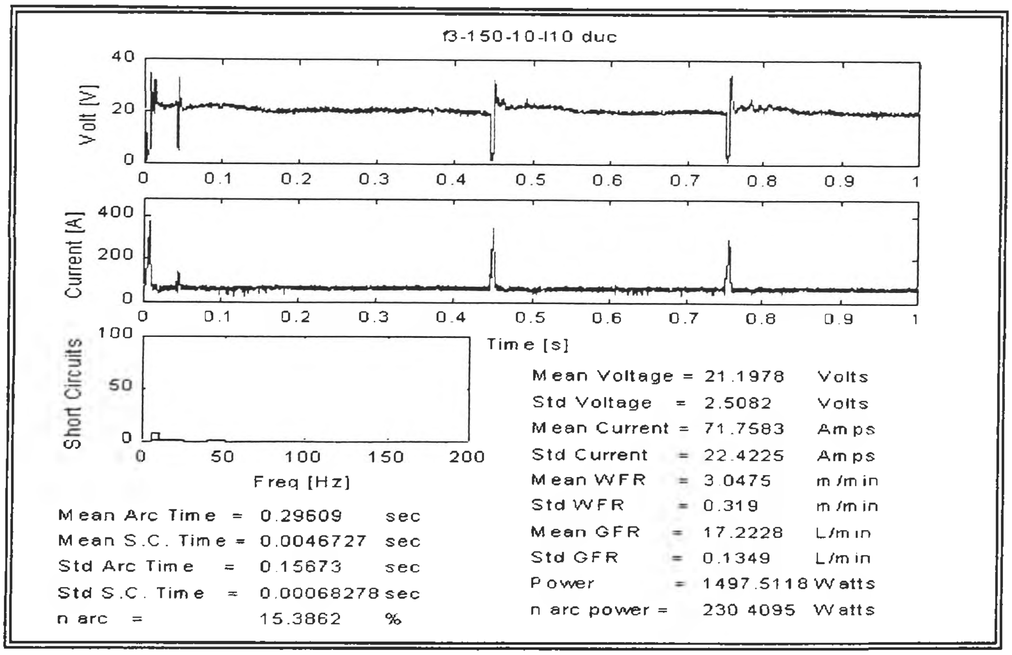

Plot F12-10

Sample f3-150-10-layer 10

F13 Wire Feed Rate of 4 m/min

Sample f4-75-10

Set Values	
Voltage [%]	75
Wire feed rate [m/min]	4
Travel speed [mm/sec]	10
Gas flow [l/min]	15

Weld Geometry		Visual Defects and Weld Property	
Weld height [mm]	12.49	Spatters	Yes
Weld width [mm]	5	Porosity	No
Stand-off at layer 1 [mm]	15	Excess material	No
Stand-off at layer 10 [mm]	15.5	Surface regularity [μm]	176.9
Temperature at layer 10 [deg.C]	200	Average hardness [HV]	176.7
Number of layers	10		

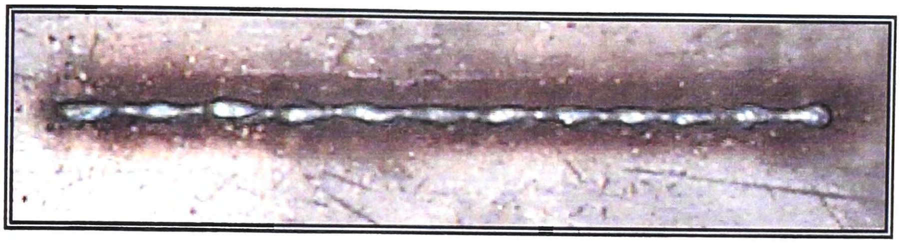

Figure F13-1

Sample f4-75-10 (top view)

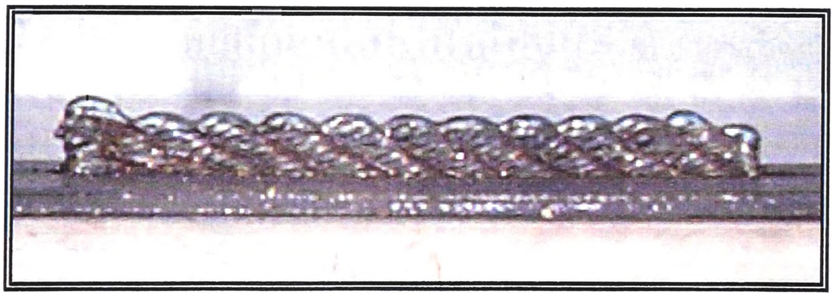

Figure F13-2

Sample f4-75-10 (front view)

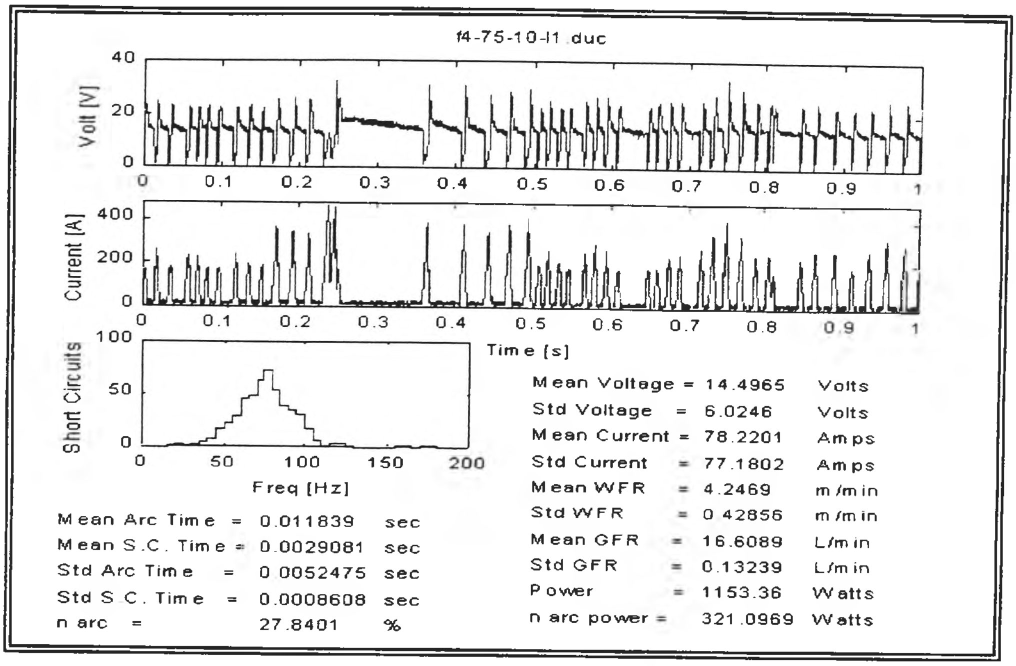

Plot F13-1

Sample f4-75-10-layer 1

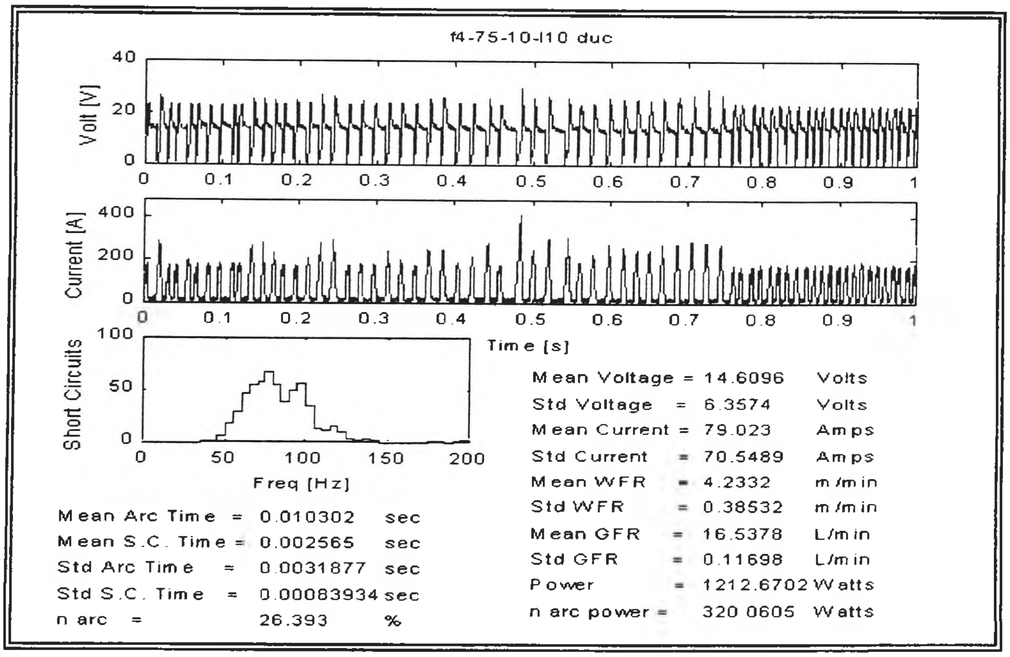

Plot F13-2

Sample f4-75-10-layer 10

Sample f4-100-10

Set Values	
Voltage [%]	100
Wire feed rate [m/min]	4
Travel speed [mm/sec]	10
Gas flow [l/min]	15

Weld Geometry		**Visual Defects and Weld Property**	
Weld height [mm]	11.5	Spatters	Yes
Weld width [mm]	4.7	Porosity	No
Stand-off at layer 1 [mm]	15	Excess material	No
Stand-off at layer 10 [mm]	15	Surface regularity [μm]	N/A
Temperature at layer 10 [deg.C]	250	Average hardness [HV]	N/A
Number of layers	10		

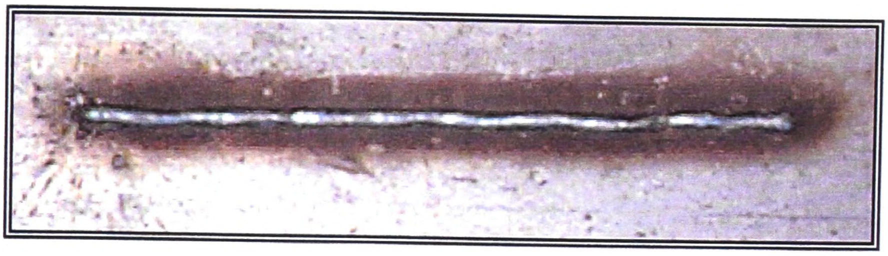

Figure F13-3

Sample f4-100-10 (top view)

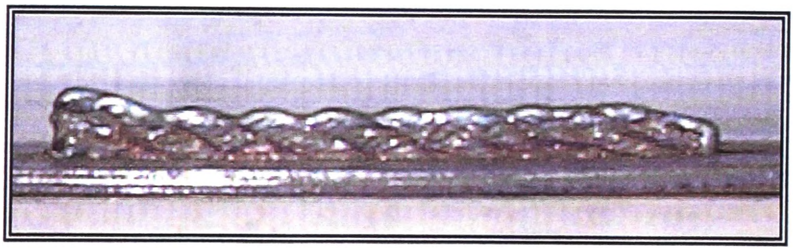

Figure F13-4

Sample f4-100-10 (front view)

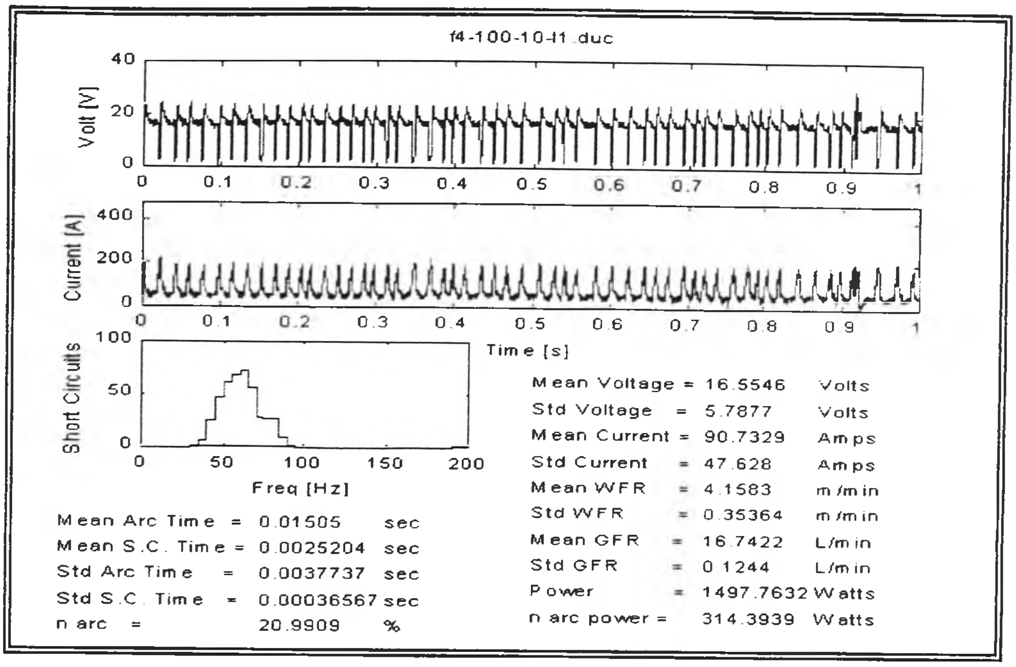

F13-3

Plot f4-100-10-layer 1

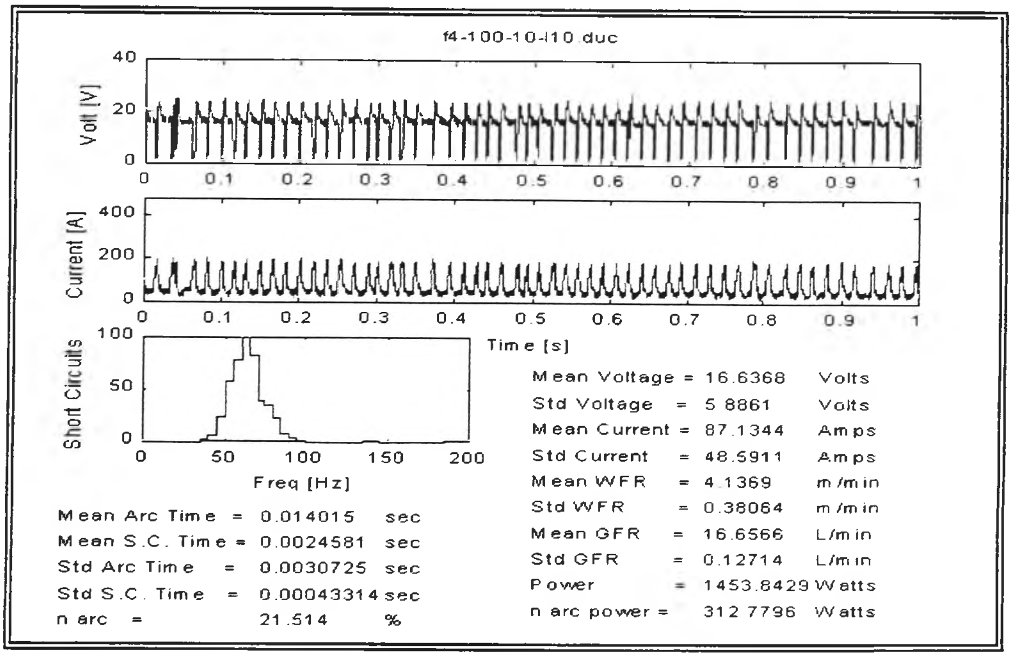

F13-4

Plot f4-100-10-layer 10

Sample f4-110-10

Set Values	
Voltage [%]	110
Wire feed rate [m/min]	4
Travel speed [mm/sec]	10
Gas flow [l/min]	15

Weld Geometry		Visual Defects and Weld Property	
Weld height [mm]	10.5	Spatters	Yes
Weld width [mm]	5	Porosity	No
Stand-off at layer 1 [mm]	15	Excess material	No
Stand-off at layer 10 [mm]	15.5	Surface regularity [μm]	N/A
Temperature at layer 10 [deg.C]	271	Average hardness [HV]	N/A
Number of layers	10		

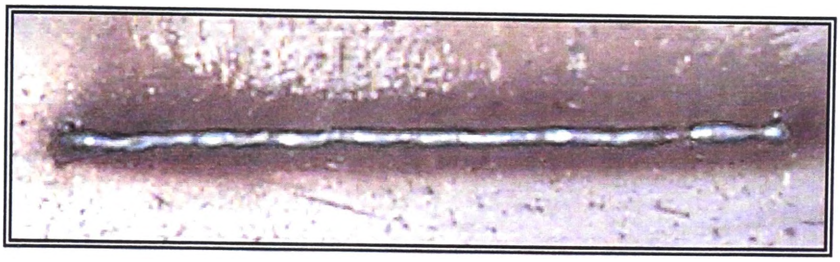

Figure F13-5

Sample f4-110-10 (top view)

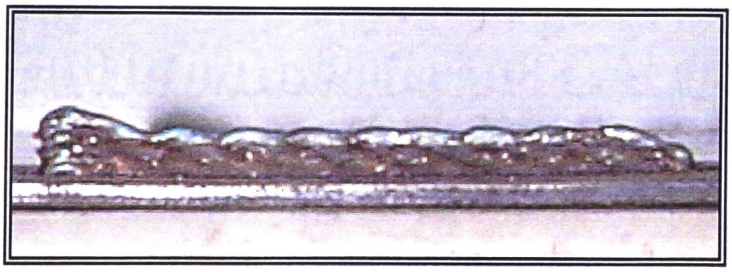

Figure F13-6

Sample f4-110-10 (front view)

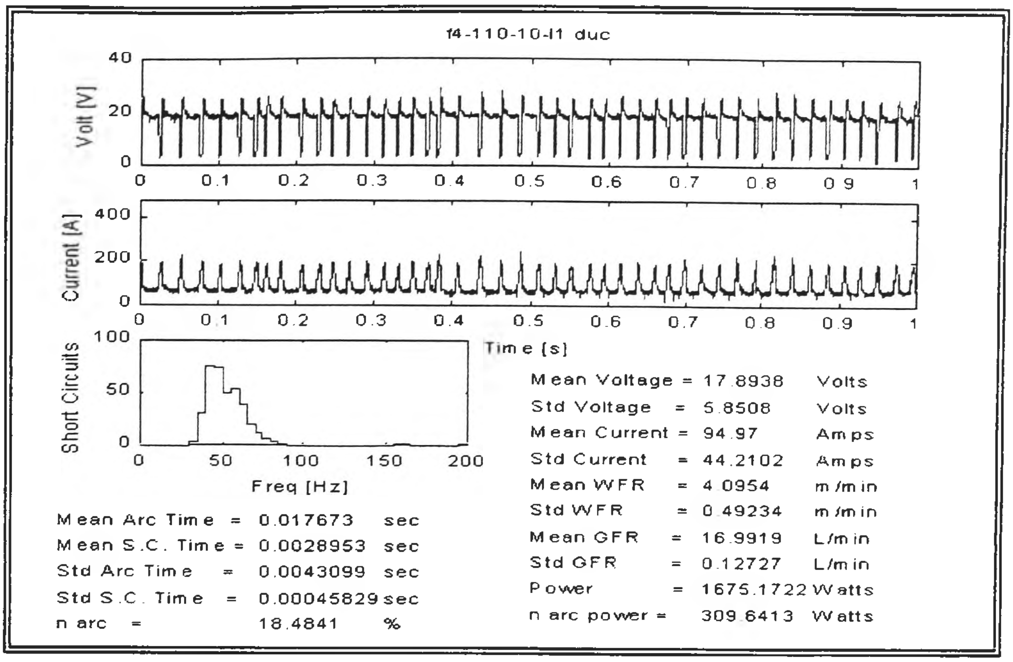

Plot F13-5

Sample f4-110-10-layer 1

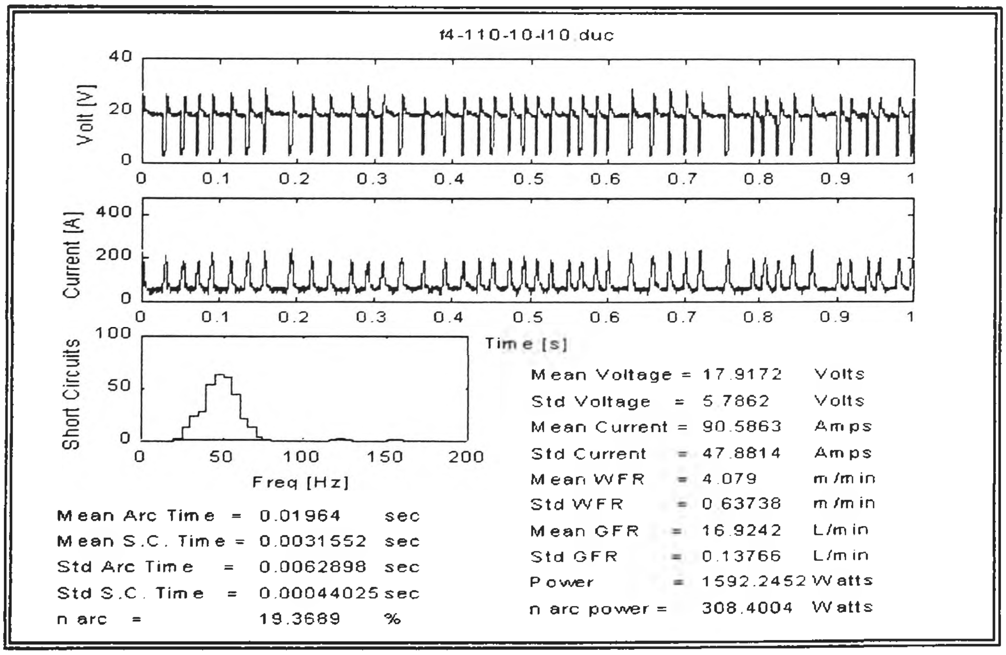

Plot F13-6

Sample f4-110-10-layer 10

Sample f4-120-10

Set Values	
Voltage [%]	120
Wire feed rate [m/min]	4
Travel speed [mm/sec]	10
Gas flow [l/min]	15

Weld Geometry		Visual Defects and Weld Property	
Weld height [mm]	9.41	Spatters	Yes
Weld width [mm]	4.7	Porosity	No
Stand-off at layer 1 [mm]	15	Excess material	No
Stand-off at layer 10 [mm]	15.5	Surface regularity [μm]	N/A
Temperature at layer 10 [deg.C]	284	Average hardness [HV]	N/A
Number of layers	10		

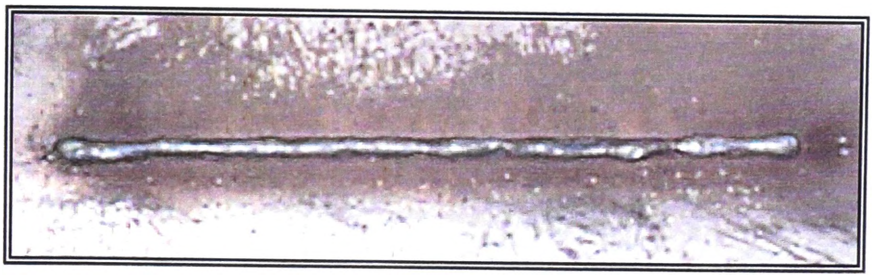

Figure F13-7

Sample f4-120-10 (top view)

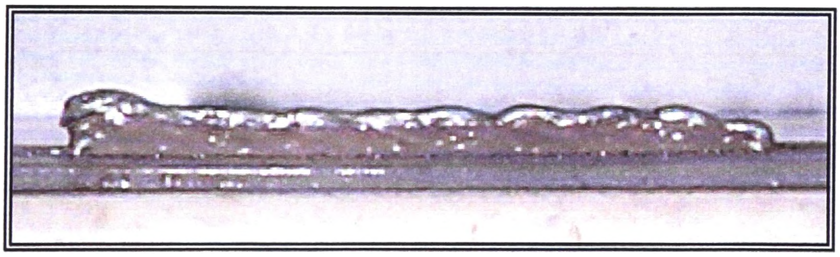

Figure F13-8

Sample f4-120-10 (front view)

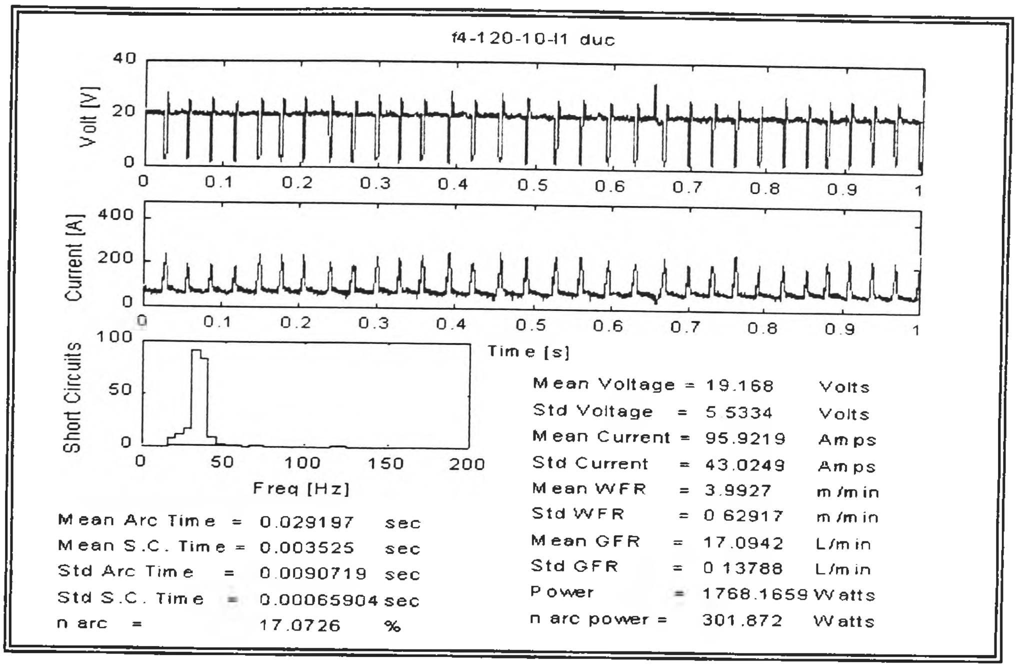

Plot F13-7

Sample f4-120-10-layer 1

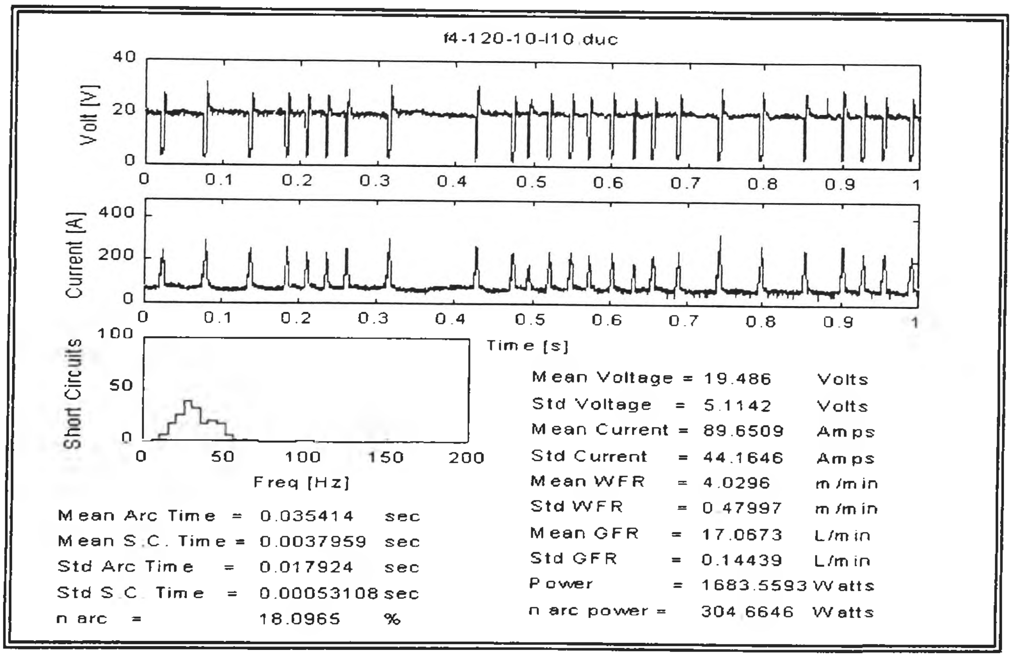

Plot F13-8

Sample f4-120-10-layer 10

Sample f4-130-10

Set Values	
Voltage [%]	130
Wire feed rate [m/min]	4
Travel speed [mm/sec]	10
Gas flow [l/min]	15

Weld Geometry		**Visual Defects and Weld Property**	
Weld height [mm]	9.3	Spatters	Yes
Weld width [mm]	5.3	Porosity	No
Stand-off at layer 1 [mm]	15	Excess material	No
Stand-off at layer 10 [mm]	17.5	Surface regularity [μm]	118.25
Temperature at layer 10 [deg.C]	295	Average hardness [HV]	163.7
Number of layers	10		

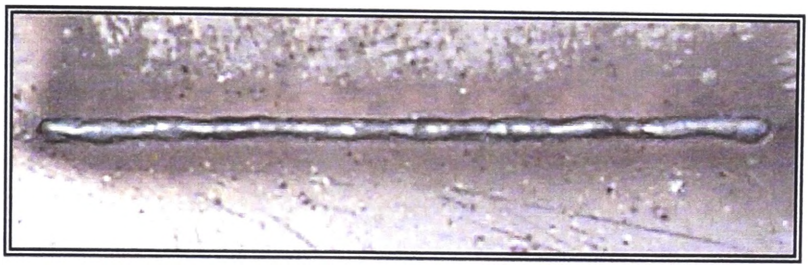

Figure F13-9

Sample f4-130-10 (top view)

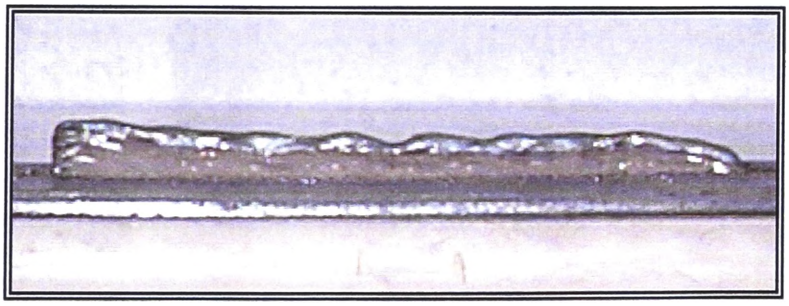

Figure F13-10

Sample f4-130-10 (front view)

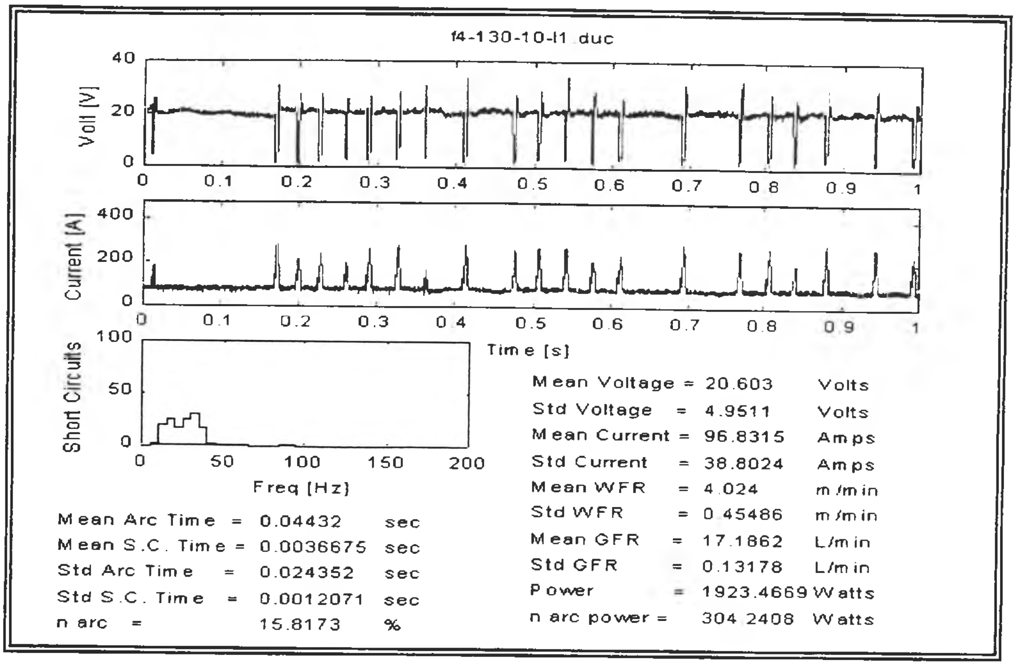

Plot F13-9

Sample f4-130-10-layer 1

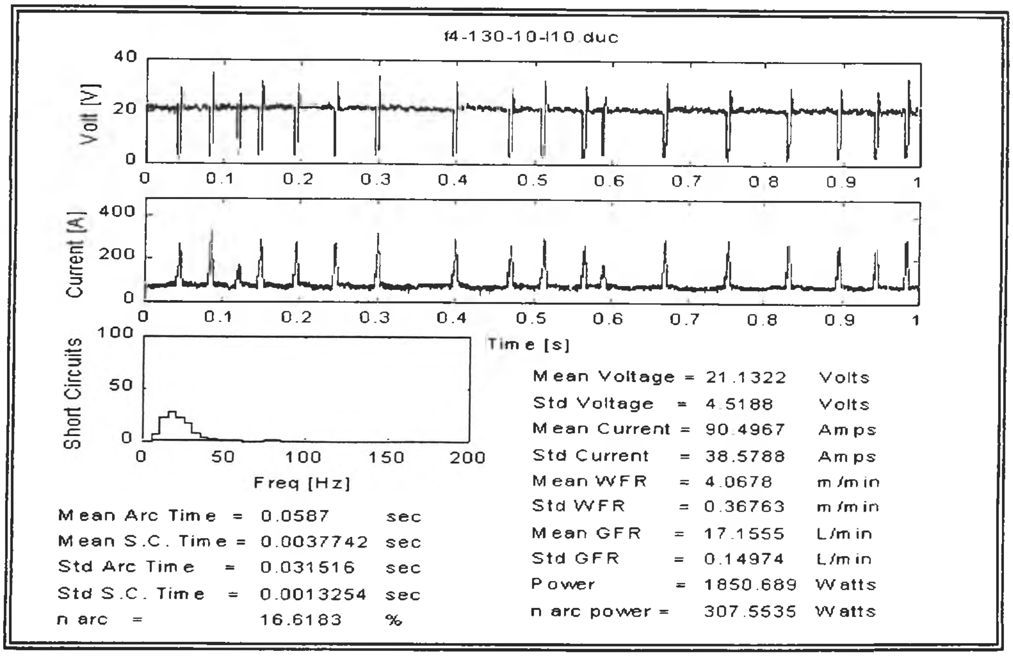

Plot F13-10

F4-130-10-layer 10

F14 Wire Feed Rate of 5 m/min

Sample f5-100-10

Set Values	
Voltage [%]	100
Wire feed rate [m/min]	5
Travel speed [mm/sec]	10
Gas flow [l/min]	15

Weld Geometry		Visual Defects and Weld Property	
Weld height [mm]	12.43	Spatters	Yes
Weld width [mm]	5.3	Porosity	No
Stand-off at layer 1 [mm]	15	Excess material	No
Stand-off at layer 10 [mm]	15	Surface regularity [µm]	75.75
Temperature at layer 10 [deg.C]	230	Average hardness [HV]	171.3
Number of layers	10		

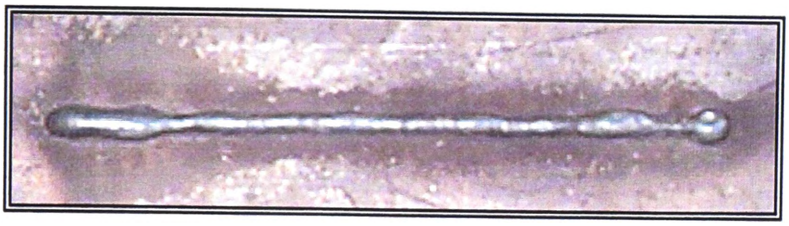

Figure F14-1

Sample f5-100-10 (top view)

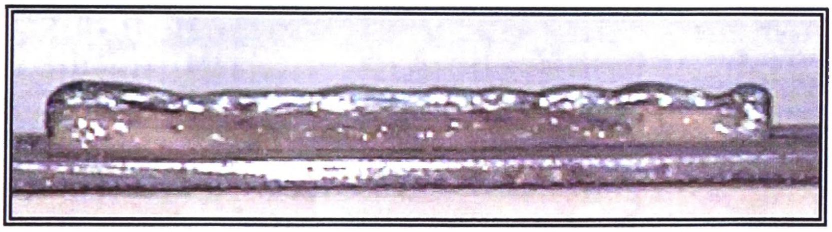

Figure F14-2

Sample f5-100-10 (front view)

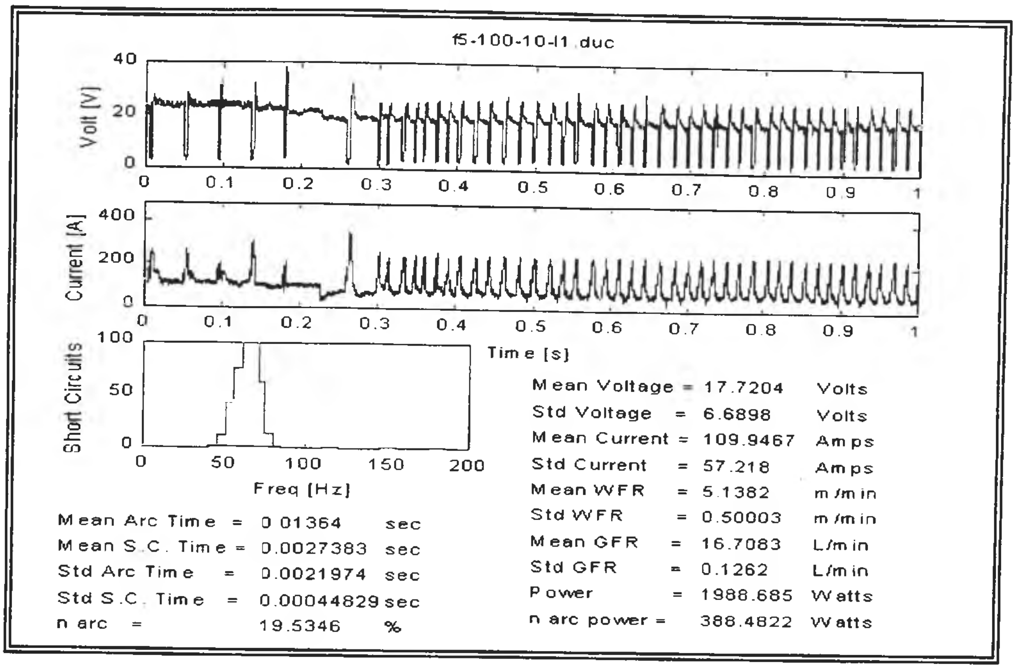

Plot F14-1

Sample f5-100-10-layer 1

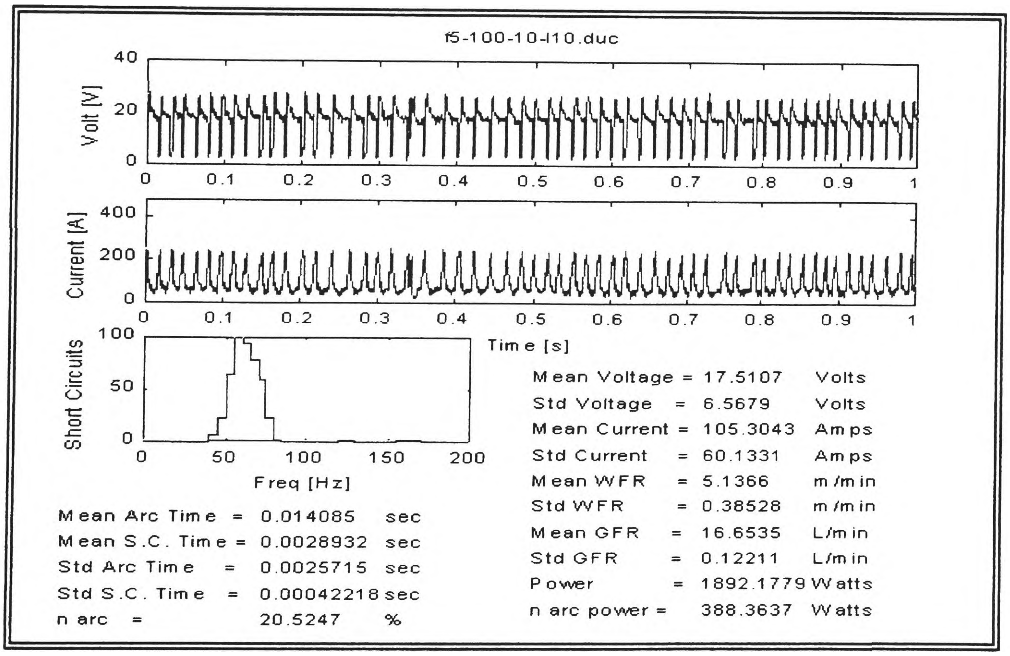

Plot F14-2

Sample f5-100-10-layer 10

Sample f5-110-10

Set Values	
Voltage [%]	110
Wire feed rate [m/min]	5
Travel speed [mm/sec]	10
Gas flow [l/min]	15

Weld Geometry		Visual Defects and Weld Property	
Weld height [mm]	12	Spatters	Yes
Weld width [mm]	5.4	Porosity	No
Stand-off at layer 1 [mm]	15	Excess material	No
Stand-off at layer 10 [mm]	15	Surface regularity [μm]	N/A
Temperature at layer 10 [deg.C]	265	Average hardness [HV]	N/A
Number of layers	10		

Figure F14-3

Sample f5-110-10 (top view)

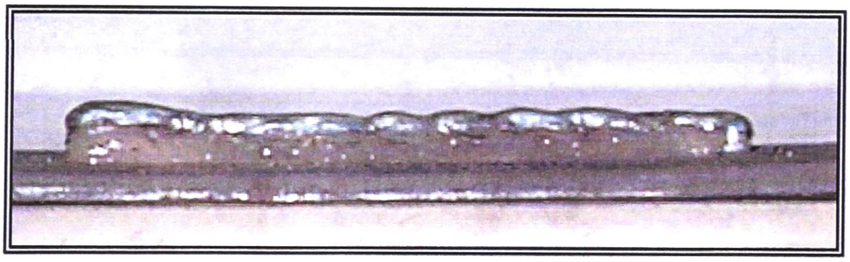

Figure F14-4

Sample f5-110-10 (front view)

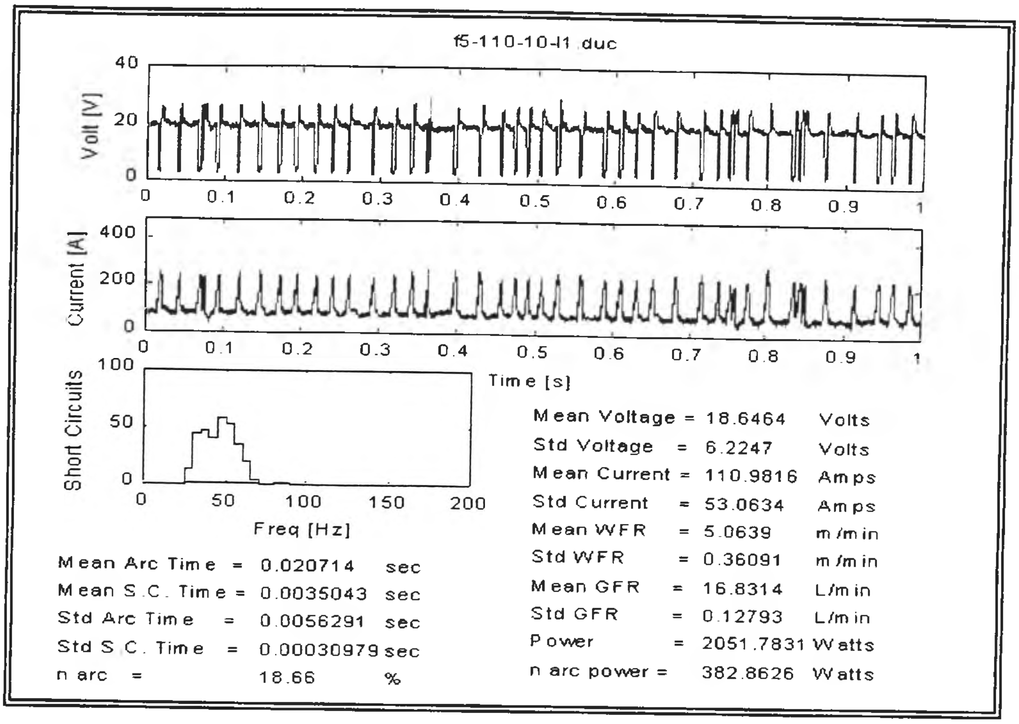

Plot F14-3

Sample f5-110-10-layer 1

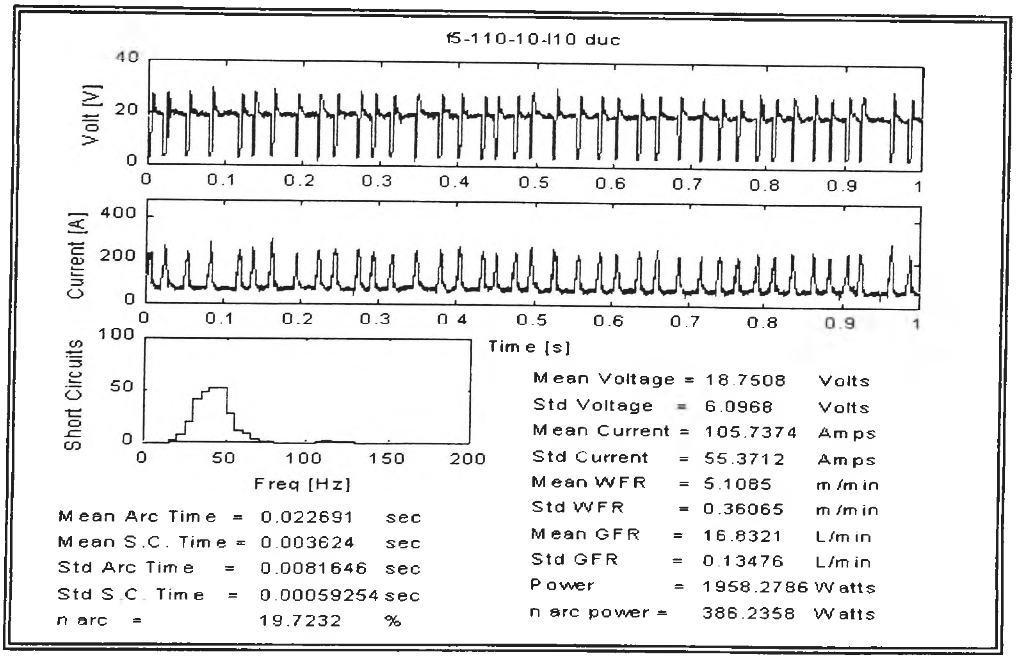

Plot F14-4

Sample f5-110-10-layer 10

Sample f5-120-10

Set Values	
Voltage [%]	120
Wire feed rate [m/min]	5
Travel speed [mm/sec]	10
Gas flow [l/min]	15

Weld Geometry		Visual Defects and Weld Property	
Weld height [mm]	11.35	Spatters	Yes
Weld width [mm]	5.8	Porosity	No
Stand-off at layer 1 [mm]	15	Excess material	No
Stand-off at layer 10 [mm]	15.5	Surface regularity [μm]	126.05
Temperature at layer 10 [deg.C]	305	Average hardness [HV]	165.7
Number of layers	10		

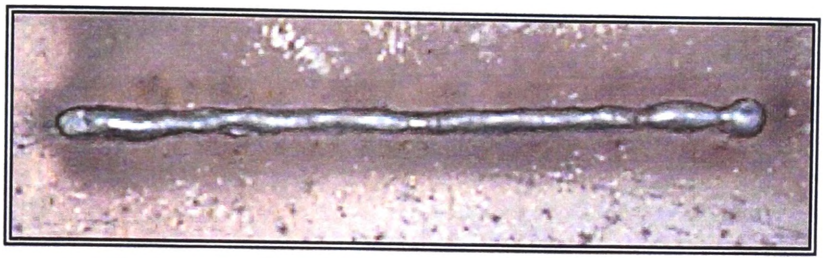

Figure F14-5

Sample f5-120-10 (top view)

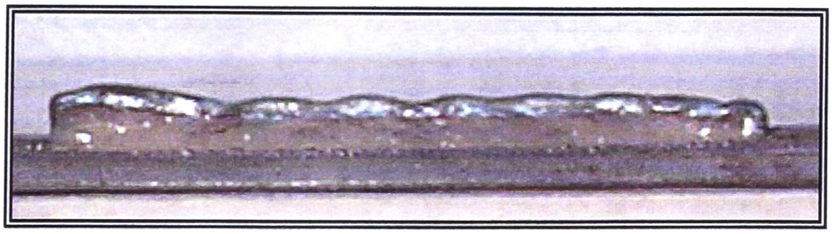

Figure F14-6

Sample f5-120-10 (front view)

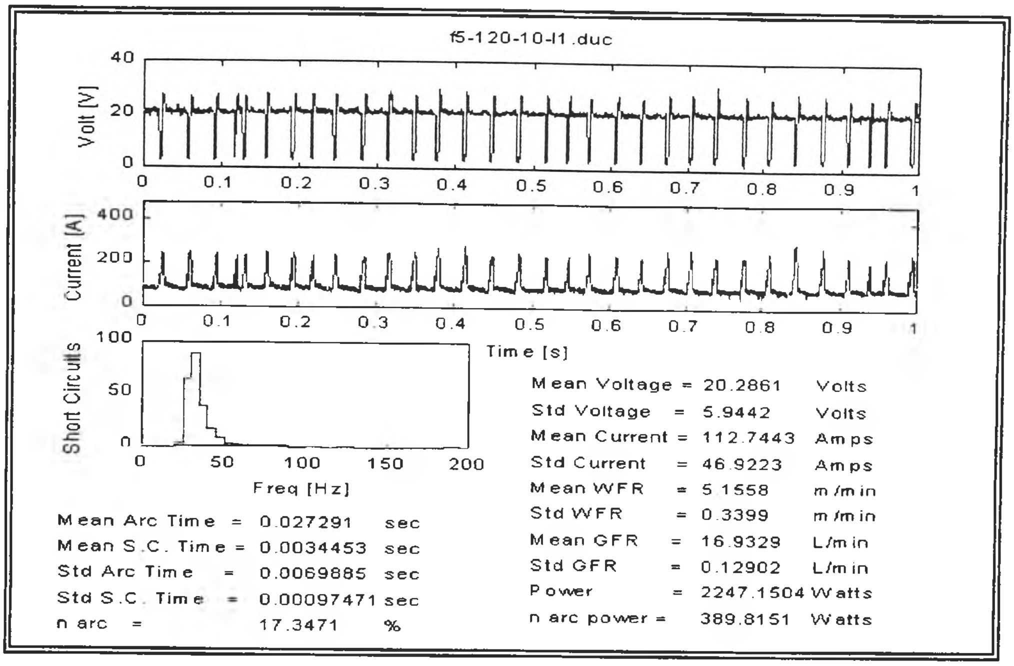

Plot F14-5

Sample f5-120-10-layer 1

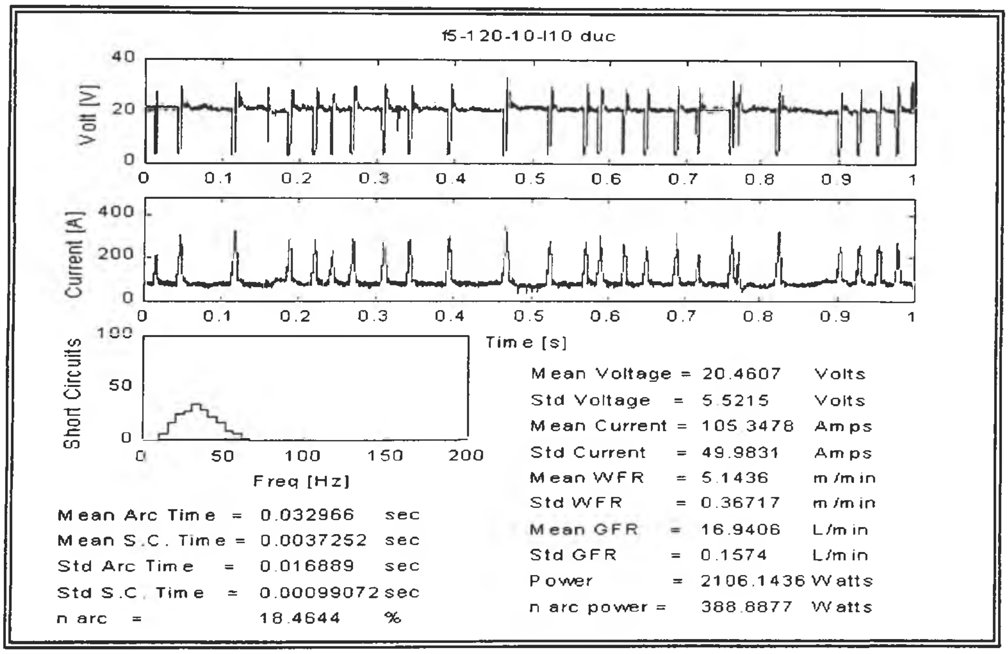

Plot F14-6

Sample f5-120-10-layer 10

F15 Wire Feed Rate of 6 m/min

Sample f6-100-10

Set Values	
Voltage [%]	100
Wire feed rate [m/min]	6
Travel speed [mm/sec]	10
Gas flow [l/min]	15

Weld Geometry		Visual Defects and Weld Property	
Weld height [mm]	11.64	Spatters	Yes
Weld width [mm]	6.2	Porosity	No
Stand-off at layer 1 [mm]	15	Excess material	No
Stand-off at layer 10 [mm]	15.5	Surface regularity [μm]	120.5
Temperature at layer 10 [deg.C]	235	Average hardness [HV]	170.5
Number of layers	10		

Figure F15-1

Sample f6-100-10 (top view)

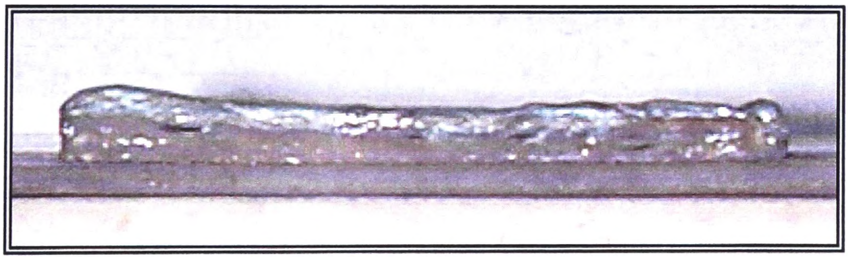

Figure F15-2

Sample f6-100-10 (front view)

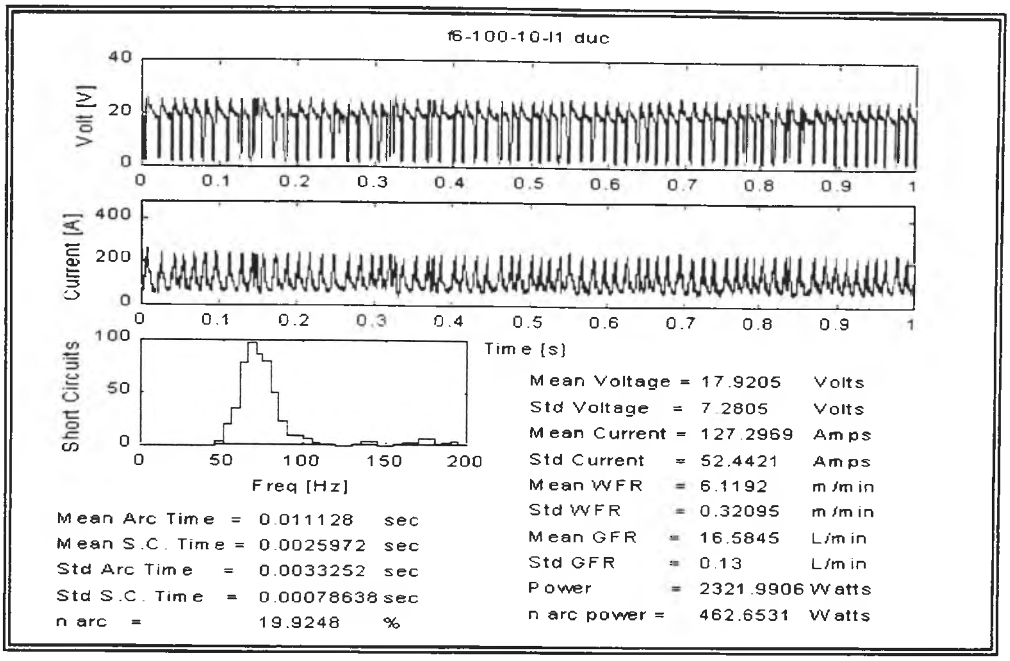

Plot F15-1

Sample f6-100-10-layer 1

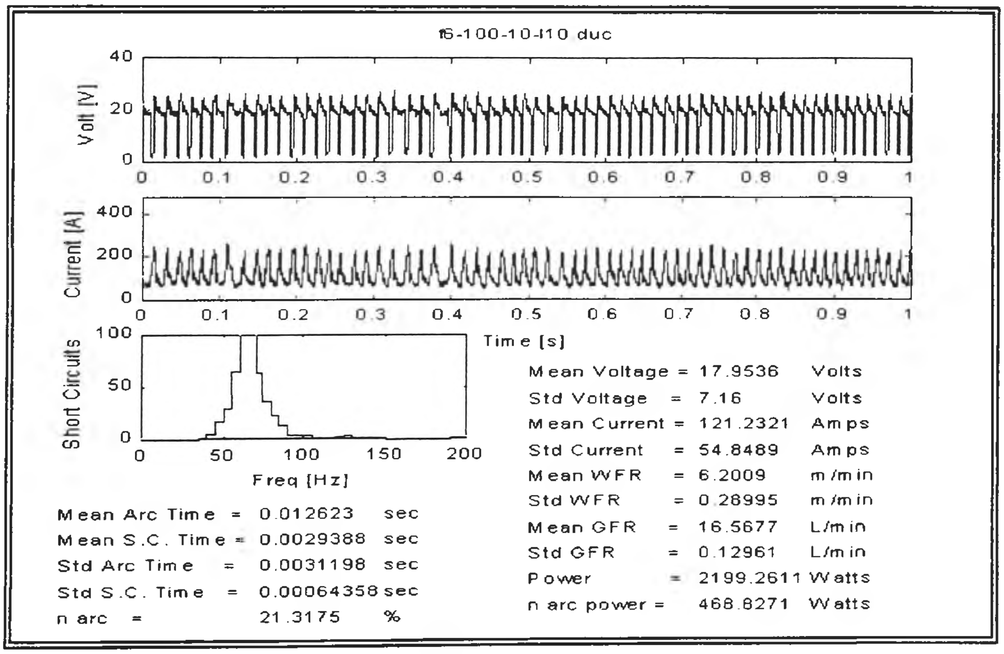

Plot F15-2

Sample f6-100-10-layer 10

Sample f6-110-10

Set Values	
Voltage [%]	110
Wire feed rate [m/min]	6
Travel speed [mm/sec]	10
Gas flow [l/min]	15

Weld Geometry		Visual Defects and Weld Property	
Weld height [mm]	11	Spatters	Yes
Weld width [mm]	6.5	Porosity	No
Stand-off at layer 1 [mm]	15	Excess material	No
Stand-off at layer 10 [mm]	15	Surface regularity [μm]	N/A
Temperature at layer 10 [deg.C]	260	Average hardness [HV]	N/A
Number of layers	10		

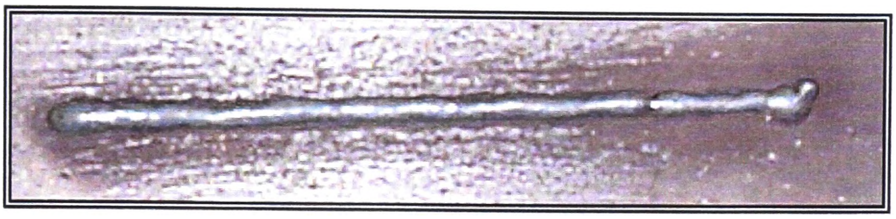

Figure F15-3

Sample f6-110-10 (top view)

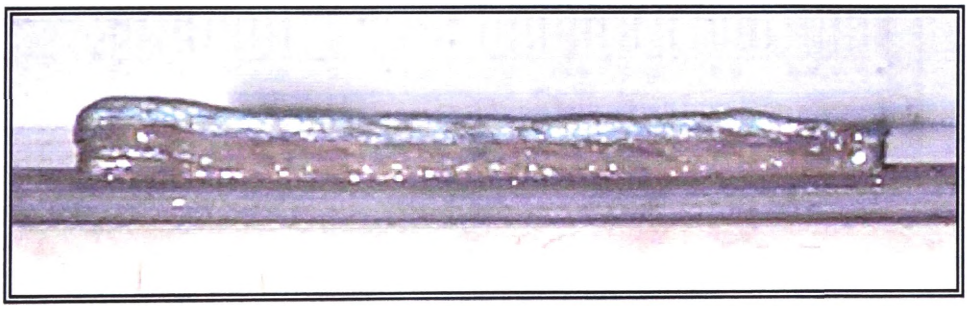

Figure F15-4

Sample f6-110-10 (front view)

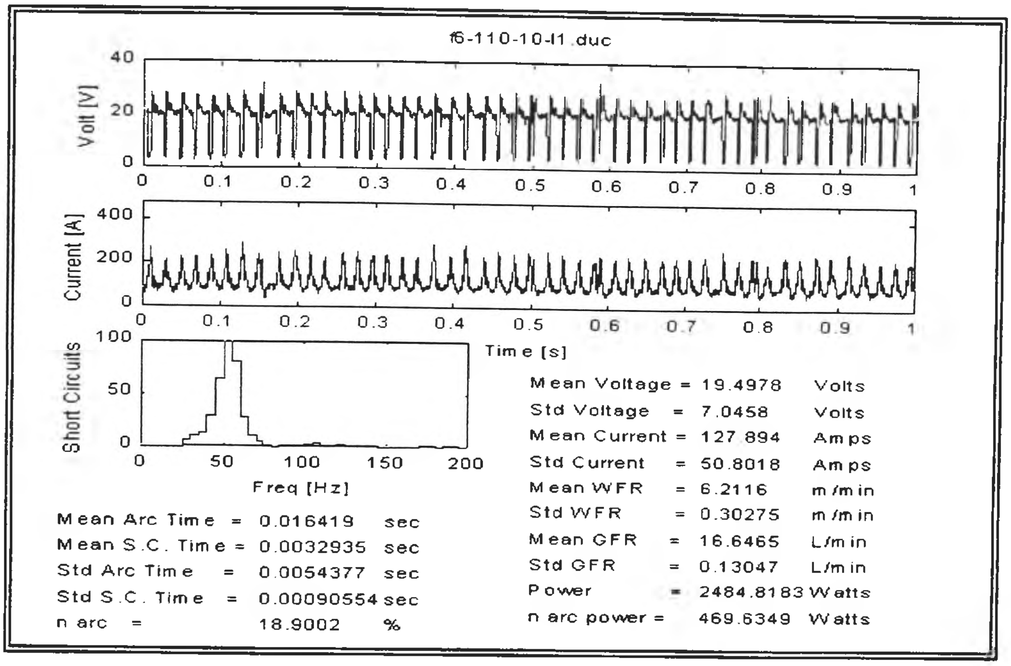

Plot F15-3

Sample f6-110-10-layer 1

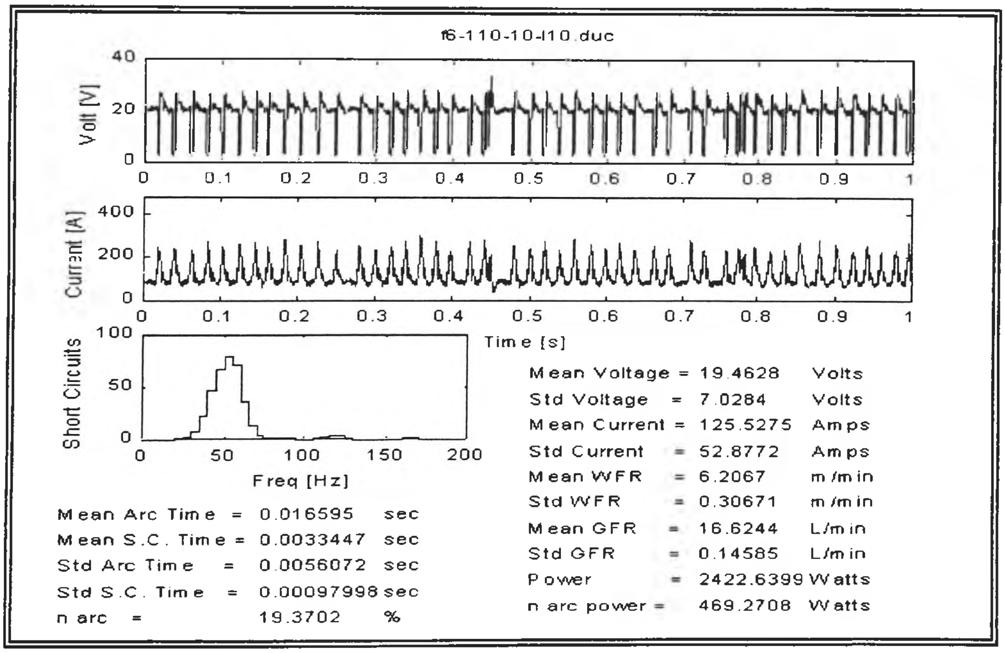

Plot F15-4

Sample f6-110-10-layer 10

Sample f6-120-10

Set Values	
Voltage [%]	120
Wire feed rate [m/min]	6
Travel speed [mm/sec]	10
Gas flow [l/min]	15

Weld Geometry		Visual Defects and Weld Property	
Weld height [mm]	10.5	Spatters	Yes
Weld width [mm]	7	Porosity	Yes
Stand-off at layer 1 [mm]	15	Excess material	No
Stand-off at layer 10 [mm]	15	Surface regularity [μm]	N/A
Temperature at layer 10 [deg.C]	275	Average hardness [HV]	N/A
Number of layers	10		

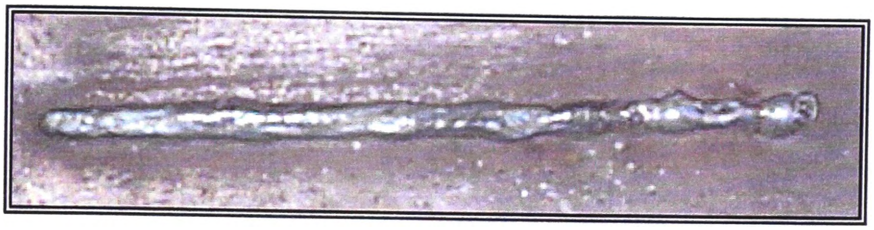

F15-5

Sample f6-120-10 (top view)

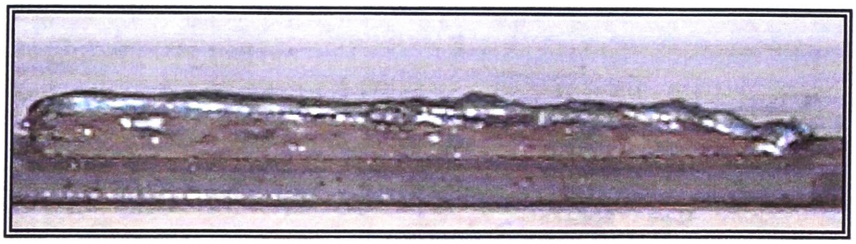

F15-6

Sample f6-120-10 (front view)

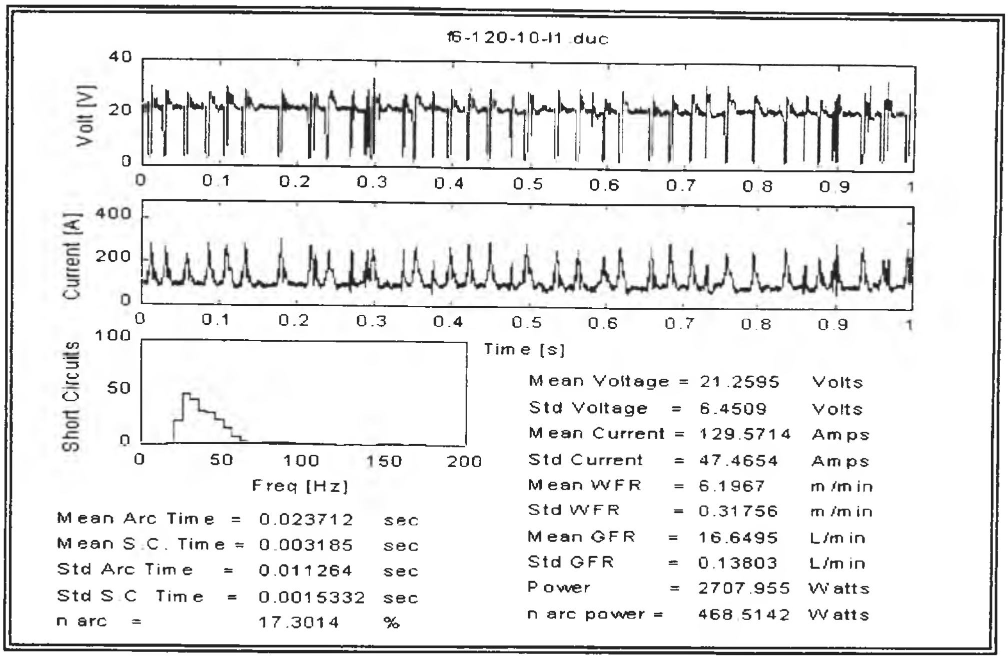

Plot F15-5

Sample f6-120-10-layer1

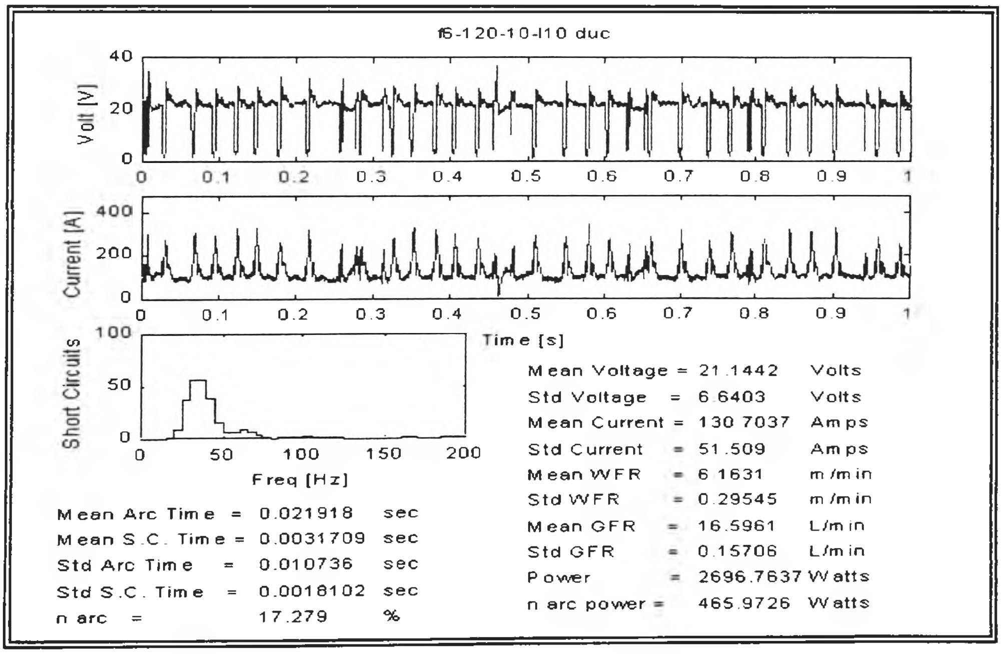

Plot F15-6

Sample f6-120-10-layer 10

Sample f6-130-10

Set Values	
Voltage [%]	130
Wire feed rate [m/min]	6
Travel speed [mm/sec]	10
Gas flow [l/min]	15

Weld Geometry		Visual Defects and Weld Property	
Weld height [mm]	10.3	Spatters	Yes
Weld width [mm]	7	Porosity	Yes
Stand-off at layer 1 [mm]	15	Excess material	No
Stand-off at layer 10 [mm]	15	Surface regularity [μm]	106.65
Temperature at layer 10 [deg.C]	300	Average hardness [HV]	166.3
Number of layers	10		

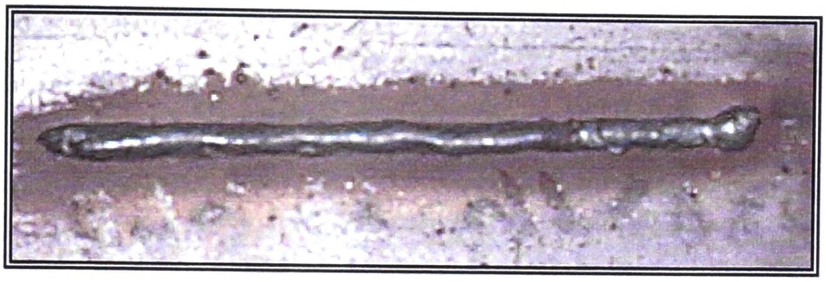

Figure F15-7

Sample f6-130-10 (top view)

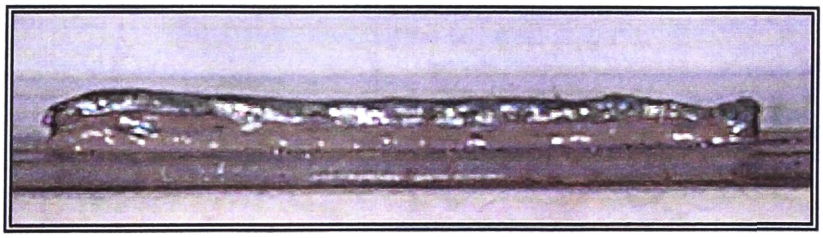

Figure F15-8

Sample f6-130-10 (front view)

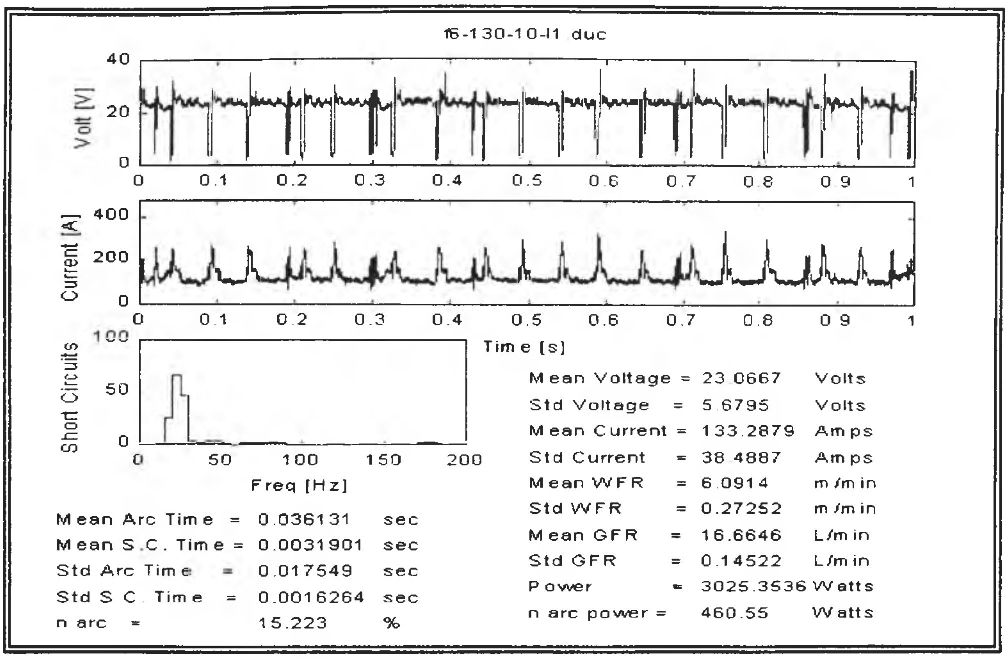

Plot F15-7

Sample f6-130-10-layer 1

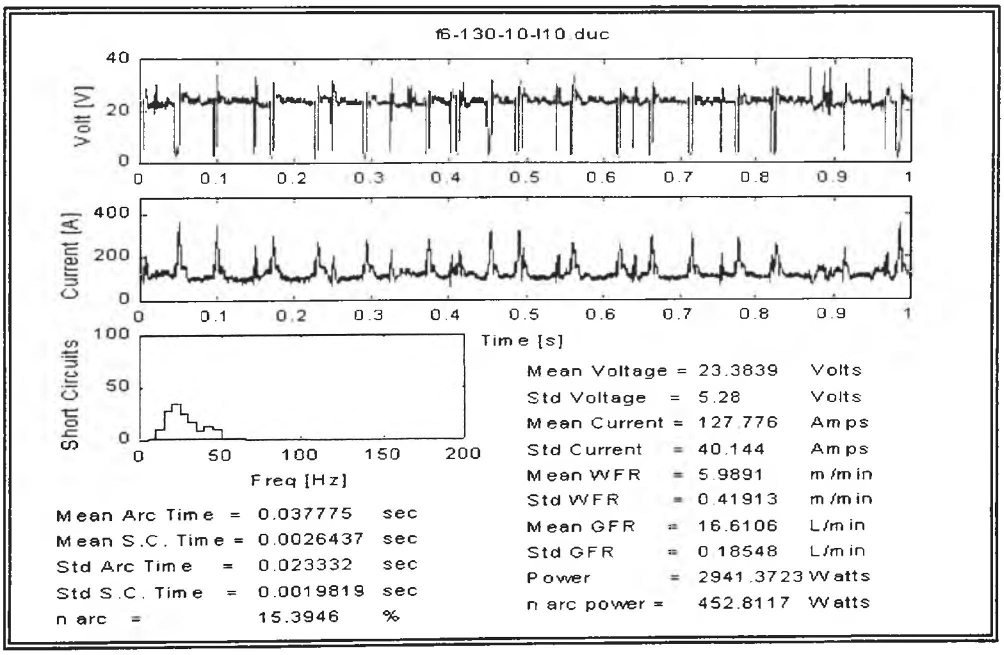

Plot F15-8

Sample f6-130-10-layer 10

F16 Wire Feed Rate of 7 m/min

Sample f7-100-10

Set Values	
Voltage [%]	100
Wire feed rate [m/min]	7
Travel speed [mm/sec]	10
Gas flow [l/min]	15

Weld Geometry		Visual Defects and Weld Property	
Weld height [mm]	12.2	Spatters	Yes
Weld width [mm]	7	Porosity	Yes
Stand-off at layer 1 [mm]	15	Excess material	No
Stand-off at layer 10 [mm]	17.5	Surface regularity [μm]	133.85
Temperature at layer 10 [deg.C]	265	Average hardness [HV]	167
Number of layers	10		

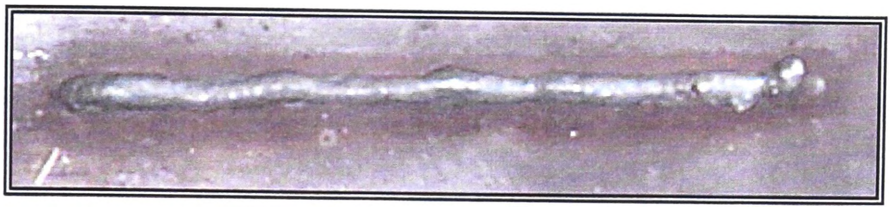

Figure F16-1

Sample f7-100-10 (top view)

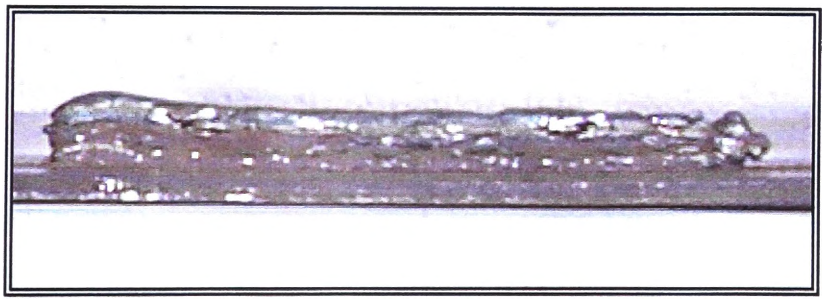

Figure F16-2

Sample f7-100-10 (front view)

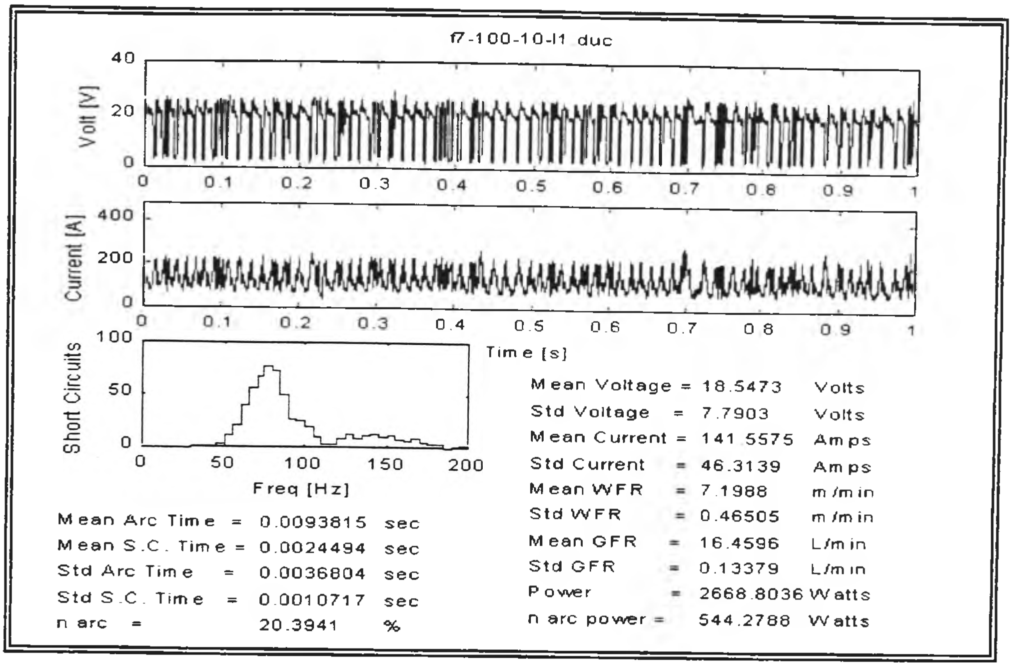

Plot F16-1

Sample f7-100-10-layer 1

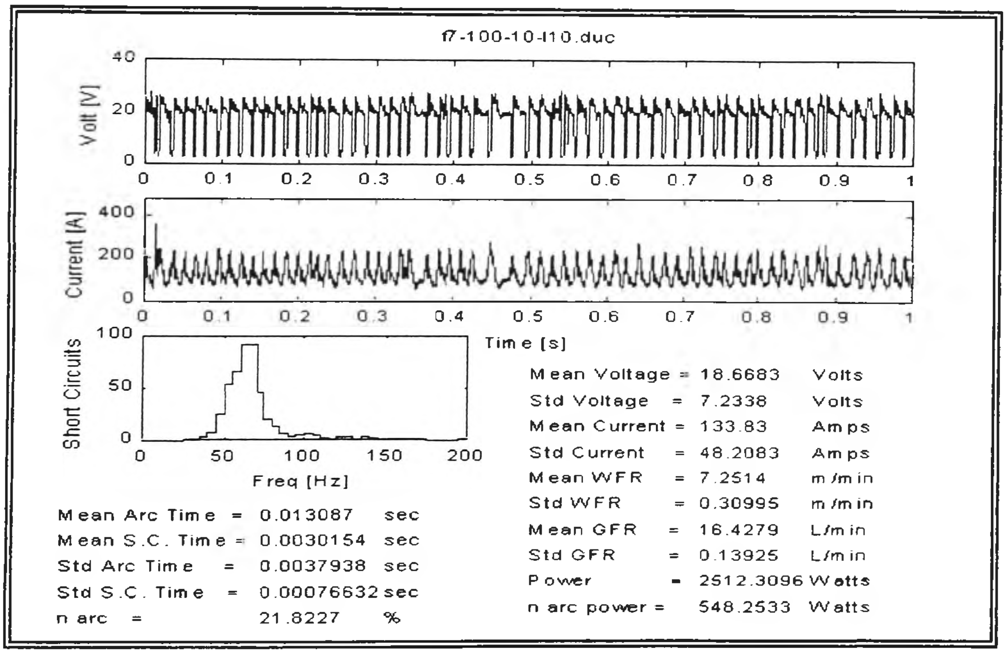

Plot F16-2

Sample f7-100-10-layer 10

Sample f7-110-10

Set Values	
Voltage [%]	110
Wire feed rate [m/min]	7
Travel speed [mm/sec]	10
Gas flow [l/min]	15

Weld Geometry		**Visual Defects and Weld Property**	
Weld height [mm]	12	Spatters	Yes
Weld width [mm]	7.2	Porosity	Yes
Stand-off at layer 1 [mm]	15	Excess material	No
Stand-off at layer 10 [mm]	15.5	Surface regularity [μm]	N/A
Temperature at layer 10 [deg.C]	280	Average hardness [HV]	N/A
Number of layers	10		

Figure F16-3

Sample f7-110-10 (top view)

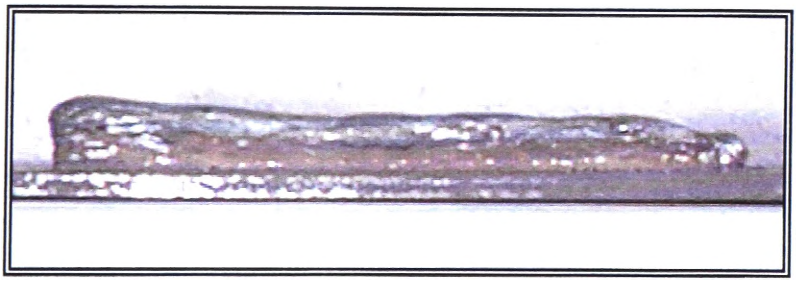

Figure F16-4

Sample f7-110-10 (front view)

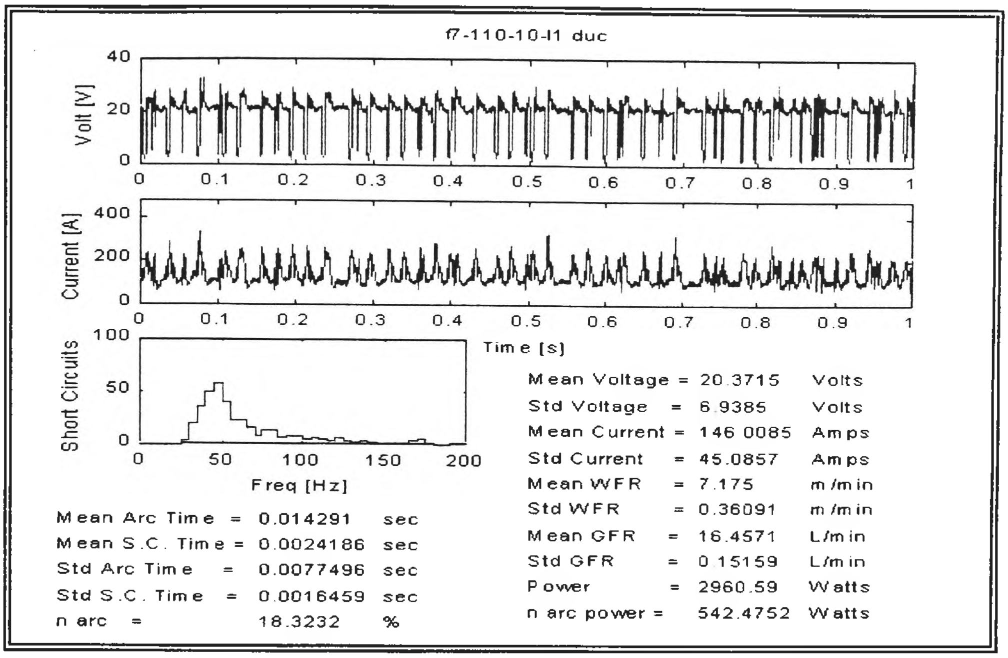

Plot F16-3

Sample f7-110-10-layer 1

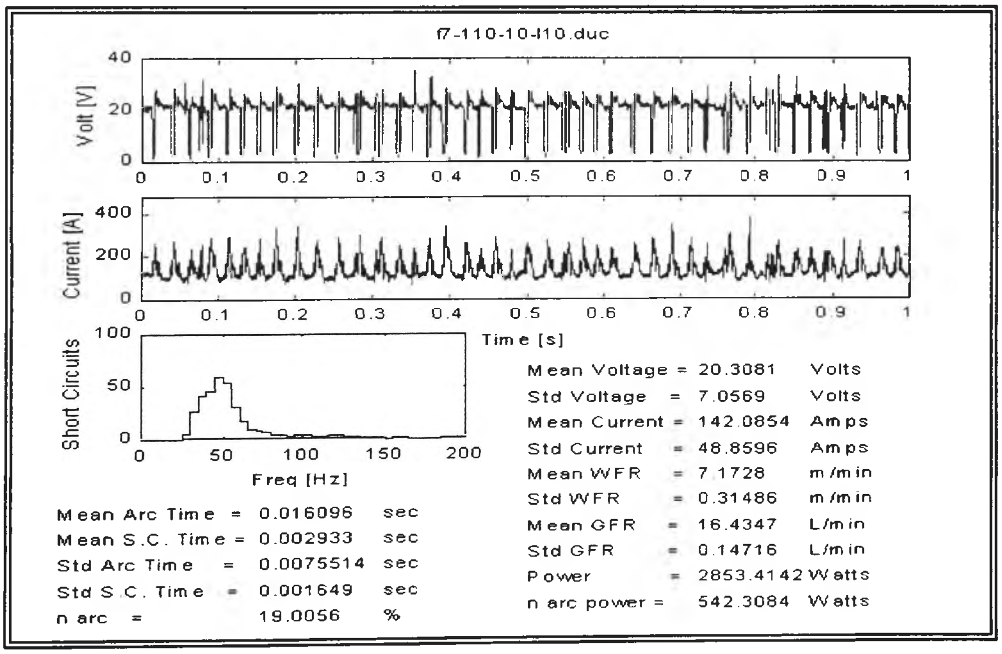

Plot F16-4

Sample f7-110-10-layer 10

Sample f7-120-10

Set Values	
Voltage [%]	120
Wire feed rate [m/min]	7
Travel speed [mm/sec]	10
Gas flow [l/min]	15

Weld Geometry		Visual Defects and Weld Property	
Weld height [mm]	11.5	Spatters	Yes
Weld width [mm]	8.5	Porosity	Yes
Stand-off at layer 1 [mm]	15	Excess material	No
Stand-off at layer 10 [mm]	16	Surface regularity [μm]	N/A
Temperature at layer 10 [deg.C]	312	Average hardness [HV]	N/A
Number of layers	10		

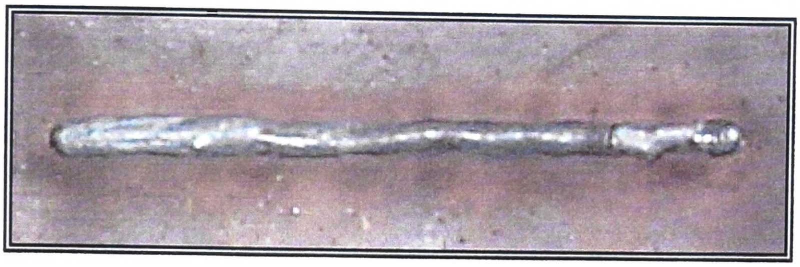

Figure F16-5

Sample f7-120-10 (top view)

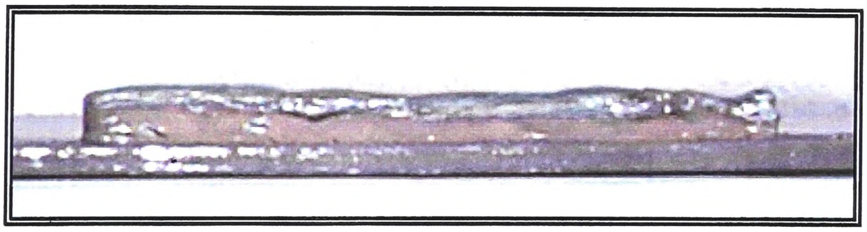

Figure F16-6

Sample f7-120-10 (front view)

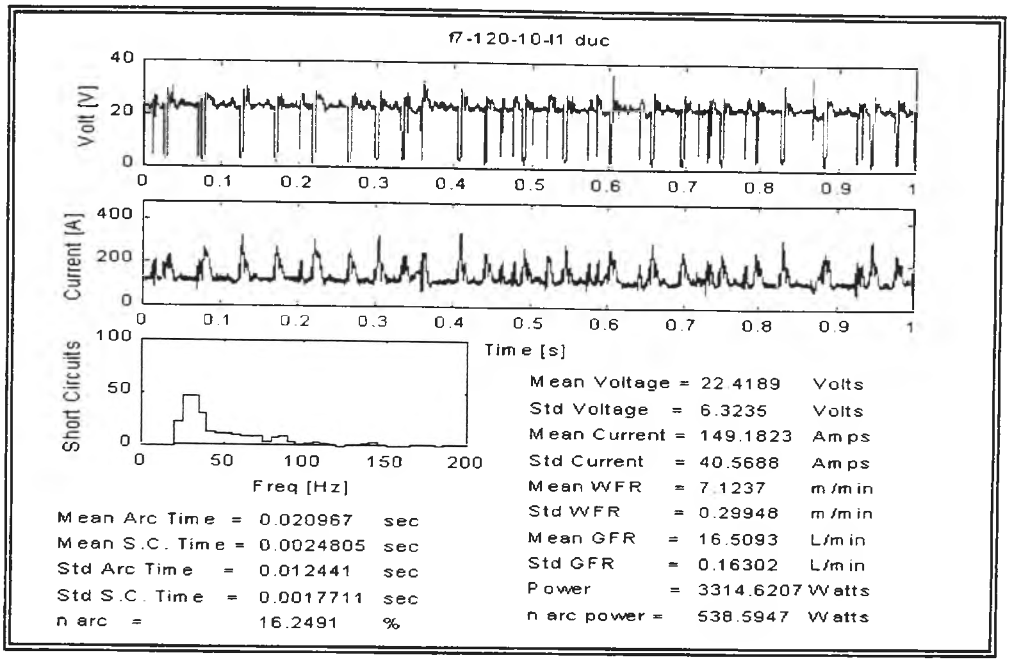

Plot F16-5

Sample f7-120-10-layer1

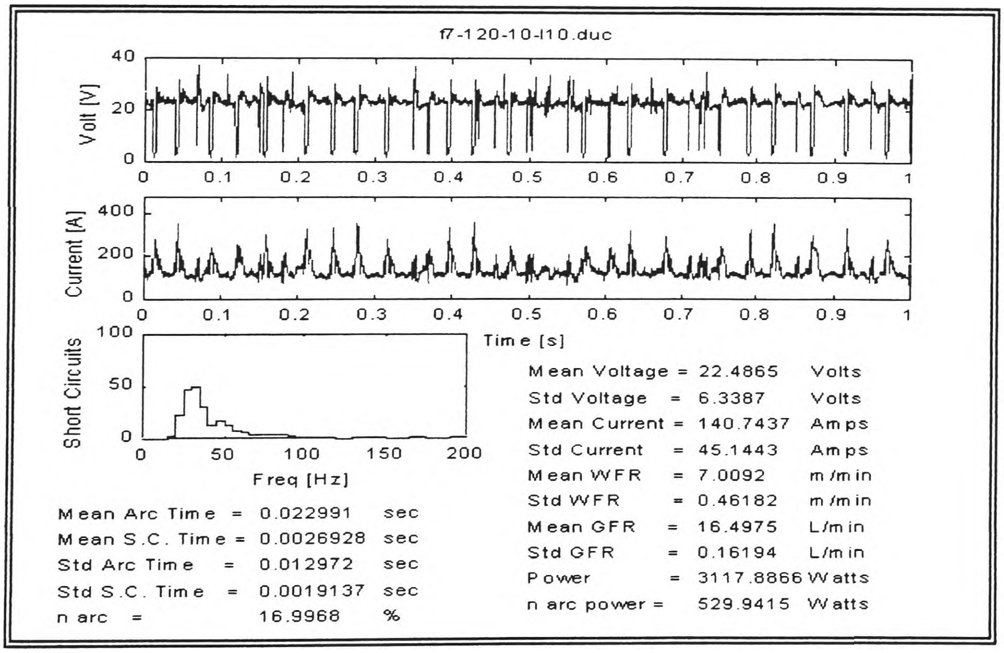

Plot F16-6

Sample f7-120-10-layer 10

Sample f7-130-10

Set Values	
Voltage [%]	130
Wire feed rate [m/min]	7
Travel speed [mm/sec]	10
Gas flow [l/min]	15

Weld Geometry		Visual Defects and Weld Property	
Weld height [mm]	11.24	Spatters	Yes
Weld width [mm]	8.6	Porosity	Yes
Stand-off at layer 1 [mm]	15	Excess material	Yes
Stand-off at layer 10 [mm]	16.5	Surface regularity [μm]	87.1
Temperature at layer 10 [deg.C]	323	Average hardness [HV]	160.4
Number of layers	10		

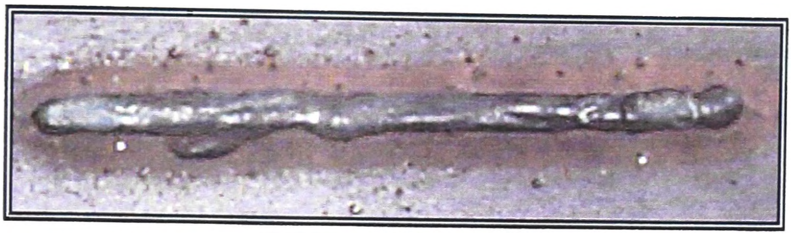

Figure F16-7

Sample f7-130-10 (top view)

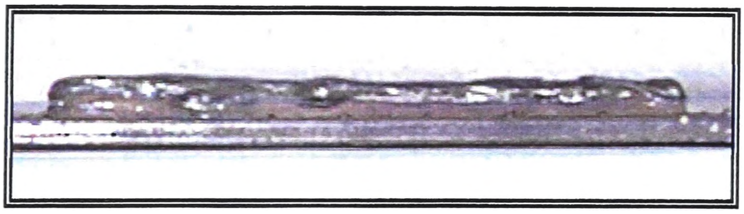

Figure F16-8

Sample f7-130-10 (front view)

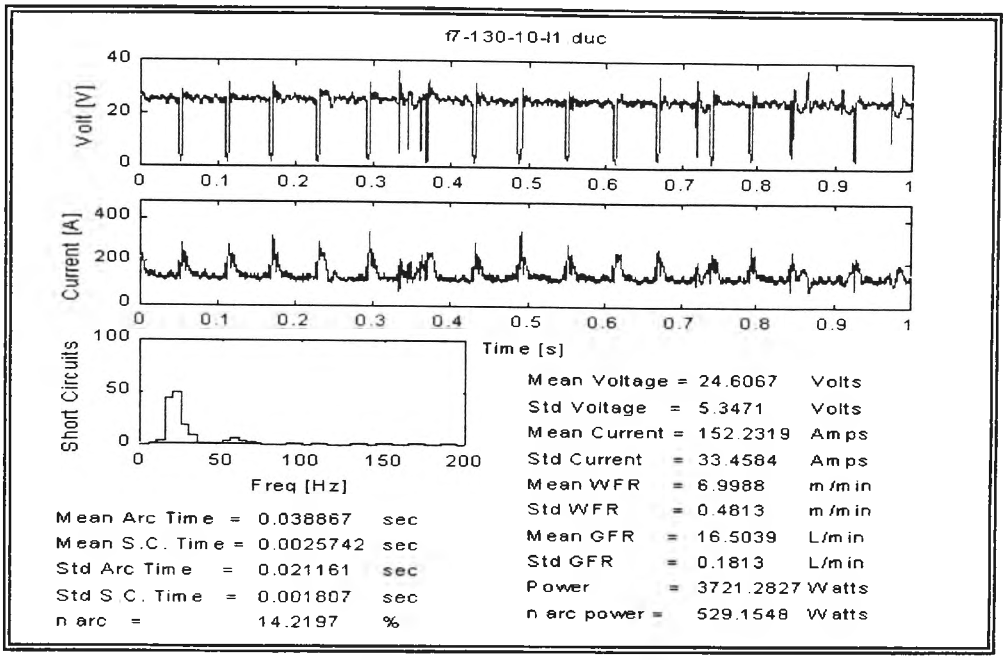

Plot F16-7

Sample f7-130-10-layer 1

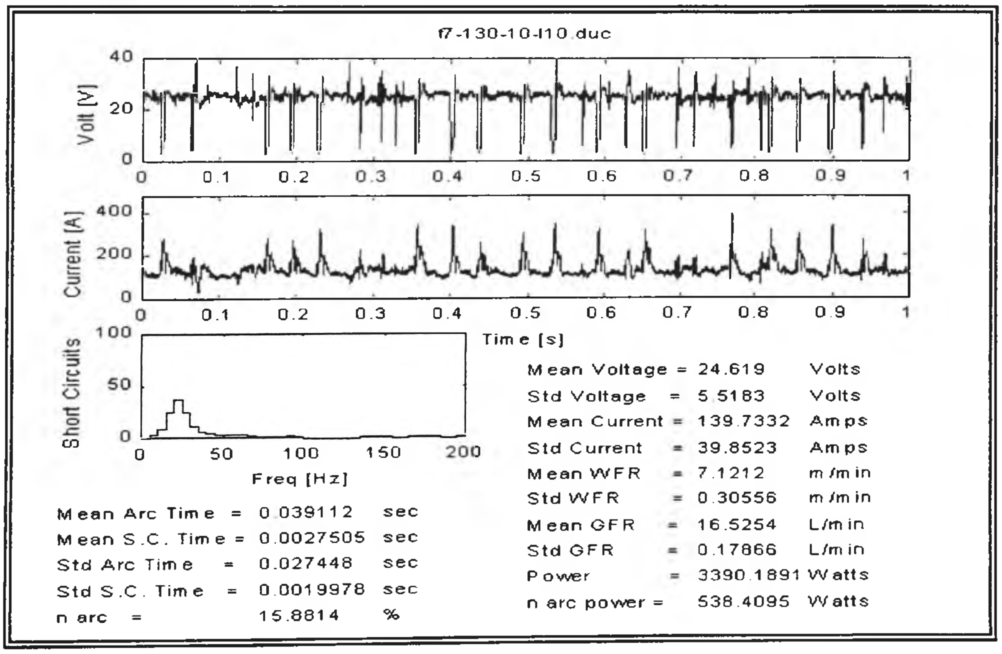

Plot F16-8

Sample f7-130-10-layer 10

F17 Wire Feed Rate of 8 m/min

Sample f8-100-10

Set Values	
Voltage [%]	100
Wire feed rate [m/min]	8
Travel speed [mm/sec]	10
Gas flow [l/min]	15

Weld Geometry		Visual Defects and Weld Property	
Weld height [mm]	14.45	Spatters	Yes
Weld width [mm]	7.4	Porosity	Yes
Stand-off at layer 1 [mm]	15	Excess material	No
Stand-off at layer 10 [mm]	16.5	Surface regularity [μm]	60.7
Temperature at layer 10 [deg.C]	290	Average hardness [HV]	166
Number of layers	10		

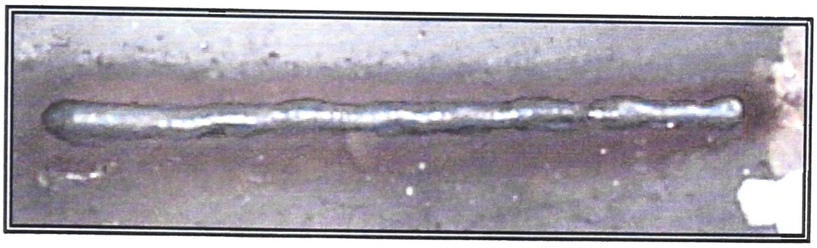

Figure F17-1

Sample f8-100-10 (top view)

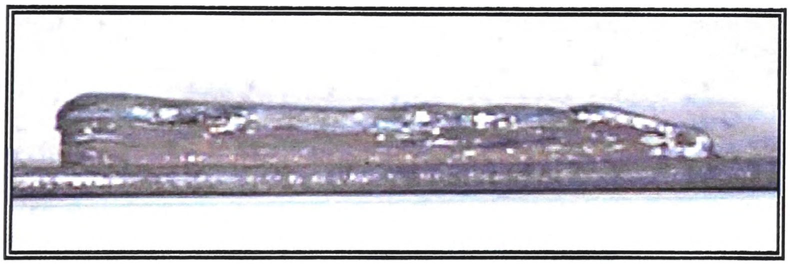

Figure F7-2

Sample f8-100-10 (front view)

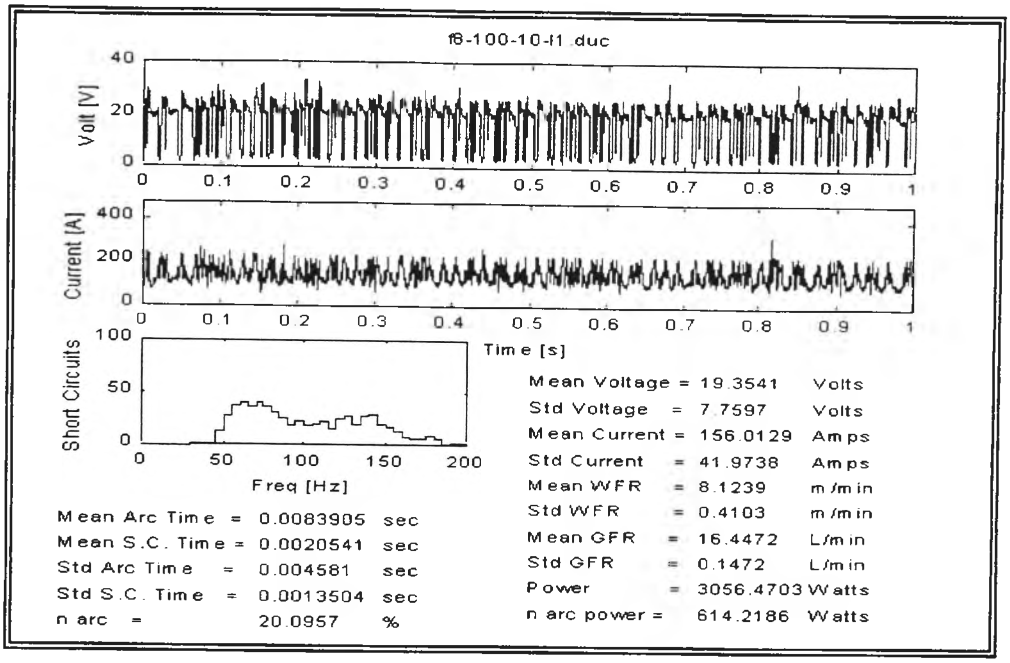

Plot F17-1

Sample f8-100-10-layer 1

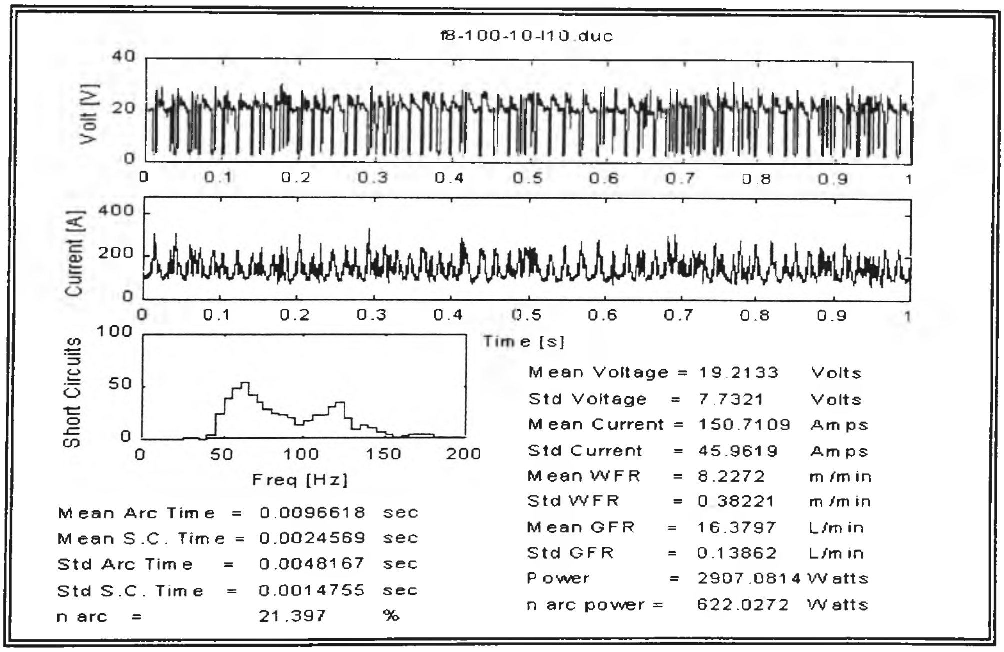

Plot F17-2

Sample f8-100-10-layer 10

F18 Wire Feed Rate of 9 m/min

Sample f9-100-10

Set Values	
Voltage [%]	100
Wire feed rate [m/min]	9
Travel speed [mm/sec]	10
Gas flow [l/min]	15

Weld Geometry		Visual Defects and Weld Property	
Weld height [mm]	14.21	Spatters	Yes
Weld width [mm]	8	Porosity	Yes
Stand-off at layer 1 [mm]	15	Excess material	Yes
Stand-off at layer 10 [mm]	17.5	Surface regularity [μm]	53.75
Temperature at layer 10 [deg.C]	302	Average hardness [HV]	164.3
Number of layers	10		

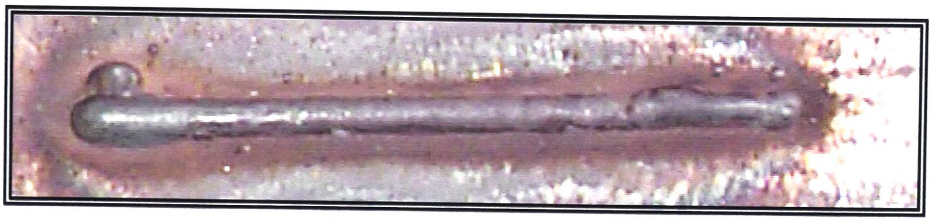

Figure F18-1

Sample f9-100-10 (top view)

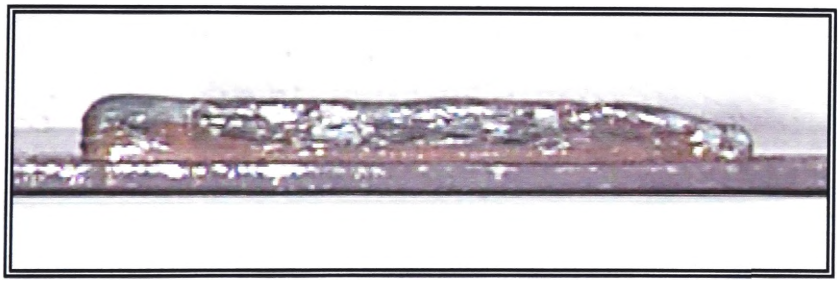

Figure F18-2

Sample f9-100-10 (front view)

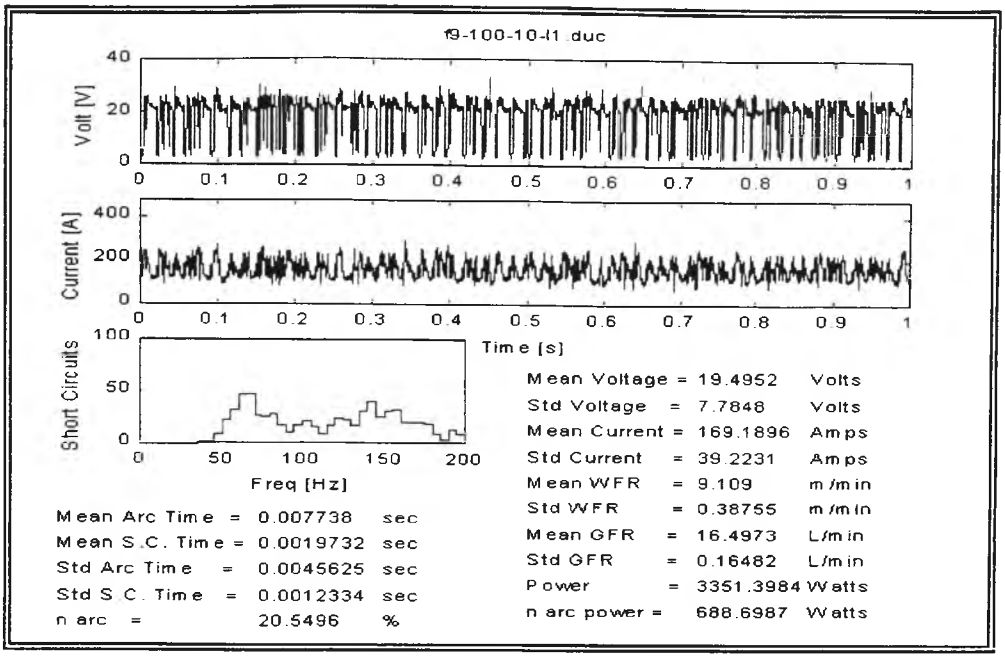

Plot F18-1

Sample f9-100-10-layer 1

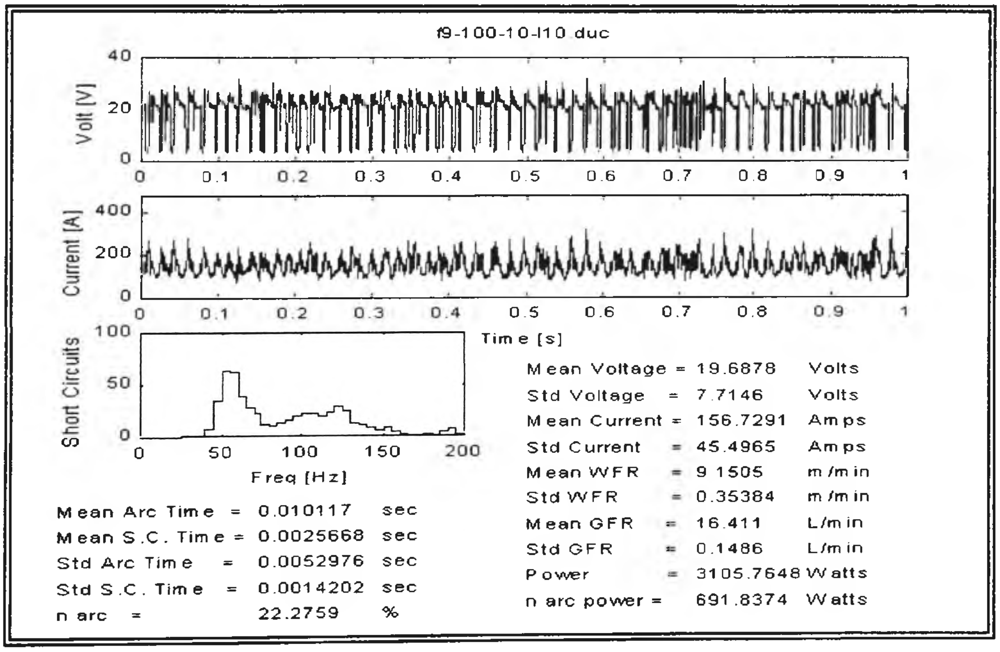

Plot F18-2

Sample f9-100-10-layer 10

Appendix G Hardness Data

Sample Code	vg Voltag [V]	Upper [VHN]	Middle [VHN]	Lower [VHN]	Average [VHN]	Base [VHN]
f1-75-05	14.1	169	167	165	167	146
f1-100-05	15.2	166	162	163	164	146
f1-110-05	16.5	162	154	156	157	140
f2-75-05	14.1	168	166	165	166	143
f2-95-05	14.6	167	165	163	165	148
f2-100-05	15.2	165	160	168	164	153
f2-105-05	15.9	168	163	161	164	146
f2-110-05	16.6	167	165	164	165	143
f2-115-05	17.6	165	162	160	162	145
f2-120-05	18.2	163	157	160	160	146
f2-135-05	20.2	159	154	156	156	148
f2-150-05	21.1	149	150	148	149	153
f3-75-05	14.1	157	157	153	156	152
f3-100-05	15.9	156	150	160	155	149
f3-150-05	21.1	152	152	152	152	155
f4-75-05	14.8	155	154	150	153	145
f4-150-05	21.2	150	151	152	151	147
f5-75-05	15.5	158	153	151	154	148
f5-125-05	21.1	152	151	151	151	151
f6-75-05	15.4	158	150	150	153	154
f6-120-05	21.4	153	149	147	150	150
f7-75-05	14.6	159	154	149	154	158
f7-120-05	22.6	153	153	151	152	147
f8-100-05	19.2	150	151	149	150	153
f9-100-05	19.2	153	148	146	149	146
Average upper			=	158.99	HV	
Average middle			=	155.95	HV	
Average Lower			=	155.53	HV	
Overal Average			=	156.10	HV	
Average Base			=	148.44	HV	

Sample Code	Avg Volta [V]	Upper [VHN]	Middle [VHN]	Lower [VHN]	Average [VHN]	Base [VHN]
f1-100-10	15.6	189.0	185.9	183.0	186.0	145.2
f2-75-10	14.3	184.0	180.0	182.0	182.0	145.7
f2-150-10	21.2	166.9	163.0	161.3	163.7	143.0
f3-75-10	14.2	186.0	180.0	182.0	182.7	149.1
f3-150-10	20.7	168.0	163.6	162.4	164.7	149.3
f4-75-10	14.6	182.0	174.0	174.0	176.7	145.0
f4-130-10	19.3	167.0	164.3	159.7	163.7	150.3
f5-100-10	17.6	174.0	171.0	169.0	171.3	158.0
f5-120-10	20.4	168.0	165.0	164.0	165.7	152.6
f6-100-10	17.9	171.0	172.4	168.0	170.5	151.7
f6-130-10	23.2	168.0	167.0	164.0	166.3	150.0
f7-100-10	18.6	168.0	165.0	168.0	167.0	151.9
f7-130-10	24.6	162.0	157.2	162.0	160.4	148.5
f8-100-10	19.3	168.0	164.0	166.0	166.0	147.0
f9-100-10	19.6	167.0	162.0	164.0	164.3	143.2
Average upper			=	172.59	HV	
Average middle			=	168.96	HV	
Average Lower			=	168.63	HV	
Overal Average			=	170.06	HV	
Average Base			=	148.70	HV	

Appendix H

Solid Block Programs

H1 F BLOCK.PRG

```
%%%
  VERSION:1
  LANGUAGE:ENGLISH
%%%

MODULE F_BLOCK
  CONST robtarget pwblock3:=[[629.71,-
28.69,1037.24],[0.350873,0.028219,0.935615,-0.026775],[-1,-
1,0,0],[9E+09,9E+09,9E+09,9E+09,9E+09,9E+09]];
  CONST robtarget p4:=[[629.75,-28.69,1037.3],[0.350925,0.02824,0.935595,-
0.026774],[-1,-1,0,0],[9E+09,9E+09,9E+09,9E+09,9E+09,9E+09]];
  VAR num iincr:=0;
  VAR num jincr:=0;
  VAR robtarget
pwinit2:=[[866.92,378.26,831.78],[0.350986,0.028254,0.935572,-0.026768],[0,-
1,0,0],[9E+09,9E+09,9E+09,9E+09,9E+09,9E+09]];
  VAR robtarget
pwinit1:=[[866.91,378.26,831.78],[0.350976,0.028264,0.935575,-0.02677],[0,-
1,0,0],[9E+09,9E+09,9E+09,9E+09,9E+09,9E+09]];
  VAR num jmax:=0;
```

```
VAR num imax:=0;
VAR robtarget
poverhead:=[[935.57,308.85,1158.55],[0.350803,0.028535,0.935634,-0.0267],[0,-
1,0,0],[9E+09,9E+09,9E+09,9E+09,9E+09,9E+09]];
VAR robtarget
pwblock2:=[[866.92,378.27,831.78],[0.350979,0.028258,0.935574,-
0.026766],[0,-1,0,0],[9E+09,9E+09,9E+09,9E+09,9E+09,9E+09]];
VAR robtarget
pwblock1:=[[866.92,378.26,831.78],[0.350983,0.028267,0.935573,-
0.026758],[0,-1,0,0],[9E+09,9E+09,9E+09,9E+09,9E+09,9E+09]];

PROC makeblock()
  FOR i FROM 1 TO imax DO
    TPErase;
    TPWrite "vertical layer:"\Num:=i;
    pwblock1:=pwinit1;
    pwblock2:=pwinit2;
    FOR j FROM 1 TO jmax DO
      TPWrite "horizontal weld pass:"\Num:=j;
      makeweld;
      pwblock1.trans.x:=pwblock1.trans.x+jincr;
      pwblock2.trans.x:=pwblock2.trans.x+jincr;
    ENDFOR
    pwinit1.trans.z:=pwinit1.trans.z+iincr;
```

```
    pwinit2.trans.z:=pwinit2.trans.z+iincr;
    poverhead.trans.z:=poverhead.trans.z+iincr;
  ENDFOR
ENDPROC

PROC makeweld()
  MoveJ poverhead,v100,z200,tool0;
  ArcL\On,pwblock1,v1000,sd2_frank,wd_frank,wvd_mike,z50,tool0;
  ArcL\Off,pwblock2,v50,sd2_frank,wd_frank,wvd_mike,fine,tool0;
  MoveJ poverhead,v100,z200,tool0;
ENDPROC

PROC main()
  TPErase;
  TPReadNum imax,"no. vertical layers:";
  TPReadNum jmax,"no. horizontal welds:";
  TPReadNum iincr,"vertical increment (mm):";
  TPReadNum jincr,"horizontal increment (mm):";
  poverhead:=[[1024.89,-290.95,855.38],[0.355091,0.028284,0.93402,-
0.026801],[-1,0,-1,0],[9E+09,9E+09,9E+09,9E+09,9E+09,9E+09]];
  pwinit1:=[[1024.88,-290.94,824.77],[0.355161,0.028312,0.933992,-
0.026808],[-1,0,-1,0],[9E+09,9E+09,9E+09,9E+09,9E+09,9E+09]];
  pwinit2:=[[1024.92,-190.08,824.35],[0.355239,0.028479,0.933959,-
0.026764],[-1,0,-1,0],[9E+09,9E+09,9E+09,9E+09,9E+09,9E+09]];
```

```
    MoveJ p4,v1000,z200,tool0;
    makeblock;
    MoveJ p4,v1000,z200,tool0;
  ENDPROC
ENDMODULE
```

H2 FBLOCKEC.PRG

```
%%%
  VERSION:1
  LANGUAGE:ENGLISH
%%%

MODULE F_BLOCEC
  VAR bool first:=FALSE;
  VAR bool dir:=FALSE;
  VAR bool last:=FALSE;
  CONST robtarget pHome:=[[618.38,-88.51,287.59],[0.00567,-
0.690109,0.723522,-0.015284],[-1,-
1,0,0],[9E+09,9E+09,9E+09,9E+09,9E+09,9E+09]];
  VAR num iincr:=0;
  VAR num hincr:=0;
  VAR num hincrx:=0;
  VAR num hincry:=0;
  VAR num crndist:=0;
  VAR num crndistx:=0;
  VAR num crndisty:=0;
  VAR robtarget
pwinit2:=[[866.92,378.26,831.78],[0.350986,0.028254,0.935572,-0.026768],[0,-
1,0,0],[9E+09,9E+09,9E+09,9E+09,9E+09,9E+09]];
```

```
VAR robtarget
pwinit1:=[[866.91,378.26,831.78],[0.350976,0.028264,0.935575,-0.02677],[0,-
1,0,0],[9E+09,9E+09,9E+09,9E+09,9E+09,9E+09]];
VAR robtarget
pwinit2c:=[[866.92,378.26,831.78],[0.350986,0.028254,0.935572,-0.026768],[0,-
1,0,0],[9E+09,9E+09,9E+09,9E+09,9E+09,9E+09]];
VAR robtarget
pwinit1c:=[[866.91,378.26,831.78],[0.350976,0.028264,0.935575,-0.02677],[0,-
1,0,0],[9E+09,9E+09,9E+09,9E+09,9E+09,9E+09]];
VAR num hmax:=0;
VAR num imax:=0;
VAR robtarget
poverhead:=[[935.57,308.85,1158.55],[0.350803,0.028535,0.935634,-0.0267],[0,-
1,0,0],[9E+09,9E+09,9E+09,9E+09,9E+09,9E+09]];
VAR robtarget
pwblock2:=[[866.92,378.27,831.78],[0.350979,0.028258,0.935574,-
0.026766],[0,-1,0,0],[9E+09,9E+09,9E+09,9E+09,9E+09,9E+09]];
VAR robtarget
pwblock1:=[[866.92,378.26,831.78],[0.350983,0.028267,0.935573,-
0.026758],[0,-1,0,0],[9E+09,9E+09,9E+09,9E+09,9E+09,9E+09]];
VAR robtarget
pwblock2c:=[[866.92,378.27,831.78],[0.350979,0.028258,0.935574,-
0.026766],[0,-1,0,0],[9E+09,9E+09,9E+09,9E+09,9E+09,9E+09]];
```

```
 VAR robtarget
pwblock1c:=[[866.92,378.26,831.78],[0.350983,0.028267,0.935573,-
0.026758],[0,-1,0,0],[9E+09,9E+09,9E+09,9E+09,9E+09,9E+09]];
 PERS welddata wldn:=[5,150,10,0,5,75,2];
 PERS seamdata smdn:=[0.1,0.1,150,10,0,5,5,25,150,10,0,2,0.5,1,150,10];
 PERS welddata wldc:=[5,150,10,0,5,75,2];
 PERS seamdata smdc:=[0.1,0.1,150,10,0,5,5,25,150,10,0,2,0.5,1,150,10];
 PERS weavedata wvdz:=[0,0,0,0,0,0,0,0,0,0,0,0,0,0,0];

 PROC makeblock()
  FOR i FROM 1 TO imax DO
   TPErase;
   TPWrite "vertical layer:"\Num:=i;
   pwblock1:=pwinit1;
   pwblock2:=pwinit2;
   pwblock1c:=pwinit1c;
   pwblock2c:=pwinit2c;
   dir:=TRUE;
   first:=TRUE;
   last:=FALSE;
   MoveJ poverhead,v100,z200,weldgun\WObj:=wbench;
   FOR j FROM 1 TO hmax DO
    TPWrite "horizontal weld pass:"\Num:=j;
    IF j=hmax last:=TRUE;
```

```
      makeweld;
      first:=FALSE;
      dir:=NOT dir;
      pwblock1:=Offs(pwblock1,hincrx,hincry,0);
      pwblock2:=Offs(pwblock2,hincrx,hincry,0);
      pwblock1c:=Offs(pwblock1c,hincrx,hincry,0);
      pwblock2c:=Offs(pwblock2c,hincrx,hincry,0);
    ENDFOR
    MoveJ poverhead,v100,z200,weldgun\WObj:=wbench;
    pwinit1:=Offs(pwinit1,0,0,iincr);
    pwinit2:=Offs(pwinit2,0,0,iincr);
    pwinit1c:=Offs(pwinit1c,0,0,iincr);
    pwinit2c:=Offs(pwinit2c,0,0,iincr);
    poverhead:=Offs(poverhead,0,0,iincr);
  ENDFOR
ENDPROC

PROC makeweld()
  VAR robtarget p2weld:=[[1023.43,-
148.28,824.36],[0.355241,0.028462,0.933959,-0.026735],[-1,0,-
1,0],[9E+09,9E+09,9E+09,9E+09,9E+09,9E+09]];
  VAR robtarget p1weld:=[[1023.44,-
148.28,824.36],[0.355237,0.028455,0.933961,-0.026741],[-1,0,-
1,0],[9E+09,9E+09,9E+09,9E+09,9E+09,9E+09]];
```

```
VAR robtarget p2weldc:=[[1023.43,-
148.28,824.36],[0.355241,0.028462,0.933959,-0.026735],[-1,0,-
1,0],[9E+09,9E+09,9E+09,9E+09,9E+09,9E+09]];
VAR robtarget p1weldc:=[[1023.44,-
148.28,824.36],[0.355237,0.028455,0.933961,-0.026741],[-1,0,-
1,0],[9E+09,9E+09,9E+09,9E+09,9E+09,9E+09]];

IF dir=TRUE THEN
  p1weld:=pwblock1;
  p2weld:=pwblock2;
  p1weldc:=pwblock1c;
  p2weldc:=pwblock2c;
ELSE
  p1weld:=pwblock2;
  p2weld:=pwblock1;
  p1weldc:=pwblock2c;
  p2weldc:=pwblock1c;
ENDIF
IF first THEN
  ArcL\On,p1weld,v50,smdc,wldc,wvdz,fine,weldgun\Wobj:=wbench;
ELSE
  ArcL p1weld,v50,smdc,wldc,wvdz,fine,weldgun\Wobj:=wbench;
  ArcL p1weldc,v50,smdc,wldc,wvdz,fine,weldgun\Wobj:=wbench;
ENDIF
```

```
 IF last=TRUE THEN
  ArcL\Off,p2weld,v50,smdn,wldn,wvdz,fine,weldgun\Wobj:=wbench;
 ELSE
  ArcL p2weldc,v50,smdn,wldn,wvdz,fine,weldgun\Wobj:=wbench;
  ArcL p2weld,v50,smdc,wldc,wvdz,fine,weldgun\Wobj:=wbench;
 ENDIF
ENDPROC

PROC setup()
 VAR num theta:=0;
 VAR num x1:=0;
 VAR num y1:=0;
 VAR num x2:=0;
 VAR num y2:=0;
 CONST orient obench:=[0,0.707107,-0.707107,0];

 poverhead.rot:=obench;
 pwinit1.rot:=obench;
 pwinit2.rot:=obench;
 x1:=pwinit1.trans.x;
 y1:=pwinit1.trans.y;
 x2:=pwinit2.trans.x;
 y2:=pwinit2.trans.y;
 theta:=ATan((y2-y1)/(x2-x1));
```

```
 hincrx:=-hincr*Sin(theta);
 hincry:=hincr*Cos(theta);
 crndistx:=crndist*Cos(theta);
 crndisty:=crndist*Sin(theta);
 pwinit1c:=pwinit1;
 pwinit2c:=pwinit2;
 IF x2>x1 THEN
   pwinit1c:=Offs(pwinit1,crndistx,crndisty,0);
   pwinit2c:=Offs(pwinit2,-crndistx,-crndisty,0);
 ELSE
   pwinit1c:=Offs(pwinit1,-crndistx,-crndisty,0);
   pwinit2c:=Offs(pwinit2,crndistx,crndisty,0);
 ENDIF
ENDPROC

PROC main()
 TPErase;
 TPReadNum imax,"no. vertical layers:";
 TPReadNum hmax,"no. horizontal welds:";
 TPReadNum iincr,"vertical increment (mm):";
 TPReadNum hincr,"horizontal increment (mm):";
 TPReadNum crndist,"pre/post corner distance (mm):";
```

```
  poverhead:=[[809.55,203.03,166.54],[0.087712,-
0.70166,0.701634,0.087693],[-1,0,-
1,0],[9E+09,9E+09,9E+09,9E+09,9E+09,9E+09]];
  pwinit1:=[[881.08,188.58,10.65],[0.005743,-0.69011,0.72352,-0.015307],[-
1,0,-1,0],[9E+09,9E+09,9E+09,9E+09,9E+09,9E+09]];
  pwinit2:=[[726.59,188.17,10.09],[0.005425,-0.690285,0.723345,-0.01581],[-
1,0,-1,0],[9E+09,9E+09,9E+09,9E+09,9E+09,9E+09]];
  wldn:=wd_frank;
  smdn:=sd10_frank;
  wldc:=wd_frankc;
  smdc:=sd10_frank;
  setup;
  MoveJ pHome,v100,z200,weldgun\WObj:=wbench;
  makeblock;
  MoveJ pHome,v100,z200,weldgun\WObj:=wbench;
 ENDPROC
ENDMODULE
```

H3 F_BLOIO2.PRG

```
%%%
  VERSION:1
  LANGUAGE:ENGLISH
%%%

MODULE F_BLOIO2
  PERS welddata wd_frankic:=[6,150,8,0,0,0,0];
  PERS welddata wd_franki:=[5,150,8,0,0,0,0];
  VAR num width:=0;
  VAR num outincr:=0;
  VAR num outcrn:=0;
  VAR num outnum:=0;
  VAR bool first:=FALSE;
  VAR bool last:=FALSE;
  VAR robtarget pHome:=[[618.38,-88.51,287.59],[0.00567,-0.690109,0.723522,-
0.015284],[-1,-1,0,0],[9E+09,9E+09,9E+09,9E+09,9E+09,9E+09]];
  VAR robtarget
poverhead:=[[935.57,308.85,1158.55],[0.350803,0.028535,0.935634,-0.0267],[0,-
1,0,0],[9E+09,9E+09,9E+09,9E+09,9E+09,9E+09]];
  VAR robtarget prect1:=[[866.92,378.26,831.78],[0.350986,0.028254,0.935572,-
0.026768],[0,-1,0,0],[9E+09,9E+09,9E+09,9E+09,9E+09,9E+09]];
  VAR robtarget prect2:=[[866.91,378.26,831.78],[0.350976,0.028264,0.935575,-
0.02677],[0,-1,0,0],[9E+09,9E+09,9E+09,9E+09,9E+09,9E+09]];
```

VAR robtarget prect3:=[[866.92,378.26,831.78],[0.350986,0.028254,0.935572,-0.026768],[0,-1,0,0],[9E+09,9E+09,9E+09,9E+09,9E+09,9E+09]];

VAR robtarget prect4:=[[866.91,378.26,831.78],[0.350976,0.028264,0.935575,-0.02677],[0,-1,0,0],[9E+09,9E+09,9E+09,9E+09,9E+09,9E+09]];

VAR robtarget prect1a:=[[866.91,378.26,831.78],[0.350976,0.028264,0.935575,-0.02677],[0,-1,0,0],[9E+09,9E+09,9E+09,9E+09,9E+09,9E+09]];

VAR robtarget prect1b:=[[866.91,378.26,831.78],[0.350976,0.028264,0.935575,-0.02677],[0,-1,0,0],[9E+09,9E+09,9E+09,9E+09,9E+09,9E+09]];

VAR robtarget prect2a:=[[866.91,378.26,831.78],[0.350976,0.028264,0.935575,-0.02677],[0,-1,0,0],[9E+09,9E+09,9E+09,9E+09,9E+09,9E+09]];

VAR robtarget prect2b:=[[866.91,378.26,831.78],[0.350976,0.028264,0.935575,-0.02677],[0,-1,0,0],[9E+09,9E+09,9E+09,9E+09,9E+09,9E+09]];

VAR robtarget prect3a:=[[866.91,378.26,831.78],[0.350976,0.028264,0.935575,-0.02677],[0,-1,0,0],[9E+09,9E+09,9E+09,9E+09,9E+09,9E+09]];

VAR robtarget prect3b:=[[866.91,378.26,831.78],[0.350976,0.028264,0.935575,-0.02677],[0,-1,0,0],[9E+09,9E+09,9E+09,9E+09,9E+09,9E+09]];

```
VAR robtarget
prect4a:=[[866.91,378.26,831.78],[0.350976,0.028264,0.935575,-0.02677],[0,-1,0,0],[9E+09,9E+09,9E+09,9E+09,9E+09,9E+09]];
VAR robtarget
prect4b:=[[866.91,378.26,831.78],[0.350976,0.028264,0.935575,-0.02677],[0,-1,0,0],[9E+09,9E+09,9E+09,9E+09,9E+09,9E+09]];
VAR num ingap:=0;
VAR num inpasses:=0;
VAR num inincr:=0;
VAR num incrn:=0;
VAR num innum:=0;
VAR num inoffs:=0;
VAR num inoffsx:=0;
VAR num inoffsy:=0;
VAR bool innerfirst:=FALSE;
VAR bool innerlast:=FALSE;
VAR bool innerdir:=FALSE;
VAR robtarget
pinner1:=[[866.91,378.26,831.78],[0.350976,0.028264,0.935575,-0.02677],[0,-1,0,0],[9E+09,9E+09,9E+09,9E+09,9E+09,9E+09]];
VAR robtarget
pinner2:=[[866.91,378.26,831.78],[0.350976,0.028264,0.935575,-0.02677],[0,-1,0,0],[9E+09,9E+09,9E+09,9E+09,9E+09,9E+09]];
```

```
VAR robtarget
pinner1c:=[[866.91,378.26,831.78],[0.350976,0.028264,0.935575,-0.02677],[0,-
1,0,0],[9E+09,9E+09,9E+09,9E+09,9E+09,9E+09]];
VAR robtarget
pinner2c:=[[866.91,378.26,831.78],[0.350976,0.028264,0.935575,-0.02677],[0,-
1,0,0],[9E+09,9E+09,9E+09,9E+09,9E+09,9E+09]];
VAR robtarget pfill1:=[[866.91,378.26,831.78],[0.350976,0.028264,0.935575,-
0.02677],[0,-1,0,0],[9E+09,9E+09,9E+09,9E+09,9E+09,9E+09]];
VAR robtarget pfill2:=[[866.91,378.26,831.78],[0.350976,0.028264,0.935575,-
0.02677],[0,-1,0,0],[9E+09,9E+09,9E+09,9E+09,9E+09,9E+09]];
VAR robtarget pfill1c:=[[866.91,378.26,831.78],[0.350976,0.028264,0.935575,-
0.02677],[0,-1,0,0],[9E+09,9E+09,9E+09,9E+09,9E+09,9E+09]];
VAR robtarget pfill2c:=[[866.91,378.26,831.78],[0.350976,0.028264,0.935575,-
0.02677],[0,-1,0,0],[9E+09,9E+09,9E+09,9E+09,9E+09,9E+09]];
PERS welddata wldn:=[5,75,4,0,5,75,2];
PERS seamdata smdn:=[0.1,0.1,120,0.5,0.1,5,5,25,75,3,0,0.5,0.5,1,75,1.5];
PERS welddata wldc:=[5,75,4,0,5,75,2];
PERS seamdata smdc:=[0.1,0.1,120,0.5,0.1,5,5,25,75,3,0,0.5,0.5,1,75,1.5];
PERS welddata wldi:=[5,150,8,0,0,0,0];
PERS seamdata smdi:=[0.1,0.1,150,8,0.1,5,5,25,150,8,0,1,0,1,150,8];
PERS welddata wldic:=[6,150,8,0,0,0,0];
PERS seamdata smdic:=[0.1,0.1,150,8,0.1,5,5,25,150,8,0,1,0,1,150,8];
PERS weavedata wvdz:=[0,0,0,0,0,0,0,0,0,0,0,0,0,0,0];
```

```
PROC makefill()
 VAR num i:=0;

 FOR i FROM 1 TO innum DO
  filllevel;
  pinner1:=Offs(pinner1,0,0,inincr);
  pinner2:=Offs(pinner2,0,0,inincr);
  pinner1c:=Offs(pinner1c,0,0,inincr);
  pinner2c:=Offs(pinner2c,0,0,inincr);
 ENDFOR
ENDPROC

PROC filllevel()
 VAR num i:=0;

 innerdir:=TRUE;
 innerfirst:=TRUE;
 innerlast:=FALSE;
 pfill1:=pinner1;
 pfill2:=pinner2;
 pfill1c:=pinner1c;
 pfill2c:=pinner2c;
 MoveJ poverhead,v100,z200,weldgun\WObj:=wbench;
 FOR i FROM 1 TO inpasses DO
```

```
    IF i=inpasses innerlast:=TRUE;
    fillweld;
    innerdir:=NOT innerdir;
    innerfirst:=FALSE;
    pfill1:=Offs(pfill1,inoffsx,inoffsy,0);
    pfill2:=Offs(pfill2,inoffsx,inoffsy,0);
    pfill1c:=Offs(pfill1c,inoffsx,inoffsy,0);
    pfill2c:=Offs(pfill2c,inoffsx,inoffsy,0);
   ENDFOR
   MoveJ poverhead,v100,z200,weldgun\WObj:=wbench;
  ENDPROC

  PROC fillweld()
   VAR robtarget
pfill1temp:=[[866.91,378.26,831.78],[0.350976,0.028264,0.935575,-0.02677],[0,-
1,0,0],[9E+09,9E+09,9E+09,9E+09,9E+09,9E+09]];
   VAR robtarget
pfill2temp:=[[866.91,378.26,831.78],[0.350976,0.028264,0.935575,-0.02677],[0,-
1,0,0],[9E+09,9E+09,9E+09,9E+09,9E+09,9E+09]];
   VAR robtarget
pfill1ctemp:=[[866.91,378.26,831.78],[0.350976,0.028264,0.935575,-
0.02677],[0,-1,0,0],[9E+09,9E+09,9E+09,9E+09,9E+09,9E+09]];
```

```
  VAR robtarget
pfill2ctemp:=[[866.91,378.26,831.78],[0.350976,0.028264,0.935575,-
0.02677],[0,-1,0,0],[9E+09,9E+09,9E+09,9E+09,9E+09,9E+09]];

  IF innerdir THEN
    pfill1temp:=pfill1;
    pfill2temp:=pfill2;
    pfill1ctemp:=pfill1c;
    pfill2ctemp:=pfill2c;
  ELSE
    pfill1temp:=pfill2;
    pfill2temp:=pfill1;
    pfill1ctemp:=pfill2c;
    pfill2ctemp:=pfill1c;
  ENDIF
  IF innerfirst THEN
    ArcL\On,pfill1temp,v50,smdic,wldic,wvdz,fine,weldgun\Wobj:=wbench;
  ELSE
    ArcL pfill1temp,v50,smdic,wldic,wvdz,fine,weldgun\Wobj:=wbench;
  ENDIF
  ArcL pfill1ctemp,v50,smdic,wldic,wvdz,fine,weldgun\Wobj:=wbench;
  ArcL pfill2ctemp,v50,smdi,wldi,wvdz,fine,weldgun\Wobj:=wbench;
  IF innerlast THEN
    ArcL\Off,pfill2temp,v50,smdic,wldic,wvdz,fine,weldgun\Wobj:=wbench;
```

```
  ELSE
   ArcL pfill2temp,v50,smdic,wldic,wvdz,fine,weldgun\Wobj:=wbench;
  ENDIF
ENDPROC


PROC makebox()
  VAR num i:=0;


  MoveJ poverhead,v100,z200,weldgun\WObj:=wbench;
  first:=TRUE;
  last:=FALSE;
  FOR i FROM 1 TO outnum DO
   IF i=outnum last:=TRUE;
   makerect;
   first:=FALSE;
   prect1:=Offs(prect1,0,0,outincr);
   prect2:=Offs(prect2,0,0,outincr);
   prect3:=Offs(prect3,0,0,outincr);
   prect4:=Offs(prect4,0,0,outincr);
   prect1a:=Offs(prect1a,0,0,outincr);
   prect1b:=Offs(prect1b,0,0,outincr);
   prect2a:=Offs(prect2a,0,0,outincr);
   prect2b:=Offs(prect2b,0,0,outincr);
   prect3a:=Offs(prect3a,0,0,outincr);
```

```
   prect3b:=Offs(prect3b,0,0,outincr);
   prect4a:=Offs(prect4a,0,0,outincr);
   prect4b:=Offs(prect4b,0,0,outincr);
  ENDFOR
  MoveJ poverhead,v100,z200,weldgun\WObj:=wbench;
ENDPROC


PROC makerect()
  IF first THEN
   ArcL\On,prect1,v50,smdc,wldc,wvdz,fine,weldgun\Wobj:=wbench;
  ELSE
   ArcL prect1,v50,smdc,wldc,wvdz,fine,weldgun\Wobj:=wbench;
  ENDIF
  ArcL prect1a,v50,smdc,wldc,wvdz,fine,weldgun\Wobj:=wbench;
  ArcL prect2a,v50,smdn,wldn,wvdz,fine,weldgun\Wobj:=wbench;
  ArcL prect2,v50,smdc,wldc,wvdz,fine,weldgun\Wobj:=wbench;
  ArcL prect2b,v50,smdc,wldc,wvdz,fine,weldgun\Wobj:=wbench;
  ArcL prect4b,v50,smdn,wldn,wvdz,fine,weldgun\Wobj:=wbench;
  ArcL prect4,v50,smdc,wldc,wvdz,fine,weldgun\Wobj:=wbench;
  ArcL prect4a,v50,smdc,wldc,wvdz,fine,weldgun\Wobj:=wbench;
  ArcL prect3a,v50,smdn,wldn,wvdz,fine,weldgun\Wobj:=wbench;
  ArcL prect3,v50,smdc,wldc,wvdz,fine,weldgun\Wobj:=wbench;
  ArcL prect3b,v50,smdc,wldc,wvdz,fine,weldgun\Wobj:=wbench;
  ArcL prect1b,v50,smdn,wldn,wvdz,fine,weldgun\Wobj:=wbench;
```

```
  IF last=TRUE THEN
    ArcL\Off,prect1,v50,smdc,wldc,wvdz,fine,weldgun\Wobj:=wbench;
  ELSE
    ArcL prect1,v50,smdc,wldc,wvdz,fine,weldgun\Wobj:=wbench;
  ENDIF
ENDPROC


PROC setup()
  VAR num theta:=0;
  VAR num x1:=0;
  VAR num y1:=0;
  VAR num x2:=0;
  VAR num y2:=0;
  CONST orient obench:=[0,0.707107,-0.707107,0];
  VAR num ingapx:=0;
  VAR num ingapy:=0;
  VAR num widthx:=0;
  VAR num widthy:=0;
  VAR num crndistx:=0;
  VAR num crndisty:=0;
  VAR num incrnx:=0;
  VAR num incrny:=0;
  VAR num innerx1:=0;
  VAR num innery1:=0;
```

```
VAR num innerx2:=0;
VAR num innery2:=0;

poverhead.rot:=obench;
prect1.rot:=obench;
prect2.rot:=obench;
x1:=prect1.trans.x;
y1:=prect1.trans.y;
x2:=prect2.trans.x;
y2:=prect2.trans.y;
theta:=ATan((y2-y1)/(x2-x1));
widthx:=-width*Sin(theta);
widthy:=width*Cos(theta);
inoffs:=width/(inpasses+1);
inoffsx:=-inoffs*Sin(theta);
inoffsy:=inoffs*Cos(theta);
incrnx:=incrn*Cos(theta);
incrny:=incrn*Sin(theta);
ingapx:=ingap*Cos(theta);
ingapy:=ingap*Sin(theta);
prect3:=Offs(prect1,widthx,widthy,0);
prect4:=Offs(prect2,widthx,widthy,0);
crndistx:=outcrn*Cos(theta);
crndisty:=outcrn*Sin(theta);
```

```
innerx1:=inoffsx+ingapx;
innery1:=inoffsy+ingapy;
innerx2:=inoffsx-ingapx;
innery2:=inoffsy-ingapy;
IF x2>x1 THEN
  prect1a:=Offs(prect1,crndistx,crndisty,0);
  prect2a:=Offs(prect2,-crndistx,-crndisty,0);
  prect3a:=Offs(prect3,crndistx,crndisty,0);
  prect4a:=Offs(prect4,-crndistx,-crndisty,0);
  pinner1:=Offs(prect1,innerx1,innery1,0);
  pinner2:=Offs(prect2,innerx2,innery2,0);
  pinner1c:=Offs(pinner1,incrnx,incrny,0);
  pinner2c:=Offs(pinner2,-incrnx,-incrny,0);
ELSE
  prect1a:=Offs(prect1,-crndistx,-crndisty,0);
  prect2a:=Offs(prect2,crndistx,crndisty,0);
  prect3a:=Offs(prect3,-crndistx,-crndisty,0);
  prect4a:=Offs(prect4,crndistx,crndisty,0);
  pinner1:=Offs(prect1,innerx2,innery2,0);
  pinner2:=Offs(prect2,innerx1,innery1,0);
  pinner1c:=Offs(pinner1,-incrnx,-incrny,0);
  pinner2c:=Offs(pinner2,incrnx,incrny,0);
ENDIF
prect1b:=Offs(prect1,-crndisty,crndistx,0);
```

```
  prect2b:=Offs(prect2,-crndisty,crndistx,0);
  prect3b:=Offs(prect3,crndisty,-crndistx,0);
  prect4b:=Offs(prect4,crndisty,-crndistx,0);
ENDPROC


PROC ask()
  TPErase;
  TPReadNum outnum,"no. consecutive outer layers:";
  TPReadNum outincr,"outer layer vertical increment (mm):";
  TPReadNum innum,"no. consecutive inner layers:";
  TPReadNum inincr,"inner layer vertical increment (mm):";
ENDPROC


PROC updatepoverhead()
  VAR num d1:=0;
  VAR num d2:=0;

  d1:=outnum*outincr;
  d2:=innum*inincr;
  IF d1>d2 THEN
    poverhead:=Offs(poverhead,0,0,d1);
  ELSE
    poverhead:=Offs(poverhead,0,0,d2);
  ENDIF
```

```
ENDPROC

PROC main()
  VAR bool continue:=TRUE;
  VAR num cntnum:=0;

  TPErase;
  TPReadNum width,"width of block (mm):";
  TPReadNum outcrn,"outer pre/post corner distance (mm):";
  TPReadNum inpasses,"no. inner filler passes:";
  TPReadNum ingap,"inner start/end to wall gap (mm):";
  TPReadNum incrn,"inner pre/post corner distance (mm):";
  pHome:=[[584.3,-2.62,353.95],[0.002779,-0.706717,0.707484,0.002998],[-1,-
1,0,0],[9E+09,9E+09,9E+09,9E+09,9E+09,9E+09]];
  poverhead:=[[795.22,193.09,120.11],[0.002759,-
0.706616,0.707586,0.003013],[-1,0,-
1,0],[9E+09,9E+09,9E+09,9E+09,9E+09,9E+09]];
  prect1:=[[876.39,170.07,10.87],[0.000124,0.707155,-0.707058,4.8E-05],[-1,0,-
1,0],[9E+09,9E+09,9E+09,9E+09,9E+09,9E+09]];
  prect2:=[[727.91,169.97,10.14],[0.000204,0.707227,-0.706987,0.000229],[-
1,0,-1,0],[9E+09,9E+09,9E+09,9E+09,9E+09,9E+09]];
  wldn:=wd_frank;
  smdn:=sd3_frank;
  wldc:=wd_frank;
```

```
smdc:=sd3_frank;
wldi:=wd_franki;
smdi:=sd8_frank;
wldic:=wd_frankic;
smdic:=sd8_frank;
setup;
MoveJ pHome,v100,z200,weldgun\WObj:=wbench;
continue:=TRUE;
WHILE continue DO
  ask;
  makebox;
  makefill;
  updatepoverhead;
  TPErase;
  TPReadFK cntnum,"Do you want to continue welding more
layers?","","","","YES","NO";
  IF cntnum=5 continue:=FALSE;
ENDWHILE
MoveJ pHome,v100,z200,weldgun\WObj:=wbench;
ENDPROC
ENDMODULE
```

Appendix I

Solid Objects Results

I1. Sample s2-75-05

I2. Sample s2-100-05

I3. Sample s3-75-05

I4. Sample s3-100-05

I5. Sample s4-75-05

I6. Sample s4-100-05

I7. Sample s2-75-05/s4-100-05

I8. Sample s2-75-05/s5-100-05

I9. Sample s4-100-05/s8-150-05

I1. Sample s2-75-05

Set Values	
Voltage [%]	75
Wire feed rate [m/min]	2
Travel speed [mm/sec]	5
Gas flow [l/min]	15

Weld Geometry		Defects and Weld Property	
Weld length [mm]	150	Spatters	No
Weld width [mm]	18.4	Porosity	Yes
Weld thickness [mm]	18	Non-metallic inclusions (Slag)	Yes
Number of adjacent welds	10	Lack of fusion	Yes
Number of layers	7	Average hardness[HV]	181.5
		Tensile Strength [Mpa]	461
		Charpy V-notch [J]	159

Hardness Data [HV]

Only in this sample, several hardness measurements from each layer were taken:

Layer 1: 188, 189, 192, 190, 190, 190

Layer 2: 167, 176, 179, 175, 175, 174

Layer 3: 177, 177, 174, 176, 175, 175

Layer 4: 179, 174, 176, 175, 177, 176

Layer 5: 175.2, 178, 179, 179,180, 183

Layer 6: 178, 178, 178, 180, 188.1, 187.6

Layer 7: 197, 191, 188, 195, 194, 195

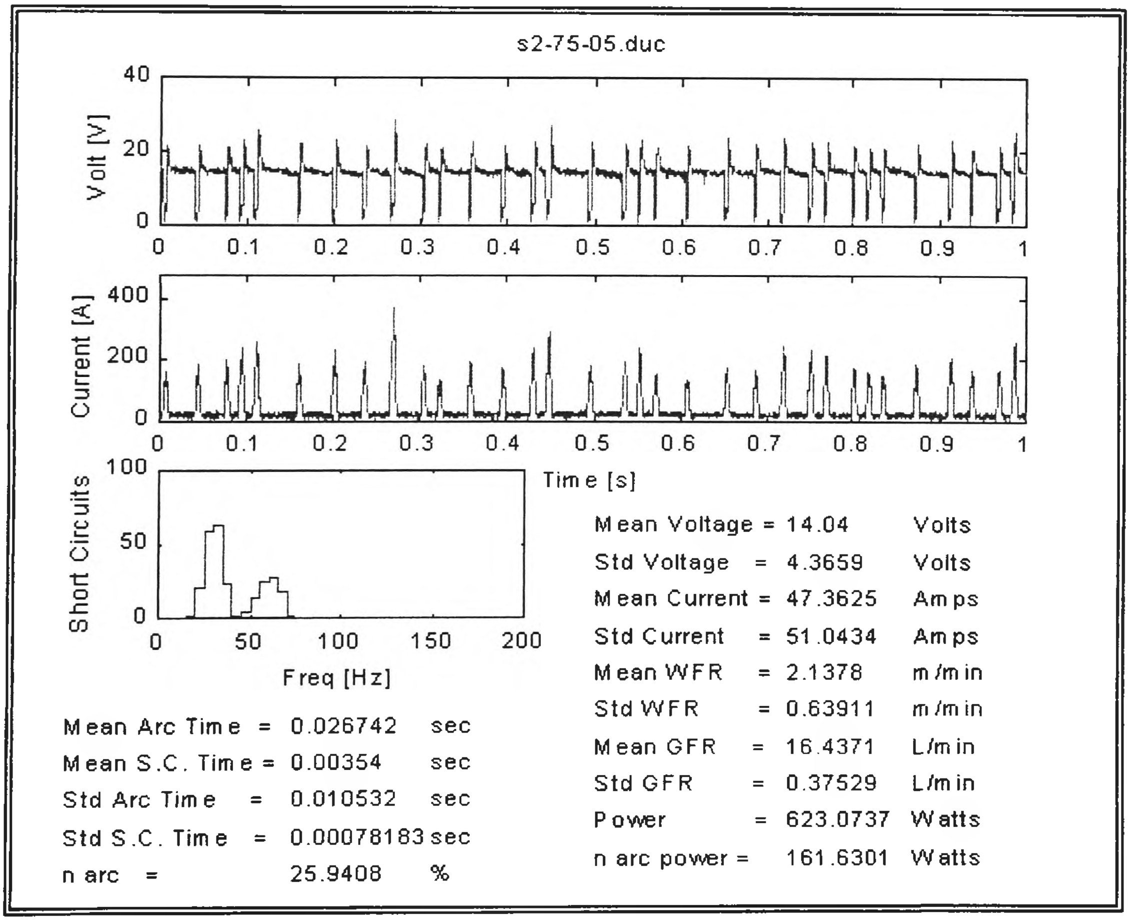

Plot I1-1

Sample s2-75-05

I2. Sample s2-100-05

Set Values	
Voltage [%]	100
Wire feed rate [m/min]	2
Travel speed [mm/sec]	5
Gas flow [l/min]	15

Weld Geometry		Defects and Weld Property	
Weld length [mm]	150	Spatters	Yes
Weld width [mm]	18.1	Porosity	Yes
Weld thickness [mm]	18.2	Non-metallic inclusions (Slag)	Yes
Number of adjacent welds	10	Lack of fusion	Yes
Number of layers	7	Average hardness[HV]	180.4
		Tensile Strength [Mpa]	481
		Charpy V-notch [J]	160

Hardness Data [HV]

Several numbers of hardness measurements were taken across the cross-section of the sample. The hardness measurements listed were taken from the top section to the bottom section of the sample: 190.7, 185.7, 178.5, 175.2, 173.5, 169.4, 185, 185.

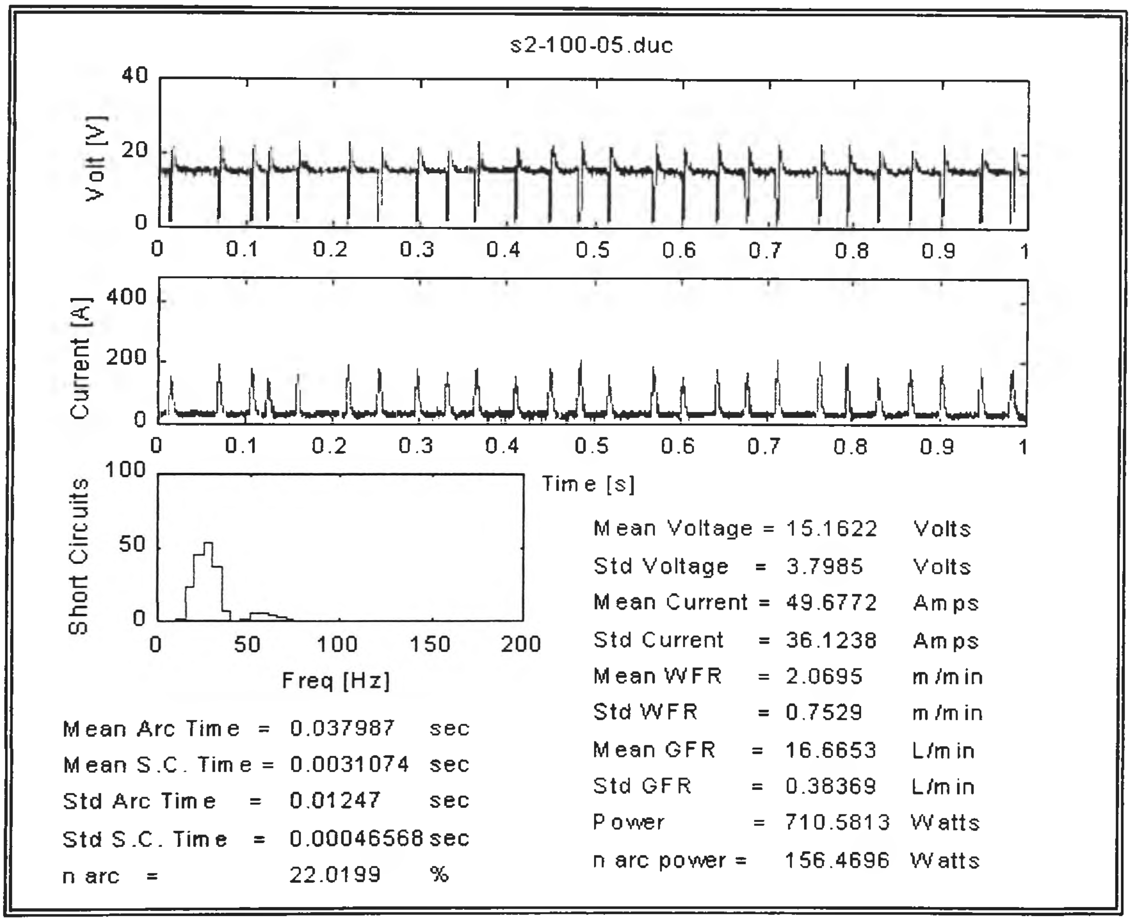

Plot I2-1

Sample s2-100-05

I3. Sample s3-75-05

Set Values	
Voltage [%]	75
Wire feed rate [m/min]	3
Travel speed [mm/sec]	5
Gas flow [l/min]	15

Weld Geometry		Defects and Weld Property	
Weld length [mm]	150	Spatters	No
Weld width [mm]	18.3	Porosity	Yes
Weld thickness [mm]	18.3	Non-metallic inclusions (Slag)	Yes
Number of adjacent welds	8	Lack of fusion	Yes
Number of layers	6	Average hardness[HV]	168.8
		Tensile Strength [Mpa]	528
		Charpy V-notch [J]	160

Hardness Data [HV]

Several numbers of hardness measurements were taken across the cross-section of the sample. The hardness measurements listed were taken from the top section to the bottom section of the sample: 170.7, 176.1, 162.5, 171.6, 166, 168.1, 168.4, 169.1, 170.7, 173.8.

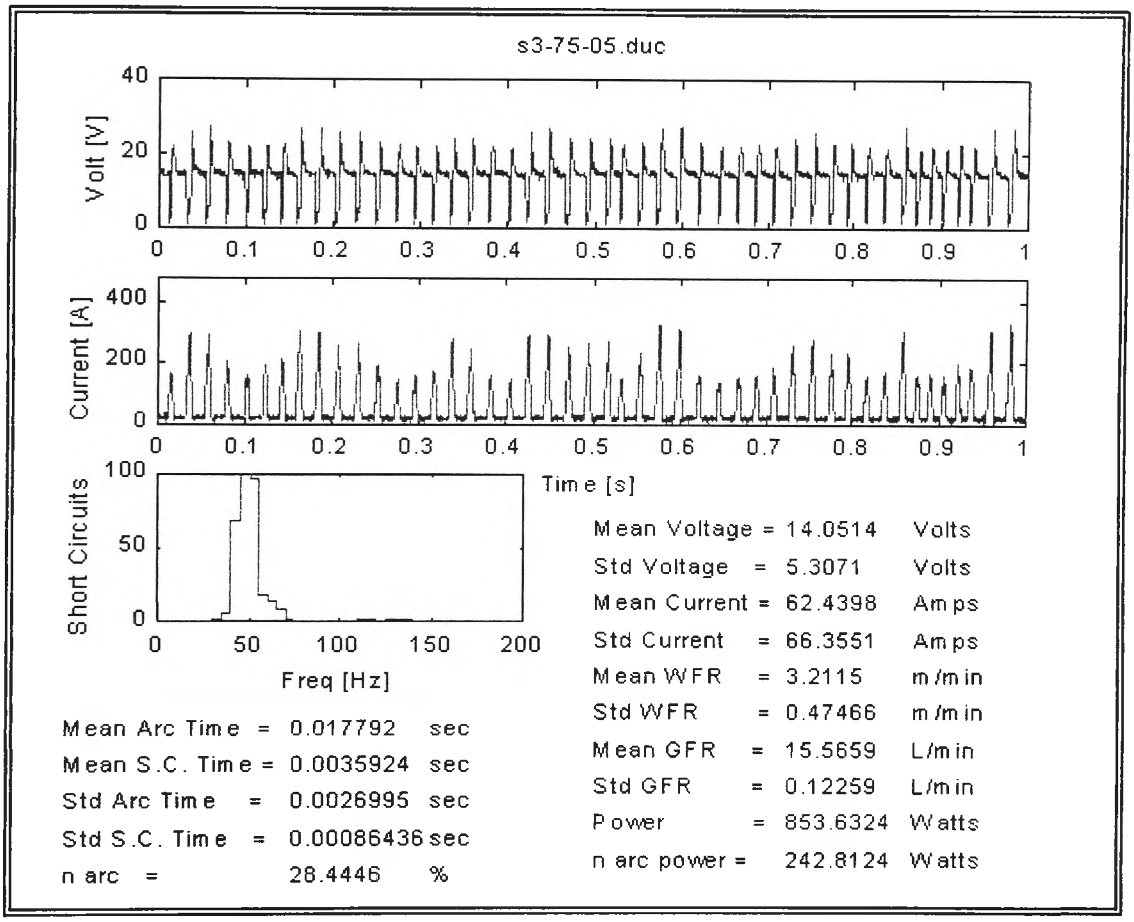

Plot I3-1

Sample s3-75-05

I4. Sample s3-100-05

Set Values	
Voltage [%]	100
Wire feed rate [m/min]	3
Travel speed [mm/sec]	5
Gas flow [l/min]	15

Weld Geometry		Defects and Weld Property	
Weld length [mm]	150	Spatters	No
Weld width [mm]	18.7	Porosity	Yes
Weld thickness [mm]	17.5	Non-metallic inclusions (Slag)	Yes
Number of adjacent welds	8	Lack of fusion	Yes
Number of layers	6	Average hardness[HV]	162
		Tensile Strength [Mpa]	517
		Charpy V-notch [J]	232

Hardness Data [HV]

Several numbers of hardness measurements were taken across the cross-section of the sample. The hardness measurements listed were taken from the top section to the bottom section of the sample: 158.5, 155, 157, 157, 157, 156.2, 158, 168.1, 168.1, 157, 162, 178.4, 164.5, 163.5, 162.8, 167.5, 165.2.

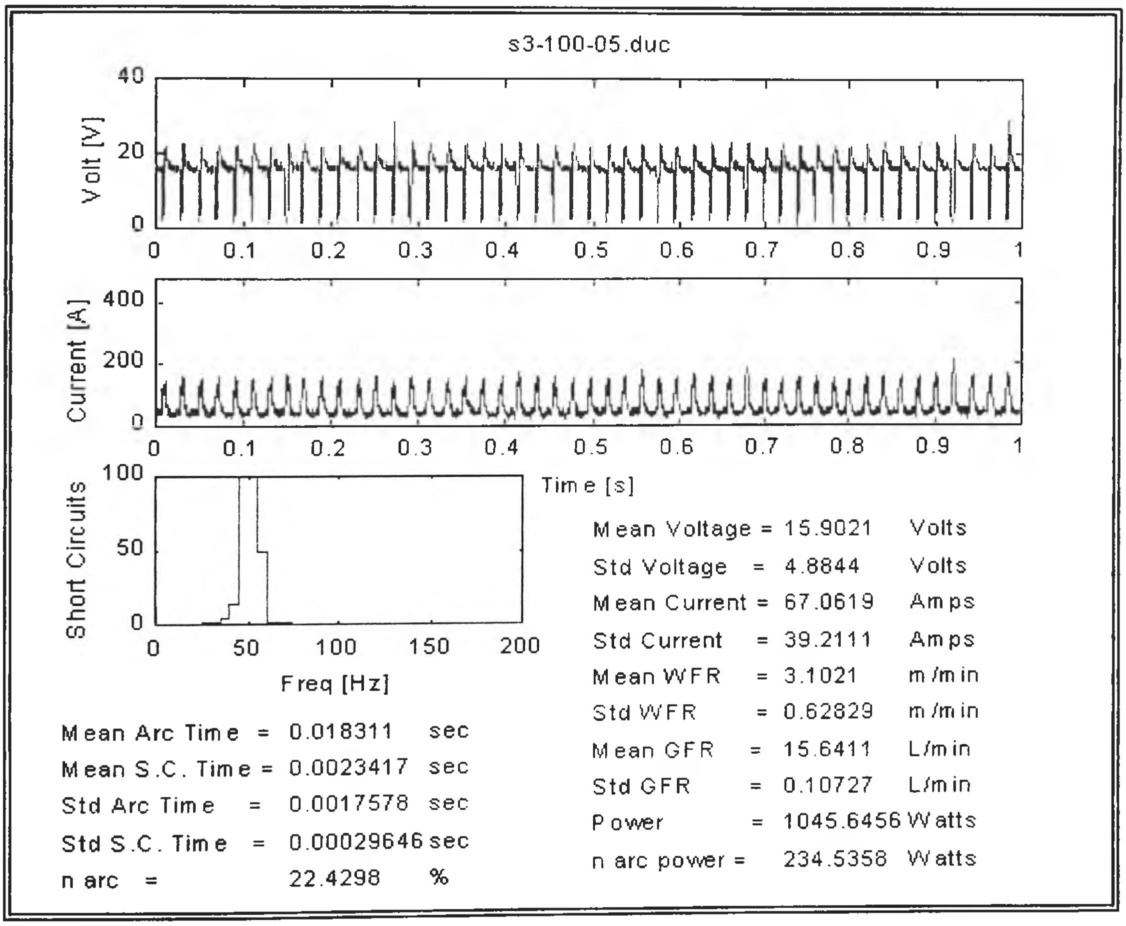

Plot I4-1

Sample s3-100-05

I5. Sample s4-75-05

Set Values	
Voltage [%]	75
Wire feed rate [m/min]	4
Travel speed [mm/sec]	5
Gas flow [l/min]	15

Weld Geometry		Defects and Weld Property	
Weld length [mm]	150	Spatters	No
Weld width [mm]	20	Porosity	Yes
Weld thickness [mm]	20	Non-metallic inclusions (Slag)	Yes
Number of adjacent welds	7	Lack of fusion	Yes
Number of layers	6	Average hardness[HV]	152.4
		Tensile Strength [Mpa]	522
		Charpy V-notch [J]	215

Hardness Data [HV]

Several numbers of hardness measurements were taken across the cross-section of the sample. The hardness measurements listed were taken from the top section to the bottom section of the sample: 157.6, 153.1, 148.2, 145.1, 152.9, 149.2, 150.8, 153.1, 158.4, 154.2, 154.1, 151.5.

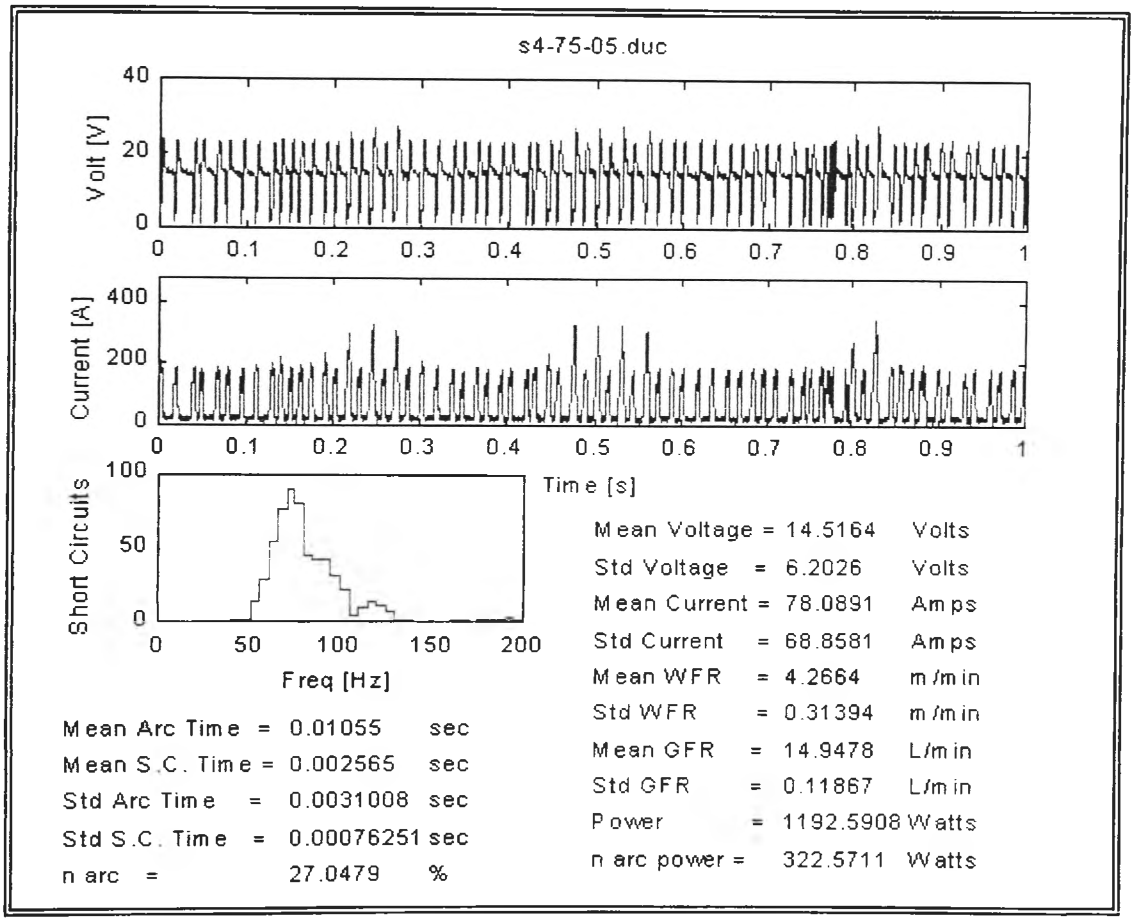

Plot I5-1

Sample s4-75-05

I6. Sample s4-100-05

Set Values	
Voltage [%]	100
Wire feed rate [m/min]	4
Travel speed [mm/sec]	5
Gas flow [l/min]	15

Weld Geometry		Defects and Weld Property	
Weld length [mm]	150	Spatters	No
Weld width [mm]	20	Porosity	No
Weld thickness [mm]	20	Non-metallic inclusions (Slag)	No
Number of adjacent welds	7	Lack of fusion	No
Number of layers	6	Average hardness[HV]	150.1
		Tensile Strength [Mpa]	486
		Charpy V-notch [J]	206

Hardness Data [HV]

Several numbers of hardness measurements were taken across the cross-section of the sample. The hardness measurements listed were taken from the top section to the bottom section of the sample: 154.2, 152.1, 150.4, 151.6, 148.4, 146.8, 147.5, 150.1, 147.5, 149.5, 151, 152.1.

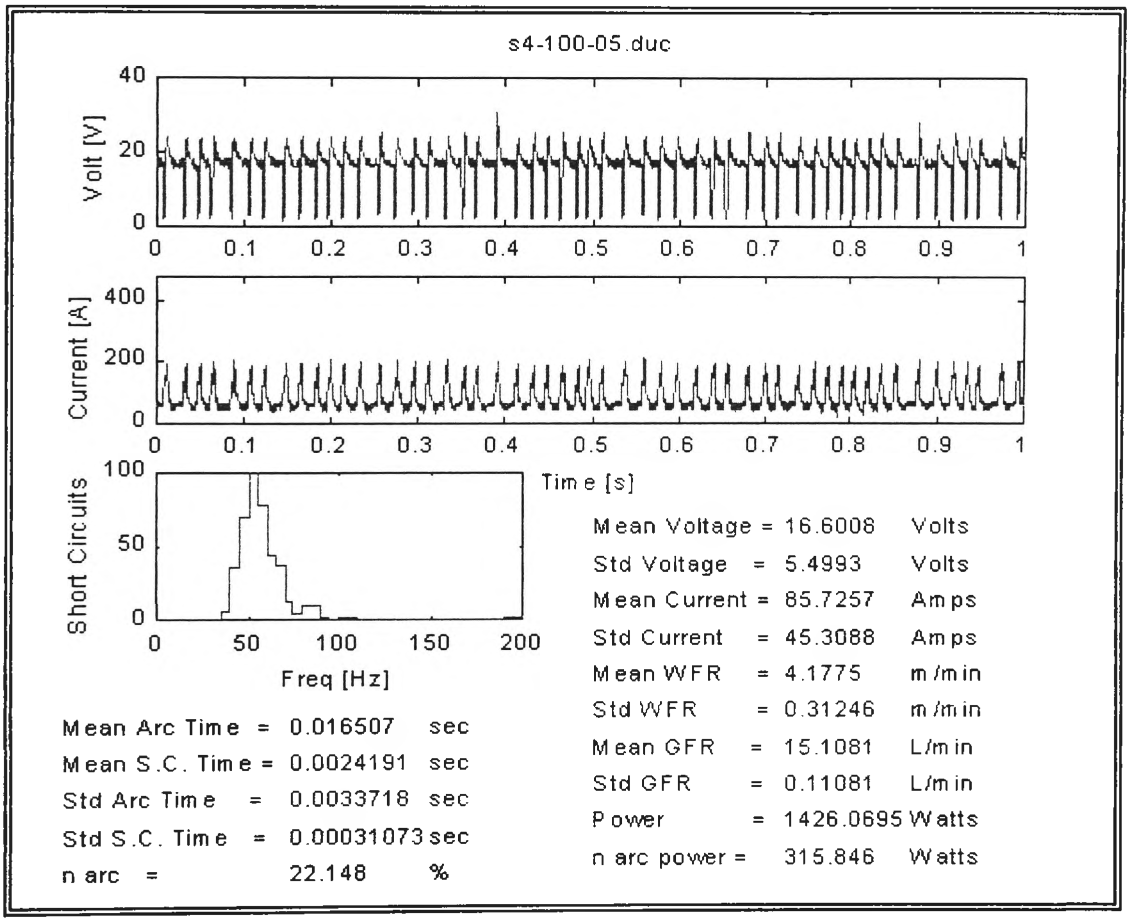

Plot 16-1

Sample s4-100-05

I7. Sample s2-75-05/s4-100-05

Set Values (Outer Wall)	
Voltage [%]	75
Wire feed rate [m/min]	2
Travel speed [mm/sec]	5
Gas flow [l/min]	15

Set Values (Filler)	
Voltage [%]	100
Wire feed rate [m/min]	4
Travel speed [mm/sec]	5
Gas flow [l/min]	15

Weld Geometry		Defects and Weld Property	
Weld length [mm]	150	Spatters	No
Weld width [mm]	21.5	Porosity	Yes
Weld thickness [mm]	16	Non-metallic inclusions (Slag)	Yes
Number of adjacent welds	6	Lack of fusion	Yes
Number of outer layers/consecutive run	2	Average hardness[HV]	152
Number of inner filler layers/consecutive run	1	Tensile Strength [Mpa]	509
Number of consecutive run	5	Charpy V-notch [J]	216

Hardness Data [HV]

Several numbers of hardness measurements were taken across the cross-section of the sample. The hardness measurements listed were taken from the top section to the bottom section of the sample: 150.8, 154.1, 149.6, 151.2, 154.1, 148.9, 157.1, 150, 153.1, 151.

Electrical Data

The electrical data of the outer setting can be obtained from sample s2-75-05 and the electrical data of the filler can be obtained from sample s4-100-05.

I8. Sample s2-75-05/s5-100-05

Set Values (Outer Wall)	
Voltage [%]	75
Wire feed rate [m/min]	2
Travel speed [mm/sec]	5
Gas flow [l/min]	15

Set Values (Filler)	
Voltage [%]	100
Wire feed rate [m/min]	5
Travel speed [mm/sec]	5
Gas flow [l/min]	15

Weld Geometry		Defects and Weld Property	
Weld length [mm]	150	Spatters	No
Weld width [mm]	22.5	Porosity	Yes
Weld thickness [mm]	16.5	Non-metallic inclusions (Slag)	Yes
Number of adjacent welds	6	Lack of fusion	Yes
Number of outer layers/consecutive run	2	Average hardness[HV]	151.4
Number of inner filler layers/consecutive run	1	Tensile Strength [Mpa]	500
Number of consecutive run	5	Charpy V-notch [J]	218

Hardness Data [HV]

Several numbers of hardness measurements were taken across the cross-section of the sample. The hardness measurements listed were taken from the top section to the bottom section of the sample: 151, 152, 148, 150, 154.1, 154, 155, 151, 150, 149.

Electrical Data

The electrical data of the outer setting can be obtained from sample s2-75-05 and the electrical data of the filler is depicted in plot I8-1.

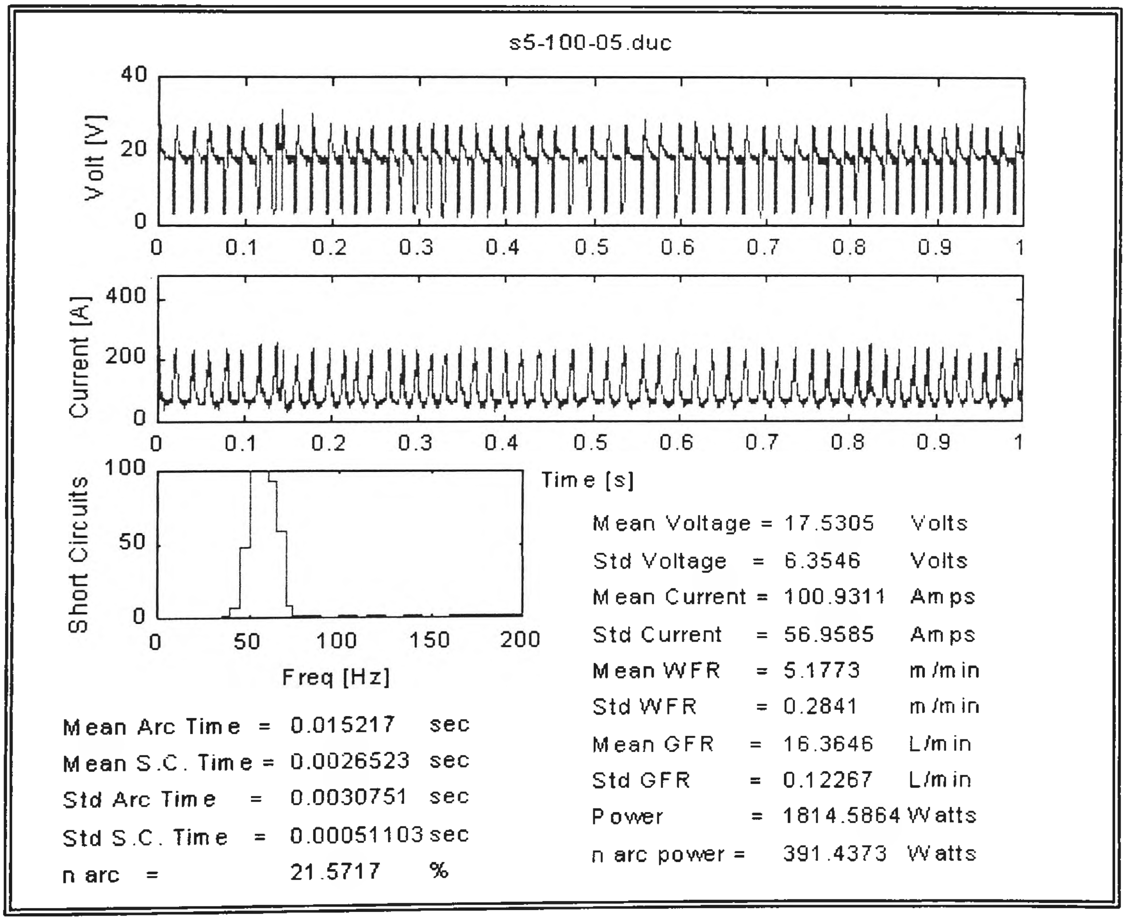

Plot I8-1

S5-100-05

I9. Sample s4-100-05/s8-150-05

Set Values (Outer Wall)	
Voltage [%]	100
Wire feed rate [m/min]	4
Travel speed [mm/sec]	5
Gas flow [l/min]	15

Set Values (Filler)	
Voltage [%]	150
Wire feed rate [m/min]	8
Travel speed [mm/sec]	5
Gas flow [l/min]	15

Weld Geometry		Defects and Weld Property	
Weld length [mm]	150	Spatters	No
Weld width [mm]	24.5	Porosity	No
Weld thickness [mm]	17.5	Non-metallic inclusions (Slag)	No
Number of adjacent welds	2	Lack of fusion	No
Number of outer layers/consecutive run	1	Average hardness[HV]	150.8
Number of inner filler layers/consecutive run	1	Tensile Strength [Mpa]	514
Number of consecutive run	8	Charpy V-notch [J]	214

Hardness Data [HV]

Several numbers of hardness measurements were taken across the cross-section of the sample. The hardness measurements listed were taken from the top section to the bottom section of the sample: 152, 151, 151, 150, 152, 151, 150, 152, 150, 149.

Electrical Data

The electrical data of the outer setting can be obtained from sample s4-100-05 and the electrical data of the filler is depicted in plot I9-1.

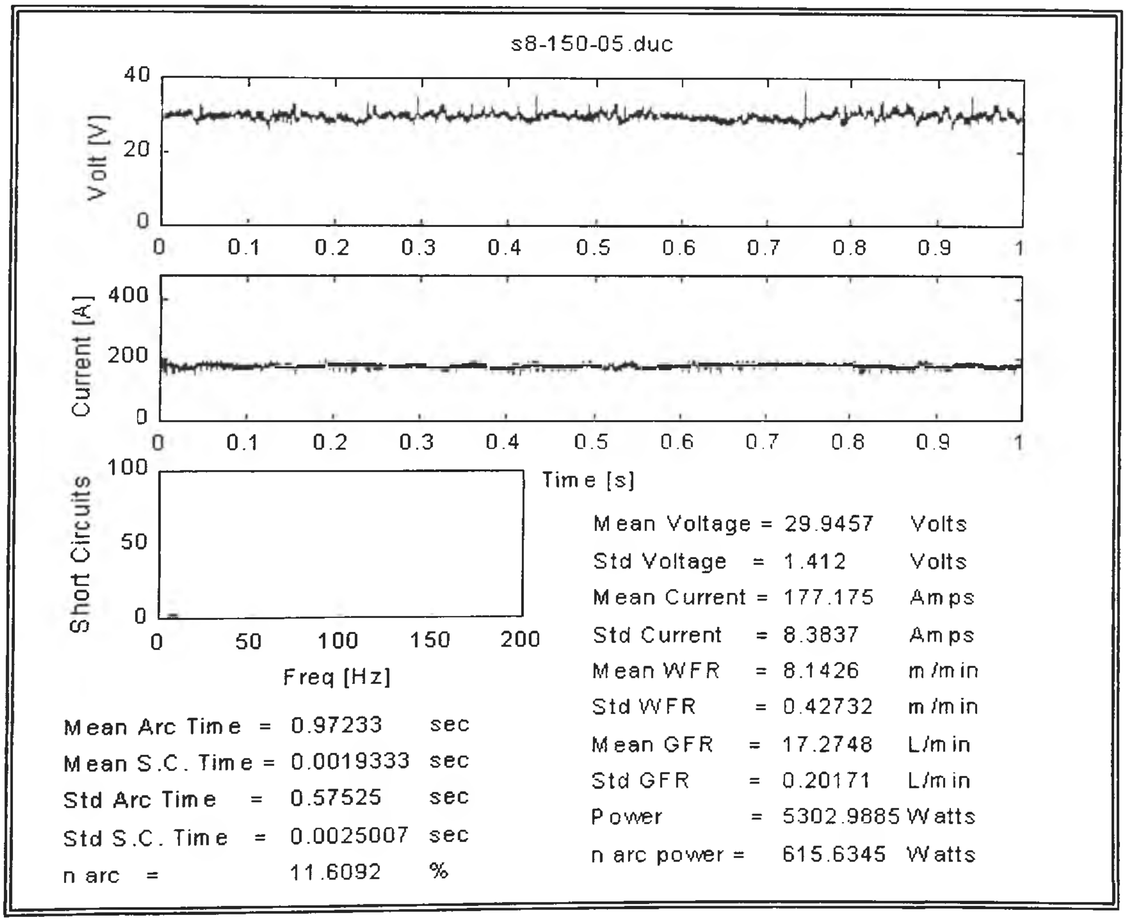

Plot I9-1

S8-150-05